

Politecnico di Milano



Scuola di Ingegneria Civile Ambientale e Territoriale

Corso di Laurea Magistrale in Ingegneria Civile

Indirizzo Strutture

***Internal Parametric Resonance and Aeroelastic
Effects for Long-Span Suspension Bridges***

Relatore: Prof. Capsoni Antonio

Correlatore: Prof. Ardito Raffaele

Tesi di Laurea Magistrale di:

Guerrieri Andrea

matr. 797216

Anno Accademico 2013/2014

Contents

Abstract	11
Introduction	13
1. Problem formulation	25
1.1. Deflection theory	25
1.1.1. General assumptions	25
1.1.2. Equilibrium conditions	25
1.1.3. Compatibility conditions	29
1.2. Extended 2 dof model	44
1.2.1. TPE formulation	44
1.2.2. Generalisation to 2dof	48
1.2.3. Dimensionless format	52
2. Modal response	63
2.1. Modal decomposition analysis	63
2.1.1. Flexural equation of motion	63
2.1.2. Torsional equation of motion	70
2.2. Parametric analysis	75
2.2.1. Flexural modes	75
2.2.2. Torsional modes	80
2.3. Numerical analysis of eigen-properties	89
2.3.1. Flexural vibrations	89
2.3.2. Torsional vibrations	104
2.4. Modal participation analysis	126
3. Nonlinear analysis	135
3.1. Direct multiple-scale perturbation technique	135
3.2. Linear contribution	137
3.3. Quadratic contribution	138
3.1.1. Skew-symmetric modes	141
3.1.2. Symmetric modes	145
3.2. Parametric analysis	155
3.2.2. Inextensible cables	156
3.2.3. Flexible deck	162
3.2.4. Free warping	170
3.4. Cubic contribution	175
3.4.1. Flexural equation	179

3.4.2	Torsional equation.....	183
3.5.	Governing equations	187
3.5.1	Free undamped vibrations	187
4.	Slackening of hangers	199
4.1	Modified equations of motion	200
4.2	Slackening development	201
4.3	Slackening initiation	206
5.	Aeroelastic model	217
5.1.	Fluid dynamics tools	217
5.1.1.	Conservation of mass	217
5.1.2.	Conservation of momentum	218
5.1.3.	Conservation of total energy	218
5.1.4.	Inviscid incompressible flows	219
5.1.5.	Potential flows.....	221
5.1.6.	Multi connected domains.....	224
5.1.7.	Kelvin theorem	225
5.1.8.	Elementary solutions for planar potential flows.....	225
5.1.9.	Stream functions	228
5.2.	Two dimensional stationary lifting flow around a circular cylinder	230
5.3.	Conformal mapping of Joukowski	238
5.4.	Theory of Theodorsen	242
5.4.1.	Non-circulatory flow component	243
5.4.2.	Circulatory flow component.....	249
5.4.3.	Circulatory intensity	253
5.4.4.	Bessel and Theodorsen functions.....	255
5.4.5.	Aeroelastic forces	258
5.5.	Static torsional divergence	263
5.6.	Dynamic flutter instability	267
5.6.1.	Analytical formulation	267
5.6.2.	Numerical results	278
6.	Parametric resonance	291
6.1	Floquet theory	291
6.1.1	The theorem.....	291
6.1.2	Hill's equation	296
6.2	Modal projection of aeroelastic equations of motion	299
6.3	Vortex shedding modelling	302

6.4	<i>Stability analysis of the complete aeroelastic model</i>	309
6.5	<i>Application to the Tacoma Narrow Bridge</i>	321
7.	Conclusion	327
	References	331

List of Figures

Figure I.1_Wynch Bridge.	13
Figure I.2_Union Bridge.	13
Figure I.3_Thomas Telford.....	14
Figure I.4_ Conwy suspension bridge.....	14
Figure I.5_ Menai strait bridge	14
Figure I.6_Isambard Kingdom Brunel.	14
Figure I.7_Clifton Bridge.	14
Figure I.8_Britannia Bridge.	15
Figure I.9_Robert Stephenson.....	15
Figure I.10_William John Macquorn Rankine.....	15
Figure I.11_Claude-Louis Navier.....	15
Figure I.12_James Finley.....	16
Figure I.13_Bridge on Jacob’s Creek.....	16
Figure I.14_Bridge on Niagara River.....	16
Figure I.15_John Augustus Roebling.....	17
Figure I.16_Brooklin Bridge.....	17
Figure I.17_Josef Melan.....	17
Figure I.18_Williamsburg Bridge.....	17
Figure I.19_Othmar Amman.....	18
Figure I.20_George Washington Bridge	18
Figure I.21_Joseph Strauss.....	18
Figure I.22_Golden Gate Bridge.....	18
Figure I.23_Deer Isle Bridge.....	19
Figure I.24_David Barnard Steinman.....	19
Figure I.25_Leon Solomon Moisseiff.....	19
Figure I.26_Bronx_Whitestone Bridge.....	19
Figure I.27_Tacoma Narrow Bridge.....	20
Figure I.28_Gilbert Roberts.....	20
Figure I.29_Severn Bridge.....	20
Figure I.30_Theodore Theodorsen.....	21
Figure I.31_Robert H. Scanlan.....	21
Figure I.32_Akashi Kaikyo Bridge.....	21
Figure I.33_Messina Strait Bridge (rendering).....	21
Figure 1.1_ Single span suspension bridge model.....	25
Figure 1.2_Cable static equilibrium configuration.....	26
Figure 1.3_Cable end forces.....	29
Figure 1.4_Cable’s elongation for large homothetic perturbation’s amplitude.....	33
Figure 1.5_ Elongation’s percentage contribution for large amplitudes.....	34
Figure 1.6_ Cable’s elongation for realistic perturbation’s amplitude.....	34
Figure 1.7_ Elongation’s percentage contribution for small amplitudes.....	35
Figure 1.8_ Exact vs approximate curvature.....	36
Figure 1.9_Cable’s elongation for large number of sinusoidal half waves.....	37
Figure 1.10_Cable’s elongation for a realistic number of sinusoidal half waves.....	38
Figure 1.11_Parametric influence of the perturbation’s amplitude.....	39

Figure 1.12_Elongation path for the first mode.....	40
Figure 1.13_Elongation path for the second mode.....	40
Figure 1.14_Elongation path for the third mode.	41
Figure 1.15_Exact vs approximate curvature.	42
Figure 1.16_Exact vs approximate curvature for the third mode.	43
Figure 2.1_Eigen function for flexural symmetric mode shape of fifth order.....	70
Figure 2.2_Flexural circular eigen-frequencies of Mode 1.....	90
Figure 2.3_Flexural circular eigen-frequencies of Mode 2.....	91
Figure 2.4_Modal shape of Mode 1 for $\lambda_L^2 = 0$ and skew-symmetric condition.	93
Figure 2.5_Modal shape of Mode 1 for $\lambda_L^2 = 100$	93
Figure 2.6_Modal shape of Mode 1 for $\lambda_L^2 = 225$	93
Figure 2.7_Modal shape of Mode 1 for $\lambda_L^2 = \infty$	94
Figure 2.8_Cross Over Frequency and Mode thresholds of Mode 1.....	96
Figure 2.9_Cross Over Modes of Mode 1.	97
Figure 2.10_Modal shape of Mode 2 for $\lambda_L^2 = 0$ and skew-symmetric condition.	98
Figure 2.11_Modal shape of Mode 2 for $\lambda_L^2 = 100$	98
Figure 2.12_Modal shape of Mode 2 for $\lambda_L^2 = 225$	99
Figure 2.13_Modal shape of Mode 2 for $\lambda_L^2 = \infty$	99
Figure 2.14_Cross Over Frequency and Mode thresholds of Mode 2.....	101
Figure 2.15_Cross Over Modes of Mode 2 for 2-0 nodes transition.....	102
Figure 2.16_Cross Over Modes of Mode 2 for 0-2 nodes transition.....	103
Figure 2.17_Cross Over Modes of Mode 2 for 2-4 nodes transition.....	103
Figure 2.18_Torsional circular eigen-frequencies of Mode 1 for $\chi^2 = 0$	105
Figure 2.19_Torsional circular eigen-frequencies of Mode 1 for $\chi^2 = \infty$	105
Figure 2.20_Torsional circular eigen-frequencies of Mode 2 for $\chi^2 = 0$	106
Figure 2.21_Torsional circular eigen-frequencies of Mode 2 for $\chi^2 = \infty$	107
Figure 2.22_Modal shape of Mode 1 for $\lambda_L^2 = 0$ and skew-symmetric condition.	108
Figure 2.23_Modal shape of Mode 1 for $\chi^2 = 0$ and $\lambda_L^2 = 100$	109
Figure 2.24_Modal shape of Mode 1 for $\chi^2 = 0$ and $\lambda_L^2 = 225$	109
Figure 2.25_Modal shape of Mode 1 for $\chi^2 = 0$ and $\lambda_L^2 = \infty$	110
Figure 2.26_Modal shape of Mode 1 for $\chi^2 = \infty$ and $\lambda_L^2 = 100$	110
Figure 2.27_Modal shape of Mode 1 for $\chi^2 = \infty$ and $\lambda_L^2 = 225$	111
Figure 2.28_Modal shape of Mode 1 for $\chi^2 = \infty$ and $\lambda_L^2 = \infty$	111
Figure 2.29_Cross Over Frequency and Mode thresholds of Mode 1 for $\chi^2 = 0$	113
Figure 2.30_Cross Over Frequency and Mode thresholds of Mode 1 for $\chi^2 = \infty$	114
Figure 2.31_Cross Over Modes of Mode 1 for $\chi^2 = 0$	115
Figure 2.32_Cross Over Modes of Mode 1 for $\chi^2 = \infty$	115
Figure 2.33_Modal shape of Mode 2 for $\lambda_L^2 = 0$ and skew-symmetric condition.	116
Figure 2.34_Modal shape of Mode 2 for $\chi^2 = 0$ and $\lambda_L^2 = 100$	116
Figure 2.35_Modal shape of Mode 2 for $\chi^2 = 0$ and $\lambda_L^2 = 225$	117
Figure 2.36_Modal shape of Mode 2 for $\chi^2 = 0$ and $\lambda_L^2 = \infty$	117
Figure 2.37_Modal shape of Mode 2 for $\chi^2 = \infty$ and $\lambda_L^2 = 100$	118
Figure 2.38_Modal shape of Mode 2 for $\chi^2 = \infty$ and $\lambda_L^2 = 225$	118
Figure 2.39_Modal shape of Mode 2 for $\chi^2 = \infty$ and $\lambda_L^2 = \infty$	119
Figure 2.40_Cross Over Frequency and Mode thresholds of Mode 2 for $\chi^2 = 0$	121
Figure 2.41_Cross Over Frequency and Mode thresholds of Mode 2 for $\chi^2 = \infty$	122
Figure 2.42_Cross Over Modes of Mode 2 for 2-0 nodes transition for $\chi^2 = 0$	123

Figure 2.43_Cross Over Modes of Mode 2 for 0-2 nodes transition for $\chi^2 = 0$	123
Figure 2.44_Cross Over Modes of Mode 2 for 2-4 nodes transition for $\chi^2 = 0$	124
Figure 2.45_Cross Over Modes of Mode 2 for 2-0 nodes transition for $\chi^2 = \infty$	124
Figure 2.46_Cross Over Modes of Mode 2 for 0-2 nodes transition for $\chi^2 = \infty$	125
Figure 2.47_Cross Over Modes of Mode 2 for 2-4 nodes transition for $\chi^2 = \infty$	125
Figure 2.48_Hyperbolic contribution on high order modal shape.....	126
Figure 2.49_Midspan displacement participation parameter for flexural symmetric mode shape 1.....	129
Figure 2.50_Quarter point displacement participation parameter for flexural symmetric mode shape 1.....	130
Figure 2.51_Midspan displacement participation parameter for flexural symmetric mode shape 2.....	130
Figure 2.52_Midspan displacement participation parameter for flexural symmetric mode shape 2.....	131
Figure 2.53_Cables tension increment for flexural symmetric mode shape 1.....	132
Figure 2.54_Cables tension increment for flexural symmetric mode shape 2.....	133
Figure 3.1_Functions governing the internal energy exchange.....	192
Figure 3.2_Amplitude modulation in time.....	192
Figure 4.1_Antinode displacement at first slackening for flexural mode 1.....	211
Figure 4.2_Antinode displacement at first slackening for flexural mode 2.....	211
Figure 4.3_Cable tension increment at first slackening for flexural mode 1.....	212
Figure 4.4_Cable tension increment at first slackening for flexural mode 2.....	212
Figure 4.5_Deck to cables forces before critical conditions.....	213
Figure 4.6_Deck to cables forces after critical conditions.....	214
Figure 4.7_Critical condition for slackening initiation.....	214
Figure 5.1_Real and imaginary part of the complex Theodorsen function.....	257
Figure 5.2_Torsional static divergence wind speed of Mode 1 for $\chi^2 = 0$	266
Figure 5.3_Aeroelastic frequency and damping of Mode 1 for Theodorsen and Steady-State formulation.....	279
Figure 5.4_Damping slope of Mode 1 for Theodorsen and Steady-State formulation.....	280
Figure 5.5_Flutter determinant of Mode 1 for generic structural conditions at null wind speed.....	281
Figure 5.6_Flutter determinant of Mode 1 for generic structural conditions at Divergent wind speed.....	282
Figure 5.7_Flutter determinant of Mode 1 for generic structural conditions at Flutter wind speed.....	282
Figure 5.8_Flutter onset of Mode 1 for Theodorsen and Steady-State formulation.....	284
Figure 5.9_Aeroelastic frequency and damping of Mode 1 for Theodorsen and Steady-State formulation.....	283
Figure 5.10_Aeroelastic modal shape of Mode 1 for generic structural conditions.....	284
Figure 5.11_Aeroelastic modal shape of Mode 1 for generic structural conditions.....	285
Figure 5.12_Aeroelastic modal shape of Mode 1 for generic structural conditions.....	285
Figure 5.13_Flutter curves of Mode 1 for Quasi-Static formulation with $\chi^2 = 0$	286
Figure 5.14_Flutter curves of Mode 1 for Quasi-Static formulation with $\chi^2 = 0$	287
Figure 5.15_Flutter curves of Mode 1 for Quasi-Static formulation with $\chi^2 = \infty$	288
Figure 5.16_Flutter curves of Mode 1 Steady-State formulation.....	288
Figure 5.17_Flutter curves of Mode 1 Theodorsen formulation.....	289
Figure 5.18_Flutter curves of Mode 1 Theodorsen formulation.....	290
Figure 6.1_Boundary layer on a flat plate.....	302
Figure 6.2_Reynolds number effect on trailing vortex street.....	303
Figure 6.3_Reynolds number effect on drag coefficient.....	306
Figure 6.4_Reynolds number effect on Strouhal number.....	307
Figure 6.5_Sectional aspect ratio effect on Strouhal number.....	308

Figure 6.6_ Strouhal model and lock-in phenomenon.....	309
Figure 6.7_ Scrouton number effect on response of cylinder.....	310
Figure 6.8_ Drag, Lift and Strouhal parameters for different cross sections.....	311
Figure 6.9_ Stability map for the Structural model with slender deck section.....	317
Figure 6.10_ Stability map for the Structural Model with bluff deck section.....	318
Figure 6.11_ Stability map for the Aeroelastic Model with slender deck section.....	319
Figure 6.12_ Stability map for the Aeroelastic Model with bluff deck section.....	320
Figure 6.13_ Unstable antinodal displacements for the Structural Model with slender deck section.....	320
Figure 6.14_ Unstable antinodal displacements for the Aeroelastic Model with slender deck section.....	321
Figure 6.15_ Unstable antinodal displacements for the Structural Model with bluff deck section.....	322
Figure 6.16_ Unstable antinodal displacements for the Aeroelastic Model with bluff deck section.....	322
Figure 6.17_ Stability map for the Aeroelastic Model of the Tacoma Narrow Bridge.....	303
Figure 6.18_ Unstable antinodal displacements for the Tacoma Narrow Bridge.....	326

Abstract

The potential occurrence of internal parametric resonance phenomena has been recently indicated as a possible contributory cause of failure for long-span suspension bridges. The peculiar non-linear behaviour of such structures entails a fundamental coupling between flexural and torsional response, with the possible occurrence of energy transfer between resonant modes. This so-called internal resonance may happen if a critical energy threshold is attained and may represent a critical issue for structural safety.

At the same time, suspension bridges, in view of their flexibility, are prone to aeroelasticity driven response, such as vortex shedding, torsional divergence and flutter.

In this work, starting from the classical Deflection Theory a non-linear dynamic model of a suspension bridge is devised, with the purpose of providing a unified framework for the study of aeroelastic and internal resonance instabilities, along with their coupled effects. The onset of unstable conditions is detected by means of stability maps traced by means of the well-known Floquet Theory. The results confirm that the interaction between aeroelastic effects and non-linear internal resonance leads to unstable phenomena for wind speed levels which are by far lower than the critical threshold provided by purely aeroelastic prediction.

Il possibile instaurarsi dei cosiddetti fenomeni di risonanza interna è stato recentemente identificato come una possibile concausa nell'instaurarsi di condizioni critiche in ponti sospesi di grande luce. L'intrinseca non linearità geometrica di tali strutture comporta un forte accoppiamento fra risposta flessionale e torsionale, con in aggiunta un possibile scambio di energia fra i modi posti in risonanza dall'azione parametrica. Questa cosiddetta risonanza interna può manifestarsi allorché si raggiunga un livello critico di energia oltre il quale la risposta strutturale può divenire instabile e divergere al passare del tempo.

Ulteriormente, i ponti sospesi, essendo strutture molto flessibili, risentono fortemente dell'azione del vento, tanto che la risposta aeroelastica può portare a distacco di vortici, divergenza torsionale e flutter.

Nel presente elaborato, partendo dalla teoria classica per la statica non lineare dei ponti sospesi nota come Deflection Theory, è stato sviluppato un modello numerico non lineare capace di analizzare la risposta dinamica di un ponte sospeso a fronte di possibili instabilità, dovute tanto all'azione aeroelastica del vento, quanto alla risonanza interna, legata alle non linearità intrinseche della struttura. L'instaurarsi di una condizione instabile è stata identificata facendo uso di mappe di stabilità, appositamente realizzata per le condizioni strutturali analizzate, facendo uso della nota Teoria di Floquet. I risultati confermano che l'interazione fra gli effetti aeroelastici e le risonanze interne portano la struttura ad instabilizzarsi in corrispondenza di velocità del vento che sono significativamente inferiori a quelle previste dalla classica trattazione che tiene in conto della sola interazione fluido-struttura.

Introduction

The first European suspension bridge is the Wynch Bridge, built in 1741 in England on the Tees River with a span of 21m and an unstiffened deck 61cm width. Four mooring chains restraint the bridge against lifting forces coming from wind action.



Figure I.1_ Wynch Bridge.

The choice of unstiffened decks remains a characteristic feature of British bridges. First in 1920 the Union Bridge, the first road bridge, designed by S. Brown with a span of 137m, lasting for six years the world record.



Figure I.2_ Union Bridge.

Later in 1826 with the Conwy and Menai suspension bridges designed by T. Telford, respectively with a span of 100m and 176m.



Figure I.4_ Conwy suspension bridge.



Figure I.3_Thomas Telford.



Figure I.5_ Menai strait bridge

Further I. K. Brunel designed the Clifton Bridge in Bristol with a central span of 214m and a very thin stiffening deck.

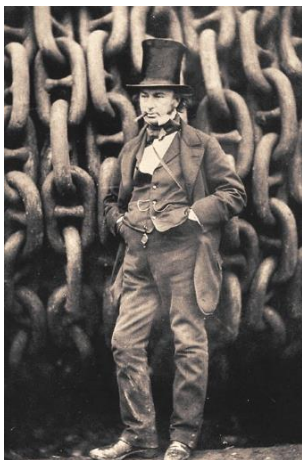


Figure I.6_ Isambard Kingdom Brunel.



Figure I.7_ Clifton Bridge.

With the advent of the first railway in first half of XIX century the stiffness of the deck become a very important issue. The classical example is the Britannia Bridge by R. Stephenson in 1850, characterised by a tubular deck that avoid the use of any suspension system, though initially expected to be necessary.

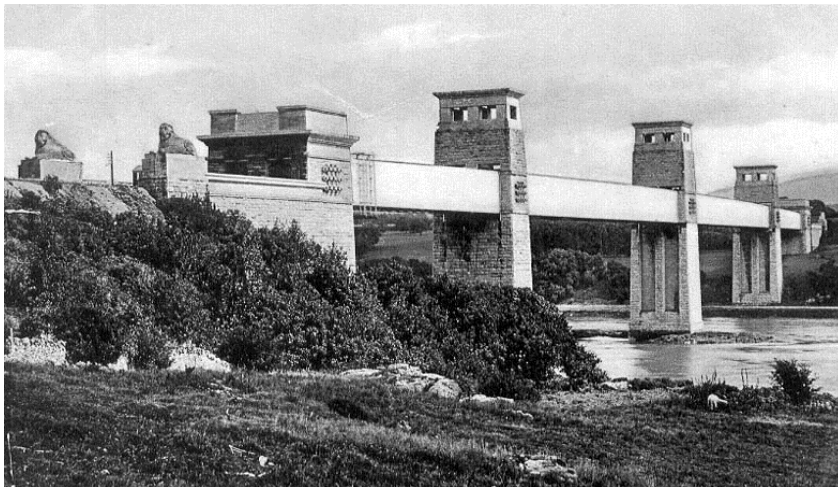


Figure I.8_Britannia Bridge.



Figure I.9_Robert Stephenson.

In 1823 Navier published the first book on statics of cables, which will be a reference for the following design of suspension bridges, up to that time based on experience and intuition of the designer. The formulation lack of the interaction between cable system and deck that will be catch only in the 1858 by Rankine. According to this theory the cables system and the deck exchange a uniformly distributed load that is equal to the accidental one. Consequently the cables system is able to reduce the bending moment on a simply supported deck of one quarter. In reality the reduction is far higher. This lead to a huge overestimation of loads acting on the stiffening structure that consequently would be oversized.

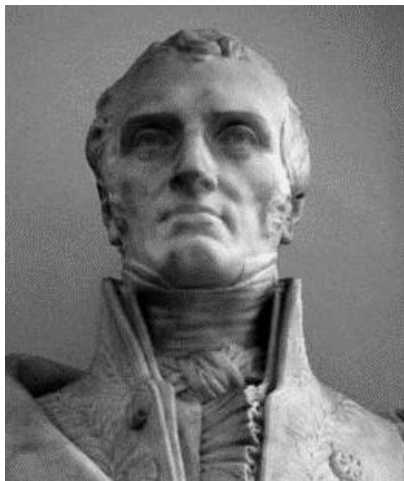


Figure I.11_Claude-Louis Navier.



Figure I.10_William John Macquorn Rankine.

Conversely in the North America stiffening girders were the norm from the first known suspension bridge, on the Jacob's Creek, designed by J. Finley in 1801. It was characterised by a three spans of 21m each, with a reticular stiffening girder of 4m width.

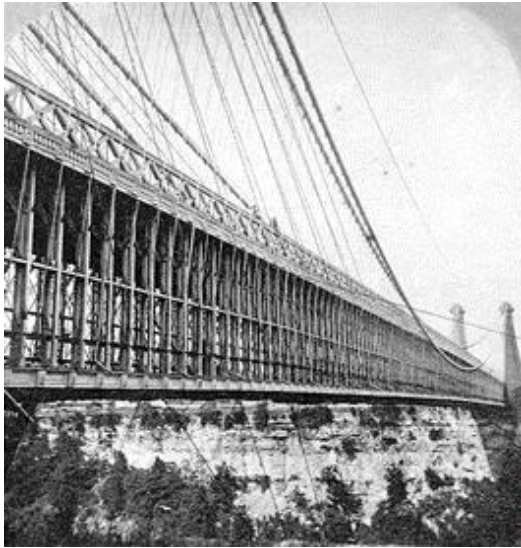


Figure I.13_Bridge on Jacob's Creek.



Figure I.12_James Finley.

Later in 1855 by J. A. Roebling designed the first suspended rail bridge of history on the Niagara River. Its reticular girder of about 5.2m depth and 251m long, and stiffening stays and moorings make it a real complicate structure. The same feature have been repeated by the same designer in 1883 for the Brooklyn Bridge spanning about 487m of clearance.



Figure I.14_Bridge on Niagara River.



Figure I.16_Brooklyn Bridge.

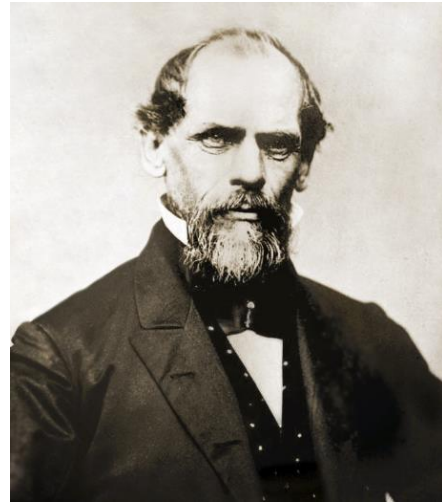


Figure I.15_John Augustus Roebling.

The theory proposed by Melan in 1888 removed the hypothesis first proposed by Rankine, since the interaction between the cables system and the deck is proportional the relative stiffness of the two parallel systems. Consequently, the loads directly acting on the deck becomes lower with respect to Rankine approach, but anyway very high, leading to large dimensions of the stiffening girders. The classical example is the Williamsburg Bridge, completed in 1903 and characterised by a deck 488m long and 12.2m deep.



Figure I.17_Josef Melan.



Figure I.18_Williamsburg Bridge.

With the advent of the so-called Deflection Theory a real evolution in the design of suspension bridges begun. The idea date back to 1888 in Melan's work but the complete theory was proposed by Steinman only in 1929. With respect to Rankine and Melan theories, the load exchanged between the cable system and the stiffening girder was no more uniformly distributed along the span. Further the geometric stiffness of cables reduces the loads acting on the deck as its stiffness reduces, leading to very thin stiffening girders.

The first application was realised in 1931 with the George Washington Bridge, designed by O. Amman, characterised by a span of 1067m.



Figure I.20_ George Washington Bridge



Figure I.19_ Othmar Amman.

Later in 1937 the Golden Gate by J. Strauss was build up. In order to achieve such a length was necessary a reticular reversed U-shaped stiffening girder that unfortunately was susceptible of large wind-induced torsional oscillations.



Figure I.21_ Joseph Strauss.



Figure I.22_ Golden Gate Bridge.

Two years later with the Deer Isle and the Bronx-Whitestone Bridges, designed by D. Steinman and O. Amman with a span of 329m and 701m respectively, continuous stiffening beams were realised.



Figure I.23_Deer Isle Bridge.



Figure I.24_David Barnard Steinman.



Figure I.25_Leon Solomon Moisseiff.



Figure I.26_Bronx_Whitestone Bridge.

This solution, already used in 1915 with the German Koln-Deutz bridge, granted both to reduce the girder stiffness and then applied loads, and to get an optimal use of materials and then a better aesthetics.

Then in the 1940 the Tacoma Narrow was realised with the same approach by the design of Moisseiff. The deck was characterised by central span 854m and side span of 355m long, 11.9m width, stiffened by two I-shaped steel bar of only 2.44m height.



Figure I.27_Tacoma Narrow Bridge.

The collapse of the TNB sanctioned the relevance of aeroelastic effects in bridge engineering practice, being the classical Theodorsen Theory known from about six years in aeronautical field. As a consequence many of the existing bridges were stiffened. An additional reticular structure realised a closed section for the deck of the Golden Gate Bridge in 1955. Similarly for the Washington Bridge in between 1958-1962 an additional lower deck was introduced. Whilst the final configuration for the Bronx-Whitestone has been realised in 2003 and foresaw a system of flow deflectors.

In the meanwhile in England G. Roberts in 1966 design the 988m long Severn Bridge, realising for the first time a closed box section for the concrete deck, properly designed for aerodynamic efficiency.



Figure I.29_Severn Bridge.



Figure I.28_Gilbert Roberts.

This solution become the standard one thanks to the work of Scanlan at the end of '60, extending the Theodorsen theory from the thin plate to the generic section geometry by means of the so-called flutter derivatives, measured experimentally with wind tunnel tests. This paves the way for modern super-long suspension bridges design, leading to the design of the Messina Bridge spanning 3300m . Though truss girders still be used, such as in the construction of the Akashi Kaikyo Bridge, 1991m long.

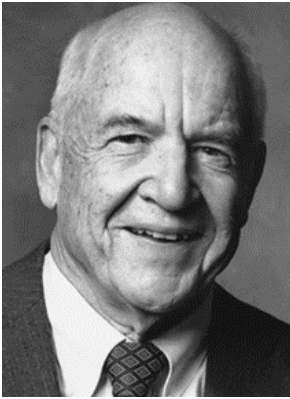


Figure I.31_Robert H. Scanlan.



Figure I.33_Messina Strait Bridge (rendering).

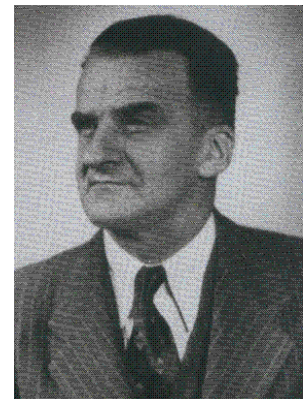


Figure I.30_Theodore Theodorsen.



Figure I.32_Akashi Kaikyo Bridge.

The emergence of new materials and advanced structural engineering technology makes suspension bridges a spontaneous answer for demands of larger spans, light weight, high strength, ease of construction, and aesthetic appearance. On one hand, the flexibility caused by the cable system and its long span makes the suspension bridges sensitive to dynamic loads; on the other hand, the relatively simple geometry of cable structures makes continuum approaches still very attractive, since can be based on a minimal number of non-dimensional parameters.

Early attempts on static equilibrium of suspension bridge were made by Steinman, who extended the elastic theory to the well-established Deflection Theory [1,2] by enforcing equilibrium in the deformed position, and accounting for the stiffening effect in the main cables.

Earliest continuum models for the linear vertical vibrations of suspension bridges reproduced the effects of the stiffening truss girder by means of an Euler–Bernoulli beam supported by the main cables through inextensible and distributed vertical hangers. In this regard, the classic continuum model for the linear vertical vibration of suspension bridges, based on the so called linearized deflection theory, was first proposed by Bleich et al. [3], and Steinman [4], which derived some formulas for computing natural frequencies and mode shapes, and recently reviewed by Luco and Turmo [5]. The last authors showed that the linear vibration of the considered suspension bridge model is completely governed by two non-dimensional parameters: the classic Irvine parameter of suspended cables, first introduced by Irvine [6] and a second parameter accounting for the relative stiffness of the girder with respect to the main cable system. Abdel-Ghaffar in the late 1970's [7-9] developed the methodology of free vertical, torsional and lateral vibration analysis of suspension bridges by means of a variational principle and a finite element approach. Then, the same author [10-12] extended the continuum formulation to include coupling between vertical–torsional vibrations, nonlinear effects occurring in the case of large vibrations and the effects of distortional deformation of the girder cross-section.

Nowadays, in the design of suspension bridges a comprehensive set of wind related responses are taken into consideration, such as static divergence, vortex-shedding, buffeting and flutter. Hence, the risk of developing aeroelastic instabilities is always the matter while designing any lightweight long-span structures, characterized by high flexibility due to a low bending/torsional stiffness and a high width-to-depth ratio. Although the phenomenon was already well known in aviation, the research on flutter in civil engineering field started as the collapse of the Tacoma Narrows Bridge (USA) in 1940, when the catastrophe was seen mainly as a direct consequence of flutter [13] that developed on the bridge deck at wind speed much lower than the design one. Flutter is generally studied within linearized aeroelastic models, which can provide the range of wind speeds where Hopf bifurcation occurs. To consider the effects due to the unsteadiness of the relative motion between the section and the air flow, indicial Theodorsen type [14,15] formulations can be adopted to predict more accurately the critical wind speed at the onset of the flutter instability [16] with respect to the quasi-steady formulation. The equations of motion for suspension bridges were employed for aeroelastic investigations in [17], where analysis are centered on experimentally determined flutter derivatives, and a full three-dimensional modal analysis of the structure.

It's well known from non-linear dynamics that, between coupled oscillators, energy transfer [18] can occur as far as the energetic levels reaches critical well established thresholds. Classically this behaviour is referred to as the *internal resonance* phenomenon. Many authors applied this principles to study the vibrations response of suspension bridges. The authors of [19,20] used the continuous model proposed by Abdel-Ghaffar [11], and solve the system of equations by means of the multiple scale perturbative technique [21]. Recently, Airoli and Gazzola [22], trying to explain why did torsional oscillations suddenly appears before the Tacoma Narrows collapse, found out that also in isolated systems as vertical oscillations become large enough they may switch to torsional ones.

The problem was already tackled by other authors [23-27] but no one was able to identify the actual causes of that sudden large torsional oscillations. Hence, they paved the way for future works concerning the interaction between internal resonance and aeroelastic phenomena, as the present paper wants to do.

The work intends to study the stability of a suspension bridge model using the continuum formulation proposed by Abdel-Ghaffar in [11] enriched by the terms coming from Theodorsen [15] indicial formulation for the wind-structure interaction. The stability will be checked in Lyapunov asymptotic sense exploiting the well-known Floquet theory [28]. The variational system of equations is obtained following the procedure proposed by Herrman [29] assuming small but finite flexural perturbations coming from vortex-shedding excitation. The possibility of parametric internal resonances such as harmonic, sub-harmonic and super-harmonic, or additive combinational and anti-resonances will be checked by means of suitable stability maps.

Following the classical Deflection Theory, it is possible to write the nonlinear static flexural response of a suspension bridge, by simply enforcing the equilibrium condition in the deformed configuration of the deck-cable system. A further step consists in the generalization of the displacement field in order to account for the torsional response of the deck-cables system. A variational formulation can be adopted, thus achieving the self-adjoint system of two equations of motion which is coupled due to non-linear (up to cubic) terms. The analytical expressions for modal shapes and frequencies of vibrations can be determined from the linear component of the complete nonlinear system of equations. A parametric analysis of the eigen-properties of the suspension bridge model allows us to detect the magnitude of influence of the main structural parameters introduced. Further the limit values for these parameters corresponding to the so-called Cross Over Frequency and Mode are analysed.

The nonlinear equations of motion are then studied by means of the method of Multiple Scales, a perturbation technique, to find approximate analytical solutions. The direct approach allows us to avoid the discretization of the equations, and to write down the analytical expressions of second order correction of classical linear modal shapes. The parametric analysis shows that, under certain structural conditions, the second order correction of linear skew-symmetric modes may be symmetric, thus introducing a trailing wave in the response of the bridge. The amplitude and phase modulation equations are then obtained for the general forced and damped vibrations. Subsequent analysis of steady state response in the case of one-to-one internal resonance focuses on the amplitude dependence of nonlinear frequency and on the stability of initial conditions.

The aeroelastic behaviour is studied by means of the Theodorsen formulation. Wind forces introduce additional mass, damping and stiffness that not only couple the linear equations of motion but also yield a system which is no longer self-adjoint. In fact, it loses its symmetries both in damping and stiffness matrices, making the structure susceptible to flutter instabilities and static divergence problems, respectively. Hence for each of the different structural conditions analysed, we are able to define a limit wind speed corresponding to torsional static Divergence and to the Flutter onset condition. For the latter case a comparison between the complete formulation of Theodorsen, the steady-state and the quasi-static ones allows us to detect the main differences of the results coming from different approaches to the same problem.

The nonlinear response of suspension bridges is caused not only by the so called global contribution given by the stiffening behaviour of the main cables system but also by the so called local one given by the slackening of hangers. Both phenomena have geometrical reasons, the first associated to quadratic and cubic terms representing the main cables curvature and the second to linear ones due to the slenderness of the elements considered. In fact as the forces transmitted by the hangers become a compressive one and overcome the initial tension given by deck self-weight, hangers buckle and are no more able to transmit forces from the deck to the main cables. A simplified perfectly tense-rigid constitutive model is assumed for hangers, in order to study the local reduction of the stiffness coming from the cables system. Hence, by means of linear equations, generalised conditions for slackening onset and development are defined introducing proper reductive parameters for the latter.

Focusing on the simple flexural motion, for the different structural conditions, we have been able to detect the modal antinode amplitude necessary to lead to the first slackening of hangers. Further the parametric analysis allows us to detect particular combinations for structural parameters such that slackening will not be feasible. This analysis confirms the fact that as the order of the mode considered increases, the required slackening amplitude onset reduces.

Finally, inspired by the pioneering work of Herrmann and Hauger, the stability analyses have been based on a linearized formulation that is able to represent the main structural non-linear effects and the coupling given by aerodynamic forces. By assuming, at a first step, null torsional vibrations and small but finite flexural ones, one can define the steady state solution of the flexural equation of motion forced by the vortex-shedding action. Then, by introducing small perturbations on the motions, a system of two variational equations is obtained, which can be used to check the stability of the motion directly applying the well-known Floquet

Theorem. The results confirm that the interaction between aeroelastic effects and non-linear internal resonance leads to unstable phenomena for wind speeds which are by far lower than the critical threshold for standard aeroelasticity. Further the analysis of stability maps confirm the possibility of parametric resonance of 2:1 type between flexural and torsional motion and the importance of bridge's deck sectional shape factor in order to explain Parametric resonance phenomenon by means of Strouhal linear law for vortex-shedding excitation.

1. Problem formulation

1.1. Deflection theory

The classical Deflection theory allows us to study the nonlinear response of a suspension bridge enforcing equilibrium in the deformed configuration.

1.1.1. General assumptions

In order to be able to define the general nonlinear equations of motion the following assumptions hold:

- 1) the self-weight of cables is negligible with respect to permanent loads acting on the deck;
- 2) cables are inextensible just in the initial condition when they carry permanent loads only;
- 3) permanent and variable loads are uniformly distributed along the length and the width of the bridge's deck;
- 4) negligible flexural stiffness of cables;
- 5) inextensible hangers;
- 6) curtain behaviour of hangers;
- 7) rigid pylons and perfect constraints.

The equilibrium equations of the two cables will consider just the central main span of the suspension bridge model.

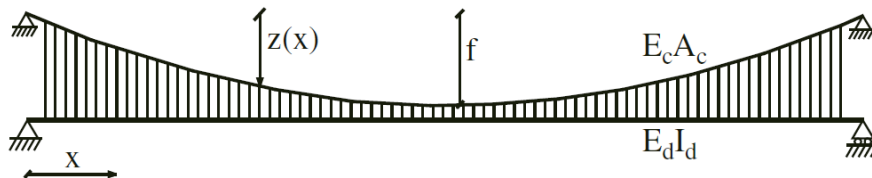


Figure 1.1_ Single span suspension bridge model.

Notice that though there are clamps at the ends of cable, thanks to (4) they behave like hinges. By the same hypothesis, cables are able to resist external vertical loads just thanks to their axial internal tension since shear and bending moments are negligible.

1.1.2. Equilibrium conditions

In the initial condition, because of assumptions (1) and (6), permanent loads acting on the bridge's deck mainly influence the shape of cables.

Then, enforce equilibrium conditions of an infinitesimal piece of cable subjected to uniformly distributed loads along the horizontal projection of its length, as suggested by the hypothesis (3).

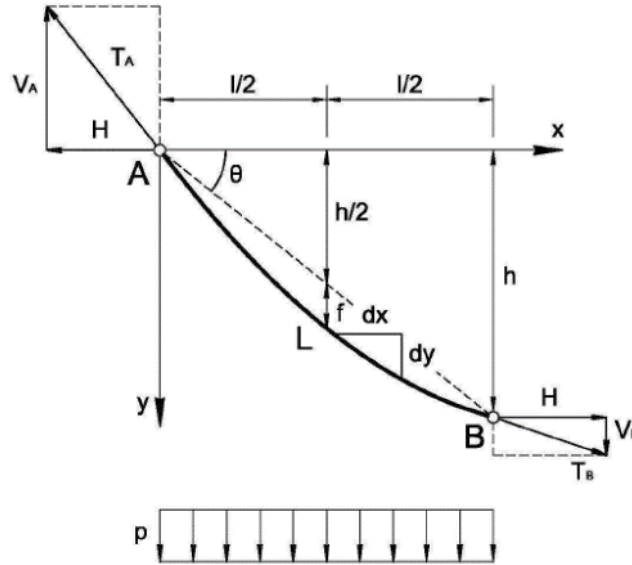


Figure 1.2_Cable static equilibrium configuration.

- cable's horizontal equilibrium in initial configuration:

$$-T \frac{dx}{ds} + T \frac{dx}{ds} + \frac{d}{ds} \left(T \frac{dx}{ds} \right) ds = 0 ;$$

$$T \frac{dx}{ds} = H = \text{constant} ;$$

Because of the absence of axial loads, the horizontal projection H of the internal tension induced by permanent loads is constant. Therefore, T has to vary along the cable's length in order to fulfil the tangential direction; hence, it reaches its maximum value in correspondence of the highest slope at cable's ends.

$$T = H \frac{dx}{ds} ;$$

- cable's vertical equilibrium in initial configuration:

$$-T \frac{dy}{ds} + T \frac{dy}{ds} - \frac{d}{ds} \left(T \frac{dy}{ds} \right) ds - \frac{p}{2} dx = 0 ;$$

The equation refers to only one of the two cables on which the total amount of permanent loads per unit length p redistributes in equal parts because of (6) and (3).

$$\frac{d}{dx} \left(T \frac{dy}{dx} \right) = -\frac{p}{2} ;$$

By substitution of $H = T \frac{dx}{ds} = \text{constant}$.

$$H \frac{d^2y}{dx^2} = -\frac{p}{2} ;$$

From the double integration of the last equation, it is possible to get the initial shape of the cable. Hence, thanks to the assumption (2), the actual parabolic shape corresponds to the exact catenary

configuration of the cable associated to uniformly distributed loads. While taking in account cable's compressibility, a parabolic shape would be just a good approximation, as axial deformations remain small. Further, it is important to notice that the validity of (1) is fundamental to get a parabolic shape; in fact, the presence of a considerable self-weight is associated to an initial configuration of the cable that follows a hyperbolic cosine function (traditionally called "catenary"). Thus, the simplification for the following developments is evident.

Because of the cable's exact catenary shape, the initial configuration of the deck is unstressed. The derivation of the catenary expression refers only to geometrical quantities of the cable layout since they are more intuitive than static quantities, like external loads.

$$\frac{d^2y}{dx^2} = A = \text{constant};$$

$$\frac{dy}{dx} = Ax + B;$$

$$y(x) = Ax^2 + Bx + C;$$

The assumptions (4) and (7) allow enforcing geometrical boundary conditions at cable's ends as in the case of perfect hinges. The others constraints refer to the point at mid-span of maximum displacement (sag f) and null slope.

$$y(0) = 0 \Rightarrow C = 0;$$

$$y\left(\frac{l}{2}\right) = f \Rightarrow A\frac{l^2}{4} + B\frac{l}{2} = f \Rightarrow A = -4\frac{f}{l^2};$$

$$\frac{dy}{dx}\left(\frac{l}{2}\right) = 0 \Rightarrow B = -Al \Rightarrow B = -4\frac{f}{l};$$

The catenary expression representative of the cable's initial configuration assumes the following parabolic shape.

$$y(x) = 4\frac{f}{l}x\left(1 - \frac{x}{l}\right);$$

The final configuration, which the cables reach after the addition of external variable loads to permanent ones, involves their compressibility, being (2) no more valid, then they lose their perfect catenary parabolic shape.

Direct consequence of the first of previous statements coupled with the nonlinear geometrical hardening response of cables led to a nonlinear increase of both cable's tension and vertical displacement.

From the second one comes out that both the deck and the cables sustain the variable loads with a contribution proportional to their relative equivalent flexural stiffness. Thus, the amount sustained by the two cables is $r(x)$, a uniform distributed load along their span thanks to (6).

In vertical equilibrium equation, nothing changes but the following quantities.

$$p \Rightarrow p + r;$$

$$H \Rightarrow H + h;$$

$$y \Rightarrow y + v;$$

Notice that since both cable's tension and slope vary with external loads, it's necessary a variation of H to grant vertical equilibrium and tangential condition of the actual $T+t$, even if $H+h$ remains constant along the cable's span.

- cable's vertical equilibrium in current configuration:

$$(H + h) \frac{d^2(y+v)}{dx^2} = -\frac{p+r}{2} ;$$

$$H \frac{d^2y}{dx^2} + (H + h) \frac{d^2v}{dx^2} + h \frac{d^2y}{dx^2} = -\frac{p}{2} - \frac{r}{2} ;$$

Enforcing initial equilibrium condition $\frac{d^2y}{dx^2} = -\frac{p}{2}$.

$$(H + h) \frac{d^2v}{dx^2} + h \frac{d^2y}{dx^2} = -\frac{r}{2} ;$$

$$r(x) = -2(H + h) \frac{d^2v}{dx^2} - 2h \frac{d^2y}{dx^2} ;$$

Since at this stage the deck sustains a partial amount of total external load equal to $q(x)-r(x)$, it undergoes to a deflection that involves its flexural stiffness.

Concerning the vertical equilibrium equation of the infinitesimal piece of bridge's deck, though the general format comes from the classical first order beam theory, it refers to the deformed configuration thanks to the dependence on $r(x)$.

- deck's vertical equilibrium in current configuration:

$$EI \frac{d^4w}{dx^4} = q - r ;$$

Since it's known the expression for $r(x) = -2(H + h) \frac{d^2v}{dx^2} - 2h \frac{d^2y}{dx^2}$.

$$EI \frac{d^4w}{dx^4} - 2(H + h) \frac{d^2v}{dx^2} - 2h \frac{d^2y}{dx^2} = q ;$$

The assumption (5) ensures that $w(x)=v(x)$.

$$EI \frac{d^4v}{dx^4} - 2(H + h) \frac{d^2v}{dx^2} - 2h \frac{d^2y}{dx^2} = q ;$$

The last equilibrium equation links the cable and the deck response coupling the horizontal component of the cable's tension with the vertical displacement of the deck. Since both previous quantities are unknown is necessary another equation in order to be able to solve the problem in close form.

1.1.3. Compatibility conditions

Let's consider an infinitesimal piece of cable undergoing to small elongation and write down the Pitagora identity in both the initial and final configuration.

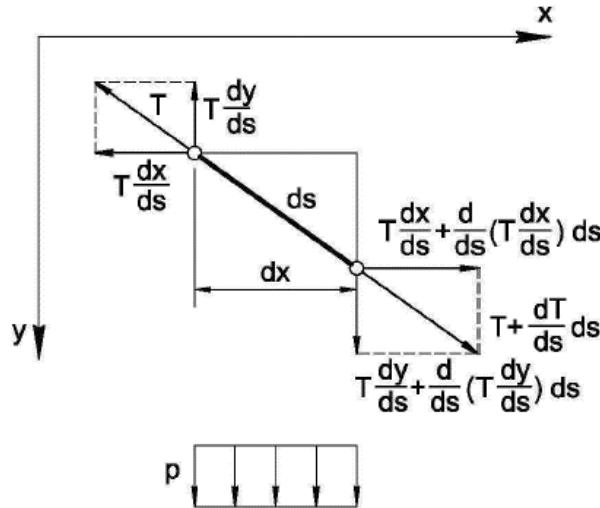


Figure 1.3_Cable end forces.

- initial infinitesimal length:

$$ds^2 = dx^2 + dy^2 ;$$

- final infinitesimal length:

$$(ds + dL)^2 = (dx + du)^2 + (dy + dv)^2 ;$$

Developing the squares and substituting the initial length's expression.

$$ds^2 + 2 \cdot ds \cdot dL + dL^2 = dx^2 + 2 \cdot dx \cdot du + du^2 + dy^2 + 2 \cdot dy \cdot dv + dv^2 ;$$

Derive two times with respect to x and collect horizontal strain component.

$$\frac{du}{dx} = \frac{ds}{dx} \frac{dL}{dx} - \frac{dy}{dx} \frac{dv}{dx} - \frac{1}{2} \left(\frac{dv}{dx} \right)^2 - \frac{1}{2} \left(\frac{dL}{dx} \right)^2 - \frac{1}{2} \left(\frac{du}{dx} \right)^2 ;$$

Write some terms in a more suitable form.

$$\frac{dx}{ds} = \cos \theta ;$$

$$\frac{dL}{dx} = \frac{dL}{ds} \frac{ds}{dx} = \frac{t(x)}{EA(x)} \frac{1}{\cos \theta} = \frac{h}{EA(x)} \frac{1}{\cos \theta^2} ;$$

Integrate the horizontal strain all over the span.

$$\Delta u = \int_0^l \frac{du}{dx} dx = h \int_0^l \frac{dx}{EA(x) \cdot \cos^3 \theta} - \int_0^l y' v' dx - \frac{1}{2} \int_0^l v'^2 dx + \frac{1}{2} \int_0^l L'^2 dx + \frac{1}{2} \int_0^l u'^2 dx ;$$

Where the last two contributions are in general negligible due to the assumption of small displacements, while the one linked to v'^2 still be important since large rotations are still taken in account.

Integrate by parts the second term on the right hand side of the equation and enforce hypothesis (7).

$$\int_0^l y' v' dx = [y' v]_{x=0}^{x=l} - \int_0^l y'' v dx ;$$

$$v(0) = v(l) = 0 ;$$

$$\Delta u = h \int_0^l \frac{dx}{EA(x) \cdot \cos^3 \theta^3} + \int_0^l y'' v dx - \frac{1}{2} \int_0^l v'^2 dx ;$$

Introduce an equivalent reference length for the cable.

$$L_c = A_c \int_0^l \frac{dx}{A(x) \cdot \cos^3 \theta^3} ;$$

$$\Delta u = \frac{h \cdot L_c}{E \cdot A_c} + \int_0^l y'' v dx - \frac{1}{2} \int_0^l v'^2 dx ;$$

The compatibility condition comes from assumption (7) and it states that pylons cannot get closer or further.

$$\Delta u = 0 \Rightarrow h = \frac{E \cdot A_c}{L_c} \cdot \left(- \int_0^l y'' v dx + \frac{1}{2} \int_0^l v'^2 dx \right) ;$$

The expression barely found it's useful to introduce the concept of equivalent length L_c and the relation between cable's elongation and the associate horizontal component h of the internal tension's increment.

$$h = EA_c \frac{\Delta L}{L_c} ;$$

Then it is important to underline the fact that the previous expression for the cable's elongation is an approximation. This is evident from the first term, representing the contribution of the cable's curvature, which neglects the contribution of the slope at the denominator typical of small perturbation approaches.

Thence it is necessary a refinement of the expression for the cable's elongation.

To fulfil compatibility is necessary to know the actual curvilinear length of the cable in its different configurations, which means before and after the vertical perturbation $v(x)$ of cable's displacement takes place.

- initial length:

$$L_i = \int_0^{L_i} ds = \int_0^l \sqrt{(dx^2 + dy^2)} = \int_0^l \sqrt{1 + \left(\frac{dy}{dx}\right)^2} dx ;$$

- final length:

$$L_f = \int_0^l \sqrt{1 + \left[\frac{d(y+v)}{dx} \right]^2} dx ;$$

Notice the implicit assumption stating that the increment in horizontal direction is negligible.

Anyway, the solution of the previous integral is not of immediate computation; an approximate solution is available through a McLaurin's series expansion truncated at second order terms of the unknown variable $v(x)$ '.

- basic function:

$$f(v') = \sqrt{1 + (y' + v')^2} = \sqrt{1 + y'^2 + 2y'v' + v'^2} ;$$

- I derivative:

$$\frac{df}{dv'} = \frac{y' + v'}{f(v')} ;$$

- II derivative:

$$\frac{d^2f}{dv'^2} = \frac{f(v') - (y' + v') \frac{df}{dv'}}{f(v')^2} = \frac{f(v') - \frac{(y' + v')^2}{f(v')}}{f(v')^2} = \frac{f(v')^2 - (y' + v')^2}{f(v')^3} = \frac{1}{[1 + (y' + v')^2]^{3/2}} ;$$

- McLaurin II order expansion:

$$f(v') \cong f(v' = 0) + \left[\frac{df}{dv'} \right]_{v'=0} \cdot v' + \left[\frac{d^2f}{dv'^2} \right]_{v'=0} \cdot \frac{v'^2}{2} + o(v'^3) ;$$

Hence.

$$f(v') \cong \sqrt{1 + y'^2} + \frac{y'v'}{\sqrt{1 + y'^2}} + \frac{v'^2}{2(1 + y'^2)^{3/2}} ;$$

- approximate expression of cable's length:

$$L_f = \int_0^l \sqrt{1 + y'^2} dx + \int_0^l \frac{y'v'}{\sqrt{1 + y'^2}} dx + \frac{1}{2} \int_0^l \frac{v'^2}{(1 + y'^2)^{3/2}} dx = L_i + \Delta L ;$$

Only the last two terms, representative of cable's elongation, are of interest in order to enforce compatibility with external constraints.

Partial integration of the first term inside ΔL allows us a simplification in following computations.

- primitive function:

$$g(x) = \frac{y'v}{\sqrt{1 + y'^2}} ;$$

- I derivative:

$$\frac{dg}{dx} = \frac{(y''v + y'v')\sqrt{1+y'^2} - \frac{y'y'^2v}{\sqrt{1+y'^2}}}{1+y'^2} = \frac{(y''v + y'v') \cdot (1+y'^2) - y'y'^2v}{(1+y'^2)^{3/2}} = \dots$$

$$\dots = \frac{y''v + y'v' \cdot (1+y'^2)}{(1+y'^2)^{3/2}} = \frac{y'v'}{\sqrt{1+y'^2}} + \frac{y''v}{(1+y'^2)^{3/2}};$$

- cable's elongation:

$$\Delta L = \left[\frac{y'v}{\sqrt{1+y'^2}} \right]_{x=0}^{x=l} - \int_0^l \frac{y''v}{(1+y'^2)^{3/2}} dx + \frac{1}{2} \int_0^l \frac{v'^2}{(1+y'^2)^{3/2}} dx;$$

- boundary conditions:

Because of the assumptions (7) and (5) respectively.

$$v(0) = v(l) = 0;$$

$$v(x) = w(x);$$

Then.

$$\Delta L = - \int_0^l \frac{y''v}{(1+y'^2)^{3/2}} dx + \frac{1}{2} \int_0^l \frac{v'^2}{(1+y'^2)^{3/2}} dx;$$

With this expression, the cable's elongation takes in consideration also the contribution of its slope but the format is identical to that previously found.

It is of interest to test the contribution of different terms in the previous series expansion.

To do that in a simple way, first analyse the case of a homothetic deformation of the parabolic cable with a main span of 1000m and a central sag of 100m.

$$v(x) = \alpha \cdot y(x);$$

$$l = 1000m;$$

$$f = 100m;$$

The amplification factor α ranges between positive and negative values to be able to take in account cable's stiffening but also loosening.

To get a higher accuracy, add further two terms to the series expansion, respectively of the third and fourth order. In this way, it is possible to maintain equal the total number of terms with pair and odd exponent, which respectively loose or not the sign of α .

$$\Delta L = - \int_0^l \frac{y'' \alpha y}{(1+y'^2)^{3/2}} dx + \frac{1}{2} \int_0^l \frac{(\alpha y)'^2}{(1+y'^2)^{3/2}} dx - \frac{1}{2} \int_0^l \frac{y'(\alpha y)'^3}{(1+y'^2)^{5/2}} dx - \frac{1}{8} \int_0^l \frac{(1-4y'^2)(\alpha y)'^4}{(1+y'^2)^{7/2}} dx ;$$

Numerical integration, by means of rectangle approximation, allows plotting the variation of the cable's elongation as the homothetic amplification changes.

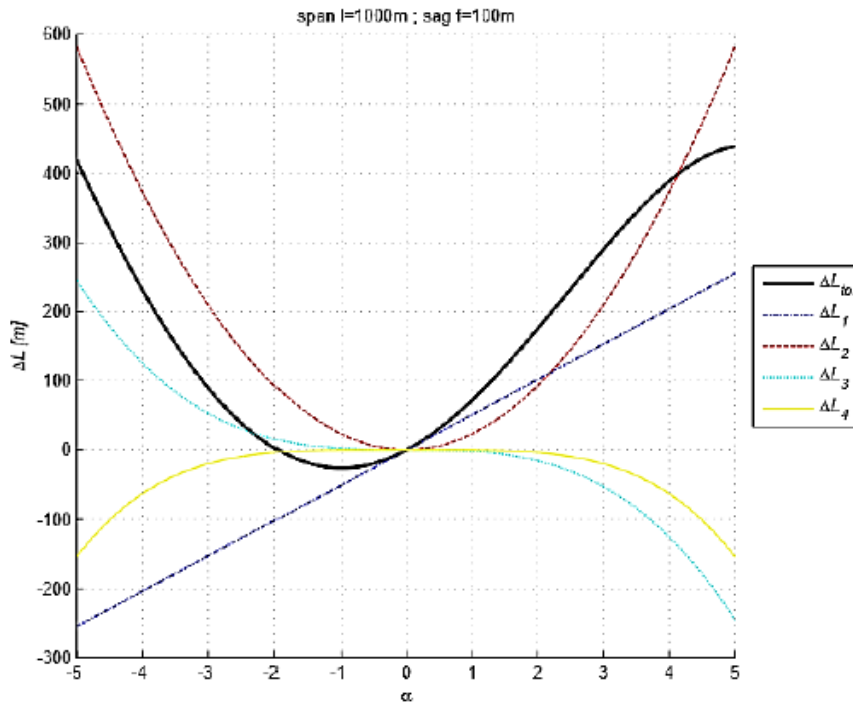


Figure 1.4_Cable's elongation for large homothetic perturbation's amplitude.

Notice that the linear contribution is dominant all over the other approximately up to $|\alpha| = 2$, beyond which the quadratic term rapidly grows and higher order ones start to become relevant.

For positive values of α , the response of the cable simply shows a monotonic stiffening behaviour. Whereas, as α starts to become negative, initially the cable reduces its length, then it slacks ($\alpha = -1$) where the elongation reach a minimum, and finally, as the perturbation doubles the initial parabolic configuration ($\alpha = -2$), the length increases again since the cable's configuration is just mirrored with respect to the initial one.

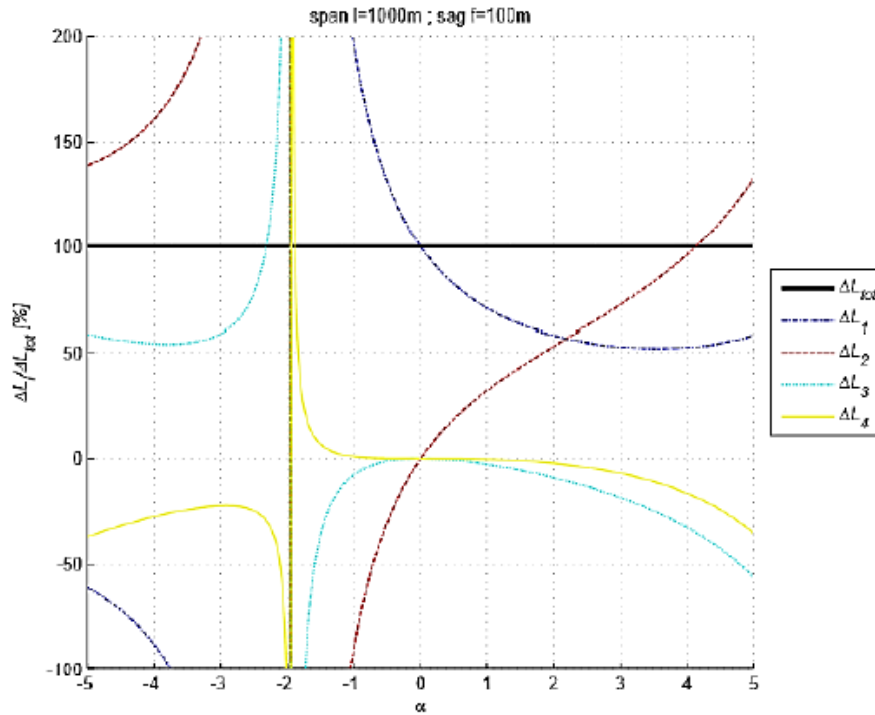


Figure 1.5_ Elongation's percentage contribution for large amplitudes.

The figure 4 tries to detect the percentage contribution of each series term to the total elongation. All the percentages explode at $\alpha=-2$ in consequence of the fact that the cable's elongation here is null. On the other hand, contributions higher than 100% or with negative sign are due to the presence of both positive and negative contributions to the overall elongation.

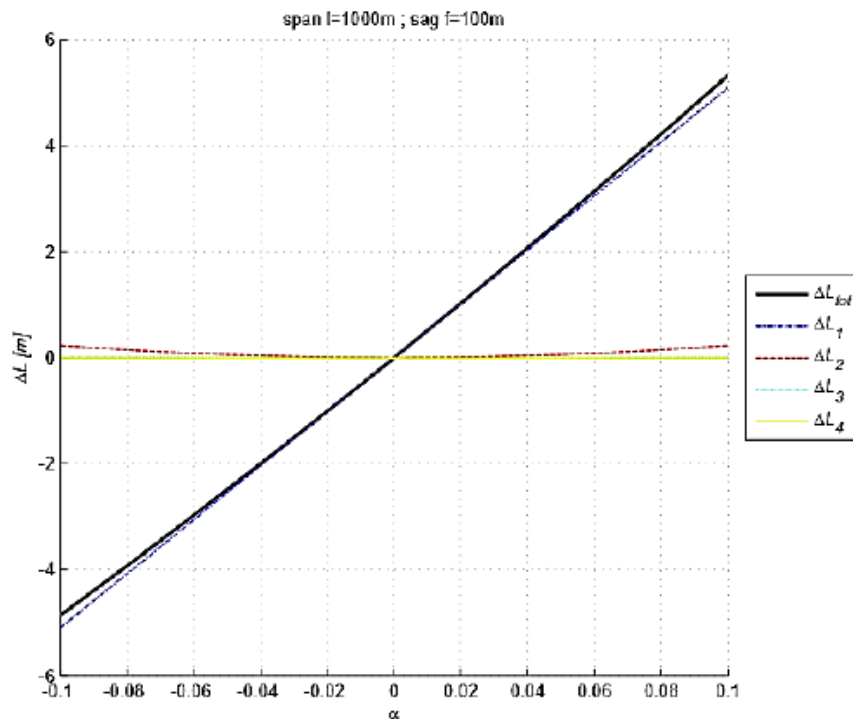


Figure 1.6_ Cable's elongation for realistic perturbation's amplitude.

The relevant observation is that in real situations perturbation $v(x)$ represents a little percentage of the initial configuration, approximately of the order of 10% the central sag. Therefore, is relevant just the contribution of the first two terms of the series.

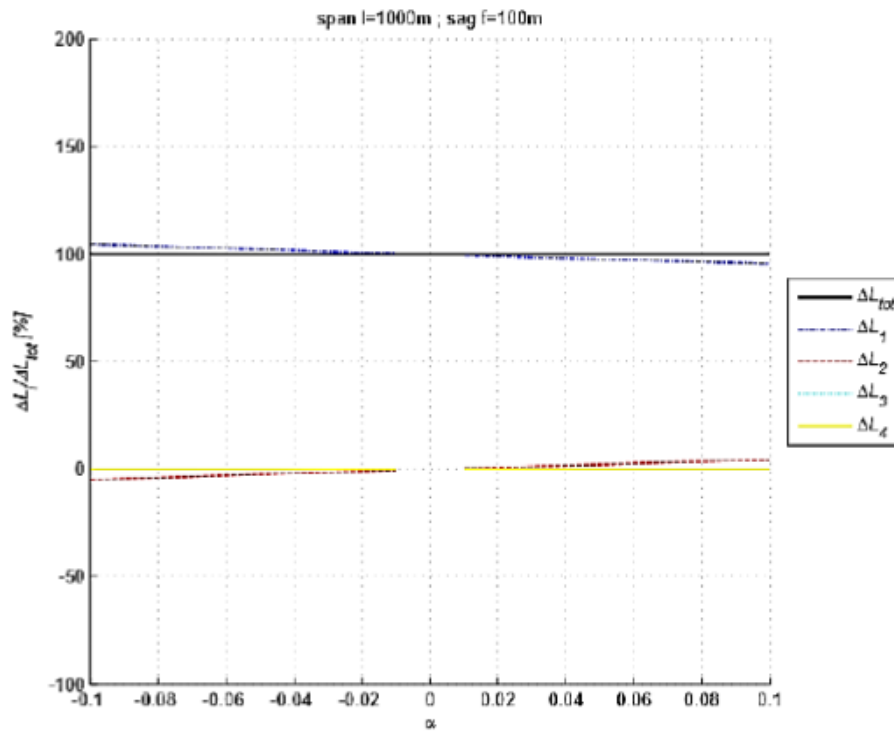


Figure 1.7_ Elongation's percentage contribution for small amplitudes.

The term proportional to v'^2 is crucial for the modelling of the cable's nonlinear stiffening response, at least with a second order approximation, though it's percentage contribution doesn't overcome the 5% even for $\alpha=10\%$.

Much more interesting is the slope contribution. In fact, it can be of critical importance because of the cable's parabolic shape has a large sag that is associated to high slope near the support's extremities.

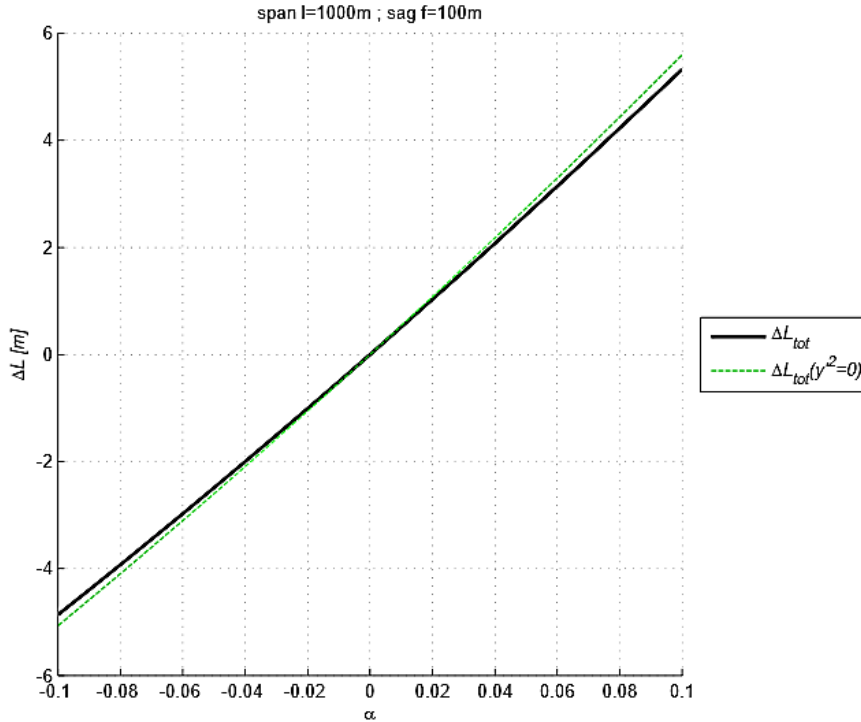


Figure 1.8_ Exact vs approximate curvature.

It is evident that neglecting the slope contribution led to results that are reliable and conservative (green line). Thus, it is possible to use the first simple and handy formulation found for ΔL to be on safe side.

$$\Delta L = - \int_0^l y''(\alpha y) dx + \frac{1}{2} \int_0^l (\alpha y)'^2 dx ;$$

We notice that neglecting the second order term but taking in account the complete curvature expression, or taking its approximate expression, it is possible to reach the same level of accuracy. In fact, both the second order term and the slope has the same weight of about 5% on the total elongation of the cable.

On the other hand, it is easy to see that as the sag f tends to infinity the asymptotic behaviour of the cable changes strongly from one model to another. In fact, taking in consideration the presence of y' the trend of ΔL is hyperbolic, whereas using the simplified expression the cable's elongation explodes with a power of two.

Concerning the influence of the cable's span l it establishes a quadratic relation with the cables' elongation in its complete formulation and a fourth order hyperbole in the simplified form.

Up to now, we have considered the presence of a unique antinode; but the dynamic response of a real cable can be very similar to that of a sinusoid. Then, the initial model would be too conservative dealing with higher order modal shapes. In order to be able to catch the actual elongation in a more generic framework, let us assume that our reference cable shapes itself as a sine function with arbitrary number of half waves.

$$w(x) = W \sin\left(\frac{n\pi x}{l}\right) ;$$

This kind of approach is a kind of assumed mode method, and allows defining each term contributing to the total elongation of the cable.

$$\Delta L = - \int_0^l \frac{y''w}{(1+y'^2)^{3/2}} dx + \frac{1}{2} \int_0^l \frac{w'^2}{(1+y'^2)^{3/2}} dx - \frac{1}{2} \int_0^l \frac{y'w'^3}{(1+y'^2)^{5/2}} dx - \frac{1}{8} \int_0^l \frac{(1-4y'^2)w'^4}{(1+y'^2)^{7/2}} dx ;$$

The first test focuses on the influence of the number of half waves, and then it is possible to assume a unitary perturbation amplitude.

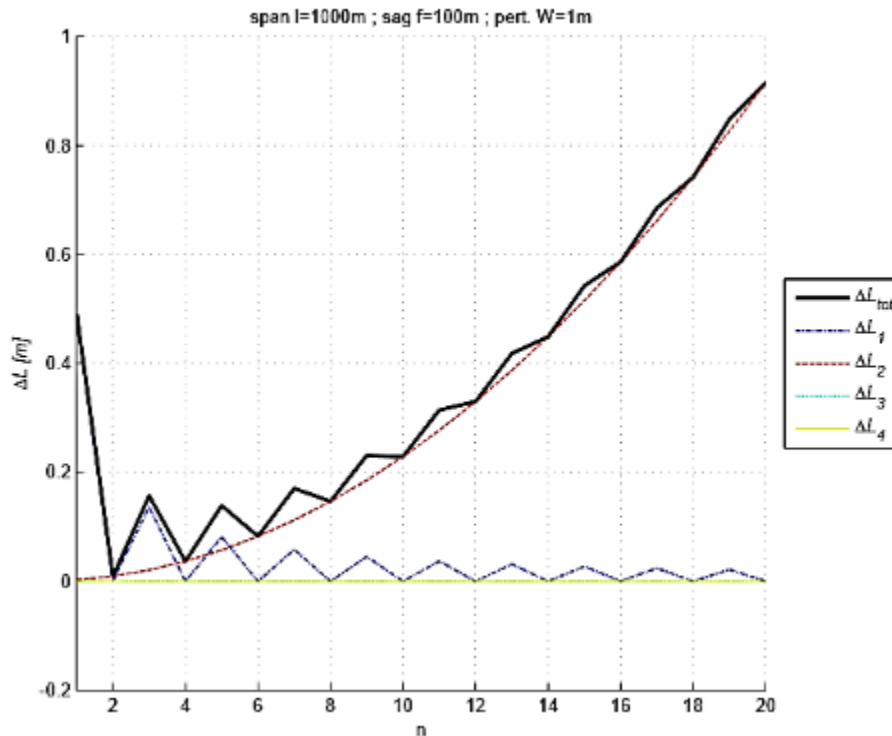


Figure 1.9_Cable's elongation for large number of sinusoidal half waves.

The choice of plotting the results for a large range of half wave's numbers allows focusing on the general path followed by each contribution.

Since the third and the fourth order terms are always negligible, let us focus on the other two.

The first order term has a strange pattern due to its analytical expression. For sake of simplicity, let's write it by means of the approximate expression for the curvature, neglecting the slope contribution.

$$\Delta L_1 = - \int_0^l (y''w) dx = \frac{8f}{l^2} W \int_0^l \sin\left(\frac{n\pi x}{l}\right) dx = -\frac{8f}{n\pi l} W (\cos(n\pi) - 1) ;$$

Then the linear contribution vanishes for each modal shape characterised by an even number of half waves, but for all the odd values it decreases along a hyperbolic path.

Contrary the second order one increases monotonically with a power of two its overall contribution. Also in this case let's write the analytical expression neglecting the slope contribution to the curvature.

$$\Delta L_2 = \frac{1}{2} \int_0^l w'^2 dx = \frac{1}{2} \left(W \frac{n\pi}{l} \right)^2 \int_0^l \left[\cos\left(\frac{n\pi x}{l}\right) \right]^2 dx ;$$

Where by means of partial integration.

$$\int_0^l \left[\cos\left(\frac{n\pi x}{l}\right) \right]^2 dx = \int_0^l \cos\left(\frac{n\pi x}{l}\right) \cos\left(\frac{n\pi x}{l}\right) dx = \frac{n\pi}{l} \left[\cos\left(\frac{n\pi x}{l}\right) \sin\left(\frac{n\pi x}{l}\right) \right]_0^l + \int_0^l \left[\sin\left(\frac{n\pi x}{l}\right) \right]^2 dx ;$$

Some simplifications hold.

$$\left[\cos\left(\frac{n\pi x}{l}\right) \sin\left(\frac{n\pi x}{l}\right) \right]_0^l = 0 ;$$

$$\int_0^l \left[\sin\left(\frac{n\pi x}{l}\right) \right]^2 dx = \int_0^l 1 - \left[\cos\left(\frac{n\pi x}{l}\right) \right]^2 dx ;$$

Hence finally.

$$\int_0^l \left[\cos\left(\frac{n\pi x}{l}\right) \right]^2 dx = \frac{l}{2} ;$$

$$\Delta L_2 = \left(W \frac{n\pi}{2\sqrt{l}} \right)^2 ;$$

As in a modal approach only the lower order modes are of practical interest, let's compare the contribution to the total elongation associated to small number of half waves.

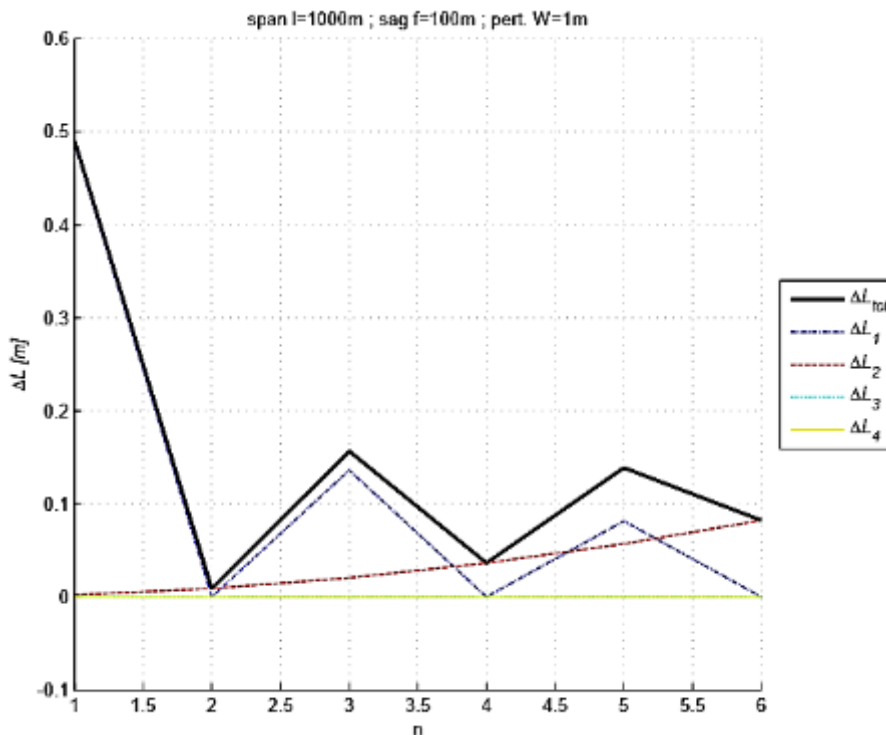


Figure 1.10_Cable's elongation for a realistic number of sinusoidal half waves.

First, it's important to underline the huge decrease of total elongation passing from just one to higher number of half waves. In fact, also considering odd "modes", in which the first order term doesn't vanish, we need to wait until the 14° one so that the second order contribution grants the same elongation of the 1°.

But this condition is purely ideal since higher order modes in general has smaller perturbation's amplitude, then it's expected even a much higher reduction of total elongation as the number of half waves increases. This considerable reduction can be easily explained thinking of the fact that in higher order modes there are region of the cable that are slackening not only with negative W . Hence, there the perturbation always counterbalance partially the initial deformation.

Because of the stress stiffening behaviour of the reference cable, higher order modes can have lower stiffness. This leads to lower frequencies of oscillations and then can happen that higher order modes appear earlier.

For the first mode is approximately valid the same discussion made for the parabolic homothetic deformation with a parameter of perturbation $\alpha=1\%$, where the second order term practically vanishes.

Now it's possible to briefly analyse the influence of other parameters as the span's length or the perturbation's amplitude.

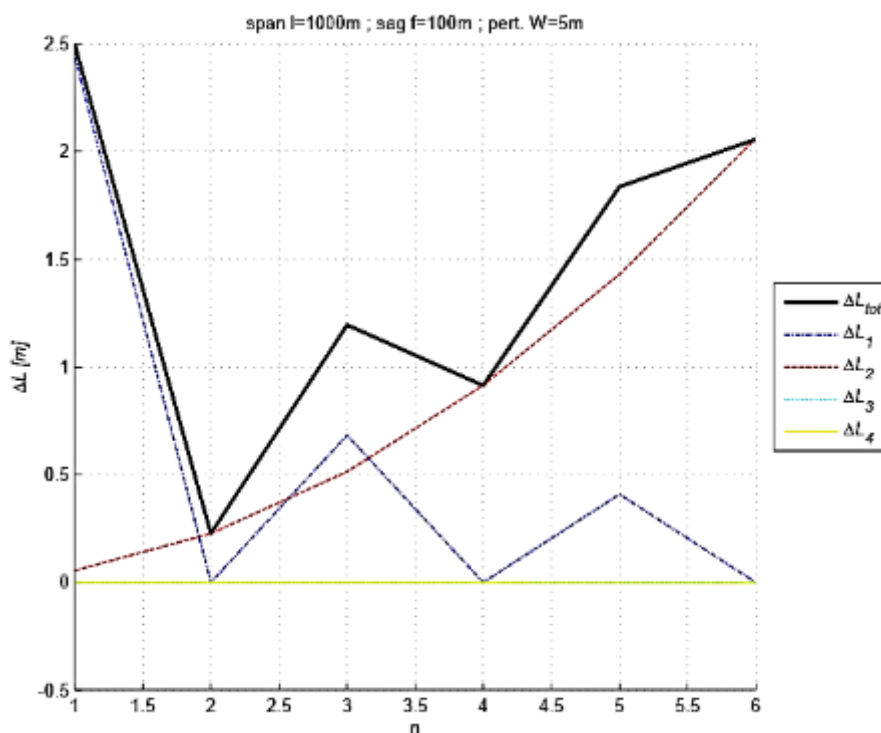


Figure 1.11_Parametric influence of the perturbation's amplitude.

Concerning the second order contribution is important to notice that its magnitude is fundamental in correspondence of all even modes since the first order one vanishes but in odd ones plays an important role another parameter. In fact, from the analytical expression of the first and second order contribution, it's possible to notice that the perturbation's amplitude enters respectively in a linear and quadratic term. Then, as W increases, the second order contribution becomes dominant on the first one in correspondence of a lower number of half waves.

For a deeper insight in the contribution of the perturbation, it's possible to plot for each number of half waves the elongation's trend as W varies.

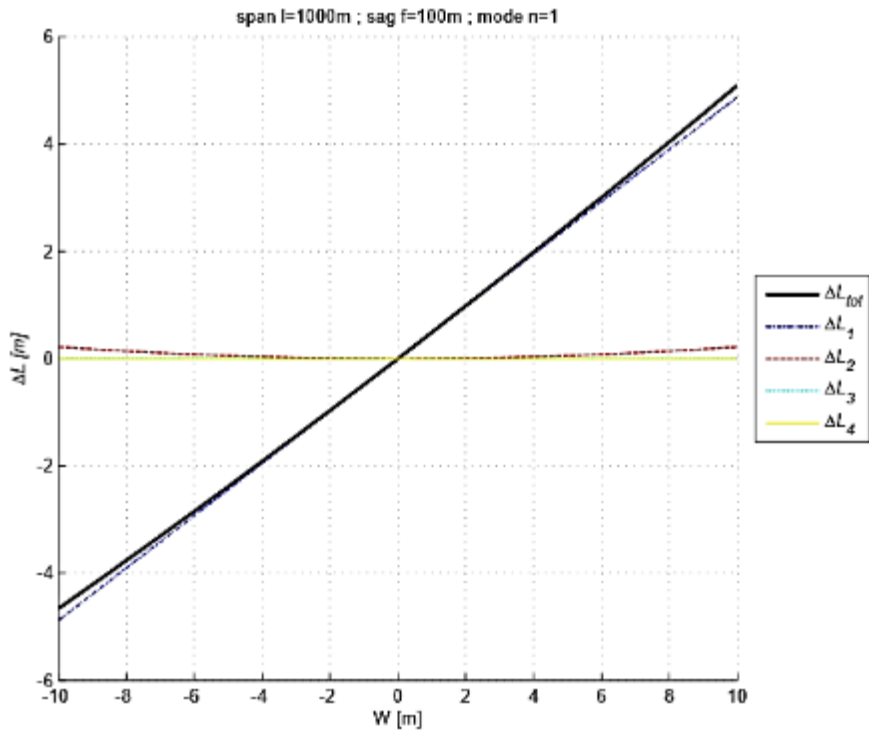


Figure 1.12_Elongation path for the first mode.

The first sinusoidal mode behaves practically in the same manner as the homothetic parabola. In fact, the first order term dominates the second one, that weights just the 5% on the total elongation, and then can be neglected also for large perturbations. Then the linear approximation gives good results also for large displacements.

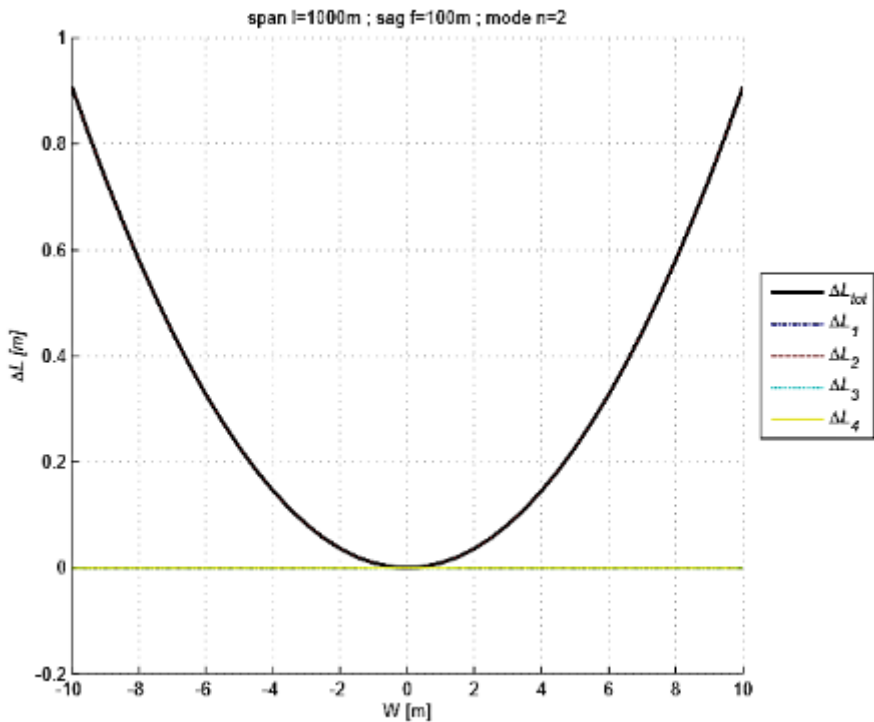


Figure 1.34_Elongation path for the second mode.

Considering the second mode, being representative of all other even ones, here the second order term is the only one that grants an increment in the cable's length since the first order contribution vanishes. Its contribution increases with the number of half waves as already stated and then neglecting it would lead to misleading and unsafe approximations. It's noticeable that there's an easy physical explanation behind the symmetry of the second mode response. In fact, it comes from the fact that the region of softening and hardening are equal along the cable. Hence, it is insensitive to the sign of the perturbation since the number of positive and negative half waves are the same.

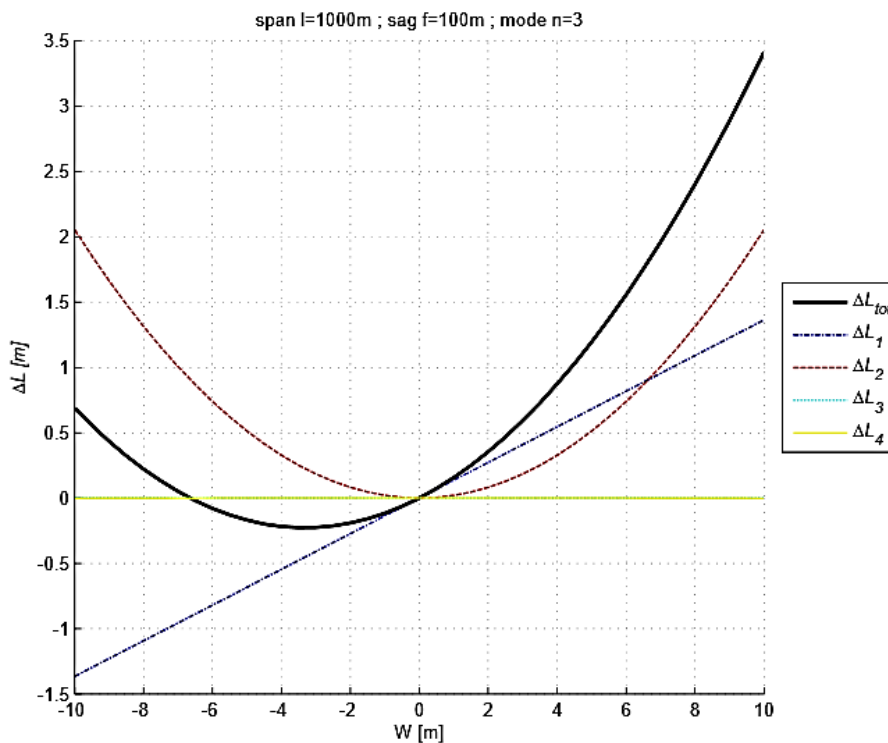


Figure 1.35_Elongation path for the third mode.

The third one can represent the odd modes. At a first glance it is easy to see that both the linear and the quadratic terms are essential to catch the actual elongation. The first one introduces a remarkable asymmetric response in correspondence of positive or negative perturbations. On physical ground, this is because the number of positive and negative half waves cannot be the same in odd modes. Therefore if W is negative, the negative contributions overcome the positive ones and the cable is shortening from the initial configuration. About this point are valid the comments made for the homothetic deformation in presence of large negative α concerning the point of null elongation. As already said for higher order odd modes the quadratic contribution becomes dominant, in fact the total elongation tends to align on a symmetric path.

Finally can be of interest to underline the influence of the slope contribution in defining the exact curvature of the reference cable.

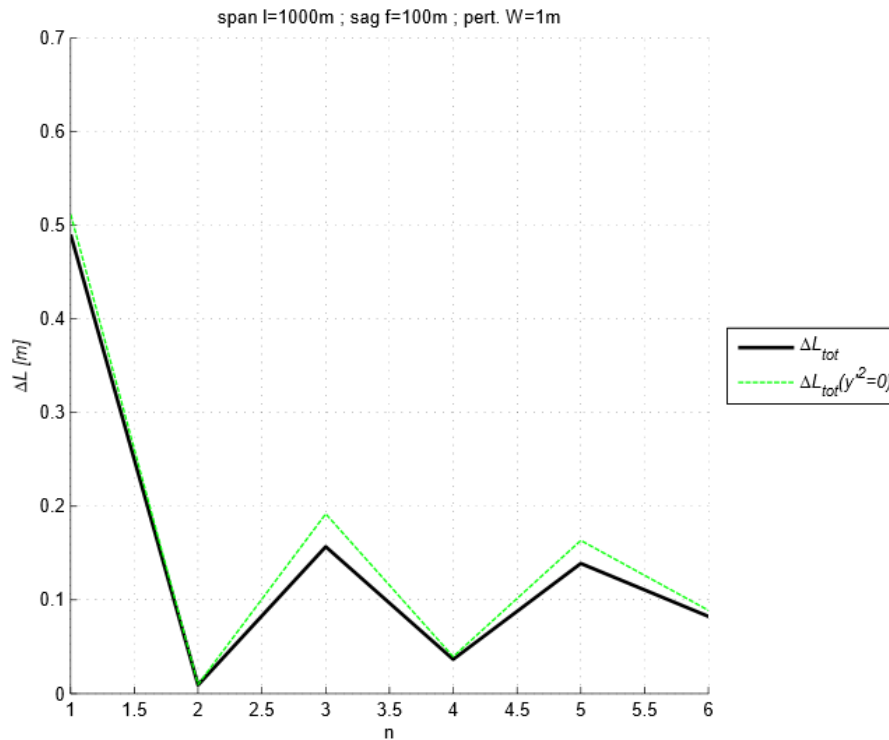


Figure 1.15 _Exact vs approximate curvature.

As can be seen from the previous graph, it's valid the same conclusion written for the case of an homothetic parabolic deformation. Hence assuming an approximate expression for the cable's curvature leads to an overestimation of its actual elongation. This is not always true in the case of odd modes; in fact, their asymmetry leads to an underestimation of cable's elongation for negative W . This is because the shortening contributions dominates the positive ones because of higher number of negative half waves, until the cable starts again to elongate.

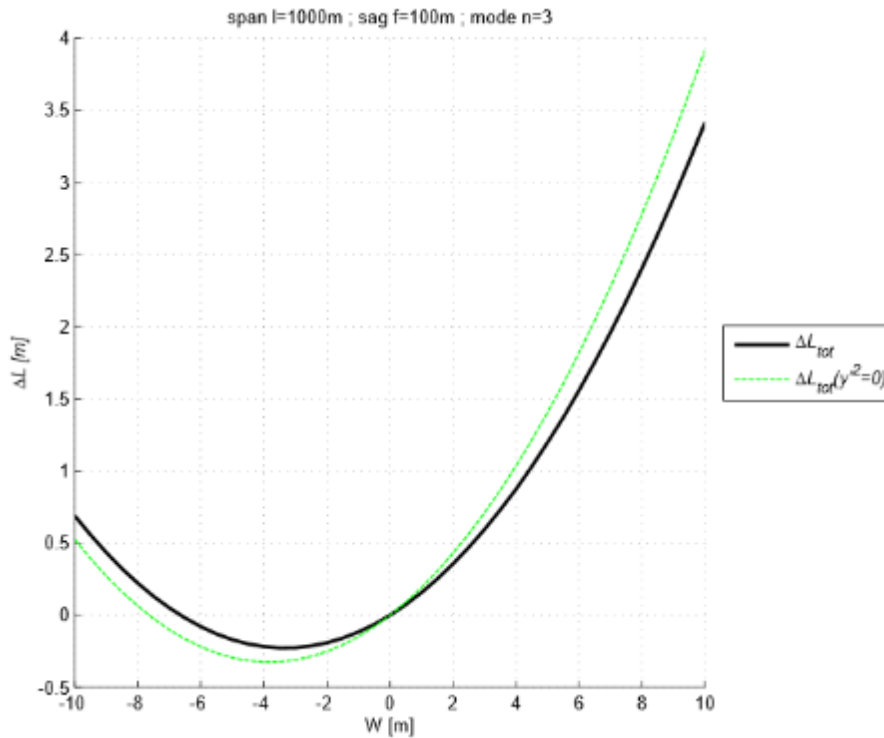


Figure 1.16_Exact vs approximate curvature for the third mode.

Nevertheless, with respect to the previous analysis is not always possible to states that this overestimation compensate the lack of the second order term contribution, since its magnitude depends on the number of half waves and the perturbation amplitude considered.

To conclude, concerning cable's compatibility it's possible to state that:

- for usual perturbation's amplitude it's always possible to neglect third and fourth order terms in the series expansion of the cable's elongation;
- for single half wave it's possible to consider just the linear term and an approximate curvature to get reliable results also in large deflections;
- for two or more half waves' number it's strictly necessary to consider both the linear and the quadratic terms;
- in the last case the approximated curvature introduces higher overestimation of cable's length than in the single half wave mode;
- for relevant higher order modes than the first, the negative contribution of antinode waves reduces drastically the cable's elongation.

1.2. Extended 2 dof model

The classical Deflection theory takes in consideration just the possibility of vertical displacement of the bridge. This is not enough accurate for very large bridges, for which the rotational degree of freedom plays an important role in the response of the structure due to its low torsional stiffness.

1.2.1. TPE formulation

The straight and simplest way to extend the classical deflection theory to a 2 dof model requires to reformulate the classical deflection Theory in energetic terms.

First of all let's write again the compatibility of an infinitesimal cable in order to introduce some fundamental quantities.

$$(ds + dL)^2 = (dx + du)^2 + (dy + dv)^2 ;$$

$$ds^2 + 2 \cdot ds \cdot dL + (dL^2) = dx^2 + 2 \cdot dx \cdot du + (du^2) + dy^2 + 2 \cdot dy \cdot dv + dv^2 ;$$

$$ds \cdot dL = dx \cdot du + dy \cdot dv + dv^2/2 ;$$

Hence it's possible to define the cable's axial strain and by the assumption of linear elasticity the associated axial tension.

$$\varepsilon(s) = \frac{dL}{ds} = \frac{u' + y'v' + v'^2/2}{s'^2} = \frac{\tilde{\varepsilon}}{ds} ;$$

$$\tau(s) = E_c A_c \cdot \varepsilon ;$$

The component of the cable's tension in the horizontal plan is given by a simple trigonometric projection of inclined axial tension, assumed to be aligned with the initial not perturbed configuration of the cable.

$$h(x) = \frac{\tau(s)}{s'} = \frac{E_c A_c}{s'^3} \cdot \tilde{\varepsilon} ;$$

Now we are ready to write the Total Potential Energy Variation of the suspension bridge starting from the initial equilibrium configuration under self-weight up to the final perturbed one under external variable loads.

$$\Delta V(u, v, q) = V(u, y + v, g + q) - V(0, y, g) = E_{deck} + 2E_{cable} - L_{ext} ;$$

Lets' analyse each single contribution starting from the elastic energy stored by the deck that is associated only to its flexural deformation. Quantitatively this involves the bending moment distribution along the bridge's span, which from the assumption of linear elastic material response is linearly dependent on the curvature by means of the flexural stiffness. Further the parametric analysis of the previous chapter allows us to consider a simplified expression for the curvature, neglecting the slope contribution.

$$E_{deck} = \frac{1}{2} \int_0^l M(x) \cdot \chi(x) dx = \frac{1}{2} \int_0^l E_d I_d \cdot \left(\frac{d^2 w}{dx^2} \right)^2 dx ;$$

Notice that up to now all sectional properties are considered generically variable along the length of the element under consideration.

On the other hand each cable has two contributions of different nature. The first one is associated to the initial constant tension needed by assumption to sustain the self-weight of the whole structure. The second takes in account the nonlinear geometrical response of the cable, introducing a higher order correction to the energy stored, that takes in account the variable increment of the cable's tension along its effective length.

$$E_{cable,H} = \int_0^L T(x) \cdot \varepsilon(x) ds = \int_0^L Hs'(x) \cdot \frac{\tilde{\varepsilon}(x)}{s'^2} ds = H \int_0^l \tilde{\varepsilon}(x) dx ;$$

$$E_{cable,h} = \frac{1}{2} \int_0^L \tau(x) \cdot \varepsilon(x) ds = \frac{1}{2} \int_0^L E_c A_c \cdot \varepsilon(x)^2 ds = \frac{1}{2} \int_0^L E_c A_c \cdot \frac{\tilde{\varepsilon}(x)^2}{s'^4} ds = \frac{1}{2} \int_0^l E_c A_c \cdot \frac{\tilde{\varepsilon}(x)^2}{s'^3} dx ;$$

From the last two expression is evident that the energetic contribution linked to cable's tension increment is nonlinear with both cable's strain and undeformed configuration.

Finally the contribution of external actions associated to permanent self-weight loads and variable ones.

$$L_{ext} = \int_0^l (g + q) \cdot w dx ; ;$$

The assumption of taut hangers allows us to write the TPE variation just in terms of the vertical displacement of the deck, being equal to that of the corresponding point on the cable.

$$v(x) = w(x) \Rightarrow \Delta V(u, w, g, q) = \left\{ \begin{array}{l} \frac{1}{2} \int_0^l E_d I_d \cdot w''^2 dx + H \int_0^l \left(u' + y' w' + \frac{w'^2}{2} \right) dx + \\ + \frac{1}{2} \int_0^l \frac{E_c A_c}{s'^3} \cdot \left(u' + y' w' + \frac{w'^2}{2} \right)^2 dx - \int_0^l (g + q) \cdot w dx \end{array} \right\} ;$$

Performing an integration by parts and enforcing the simply supports boundary conditions it's possible to extract from the TPE formulation the initial equilibrium equation.

$$\int_0^l y' w' dx = [y' w]_0^l - \int_0^l y'' w dx = y'(l)w(l) - y'(0)w(0) - \int_0^l y'' w dx = - \int_0^l y'' w dx ;$$

$$H \int_0^l y' w' dx - \int_0^l g \cdot w dx = - \int_0^l (H y'' + g) \cdot w dx = 0$$

Hence it's possible to simplify the TPE formulation as follows.

$$\Delta V(u, w, q) = \left\{ \begin{array}{l} \frac{1}{2} \int_0^l E_d I_d \cdot w''^2 dx + 2H \int_0^l \left(u' + \frac{w'^2}{2} \right) dx + \\ + 2 \left[\frac{1}{2} \int_0^l \frac{E_c A_c}{s'^3} \cdot \left(u' + y' w' + \frac{w'^2}{2} \right)^2 dx \right] - \int_0^l q \cdot w dx \end{array} \right\} ;$$

Enforcing the stationarity of the variational formulation along with suitable boundary conditions both for the suspension cables and the stiffening deck, leads to the equilibrium equations in the longitudinal and vertical directions.

Suitable boundary conditions for the longitudinal equilibrium are those that grant fixed perfectly rigid pylons. Otherwise taking in account also the possible motion of pylons we should consider that the cables curvature increases as pylons comes near and vice versa.

$$b. c. = \begin{cases} u(0) = u(l) = 0 \Rightarrow du(0) = du(l) = 0 \\ H = const \Rightarrow H' = 0 \end{cases} ;$$

$$\delta_u V = \left\{ \begin{aligned} & 2H \int_0^l du' dx + \int_0^l \frac{E_c A_c}{s'^3} \cdot 2 \left(u' + y' w' + \frac{w'^2}{2} \right) du' dx = 2 \int_0^l (H + h) du' dx = \\ & = 2[(H + h)du]_0^l - 2 \int_0^l (H + h)' du dx = \\ & = 2[(H + h(l))du(l) - (H + h(0))du(0)] - 2 \int_0^l h' du dx = \\ & = -2 \int_0^l h' du dx \end{aligned} \right\} ;$$

$$\delta_u V = 0 \quad \forall \delta u \Leftrightarrow h(x) = const ;$$

The final statement is coherent with the assumptions of fixed pylons and the absence of longitudinal loadings, and it allows us to define an important term related to the main cable's tension increment. This term is in general called global or non-local term since has to be distinguished from the local one typical of 4 dof models that takes in account also the actual stiffness of hanger. Since in 2 dof model hangers are considered as perfectly rigid not only in tension but also in compression, the cable's stiffening action has a distributed effect on all the structure. In fact the cable can be seen as a non-uniform distributed set of springs that smear out local effects of external loads along the whole length of the stiffening deck.

Hence the global increment of the cable's tension is not dependent on the position along the cable but only on the integral contributions along all its length.

$$h(w) = \int_0^l h(x) dx = \left\{ \begin{aligned} & \int_0^l \frac{E_c A_c}{s'^3} dx \cdot \int_0^l \left(u' + y' w' + \frac{w'^2}{2} \right) dx = \\ & = \frac{\overline{E_c A_c}}{L_c} \cdot \left[u(l) - u(0) + \int_0^l \left(y' w' + \frac{w'^2}{2} \right) dx \right] = \\ & = \frac{\overline{E_c A_c}}{L_c} \cdot \int_0^l \left(y' w' + \frac{w'^2}{2} \right) dx \end{aligned} \right\} ;$$

As can be seen has been introduced an equivalent cable's length that takes in account also the variation of its sectional axial stiffness.

$$L_c = \int_0^l \frac{\overline{E_c A_c}}{E_c A_c} \cdot s'^3 dx ;$$

Then for the vertical direction are sufficient the boundary conditions associated to a simply supported beam.

$$b. c. = \begin{cases} w(0) = w(l) = 0 \Rightarrow dw(0) = dw(l) = 0 \\ w''(0) = w''(l) = 0 \\ H, h(w) = \text{const}(x) \end{cases} ;$$

$$\delta_w V = \left\{ \begin{aligned} & \frac{1}{2} \int_0^l E_d I_d \cdot 2w'' dw'' dx + 2H \int_0^l \frac{2w' dw'}{2} dx + \\ & + 2 \left[\frac{1}{2} \int_0^l \frac{E_c A_c}{s'^3} \cdot 2 \left(u' + y' w' + \frac{w'^2}{2} \right) \left(y' + \frac{2w'}{2} \right) dw' dx \right] - \int_0^l q \cdot dw dx = \\ & = \int_0^l E_d I_d \cdot w'' dw'' dx + 2H \int_0^l w' dw' dx + \\ & + 2h(w) \cdot \int_0^l (y' + w') dw' dx - \int_0^l q \cdot dw dx \end{aligned} \right\} ;$$

$$\delta_w V = 0 \quad \forall \delta w \Leftrightarrow \left\{ \begin{aligned} & \int_0^l E_d I_d \cdot w'' dw'' dx + 2H \int_0^l w' dw' dx + \\ & + 2h(w) \cdot \int_0^l (y' + w') dw' dx - \int_0^l q \cdot dw dx \end{aligned} \right\} = 0 \quad \forall \delta w ;$$

Hence we need to pass all derivatives from the differential terms to the associated ones by means of integration by parts and enforcing proper boundary conditions.

$$\int_0^l E_d I_d w'' dw'' dx = \left\{ \begin{aligned} & [E_d I_d \cdot w'' dw']_0^l - \int_0^l (E_d I_d \cdot w'')' dw' dx = \\ & = E_d I_d(l) \cdot w''(l) dw'(l) - E_d I_d(0) \cdot w''(0) dw'(0) + \\ & - [(E_d I_d \cdot w'')' dw]_0^l + \int_0^l (E_d I_d \cdot w'')'' dw dx = \\ & = -[E_d I_d \cdot w'']'_{x=l} \cdot dw(l) + [E_d I_d \cdot w'']'_{x=0} \cdot dw(0) + \int_0^l (E_d I_d \cdot w'')'' dw dx = \\ & = \int_0^l (E_d I_d \cdot w'')'' dw dx \end{aligned} \right\} ;$$

$$H \int_0^l w' dw' dx = H \left\{ \begin{aligned} & [w' dw]_0^l - \int_0^l w'' dw dx = \\ & = w'(l) dw(l) - w'(0) dw(0) - \int_0^l w'' dw dx = \\ & = - \int_0^l w'' dw dx \end{aligned} \right\} ;$$

$$\int_0^l h(x) \cdot (y' + w') dw' dx = \left\{ \begin{array}{l} [h(w) \cdot (y' + w') dw]_0^l - \int_0^l h(w) \cdot (y' + w')' dw dx = \\ = \left[h(w(l)) \cdot (y'(l) + w'(l)) dw(l) + \right. \\ \left. - h(w(0)) \cdot (y'(0) + w'(0)) dw(0) \right] + \\ - h(w) \cdot \int_0^l (y'' + w'') dw dx = \\ = -h(w) \cdot \int_0^l (y'' + w'') dw dx \end{array} \right\};$$

Hence.

$$\delta_w V = 0 \quad \forall \delta w \Leftrightarrow \int_0^l [(E_d I_d \cdot w'')'' - 2(H + h(w)) \cdot w'' - 2h(w) \cdot y'' - q] dw dx = 0 \quad \forall \delta w;$$

Finally we obtain again the equilibrium equation in the perturbed configuration.

$$(E_d I_d \cdot w'')'' - 2(H + h(w)) \cdot w'' - 2h(w) \cdot y'' = q;$$

But for the following treatment is much more important to return to the TPE formulation taking in account just important information concerning perturbed vertical displacements.

$$\Delta V(w, q) = \left\{ \begin{array}{l} \left[\frac{1}{2} \int_0^l E_d I_d \cdot w''^2 dx + 2H \int_0^l \frac{w'^2}{2} dx + 2 \left[\frac{1}{2} \int_0^l \frac{E_c A_c}{s'^3} \cdot (y' w' + \frac{w'^2}{2})^2 dx \right] - \int_0^l q \cdot w dx \right] = \\ = \int_0^l \left[\frac{1}{2} E_d I_d \cdot w''^2 + \frac{1}{2} H \cdot (2w'^2) + \int_0^{w'} h(w) \cdot (y' + w') dw' - q \cdot w \right] dx \end{array} \right\};$$

The redundant expression for the initial tension in the cable wants to stress the fact that in the single dof model each of the two main cables introduces the same elastic energy in the structural system. On the contrary in the following 2dofs model each cable introduces a different amount of elastic energy as a direct consequence of the difference in the kinematics of the two elements.

1.2.2. Generalisation to 2dof

Once we get the general expression for the TPE of the single dof flexural model it's straightforward to generalise it for the 2 dof one. The new model not only takes trace of the vertical displacement in correspondence of the axis of the deck but also of the rotation around the same axis.

First of all it's necessary to introduce a new coordinate that takes in account for the rotation of the deck in its section. If the flexural motions are assumed to be positive when downward, for the torsional one we will assume to be positive if clockwise.

Hence it's possible to write down the displacements at the two extreme sides of the deck where are assume to be located the plans of the two main cables.

$$\begin{cases} w_R = w_d + \vartheta_d \cdot b \\ w_L = w_d - \vartheta_d \cdot b \end{cases};$$

The introduction of a new degree of freedom not only changes the kinematics of the model but also introduces additional elastic energy, being the model more deformable than previously, that has to be added to the TPE variation.

$$E_{deck, \vartheta_d} = \frac{1}{2} \int_0^l G_d J_d \cdot \vartheta_d'^2 dx + \frac{1}{2} \int_0^l E_d \Gamma_d \cdot \vartheta_d''^2 dx ;$$

The first term is the classical one related to the primary torsion given by the S. Venant theory of beams. The second one on the other hand is associated to secondary torsion effects that are relevant just in thin open section elements and can be studied by means of the Vlasov-Wagner theory.

Generally modern bridges has closed box sections that allows to get high torsional rigidities saving a lot of material and hence reducing drastically self-weight of the stiffening deck. Hence the so called warping deformation it's relevant just in those bridges characterised by very thin decks and few longitudinal I shaped beams in order to restrain possible torsional motions. The design of such kind of bridges can be located in time just after the Deflection Theory took hold in the design practice allowing to use larger structural resources but just before the Tacoma Narrows Bridge collapse when the aerodynamic effects on bridges became of fundamental importance.

The presence of an additional dof allows also to introduce the associated external action linked in terms of external work.

Replacing inside the expression for the single dof TPE variation and adding the terms related to the additional elastic energy stored by the torsional deformation we get.

$$\Delta V(w_d, \vartheta_d, q, m) = \int_0^l \left\{ \begin{array}{l} \frac{1}{2} E_d I_d \cdot w_d''^2 + \frac{1}{2} E_d \Gamma_d \cdot \vartheta_d''^2 + \frac{1}{2} G_d J_d \cdot \vartheta_d'^2 + \\ + \frac{1}{2} H \cdot (w_R'^2 + w_L'^2) + \\ + \int_0^{w_R'} h(w_R) \cdot (y' + w_R') dw_R' + \int_0^{w_L'} h(w_L) \cdot (y' + w_L') dw_L' + \\ - q \cdot w_d - m \cdot \vartheta_d \end{array} \right\} dx ;$$

In order to get the general expression for the static equilibrium equations the following passages are needed.

First of all notice that from the kinematic model we get the total elastic energy stored by the two main cables.

$$H \cdot (w_R'^2 + w_L'^2) = H \cdot \left\{ \begin{array}{l} [(w_d' + \vartheta_d' \cdot b)^2 + (w_d' - \vartheta_d' \cdot b)^2] = \\ = w_d'^2 + 2w_d' \cdot \vartheta_d' b^2 + \vartheta_d'^2 \cdot b^2 + w_d'^2 - 2w_d' \cdot \vartheta_d' b^2 + \vartheta_d'^2 \cdot b^2 = \\ = 2 \cdot (w_d'^2 + \vartheta_d'^2 \cdot b^2) \end{array} \right\} ;$$

Then we need to find the first differential of the TPE variation.

$$\delta V = \int_0^l \left\{ \begin{aligned} & \frac{1}{2} E_d I_d \cdot 2w_d'' dw_d'' + \frac{1}{2} E_d \Gamma_d \cdot 2\vartheta_d'' d\vartheta_d'' + \frac{1}{2} G_d J_d \cdot 2\vartheta_d' d\vartheta_d' + \\ & + \frac{1}{2} H \cdot 2 \cdot (2w_d' dw_d' + 2\vartheta_d' d\vartheta_d' \cdot b^2) + \\ & + h(w_R) \cdot (y' + w_d' + \vartheta_d' \cdot b) \cdot d(w_d' + \vartheta_d' \cdot b) + \\ & + h(w_L) \cdot (y' + w_d' - \vartheta_d' \cdot b) \cdot d(w_d' - \vartheta_d' \cdot b) + \\ & - q \cdot dw_d - m \cdot d\vartheta_d \end{aligned} \right\} dx ;$$

Integration by parts leads to the following statement.

$$\delta V = \int_0^l \left\{ \begin{aligned} & (E_d I_d \cdot w_d'')'' \cdot dw_d + (E_d \Gamma_d \cdot \vartheta_d'')'' \cdot d\vartheta_d - (G_d J_d \cdot \vartheta_d')' \cdot d\vartheta_d + \\ & - 2H \cdot (w_d'' dw_d + \vartheta_d'' d\vartheta_d \cdot b^2) + \\ & - h(w_R) \cdot (y'' + w_d'' + \vartheta_d'' \cdot b) \cdot d(w_d + \vartheta_d \cdot b) + \\ & - h(w_L) \cdot (y'' + w_d'' - \vartheta_d'' \cdot b) \cdot d(w_d - \vartheta_d \cdot b) + \\ & - q \cdot dw_d - m \cdot d\vartheta_d \end{aligned} \right\} dx ;$$

Let's now analyse the non-local term associated to the stiffening behaviour of the main cables.

$$h(w_d \pm \vartheta_d \cdot b) = \frac{\overline{E_c A_c}}{L_c} \cdot \int_0^l \left\{ \begin{aligned} & y' \cdot (w_d' \pm \vartheta_d' \cdot b) + \frac{1}{2} (w_d' \pm \vartheta_d' \cdot b)^2 = \\ & = y' w_d' \pm y' \vartheta_d' \cdot b + \frac{1}{2} (w_d'^2 \pm 2w_d' \vartheta_d' \cdot b + \vartheta_d'^2 \cdot b^2) = \\ & = \left(y' w_d' + \frac{w_d'^2}{2} \right) \pm (y' \vartheta_d' + w_d' \vartheta_d') \cdot b + \left(\frac{\vartheta_d'^2}{2} \cdot b^2 \right) \end{aligned} \right\} dx ;$$

Hence for sake of brevity we can introduce few parameters, taking in account of the effect on cable's additional tension respectively for contribution given by pure flexure, coupled flexure-torsion and pure torsion.

$$h(w_d \pm \vartheta_d \cdot b) = h(w^\pm) = h_w \pm h_{w\vartheta} + h_\vartheta ;$$

Where each term can be define as follows.

$$\left\{ \begin{aligned} & h_w(w_d) = \frac{\overline{E_c A_c}}{L_c} \cdot \int_0^l \left(y' w_d' + \frac{w_d'^2}{2} \right) dx = \frac{\overline{E_c A_c}}{L_c} \cdot \int_0^l \left(-y'' w_d + \frac{w_d'^2}{2} \right) dx \\ & h_{w\vartheta}(w_d, \vartheta_d) = \frac{\overline{E_c A_c}}{L_c} \cdot \int_0^l (y' \vartheta_d' + w_d' \vartheta_d') \cdot b dx = \frac{\overline{E_c A_c}}{L_c} \cdot \int_0^l (-y'' \vartheta_d + w_d' \vartheta_d') \cdot b dx ; \\ & h_\vartheta(\vartheta_d) = \frac{\overline{E_c A_c}}{L_c} \cdot \int_0^l \frac{\vartheta_d'^2}{2} \cdot b^2 dx \end{aligned} \right.$$

Hence it's easy to compute the stiffening contributions of both cables to the TPE variation.

$$h(w^\pm)(y'' + w_d'' \pm \vartheta_d'' \cdot b)(dw_d \pm d\vartheta_d \cdot b) = 2 \cdot \left\{ \begin{array}{l} (h_w + h_\vartheta) \cdot [(y'' + w_d'') \cdot dw_d + \vartheta_d'' b^2 \cdot d\vartheta_d] + \\ + h_{w\vartheta} \cdot b[(y'' + w_d'') \cdot d\vartheta_d + \vartheta_d'' \cdot dw_d] \end{array} \right\};$$

Now we are able to enforce the stationarity of the TPE variation.

$$\delta_{w_d} V = 0 \quad \forall \delta w_d \Leftrightarrow \left\{ \begin{array}{l} (E_d I_d(x) \cdot w_d''(x))'' + \\ -2H \cdot w_d''(x) + \\ -2(h_w + h_\vartheta) \cdot (y'' + w_d''(x)) + \\ -2h_{w\vartheta} b \cdot \vartheta_d''(x) \end{array} \right\} = q(x);$$

$$\delta_{\vartheta_d} V = 0 \quad \forall \delta \vartheta_d \Leftrightarrow \left\{ \begin{array}{l} (E_d \Gamma_d(x) \cdot \vartheta_d''(x))'' + \\ -(G_d J_d(x) \cdot \vartheta_d'(x))' + \\ -2H b^2 \cdot \vartheta_d''(x) + \\ -2(h_w + h_\vartheta) b^2 \cdot \vartheta_d''(x) + \\ -2h_{w\vartheta} b \cdot (y'' + w_d''(x)) \end{array} \right\} = m(x);$$

Once again we have obtained a self-adjoint system of equations that grants the static equilibrium of the structural system.

In order to extend the present treatment to the dynamic field is simply necessary to add the inertial terms.

$$\delta_{w_d} V = 0 \quad \forall \delta w_d \Leftrightarrow \left\{ \begin{array}{l} (m_d + 2m_c) \cdot \ddot{w}_d(x, t) + \\ + (E_d I_d(x) \cdot w_d''(x, t))'' + \\ -2H \cdot w_d''(x, t) + \\ -2(h_w + h_\vartheta) \cdot (y'' + w_d''(x, t)) + \\ -2h_{w\vartheta} b \cdot \vartheta_d''(x, t) \end{array} \right\} = q(x, t);$$

$$\delta_{\vartheta_d} V = 0 \quad \forall \delta \vartheta_d \Leftrightarrow \left\{ \begin{array}{l} (J_t + 2m_c b^2) \cdot \ddot{\vartheta}_d(x, t) + \\ + (E_d \Gamma_d(x) \cdot \vartheta_d''(x, t))'' + \\ - (G_d J_d(x) \cdot \vartheta_d'(x, t))' + \\ - 2Hb^2 \cdot \vartheta_d''(x, t) + \\ - 2(h_w + h_\vartheta) b^2 \cdot \vartheta_d''(x, t) + \\ - 2h_{w\vartheta} b \cdot (y'' + w_d''(x, t)) \end{array} \right\} = m(x, t);$$

Notice that the equations just obtained refers to the generic situation where the sectional properties of both the deck and the cables can vary along their respective length. But for sake of simplicity, in the following we will assume to consider constant values.

It's evident that the two equations of motion so obtained are not linear with the actual configuration of the structural system. This is a consequence of the presence of the non-local cable term, that is function itself of the bridge configuration though in integral form.

The second remark concerns the coupling of the two equations of motions. This is a common property of nonlinear mechanical systems, and in the actual structural system it's due once again by the non-local term.

Thence can be of interest first to separate the terms with different order of magnitude and secondly to have an estimate of the degree of coupling of the 2 dofs, mainly related to the order of non-linearity of the problem.

1.2.3. Dimensionless format

For a better comprehension of the following treatment let's introduce the dimensionless format for the equation of motions.

First of all let's define some fundamental dimensionless quantities.

$$\left\{ \begin{array}{l} \xi = \frac{x}{l} \in [0,1] \\ \tilde{w}_d(\xi, \tau) = \frac{w_d(x,t)}{f} ; \\ \tilde{\vartheta}_d(\xi, \tau) = \frac{\vartheta_d(x,t) \cdot b}{f} \end{array} \right.$$

Notice that the dimensionless time variable will be define subsequently.

Before considering separately each equation of motion, it's better to expand some terms.

$$2(h_w + h_\vartheta) \cdot (y'' + w_d'') = 2 \cdot \left\{ \begin{array}{l} \left[\begin{array}{l} h_w \cdot y'' = \frac{E_c A_c}{L_c} \cdot \int_0^l \left(-y'' w_d + \frac{w_d'^2}{2} \right) dx \cdot y'' = \\ = \frac{E_c A_c}{L_c} y'' \left(-y'' \cdot fl \int_0^1 \tilde{w}_d d\xi + \frac{1}{2} \frac{f^2}{l^2} l \int_0^1 \tilde{w}_d'^2 d\xi \right) = \\ = -\frac{E_c A_c}{L_c} y''^2 fl \cdot \int_0^1 \tilde{w}_d d\xi + \frac{1}{2} \frac{E_c A_c}{L_c} y'' \frac{f^2}{l} \cdot \int_0^1 \tilde{w}_d'^2 d\xi \end{array} \right] \\ + \left[\begin{array}{l} h_w \cdot w_d'' = \frac{E_c A_c}{L_c} \cdot \int_0^l \left(-y'' w_d + \frac{w_d'^2}{2} \right) dx \cdot w_d'' = \\ = \frac{E_c A_c}{L_c} \cdot \frac{f}{l^2} \tilde{w}_d'' \left(-y'' \cdot fl \int_0^1 \tilde{w}_d d\xi + \frac{1}{2} \frac{f^2}{l^2} l \int_0^1 \tilde{w}_d'^2 d\xi \right) = \\ = -\frac{E_c A_c}{L_c} y'' \frac{f^2}{l} \cdot \tilde{w}_d'' \int_0^1 \tilde{w}_d d\xi + \frac{1}{2} \frac{E_c A_c}{L_c} \frac{f^3}{l^3} \cdot \tilde{w}_d'' \int_0^1 \tilde{w}_d'^2 d\xi \end{array} \right] \\ + \left[\begin{array}{l} h_\vartheta \cdot y'' = \frac{E_c A_c}{L_c} \cdot \int_0^l \frac{\vartheta_d'^2}{2} \cdot b^2 dx \cdot y'' = \\ = \frac{1}{2} \frac{E_c A_c}{L_c} y'' \cdot \frac{f^2 l}{b^2 l^2} \int_0^1 \tilde{\vartheta}_d'^2 d\xi \cdot b^2 = \\ = \frac{1}{2} \frac{E_c A_c}{L_c} y'' \frac{f^2}{l} \cdot \int_0^1 \tilde{\vartheta}_d'^2 d\xi \end{array} \right] \\ + \left[\begin{array}{l} h_\vartheta \cdot w_d'' = \frac{E_c A_c}{L_c} \cdot \int_0^l \frac{\vartheta_d'^2}{2} \cdot b^2 dx \cdot w_d'' = \\ = \frac{1}{2} \frac{E_c A_c}{L_c} \cdot \frac{f}{l^2} \tilde{w}_d'' \cdot \frac{f^2 l}{b^2 l^2} \int_0^1 \tilde{\vartheta}_d'^2 d\xi \cdot b^2 = \\ = \frac{1}{2} \frac{E_c A_c}{L_c} \frac{f^3}{l^3} \cdot \tilde{w}_d'' \int_0^1 \tilde{\vartheta}_d'^2 d\xi \end{array} \right] \end{array} \right\};$$

$$2h_{w\vartheta} b \cdot \vartheta_d'' = 2 \cdot \left\{ \begin{array}{l} \frac{E_c A_c}{L_c} \cdot \int_0^l \left(-y'' \vartheta_d + w_d' \vartheta_d' \right) \cdot b dx \cdot b \vartheta_d'' = \\ = \frac{E_c A_c}{L_c} b \cdot \frac{f}{bl^2} \tilde{\vartheta}_d'' \cdot \left[-y'' \frac{fl}{b} \int_0^1 \tilde{\vartheta}_d d\xi + \frac{f^2 l}{bl^2} \int_0^1 \tilde{w}_d' \tilde{\vartheta}_d' d\xi \right] \cdot b = \\ = -\frac{E_c A_c}{L_c} y'' \frac{f^2}{l} \cdot \tilde{\vartheta}_d'' \int_0^1 \tilde{\vartheta}_d d\xi + \frac{E_c A_c}{L_c} \frac{f^3}{l^3} \cdot \tilde{\vartheta}_d'' \int_0^1 \tilde{w}_d' \tilde{\vartheta}_d' d\xi \end{array} \right\};$$

$$2(h_w + h_\vartheta)b^2 \cdot \vartheta_d'' = 2 \cdot \left\{ \begin{array}{l} \left[\begin{array}{l} h_w b^2 \cdot \vartheta_d'' = \frac{E_c A_c}{L_c} \cdot \int_0^l \left(-y'' w_d + \frac{w_d'^2}{2} \right) dx b^2 \cdot \vartheta_d'' = \\ = \frac{E_c A_c}{L_c} b^2 \cdot \frac{f}{bl^2} \tilde{\vartheta}_d'' \left(-y'' \cdot fl \int_0^1 \tilde{w}_d d\xi + \frac{1}{2} \frac{f^2}{l^2} l \int_0^1 \tilde{w}_d'^2 d\xi \right) = + \\ = -\frac{E_c A_c}{L_c} y'' \frac{f^2 b}{l} \cdot \tilde{\vartheta}_d'' \int_0^1 \tilde{w}_d d\xi + \frac{1}{2} \frac{E_c A_c f^3 b}{L_c l^3} \cdot \tilde{\vartheta}_d'' \int_0^1 \tilde{w}_d'^2 d\xi \end{array} \right] \\ + \left[\begin{array}{l} h_\vartheta b^2 \cdot \vartheta_d'' = \frac{E_c A_c}{L_c} \cdot \int_0^l \frac{\vartheta_d'^2}{2} \cdot b^2 dx b^2 \cdot \vartheta_d'' = \\ = \frac{1}{2} \frac{E_c A_c}{L_c} b^4 \cdot \frac{f}{bl^2} \tilde{\vartheta}_d'' \cdot \frac{f^2 l}{b^2 l^2} \int_0^1 \tilde{\vartheta}_d'^2 d\xi = \\ = \frac{1}{2} \frac{E_c A_c f^3 b}{L_c l^3} \cdot \tilde{\vartheta}_d'' \int_0^1 \tilde{\vartheta}_d'^2 d\xi \end{array} \right] \end{array} \right\};$$

$$2h_{w\vartheta}b \cdot (y'' + w_d'') = 2 \cdot \left\{ \begin{array}{l} \left[\begin{array}{l} h_{w\vartheta} b \cdot y'' = \frac{E_c A_c}{L_c} \cdot \int_0^l (-y'' \vartheta_d + w_d' \vartheta_d') \cdot b dx \cdot b y'' = \\ = \frac{E_c A_c}{L_c} b y'' \cdot \left(-y'' \frac{fl}{b} \int_0^1 \tilde{\vartheta}_d d\xi + \frac{f^2 l}{bl^2} \int_0^1 \tilde{w}_d' \tilde{\vartheta}_d' d\xi \right) \cdot b = \\ = -\frac{E_c A_c}{L_c} y''^2 fl b \int_0^1 \tilde{\vartheta}_d d\xi + \frac{E_c A_c}{L_c} y'' \frac{f^2 b}{l} \int_0^1 \tilde{w}_d' \tilde{\vartheta}_d' d\xi \end{array} \right] \\ \left[\begin{array}{l} h_{w\vartheta} b \cdot w_d'' = \frac{E_c A_c}{L_c} \cdot \int_0^l (-y'' \vartheta_d + w_d' \vartheta_d') \cdot b dx \cdot b w_d'' = \\ = \frac{E_c A_c}{L_c} b \cdot \frac{f}{l^2} \tilde{w}_d'' \cdot \left(-y'' \frac{fl}{b} \int_0^1 \tilde{\vartheta}_d d\xi + \frac{f^2 l}{bl^2} \int_0^1 \tilde{w}_d' \tilde{\vartheta}_d' d\xi \right) \cdot b = \\ = -\frac{E_c A_c}{L_c} y'' \frac{f^2 b}{l} \cdot \tilde{w}_d'' \int_0^1 \tilde{\vartheta}_d d\xi + \frac{E_c A_c f^3 b}{L_c l^3} \cdot \tilde{w}_d'' \int_0^1 \tilde{w}_d' \tilde{\vartheta}_d' d\xi \end{array} \right] \end{array} \right\};$$

➤ Flexural equation of motion:

$$\left. \begin{aligned}
 & \left[(m_d + 2m_c) \cdot \frac{d^2 w_d}{dt^2} = (m_d + 2m_c) f \cdot \frac{d^2 \tilde{w}_d}{dt^2} \right] + \\
 & + \left[E_d I_d \cdot \frac{d^4 w_d}{dx^4} = E_d I_d \frac{f}{l^4} \cdot \frac{d^4 \tilde{w}_d}{d\xi^4} \right] + \\
 & - \left[2H \cdot \frac{d^2 w_d}{dx^2} = 2H \frac{f}{l^2} \cdot \frac{d^2 \tilde{w}_d}{d\xi^2} \right] + \\
 & - 2(h_w + h_\vartheta) \cdot (y'' + w_d'') = 2 \cdot \left[\begin{aligned}
 & - \frac{E_c A_c}{L_c} y''^2 f l \cdot \int_0^1 \tilde{w}_d d\xi + \\
 & + \frac{1}{2} \frac{E_c A_c}{L_c} y'' \frac{f^2}{l} \cdot \int_0^1 \tilde{w}_d'^2 d\xi + \\
 & - \frac{E_c A_c}{L_c} y'' \frac{f^2}{l} \cdot \tilde{w}_d'' \int_0^1 \tilde{w}_d d\xi + \\
 & + \frac{1}{2} \frac{E_c A_c}{L_c} \frac{f^3}{l^3} \cdot \tilde{w}_d'' \int_0^1 \tilde{w}_d'^2 d\xi + \\
 & + \frac{1}{2} \frac{E_c A_c}{L_c} y'' \frac{f^2}{l} \cdot \int_0^1 \tilde{\vartheta}_d'^2 d\xi + \\
 & + \frac{1}{2} \frac{E_c A_c}{L_c} \frac{f^3}{l^3} \cdot \tilde{w}_d'' \int_0^1 \tilde{\vartheta}_d'^2 d\xi
 \end{aligned} \right] + \\
 & - \left[2h_{w\vartheta} b \cdot \vartheta_d'' = 2 \cdot \left(\begin{aligned}
 & - \frac{E_c A_c}{L_c} y'' \frac{f^2}{l} \cdot \tilde{\vartheta}_d'' \int_0^1 \tilde{\vartheta}_d d\xi + \\
 & + \frac{E_c A_c}{L_c} \frac{f^3}{l^3} \cdot \tilde{\vartheta}_d'' \int_0^1 \tilde{w}_d' \tilde{\vartheta}_d' d\xi
 \end{aligned} \right) \right]
 \end{aligned} \right\} = q(\xi, \tau);$$

It can be noticed that the choice of the cable's initial arrow, as reference length for the flexural perturbations, doesn't affect the format of the dimensionless equations in the special case of free-vibrations.

On the other hand for the forced case is important to remember that also the forcing terms has to be dimensionless.

Hence collecting the modulus of the coefficient of the third term, that is associated to the initial tension in the cable, we get.

$$\left. \begin{aligned}
& \frac{(m_d+2m_c)}{2H} l^2 \cdot \frac{d^2 \tilde{w}_d}{dt^2} + \\
& + \frac{E_d l_d}{2H l^2} \cdot \frac{d^4 \tilde{w}_d}{d\xi^4} + \\
& - \frac{d^2 \tilde{w}_d}{d\xi^2} + \\
& \left(+ \frac{E_c A_c}{H} \frac{l}{L_c} (y'' l)^2 \cdot \int_0^1 \tilde{w}_d d\xi + \right. \\
& - \frac{1}{2} \frac{E_c A_c}{H} \frac{l}{L_c} y'' f \cdot \int_0^1 \tilde{w}_d '2 d\xi + \\
& + \frac{E_c A_c}{H} \frac{l}{L_c} y'' f \cdot \tilde{w}_d '' \int_0^1 \tilde{w}_d d\xi + \\
& \left. - \frac{1}{2} \frac{E_c A_c}{H} \frac{l}{L_c} \left(\frac{f}{l}\right)^2 \cdot \tilde{w}_d '' \int_0^1 \tilde{w}_d '2 d\xi + \right. \\
& - \frac{1}{2} \frac{E_c A_c}{H} \frac{l}{L_c} y'' f \cdot \int_0^1 \tilde{\vartheta}_d '2 d\xi + \\
& \left. - \frac{1}{2} \frac{E_c A_c}{H} \frac{l}{L_c} \left(\frac{f}{l}\right)^2 \cdot \tilde{w}_d '' \int_0^1 \tilde{\vartheta}_d '2 d\xi \right) \\
& + \left(+ \frac{E_c A_c}{H} \frac{l}{L_c} y'' f \cdot \tilde{\vartheta}_d '' \int_0^1 \tilde{\vartheta}_d d\xi + \right. \\
& \left. - \frac{E_c A_c}{H} \frac{l}{L_c} \left(\frac{f}{l}\right)^2 \cdot \tilde{\vartheta}_d '' \int_0^1 \tilde{w}_d ' \tilde{\vartheta}_d ' d\xi \right)
\end{aligned} \right\} = \frac{l^2}{2Hf} q(\xi, \tau);$$

Let's define other fundamental dimensionless parameters.

$$\left\{ \begin{aligned}
\tau &= t \cdot \frac{1}{l} \sqrt{\frac{2H}{(m_d+2m_c)}} \\
\tilde{q}(\xi, \tau) &= \frac{l^2}{2Hf} q(\xi, \tau) \\
\mu^2 &= \frac{E_d l_d}{2H l^2} \\
\lambda_L^2 &= \frac{E_c A_c}{H} \frac{l}{L_c} (y'' l)^2 \\
\lambda_Q^2 &= -\frac{E_c A_c}{H} \frac{l}{L_c} y'' f \\
\lambda_C^2 &= \frac{E_c A_c}{H} \frac{l}{L_c} \left(\frac{f}{l}\right)^2
\end{aligned} \right. ;$$

The first two terms simply define respectively the dimensionless time coordinate and the equivalent flexural external forcing.

Regarding the first one, can be of interest to have an estimate of the term collected in order to get dimensionless time variable. In fact, this will be used in the following defining the dimensionless circular eigen-frequency. From literature [31-40] we can give a reasonable range of variation.

$$l \sqrt{\frac{(m_d + 2m_c)}{2H}} \cong (5 \div 20) \text{ [s]};$$

The range is very large but it's useful to get the order of magnitude of real values passing from the dimensionless to dimensional values.

The third is the ratio between the deck and cables flexural stiffness, hence it's an important parameter giving us directly the weight of each contribution to the whole bridge flexural stiffness. In the following a bibliographical research will allow us to give it reasonable values.

The last three terms measure the extensibility of cables in relation to the initial tension needed to sustain the whole self-weight of the suspended structure.

Each can only multiply respectively linear, quadratic and cubic terms of the deck configuration. Thus are clear the subscript given to each, and it's also clear that the equation of motions would be nonlinear up to the third order.

The parabolic initial cable shape allows us to give also an estimation of the degree of nonlinear terms, thanks to the fact that this particular cable configuration has a constant curvature.

$$y'' = -\frac{8f}{l^2} \Rightarrow \begin{cases} \lambda_L^2 = 64 \frac{E_c A_c}{H} \frac{l}{L_c} \left(\frac{f}{l}\right)^2 \\ \lambda_Q^2 = 8 \frac{E_c A_c}{H} \frac{l}{L_c} \left(\frac{f}{l}\right)^2 \Rightarrow \lambda_L^2 = 8\lambda_Q^2 = 64\lambda_C^2; \\ \lambda_C^2 = \frac{E_c A_c}{H} \frac{l}{L_c} \left(\frac{f}{l}\right)^2 \end{cases}$$

It's evident that the higher order terms are very smooth; this is an intrinsic structural property of the 2 dof model proposed since the only nonlinearities are related to the nonlinear response of the main cables. This has been already evidenced in the previous chapter where the parametric analysis of a cable shows that second order terms are the only that can be appreciated within reasonable deformations.

Larger contributions comes from nonlinearities in 4 dofs model where the possible local slackening of hangers introduces a hard type of nonlinearity in the response. This behaviour is due to the intrinsic geometrical property of these structural elements, characterised by values of slenderness so high that makes it unable to react in compression.

Hence we can say that the proposed 2 dofs mathematical model of the suspension bridge is characterised by soft nonlinearities. This property will be useful in the further study of the model once we try to find an analytical solution for the structural response by means of a perturbative technique.

Generally the linear term is called Irvine parameter [5] being the first one that discover it importance in the vibrations of suspended cables.

Let's introduce some further parameters.

$$\left\{ \begin{array}{l} \tilde{h}_w = \int_0^1 \tilde{w}_d d\xi \\ \tilde{h}_\vartheta = \int_0^1 \tilde{\vartheta}_d d\xi \\ \tilde{h}_{w'w'} = \int_0^1 \tilde{w}_d' \cdot \tilde{w}_d' d\xi ; \\ \tilde{h}_{\vartheta'\vartheta'} = \int_0^1 \tilde{\vartheta}_d' \cdot \tilde{\vartheta}_d' d\xi \\ \tilde{h}_{w'\vartheta'} = \int_0^1 \tilde{w}_d' \cdot \tilde{\vartheta}_d' d\xi \end{array} \right.$$

Now we are able to rewrite the flexural equation of motion in a more compact form collecting terms with the same order.

$$\left\{ \begin{array}{l} \frac{d^2 \tilde{w}_d}{d\tau^2} + \mu^2 \cdot \tilde{w}_d'^v - \tilde{w}_d'' + \lambda_L^2 \tilde{h}_w + \\ -\lambda_Q^2 \cdot \left[\tilde{h}_w \cdot \tilde{w}_d'' + \tilde{h}_\vartheta \cdot \tilde{\vartheta}_d'' - \frac{1}{2} (\tilde{h}_{w'w'} + \tilde{h}_{\vartheta'\vartheta'}) \right] + \\ -\lambda_C^2 \cdot \left[\frac{1}{2} (\tilde{h}_{w'w'} + \tilde{h}_{\vartheta'\vartheta'}) \cdot \tilde{w}_d'' + \tilde{h}_{w'\vartheta'} \cdot \tilde{\vartheta}_d'' \right] \end{array} \right\} = \tilde{q}(\xi, \tau) ;$$

From a first analysis of parameters we can say that the dominant one will be the cables stiffening term associated to λ_L^2 (linear component), then the quadratic and the cubic components. Of two order of magnitude lower will be the inertial and the curvature contributions and finally of five order of magnitude lower the terms associated to the deck relative flexural stiffness μ^2 .

$$\lambda_L^2 = 8 \cdot \lambda_Q^2 = 64 \cdot \lambda_C^2 \cong 10^2 \cdot \left\{ \begin{array}{l} \frac{d^2 \tilde{w}_d}{d\tau^2} \\ \tilde{w}_d'' \end{array} \right. \cong (10^5 \div 10^6) \cdot \mu^2$$

➤ Torsional equation of motion:

$$\left\{ \begin{array}{l}
 \left[(J_t + 2m_c b^2) \cdot \frac{d^2 \vartheta_d}{dt^2} = (J_t + 2m_c b^2) \frac{f}{b} \cdot \frac{d^2 \tilde{w}_d}{dt^2} \right] + \\
 + \left[E_d \Gamma_d \cdot \frac{d^4 \vartheta_d}{dx^4} = E_d \Gamma_d \frac{f}{bl^4} \cdot \frac{d^4 \tilde{\vartheta}_d}{d\xi^4} \right] + \\
 - \left[G_d J_d \cdot \frac{d^2 \vartheta_d}{dx^2} = G_d J_d \frac{f}{bl^2} \cdot \frac{d^2 \tilde{\vartheta}_d}{d\xi^2} \right] + \\
 - \left[2Hb^2 \cdot \frac{d^2 \vartheta_d}{dx^2} = 2Hb^2 \frac{f}{bl^2} \cdot \frac{d^2 \tilde{\vartheta}_d}{d\xi^2} = 2H \frac{fb}{l^2} \cdot \frac{d^2 \tilde{\vartheta}_d}{d\xi^2} \right] + \\
 - \left[2(h_w + h_\vartheta) b^2 \cdot \vartheta_d'' = 2 \cdot \left(\begin{array}{l}
 -\frac{E_c A_c}{L_c} y'' \frac{f^2 b}{l} \cdot \tilde{\vartheta}_d'' \int_0^1 \tilde{w}_d d\xi + \\
 + \frac{1}{2} \frac{E_c A_c f^3 b}{L_c l^3} \cdot \tilde{\vartheta}_d'' \int_0^1 \tilde{w}_d'^2 d\xi + \\
 + \frac{1}{2} \frac{E_c A_c f^3 b}{L_c l^3} \cdot \tilde{\vartheta}_d'' \int_0^1 \tilde{\vartheta}_d'^2 d\xi
 \end{array} \right) \right] + \\
 - \left[2h_{w\vartheta} b \cdot (y'' + w_d''(x, t)) = 2 \cdot \left(\begin{array}{l}
 -\frac{E_c A_c}{L_c} y''^2 f l b \int_0^1 \tilde{\vartheta}_d d\xi + \\
 + \frac{E_c A_c}{L_c} y'' \frac{f^2 b}{l} \int_0^1 \tilde{w}_d' \tilde{\vartheta}_d' d\xi + \\
 -\frac{E_c A_c}{L_c} y'' \frac{f^2 b}{l} \cdot \tilde{w}_d'' \int_0^1 \tilde{\vartheta}_d d\xi + \\
 + \frac{E_c A_c f^3 b}{L_c l^3} \cdot \tilde{w}_d'' \int_0^1 \tilde{w}_d' \tilde{\vartheta}_d' d\xi
 \end{array} \right) \right]
 \end{array} \right\} = m(\xi, \tau);$$

Once again let's collect the modulus of the second term coefficient.

$$\left\{ \begin{array}{l} \frac{(J_t+2m_c b^2)}{2Hb^2} l^2 \cdot \frac{d^2 \tilde{w}_d}{dt^2} + \\ + \frac{E_d \Gamma_d}{2Hb^2 l^2} \cdot \frac{d^4 \tilde{\vartheta}_d}{d\xi^4} + \\ - \frac{G_d J_d}{2Hb^2} \cdot \frac{d^2 \tilde{\vartheta}_d}{d\xi^2} + \\ - \frac{d^2 \tilde{\vartheta}_d}{d\xi^2} + \\ - \left(\begin{array}{l} - \frac{E_c A_c}{H} \frac{l}{L_c} y'' f \cdot \tilde{\vartheta}_d'' \int_0^1 \tilde{w}_d d\xi + \\ + \frac{1}{2} \frac{E_c A_c}{H} \frac{l}{L_c} \left(\frac{f}{l}\right)^2 \cdot \tilde{\vartheta}_d'' \int_0^1 \tilde{w}_d'^2 d\xi + \\ + \frac{1}{2} \frac{E_c A_c}{H} \frac{l}{L_c} \left(\frac{f}{l}\right)^2 \cdot \tilde{\vartheta}_d'' \int_0^1 \tilde{\vartheta}_d'^2 d\xi \end{array} \right) + \\ - \left(\begin{array}{l} - \frac{E_c A_c}{H} \frac{l}{L_c} (y'' l)^2 \int_0^1 \tilde{\vartheta}_d d\xi + \\ + \frac{E_c A_c}{H} \frac{l}{L_c} y'' f \int_0^1 \tilde{w}_d' \tilde{\vartheta}_d' d\xi + \\ - \frac{E_c A_c}{H} \frac{l}{L_c} y'' f \cdot \tilde{w}_d'' \int_0^1 \tilde{\vartheta}_d d\xi + \\ + \frac{E_c A_c}{H} \frac{l}{L_c} \left(\frac{f}{l}\right)^2 \cdot \tilde{w}_d'' \int_0^1 \tilde{w}_d' \tilde{\vartheta}_d' d\xi \end{array} \right) \end{array} \right\} = \frac{l^2}{2Hfb} m(\xi, \tau);$$

It's necessary to define others few parameters.

$$\left\{ \begin{array}{l} \frac{(J_t+2m_c b^2)}{b^2} \frac{l^2}{2H} = \frac{(J_t+2m_c b^2)}{(m_d+2m_c) \cdot b^2} \left(\frac{t}{\tau}\right)^2 \Rightarrow \tilde{J}_t = \frac{(J_t+2m_c b^2)}{(m_d+2m_c) \cdot b^2} = \left(\frac{\rho_d}{b}\right)^2 \\ \tilde{m}(\xi, \tau) = \frac{l^2}{2Hfb} m(\xi, \tau) \\ \beta^2 = \frac{G_d J_d}{2Hb^2} \\ \gamma^2 = \frac{E_d \Gamma_d}{2Hb^2 l^2} = \frac{E_d \Gamma_d}{G_d J_d l^2} \beta^2 = \frac{\beta^2}{\chi^2} \end{array} \right. ;$$

The first term represent respectively the ratio between the actual torsional inertia of the deck and cables system and the maximum one corresponding to ideal condition with all the masses lumped at the two deck sectional sides. Hence it can be seen as a sort of dimensionless gyration radius normalised with respect to the half width of the deck.

While the second one represent just the dimensionless format of the external torsional moment.

The last two terms relate respectively the torsional and warping stiffness contribution given by the deck and that given by the two cables. Also these terms will play an important role in further analysis thence will be given realistic values to it.

Hence the torsional equation of motion can be written synthetically as follows, separating different order terms.

$$\left\{ \begin{array}{l} \tilde{J}_t \cdot \frac{d^2 \tilde{\vartheta}_d}{dt^2} + \frac{\beta^2}{\chi^2} \cdot \tilde{\vartheta}_d'' - (1 + \beta^2) \cdot \tilde{\vartheta}_d'' + \lambda_L^2 \tilde{h}_\vartheta + \\ -\lambda_Q^2 \cdot [\tilde{h}_\vartheta \cdot \tilde{w}_d'' + \tilde{h}_w \cdot \tilde{\vartheta}_d'' - \tilde{h}_{w'\vartheta'}] + \\ -\lambda_C^2 \cdot [\tilde{h}_{w'\vartheta'} \cdot \tilde{w}_d'' + \frac{1}{2}(\tilde{h}_{w'w'} + \tilde{h}_{\vartheta'\vartheta'}) \cdot \tilde{\vartheta}_d''] \end{array} \right\} = \tilde{m}(\xi, \tau);$$

It's important to notice that only the linear terms of both the flexural and torsional equations of motion are uncoupled. This is an important feature of the structural system that allows us to get into analytical solutions by means of modal analysis.

Once again the dominant term is the cables stiffening associated to λ_L^2 (linear component), then the quadratic and the cubic components. Of three order of magnitude lower will be the inertial and of four order of magnitude lower the terms associated to the deck relative torsional stiffness $\frac{\beta^2}{\chi^2}$. Whilst the curvature contribution, depending on the structural configuration, can be of the same order of magnitude of the dominant λ_L^2 or nearly negligible being of six order of magnitude lower.

$$\lambda_L^2 = 8 \cdot \lambda_Q^2 = 64 \cdot \lambda_C^2 \cong 10^3 \cdot \tilde{J}_t \cong (10^4 \div 10^5) \cdot \frac{\beta^2}{\chi^2} \cong (1 \div 10^6) \cdot (1 + \beta^2)$$

Hence we have defined the governing equations for both the flexural and the torsional motion of the simplified model for a suspension bridge. In the following we will analyse the fundamental modal characteristic.

2. Modal response

Modal analysis is usually seen as a simple separation of variable process, since it's able to split the spatial and time dependence of variables, allowing to study their variation in those spaces separately and in an easy way. Hence permitting to pass from partial differential equations to ordinary ones.

The only requirement is that the field of application has to be linear where the superposition principle is still valid. In fact modal decomposition describe the actual configuration of the system summing ideally an infinite number of products between a modal shape variable in space and function variable in time.

2.1. Modal decomposition analysis

It's important to underline also the fact that we are going to define structural properties, hence the external forcing cannot affect them in a structural model that doesn't consider the effects of the external world on the structure itself (as can be done for example with an aeroelastic model).

Hence the modal approach can be applied just to the linear component of the free equations of motion.

In general is not useful to get all terms of this series since the first modes are sufficient to represent accurately the actual behaviour of the structure.

2.1.1. Flexural equation of motion

First of all let's introduce the modal decomposition for flexural modes.

$$\tilde{w}_d(\xi, \tau) = \sum_{n=1}^{\infty} W_n(\xi) \cdot z_n(\tau) \quad \text{with } n \in \mathbb{N} \setminus \{0\};$$

Hence Euler formula allows us to use a simple representation of the time variant function by means of an exponential function that is a sin and cosine time series.

$$z_n(\tau) = Z_n \cdot \exp(i \cdot \tilde{\omega}_{w,n} \cdot \tau) + \bar{Z}_n \cdot \exp(-i \cdot \tilde{\omega}_{w,n} \cdot \tau);$$

Notice that in order to get a structural response in the real field is necessary to consider also the complex conjugate of the time function that otherwise would be a complex value as shown by the Euler formula.

$$z_n(\tau) = \left\{ \begin{array}{l} \left[(Z_n^R + iZ_n^I) \cdot [\cos(\tilde{\omega}_{w,n} \cdot \tau) + i \cdot \sin(\tilde{\omega}_{w,n} \cdot \tau)] + \right. \\ \left. + (Z_n^R - iZ_n^I) \cdot [\cos(\tilde{\omega}_{w,n} \cdot \tau) - i \cdot \sin(\tilde{\omega}_{w,n} \cdot \tau)] \right] = \\ = 2 \cdot [Z_n^R \cdot \cos(\tilde{\omega}_{w,n} \cdot \tau) - Z_n^I \cdot \sin(\tilde{\omega}_{w,n} \cdot \tau)] = \\ = \bar{Z}_n \cdot \cos(\tilde{\omega}_{w,n} \cdot \tau + \varphi_{w,n}) \end{array} \right\};$$

Where new terms has been introduced.

$$\left\{ \begin{array}{l} \bar{Z}_n = 2 \cdot \sqrt{(Z_n^R)^2 + (Z_n^I)^2} \\ \tan \varphi_{w,n} = \frac{Z_n^I}{Z_n^R} \end{array} \right. ;$$

First has to be notice that the amplitude of oscillations becomes a real quantity and that to account for the effect of imaginary terms we need to introduce a phase lag. This term could be useful once we superimpose the effects of flexural and torsional motions, where a time lag between the two modal shapes can change the response of the structure.

Notice that in principle also the modal shapes could be complex functions of spatial coordinate but the assumption to be real allow us to follow an analytical treatment.

Before proceeding is important to notice that the time function contains a dimensionless term related to the circular eigen-frequency of each specific mode.

$$\tilde{\omega}_{w,n} = \omega_{w,n} \cdot l \sqrt{\frac{(m_d + 2m_c)}{2H}} ;$$

Now we are able to introduce the modal decomposition in the linear flexural equation of motion of the free vibrating system.

$$F(\xi, \tau) = \frac{d^2 \tilde{w}_d}{d\tau^2} + \mu^2 \cdot \tilde{w}_d{}'' - \tilde{w}_d'' + \lambda_L^2 \tilde{h}_w = \sum_{n=1}^{\infty} \left\{ \begin{array}{l} -\tilde{\omega}_{w,n}^2 \cdot W_n(\xi) + \mu^2 \cdot W_n{}''(\xi) + \\ -W_n''(\xi) + \lambda_L^2 \int_0^1 W_n(\xi) d\xi \end{array} \right\} \cdot z_n(\tau) ;$$

Hence in order to satisfy dynamic equilibrium at each instant of time we need to grant the following relation for each mode.

$$F_n(\xi, \tau, n) = 0 \quad \forall(\xi, \tau, n) \Leftrightarrow F_n(\xi) = \left\{ \begin{array}{l} \mu^2 \cdot W_n{}''(\xi) - W_n''(\xi) + \\ -\tilde{\omega}_{w,n}^2 \cdot W_n(\xi) + \lambda_L^2 \cdot \tilde{h}_{w,n} \end{array} \right\} = F_{n,o}(\xi) + \lambda_L^2 \cdot \tilde{h}_{w,n} = 0 \quad \forall(\xi, n)$$

We have just found the ordinary differential equation of fourth order that can be solved analytically and find out both the unknowns that are the modal shape and the circular eigen-frequencies. The fact that from a single equation is possible to define two unknowns is not so surprising if we think that the two variables are implicitly linked together. In fact the procedure is the usual one used to solve eigen-values problems.

In order to solve an ode with spatial variable are necessary proper boundary conditions, that in this case has to be four and are those associate to the simply supported beam.

The analytical procedure allows us to detect particular conditions that a numerical approach will risk to neglect.

First of all is the distinction between symmetric and skew-symmetric modal shapes.

i. Skew-symmetric modes:

In the parametric analysis of the previous Chapter 1 we have already notice that in correspondence of even wave numbers the linear contribution to the cable's elongation vanishes. Hence, this means that the initial tension in the cable doesn't change when the structure vibrates following a skew-symmetric shape along its length.

As a consequence the stiffening term would be null and the equation of motion reduce to that of a tensioned simply supported Euler-Bernoulli beam or to that of a taut string depending on the values assumed by the parameters.

$$\tilde{h}_{W,n} = 0 \quad \forall n \Rightarrow F_n(\xi) = \mu^2 \cdot W_n''(\xi) - W_n''(\xi) - \tilde{\omega}_{w,n}^2 \cdot W_n(\xi) = 0 \quad \forall(\xi, n);$$

This equation admits a simple sinusoidal motion with even number of half waves.

$$W_n(\xi) = \sin(2n \cdot \pi \cdot \xi);$$

Notice that we have found a modal shape, hence it's not important the actual amplitude of vibration, since it will be given by the time dependent function after a time integration of the equation of motion.

Thus, all modal shapes will be normalised with respect to the maximum positive downward displacement.

It's simple to show that effectively the stiffening term vanishes for any choice of half wave number.

$$\tilde{h}_{W,n} = \int_0^1 W_n(\xi) d\xi = \int_0^1 \sin(2n \cdot \pi \cdot \xi) d\xi = \left\{ \begin{array}{l} = -\frac{1}{2n\pi} [\cos(2n \cdot \pi \cdot \xi)]_0^1 = \\ = -\frac{1}{2n\pi} [\cos(2\pi \cdot n) - 1] \end{array} \right\} = 0 \quad \forall n;$$

Substituting inside the equation of motion we get the expression for the circular eigen-frequencies.

$$F_n(\xi) = \{\mu^2 \cdot (2n\pi)^4 + (2n\pi)^2 - \tilde{\omega}_{w,n}^2\} \cdot \sin(2n\pi \cdot \xi);$$

It's evident that the format is the usual one used in discrete systems to study the eigen-value solutions.

$$F_n(\xi) = 0 \quad \forall(\xi, n) \Leftrightarrow \mu^2 \cdot (2n\pi)^4 + (2n\pi)^2 - \tilde{\omega}_{w,n}^2 = 0 \quad \forall n \Leftrightarrow \tilde{\omega}_{w,n} = 2n\pi \cdot \sqrt{1 + \mu^2 \cdot (2n\pi)^2};$$

As previously mentioned two extreme situations can be described respectively when the cable's or deck flexural stiffness is dominant on the whole system response.

$$\text{if } \mu^2 \ll \frac{1}{(2n\pi)^2} \Rightarrow \tilde{\omega}_{w,n} = 2n\pi \quad (\text{taut string});$$

$$\text{if } \mu^2 \gg \frac{1}{(2n\pi)^2} \Rightarrow \tilde{\omega}_{w,n} = (2n\pi)^2 \cdot \mu \quad (\text{tensioned beam});$$

ii. Symmetric modes:

In this case the linear contribution of the stiffening term becomes relevant on the flexural response. As direct consequence the equation of motion becomes a complete ODE in spatial variable. Hence the solution is a combination of a homogeneous and a particular integral.

Since the stiffening term is constant once we fix the modal shape to be analysed, then the particular solution required is a constant, since has to be able to solve by itself the complete ODE without any need for boundary conditions.

$$W_{n,p} = C_n \Rightarrow F_n(\xi) = 0 \quad \forall(\xi, n) \Leftrightarrow C_n = \frac{\lambda_L^2}{\tilde{\omega}_{w,n}^2} \tilde{h}_{W,n} ;$$

Notice that in the stiffening term we need to consider the complete solution and not only the particular one, though up to now it's unknown.

On the other hand the Euler method is the easiest way to find out the homogeneous integral for ODE with constant coefficients. This method exploits the linearity of the equation, trying to find the homogeneous solution as a linear combination of exponential terms.

The terms necessary to describe exactly the modal shape under consideration are equal to the number of boundary conditions that affects its shape, that in the present general case are the four ones proper of a simply supported beam. In fact with respect to the particular integral, the homogeneous one has to satisfy both the homogeneous equation and all the boundary conditions.

$$W_{n,o}(\xi) = \sum_{i=1}^4 c_{n,i} \cdot \exp(\alpha_{n,i} \cdot \xi) ;$$

Replacing in the homogeneous equation of motion we get the expression for the exponential coefficient.

$$F_{n,o}(\xi) = \sum_{i=1}^4 c_{n,i} \cdot \{\mu^2 \cdot \alpha_{n,i}^4 - \alpha_{n,i}^2 - \tilde{\omega}_{w,n}^2\} \cdot \exp(\alpha_{n,i} \xi) ;$$

Hence.

$$F_{n,o}(\xi) = 0 \quad \forall(\xi, i, n) \Leftrightarrow \{\mu^2 \cdot \alpha_{n,i}^4 - \alpha_{n,i}^2 - \tilde{\omega}_{w,n}^2\} = 0 \quad \forall(i, n) ;$$

$$\Leftrightarrow \alpha_{n,i}^2 = \frac{1}{2\mu^2} \left(1 \pm \sqrt{1 + 4\mu^2 \cdot \tilde{\omega}_{w,n}^2} \right) ;$$

In the following will be useful to manage easily these coefficients.

$$\eta_{w,n}^2 = \frac{1}{2\mu^2} \left(\sqrt{1 + 4\mu^2 \cdot \tilde{\omega}_{w,n}^2} - 1 \right) ;$$

$$\psi_{w,n}^2 = \frac{1}{2\mu^2} \left(\sqrt{1 + 4\mu^2 \cdot \tilde{\omega}_{w,n}^2} + 1 \right) ;$$

The previous definition allow us to define respectively the so called trigonometric and hyperbolic exponential coefficient.

The following relation will be useful in the following.

$$\Psi_{w,n}^2 = \eta_{w,n}^2 + \frac{1}{\mu^2};$$

Then we are able to superimpose effects of both the particular and homogeneous integrals in order to obtain the complete solution of the equation of motion.

$$W_n(\xi) = W_{n,p} + W_{n,o}(\xi) = \left\{ \begin{array}{l} \frac{\lambda_L^2}{\tilde{\omega}_{w,n}^2} \tilde{h}_{W,n} + \\ + c_{n,1} \cdot \exp(\Psi_{w,n}\xi) + c_{n,2} \cdot \exp(-\Psi_{w,n}\xi) + \\ + c_{n,3} \cdot \exp(i \cdot \eta_{w,n}\xi) + c_{n,4} \cdot \exp(-i \cdot \eta_{w,n}\xi) \end{array} \right\};$$

Now it's evident that we are searching for real modal shapes, in fact the last two contributions if taken separately would be a complex combination of sine and cosine spatial functions, while together grant the solution to be a real function, being complex conjugate number.

At this point is necessary to enforce the following boundary conditions in order to find the values of the constant coefficients necessary to linearly combine each contribution.

$$b. c. (support) \left\{ \begin{array}{l} W_n(0) = W_n(1) = 0 \quad (null \ displacement) \\ W_n''(0) = W_n''(1) = 0 \quad (free \ curvature) \end{array} \right. \quad \forall n;$$

It's possible to study separately the conditions at the two ends.

$$\left\{ \begin{array}{l} W_n(0) = 0 \Leftrightarrow c_{n,1} + c_{n,2} + c_{n,3} + c_{n,4} + \frac{\lambda_L^2}{\tilde{\omega}_{w,n}^2} \tilde{h}_{W,n} = 0 \\ W_n''(0) = 0 \Leftrightarrow (c_{n,1} + c_{n,2}) \cdot \Psi_{w,n}^2 - (c_{n,3} + c_{n,4}) \cdot \eta_{w,n}^2 = 0 \end{array} \right. ;$$

$$\Rightarrow c_{n,3} = - \left(c_{n,4} + \frac{\Psi_{w,n}^2}{\Psi_{w,n}^2 + \eta_{w,n}^2} \cdot \frac{\lambda_L^2}{\tilde{\omega}_{w,n}^2} \tilde{h}_{W,n} \right);$$

$$\left\{ \begin{array}{l} W_n(1) = 0 \Leftrightarrow c_{n,1} \cdot e^{\Psi_{w,n}} + c_{n,2} \cdot e^{-\Psi_{w,n}} + c_{n,3} \cdot e^{i\eta_{w,n}} + c_{n,4} \cdot e^{-i\eta_{w,n}} + \frac{\lambda_L^2}{\tilde{\omega}_{w,n}^2} \tilde{h}_{W,n} = 0 \\ W_n''(1) = 0 \Leftrightarrow (c_{n,1} \cdot e^{\Psi_{w,n}} + c_{n,2} \cdot e^{-\Psi_{w,n}}) \cdot \Psi_{w,n}^2 - (c_{n,3} \cdot e^{i\eta_{w,n}} + c_{n,4} \cdot e^{-i\eta_{w,n}}) \cdot \eta_{w,n}^2 = 0 \end{array} \right. ;$$

$$\Rightarrow c_{n,3} = - \left(c_{n,4} + \frac{\Psi_{w,n}^2}{\Psi_{w,n}^2 + \eta_{w,n}^2} \cdot e^{-i\eta_{w,n}} \cdot \frac{\lambda_L^2}{\tilde{\omega}_{w,n}^2} \tilde{h}_{W,n} \right);$$

Hence the constant parameters assume the following expression.

$$c_{n,4} = \frac{\lambda_L^2}{\tilde{\omega}_{w,n}^2} \tilde{h}_{W,n} \cdot \frac{\Psi_{w,n}^2}{\Psi_{w,n}^2 + \eta_{w,n}^2} \cdot \frac{1 - e^{i\eta_{w,n}}}{e^{i\eta_{w,n}} - e^{-i\eta_{w,n}}};$$

$$c_{n,3} = -\frac{\lambda_L^2}{\tilde{\omega}_{w,n}^2} \tilde{h}_{W,n} \cdot \frac{\Psi_{w,n}^2}{\Psi_{w,n}^2 + \eta_{w,n}^2} \cdot \frac{1 - e^{-i\eta_{w,n}}}{e^{i\eta_{w,n}} - e^{-i\eta_{w,n}}};$$

$$c_{n,2} = \frac{\lambda_L^2}{\tilde{\omega}_{w,n}^2} \tilde{h}_{W,n} \cdot \frac{\eta_{w,n}^2}{\Psi_{w,n}^2 + \eta_{w,n}^2} \cdot \frac{1 - e^{\Psi_{w,n}}}{e^{\Psi_{w,n}} - e^{-\Psi_{w,n}}};$$

$$c_{n,1} = -\frac{\lambda_L^2}{\tilde{\omega}_{w,n}^2} \tilde{h}_{W,n} \cdot \frac{\eta_{w,n}^2}{\Psi_{w,n}^2 + \eta_{w,n}^2} \cdot \frac{1 - e^{-\Psi_{w,n}}}{e^{\Psi_{w,n}} - e^{-\Psi_{w,n}}};$$

The substitution in the general solution leads to the following expression.

$$W_n(\xi) = \frac{\lambda_L^2}{\tilde{\omega}_{w,n}^2} \tilde{h}_{W,n} \cdot \left\{ 1 - \frac{1}{\Psi_{w,n}^2 + \eta_{w,n}^2} \cdot \left(\eta_{w,n}^2 \cdot \frac{e^{\Psi_{w,n} \cdot \xi} - e^{\Psi_{w,n} \cdot (\xi-1)} + e^{-\Psi_{w,n} \cdot \xi} - e^{-\Psi_{w,n} \cdot (\xi-1)}}{e^{\Psi_{w,n}} - e^{-\Psi_{w,n}}} + \right. \right. \\ \left. \left. + \Psi_{w,n}^2 \cdot \frac{e^{i\eta_{w,n} \cdot \xi} - e^{i\eta_{w,n} \cdot (\xi-1)} + e^{-i\eta_{w,n} \cdot \xi} - e^{-i\eta_{w,n} \cdot (\xi-1)}}{e^{i\eta_{w,n}} - e^{-i\eta_{w,n}}} \right) \right\};$$

Some trigonometric relations allow us to reformulate the solution in a more compact form.

$$\begin{cases} \sinh(\alpha) = \frac{1}{2}(e^\alpha - e^{-\alpha}) \\ \sin(\alpha) = \frac{1}{2}(e^{i\alpha} - e^{-i\alpha}) \end{cases};$$

$$\Rightarrow W_n(\xi) = \frac{\lambda_L^2}{\tilde{\omega}_{w,n}^2} \tilde{h}_{W,n} \cdot \left\{ 1 - \frac{1}{\Psi_{w,n}^2 + \eta_{w,n}^2} \cdot \left(\eta_{w,n}^2 \cdot \frac{\sinh(\Psi_{w,n} \cdot \xi) - \sinh(\Psi_{w,n} \cdot (\xi-1))}{\sinh(\Psi_{w,n})} + \right. \right. \\ \left. \left. + \Psi_{w,n}^2 \cdot \frac{\sin(\eta_{w,n} \cdot \xi) - \sin(\eta_{w,n} \cdot (\xi-1))}{\sin(\eta_{w,n})} \right) \right\};$$

$$\begin{cases} \sinh(\alpha) \pm \sinh(\beta) = 2 \cdot \sinh\left(\frac{\alpha \pm \beta}{2}\right) \cdot \cosh\left(\frac{\alpha \mp \beta}{2}\right) \\ \sin(\alpha) \pm \sin(\beta) = 2 \cdot \sin\left(\frac{\alpha \pm \beta}{2}\right) \cdot \cos\left(\frac{\alpha \mp \beta}{2}\right) \end{cases};$$

$$\Rightarrow \begin{cases} \sinh(\Psi_{w,n} \cdot \xi) - \sinh(\Psi_{w,n} \cdot (\xi-1)) = 2 \cdot \sinh\left(\frac{\Psi_{w,n}}{2}\right) \cdot \cosh\left(\Psi_{w,n} \cdot \left(\xi - \frac{1}{2}\right)\right) \\ \sin(\eta_{w,n} \cdot \xi) - \sin(\eta_{w,n} \cdot (\xi-1)) = 2 \cdot \sin\left(\frac{\eta_{w,n}}{2}\right) \cdot \cos\left(\eta_{w,n} \cdot \left(\xi - \frac{1}{2}\right)\right) \end{cases};$$

$$\begin{cases} \sinh(2\alpha) = 2 \cdot \sinh(\alpha) \cdot \cosh(\alpha) \\ \sin(2\alpha) = 2 \cdot \sin(\alpha) \cdot \cos(\alpha) \end{cases};$$

$$\Rightarrow \begin{cases} \frac{\sinh(\Psi_{w,n})}{\sinh\left(\frac{\Psi_{w,n}}{2}\right)} = 2 \cdot \cosh\left(\frac{\Psi_{w,n}}{2}\right) \\ \frac{\sin(\eta_{w,n})}{\sin\left(\frac{\eta_{w,n}}{2}\right)} = 2 \cdot \cos\left(\frac{\eta_{w,n}}{2}\right) \end{cases};$$

Hence the final expression for the eigen-modes is the following.

$$W_n(\xi) = \frac{\lambda_L^2}{\tilde{\omega}_{w,n}^2} \tilde{h}_{W,n} \cdot \left\{ 1 - \frac{1}{\psi_{w,n}^2 + \eta_{w,n}^2} \cdot \left(\eta_{w,n}^2 \cdot \frac{\cosh\left(\psi_{w,n} \cdot \left(\xi - \frac{1}{2}\right)\right)}{\cosh\left(\frac{\psi_{w,n}}{2}\right)} + \psi_{w,n}^2 \cdot \frac{\cos\left(\eta_{w,n} \cdot \left(\xi - \frac{1}{2}\right)\right)}{\cos\left(\frac{\eta_{w,n}}{2}\right)} \right) \right\};$$

It's evident that the actual expression is implicit due to the presence of the stiffening term that depends itself by the modal shape, but as already said the eigen-modes has to be normalised, hence all common constant terms can be neglected.

Effectively the modal shape is not already known, since the parameters inside the parenthesis are all functions of the unknown circular eigen-frequency.

In fact the only reason why is important to takes in account for the stiffening implicit term is that only in this way it is possible to find the eigen-function giving us the circular frequency associated to that particular modal shape.

Thence from the definition of the stiffening term we get the following relation.

$$\tilde{h}_{W,n} = \int_0^1 W_n(\xi) d\xi = \frac{\lambda_L^2}{\tilde{\omega}_{w,n}^2} \tilde{h}_{W,n} \cdot \int_0^1 \left\{ 1 - \frac{1}{\psi_{w,n}^2 + \eta_{w,n}^2} \cdot \left(\eta_{w,n}^2 \cdot \frac{\cosh\left(\psi_{w,n} \cdot \left(\xi - \frac{1}{2}\right)\right)}{\cosh\left(\frac{\psi_{w,n}}{2}\right)} + \psi_{w,n}^2 \cdot \frac{\cos\left(\eta_{w,n} \cdot \left(\xi - \frac{1}{2}\right)\right)}{\cos\left(\frac{\eta_{w,n}}{2}\right)} \right) \right\} d\xi;$$

It's evident the implicit nature of the actual problem, since the stiffening term can be cancelled out to find the general eigen-function of the problem.

$$\frac{\tilde{\omega}_{w,n}^2}{\lambda_L^2} = 1 - \frac{1}{\psi_{w,n}^2 + \eta_{w,n}^2} \cdot \left(\eta_{w,n}^2 \cdot \frac{\tanh\left(\frac{\psi_{w,n}}{2}\right)}{\frac{\psi_{w,n}}{2}} + \psi_{w,n}^2 \cdot \frac{\tan\left(\frac{\eta_{w,n}}{2}\right)}{\frac{\eta_{w,n}}{2}} \right);$$

The last expression is once again an implicit equation that can be solved numerically by an iterative trial and error process.

We have to underline the fact that this eigen-function is general in the sense that its expression is valid for any symmetrical flexural modes we want to consider.

Hence we expect that function to have an infinite number of zeros, since it has to be able to describe all the infinite set of eigen-solution that characterise the problem.

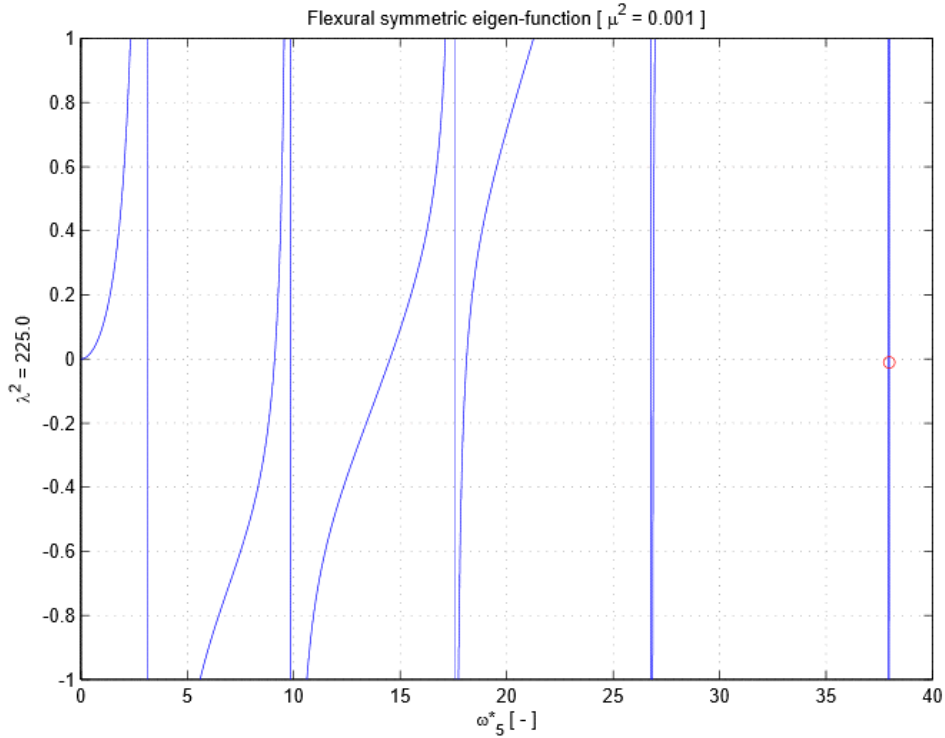


Figure 2.1_Eigen function for flexural symmetric mode shape of fifth order.

As can be seen from the figure above that eigen-function has asymptotic vertical discontinuities that make the rooting a little bit cumbersome. The complexity grows with the order of the mode since for higher orders the continuous branch tends to move the zero nearer and nearer to the discontinuity point. In that way the slope of the function become so high that it's hard to distinguish numerically between the zero given by the vertical asymptote and the one given by the continuous branch of the eigen- function. Fortunately each "true" zero is always in between two asymptotes hence a simple rudimental counter allows us to write a code capable to capture automatically any circular eigen-frequency also for very high modal order.

Once we get the actual eigen-value of interest we can compute both the trigonometric and hyperbolic exponential coefficient and get the associated normalised modal shape.

2.1.2. Torsional equation of motion

The steps to be followed are the same as for the flexural counterpart, hence we will report just the fundamental passages.

First of all introduce the modal decomposition for torsional vibrations.

$$\tilde{\vartheta}_d(\xi, \tau) = \sum_{m=1}^{\infty} \theta_m(\xi) \cdot \gamma_m(\tau) \quad \text{with } m \in \mathbb{N} \setminus \{0\};$$

$$\gamma_m(\tau) = \Gamma_m \cdot \exp(i \cdot \tilde{\omega}_{\vartheta,m} \cdot \tau) + \hat{\Gamma}_m \cdot \exp(-i \cdot \tilde{\omega}_{\vartheta,m} \cdot \tau) = \bar{\Gamma}_m \cdot \cos(\tilde{\omega}_{\vartheta,m} \cdot \tau + \varphi_{\vartheta,m});$$

Where the following parameters has been used.

$$\left\{ \begin{array}{l} \bar{\Gamma}_m = 2 \cdot \sqrt{(\Gamma_m^R)^2 + (\Gamma_m^I)^2} \\ \tan \varphi_{\vartheta, m} = \frac{\Gamma_m^I}{\Gamma_m^R} \end{array} \right. ;$$

$$\tilde{\omega}_{\vartheta, m} = \omega_{\vartheta, m} \cdot l \sqrt{\frac{(m_d + 2m_c)}{2H}} ;$$

Substitution in the linear component of the free torsional equation of motion leads to its modal format.

$$T(\xi, \tau) = \left\{ \begin{array}{l} \tilde{J}_t \cdot \frac{d^2 \tilde{\omega}_d}{dt^2} + \frac{\beta^2}{\chi^2} \cdot \tilde{\vartheta}_d{}^{iv} + \\ -(1 + \beta^2) \cdot \tilde{\vartheta}_d{}'' + \lambda_L^2 \tilde{h}_{\vartheta} \end{array} \right\} = \sum_{m=1}^{\infty} \left\{ \begin{array}{l} -\tilde{J}_t \cdot \tilde{\omega}_{\vartheta, m}^2 \cdot \Theta_m(\xi) + \frac{\beta^2}{\chi^2} \cdot \Theta_m{}^{iv}(\xi) + \\ -(1 + \beta^2) \Theta_m{}''(\xi) + \lambda_L^2 \int_0^1 \Theta_m(\xi) d\xi \end{array} \right\} \cdot \gamma_m(\tau) ;$$

$$T(\xi, \tau) = 0 \quad \forall(\xi, \tau, m) \Leftrightarrow T_m(\xi) = \left\{ \begin{array}{l} \frac{\beta^2}{\chi^2} \cdot \Theta_m{}^{iv}(\xi) + \\ -(1 + \beta^2) \Theta_m{}''(\xi) + \\ -\tilde{J}_t \cdot \tilde{\omega}_{\vartheta, m}^2 \cdot \Theta_m(\xi) + \\ + \lambda_L^2 \tilde{h}_{\vartheta, m} \end{array} \right\} = T_{m, o}(\xi) + \lambda_L^2 \tilde{h}_{\vartheta, m} = 0 \quad \forall(\xi, m) ;$$

i. Skew-symmetric modes:

The vanishing of the stiffening parameter allows us to define both the modal shapes and the corresponding circular eigen-frequencies.

$$\tilde{h}_{\vartheta, m} = 0 \quad \forall m \Rightarrow T_m(\xi) = \frac{\beta^2}{\chi^2} \cdot \Theta_m{}^{iv}(\xi) - (1 + \beta^2) \Theta_m{}''(\xi) - \tilde{J}_t \cdot \tilde{\omega}_{\vartheta, m}^2 \cdot \Theta_m(\xi) = 0 \quad \forall(\xi, m) ;$$

$$\Theta_m(\xi) = \sin(2m \cdot \pi \cdot \xi) ;$$

$$T_m(\xi) = \left\{ \frac{\beta^2}{\chi^2} \cdot (2m\pi)^4 + (1 + \beta^2) \cdot (2m\pi)^2 - \tilde{J}_t \cdot \tilde{\omega}_{\vartheta, m}^2 \right\} \cdot \sin(2m\pi \cdot \xi) ;$$

$$T_m(\xi) = 0 \quad \forall(\xi, m) \Leftrightarrow \frac{\beta^2}{\chi^2} \cdot (2m\pi)^4 + (1 + \beta^2) \cdot (2m\pi)^2 - \tilde{J}_t \cdot \tilde{\omega}_{\vartheta, m}^2 = 0 \quad \forall m ;$$

$$\Leftrightarrow \sqrt{\tilde{J}_t} \cdot \tilde{\omega}_{\vartheta, m} = 2m\pi \cdot \sqrt{1 + \beta^2 + \frac{\beta^2}{\chi^2} \cdot (2m\pi)^2} ;$$

The fact that the dimensionless torsional inertia is not on the right hand side is not casual but the reason of this choice will be clear in the following treatment.

Also for torsional skew-symmetric modes we can distinguish some fundamental situations.

$$\text{if } \beta^2 \ll \frac{1}{1 + \frac{(2m\pi)^2}{\chi^2}} \Rightarrow \sqrt{\tilde{J}_t} \cdot \tilde{\omega}_{\vartheta,m} = 2m\pi \quad (2 \text{ coupled taut strings});$$

$$\text{if } \beta^2 \gg \frac{1}{1 + \frac{(2m\pi)^2}{\chi^2}} \Rightarrow \sqrt{\tilde{J}_t} \cdot \tilde{\omega}_{\vartheta,m} = 2m\pi \cdot \sqrt{1 + \frac{(2m\pi)^2}{\chi^2}} \cdot \beta \quad (\text{tensioned beam});$$

Notice that the threshold for the ratio between the torsional stiffness given by the deck and that given by the cables is strongly influenced by the warping stiffness of the deck's section, being a parameter that can assume very different values.

$$\text{if } \chi^2 \gg \frac{(2m\pi)^2}{1 + \frac{1}{\beta^2}} \Rightarrow \sqrt{\tilde{J}_t} \cdot \tilde{\omega}_{\vartheta,m} = 2m\pi \cdot \sqrt{1 + \beta^2} \quad (\text{tensioned beam with closed box section});$$

$$\text{if } \chi^2 \ll \frac{(2m\pi)^2}{1 + \frac{1}{\beta^2}} \Rightarrow \sqrt{\tilde{J}_t} \cdot \tilde{\omega}_{\vartheta,m} = (2m\pi)^2 \cdot \frac{\beta}{\chi} \quad (\text{tensioned beam with thin open section});$$

ii. Symmetric modes:

Let's introduce the general expression for the complete solution composed by the particular integral and the homogeneous one.

$$\Theta_{m,p} = C_m \Rightarrow T_m(\xi) = 0 \quad \forall(\xi, m) \Leftrightarrow C_m = \frac{\lambda_L^2}{\tilde{J}_t \cdot \tilde{\omega}_{\vartheta,m}^2} \tilde{h}_{\Theta,m};$$

$$\Theta_{m,o}(\xi) = \sum_{i=1}^4 c_{m,i} \cdot \exp(\alpha_{m,i} \cdot \xi);$$

$$T_{m,o}(\xi) = \sum_{i=1}^4 c_{m,i} \cdot \left\{ \frac{\beta^2}{\chi^2} \cdot \alpha_{m,i}^4 - (1 + \beta^2) \cdot \alpha_{m,i}^2 - \tilde{J}_t \cdot \tilde{\omega}_{\vartheta,m}^2 \right\} \cdot \exp(\alpha_{m,i} \xi);$$

$$T_{m,o}(\xi) = 0 \quad \forall(\xi, i, m) \Leftrightarrow \left\{ \frac{\beta^2}{\chi^2} \cdot \alpha_{m,i}^4 - (1 + \beta^2) \cdot \alpha_{m,i}^2 - \tilde{J}_t \cdot \tilde{\omega}_{\vartheta,m}^2 \right\} = 0 \quad \forall(i, m);$$

$$\Leftrightarrow \alpha_{m,i}^2 = \frac{\chi^2}{2\beta^2} \left(1 + \beta^2 \pm \sqrt{(1 + \beta^2)^2 + 4 \frac{\beta^2}{\chi^2} \cdot \tilde{J}_t \cdot \tilde{\omega}_{\vartheta,m}^2} \right);$$

Define the trigonometric and hyperbolic exponential parameters.

$$\eta_{\vartheta,m}^2 = \frac{\chi^2}{2\beta^2} \left(\sqrt{(1 + \beta^2)^2 + 4 \frac{\beta^2}{\chi^2} \cdot \tilde{J}_t \cdot \tilde{\omega}_{\vartheta,m}^2} - (1 + \beta^2) \right);$$

$$\Psi_{\vartheta,m}^2 = \frac{\chi^2}{2\beta^2} \left(\sqrt{(1 + \beta^2)^2 + 4 \frac{\beta^2}{\chi^2} \cdot \tilde{J}_t \cdot \tilde{\omega}_{\vartheta,m}^2} + (1 + \beta^2) \right) = \eta_{\vartheta,m}^2 + \frac{\chi^2}{\beta^2} (1 + \beta^2);$$

$$\Theta_m(\xi) = \Theta_{m,p} + \Theta_{m,o}(\xi) = \left\{ \begin{array}{l} \frac{\lambda_L^2}{\tilde{J}_t \cdot \tilde{\omega}_{\vartheta,m}^2} \tilde{h}_{\vartheta,m} + \\ + c_{m,1} \cdot \exp(\Psi_{\vartheta,m} \xi) + c_{m,2} \cdot \exp(-\Psi_{\vartheta,m} \xi) + \\ + c_{m,3} \cdot \exp(i \cdot \eta_{\vartheta,m} \xi) + c_{m,4} \cdot \exp(-i \cdot \eta_{\vartheta,m} \xi) \end{array} \right\};$$

Hence enforcing proper boundary conditions for the fork support and by means of proper trigonometric relations we can get the expression for the eigen-modes.

$$b. c. (fork) \left\{ \begin{array}{l} \Theta_m(0) = \Theta_m(1) = 0 \quad (null \ torsion) \\ \Theta_m''(0) = \Theta_m''(1) = 0 \quad (free \ warping) \end{array} \right. \quad \forall m;$$

$$\left\{ \begin{array}{l} \Theta_m(0) = 0 \Leftrightarrow c_{m,1} + c_{m,2} + c_{m,3} + c_{m,4} + \frac{\lambda_L^2}{\tilde{J}_t \cdot \tilde{\omega}_{\vartheta,m}^2} \tilde{h}_{\vartheta,m} = 0 \\ \Theta_m''(0) = 0 \Leftrightarrow (c_{m,1} + c_{m,2}) \cdot \Psi_{\vartheta,m}^2 - (c_{m,3} + c_{m,4}) \cdot \eta_{\vartheta,m}^2 = 0 \end{array} \right. ;$$

$$\Rightarrow c_{m,3} = - \left(c_{m,4} + \frac{\Psi_{\vartheta,m}^2}{\Psi_{\vartheta,m}^2 + \eta_{\vartheta,m}^2} \cdot \frac{\lambda_L^2}{\tilde{J}_t \cdot \tilde{\omega}_{\vartheta,m}^2} \tilde{h}_{\vartheta,m} \right);$$

$$\left\{ \begin{array}{l} \Theta_m(1) = 0 \Leftrightarrow c_{m,1} \cdot e^{\Psi_{\vartheta,m}} + c_{m,2} \cdot e^{-\Psi_{\vartheta,m}} + c_{m,3} \cdot e^{i \cdot \eta_{\vartheta,m}} + c_{m,4} \cdot e^{-i \cdot \eta_{\vartheta,m}} + \frac{\lambda_L^2}{\tilde{J}_t \cdot \tilde{\omega}_{\vartheta,m}^2} \tilde{h}_{\vartheta,m} = 0 \\ \Theta_m''(1) = 0 \Leftrightarrow (c_{m,1} \cdot e^{\Psi_{\vartheta,m}} + c_{m,2} \cdot e^{-\Psi_{\vartheta,m}}) \cdot \Psi_{\vartheta,m}^2 - (c_{m,3} \cdot e^{i \cdot \eta_{\vartheta,m}} + c_{m,4} \cdot e^{-i \cdot \eta_{\vartheta,m}}) \cdot \eta_{\vartheta,m}^2 = 0 \end{array} \right. ;$$

$$\Rightarrow c_{m,3} = - \left(c_{m,4} + \frac{\Psi_{\vartheta,m}^2}{\Psi_{\vartheta,m}^2 + \eta_{\vartheta,m}^2} \cdot e^{-i \cdot \eta_{\vartheta,m}} \cdot \frac{\lambda_L^2}{\tilde{J}_t \cdot \tilde{\omega}_{\vartheta,m}^2} \tilde{h}_{\vartheta,m} \right);$$

Find the constant coefficients.

$$c_{m,4} = \frac{\lambda_L^2}{\tilde{J}_t \cdot \tilde{\omega}_{\vartheta,m}^2} \tilde{h}_{\vartheta,m} \cdot \frac{\Psi_{\vartheta,m}^2}{\Psi_{\vartheta,m}^2 + \eta_{\vartheta,m}^2} \cdot \frac{1 - e^{i \cdot \eta_{\vartheta,m}}}{e^{i \cdot \eta_{\vartheta,m}} - e^{-i \cdot \eta_{\vartheta,m}}};$$

$$c_{m,3} = - \frac{\lambda_L^2}{\tilde{J}_t \cdot \tilde{\omega}_{\vartheta,m}^2} \tilde{h}_{\vartheta,m} \cdot \frac{\Psi_{\vartheta,m}^2}{\Psi_{\vartheta,m}^2 + \eta_{\vartheta,m}^2} \cdot \frac{1 - e^{i \cdot \eta_{\vartheta,m}}}{e^{i \cdot \eta_{\vartheta,m}} - e^{-i \cdot \eta_{\vartheta,m}}};$$

$$c_{m,2} = \frac{\lambda_L^2}{\tilde{J}_t \cdot \tilde{\omega}_{\vartheta,m}^2} \tilde{h}_{\vartheta,m} \cdot \frac{\eta_{\vartheta,m}^2}{\Psi_{\vartheta,m}^2 + \eta_{\vartheta,m}^2} \cdot \frac{1 - e^{\Psi_{\vartheta,m}}}{e^{\Psi_{\vartheta,m}} - e^{-\Psi_{\vartheta,m}}};$$

$$c_{m,1} = - \frac{\lambda_L^2}{\tilde{J}_t \cdot \tilde{\omega}_{\vartheta,m}^2} \tilde{h}_{\vartheta,m} \cdot \frac{\eta_{\vartheta,m}^2}{\Psi_{\vartheta,m}^2 + \eta_{\vartheta,m}^2} \cdot \frac{1 - e^{\Psi_{\vartheta,m}}}{e^{\Psi_{\vartheta,m}} - e^{-\Psi_{\vartheta,m}}};$$

Exploiting some trigonometric relations.

$$\Theta_m(\xi) = \frac{\lambda_L^2}{\tilde{J}_t \cdot \tilde{\omega}_{\vartheta,m}^2} \tilde{h}_{\vartheta,m} \cdot \left\{ 1 - \frac{1}{\Psi_{\vartheta,m}^2 + \eta_{\vartheta,m}^2} \cdot \left(\eta_{\vartheta,m}^2 \cdot \frac{e^{\Psi_{\vartheta,m} \cdot \xi} - e^{\Psi_{\vartheta,m} \cdot (\xi-1)} + e^{-\Psi_{\vartheta,m} \cdot \xi} - e^{-\Psi_{\vartheta,m} \cdot (\xi-1)}}{e^{\Psi_{\vartheta,m}} - e^{-\Psi_{\vartheta,m}}} + \right. \right. \\ \left. \left. + \Psi_{\vartheta,m}^2 \cdot \frac{e^{i \cdot \eta_{\vartheta,m} \cdot \xi} - e^{i \cdot \eta_{\vartheta,m} \cdot (\xi-1)} + e^{-i \cdot \eta_{\vartheta,m} \cdot \xi} - e^{-i \cdot \eta_{\vartheta,m} \cdot (\xi-1)}}{e^{\eta_{\vartheta,m}} - e^{-\eta_{\vartheta,m}}} \right) \right\};$$

$$\Theta_m(\xi) = \frac{\lambda_L^2}{\tilde{J}_t \cdot \tilde{\omega}_{\vartheta,m}^2} \tilde{h}_{\vartheta,m} \cdot \left\{ 1 - \frac{1}{\Psi_{\vartheta,m}^2 + \eta_{\vartheta,m}^2} \cdot \left(\eta_{\vartheta,m}^2 \cdot \frac{\sinh(\Psi_{\vartheta,m} \cdot \xi) - \sinh(\Psi_{\vartheta,m} \cdot (\xi-1))}{\sinh(\Psi_{\vartheta,m})} + \right. \right. \\ \left. \left. + \Psi_{\vartheta,m}^2 \cdot \frac{\sin(\eta_{\vartheta,m} \cdot \xi) - \sin(\eta_{\vartheta,m} \cdot (\xi-1))}{\sin(\eta_{\vartheta,m})} \right) \right\};$$

$$\Theta_m(\xi) = \frac{\lambda_L^2}{\tilde{J}_t \cdot \tilde{\omega}_{\vartheta,m}^2} \tilde{h}_{\vartheta,m} \cdot \left\{ 1 - \frac{1}{\Psi_{\vartheta,m}^2 + \eta_{\vartheta,m}^2} \cdot \left(\eta_{\vartheta,m}^2 \cdot \frac{\cosh(\Psi_{\vartheta,m} \cdot (\xi - \frac{1}{2}))}{\cosh(\frac{\Psi_{\vartheta,m}}{2})} + \Psi_{\vartheta,m}^2 \cdot \frac{\cos(\eta_{\vartheta,m} \cdot (\xi - \frac{1}{2}))}{\cos(\frac{\eta_{\vartheta,m}}{2})} \right) \right\};$$

Hence enforcing the definition of the stiffening term we get the eigen-function for circular torsional frequencies.

$$\tilde{h}_{\vartheta,m} = \int_0^1 \Theta_m(\xi) d\xi = \frac{\lambda_L^2}{\tilde{J}_t \cdot \tilde{\omega}_{\vartheta,m}^2} \tilde{h}_{\vartheta,m} \cdot \int_0^1 \left\{ 1 - \frac{1}{\Psi_{\vartheta,m}^2 + \eta_{\vartheta,m}^2} \cdot \left(\eta_{\vartheta,m}^2 \cdot \frac{\cosh(\Psi_{\vartheta,m} \cdot (\xi - \frac{1}{2}))}{\cosh(\frac{\Psi_{\vartheta,m}}{2})} + \right. \right. \\ \left. \left. + \Psi_{\vartheta,m}^2 \cdot \frac{\cos(\eta_{\vartheta,m} \cdot (\xi - \frac{1}{2}))}{\cos(\frac{\eta_{\vartheta,m}}{2})} \right) \right\} d\xi;$$

$$\frac{\tilde{J}_t \cdot \tilde{\omega}_{\vartheta,m}^2}{\lambda_L^2} = 1 - \frac{1}{\Psi_{\vartheta,m}^2 + \eta_{\vartheta,m}^2} \cdot \left(\eta_{\vartheta,m}^2 \cdot \frac{\tanh(\frac{\Psi_{\vartheta,m}}{2})}{\frac{\Psi_{\vartheta,m}}{2}} + \Psi_{\vartheta,m}^2 \cdot \frac{\tan(\frac{\eta_{\vartheta,m}}{2})}{\frac{\eta_{\vartheta,m}}{2}} \right);$$

It's now evident that the solution of the eigen-function can be found taking as unknown the dimensionless torsional inertia and circular frequency together. In fact both the trigonometric and the hyperbolic exponential coefficients depends on that product.

This trick allows us to define the eigen-values and vectors of the problem without necessary specify the torsional inertia of the structural system that in general could be not so easily found in literature.

2.2. Parametric analysis

Once the general solutions have been defined both for the flexural and the torsional equation of motion, could be interesting to analyse some special cases. In fact, considering extreme values for the fundamental parameters entering in the equation of motion, we can get in some cases simpler solution than in the general situation and then we will use those results to validate and bound the latter.

2.2.1. Flexural modes

Let's start to analyse the parametric influence of the so called Irvine parameter and of the deck to cable flexural stiffness on the flexural vibrations.

First of all it's useful to recall their definitions.

$$\lambda_L^2 = \frac{E_c A_c}{H} \frac{l}{L_c} (y'' l)^2 \quad \text{and} \quad \mu^2 = \frac{E_d I_d}{2 H l^2};$$

i. Flat cable:

As far as the initial tension in the cable grows the cable's stretch increases too, hence its curvature reduces as its effective curvilinear length tends to reach the rectilinear distance between pylons.

In the extreme situation the initial tension would be so high that prevent the cable to have any curvature and behaves like a taut string.

$$\lim_{H \rightarrow \infty} \lambda_L^2 = 0 \Rightarrow \lim_{H \rightarrow \infty} F_n(\xi) = \mu^2 \cdot W_n''''(\xi) - W_n''(\xi) - \tilde{\omega}_{w,n}^2 \cdot W_n(\xi);$$

$$F_n(\xi) = 0 \quad \forall(\xi, n) \Leftrightarrow \mu^2 \cdot W_n''''(\xi) - W_n''(\xi) - \tilde{\omega}_{w,n}^2 \cdot W_n(\xi) = 0 \quad \forall(\xi, n);$$

It's evident that the equation of motion reduces to that of skew-symmetric modes. Hence the solution will be in the same format, with the exception that now we are considering symmetric modes and consequently the number of sinusoidal half-waves has to be odd and no more even.

$$W_n(\xi) = \sin((2n - 1) \cdot \pi \cdot \xi);$$

$$\tilde{\omega}_{w,n} = (2n - 1)\pi \cdot \sqrt{1 + \mu^2 \cdot ((2n - 1)\pi)^2};$$

Also in this special condition there are two special situations.

$$\text{if } \mu^2 \ll \frac{1}{((2n-1)\pi)^2} \Rightarrow \tilde{\omega}_{w,n} = (2n - 1)\pi \quad (\text{taut string});$$

$$\text{if } \mu^2 \gg \frac{1}{((2n-1)\pi)^2} \Rightarrow \tilde{\omega}_{w,n} = ((2n - 1)\pi)^2 \cdot \mu \quad (\text{tensioned beam});$$

ii. Inextensible cable:

The inverse situation happens when the axial stiffness of the cable is so high with respect to the initial tension that it can be assumed to be inextensible. This kind of assumption is a classical one that is generally assumed for preliminary analysis of cables with large diameter.

$$\lim_{E_c A_c \rightarrow \infty} \lambda_L^2 = \infty \Rightarrow \lim_{E_c A_c \rightarrow \infty} F_n(\xi) = \mu^2 \cdot W_n{}^{iv}(\xi) - W_n''(\xi) - \tilde{\omega}_{w,n}^2 \cdot W_n(\xi) + \lambda_L^2 \cdot \tilde{h}_{W,n};$$

Since the equation of motion doesn't change then the expression for the eigen-modes remains the same as for the general case, in fact would be normalised with respect the Irvine parameter.

$$W_n(\xi) = \frac{\lambda_L^2}{\tilde{\omega}_{w,n}^2} \tilde{h}_{W,n} \cdot \left\{ 1 - \frac{1}{\Psi_{w,n}^2 + \eta_{w,n}^2} \cdot \left(\eta_{w,n}^2 \cdot \frac{\cosh\left(\Psi_{w,n}\left(\xi - \frac{1}{2}\right)\right)}{\cosh\left(\frac{\Psi_{w,n}}{2}\right)} + \Psi_{w,n}^2 \cdot \frac{\cos\left(\eta_{w,n}\left(\xi - \frac{1}{2}\right)\right)}{\cos\left(\frac{\eta_{w,n}}{2}\right)} \right) \right\};$$

On the other hand the same parameter affect those modal shapes indirectly by means of the circular eigen-frequency, due to the fact that the eigen-function changes as follows.

$$\lim_{E_c A_c \rightarrow \infty} \frac{\tilde{\omega}_{w,n}^2}{\lambda_L^2} = 0 \Rightarrow 1 - \frac{1}{\Psi_{w,n}^2 + \eta_{w,n}^2} \cdot \left(\eta_{w,n}^2 \cdot \frac{\tanh\left(\frac{\Psi_{w,n}}{2}\right)}{\frac{\Psi_{w,n}}{2}} + \Psi_{w,n}^2 \cdot \frac{\tan\left(\frac{\eta_{w,n}}{2}\right)}{\frac{\eta_{w,n}}{2}} \right) = 0;$$

Further, substituting the expression relating the hyperbolic exponential parameter to the trigonometric one, after some passage we can get the following expression proposed by [5].

$$\Psi_{w,n}^2 = \eta_{w,n}^2 + \frac{1}{\mu^2} \Rightarrow \tilde{\omega}_{w,n}^2 = \frac{1}{2\mu^2} \left\{ (1 + 2\mu^2 \eta_{w,n}^2)^2 - 1 \right\};$$

iii. Flexible deck:

This situation wants to make evident that hidden in the model there is also the elastic suspension cable formulation. In fact once the deck is assumed to have a negligible flexural stiffness with respect to the cable's one, external loads are mainly sustained just by the cables system.

In the limit case the deck loose completely its flexural stiffness and hence cannot behave like an equivalent cable since in the formulation of the model we assume that it has not axially fixed ends.

$$\lim_{E_d I_d \rightarrow 0} \mu^2 = 0 \Rightarrow \lim_{E_d I_d \rightarrow 0} F_n(\xi) = -W_n''(\xi) - \tilde{\omega}_{w,n}^2 \cdot W_n(\xi) + \lambda_L^2 \cdot \tilde{h}_{W,n} = F_{n,0}(\xi) + \lambda_L^2 \cdot \tilde{h}_{W,n};$$

Since the equation of motion changes drastically it's better to follow all the passages.

$$W_{n,p} = C_n \Rightarrow F_n(\xi) = 0 \quad \forall(\xi, n) \Leftrightarrow C_n = \frac{\lambda_L^2}{\tilde{\omega}_{w,n}^2} \tilde{h}_{W,n};$$

It's important to notice that in this particular situation has no sense to enforce free curvature at the two end of the bridge. In fact we are dealing with a suspension cable system that by hypothesis has null flexural sectional stiffness. Hence the free curvature condition is automatically satisfied by the modal shape. As direct consequence in the homogeneous integral we need no more four terms but only two.

$$W_{n,o}(\xi) = \sum_{i=1}^2 c_{n,i} \cdot \exp(\alpha_{n,i} \cdot \xi)$$

$$F_{n,o}(\xi) = \sum_{i=1}^2 c_{n,i} \cdot \{-\alpha_{n,i}^2 - \tilde{\omega}_{w,n}^2\} \cdot \exp(\alpha_{n,i} \xi);$$

Hence we can enforce.

$$F_{n,o}(\xi) = 0 \quad \forall(\xi, i, n) \Leftrightarrow \{-\alpha_{n,i}^2 - \tilde{\omega}_{w,n}^2\} = 0 \quad \forall(i, n) \Leftrightarrow \alpha_{n,i} = \pm i \cdot \tilde{\omega}_{w,n};$$

It's evident that the contribution of the hyperbolic exponential term vanishes, hence the modal shapes will be characterised by a trigonometric function.

$$\lim_{\mu^2 \rightarrow 0} \eta_{w,n}^2 = \lim_{\mu^2 \rightarrow 0} \frac{1}{2\mu^2} \left(\sqrt{1 + 4\mu^2 \cdot \tilde{\omega}_{w,n}^2} - 1 \right) = \tilde{\omega}_{w,n}^2;$$

$$\lim_{\mu^2 \rightarrow 0} \Psi_{w,n}^2 = \lim_{\mu^2 \rightarrow 0} \frac{1}{2\mu^2} \left(\sqrt{1 + 4\mu^2 \cdot \tilde{\omega}_{w,n}^2} + 1 \right) = \lim_{\mu^2 \rightarrow 0} \frac{1}{\mu^2} = \infty;$$

The complete solution becomes.

$$W_n(\xi) = W_{n,p} + W_{n,o}(\xi) = \frac{\lambda_L^2}{\tilde{\omega}_{w,n}^2} \tilde{h}_{W,n} + c_{n,1} \cdot \exp(i \cdot \eta_{w,n} \xi) + c_{n,2} \cdot \exp(-i \cdot \eta_{w,n} \xi);$$

Enforcing the following boundary conditions.

$$b. c. \begin{cases} W_n(0) = 0 \\ W_n(1) = 0 \end{cases} \quad \forall n \Rightarrow \begin{cases} W_n(0) = 0 \Leftrightarrow c_{n,1} + c_{n,2} + \frac{\lambda_L^2}{\tilde{\omega}_{w,n}^2} \tilde{h}_{W,n} = 0 \\ W_n(1) = 0 \Leftrightarrow c_{n,1} \cdot e^{i\eta_{w,n}} + c_{n,2} \cdot e^{-i\eta_{w,n}} + \frac{\lambda_L^2}{\tilde{\omega}_{w,n}^2} \tilde{h}_{W,n} = 0 \end{cases};$$

Hence the constant parameters assume the following expression.

$$c_{n,2} = \frac{\lambda_L^2}{\tilde{\omega}_{w,n}^2} \tilde{h}_{W,n} \cdot \frac{1 - e^{i\eta_{w,n}}}{e^{i\eta_{w,n}} - e^{-i\eta_{w,n}}};$$

$$c_{n,1} = -\frac{\lambda_L^2}{\tilde{\omega}_{w,n}^2} \tilde{h}_{W,n} \cdot \frac{1 - e^{-i\eta_{w,n}}}{e^{i\eta_{w,n}} - e^{-i\eta_{w,n}}};$$

The substitution in the general solution leads to the following expression.

$$W_n(\xi) = \frac{\lambda_L^2}{\tilde{\omega}_{w,n}^2} \tilde{h}_{W,n} \cdot \left\{ 1 - \frac{e^{i\eta_{w,n} \cdot \xi} - e^{i\eta_{w,n} \cdot (\xi-1)} + e^{-i\eta_{w,n} \cdot \xi} - e^{-i\eta_{w,n} \cdot (\xi-1)}}{e^{i\eta_{w,n}} - e^{-i\eta_{w,n}}} \right\};$$

The usual trigonometric relations allow us to reformulate the solution in a more compact form.

$$W_n(\xi) = \frac{\lambda_L^2}{\tilde{\omega}_{w,n}^2} \tilde{h}_{W,n} \cdot \left\{ 1 - \frac{\sin(\eta_{w,n} \cdot \xi) - \sin(\eta_{w,n} \cdot (\xi-1))}{\sin(\eta_{w,n})} \right\} = \frac{\lambda_L^2}{\tilde{\omega}_{w,n}^2} \tilde{h}_{W,n} \cdot \left\{ 1 - \frac{\cos\left(\tilde{\omega}_{w,n} \cdot \left(\xi - \frac{1}{2}\right)\right)}{\cos\left(\frac{\tilde{\omega}_{w,n}}{2}\right)} \right\};$$

From the definition of the stiffening term we get the eigen-function of the problem.

$$\tilde{h}_{W,n} = \int_0^1 W_n(\xi) d\xi \Rightarrow \frac{\tilde{\omega}_{w,n}^2}{\lambda_L^2} = 1 - \frac{\tan\left(\frac{\tilde{\omega}_{w,n}}{2}\right)}{\frac{\tilde{\omega}_{w,n}}{2}};$$

iv. Rigid deck:

Let's consider the opposite case in which it's the deck the main stiffening structure for the flexural vibration of the suspension bridge.

$$\lim_{EdI_d \rightarrow \infty} \mu^2 = \infty \Rightarrow \lim_{EdI_d \rightarrow \infty} F_n(\xi) = \mu^2 \cdot W_n''(\xi) - W_n''(\xi) - \tilde{\omega}_{w,n}^2 \cdot W_n(\xi) + \lambda_L^2 \cdot \tilde{h}_{W,n};$$

As before since the equation of motion doesn't change its shape we expect the modal shape to be influenced by the actual condition indirectly by means of the circular eigen-frequency.

$$\text{if } \mu^2 \gg \frac{1}{4 \cdot \tilde{\omega}_{w,n}^2} \Rightarrow (\eta_{w,n}^2, \Psi_{w,n}^2) = \frac{\tilde{\omega}_{w,n}}{\mu} \Rightarrow \frac{(\eta_{w,n}^2, \Psi_{w,n}^2)}{\Psi_{w,n}^2 + \eta_{w,n}^2} = \frac{1}{2};$$

Hence we can find the following expression for the modal shapes and the eigen-function.

$$W_n(\xi) = \frac{\lambda_L^2}{\tilde{\omega}_{w,n}^2} \tilde{h}_{W,n} \cdot \left\{ 1 - \frac{1}{2} \cdot \left(\frac{\cosh\left(\sqrt{\frac{\tilde{\omega}_{w,n}}{\mu}} \cdot \left(\xi - \frac{1}{2}\right)\right)}{\cosh\left(\frac{1}{2} \sqrt{\frac{\tilde{\omega}_{w,n}}{\mu}}\right)} + \frac{\cos\left(\sqrt{\frac{\tilde{\omega}_{w,n}}{\mu}} \cdot \left(\xi - \frac{1}{2}\right)\right)}{\cos\left(\frac{1}{2} \sqrt{\frac{\tilde{\omega}_{w,n}}{\mu}}\right)} \right) \right\};$$

$$\tilde{h}_{W,n} = \int_0^1 W_n(\xi) d\xi \Rightarrow \frac{\tilde{\omega}_{w,n}^2}{\lambda_L^2} = 1 - \frac{1}{2} \cdot \left(\frac{\tanh\left(\frac{1}{2} \sqrt{\frac{\tilde{\omega}_{w,n}}{\mu}}\right)}{\frac{1}{2} \sqrt{\frac{\tilde{\omega}_{w,n}}{\mu}}} + \frac{\tan\left(\frac{1}{2} \sqrt{\frac{\tilde{\omega}_{w,n}}{\mu}}\right)}{\frac{1}{2} \sqrt{\frac{\tilde{\omega}_{w,n}}{\mu}}} \right);$$

Let's now try to combine those particular conditions in order to find the limiting cases.

v. Flat cable & Flexible deck:

$$\lim_{H \rightarrow \infty} \lambda_L^2 = 0 \text{ and } \lim_{EdI_d \rightarrow 0} \mu^2 = 0 \Rightarrow \lim_{H \rightarrow \infty} \lim_{EdI_d \rightarrow 0} F_n(\xi) = -W_n''(\xi) - \tilde{\omega}_{w,n}^2 \cdot W_n(\xi);$$

$$F_n(\xi) = 0 \quad \forall(\xi, n) \Leftrightarrow -W_n''(\xi) - \tilde{\omega}_{w,n}^2 \cdot W_n(\xi) = 0 \quad \forall(\xi, n);$$

Hence we get the same sinusoidal modal shape obtained by the only flat cable condition and a slightly different circular eigen-frequency.

$$W_n(\xi) = \sin((2n - 1) \cdot \pi \cdot \xi);$$

$$\tilde{\omega}_{w,n} = (2n - 1)\pi;$$

Notice that this case has been already analysed for the flat cable limit condition. Hence the condition on the deck to cable flexural stiffness parameter can be smoother.

$$\text{from } \lim_{E_d I_d \rightarrow 0} \mu^2 = 0 \Rightarrow \text{to } \mu^2 \ll \frac{1}{((2n-1)\pi)^2};$$

vi. Flat cable & Rigid deck:

$$\lim_{H \rightarrow \infty} \lambda_L^2 = 0 \text{ and } \lim_{E_d I_d \rightarrow \infty} \mu^2 = \infty \Rightarrow \lim_{H \rightarrow \infty} F_n(\xi) = \mu^2 W_n''(\xi) - W_n''(\xi) - \tilde{\omega}_{w,n}^2 \cdot W_n(\xi);$$

$$E_d I_d \rightarrow \infty$$

$$F_n(\xi) = 0 \quad \forall(\xi, n) \Leftrightarrow \mu^2 W_n''(\xi) - W_n''(\xi) - \tilde{\omega}_{w,n}^2 \cdot W_n(\xi) = 0 \quad \forall(\xi, n);$$

Hence we get the same condition already seen for the flat cable condition.

$$W_n(\xi) = \sin((2n-1) \cdot \pi \cdot \xi);$$

$$\tilde{\omega}_{w,n} = ((2n-1)\pi)^2 \cdot \mu;$$

So the sufficient condition for flexural stiffness becomes as follows.

$$\text{from } \lim_{E_d I_d \rightarrow \infty} \mu^2 = \infty \Rightarrow \text{to } \mu^2 \gg \frac{1}{((2n-1)\pi)^2};$$

vii. Inextensible cable & Flexible deck:

$$\lim_{E_c A_c \rightarrow \infty} \lambda_L^2 = 0 \text{ and } \lim_{E_d I_d \rightarrow 0} \mu^2 = 0 \Rightarrow \lim_{E_c A_c \rightarrow \infty} F_n(\xi) = -W_n''(\xi) - \tilde{\omega}_{w,n}^2 \cdot W_n(\xi) + \lambda_L^2 \cdot \tilde{h}_{W,n};$$

$$E_d I_d \rightarrow 0$$

$$F_n(\xi) = 0 \quad \forall(\xi, n) \Leftrightarrow -W_n''(\xi) - \tilde{\omega}_{w,n}^2 \cdot W_n(\xi) + \lambda_L^2 \cdot \tilde{h}_{W,n} = 0 \quad \forall(\xi, n);$$

Hence obtain eigen-modes that are identical to that found for the flexible deck limit condition and eigen-functions similar to the case of inextensible cables.

$$W_n(\xi) = \frac{\lambda_L^2}{\tilde{\omega}_{w,n}^2} \tilde{h}_{W,n} \cdot \left\{ 1 - \frac{\cos(\tilde{\omega}_{w,n}(\xi - \frac{1}{2}))}{\cos(\frac{\tilde{\omega}_{w,n}}{2})} \right\};$$

$$\tilde{h}_{W,n} = \int_0^1 W_n(\xi) d\xi \Rightarrow \lim_{E_c A_c \rightarrow \infty} \frac{\tilde{\omega}_{w,n}^2}{\lambda_L^2} = 0 \Rightarrow 1 - \frac{\tan(\frac{\tilde{\omega}_{w,n}}{2})}{\frac{\tilde{\omega}_{w,n}}{2}} = 0;$$

viii. Inextensible cable & Rigid deck:

$$\lim_{E_c A_c \rightarrow \infty} \lambda_L^2 = 0 \quad \text{and} \quad \lim_{E_d I_d \rightarrow \infty} \mu^2 = \infty \Rightarrow \lim_{E_c A_c \rightarrow \infty} F_n(\xi) = \left\{ \begin{array}{l} \mu^2 W_n''(\xi) - W_n''(\xi) + \\ -\tilde{\omega}_{w,n}^2 \cdot W_n(\xi) + \lambda_L^2 \cdot \tilde{h}_{W,n} \end{array} \right\};$$

$$F_n(\xi) = 0 \quad \forall(\xi, n) \Leftrightarrow \mu^2 W_n''(\xi) - W_n''(\xi) - \tilde{\omega}_{w,n}^2 \cdot W_n(\xi) + \lambda_L^2 \cdot \tilde{h}_{W,n} = 0 \quad \forall(\xi, n);$$

Once again since the equation of motion is unchanged with respect to the general situation, we expect a slight modification of both the modal shape with respect to the general case and of the expression for the eigen-function that takes some feature of the rigid deck condition.

$$\text{if } \mu^2 \gg \frac{1}{4 \cdot \tilde{\omega}_{w,n}^2} \Rightarrow (\eta_{w,n}^2, \Psi_{w,n}^2) = \frac{\tilde{\omega}_{w,n}}{\mu} \Rightarrow \frac{(\eta_{w,n}^2, \Psi_{w,n}^2)}{\Psi_{w,n}^2 + \eta_{w,n}^2} = \frac{1}{2};$$

$$W_n(\xi) = \frac{\lambda_L^2}{\tilde{\omega}_{w,n}^2} \tilde{h}_{W,n} \cdot \left\{ 1 - \frac{1}{2} \cdot \left(\frac{\cosh\left(\sqrt{\frac{\tilde{\omega}_{w,n}}{\mu}} \left(\xi - \frac{1}{2}\right)\right)}{\cosh\left(\frac{1}{2} \sqrt{\frac{\tilde{\omega}_{w,n}}{\mu}}\right)} + \frac{\cos\left(\sqrt{\frac{\tilde{\omega}_{w,n}}{\mu}} \left(\xi - \frac{1}{2}\right)\right)}{\cos\left(\frac{1}{2} \sqrt{\frac{\tilde{\omega}_{w,n}}{\mu}}\right)} \right) \right\};$$

$$\tilde{h}_{W,n} = \int_0^1 W_n(\xi) d\xi \Rightarrow \lim_{E_c A_c \rightarrow \infty} \frac{\tilde{\omega}_{w,n}^2}{\lambda_L^2} = 0 \Rightarrow 1 - \frac{1}{2} \cdot \left(\frac{\tanh\left(\frac{1}{2} \sqrt{\frac{\tilde{\omega}_{w,n}}{\mu}}\right)}{\frac{1}{2} \sqrt{\frac{\tilde{\omega}_{w,n}}{\mu}}} + \frac{\tan\left(\frac{1}{2} \sqrt{\frac{\tilde{\omega}_{w,n}}{\mu}}\right)}{\frac{1}{2} \sqrt{\frac{\tilde{\omega}_{w,n}}{\mu}}} \right) = 0;$$

An important conclusion of this first parametric analysis is that the Irvine parameter strongly influences both the modal shapes and the circular frequencies only in the special case of flat cables, while the deck to cable flexural stiffness parameter plays just a secondary role tuning the structural frequencies. In all the other extreme situations the Irvine parameter cannot influence directly the modal shapes, but indirectly since it can strongly influence the expression for eigen-functions. The flexural stiffness parameter now plays an important role in the definition of the modal shapes mainly by its direct effect on the eigen-modes expression adding or not the hyperbolic contribution.

2.2.2. Torsional modes

Regarding the torsional modes the fundamental parameters to be taken in account are the Irvine and the deck to cables torsional stiffness parameters, with the deck warping coefficient.

$$\lambda_L^2 = \frac{E_c A_c}{H} \frac{l}{L_c} (y''l)^2 \quad \text{and} \quad \beta^2 = \frac{G_d I_d}{2Hb^2} \quad \text{and} \quad \chi^2;$$

i. Flat cable:

As for flexural modes, if the cable tension grows very much at limit condition can lead the cable's curvature to vanish.

$$\lim_{H \rightarrow \infty} \lambda_L^2 = 0 \Rightarrow \lim_{H \rightarrow \infty} T_m(\xi) = \frac{\beta^2}{\chi^2} \cdot \Theta_m''(\xi) - (1 + \beta^2) \Theta_m''(\xi) - \tilde{J}_t \cdot \tilde{\omega}_{\vartheta,m}^2 \cdot \Theta_m(\xi);$$

$$T_m(\xi) = 0 \quad \forall(\xi, m) \Leftrightarrow \frac{\beta^2}{\chi^2} \cdot \Theta_m''(\xi) - (1 + \beta^2) \Theta_m''(\xi) - \tilde{J}_t \cdot \tilde{\omega}_{\vartheta,m}^2 \cdot \Theta_m(\xi) = 0 \quad \forall(\xi, m);$$

Both the equation of motion and the eigen-solutions reduces to that of skew-symmetric modes, with the exception that now the number of sinusoidal half-waves has to be odd.

$$\Theta_m(\xi) = \sin((2m - 1) \cdot \pi \cdot \xi) ;$$

$$\sqrt{\tilde{J}_t} \cdot \tilde{\omega}_{\vartheta,m} = (2m - 1)\pi \cdot \sqrt{1 + \beta^2 + \frac{\beta^2}{\chi^2} \cdot ((2m - 1)\pi)^2} ;$$

The associated special situations are as follows.

$$\text{if } \beta^2 \ll \frac{1}{1 + \frac{((2m-1)\pi)^2}{\chi^2}} \Rightarrow \sqrt{\tilde{J}_t} \cdot \tilde{\omega}_{\vartheta,m} = (2m - 1)\pi \quad (2 \text{ coupled taut strings}) ;$$

$$\text{if } \beta^2 \gg \frac{1}{1 + \frac{((2m-1)\pi)^2}{\chi^2}} \Rightarrow \sqrt{\tilde{J}_t} \cdot \tilde{\omega}_{\vartheta,m} = (2m - 1)\pi \cdot \sqrt{1 + \frac{((2m-1)\pi)^2}{\chi^2} \cdot \beta} \quad (\text{tensioned beam}) ;$$

$$\text{if } \chi^2 \gg \frac{((2m-1)\pi)^2}{1 + \frac{1}{\beta^2}} \Rightarrow \sqrt{\tilde{J}_t} \cdot \tilde{\omega}_{\vartheta,m} = (2m - 1)\pi \cdot \sqrt{1 + \beta^2} \quad (\text{tensioned beam with closed box section}) ;$$

$$\text{if } \chi^2 \ll \frac{((2m-1)\pi)^2}{1 + \frac{1}{\beta^2}} \Rightarrow \sqrt{\tilde{J}_t} \cdot \tilde{\omega}_{\vartheta,m} = ((2m - 1)\pi)^2 \cdot \frac{\beta}{\chi} \quad (\text{tensioned beam with thin open section}) ;$$

ii. Inextensible cable:

The inverse situation happens when the cable can be assumed to be inextensible.

$$\lim_{E_c A_c \rightarrow \infty} \lambda_L^2 = \infty \Rightarrow \lim_{E_c A_c \rightarrow \infty} T_m(\xi) = \frac{\beta^2}{\chi^2} \cdot \Theta_m{}''''(\xi) - (1 + \beta^2)\Theta_m''(\xi) - \tilde{J}_t \cdot \tilde{\omega}_{\vartheta,m}^2 \cdot \Theta_m(\xi) + \lambda_L^2 \cdot \tilde{h}_{\vartheta,m} ;$$

The expression for the eigen-modes remains the same as for the general case, in fact would be normalised with respect the Irvine parameter.

$$\Theta_m(\xi) = \frac{\lambda_L^2}{\tilde{J}_t \cdot \tilde{\omega}_{\vartheta,m}^2} \tilde{h}_{\vartheta,m} \cdot \left\{ 1 - \frac{1}{\Psi_{\vartheta,m}^2 + \eta_{\vartheta,m}^2} \cdot \left(\eta_{\vartheta,m}^2 \cdot \frac{\cosh(\Psi_{\vartheta,m} \cdot (\xi - \frac{1}{2}))}{\cosh(\frac{\Psi_{\vartheta,m}}{2})} + \Psi_{\vartheta,m}^2 \cdot \frac{\cos(\eta_{\vartheta,m} \cdot (\xi - \frac{1}{2}))}{\cos(\frac{\eta_{\vartheta,m}}{2})} \right) \right\} ;$$

On the other hand the eigen-function changes as follows.

$$\lim_{E_c A_c \rightarrow \infty} \frac{\tilde{J}_t \cdot \tilde{\omega}_{\vartheta,m}^2}{\lambda_L^2} = 0 \Rightarrow 1 - \frac{1}{\Psi_{\vartheta,m}^2 + \eta_{\vartheta,m}^2} \cdot \left(\eta_{\vartheta,m}^2 \cdot \frac{\tanh(\frac{\Psi_{\vartheta,m}}{2})}{\frac{\Psi_{\vartheta,m}}{2}} + \Psi_{\vartheta,m}^2 \cdot \frac{\tan(\frac{\eta_{\vartheta,m}}{2})}{\frac{\eta_{\vartheta,m}}{2}} \right) = 0 ;$$

Further, substituting the expression relating the hyperbolic exponential parameter to the trigonometric one, by analogy with the expression previously found for flexural modes in the inextensible condition we get the following expression.

$$\Psi_{\vartheta,m}^2 = \eta_{\vartheta,m}^2 + \frac{\chi^2}{\beta^2} (1 + \beta^2) \Rightarrow \tilde{J}_t \cdot \tilde{\omega}_{\vartheta,m}^2 = \frac{\chi^2}{2\beta^2} \left\{ \left((1 + \beta^2)^2 + 2 \frac{\beta^2}{\chi^2} \cdot \eta_{\vartheta,m}^2 \right)^2 - 1 \right\};$$

iii. Free warping deck:

As previously mentioned this is the usual condition for modern suspension bridges, characterised by thin walled box girders for which the secondary torsional stiffness given by the Vlasov-Wagner theory is negligible with respect to the primary contribution from the de S. Venant theory.

$$\text{if } \chi^2 \rightarrow \infty \Rightarrow \lim_{\chi^2 \rightarrow \infty} T_m(\xi) = -(1 + \beta^2) \theta_m''(\xi) - \tilde{J}_t \cdot \tilde{\omega}_{\vartheta,m}^2 \cdot \theta_m(\xi) + \lambda_L^2 \cdot \tilde{h}_{\theta,m};$$

In reality the most proper condition would be the one that takes in consideration also the value reached by the deck to cables torsional stiffness parameter. Hence this relative condition will be in the following form and avoid to fall into mathematical indeterminate conditions of the kind infinite over infinite.

$$\text{from } \chi^2 \rightarrow \infty \Rightarrow \text{to } \frac{\chi^2}{\beta^2} \rightarrow \infty;$$

This means that if we are dealing with a closed box girder is not possible to neglect the torsional stiffness contribution given by the cable system with respect to the primary torsional stiffness of the deck.

The modifications of the equation of motion are similar to the ones of flexural modes under the flexible deck condition. In fact disappear the term related to the fourth order derivative that grant the presence of the hyperbolic contribution both to the modal shapes and to the eigen-functions, that consequently changes as follows.

Starting from the particular and homogeneous solution we get.

$$\theta_{m,p} = C_m \Rightarrow T_m(\xi) = 0 \quad \forall(\xi, m) \Leftrightarrow C_m = \frac{\lambda_L^2}{\tilde{J}_t \cdot \tilde{\omega}_{\vartheta,m}^2} \tilde{h}_{\theta,m};$$

$$\theta_{m,o}(\xi) = \sum_{i=1}^2 c_{m,i} \cdot \exp(\alpha_{m,i} \cdot \xi);$$

$$T_{m,o}(\xi) = \sum_{i=1}^2 c_{m,i} \cdot \left\{ -(1 + \beta^2) \alpha_{m,i}^2 - \tilde{J}_t \cdot \tilde{\omega}_{\vartheta,m}^2 \right\} \cdot \exp(\alpha_{m,i} \xi);$$

$$T_{m,o}(\xi) = 0 \quad \forall(\xi, i, m) \Leftrightarrow \left\{ -(1 + \beta^2) \alpha_{m,i}^2 - \tilde{J}_t \cdot \tilde{\omega}_{\vartheta,m}^2 \right\} = 0 \quad \forall(i, m) \Leftrightarrow \alpha_{m,i}^2 = -\frac{\tilde{J}_t \cdot \tilde{\omega}_{\vartheta,m}^2}{(1 + \beta^2)};$$

It's evident that the contribution of the hyperbolic exponential term vanishes.

$$\lim_{\chi^2 \rightarrow \infty} \eta_{\vartheta,m}^2 = \lim_{\chi^2 \rightarrow \infty} \frac{\chi^2}{2\beta^2} \left(\sqrt{(1 + \beta^2)^2 + 4 \frac{\beta^2}{\chi^2} \cdot \tilde{J}_t \cdot \tilde{\omega}_{\vartheta,m}^2} - (1 + \beta^2) \right) = \frac{\tilde{J}_t \cdot \tilde{\omega}_{\vartheta,m}^2}{(1 + \beta^2)};$$

$$\lim_{\chi^2 \rightarrow \infty} \Psi_{\vartheta,m}^2 = \lim_{\chi^2 \rightarrow \infty} \frac{\chi^2}{2\beta^2} \left(\sqrt{(1+\beta^2)^2 + 4 \frac{\beta^2}{\chi^2} \cdot \tilde{J}_t \cdot \tilde{\omega}_{\vartheta,m}^2} + (1+\beta^2) \right) = \lim_{\mu^2 \rightarrow 0} \chi^2 \left(1 + \frac{1}{\beta^2} \right) = \infty;$$

The complete solution becomes.

$$\Theta_m(\xi) = \Theta_{m,p} + \Theta_{m,o}(\xi) = \frac{\lambda_L^2}{\tilde{J}_t \cdot \tilde{\omega}_{\vartheta,m}^2} \tilde{h}_{\Theta,m} + c_{m,1} \cdot \exp(i \cdot \eta_{\vartheta,m} \xi) + c_{m,2} \cdot \exp(-i \cdot \eta_{\vartheta,m} \xi);$$

Enforcing the boundary conditions it's important to notice that in this particular situation has no sense to enforce free warping condition at the two end of the bridge, since satisfied by hypothesis.

$$b. c. \begin{cases} \Theta_m(0) = 0 \\ \Theta_m(1) = 0 \end{cases} \forall m \Rightarrow \begin{cases} \Theta_m(0) = 0 \Leftrightarrow c_{m,1} + c_{m,2} + \frac{\lambda_L^2}{\tilde{J}_t \cdot \tilde{\omega}_{\vartheta,m}^2} \tilde{h}_{\Theta,m} = 0 \\ \Theta_m(1) = 0 \Leftrightarrow c_{m,1} \cdot e^{i \cdot \eta_{\vartheta,m}} + c_{m,2} \cdot e^{-i \cdot \eta_{\vartheta,m}} + \frac{\lambda_L^2}{\tilde{J}_t \cdot \tilde{\omega}_{\vartheta,m}^2} \tilde{h}_{\Theta,m} = 0 \end{cases};$$

Hence the constant parameters assume the following expression.

$$c_{n,2} = \frac{\lambda_L^2}{\tilde{J}_t \cdot \tilde{\omega}_{\vartheta,m}^2} \tilde{h}_{\Theta,m} \cdot \frac{1 - e^{i \cdot \eta_{\vartheta,m}}}{e^{i \cdot \eta_{\vartheta,m}} - e^{-i \cdot \eta_{\vartheta,m}}};$$

$$c_{n,1} = - \frac{\lambda_L^2}{\tilde{J}_t \cdot \tilde{\omega}_{\vartheta,m}^2} \tilde{h}_{\Theta,m} \cdot \frac{1 - e^{-i \cdot \eta_{\vartheta,m}}}{e^{i \cdot \eta_{\vartheta,m}} - e^{-i \cdot \eta_{\vartheta,m}}};$$

The substitution in the general solution leads to the following expression.

$$\Theta_m(\xi) = \frac{\lambda_L^2}{\tilde{J}_t \cdot \tilde{\omega}_{\vartheta,m}^2} \tilde{h}_{\Theta,m} \cdot \left\{ 1 - \frac{e^{i \cdot \eta_{\vartheta,m} \cdot \xi} - e^{i \cdot \eta_{\vartheta,m} \cdot (\xi-1)} + e^{-i \cdot \eta_{\vartheta,m} \cdot \xi} - e^{-i \cdot \eta_{\vartheta,m} \cdot (\xi-1)}}{e^{i \cdot \eta_{\vartheta,m}} - e^{-i \cdot \eta_{\vartheta,m}}} \right\};$$

The usual trigonometric relations allow us to reformulate the solution in a more compact form.

$$\Theta_m(\xi) = \frac{\lambda_L^2}{\tilde{J}_t \cdot \tilde{\omega}_{\vartheta,m}^2} \tilde{h}_{\Theta,m} \cdot \left\{ 1 - \frac{\sin(\eta_{\vartheta,m} \cdot \xi) - \sin(\eta_{\vartheta,m} \cdot (\xi-1))}{\sin(\eta_{\vartheta,m})} \right\} = \frac{\lambda_L^2}{\tilde{J}_t \cdot \tilde{\omega}_{\vartheta,m}^2} \tilde{h}_{\Theta,m} \cdot \left\{ 1 - \frac{\cos\left(\sqrt{\frac{\tilde{J}_t}{(1+\beta^2)}} \tilde{\omega}_{\vartheta,m} \cdot \left(\xi - \frac{1}{2}\right)\right)}{\cos\left(\frac{1}{2} \sqrt{\frac{\tilde{J}_t}{(1+\beta^2)}} \tilde{\omega}_{\vartheta,m}\right)} \right\};$$

From the definition of the stiffening term we get the eigen-function of the problem.

$$\tilde{h}_{\Theta,m} = \int_0^1 \Theta_m(\xi) d\xi \Rightarrow \frac{\tilde{J}_t \cdot \tilde{\omega}_{\vartheta,m}^2}{\lambda_L^2} = 1 - \frac{\tan\left(\frac{1}{2} \sqrt{\frac{\tilde{J}_t}{(1+\beta^2)}} \tilde{\omega}_{\vartheta,m}\right)}{\left(\frac{1}{2} \sqrt{\frac{\tilde{J}_t}{(1+\beta^2)}} \tilde{\omega}_{\vartheta,m}\right)};$$

iv. Flexible deck:

This occurs any time that the torsional stiffness contribution given by the deck becomes negligible with respect to the one given by the action of the couple of cables.

In the limit case the deck loose completely its torsional stiffness and hence cannot behave like an equivalent couple of cables since in the formulation of the model we assume that it has not axially fixed ends.

$$\lim_{G_d J_d \rightarrow 0} \beta^2 = 0 \Rightarrow \lim_{G_d J_d \rightarrow 0} T_m(\xi) = -\Theta_m''(\xi) - \tilde{J}_t \cdot \tilde{\omega}_{\vartheta, m}^2 \cdot \Theta_m(\xi) + \lambda_L^2 \cdot \tilde{h}_{\Theta, m} ;$$

In this case in order to avoid indeterminate condition we need to specify the following additional condition.

$$\beta^2 \rightarrow 0 \quad \text{and} \quad \frac{\beta^2}{\chi^2} \rightarrow 0 ;$$

This additional condition has the physical meaning that when the primary torsional stiffness of the deck is negligible with respect to the cable system contribution then we cannot consider a thin walled open section girder.

Since the equation of motion is identical to the one obtained just previously in the case of free warping condition, with the exception that the deck to cables torsional stiffness parameter is now vanished. Thence we can conclude that the modal shapes and eigen-function expression are just slightly modified as follows.

$$\Theta_m(\xi) = \frac{\lambda_L^2}{\tilde{J}_t \cdot \tilde{\omega}_{\vartheta, m}^2} \tilde{h}_{\Theta, m} \cdot \left\{ 1 - \frac{\cos\left(\sqrt{\tilde{J}_t} \cdot \tilde{\omega}_{\vartheta, m} \cdot \left(\xi - \frac{1}{2}\right)\right)}{\cos\left(\frac{1}{2} \sqrt{\tilde{J}_t} \cdot \tilde{\omega}_{\vartheta, m}\right)} \right\} ;$$

$$\tilde{h}_{\Theta, m} = \int_0^1 \Theta_m(\xi) d\xi \Rightarrow \frac{\tilde{J}_t \cdot \tilde{\omega}_{\vartheta, m}^2}{\lambda_L^2} = 1 - \frac{\tan\left(\frac{1}{2} \sqrt{\tilde{J}_t} \cdot \tilde{\omega}_{\vartheta, m}\right)}{\left(\frac{1}{2} \sqrt{\tilde{J}_t} \cdot \tilde{\omega}_{\vartheta, m}\right)} ;$$

v. Stiff warping deck:

The typical girders characterised by low values of the warping coefficient are those with thin walled open cross section, where the primary torsional stiffness by de S. Venant is negligible with respect to the secondary Vlasov-Wagner contribution.

$$\text{if } \chi^2 \rightarrow 0 \Rightarrow \lim_{\chi^2 \rightarrow 0} T_m(\xi) = \frac{\beta^2}{\chi^2} \cdot \Theta_m''''(\xi) - (1 + \beta^2) \Theta_m''(\xi) - \tilde{J}_t \cdot \tilde{\omega}_{\vartheta, m}^2 \cdot \Theta_m(\xi) + \lambda_L^2 \cdot \tilde{h}_{\Theta, m} ;$$

Once again to avoid indeterminate situations let's reformulate the previous condition as follows.

$$\text{from } \chi^2 \rightarrow 0 \Rightarrow \text{to } \frac{\chi^2}{\beta^2} \rightarrow 0 ;$$

This states that for thin open sections is not possible to neglect the primary torsional stiffness contribution given by the deck with respect to the one of cable system.

Since the equation of motion format is not directly sensible to this limit condition let's analyse the trigonometric and hyperbolic exponential coefficients.

The previous limit condition is too stringent hence a more relaxed condition will suffice.

$$\text{if } \chi^2 \ll \frac{4\beta^2 \cdot \tilde{J}_t \cdot \tilde{\omega}_{\vartheta, m}^2}{(1 + \beta^2)^2} \Rightarrow (\eta_{\vartheta, m}^2, \Psi_{\vartheta, m}^2) = \sqrt{\tilde{J}_t} \cdot \tilde{\omega}_{\vartheta, m} \cdot \frac{\chi}{\beta} \Rightarrow \frac{(\eta_{\vartheta, m}^2, \Psi_{\vartheta, m}^2)}{\Psi_{\vartheta, m}^2 + \eta_{\vartheta, m}^2} = \frac{1}{2} ;$$

Hence we can find expression for modal shapes and eigen-functions similar to the flexural modes under stiff deck hypothesis.

$$\Theta_m(\xi) = \frac{\lambda_L^2}{\tilde{J}_t \cdot \tilde{\omega}_{\vartheta,m}^2} \tilde{h}_{\vartheta,m} \cdot \left\{ 1 - \frac{1}{2} \cdot \left(\frac{\cosh\left(\sqrt{\tilde{J}_t} \cdot \tilde{\omega}_{\vartheta,m} \cdot \frac{\chi}{\beta} \cdot \left(\xi - \frac{1}{2}\right)\right)}{\cosh\left(\frac{1}{2}\sqrt{\tilde{J}_t} \cdot \tilde{\omega}_{\vartheta,m} \cdot \frac{\chi}{\beta}\right)} + \frac{\cos\left(\sqrt{\tilde{J}_t} \cdot \tilde{\omega}_{\vartheta,m} \cdot \frac{\chi}{\beta} \cdot \left(\xi - \frac{1}{2}\right)\right)}{\cos\left(\frac{1}{2}\sqrt{\tilde{J}_t} \cdot \tilde{\omega}_{\vartheta,m} \cdot \frac{\chi}{\beta}\right)} \right) \right\};$$

$$\tilde{h}_{\vartheta,m} = \int_0^1 \Theta_m(\xi) d\xi \Rightarrow \frac{\tilde{J}_t \cdot \tilde{\omega}_{\vartheta,m}^2}{\lambda_L^2} = 1 - \frac{1}{2} \cdot \left(\frac{\tanh\left(\frac{1}{2}\sqrt{\tilde{J}_t} \cdot \tilde{\omega}_{\vartheta,m} \cdot \frac{\chi}{\beta}\right)}{\left(\frac{1}{2}\sqrt{\tilde{J}_t} \cdot \tilde{\omega}_{\vartheta,m} \cdot \frac{\chi}{\beta}\right)} + \frac{\tan\left(\frac{1}{2}\sqrt{\tilde{J}_t} \cdot \tilde{\omega}_{\vartheta,m} \cdot \frac{\chi}{\beta}\right)}{\left(\frac{1}{2}\sqrt{\tilde{J}_t} \cdot \tilde{\omega}_{\vartheta,m} \cdot \frac{\chi}{\beta}\right)} \right);$$

vi. Rigid deck:

As the primary torsional stiffness of the deck is dominant on the contribution given by the cable system we can state the following relations.

$$\lim_{GdJd \rightarrow \infty} \beta^2 = \infty \Rightarrow \lim_{GdJd \rightarrow \infty} T_m(\xi) = \frac{\beta^2}{\chi^2} \cdot \Theta_m{}''''(\xi) - (1 + \beta^2) \Theta_m''(\xi) - \tilde{J}_t \cdot \tilde{\omega}_{\vartheta,m}^2 \cdot \Theta_m(\xi) + \lambda_L^2 \cdot \tilde{h}_{\vartheta,m};$$

In order to avoid indeterminate condition the following additional relation holds.

$$\beta^2 \rightarrow \infty \quad \text{and} \quad \frac{\beta^2}{\chi^2} \rightarrow \infty;$$

Meaning that once the torsional stiffness contribution coming from the cable system is negligible with respect to the primary one from of the deck, thence the latter cannot be of the close box section type.

As for the previous case the equation of motion format doesn't change, hence let's analyse the exponential coefficients, introducing by the way a more general limiting condition.

$$\text{if } \beta^2 \gg 1 \Rightarrow (\eta_{\vartheta,m}^2, \Psi_{\vartheta,m}^2) = \frac{\chi^2}{2} \left(\sqrt{1 + \frac{4}{\chi^2 \cdot \beta^2} \cdot \tilde{J}_t \cdot \tilde{\omega}_{\vartheta,m}^2} \mp 1 \right);$$

$$\text{if } \beta^2 \gg \frac{4}{\chi^2} \cdot \tilde{J}_t \cdot \tilde{\omega}_{\vartheta,m}^2 \Rightarrow (\eta_{\vartheta,m}^2, \Psi_{\vartheta,m}^2) = (0, \chi^2);$$

Hence the expression for modal shapes and eigen-function can be found.

$$\Theta_m(\xi) = \frac{\lambda_L^2}{\tilde{J}_t \cdot \tilde{\omega}_{\vartheta,m}^2} \tilde{h}_{\vartheta,m} \cdot \left\{ 1 - \frac{\cosh\left(\chi \cdot \left(\xi - \frac{1}{2}\right)\right)}{\cosh\left(\frac{\chi}{2}\right)} \right\};$$

$$\tilde{h}_{\vartheta,m} = \int_0^1 \Theta_m(\xi) d\xi \Rightarrow \frac{\tilde{J}_t \cdot \tilde{\omega}_{\vartheta,m}^2}{\lambda_L^2} = 1 - \frac{\cosh\left(\chi \cdot \left(\xi - \frac{1}{2}\right)\right)}{\cosh\left(\frac{\chi}{2}\right)};$$

Is interesting to notice that this is the first case in which the hyperbolic term survive on the trigonometric one.

Finally let's consider very special case situations.

vii. Flat cables & Free warping deck & Flexible deck:

First of all consider the more general case of flat cable and free warping deck conditions.

$$\lim_{H \rightarrow \infty} \lambda_L^2 = 0 \text{ and } \chi^2 \rightarrow \infty \Rightarrow \lim_{H \rightarrow \infty} T_m(\xi) = -(1 + \beta^2)\theta_m''(\xi) - \tilde{J}_t \cdot \tilde{\omega}_{\vartheta, m}^2 \cdot \theta_m(\xi);$$

$$\chi^2 \rightarrow \infty$$

$$T_m(\xi) = 0 \quad \forall(\xi, m) \Leftrightarrow -(1 + \beta^2)\theta_m''(\xi) - \tilde{J}_t \cdot \tilde{\omega}_{\vartheta, m}^2 \cdot \theta_m(\xi) = 0 \quad \forall(\xi, m);$$

Hence we get the same sinusoidal modal shape obtained by the only flat cable condition and a slightly different circular eigen-frequency.

$$\theta_m(\xi) = \sin((2m - 1) \cdot \pi \cdot \xi);$$

$$\sqrt{\tilde{J}_t} \cdot \tilde{\omega}_{\vartheta, m} = (2m - 1)\pi \cdot \sqrt{1 + \beta^2};$$

Notice that this case has been already analysed for the flat cable limit condition. Hence the condition on the deck warping coefficient can be reformulate as follows.

$$\text{from } \chi^2 \rightarrow \infty \Rightarrow \text{to } \frac{\chi^2}{\beta^2} \rightarrow \infty \Rightarrow \text{to } \chi^2 \gg \frac{((2m-1) \cdot \pi)^2}{1 + \frac{1}{\beta^2}};$$

If also the deck becomes extremely flexible under torsional actions then we get similar results, in fact only the circular eigen-frequencies and the limit condition are slightly modified.

$$\lim_{G_d J_d \rightarrow 0} \beta^2 = 0 \Rightarrow \chi^2 \gg ((2m - 1) \cdot \pi)^2 \Rightarrow \sqrt{\tilde{J}_t} \cdot \tilde{\omega}_{\vartheta, m} = (2m - 1)\pi;$$

Notice that we get the same sinusoidal modal shape and the latter circular eigen-frequency expression also for the simpler combination flat cables and torsional flexible deck. While the limiting condition for a generic warping coefficient is that already obtained from the flat cables condition.

$$\text{from } \beta^2 \rightarrow 0 \Rightarrow \text{to } \frac{\beta^2}{\chi^2} \rightarrow 0 \Rightarrow \text{to } \beta^2 \ll \frac{1}{1 + \frac{((2m-1) \cdot \pi)^2}{\chi^2}};$$

viii. Flat cables & Stiff warping deck & Flexible deck:

First of all consider the more general case of flat cable and stiff warping deck conditions.

$$\lim_{H \rightarrow \infty} \lambda_L^2 = 0 \text{ and } \chi^2 \rightarrow 0 \Rightarrow \lim_{H \rightarrow \infty} T_m(\xi) = \frac{\beta^2}{\chi^2} \cdot \theta_m''''(\xi) - (1 + \beta^2)\theta_m''(\xi) - \tilde{J}_t \cdot \tilde{\omega}_{\vartheta, m}^2 \cdot \theta_m(\xi);$$

$$\chi^2 \rightarrow 0$$

$$T_m(\xi) = 0 \quad \forall(\xi, m) \Leftrightarrow \frac{\beta^2}{\chi^2} \cdot \theta_m''''(\xi) - (1 + \beta^2)\theta_m''(\xi) - \tilde{J}_t \cdot \tilde{\omega}_{\vartheta, m}^2 \cdot \theta_m(\xi) = 0 \quad \forall(\xi, m);$$

Hence we get the same sinusoidal modal shape obtained by the only flat cable condition and a slightly modified circular eigen-frequency.

$$\Theta_m(\xi) = \sin((2m - 1) \cdot \pi \cdot \xi);$$

$$\chi^2 \rightarrow 0 \Rightarrow \sqrt{\tilde{J}_t} \cdot \tilde{\omega}_{\vartheta,m} = ((2m - 1)\pi)^2 \cdot \frac{\beta}{\chi};$$

Notice that this case has been already analysed for the flat cable limit condition. Hence the condition on the deck warping coefficient can be reformulate as follows.

$$\text{from } \chi^2 \rightarrow 0 \Rightarrow \text{to } \frac{\chi^2}{\beta^2} \rightarrow 0 \Rightarrow \text{to } \chi^2 \ll \frac{((2m-1)\pi)^2}{(1+\frac{1}{\beta^2})};$$

If also the deck becomes extremely rigid under torsional actions then we get identical results, in fact only the limit condition is slightly modified.

$$\lim_{G_d J_d \rightarrow \infty} \beta^2 = \infty \Rightarrow \chi^2 \ll ((2m - 1) \cdot \pi)^2;$$

For the simpler combination flat cables and torsional rigid deck the expression for the modal shapes remains the same. While change a little bit both the circular eigen-frequency and the limiting condition, that for a generic warping coefficient are that obtained from the flat cables condition.

$$\beta^2 \rightarrow \infty \Rightarrow \sqrt{\tilde{J}_t} \cdot \tilde{\omega}_{\vartheta,m} = (2m - 1)\pi \cdot \sqrt{1 + \frac{((2m-1)\pi)^2}{\chi^2}} \cdot \beta;$$

$$\text{from } \beta^2 \rightarrow \infty \Rightarrow \text{to } \frac{\beta^2}{\chi^2} \rightarrow \infty \Rightarrow \text{to } \beta^2 \gg \frac{1}{1 + \frac{((2m-1)\pi)^2}{\chi^2}};$$

ix. Inextensible cables & Free warping deck & Flexible deck:

First of all consider the more general case of inextensible cables and free warping deck conditions.

$$\lim_{E_c A_c \rightarrow \infty} \lambda_L^2 = \infty \text{ and } \chi^2 \rightarrow \infty \Rightarrow \lim_{\substack{E_c A_c \rightarrow \infty \\ \chi^2 \rightarrow \infty}} T_m(\xi) = -(1 + \beta^2)\Theta_m''(\xi) - \tilde{J}_t \cdot \tilde{\omega}_{\vartheta,m}^2 \cdot \Theta_m(\xi) + \lambda_L^2 \cdot \tilde{h}_{\vartheta,m};$$

$$T_m(\xi) = 0 \quad \forall(\xi, m) \Leftrightarrow -(1 + \beta^2)\Theta_m''(\xi) - \tilde{J}_t \cdot \tilde{\omega}_{\vartheta,m}^2 \cdot \Theta_m(\xi) + \lambda_L^2 \cdot \tilde{h}_{\vartheta,m} = 0 \quad \forall(\xi, m);$$

Hence we get the same modal shapes of the free warping deck condition and a slightly modified eigen-functions.

$$\Theta_m(\xi) = \frac{\lambda_L^2}{\tilde{J}_t \cdot \tilde{\omega}_{\vartheta,m}^2} \tilde{h}_{\Theta,m} \cdot \left\{ 1 - \frac{\cos\left(\sqrt{\frac{\tilde{J}_t}{(1+\beta^2)}} \tilde{\omega}_{\vartheta,m} \cdot \left(\xi - \frac{1}{2}\right)\right)}{\cos\left(\frac{1}{2} \sqrt{\frac{\tilde{J}_t}{(1+\beta^2)}} \tilde{\omega}_{\vartheta,m}\right)} \right\};$$

$$\tilde{h}_{\Theta,m} = \int_0^1 \Theta_m(\xi) d\xi \Rightarrow \lim_{\lambda_L^2 \rightarrow \infty} \frac{\tilde{J}_t \cdot \tilde{\omega}_{\vartheta,m}^2}{\lambda_L^2} = 0 \Rightarrow 1 - \frac{\tan\left(\frac{1}{2} \sqrt{\frac{\tilde{J}_t}{(1+\beta^2)}} \tilde{\omega}_{\vartheta,m}\right)}{\left(\frac{1}{2} \sqrt{\frac{\tilde{J}_t}{(1+\beta^2)}} \tilde{\omega}_{\vartheta,m}\right)} = 0;$$

As the flexible deck condition is taken in account we need just to substitute inside the previous expression the condition that make vanish the deck to cable system torsional stiffness ratio.

Although this last condition can be generalised as follows.

$$\text{from } \beta^2 \rightarrow 0 \Rightarrow \text{to } \frac{\beta^2}{\chi^2} \rightarrow 0 \Rightarrow \text{to } \beta^2 \ll 1;$$

The last step allows us to find also the right expression valid for the inextensible cable system and flexible deck condition with generic warping coefficient.

While if we consider just the conditions of free warping and flexible deck we get the same expressions for the modal shapes but cannot neglect the contribution of the Irvine parameter on the eigen-function expression.

x. Inextensible cables & Stiff warping deck & Rigid deck:

First of all consider the more general case of inextensible cables and stiff warping deck conditions.

$$\lim_{E_c A_c \rightarrow \infty} \lambda_L^2 = \infty \text{ and } \chi^2 \rightarrow 0 \Rightarrow \lim_{E_c A_c \rightarrow \infty} T_m(\xi) = \left\{ \begin{array}{l} \frac{\beta^2}{\chi^2} \cdot \Theta_m{}^{iv}(\xi) - (1 + \beta^2) \Theta_m''(\xi) + \\ -\tilde{J}_t \cdot \tilde{\omega}_{\vartheta,m}^2 \cdot \Theta_m(\xi) + \lambda_L^2 \cdot \tilde{h}_{\Theta,m} \end{array} \right\};$$

$$T_m(\xi) = 0 \quad \forall(\xi, m) \Leftrightarrow \left\{ \begin{array}{l} \frac{\beta^2}{\chi^2} \cdot \Theta_m{}^{iv}(\xi) - (1 + \beta^2) \Theta_m''(\xi) + \\ -\tilde{J}_t \cdot \tilde{\omega}_{\vartheta,m}^2 \cdot \Theta_m(\xi) + \lambda_L^2 \cdot \tilde{h}_{\Theta,m} \end{array} \right\} = 0 \quad \forall(\xi, m);$$

Hence we get the same modal shapes of the stiff warping deck condition and a slightly modified eigen-functions.

$$\Theta_m(\xi) = \frac{\lambda_L^2}{\tilde{J}_t \cdot \tilde{\omega}_{\vartheta,m}^2} \tilde{h}_{\Theta,m} \cdot \left\{ 1 - \frac{1}{2} \cdot \left(\frac{\cosh\left(\sqrt{\tilde{J}_t} \cdot \tilde{\omega}_{\vartheta,m} \cdot \frac{\chi}{\beta} \cdot \left(\xi - \frac{1}{2}\right)\right)}{\cosh\left(\frac{1}{2} \sqrt{\tilde{J}_t} \cdot \tilde{\omega}_{\vartheta,m} \cdot \frac{\chi}{\beta}\right)} + \frac{\cos\left(\sqrt{\tilde{J}_t} \cdot \tilde{\omega}_{\vartheta,m} \cdot \frac{\chi}{\beta} \cdot \left(\xi - \frac{1}{2}\right)\right)}{\cos\left(\frac{1}{2} \sqrt{\tilde{J}_t} \cdot \tilde{\omega}_{\vartheta,m} \cdot \frac{\chi}{\beta}\right)} \right) \right\};$$

$$\tilde{h}_{\theta,m} = \int_0^1 \theta_m(\xi) d\xi \Rightarrow \lim_{\lambda_L^2 \rightarrow \infty} \frac{\tilde{J}_t \cdot \tilde{\omega}_{\theta,m}^2}{\lambda_L^2} = 0 \Rightarrow 1 - \frac{1}{2} \cdot \left(\frac{\tanh\left(\frac{1}{2}\sqrt{\tilde{J}_t} \cdot \tilde{\omega}_{\theta,m} \frac{\lambda}{\beta}\right)}{\left(\frac{1}{2}\sqrt{\tilde{J}_t} \cdot \tilde{\omega}_{\theta,m} \frac{\lambda}{\beta}\right)} + \frac{\tan\left(\frac{1}{2}\sqrt{\tilde{J}_t} \cdot \tilde{\omega}_{\theta,m} \frac{\lambda}{\beta}\right)}{\left(\frac{1}{2}\sqrt{\tilde{J}_t} \cdot \tilde{\omega}_{\theta,m} \frac{\lambda}{\beta}\right)} \right) = 0 ;$$

Taking in account also for the rigid deck condition any variation to previous expression is needed.

The last statement is valid also for the inextensible cable system and rigid deck condition with generic warping coefficient.

While if we consider just the conditions of stiff warping and rigid deck we get the same expressions for the modal shapes but cannot neglect the contribution of the Irvine parameter on the eigen-function expression.

What is really important to notice is that in the combined limit situations what really governs format of the fundamental expressions are those parameters that make vanish some terms in the equation of motion.

2.3. Numerical analysis of eigen-properties

Once the solutions for both the flexural and the torsional equation of motion has been defined for the general and the extreme situations is possible to analyse some numerical result in order to see the influence of the mechanical and structural parameters on the response of the system.

2.3.1. Flexural vibrations

The parameters affecting the flexural equation of motion change depending if we are considering symmetric or skew symmetric modes.

For the symmetric ones is necessary to define both the deck to cable flexural stiffness ratio μ^2 and the Irvine parameter λ_L^2 in order to compute circular eigen-frequencies and the associate modal shapes.

On contrary for skew-symmetric modes the eigen-vectors are simply sinusoidal with a prescribed half wave length proportional to the modal number and it's not influenced directly by the circular eigen-frequency that depends only on the modal number and on the deck to cable stiffness parameter.

Concluding, the parameters of interest would be the following.

$$n \quad ; \quad \lambda_L^2 = \frac{E_c A_c}{H} \frac{l}{L_c} (y''l)^2 \quad ; \quad \mu^2 = \frac{E_d I_d}{2Hl^2} ;$$

From literature has been possible to define reliable values for such parameters.

In their paper [38], Cobo and Aparicio collect the values such parameters in relation to 13 three span bridges with different peculiarities. They include the Bronx-Withestone, Tacoma Narrows, Severn, Forth Road, George Washingtonj, Bosforus I, Mackinac, Golden Gate, Verrazzano, Humber, Great Belt and Akashi-Kaikyo Bridges.

Further from the work [5] done by Luco and Lo Turmo has been possible to introduce also data related to Innoshima Bridge.

The center –span ranges from 700 to 1990 meters, hence the Irvine parameter has a bimodal distribution, ranging from 90 up to 132 for ten of the bridges and for the remaining from 171 to 231, with a global average value of 198. We must remember that these are results referring to three span bridges but our structural model takes in account just the central main span neglecting the presence of backstays. Hence if we account just for the data related to the central span we get Irvine parameters ranging from 148 to 376 with an average of 220.

Hence in the following we will consider values for the cables parameter corresponding to 0 to take in account for the flat cables condition, 100 and 225 to represent the bimodal behaviour seen from real data, and ∞ for the inextensible cables situation.

$$\lambda_L^2 = [0 ; 100 ; 225 ; \infty];$$

The relative deck flexural stiffness parameter ranges from $0.4 \cdot 10^{-3}$ for the Tacoma Narrows Bridge to $11.4 \cdot 10^{-3}$ for the Tagus Bridge, but is also important to notice that for nine of the bridges this parameter has an average value close to $1.17 \cdot 10^{-3}$.

Hence seems that values ranging from $0.5 \cdot 10^{-3}$ up to $10 \cdot 10^{-3}$ would span most of the typical situations, but in the following this array will be enlarged in order to take in account some extreme conditions from 0 to include the flexible deck condition and 1 for the opposite rigid deck condition.

$$\mu^2 = [0 \dots 0.5 \cdot 10^{-3} \dots 10^{-2} \dots 1];$$

Let's analyse the results obtained for the first two relevant modes.

i. Circular eigen-frequencies:

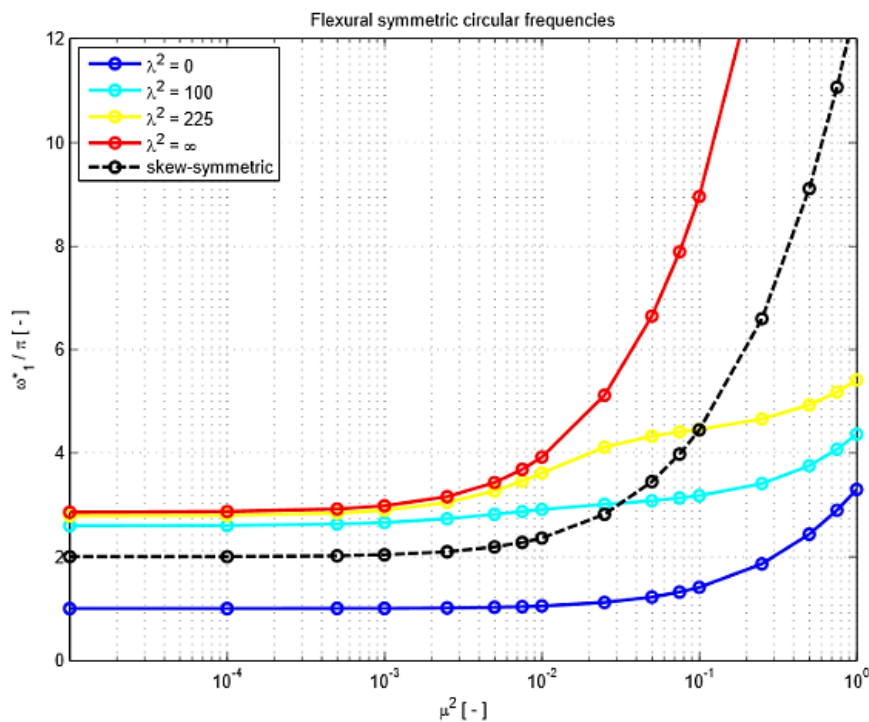


Figure 2.2_ Flexural circular eigen-frequencies of Mode 1.

For the first mode it's evident that for $\mu^2 < 10^{-3}$ the circular eigen-frequencies remains constant meaning that the deck relative stiffness μ^2 is no more influent on them, becoming dominant the cables contribution. This threshold reduces in higher order modes.

On the contrary the effect of μ^2 becomes more and more relevant increasing the cable parameter λ_L^2 and the modal order as it's evident from next figures.

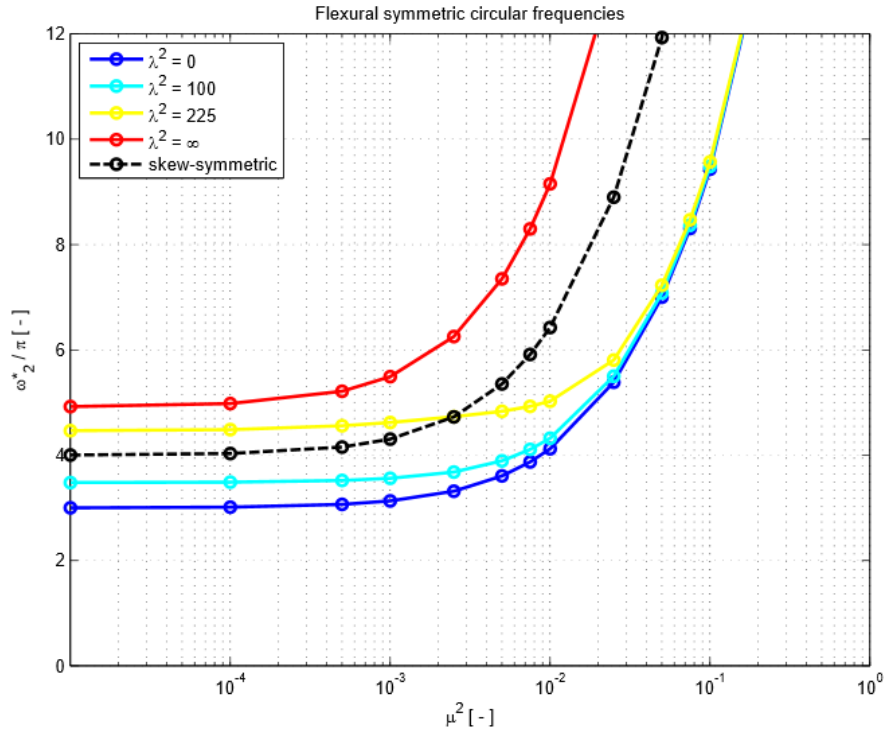


Figure 2.3_ Flexural circular eigen-frequencies of Mode 2.

As mentioned above is evident that the deck stiffness parameter threshold reduces to $\mu^2 < 10^{-4}$ in fact its influence on frequencies increases.

From the second mode plot it's evident that for finite values of λ_L^2 as the deck relative flexural stiffness parameter increases, all curves of the circular eigen-frequencies tend to collapse on that one characterised by $\lambda_L^2 = 0$. This means that beyond certain level of deck rigidity ($\mu^2 > 5 \cdot 10^{-2}$) the cables contribution to flexural vibrations has no more effects on the structural response in time.

It's interesting to notice that in correspondence of any μ^2 hold a relation between the frequencies of subsequent modes.

$$\omega_{n+1}^*(\lambda_L^2 = 0, \forall \mu^2) \approx \omega_n^*(\lambda_L^2 = \infty, \forall \mu^2);$$

Can be of interest to find the critical conditions that leads a symmetric modal shape to vibrate according to the circular eigen-frequency of the corresponding skew symmetric one. Consequently being the eigen-value associated to a unique eigen-vector, as the vibration frequency coalesce with the skew-symmetric one, as a consequence also the modal shape is forced to be skew-symmetric. Further we must underline the fact that generally for real structures we should expect skew-symmetric modes. In fact in this condition, cables do not elongate, leading the structure on to a minimum energetic level, which usually is much more stable.

It is evident from the previous figures that tuning properly the structural properties it's possible to reach this condition that we will call Cross Over Frequency (COF).

Let's analyse analytically the conditions that leads to this particular situation.

$$(\tilde{\omega}_{w,n}^a)^2 = (2n\pi)^2 \cdot [1 + \mu^2 \cdot (2n\pi)^2];$$

$$(\tilde{\omega}_{w,n}^s)^2 = \lambda_L^2 \cdot \left[1 - \frac{1}{\Psi_{w,n}^2 + \eta_{w,n}^2} \cdot \left(\eta_{w,n}^2 \cdot \frac{\tanh\left(\frac{\Psi_{w,n}}{2}\right)}{\frac{\Psi_{w,n}}{2}} + \Psi_{w,n}^2 \cdot \frac{\tan\left(\frac{\eta_{w,n}}{2}\right)}{\frac{\eta_{w,n}}{2}} \right) \right];$$

In the general situation the COF condition requires an iterative solution of the following equality.

$$(\lambda_L^2)_{cr} = (2n\pi)^2 \cdot [1 + \mu^2 \cdot (2n\pi)^2] \cdot \left[1 - \frac{1}{\Psi_{w,n}^2 + \eta_{w,n}^2} \cdot \left(\eta_{w,n}^2 \cdot \frac{\tanh\left(\frac{\Psi_{w,n}}{2}\right)}{\frac{\Psi_{w,n}}{2}} + \Psi_{w,n}^2 \cdot \frac{\tan\left(\frac{\eta_{w,n}}{2}\right)}{\frac{\eta_{w,n}}{2}} \right) \right]^{-1};$$

Hence for each values of the deck relative flexural stiffness parameter μ^2 is possible to define a critical value for the Irvine parameter that grant the cross over condition.

Let's simplify the treatment considering the case of perfectly flexible deck $\mu^2 = 0$.

$$(\tilde{\omega}_{w,n}^a)^2 = (2n\pi)^2;$$

$$(\tilde{\omega}_{w,n}^s)^2 = \lambda_L^2 \cdot \left[1 - \frac{\tan\left(\frac{\tilde{\omega}_{w,n}^s}{2}\right)}{\frac{\tilde{\omega}_{w,n}^s}{2}} \right];$$

Enforcing the COF threshold condition we get the following relation.

$$(\tilde{\omega}_{w,n}^s)^2 = (\tilde{\omega}_{w,n}^a)^2 \Rightarrow \lambda_L^2 \cdot \left[1 - \frac{\tan(n\pi)}{n\pi} \right] = (2n\pi)^2 \Rightarrow (\lambda_L^2)_{cr,0} = (2n\pi)^2;$$

ii. Modal shapes:

Let's analyse the modal shapes associate to the first order mode.

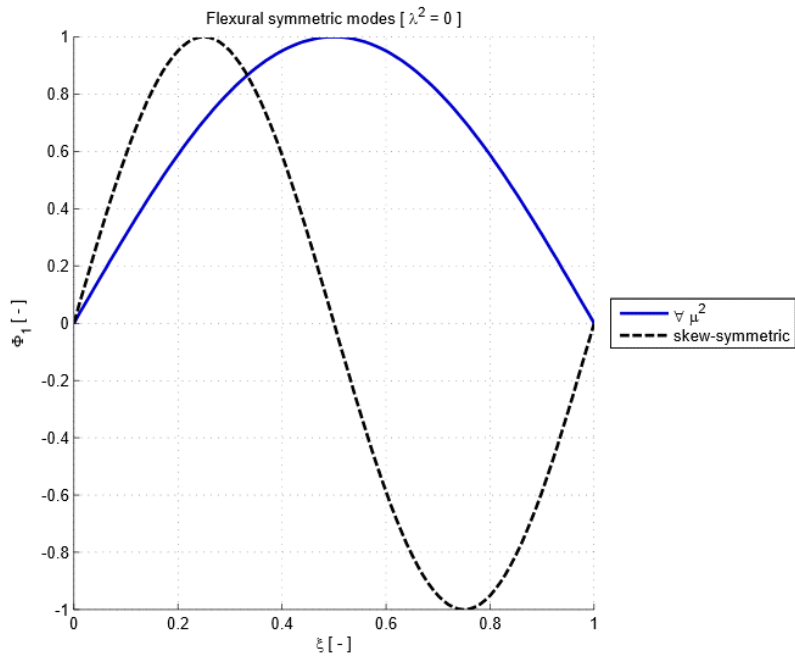


Figure 2.4_ Modal shape of Mode 1 for $\lambda_L^2 = 0$ and skew-symmetric condition.

In both the situation of skew symmetric modes or very taut cables, the stiffening contribution vanishes and hence the bridge vibrates according to a sinusoidal shape proper of strings. In fact the deck stiffness parameter has no effect on the modal shape.

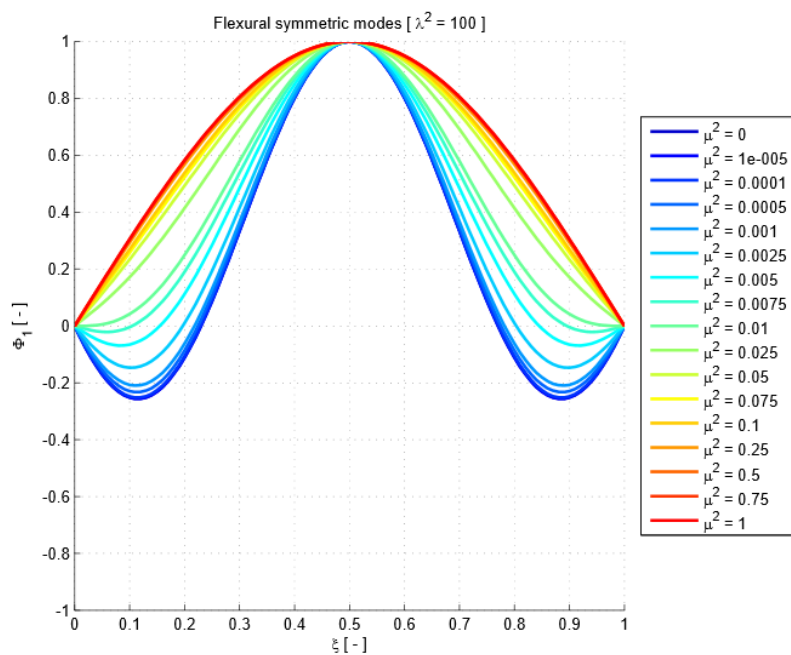


Figure 2.5_ Modal shape of Mode 1 for $\lambda_L^2 = 100$.

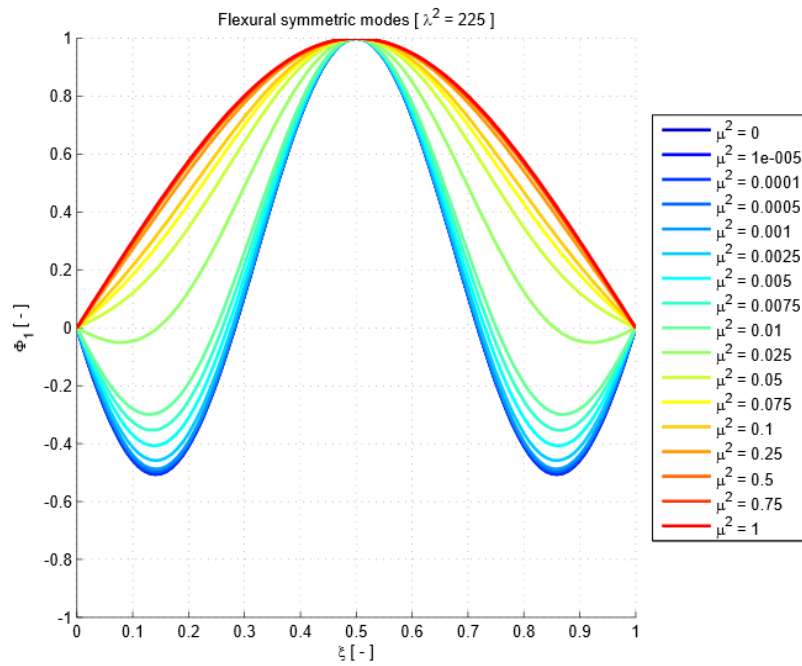


Figure 2.6_ Modal shape of Mode 1 for $\lambda_L^2 = 225$.

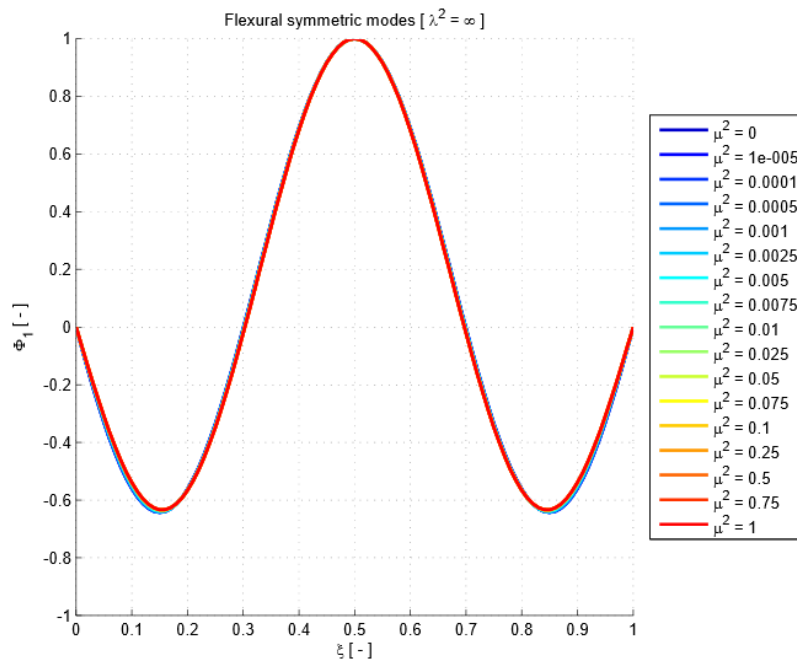


Figure 2.7_ Modal shape of Mode 1 for $\lambda_L^2 = \infty$.

As can be seen from the last three figures the increase of the Irvine parameter λ_L^2 leads to higher negative displacements. In fact as the cables axial stiffness increases the geometrical contribution to the flexural stiffness increases too. Hence enforcing a downward displacement to the centre span of the deck would lead to an increment to the cable's sag. Consequently the original parabolic shape is more distorted as compressibility decreases.

In fact in the limit condition of incompressible cable being not able to increase its length it must assume a V shape that leads the lateral sides to undergo an upward displacement with respect to the initial parabolic shape. The inextensibility of hangers grants that the deck follow exactly the same path from the initial undeformed straight configuration.

The deck relative stiffness parameter μ^2 has a great influence on standard symmetric modal shapes, and this peculiarity increases as it assumes values far from extreme conditions and the cables stiffness parameter decreases. In fact as the latter increases the modal shapes collapses to the lower curves meaning that as the cable inextensibility grows the influence of the deck relative flexural stiffness become more and more negligible.

Another interesting feature is evident as λ_L^2 increases. In fact is possible to define a critical value beyond which the modal shape internal nodes number changes. In general we will refer to it as to the Cross Over Mode (COM), that for the first symmetric modes ensure the passage from a zero to a two node modal shape. This critical condition changes with μ^2 and can be define by the following relation that enforce the vanishing of the first derivative at the two extremities of the span.

$$\begin{aligned} \left[\frac{d}{d\xi} W_n(\xi) \right]_{\xi=0} &= \frac{\lambda_L^2}{\tilde{\omega}_{w,n}^2} \tilde{h}_{W,n} \cdot \left\{ -\frac{\eta_{w,n} \cdot \Psi_{w,n}}{\Psi_{w,n}^2 + \eta_{w,n}^2} \cdot \left(\begin{array}{l} \eta_{w,n} \cdot \frac{\sinh\left(\frac{\Psi_{w,n}}{2} \left(\xi - \frac{1}{2}\right)\right)}{\cosh\left(\frac{\Psi_{w,n}}{2}\right)} + \\ + \Psi_{w,n} \cdot \frac{\sin\left(\eta_{w,n} \left(\xi - \frac{1}{2}\right)\right)}{\cos\left(\frac{\eta_{w,n}}{2}\right)} \end{array} \right) \right\}_{\xi=0} = \\ &= \frac{\lambda_L^2}{\tilde{\omega}_{w,n}^2} \tilde{h}_{W,n} \cdot \left\{ -\frac{\eta_{w,n} \cdot \Psi_{w,n}}{\Psi_{w,n}^2 + \eta_{w,n}^2} \cdot \left(\begin{array}{l} \eta_{w,n} \cdot \tanh\left(\frac{\Psi_{w,n}}{2}\right) + \\ + \Psi_{w,n} \cdot \tan\left(\frac{\eta_{w,n}}{2}\right) \end{array} \right) \right\} \geq 0 ; \end{aligned}$$

That reduces to the following condition that grants upward slope at the two ends.

$$\eta_{w,n} \cdot \tanh\left(\frac{\Psi_{w,n}}{2}\right) \geq \Psi_{w,n} \cdot \tan\left(\frac{\eta_{w,n}}{2}\right) ;$$

Notice that the symmetry of the problem allows to consider simply one side of the deck.

The last condition can be solved only iteratively, hence to get an analytical expression let's consider the usual flexible deck limit condition ($\mu^2 = 0$).

$$W_n(\xi) = \frac{\lambda_L^2}{\tilde{\omega}_{w,n}^2} \tilde{h}_{W,n} \cdot \left\{ 1 - \frac{\cos\left(\tilde{\omega}_{w,n} \left(\xi - \frac{1}{2}\right)\right)}{\cos\left(\frac{\tilde{\omega}_{w,n}}{2}\right)} \right\} \Rightarrow \left[\frac{d}{d\xi} W_n(\xi) \right]_{\xi=0} = \frac{\lambda_L^2}{\tilde{\omega}_{w,n}^2} \tilde{h}_{W,n} \cdot \left\{ -\tilde{\omega}_{w,n} \cdot \tan\left(\frac{\tilde{\omega}_{w,n}}{2}\right) \right\} ;$$

Hence enforcing the COM condition for the 0 to 2 node transition leads to.

$$\left[\frac{d}{d\xi} W_n(\xi) \right]_{\xi=0} \geq 0 \Leftrightarrow \tan\left(\frac{\tilde{\omega}_{w,n}}{2}\right) \leq 0 \Leftrightarrow \left(\frac{\pi}{2} + n\pi\right) \leq \left(\frac{\tilde{\omega}_{w,n}}{2}\right) \leq (\pi + n\pi)$$

Notice that in the last condition is implicitly assumed that the cables stiffening term is positive as generally happens.

After few computations we can find the following final expression.

$$(2n + 1) \cdot \pi \leq \tilde{\omega}_{w,n} \leq (2n + 1) \cdot \pi + \pi \Rightarrow \tilde{\omega}_{w,n}^a \leq \tilde{\omega}_{w,n}^s \leq \tilde{\omega}_{w,n}^a + \pi ;$$

Hence it's evident that at the limit condition the last relation correspond to the COF condition. This means that for infinitely flexible deck ($\mu^2 = 0$) is possible to tune the structural parameters in such a way that at the same time the bridge oscillates according to a symmetric mode characterised by null side slope and with the same frequency of vibration of the corresponding skew-symmetric mode. However as previously mentioned this would not be possible since in correspondence of a skew-symmetric frequency would be located a similar modal shape.

For the general case has been performed a numerical rooting of the first COM condition.

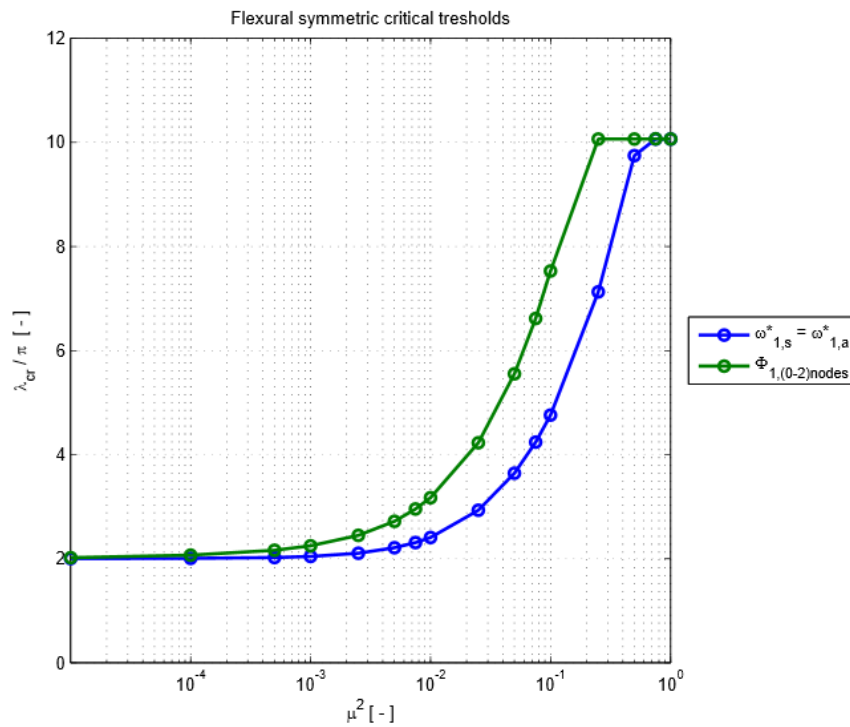


Figure 2.8_ Cross Over Frequency and Mode thresholds of Mode 1.

As it can be seen the COF limit for the flexible deck condition holds up to $\mu^2 = 10^{-3}$, corresponding to the limit before that the circular eigen-frequencies of the first mode are practically constant with the deck relative stiffness parameter.

Notice that the max admissible values for normalised critical $\frac{\lambda_L}{\pi}$ is fixed to 10 since the corresponding value of λ_L^2 is equal to 1000, that is an excellent numerical representation of the inextensible cables limit condition $\lambda_L^2 = \infty$. In fact as can be seen for $\mu^2 > 0.75$ the values of $\frac{\lambda_L}{\pi}$ collapse to 10, meaning that for very stiff decks the Cross Over Frequency cannot be reached for any level of tension inside the cables.

On the other hand the limits for the Cross Over Modes are practically equal to that of COF as long as $\mu^2 \leq 10^{-4}$, but beyond that limit it diverges until collapse to the limit value of 10. This means that in general is not possible to get a symmetric mode oscillating according to the same circular frequency of the associate skew-symmetric counterpart and with null slope at the two end. Hence tuning properly the structural parameters for the COF condition we get a symmetric modal shape with upward slope at the two ends.

Vice versa tuning those parameters for the COM condition leads to oscillations characterised with frequencies higher than that proper of the associate skew-symmetric mode.

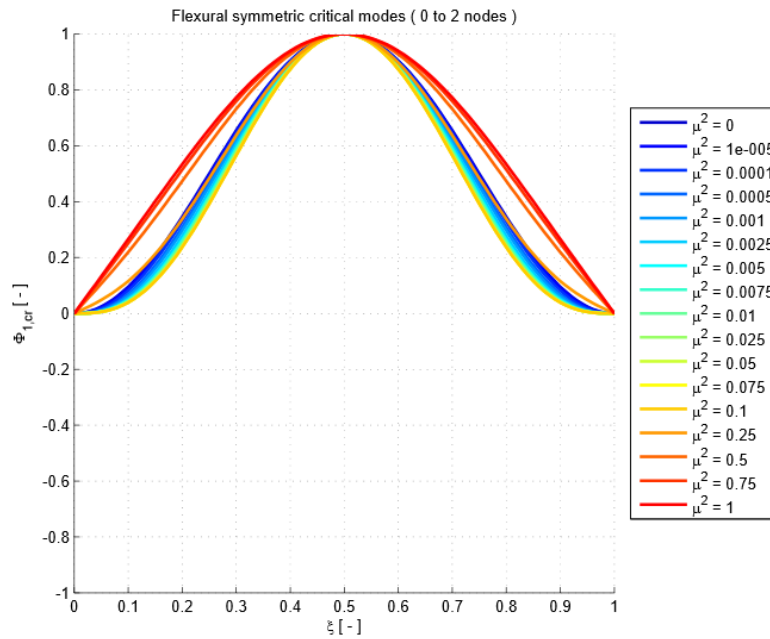


Figure 2.9_ Cross Over Modes of Mode 1.

Plotting the critical modal shape with null side slope it's evident that beyond a certain limit ($\mu^2 = 0.1 \Rightarrow \frac{\lambda_L}{\pi} = 7.5$) the increment of the cables initial tension is no more able to grant the vanishing of the slope at the two ends. This means that for too rigid deck is not possible to grant the COM condition also for cables tension lower than the limit taut cables situation ($\frac{\lambda_L}{\pi} = 10$).

Let's now analyse the modal shapes assumed by the second order mode.

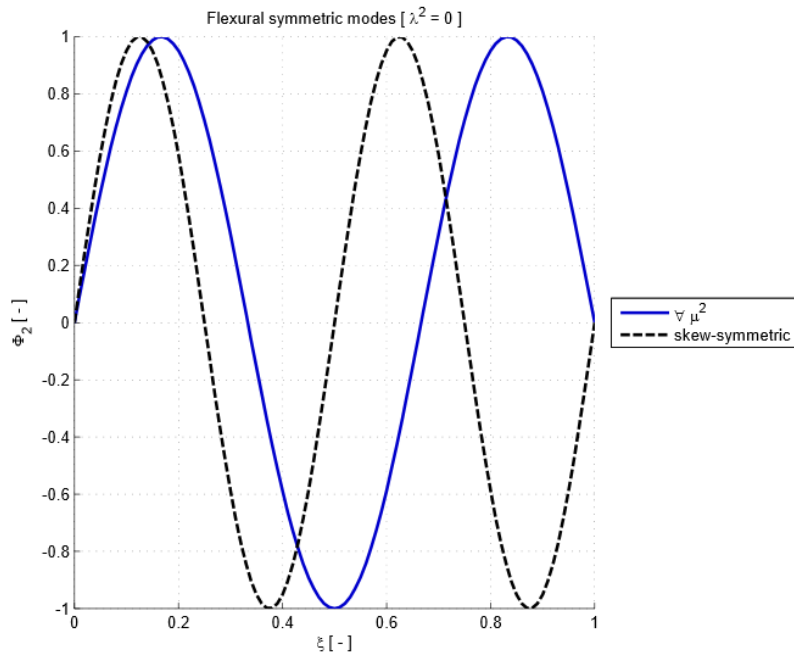


Figure 2.10_ Modal shape of Mode 2 for $\lambda_L^2 = 0$ and skew-symmetric condition.

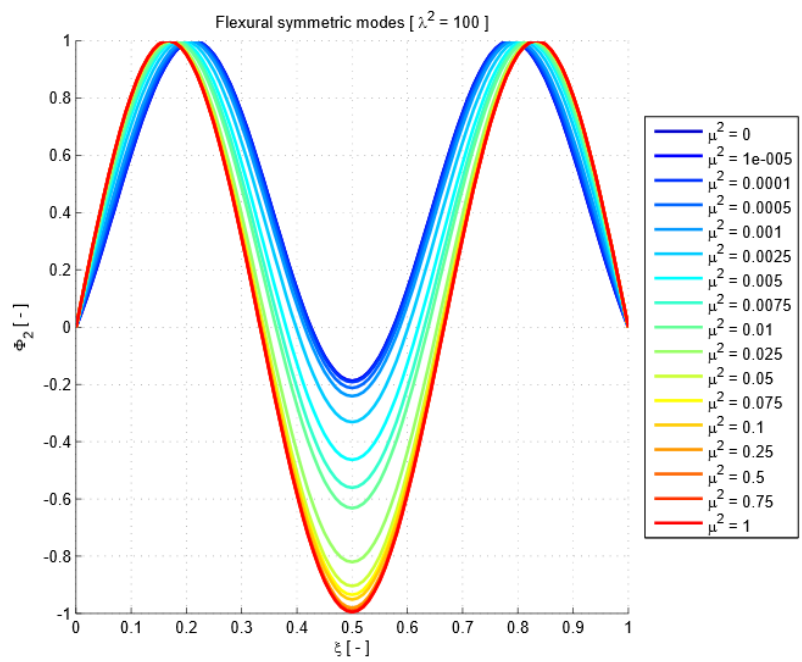


Figure 2.11_ Modal shape of Mode 2 for $\lambda_L^2 = 100$.

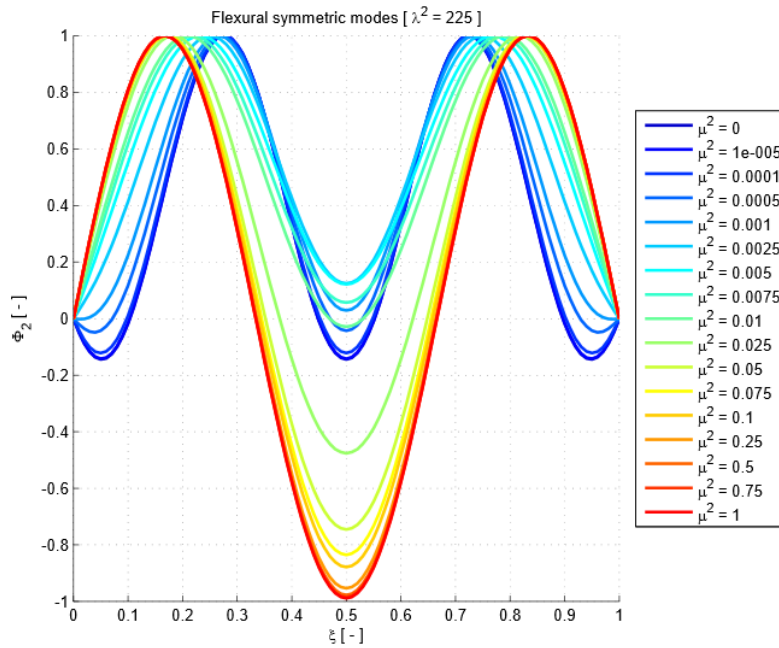


Figure 2.12_ Modal shape of Mode 2 for $\lambda_L^2 = 225$.

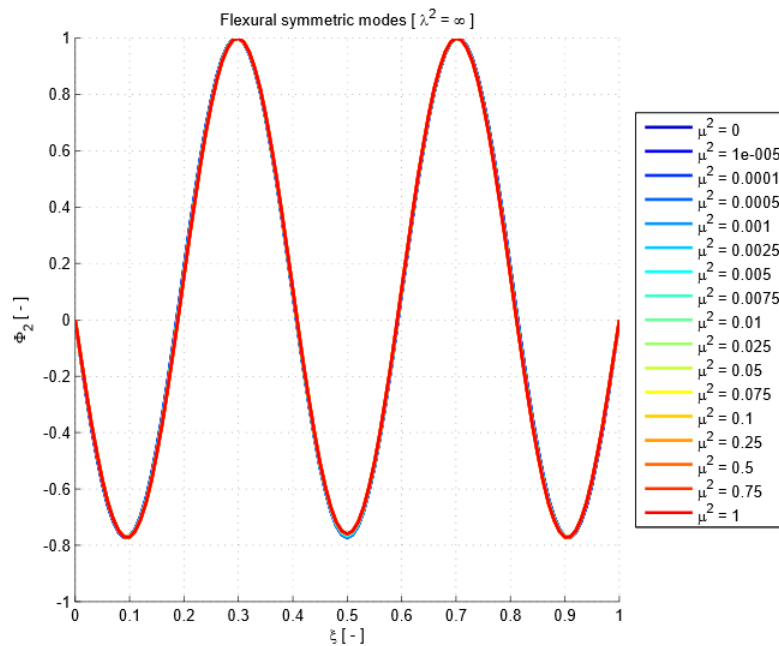


Figure 2.13_ Modal shape of Mode 2 for $\lambda_L^2 = \infty$.

With respect to the mode 1 here is evident how much is influenced the deck relative stiffness parameter on the position of peak antinode displacement, that moves farther to the midspan section as μ^2 increases. The same parameter affects the antinode upward displacements that increase with the deck relative stiffness. In fact as the cables initial tension reduce consequently the geometric flexural stiffness contribution reduces too, hence their deformed shape is much more pronounced.

Since the second order of a suspension string alone would be a double wave sinusoidal with the central part uplifted. Consequently, the lower is the cables flexural stiffness contribution the higher is that uplift.

Much more interesting is the evolution of modal shapes as the main parameters μ^2 and λ_L^2 are tuned. In fact the transition is now much more complex, passing from a mode characterised by 2 then by 0 and finally by 4 internal nodes as the Irvine parameter increases.

This requires further investigations of the modal properties in order to find a second Cross Over Mode in correspondence of null midspan displacement and making the modal shape transit from a 2 node to a 0 node condition; and a third COM condition again as the midspan displacement vanishes but characterising the passage from a 0 to a four node modal shape.

Hence the condition required for a generic mode is the vanishing of the negative antinode displacement.

$$W_n(\xi) = \frac{\lambda_L^2}{\tilde{\omega}_{w,n}^2} \tilde{h}_{W,n} \cdot \left\{ 1 - \frac{1}{\psi_{w,n}^2 + \eta_{w,n}^2} \cdot \left(\eta_{w,n}^2 \cdot \frac{\cosh\left(\psi_{w,n} \cdot \left(\xi - \frac{1}{2}\right)\right)}{\cosh\left(\frac{\psi_{w,n}}{2}\right)} + \psi_{w,n}^2 \cdot \frac{\cos\left(\eta_{w,n} \cdot \left(\xi - \frac{1}{2}\right)\right)}{\cos\left(\frac{\eta_{w,n}}{2}\right)} \right) \right\}_{\xi=\xi_{min}} = 0 ;$$

Notice that this condition is not required by the first order modes since the vanishing of lateral slopes grant it automatically.

Since in general the position of the antinode points varies with the actual values of the parameters μ^2 and λ_L^2 need to enforce the vanishing of the slope in order to find the stationary point and then find the minima searching for negative curvatures.

The only cases that allows simpler treatment are those related to the usual flexible deck condition ($\mu^2 = 0$) and the generic condition ($\forall \mu^2$) for the mode 2.

Let's start from the latter one. The fact that we are dealing with the second order mode simplify the treatment since the position of the minimum antinode displacement is known a priori ($\xi_{min} = \frac{1}{2}$).

On the contrary the first case as usual the flexible deck condition allows analytical results. In fact the COM condition reduces to the following relation.

$$W_n(\xi_{min}) = \frac{\lambda_L^2}{\tilde{\omega}_{w,n}^2} \tilde{h}_{W,n} \cdot \left\{ 1 - \frac{\cos\left(\tilde{\omega}_{w,n} \cdot \left(\xi - \frac{1}{2}\right)\right)}{\cos\left(\frac{\tilde{\omega}_{w,n}}{2}\right)} \right\}_{\xi=\xi_{min}} ;$$

First if all need to define the position of the antinode displacement.

$$\frac{d}{d\xi} W_n(\xi) = \frac{\lambda_L^2}{\tilde{\omega}_{w,n}^2} \tilde{h}_{W,n} \cdot \left\{ \tilde{\omega}_{w,n} \cdot \frac{\sin\left(\tilde{\omega}_{w,n} \cdot \left(\xi - \frac{1}{2}\right)\right)}{\cos\left(\frac{\tilde{\omega}_{w,n}}{2}\right)} \right\} = 0 \Leftrightarrow \tilde{\omega}_{w,n} \cdot \left(\xi - \frac{1}{2}\right) = k\pi \text{ with } k \in \mathbb{N} \setminus \{0\} ;$$

Hence.

$$\xi = \xi_{staz} = \frac{1}{2} + \frac{k\pi}{\tilde{\omega}_{w,n}} ;$$

It's evident that the latter relation gives the actual position of the minimum antinode point of the 2 order mode as $= 0$. Hence it's possible to link the parameter k to the actual modal order.

$$k = n - 2 ;$$

Then enforce positive curvature since the positive displacements convention is downward, and hence upward min displacements are characterised by such kind of curvatures.

$$\frac{d^2}{d\xi^2} W_n(\xi_{min}) = \frac{\lambda_L^2}{\tilde{\omega}_{w,n}^2} \tilde{h}_{W,n} \cdot \left\{ \tilde{\omega}_{w,n}^2 \cdot \frac{\cos\left(\tilde{\omega}_{w,n} \cdot \left(\xi_{staz} - \frac{1}{2}\right)\right)}{\cos\left(\frac{\tilde{\omega}_{w,n}}{2}\right)} \right\} \geq 0 \Leftrightarrow \cos(k\pi) \geq 0 \Leftrightarrow k = \text{even} ;$$

Hence the previous relation becomes as follows.

$$k = 2 \cdot (n - 2) \Rightarrow \xi_{min} = \frac{1}{2} \pm \frac{2 \cdot (n-2)\pi}{\tilde{\omega}_{w,n}} ;$$

Finally substituting in the initial modal shape we get the following condition.

$$W_n\left(\xi_{min} = \frac{1}{2} + \frac{2 \cdot (n-2)\pi}{\tilde{\omega}_{w,n}}\right) = \frac{\lambda_L^2}{\tilde{\omega}_{w,n}^2} \tilde{h}_{W,n} \cdot \left\{ 1 - \frac{\cos(2 \cdot (n-2)\pi)}{\cos\left(\frac{\tilde{\omega}_{w,n}}{2}\right)} \right\} = 0 \quad \forall n$$

The meaning of the last statement is that for perfectly flexible deck the transition from a 2 to a 0 node condition is doesn't depend on the actual value of the Irvine parameter λ_L^2 .

Lets' comment some numerical results obtained for the second mode of vibration.

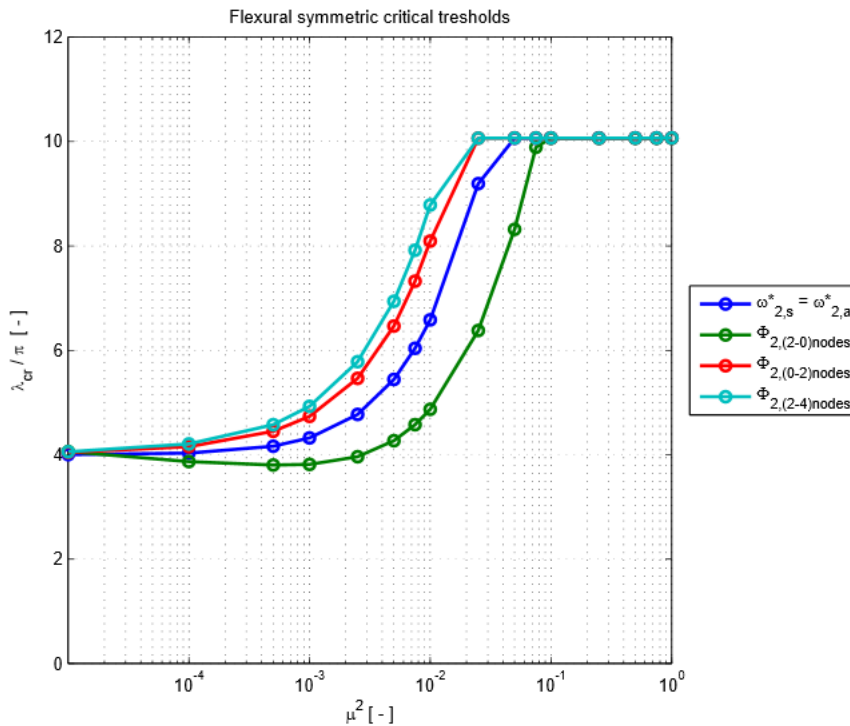


Figure 2.14_ Cross Over Frequency and Mode thresholds of Mode 2.

As for circular eigen-frequencies the Cross Over Frequency is constant for very flexible decks ($\mu^2 \leq 10^{-4}$) and cannot be tuned beyond $\mu^2 = 2 \cdot 10^{-2}$.

With respect to the first symmetric mode the transition of modal shapes for higher order modes are always three as the Irvine parameter increases. Starting from the one with $2 \cdot (n - 1)$ internal nodes, then passing by Cross Over Frequency condition to increase further to reach the one with 0 internal nodes and ending with the last one with $2 \cdot n$ internal nodes.

Here the transition from 2 to 0 internal nodes occurs in correspondence of values for the critical Irvine parameter lower than the Cross Over Frequency, at least for not perfectly flexible deck. In fact all the curves collapse to the same critical λ_L^2 only for deck relative stiffnesses lower than ($\mu^2 = 10^{-5}$).

This means that for the special case of perfectly flexible deck both the Cross Over Frequency and the three Cross Over Mode conditions occurs at the same critical value for λ_L^2 .

This explain why we found that for $\mu^2 = 0$ the condition for null negative antinodal displacement is satisfied for any modes independently from the value assumed by the Irvine parameter. In fact once we reach the COF we satisfy all four possible conditions simultaneously.

Focusing on the 2 to 0 nodes transition curve, is possible to see that approximately for μ^2 belonging to the interval ($10^{-5} \div 2 \cdot 10^{-3}$) the critical λ_L^2 required is lower than the one required for perfectly flexible deck. This means that the initial increase of the flexural stiffness of the deck gives a huge contribution to grant null midspan displacement, but beyond a certain threshold ($\mu^2 = 2 \cdot 10^{-3}$) since the midspan uplift increases higher values for λ_L^2 are required.

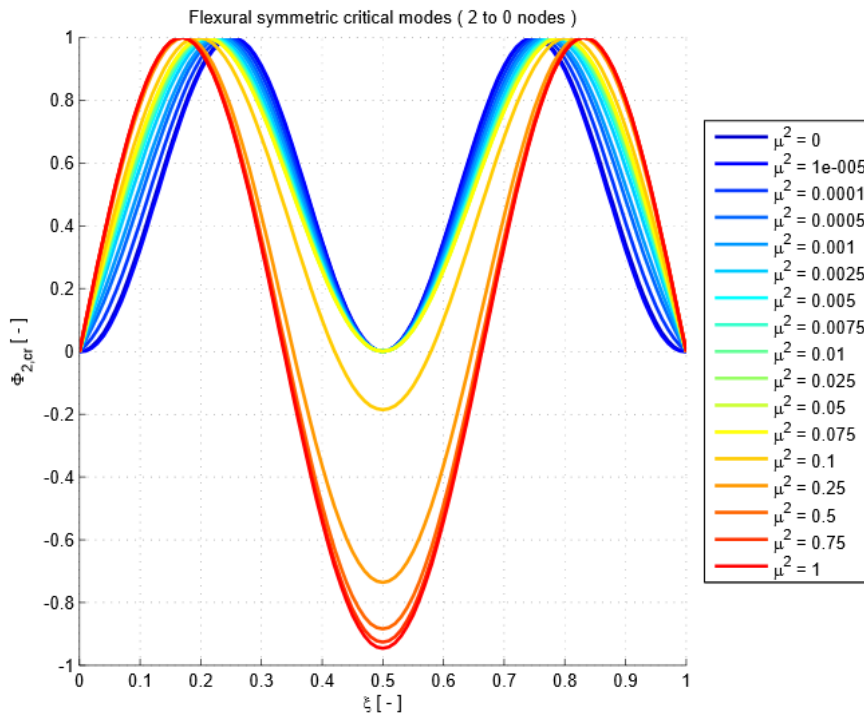


Figure 2.15_ Cross Over Modes of Mode 2 for 2-0 nodes transition.

From the last image is evident that beyond ($\mu^2 = 0.1$) is no more possible to tune the Irvine parameter in order to obtain null midspan displacements.

With respect to the previous limit curve the ones associated to the 0 to 2 and the 2 to 4 internal nodes transitions are both monotonically increasing and with a threshold value of $\mu^2 = 10^{-2}$ beyond which those transitions are no more feasible. The last statement is much clearer from the next two figures.

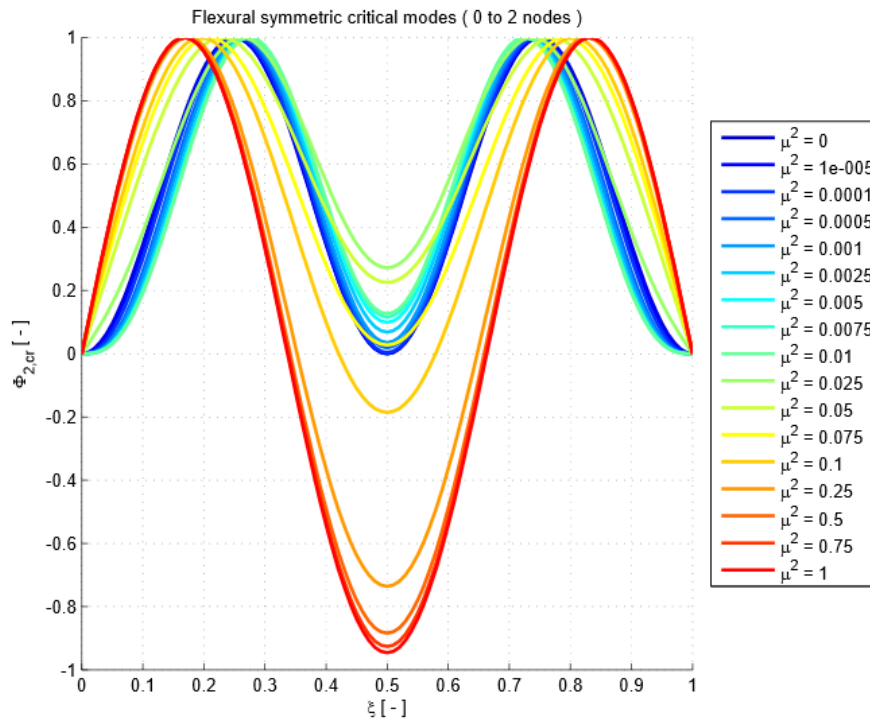


Figure 2.16_ Cross Over Modes of Mode 2 for 0-2 nodes transition.

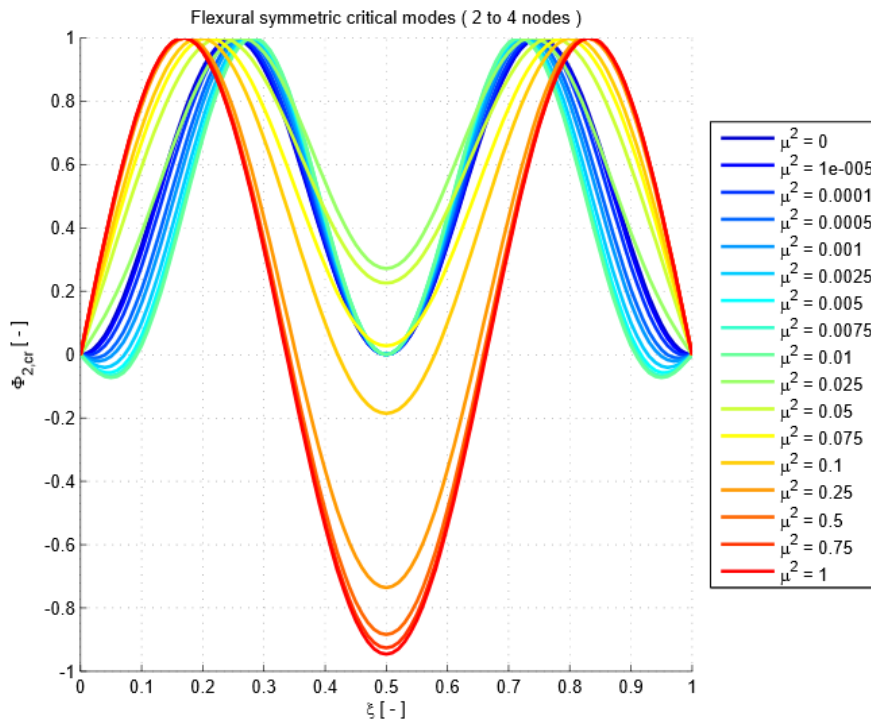


Figure 2.17_ Cross Over Modes of Mode 2 for 2-4 nodes transition.

Another important thing that can be notice for any choice of the modal order is that once λ_L^2 overcome the last COM condition that grants generally the transition to the $2 \cdot n$ internal nodes modal shape, rapidly all the negative antinodal displacements becomes equal and remains for any higher value of λ_L^2 .

2.3.2. Torsional vibrations

As for the flexural counterpart the parameters affecting the torsional equation of motion change depending if we are considering symmetric or skew symmetric modes.

For the symmetric ones is necessary to define the warping coefficient χ^2 together with the deck to cable torsional stiffness ratio β^2 and the Irvine parameter in order to compute circular eigen-frequencies and the associate modal shapes.

On contrary for skew-symmetric modes the eigen-vectors are simply sinusoidal with a prescribed half wave length proportional to the modal number and it's not influenced directly by the circular eigen-frequency that depends only on the modal number and on χ^2 and β^2 .

Concluding, the parameters of interest would be the following.

$$n \quad ; \quad \lambda_L^2 = \frac{E_c A_c l}{H L_c} (y'' l)^2 \quad ; \quad \chi^2 \quad ; \quad \beta^2 = \frac{G_d J_d}{2 H b^2} ;$$

From literature has been possible to define reliable values for such parameters, from different [31-40] we take the values of 10 bridges including the Innoshima, Runyang, HuMen, Takoma Narrows, Golden Gate, Vincent Thomas, Bosphorus I, Fatih Sultan Mehmet, Great Belt, Humber and Taizhou Bridges.

The center –span ranges from 458 to 1624 meters, hence the Irvine parameter has a bimodal distribution, ranging from 61 up to 134 for six of the bridges and for the remaining from 168 to 304, with a global average value of 162. In this case the cables data refer directly to the central main span.

Hence as for the flexural motion in the following we will consider values for the cables parameter corresponding to 0 to take in account for the flat cables condition, 100 and 225 to represent the bimodal behaviour seen from real data, and ∞ for the inextensible cables situation.

$$\lambda_L^2 = [0 \quad ; \quad 100 \quad ; \quad 225 \quad ; \quad \infty \quad] ;$$

The relative deck torsional stiffness parameter ranges from $1.2 \cdot 10^{-4}$ for the Tacoma Narrows Bridge to 65.3 for the Bosphorus I, with an average value for the remaining bridges close to 10.

Hence seems that values ranging from $0.5 \cdot 10^{-4}$ up to 50 would span most of the typical situations, but in the following this array will be enlarged in order to take in account some extreme conditions from 0 to include the flexible deck condition and 100 for the opposite rigid deck condition.

$$\beta^2 = [0 \quad \dots \quad 0.5 \cdot 10^{-4} \quad \dots \quad 50 \quad \dots \quad 100 \quad] ;$$

By last we leave the warping coefficient that generally can be neglected when dealing with closed box section girders for which the primary S. Venant torsional stiffness is predominant on the secondary one related to Vlasov-Wagner theory. But when dealing with thin walled open section girders as that of the Takoma Narrows things changes drastically with values of the warping coefficient nearly to vanish.

From literature has been possible to find data referring to the Innoshima, Golden Gate, Tacoma Narrows and Vincent Thomas Bridges. Except for the Tacoma Narrows bridge characterised by a warping coefficient of about 0.31 the others three values ranges from 805.7 to 2941.28.

Hence in order to be able to describe both the situation we assume to consider the extreme situations.

$$\chi^2 = [0 ; \infty]$$

Let's analyse the results obtained for the first two relevant modes.

i. Circular eigen-frequencies:

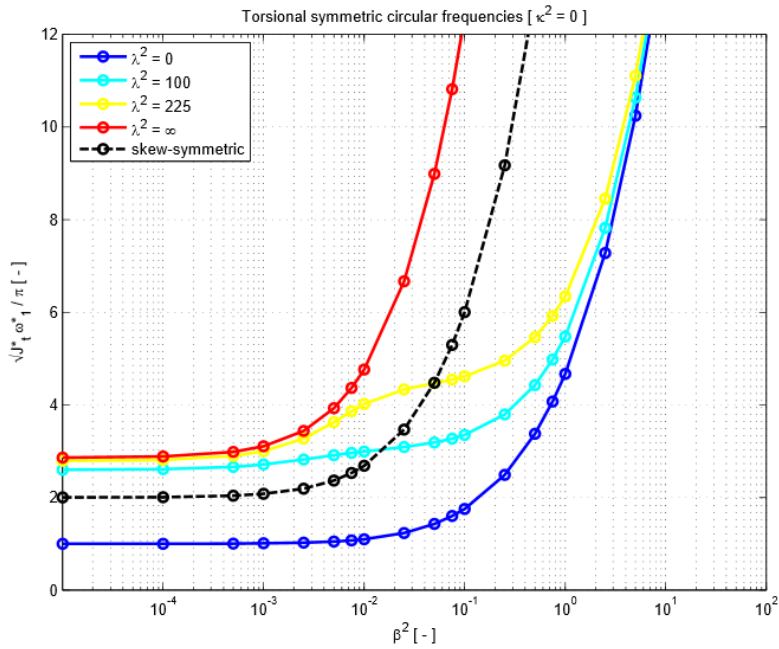


Figure 2.18_Torsional circular eigen-frequencies of Mode 1 for $\chi^2 = 0$.

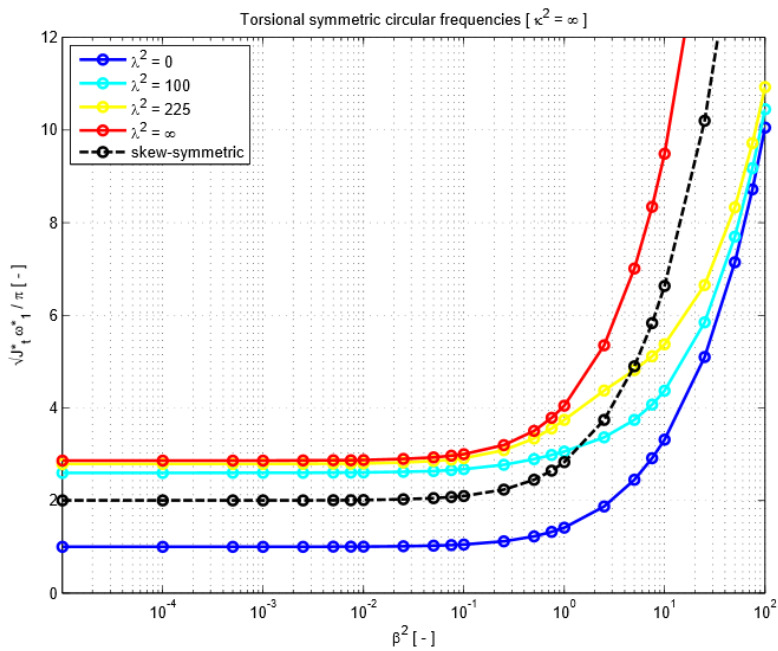


Figure 2.19_Torsional circular eigen-frequencies of Mode 1 for $\chi^2 = \infty$.

First of all notice that increasing the warping coefficient the structure is more and more flexible and consequently we get higher lower eigen-frequencies.

For $\chi^2 = 0$ and $\chi^2 = \infty$ the circular eigen-frequencies remains constant as long as $\beta^2 < 10^{-4}$ and $\beta^2 < 10^{-1}$ respectively meaning that the deck torsional relative stiffness β^2 is no more influent on them, becoming dominant the cables contribution. This threshold reduces in higher order modes. On the contrary the effect of β^2 become more and more relevant increasing the cable parameter λ_L^2 and the modal order as it's evident from next figures.

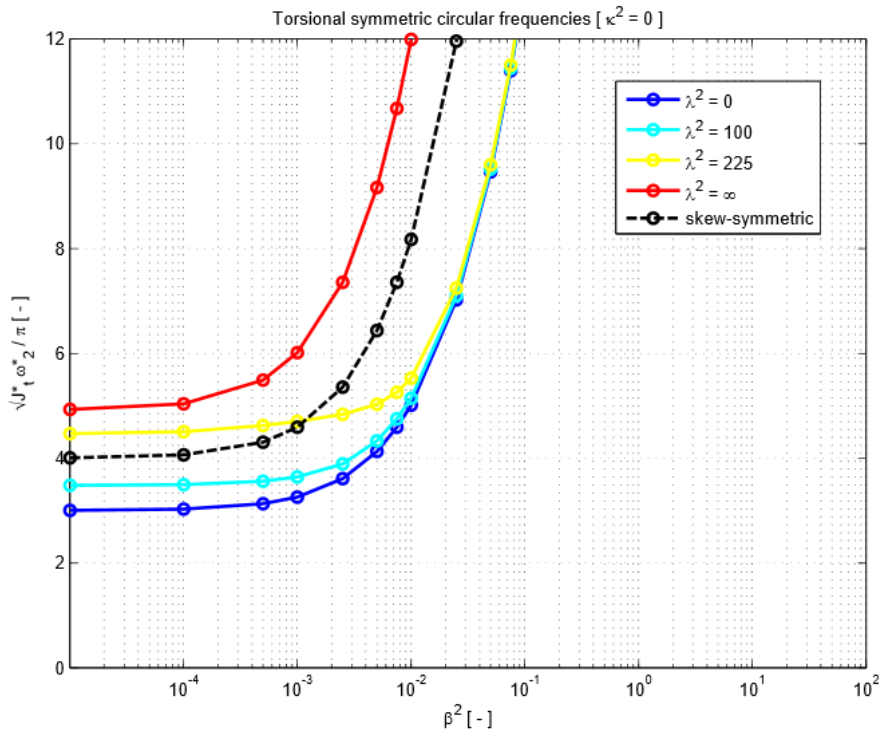


Figure 2.20_Torsional circular eigen-frequencies of Mode 2 for $\chi^2 = 0$.

Also for the torsional motion it's evident that for finite values of λ_L^2 as the deck relative torsional stiffness parameter increases, all curves of the circular eigen-frequencies tend to collapse on that one characterised by $\lambda_L^2 = 0$. This means that beyond certain level of deck rigidity the cables contribution to torsional vibrations has no more effects on the structural response in time. These limits are $\beta^2 > 5$ for the second symmetric modes characterised by $\chi^2 = 0$ and $\beta^2 > 7.5$ for the one associated to $\chi^2 = \infty$.

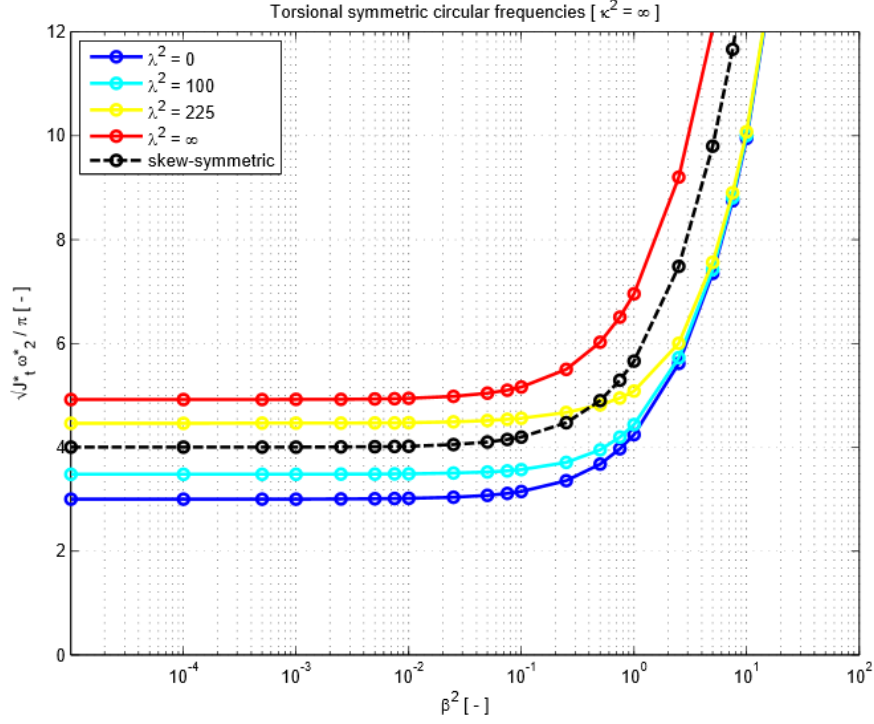


Figure 2.21_ Torsional circular eigen-frequencies of Mode 2 for $\chi^2 = \infty$.

As mentioned above is evident that the deck torsional stiffness parameter threshold reduces to $\beta^2 < 10^{-5}$ and $\beta^2 < 10^{-2}$ respectively for $\chi^2 = 0$ and $\chi^2 = \infty$.

The same relation between the frequencies of subsequent modes found for flexural motion is valid for the torsional case.

$$\omega_{m+1}^*(\lambda_L^2 = 0, \forall \chi^2, \forall \beta^2) \approx \omega_m^*(\lambda_L^2 = \infty, \forall \chi^2, \forall \beta^2);$$

Can be of interest to find the critical conditions that leads a symmetric modal shape to vibrate according to the circular eigen-frequency of the corresponding skew symmetric one.

In fact is evident from the previous figures that tuning properly the structural properties it's possible to reach this condition that we will call Cross Over Frequency (COF).

Let's analyse analytically the conditions that leads to this particular situation.

$$\tilde{J}_t \cdot (\tilde{\omega}_{\vartheta,m}^a)^2 = (2m\pi)^2 \cdot \left[1 + \beta^2 + \frac{\beta^2}{\chi^2} \cdot (2m\pi)^2 \right];$$

$$\tilde{J}_t \cdot (\tilde{\omega}_{\vartheta,m}^s)^2 = \lambda_L^2 \cdot \left[1 - \frac{1}{\psi_{\vartheta,m}^2 + \eta_{\vartheta,m}^2} \cdot \left(\eta_{\vartheta,m}^2 \cdot \frac{\tanh\left(\frac{\psi_{\vartheta,m}}{2}\right)}{\frac{\psi_{\vartheta,m}}{2}} + \psi_{\vartheta,m}^2 \cdot \frac{\tan\left(\frac{\eta_{\vartheta,m}}{2}\right)}{\frac{\eta_{\vartheta,m}}{2}} \right) \right];$$

In the general situation the COF condition requires an iterative solution of the following equality.

$$(\lambda_L^2)_{cr} = (2m\pi)^2 \cdot \left[1 + \beta^2 + \frac{\beta^2}{\chi^2} \cdot (2m\pi)^2 \right] \cdot \left[1 - \frac{1}{\Psi_{\vartheta,m}^2 + \eta_{\vartheta,m}^2} \cdot \left(\eta_{\vartheta,m}^2 \cdot \frac{\tanh\left(\frac{\Psi_{\vartheta,m}}{2}\right)}{\frac{\Psi_{\vartheta,m}}{2}} + \Psi_{\vartheta,m}^2 \cdot \frac{\tan\left(\frac{\eta_{\vartheta,m}}{2}\right)}{\frac{\eta_{\vartheta,m}}{2}} \right) \right]^{-1};$$

Hence for each values of the deck relative torsional stiffness parameter β^2 is possible to define a critical value for the Irvine parameter that grant the cross over condition.

Let's simplify the treatment considering the case of perfectly free warping deck $\chi^2 = \infty$.

$$\tilde{J}_t \cdot (\tilde{\omega}^a_{\vartheta,m})^2 = (2m\pi)^2 \cdot (1 + \beta^2);$$

$$\tilde{J}_t \cdot (\tilde{\omega}^s_{\vartheta,m})^2 = \lambda_L^2 \cdot \left[1 - \frac{\tan\left(\frac{1}{2} \sqrt{\frac{\tilde{J}_t}{(1+\beta^2)}} \tilde{\omega}^s_{\vartheta,m}\right)}{\left(\frac{1}{2} \sqrt{\frac{\tilde{J}_t}{(1+\beta^2)}} \tilde{\omega}^s_{\vartheta,m}\right)} \right];$$

Enforcing the COF threshold condition we get the following relation.

$$(\tilde{\omega}^s_{\vartheta,m})^2 = (\tilde{\omega}^a_{\vartheta,m})^2 \Rightarrow \lambda_L^2 \cdot \left[1 - \frac{\tan(m\pi)}{m\pi} \right] = (2m\pi)^2 \cdot (1 + \beta^2) \Rightarrow (\lambda_L^2)_{cr,0} = (2m\pi)^2 \cdot (1 + \beta^2);$$

ii. Modal shapes:

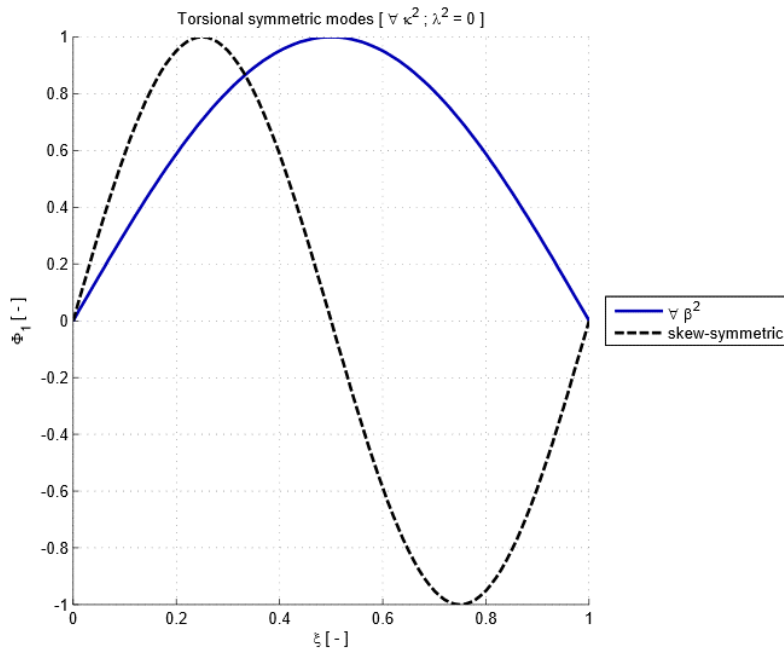


Figure 2.22_ Modal shape of Mode 1 for $\lambda_L^2 = 0$ and skew-symmetric condition.

In both the situation of skew symmetric modes or very taut cables, the stiffening contribution vanishes and hence the bridge vibrates according to a sinusoidal shape proper of strings. Notice that the modal shapes are identical to that found for flexural motion under the same conditions in terms of flexural parameters, since both the deck torsional stiffness parameter β^2 and the warping coefficient χ^2 have no effect on the modal shape.

Let's sketch the modal shapes associate to $\chi^2 = 0$.

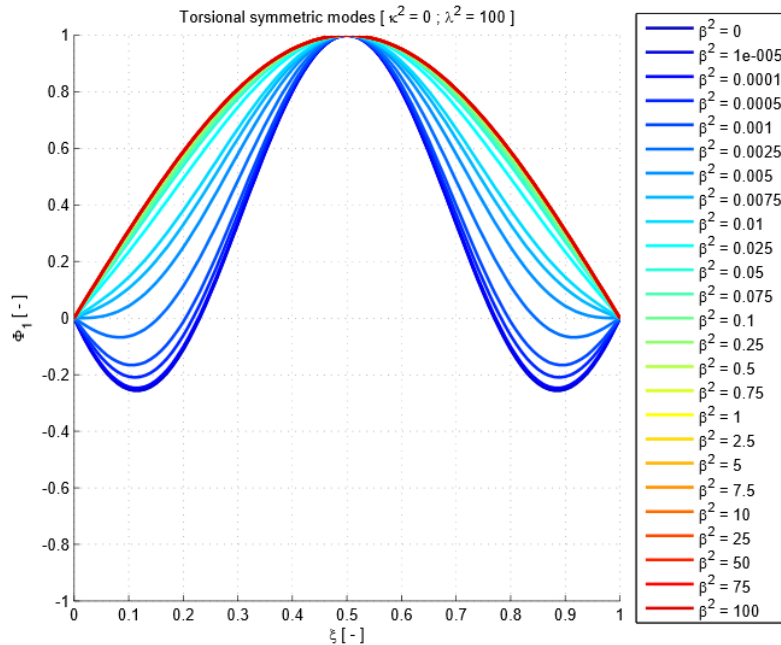


Figure 2.23_ Modal shape of Mode 1 for $\chi^2 = 0$ and $\lambda_L^2 = 100$.

At first sight it's clear that for finite values of the Irvine parameter λ_L^2 beyond $\beta^2 = 1$ the effect of cables has no more effect on the torsional modal shape.

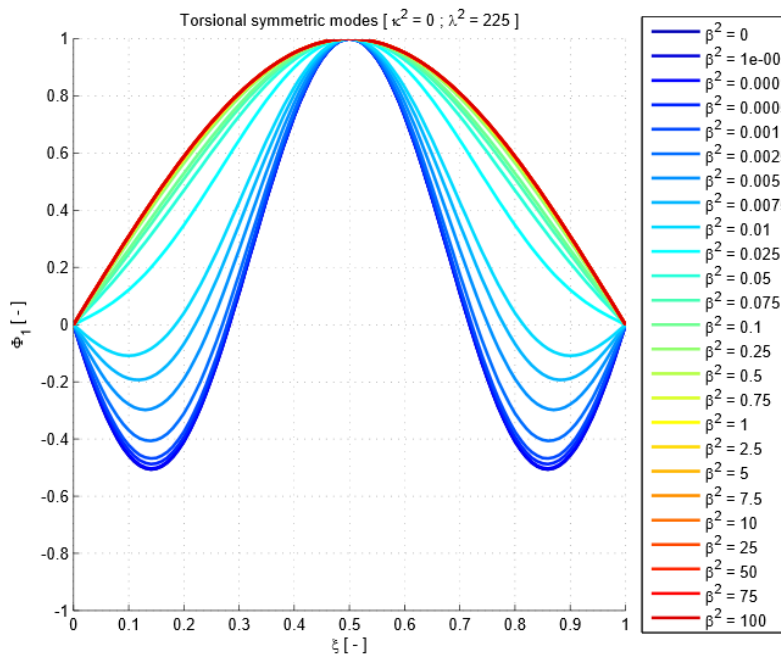


Figure 2.24_ Modal shape of Mode 1 for $\chi^2 = 0$ and $\lambda_L^2 = 225$.

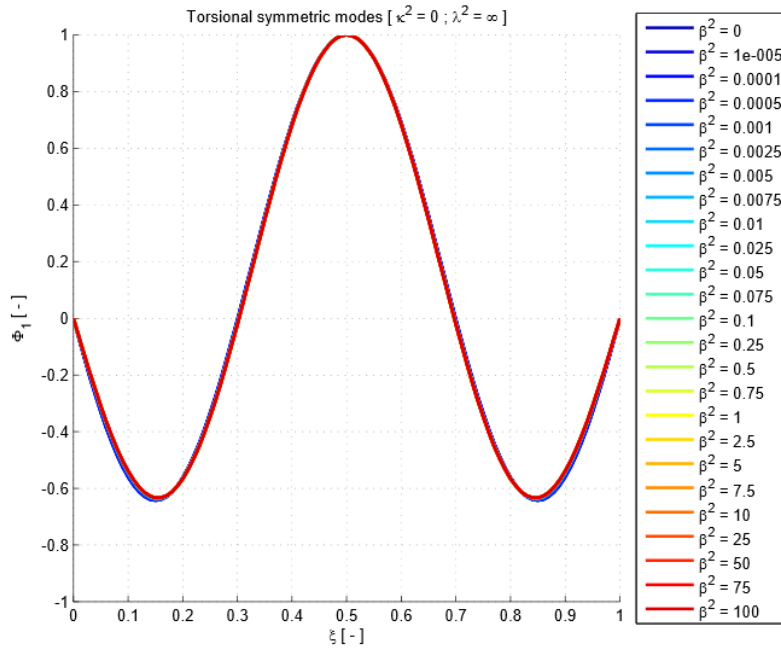


Figure 2.25_ Modal shape of Mode 1 for $\chi^2 = 0$ and $\lambda_L^2 = \infty$.

Then the free warping condition $\chi^2 = \infty$ leads to the following modal shapes.

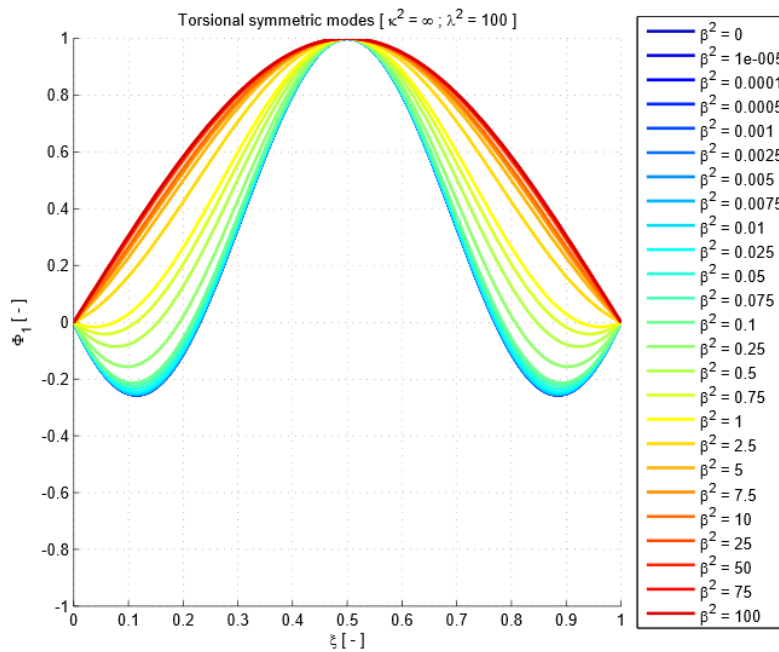


Figure 2.26_ Modal shape of Mode 1 for $\chi^2 = \infty$ and $\lambda_L^2 = 100$.

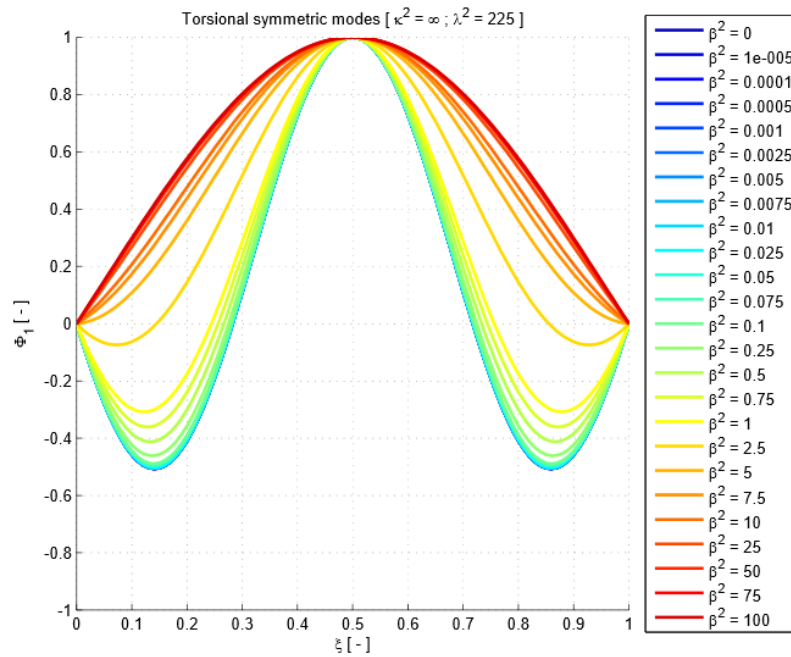


Figure 2.27_Modal shape of Mode 1 for $\chi^2 = \infty$ and $\lambda_L^2 = 225$.

Again for finite values of the Irvine parameter λ_L^2 there exist a threshold beyond which the deck relative torsional stiffness ($\beta^2 > 50$) has no more influence on the modal shapes, but with respect to the case $\chi^2 = 0$ is an order of magnitude higher due to the flexibility introduced by the free warping condition.

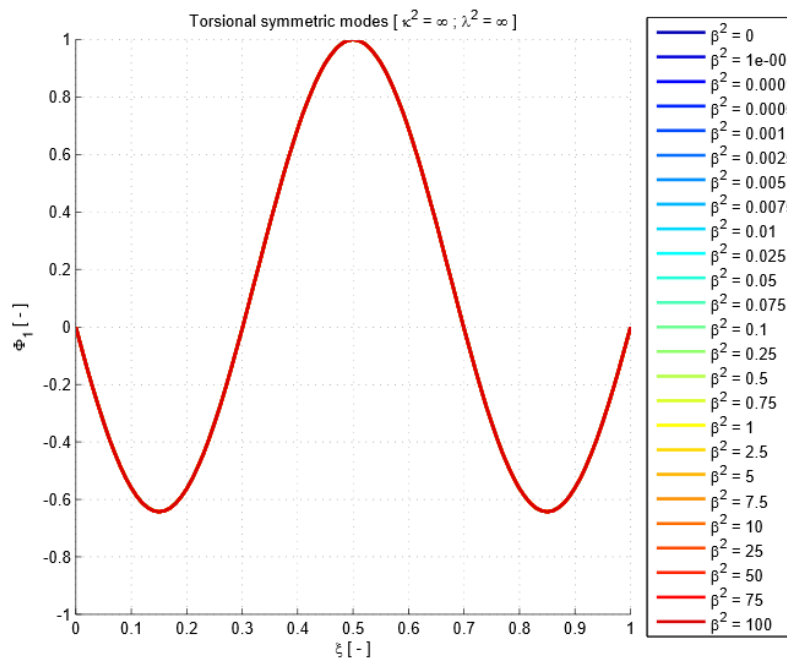


Figure 2.28_Modal shape of Mode 1 for $\chi^2 = \infty$ and $\lambda_L^2 = \infty$.

On the contrary for perfectly inextensible cables the torsional response in space is practically unaffected by the deck relative stiffness β^2 in both the cases char characterised by $\chi^2 = \infty$ and $\chi^2 = 0$, although in the second condition a slight contribution can be seen since because of the extremely high warping rigidity of the deck.

For both the cases $\chi^2 = \infty$ and $\chi^2 = 0$ the increase of the Irvine parameter λ_L^2 leads to higher negative rotations as consequence of the combined action of two opposite flexural motion of the deck and cables system.

The deck relative stiffness parameter β^2 has a great influence on standard symmetric modal shapes, and this peculiarity increases as it assumes values far from extreme conditions and the cables stiffness parameter decreases. In fact as the latter increases the modal shapes collapses to the lower curves meaning that the as the cable inextensibility grows the influence of the deck relative torsional stiffness become more and more negligible.

Another interesting feature is evident as λ_L^2 increases. In fact is possible to define a critical value beyond which the modal shape internal nodes number changes. In general we will refer to it as to the Cross Over Mode (COM), that for the first symmetric modes ensure the passage from a zero to a two node modal shape. This critical condition changes with β^2 and can be define by the following relation that enforce the vanishing of the first derivative at the two extremities of the span.

$$\begin{aligned} \left[\frac{d}{d\xi} \Theta_m(\xi) \right]_{\xi=0} &= \frac{\lambda_L^2}{\tilde{J}_t \cdot \tilde{\omega}_{\vartheta,m}^2} \tilde{h}_{\vartheta,m} \cdot \left\{ -\frac{\eta_{\vartheta,m} \cdot \Psi_{\vartheta,m}}{\Psi_{\vartheta,m}^2 + \eta_{\vartheta,m}^2} \cdot \left(\eta_{\vartheta,m} \cdot \frac{\sinh\left(\Psi_{\vartheta,m} \cdot \left(\xi - \frac{1}{2}\right)\right)}{\cosh\left(\frac{\Psi_{\vartheta,m}}{2}\right)} + \right) \right\}_{\xi=0} = \\ &= \frac{\lambda_L^2}{\tilde{J}_t \cdot \tilde{\omega}_{\vartheta,m}^2} \tilde{h}_{\vartheta,m} \cdot \left\{ -\frac{\eta_{\vartheta,m} \cdot \Psi_{\vartheta,m}}{\Psi_{\vartheta,m}^2 + \eta_{\vartheta,m}^2} \cdot \left(\eta_{\vartheta,m} \cdot \tanh\left(\frac{\Psi_{\vartheta,m}}{2}\right) + \right) \right\} \geq 0 ; \end{aligned}$$

That reduces to the following condition that grants counter-clockwise torsion at the two ends.

$$\eta_{\vartheta,m} \cdot \tanh\left(\frac{\Psi_{\vartheta,m}}{2}\right) \geq \Psi_{\vartheta,m} \cdot \tan\left(\frac{\eta_{\vartheta,m}}{2}\right) ;$$

Notice that the symmetry of the problem allows to consider simply one side of the deck.

The last condition can be solved only iteratively, hence to get an analytical expression let's consider the usual free warping deck limit condition ($\chi^2 = \infty$).

$$\begin{aligned} \Theta_m(\xi) &= \frac{\lambda_L^2}{\tilde{J}_t \cdot \tilde{\omega}_{\vartheta,m}^2} \tilde{h}_{\vartheta,m} \cdot \left\{ 1 - \frac{\cos\left(\sqrt{\frac{\tilde{J}_t}{(1+\beta^2)}} \tilde{\omega}_{\vartheta,m} \cdot \left(\xi - \frac{1}{2}\right)\right)}{\cos\left(\frac{1}{2} \sqrt{\frac{\tilde{J}_t}{(1+\beta^2)}} \tilde{\omega}_{\vartheta,m}\right)} \right\} \\ \Rightarrow \left[\frac{d}{d\xi} \Theta_m(\xi) \right]_{\xi=0} &= \frac{\lambda_L^2}{\tilde{J}_t \cdot \tilde{\omega}_{\vartheta,m}^2} \tilde{h}_{\vartheta,m} \cdot \left\{ -\sqrt{\frac{\tilde{J}_t}{(1+\beta^2)}} \cdot \tilde{\omega}_{\vartheta,m} \cdot \tan\left(\frac{1}{2} \sqrt{\frac{\tilde{J}_t}{(1+\beta^2)}} \cdot \tilde{\omega}_{\vartheta,m}\right) \right\} ; \end{aligned}$$

Hence enforcing the COM condition for the 0 to 2 node transition leads to.

$$\left[\frac{d}{d\xi} \theta_m(\xi) \right]_{\xi=0} \geq 0 \Leftrightarrow \tan \left(\frac{1}{2} \sqrt{\frac{\tilde{J}_t}{(1+\beta^2)}} \cdot \tilde{\omega}_{\vartheta,m} \right) \leq 0 \Leftrightarrow \left(\frac{\pi}{2} + m\pi \right) \leq \left(\frac{1}{2} \sqrt{\frac{\tilde{J}_t}{(1+\beta^2)}} \cdot \tilde{\omega}_{\vartheta,m} \right) \leq (\pi + m\pi)$$

Notice that in the last condition is implicitly assumed that the cables stiffening term is positive as generally happens.

After few computations we can find the following final expression.

$$(2m + 1) \cdot \pi \cdot \sqrt{(1 + \beta^2)} \leq \sqrt{\tilde{J}_t} \cdot \tilde{\omega}_{\vartheta,m} \leq (2m + 1) \cdot \pi \cdot \sqrt{(1 + \beta^2)} + \pi \cdot \sqrt{(1 + \beta^2)}$$

$$\Rightarrow \sqrt{\tilde{J}_t} \cdot \tilde{\omega}^a_{\vartheta,m} \leq \sqrt{\tilde{J}_t} \cdot \tilde{\omega}^s_{\vartheta,m} \leq \sqrt{\tilde{J}_t} \cdot \tilde{\omega}^a_{\vartheta,m} + \pi \cdot \sqrt{(1 + \beta^2)};$$

Hence it's evident that at the limit condition the last relation correspond to the COF condition. This means that for infinitely free warping deck ($\chi^2 = \infty$) is possible to tune the structural parameters in such a way that at the same time the bridge oscillates according to a symmetric mode characterised by null side torsional slope and with the same frequency of vibration of the corresponding skew-symmetric mode. Again this is not feasible since both the frequency and the modal shape will be of symmetric case.

Hence the situation of perfectly flexible deck ($\beta^2 = 0$) is a subcase of the previous one, and it's not strictly require to get the satisfaction of both the COF and COM at the same time.

Has been performed a numerical rooting of the first COM condition for both perfectly rigid and flexible warping deck condition.

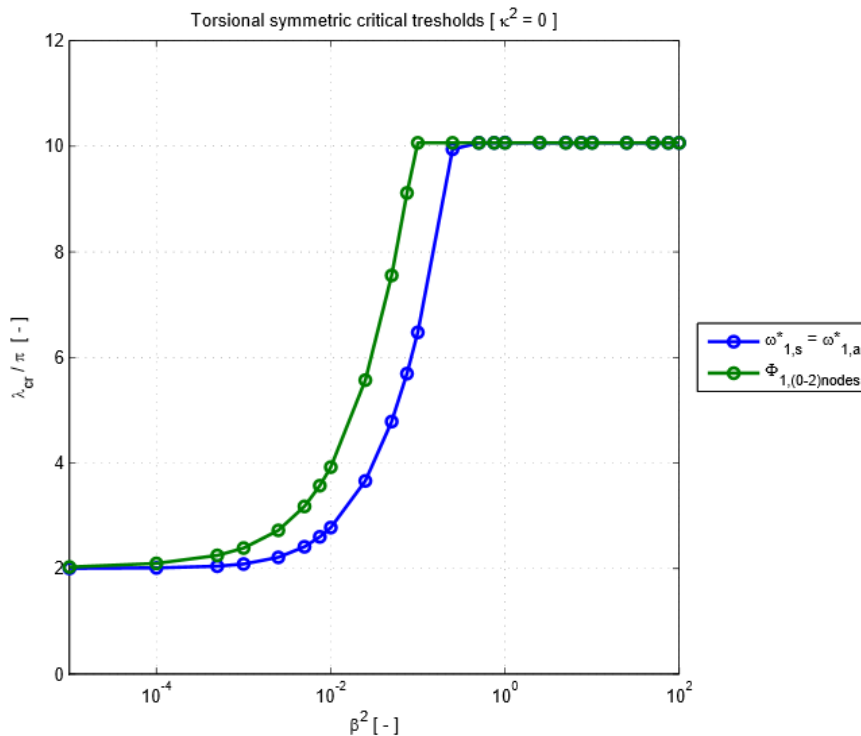


Figure 2.2936_Cross Over Frequency and Mode thresholds of Mode 1 for $\chi^2 = 0$.

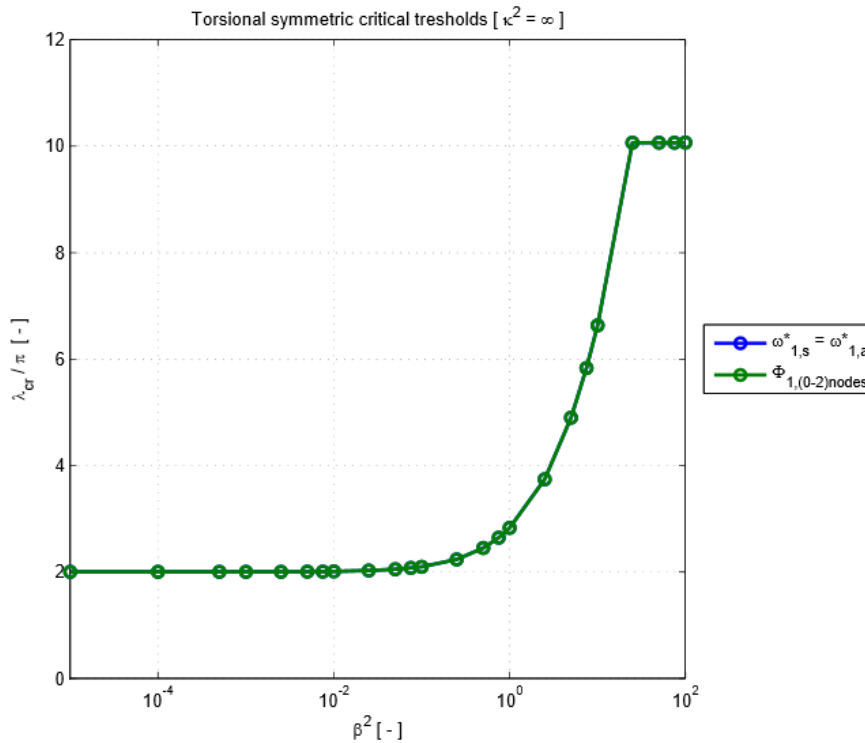


Figure 2.30_ Cross Over Frequency and Mode thresholds of Mode 1 for $\chi^2 = \infty$.

As it can be seen both the COF and COM limit for the flexible deck condition holds up to $\beta^2 = 10^{-2}$ only for $\chi^2 = \infty$, corresponding to the limit before which the circular eigen-frequencies of the first mode are practically constant with the deck relative stiffness parameter. For the opposite condition ($\chi^2 = 0$) we can find such threshold only for both the COF corresponding to $\beta^2 = 10^{-4}$ as for the circular eigen-frequencies curves.

Hence the main conclusion is that for finite values of χ^2 we can get different critical values for λ_L^2 for the COF and COM limit conditions, as happen for the flexural motion with different parameters.

Once again the max admissible values for normalised critical $\frac{\lambda_L}{\pi}$ is fixed to 10 since the corresponding value of λ_L^2 is equal to 1000, that is an excellent numerical representation of the inextensible cables limit condition $\lambda_L^2 = \infty$. In fact as can be seen for $\beta^2 > 10$ as $\chi^2 = \infty$ and $\beta^2 > 0.1$ as $\chi^2 = 0$ the values of $\frac{\lambda_L}{\pi}$ collapse to 10, meaning that for very stiff decks the Cross Over Frequency cannot be reached for any level of tension inside the cables.

On the other hand the limits for the Cross Over Modes are practically equal to that of COF as long as $\beta^2 \leq 10^{-5}$ for $\chi^2 = 0$ and for any β^2 if $\chi^2 = \infty$, but beyond that limit it diverges until collapse to the limit value of 10.

This means that in general ($\chi^2 < \infty$) is not possible to get a symmetric mode oscillating according to the same circular frequency of the associate skew-symmetric counterpart and with null torsional slope at the two end. Hence tuning properly the structural parameters for the COF condition we get a symmetric modal shape with counter-clockwise torsion at the two ends. Vice versa tuning those parameters for the COM condition leads to oscillations characterised with frequencies higher than that proper of the associate skew-symmetric mode.

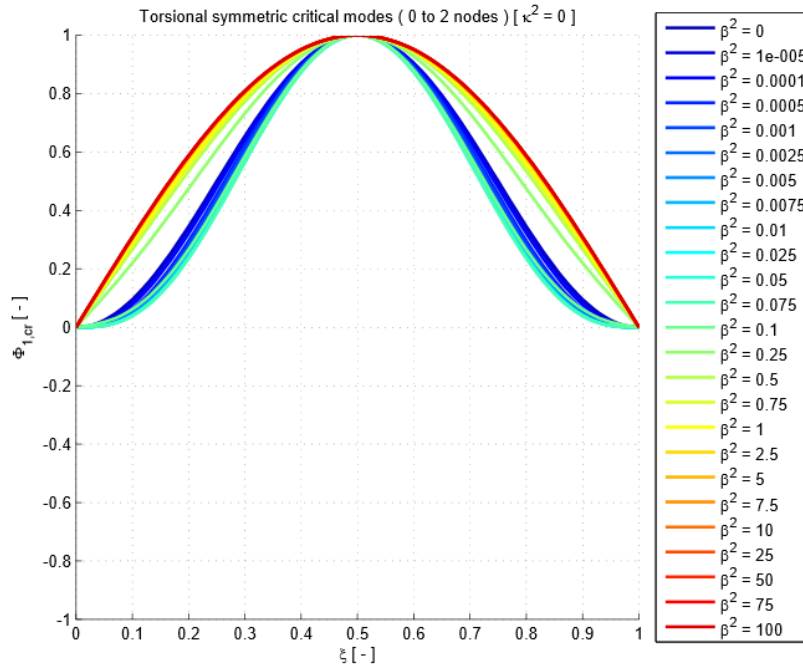


Figure 2.31_Cross Over Modes of Mode 1 for $\chi^2 = 0$.

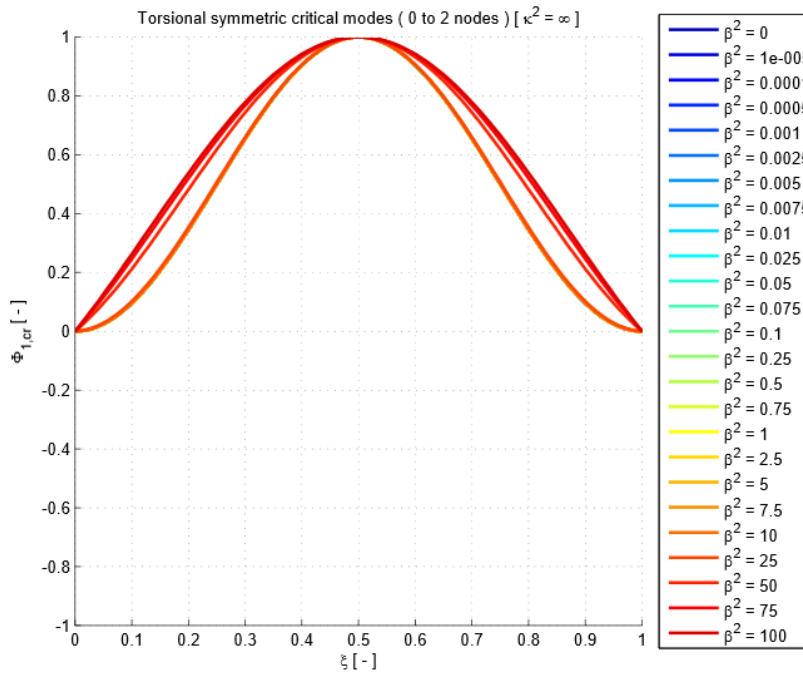


Figure 2.32_Cross Over Modes of Mode 1 for $\chi^2 = \infty$.

Plotting the critical modal shape with null side torsional slope for $\chi^2 = 0$ it's evident that beyond a certain limit ($\beta^2 = 0.1 \Rightarrow \frac{\lambda_L}{\pi} = 8.5$) the increment of the cables initial tension is no more able to grant the vanishing of the torsional slope at the two ends. This means that for too rigid deck is not possible to grant the COM condition also for cables tension lower than the limit taut cables situation ($\frac{\lambda_L}{\pi} = 10$).

On the other hand for $\chi^2 = \infty$ all the modal shapes collapses to the same curve if the COM can be reached ($\beta^2 < 10 \Rightarrow \frac{\lambda_L}{\pi} < 7$).

Let's now analyse the second order modal shapes.

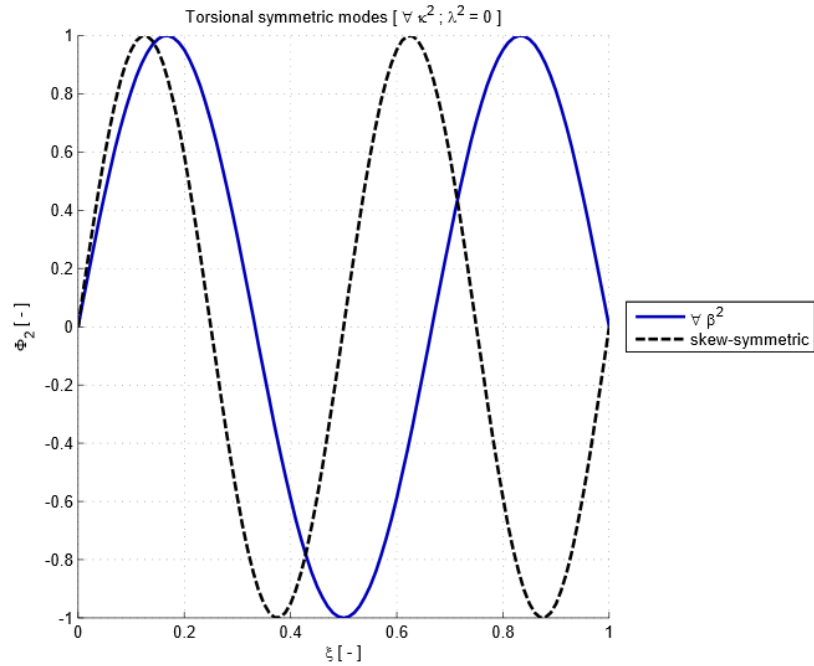


Figure 2.33_Modal shape of Mode 2 for $\lambda_L^2 = 0$ and skew-symmetric condition.

First analyse the perfectly rigid warping condition.

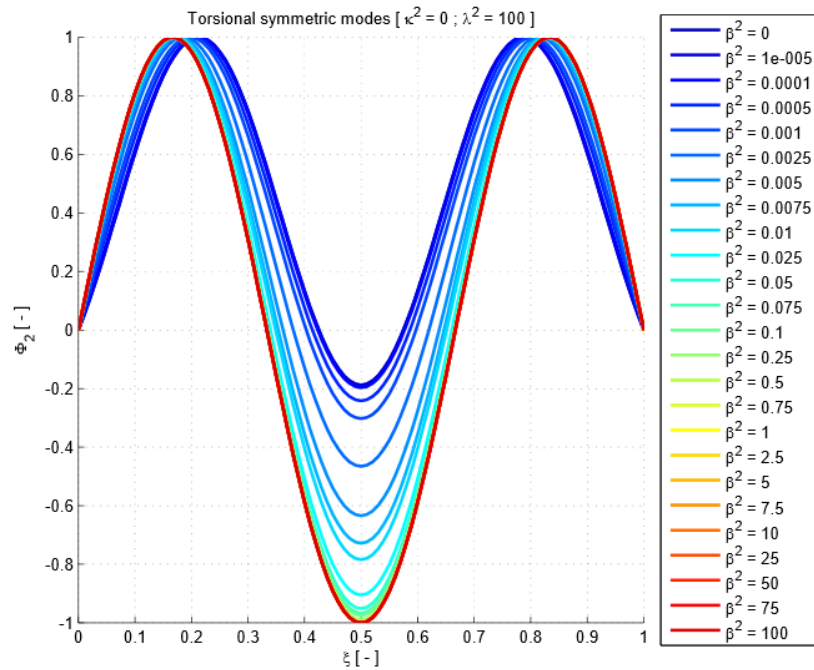


Figure 2.34_Modal shape of Mode 2 for $\chi^2 = 0$ and $\lambda_L^2 = 100$.

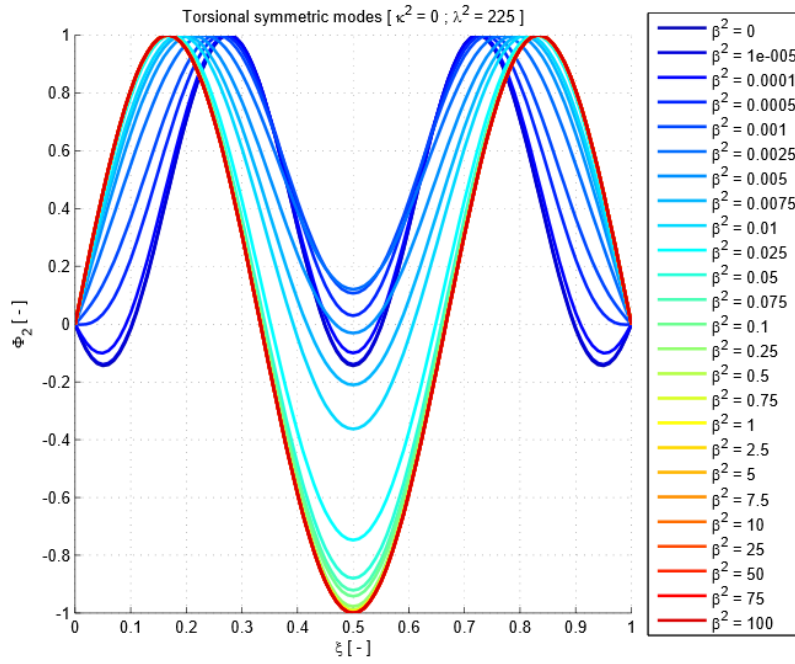


Figure 2.35_Modal shape of Mode 2 for $\chi^2 = 0$ and $\lambda_L^2 = 225$.

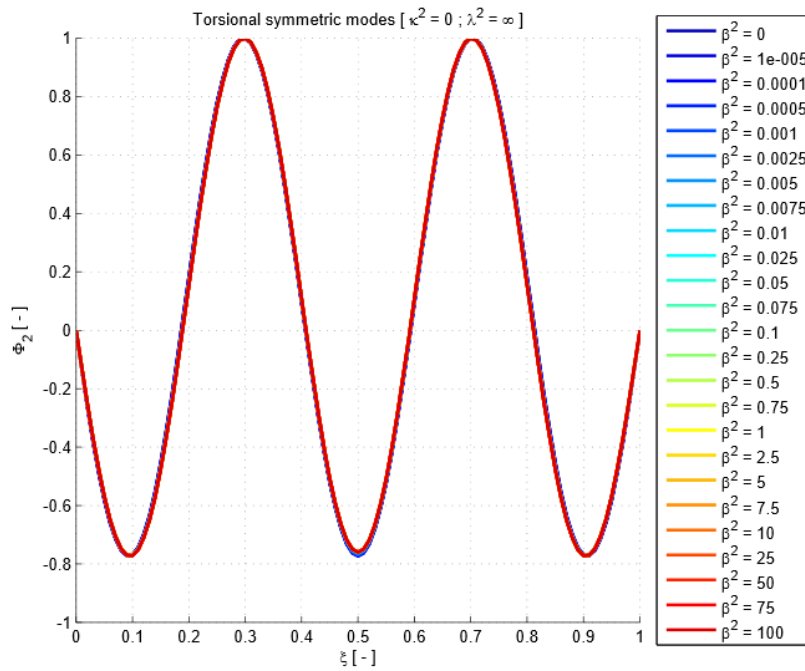


Figure 2.36_Modal shape of Mode 2 for $\chi^2 = 0$ and $\lambda_L^2 = \infty$.

Then the modes associate to the perfectly free warping condition.

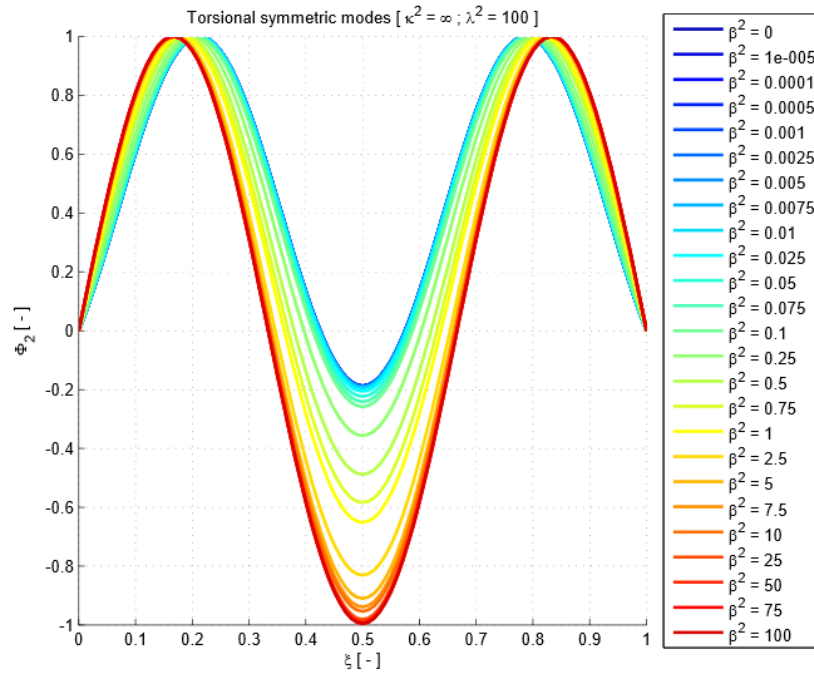


Figure 2.37_Modal shape of Mode 2 for $\chi^2 = \infty$ and $\lambda_L^2 = 100$.

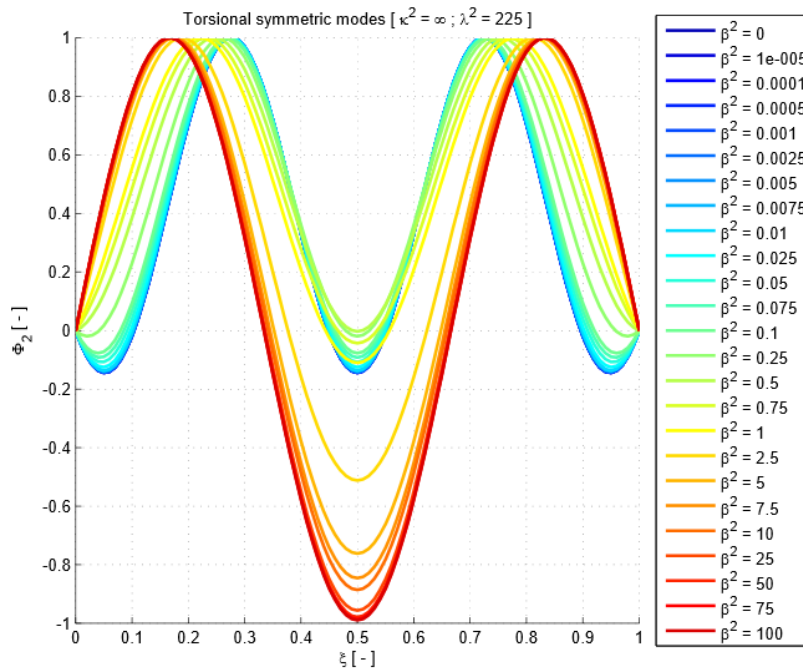


Figure 2.38_Modal shape of Mode 2 for $\chi^2 = \infty$ and $\lambda_L^2 = 225$.

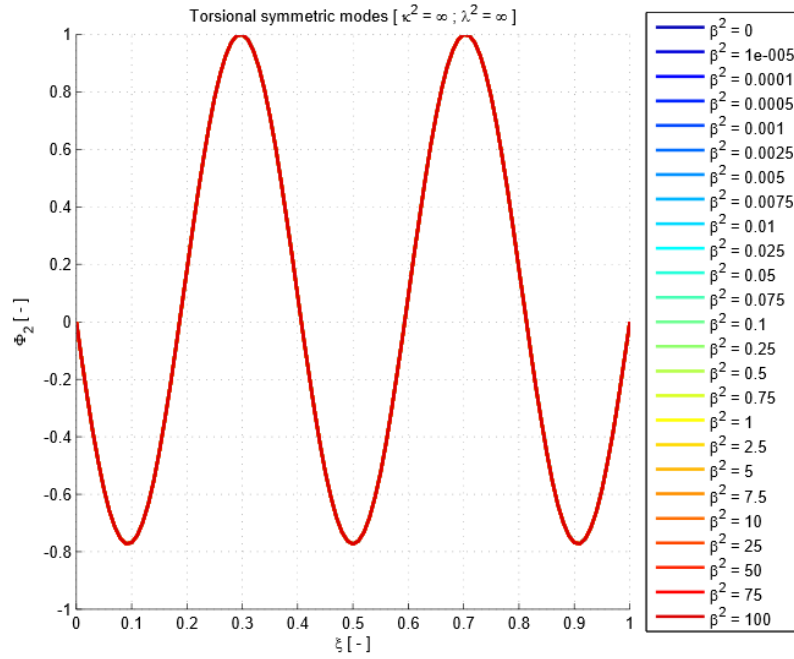


Figure 2.39_Modal shape of Mode 2 for $\chi^2 = \infty$ and $\lambda_L^2 = \infty$.

Comparing the two limit conditions $\chi^2 = 0$ and $\chi^2 = \infty$ is evident that increasing the warping stiffness the deck relative torsional stiffness β^2 influence on negative rotations reduces itself. In fact for $\chi^2 = 0$ we get many modes collapsed to the one proper of a stiff deck condition characterised by high counter-clockwise torsion. This is linked to the fact that the torsional stiffness contribution given by warping become dominant on both the primary de S Venant and cables system.

With respect to the mode 1 here is evident how much is influent the deck relative stiffness parameter on the position of peak antinode displacement, that moves farther to the midspan section as β^2 increases. While no evident effect on this feature is associate to χ^2 .

The same parameter β^2 affects the antinode counter-clockwise rotation that increases with the deck relative stiffness, due to the combined action of two opposite flexural motion of the main cables.

Much more interesting is the evolution of modal shapes as the main parameters χ^2 , β^2 and λ_L^2 are tuned. In fact the transition is now much more complex, passing from a mode characterised by 2 then by 0 and finally by 4 internal nodes as the Irvine parameter increases.

This requires further investigations of the modal properties in order to find a second Cross Over Mode in correspondence of null midspan rotation and making the modal shape transit from a 2 node to a 0 node condition; and a third COM condition again as the midspan rotation vanishes but characterising the passage from a 0 to a four node modal shape.

Hence the condition required for a generic mode is the vanishing of the negative antinode rotation.

$$\theta_m(\xi_{min}) = \frac{\lambda_L^2}{\bar{J}_t \cdot \bar{\omega}_{\vartheta,m}^2} \tilde{h}_{\theta,m} \cdot \left\{ 1 - \frac{1}{2} \cdot \left(\frac{\cosh\left(\sqrt{\bar{J}_t} \cdot \bar{\omega}_{\vartheta,m} \cdot \frac{\chi}{\beta} \left(\xi - \frac{1}{2}\right)\right)}{\cosh\left(\frac{1}{2} \sqrt{\bar{J}_t} \cdot \bar{\omega}_{\vartheta,m} \cdot \frac{\chi}{\beta}\right)} + \frac{\cos\left(\sqrt{\bar{J}_t} \cdot \bar{\omega}_{\vartheta,m} \cdot \frac{\chi}{\beta} \left(\xi - \frac{1}{2}\right)\right)}{\cos\left(\frac{1}{2} \sqrt{\bar{J}_t} \cdot \bar{\omega}_{\vartheta,m} \cdot \frac{\chi}{\beta}\right)} \right) \right\}_{\xi=\xi_{min}} = 0 ;$$

Notice that this condition is not required by the first order modes since the vanishing of lateral torsional slopes grant it automatically.

Since in general the position of the antinode points varies with the actual values of the parameters χ^2 , β^2 and λ_L^2 need to enforce the vanishing of the slope in order to find the stationary point and then find the minima searching for negative curvatures.

The only cases that allows simpler treatment are those related to the usual free warping deck condition ($\chi^2 = 0$) and the generic condition ($\forall \chi^2, \forall \beta^2$) for the mode 2.

Let's start from the latter one. The fact that we are dealing with the second order mode simplify the treatment since the position of the minimum antinode displacement is known a priori ($\xi_{min} = \frac{1}{2}$).

On the contrary the first case as usual the free warping condition allows analytical results. In fact the COM condition reduces to the following relation.

$$\Theta_m(\xi_{min}) = \frac{\lambda_L^2}{\tilde{J}_t \tilde{\omega}_{\vartheta,m}^2} \tilde{h}_{\vartheta,m} \cdot \left\{ 1 - \frac{\cos\left(\sqrt{\frac{\tilde{J}_t}{(1+\beta^2)}} \tilde{\omega}_{\vartheta,m} \cdot \left(\xi - \frac{1}{2}\right)\right)}{\cos\left(\frac{1}{2} \sqrt{\frac{\tilde{J}_t}{(1+\beta^2)}} \tilde{\omega}_{\vartheta,m}\right)} \right\}_{\xi=\xi_{min}} ;$$

First if all need to define the position of the antinode rotations.

$$\frac{d}{d\xi} \Theta_m(\xi) = \frac{\lambda_L^2}{\tilde{J}_t \tilde{\omega}_{\vartheta,m}^2} \tilde{h}_{\vartheta,m} \cdot \left\{ \sqrt{\frac{\tilde{J}_t}{(1+\beta^2)}} \cdot \tilde{\omega}_{\vartheta,m} \cdot \frac{\sin\left(\sqrt{\frac{\tilde{J}_t}{(1+\beta^2)}} \tilde{\omega}_{\vartheta,m} \cdot \left(\xi - \frac{1}{2}\right)\right)}{\cos\left(\frac{1}{2} \sqrt{\frac{\tilde{J}_t}{(1+\beta^2)}} \tilde{\omega}_{\vartheta,m}\right)} \right\} = 0$$

$$\Leftrightarrow \sqrt{\frac{\tilde{J}_t}{(1+\beta^2)}} \cdot \tilde{\omega}_{\vartheta,m} \cdot \left(\xi - \frac{1}{2}\right) = k\pi \text{ with } k \in \mathbb{N} \setminus \{0\} \Rightarrow \xi = \xi_{staz} = \frac{1}{2} + \frac{k\pi \cdot \sqrt{(1+\beta^2)}}{\sqrt{\tilde{J}_t} \tilde{\omega}_{\vartheta,m}} ;$$

It's evident that the latter relation gives the actual position of the minimum antinode point of the 2 order mode as = 0 . Hence it's possible to link the parameter k to the actual modal order.

$$k = m - 2 ;$$

Then enforce positive curvature since the positive rotation convention is clockwise, and hence counter-clockwise min rotations are characterised by such kind of curvatures.

$$\frac{d^2}{d\xi^2} \Theta_m(\xi) = \frac{\lambda_L^2}{\tilde{J}_t \tilde{\omega}_{\vartheta,m}^2} \tilde{h}_{\vartheta,m} \cdot \left\{ \frac{\tilde{J}_t}{(1+\beta^2)} \cdot \tilde{\omega}_{\vartheta,m}^2 \cdot \frac{\cos\left(\sqrt{\frac{\tilde{J}_t}{(1+\beta^2)}} \tilde{\omega}_{\vartheta,m} \cdot \left(\xi_{staz} - \frac{1}{2}\right)\right)}{\cos\left(\frac{1}{2} \sqrt{\frac{\tilde{J}_t}{(1+\beta^2)}} \tilde{\omega}_{\vartheta,m}\right)} \right\} \geq 0 \Leftrightarrow \cos(k\pi) \geq 0 \Leftrightarrow k = \text{even};$$

Hence the previous relation becomes as follows.

$$k = 2 \cdot (m - 2) \Rightarrow \xi_{min} = \frac{1}{2} \pm \frac{2 \cdot (m-2) \pi \cdot \sqrt{(1+\beta^2)}}{\sqrt{J_t} \cdot \tilde{\omega}_{w,n}};$$

Finally substituting in the initial modal shape we get the following condition.

$$\Theta_m \left(\xi_{min} = \frac{1}{2} + \frac{2 \cdot (m-2) \pi \cdot \sqrt{(1+\beta^2)}}{\sqrt{J_t} \cdot \tilde{\omega}_{w,n}} \right) = \frac{\lambda_L^2}{J_t \cdot \tilde{\omega}_{\vartheta,m}^2} \tilde{h}_{\Theta,m} \cdot \left\{ 1 - \frac{\cos(2 \cdot (m-2) \pi)}{\cos\left(\frac{1}{2} \sqrt{\frac{J_t}{(1+\beta^2)}} \tilde{\omega}_{\vartheta,m}\right)} \right\} = 0 \quad \forall m \text{ and } \forall \beta^2;$$

The meaning of the last statement is that for perfectly free warping deck the transition from a 2 to a 0 node condition is doesn't depend on the actual value of the Irvine parameter λ_L^2 .

Lets' comment some numerical results obtained for the second mode of vibrations.

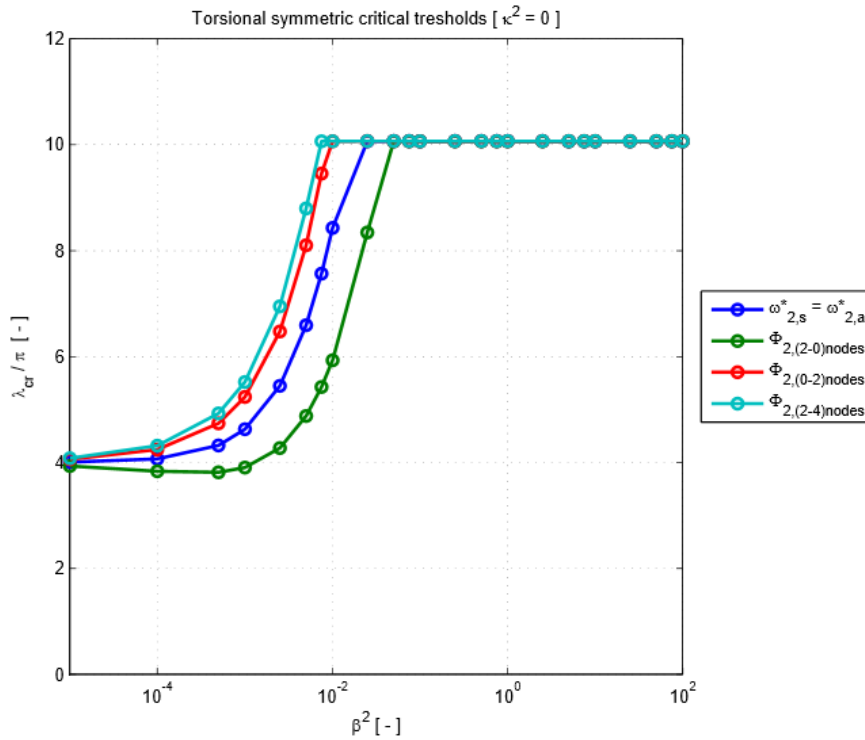


Figure 2.40_Cross Over Frequency and Mode thresholds of Mode 2 for $\chi^2 = 0$.

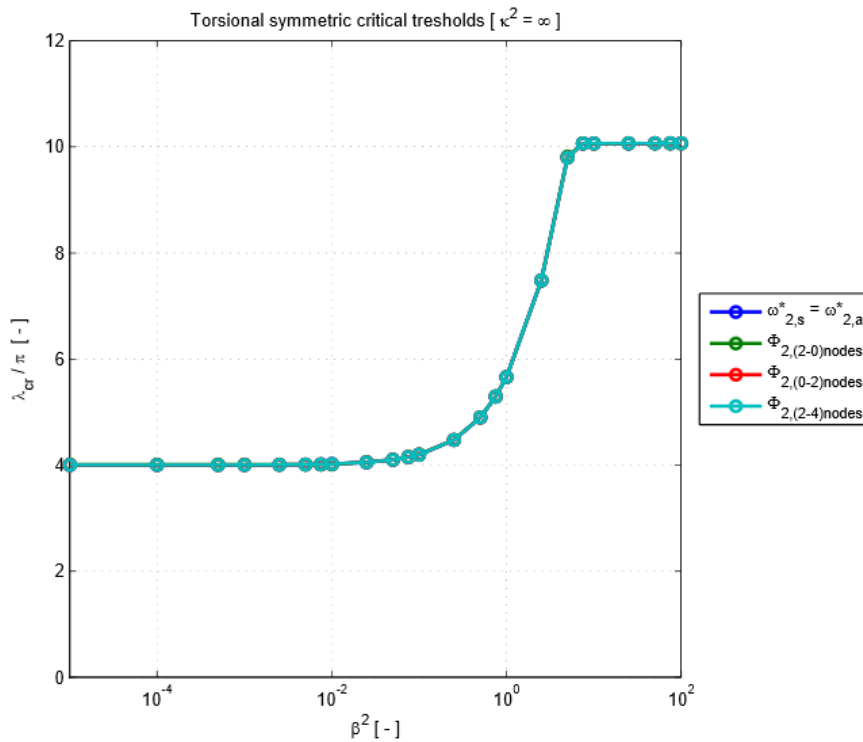


Figure 2.41_Cross Over Frequency and Mode thresholds of Mode 2 for $\chi^2 = \infty$.

Let's first analyse the $\chi^2 = 0$ condition.

As for circular eigen-frequencies the Cross Over Frequency is constant for very flexible decks ($\beta^2 \leq 10^{-4}$) and cannot be tuned beyond $\beta^2 = 10^{-2}$.

With respect to the first symmetric mode the transition of modal shapes for higher order modes are always three as the Irvine parameter increases. Starting from the one with $2 \cdot (m - 1)$ internal nodes, then passing by Cross Over Frequency condition to increase further to reach the one with 0 internal nodes and ending with the last one with $2 \cdot m$ internal nodes.

Here the transition from 2 to 0 internal nodes occurs in correspondence of values for the critical Irvine parameter lower than the Cross Over Frequency, at least for not perfectly flexible deck. In fact all the curves collapse to the same critical λ_L^2 only for deck relative stiffnesses lower than ($\beta^2 = 10^{-5}$).

This means that for the special case of perfectly flexible deck both the Cross Over Frequency and the three Cross Over Mode conditions occurs at the same critical value for λ_L^2 .

Focusing on the 2 to 0 nodes transition curve, is possible to see that approximately for β^2 belonging to the interval ($10^{-5} \div 2 \cdot 10^{-3}$) the critical λ_L^2 required is lower than the one required for perfectly flexible deck. This means that the initial increase of the flexural stiffness of the deck gives a huge contribution to grant null midspan rotation, but beyond a certain threshold ($\beta^2 = 2 \cdot 10^{-3}$) since the midspan rotation increases then higher values for λ_L^2 are required.

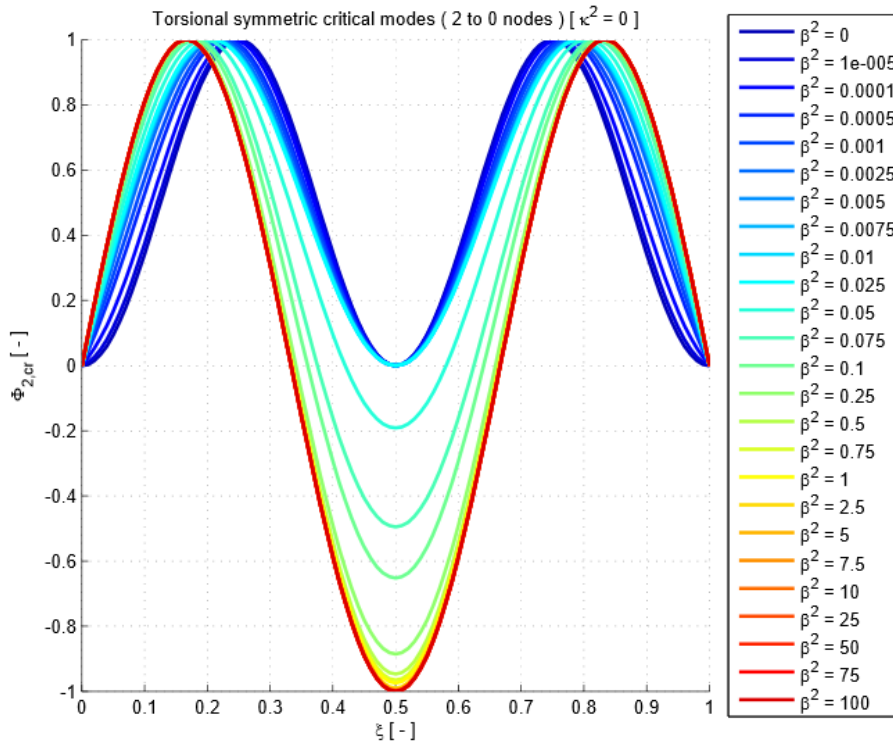


Figure 2.42_Cross Over Modes of Mode 2 for 2-0 nodes transition for $\chi^2 = 0$.

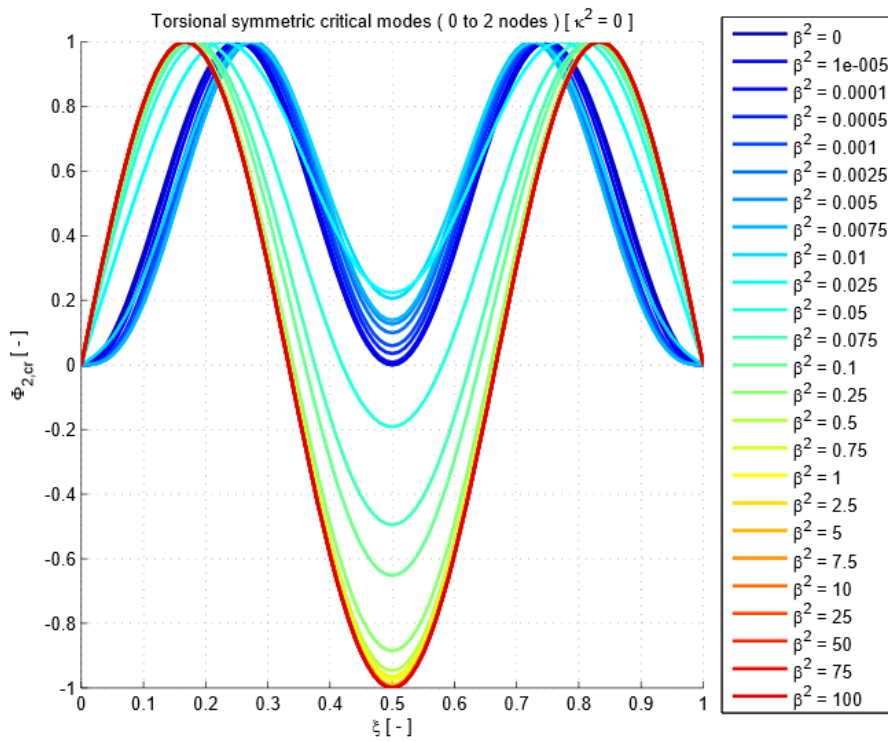


Figure 2.43_Cross Over Modes of Mode 2 for 0-2 nodes transition for $\chi^2 = 0$.

Notice that for $\beta^2 > 0.025$ is no more possible to tune the Irvine parameter in order to satisfy the first COM condition, for $\beta^2 > 0.0075$ the second and for $\beta^2 > 0.005$ the third.

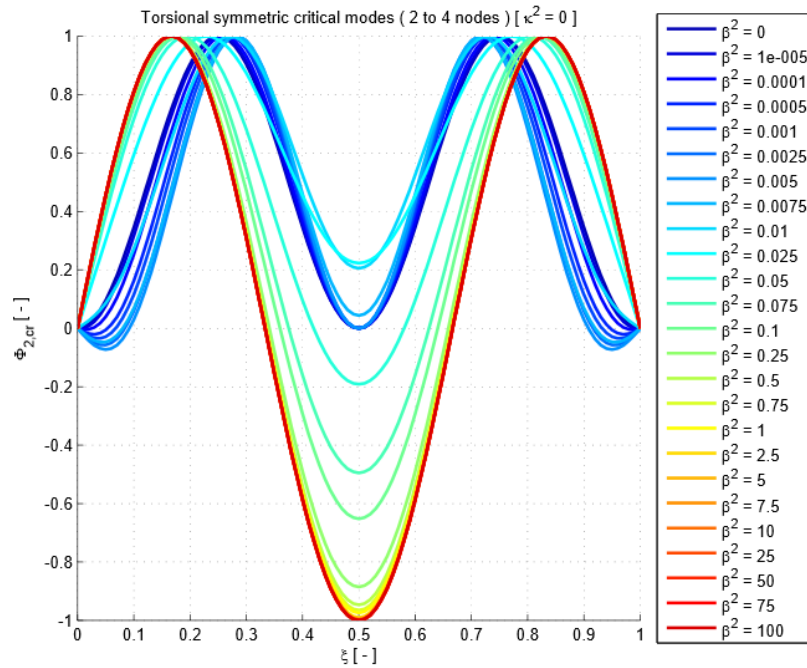


Figure 2.44_Cross Over Modes of Mode 2 for 2-4 nodes transition for $\chi^2 = 0$.

For the limit case $\chi^2 = \infty$ the curve is unique for all the critical conditions taken in consideration as just demonstrated before saying that the vanishing of the midspan rotation is not dependent on the actual mode considered and on the other structural parameters. This means that for any β^2 we can satisfy both the COF and the three COM conditions simultaneously.

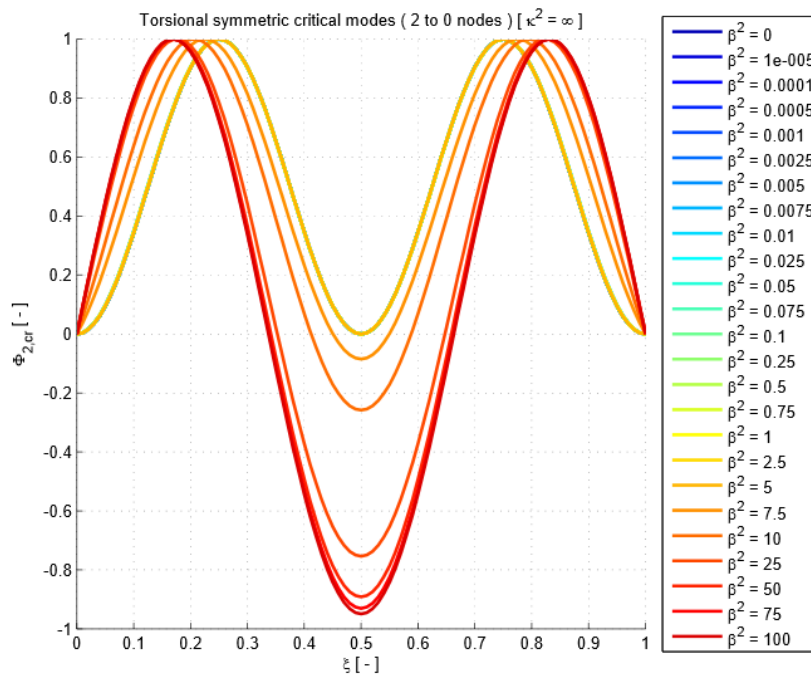


Figure 2.45_Cross Over Modes of Mode 2 for 2-0 nodes transition for $\chi^2 = \infty$.

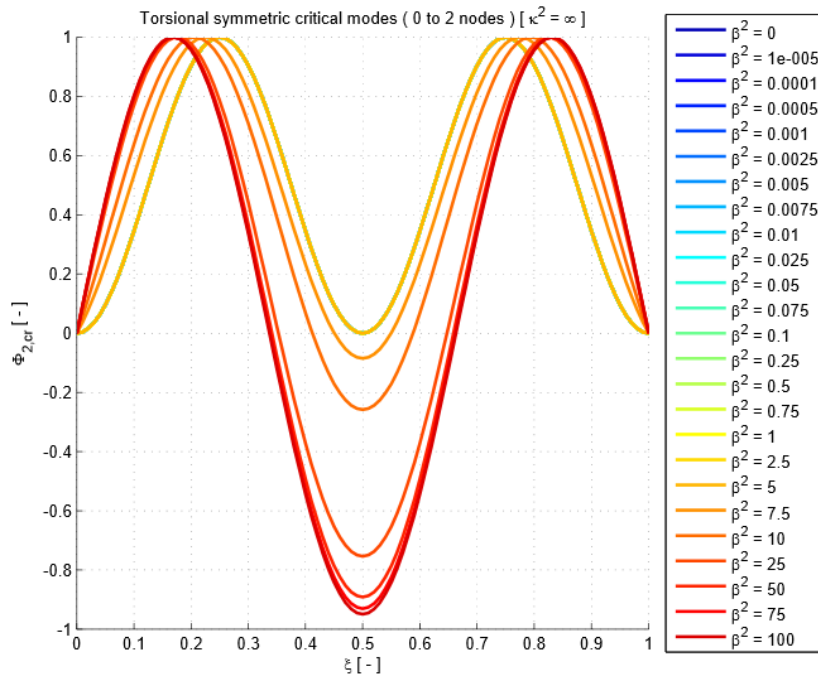


Figure 2.46_Cross Over Modes of Mode 2 for 0-2 nodes transition for $\chi^2 = \infty$.

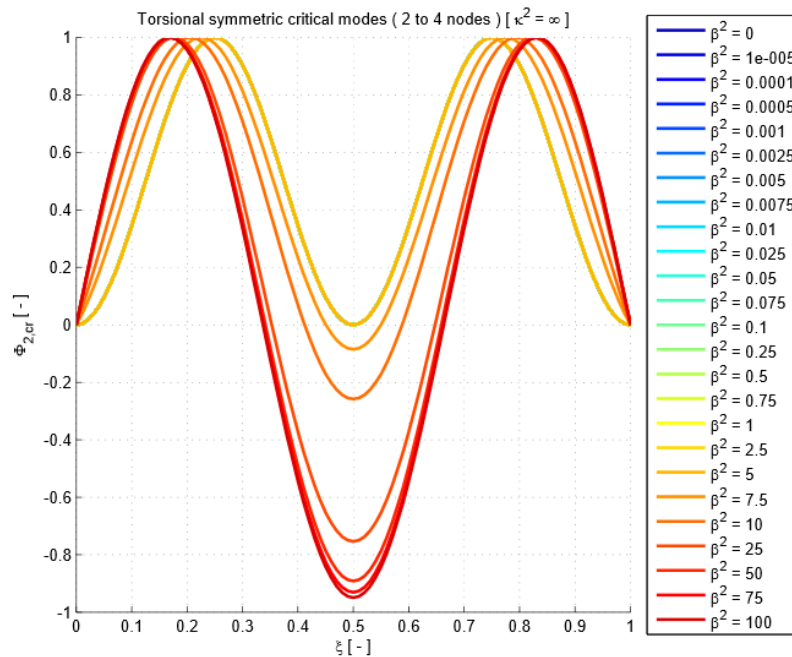


Figure 2.47_Cross Over Modes of Mode 2 for 2-4 nodes transition for $\chi^2 = \infty$.

In this second limit condition when it is possible to satisfy the COF at the same time are satisfied the three COM condition. Hence the modal shapes are identical as the Irvine parameter for any choice of β^2 . Any condition can be satisfied once $\beta^2 > 5$.

Also for the torsional modes can be notice that for any choice of the modal order is that once λ_L^2 overcome the last COM condition that grants generally the transition to the $2 \cdot n$ internal nodes modal shape, immediately all the negative antinodal rotations becomes equal and remains so for any higher value of λ_L^2 .

Before concluding this section we want to mention the fact that the hyperbolic contribution associated to the deck stiffness contribution is responsible for the distortion of modal shapes from the sinusoidal one typical of strings. But as the modal order increases its effect reduces, and from numerical analysis can be seen that sinusoidal shape is a very good approximation beyond the fourth order mode.

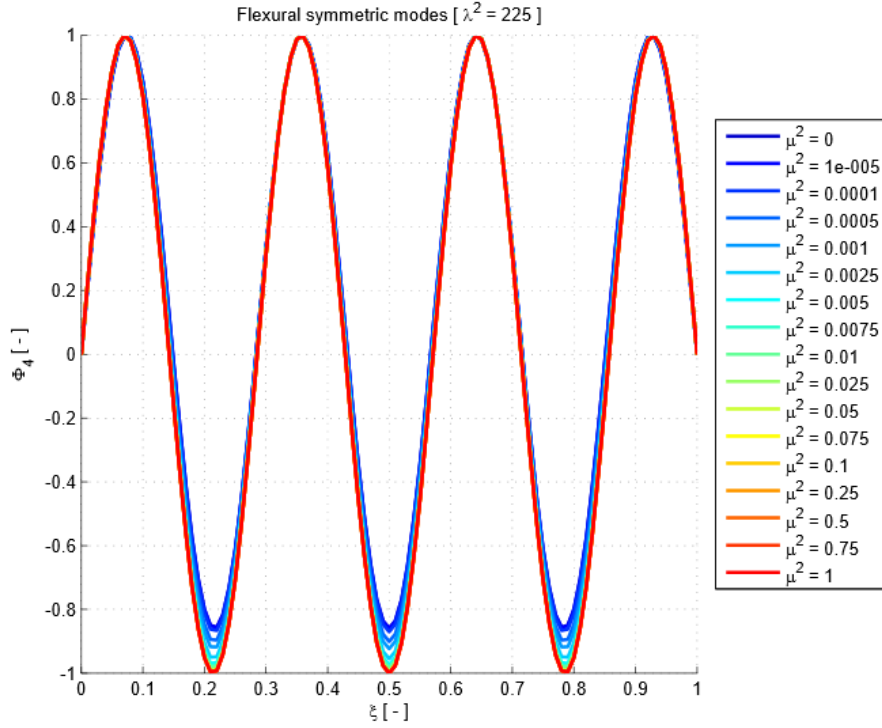


Figure 2.48_Hyperbolic contribution on high order modal shape.

2.4. Modal participation analysis

The modal expansion has the great advantage that allows us to decouple the spatial and time variable. As a consequence on one hand the vibration analysis becomes much more easily but on the other hand it gives us the response of each mode separately. Since the real structural response would be a superposition of all modal contributions is important to find out how much each modes weight on the global solution. These parameters are in general called modal participation parameters.

In order to obtain those parameters is necessary first of all to perform a modal expansion of the equation of motion. We have already done it for the linear dimensionless undamped free vibrations assuming an exponential format for the time variables.

We remember once again that the modal superposition is allowed thanks to the linearity of the equations.

Now we will analyse the more general situation of forced damped vibrations hence we will not specify the time variation format.

$$\tilde{w}_d(\xi, \tau) = \sum_{n=1}^{\infty} W_n(\xi) \cdot z_n(\tau) \quad \text{with } n \in \mathbb{N} \setminus \{0\};$$

$$\tilde{v}_d(\xi, \tau) = \sum_{m=1}^{\infty} \theta_m(\xi) \cdot \gamma_m(\tau) \quad \text{with } m \in \mathbb{N} \setminus \{0\};$$

Hence substituting in the generalised linear dimensionless equations of motion we get the following expressions.

$$\frac{d^2\tilde{w}_d}{d\tau^2} + \tilde{c}_w \cdot \frac{d\tilde{w}_d}{d\tau} + \mu^2 \cdot \tilde{w}_d'^v - \tilde{w}_d'' + \lambda_L^2 \tilde{h}_w = \tilde{q}(\xi, \tau);$$

$$\tilde{J}_t \cdot \frac{d^2\tilde{\vartheta}_d}{dt^2} + \tilde{c}_\vartheta \cdot \frac{d\tilde{\vartheta}_d}{d\tau} + \frac{\beta^2}{\chi^2} \cdot \tilde{\vartheta}_d'^v - (1 + \beta^2) \cdot \tilde{\vartheta}_d'' + \lambda_L^2 \tilde{h}_\vartheta = \tilde{m}(\xi, \tau);$$

The new parameters introduced are the dimensionless damping parameters that can be define as follows.

$$c_w \cdot \frac{dw_d}{dt} = c_w \cdot f \cdot \frac{1}{l} \sqrt{\frac{2H}{m_d+2 \cdot m_c}} \cdot \frac{l^2}{2Hf} \cdot \frac{d\tilde{w}_d}{d\tau} = c_w \cdot \frac{l}{\sqrt{2H(m_d+2 \cdot m_c)}} \cdot \frac{d\tilde{w}_d}{d\tau} = \tilde{c}_w \cdot \frac{d\tilde{w}_d}{d\tau};$$

$$c_\vartheta \cdot \frac{d\vartheta_d}{dt} = c_\vartheta \cdot \frac{f}{b} \cdot \frac{1}{l} \sqrt{\frac{2H}{m_d+2 \cdot m_c}} \cdot \frac{l^2}{2Hfb} \cdot \frac{d\tilde{\vartheta}_d}{d\tau} = c_\vartheta \cdot \frac{l}{b^2 \sqrt{2H(m_d+2 \cdot m_c)}} \cdot \frac{d\tilde{\vartheta}_d}{d\tau} = \tilde{c}_\vartheta \cdot \frac{d\tilde{\vartheta}_d}{d\tau};$$

The next step consists in the projection on the modal space of the previous equations. In continuous mechanics this can be done simply multiplying each equation by the respective modals shape and then integrating over the spatial domain. The counterpart in discrete mechanics is the diagonalization of the mass, damping and stiffness matrix multiplying and pre-multiplying each of them by the modal matrix whose columns should be all the possible modal shapes allowed by discretisation but in general has much more limited dimensions since few modes are sufficient to define sufficiently accurately the structural response.

In the present case, hence, we will multiply respectively the first and the second linear dimensionless equations of motion by $W_n(\xi)$ and $\Theta_m(\xi)$ and then integrate them over the domain [0,1].

We obtain the following modal equations of motion.

$$M_{w,n} \cdot \ddot{z}_n(\tau) + 2\xi_{w,n} \tilde{\omega}_{w,n} M_{w,n} \cdot \dot{z}_n(\tau) + K_{w,n} \cdot z_n(\tau) = \Gamma_{w,n}(\tau);$$

$$J_{\vartheta,m} \cdot \ddot{\gamma}_m(\tau) + 2\xi_{\vartheta,m} \tilde{\omega}_{\vartheta,m} J_{\vartheta,m} \cdot \dot{\gamma}_m(\tau) + K_{\vartheta,m} \cdot \gamma_m(\tau) = \Gamma_{\vartheta,m}(\tau);$$

Where the new parameters defined are modal masses, damping ratios, stiffness and forcing terms.

$$M_{w,n} = \int_0^1 W_n^2(\xi) d\xi;$$

$$M_{\vartheta,m} = \int_0^1 \Theta_m^2(\xi) d\xi \Rightarrow J_{\vartheta,m} = \tilde{J}_t M_{\vartheta,m};$$

$$\xi_{w,n} = \frac{\tilde{c}_w}{2\sqrt{K_{w,n} \cdot M_{w,n}}} = \frac{\tilde{c}_w}{2\tilde{\omega}_{w,n} M_{w,n}};$$

$$\xi_{\vartheta,m} = \frac{\tilde{c}_\vartheta}{2\sqrt{K_{\vartheta,m} \cdot J_{\vartheta,m}}} = \frac{\tilde{c}_\vartheta}{2\tilde{\omega}_{\vartheta,m} J_{\vartheta,m}};$$

$$K_{w,n} = \int_0^1 W_n(\xi) \cdot [\mu^2 \cdot W_n'^v(\xi) - W_n''(\xi)] d\xi + \lambda_L^2 \tilde{h}_{w,n}^2 = \tilde{\omega}_{w,n}^2 \cdot M_{w,n};$$

$$K_{\vartheta,m} = \int_0^1 \Theta_m(\xi) \cdot \left[\frac{\beta^2}{\chi^2} \cdot \Theta_m'^v(\xi) - (1 + \beta^2) \cdot \Theta_m''(\xi) \right] d\xi + \lambda_L^2 \tilde{h}_{\vartheta,m}^2 = \tilde{\omega}_{\vartheta,m}^2 \cdot J_{\vartheta,m};$$

$$\Gamma_{w,n}(\tau) = \int_0^1 W_n(\xi) \cdot \tilde{q}(\xi, \tau) d\xi;$$

$$\Gamma_{\vartheta,m}(\tau) = \int_0^1 \Theta_m(\xi) \cdot \tilde{m}(\xi, \tau) d\xi ;$$

It's evident that the modal projection allows us to reduce the equations of motion to the same format of 2 single degree of freedom systems. The fact that the dofs are independent is due to the fact that we are considering just the linear component of the structural response.

The analytical solution of a general forced and damped system can be found performing the Convolution Integration proposed by Duhamel. The theory is based on the assumption that a generic forcing can be seen as an infinite series of unitary impulses adequately scaled in order to map the actual external forcing term. The superposition once again is allowed by the linearity of the problem. The second principal hypothesis is that each impulse has effect only on subsequent instant since the system considered is causal. We must remember that in nature not all the process are causal, since we can feel the effect of events that are going to happen.

Anyway, the convolution integral is able to give us not only the forced response of the system but superimposing the well-known free vibration response of a generic single degree of freedom oscillator we can get the generic response of a forced and damped system starting from non-trivial initial conditions.

In the present case is not of interest the free vibration response hence we will assume null initial conditions. Consequently we need to consider just the Duhamel Integral that has the following expression.

$$z_n(\tau) = \frac{1}{\tilde{\omega}_{w,n} M_{w,n}} \int_0^{\bar{\tau}} \Gamma_{w,n}(\tau) \cdot \exp\{-\xi_{w,n} \tilde{\omega}_{w,n} \cdot (\tau - \bar{\tau})\} \cdot \sin\{\tilde{\omega}_{w,n} \sqrt{1 - \xi_{w,n}^2} \cdot (\tau - \bar{\tau})\} d\bar{\tau} ;$$

$$\gamma_m(\tau) = \frac{1}{\tilde{\omega}_{\vartheta,m} J_{\vartheta,m}} \int_0^{\bar{\tau}} \Gamma_{\vartheta,m}(\tau) \cdot \exp\{-\xi_{\vartheta,m} \tilde{\omega}_{\vartheta,m} \cdot (\tau - \bar{\tau})\} \cdot \sin\{\tilde{\omega}_{\vartheta,m} \sqrt{1 - \xi_{\vartheta,m}^2} \cdot (\tau - \bar{\tau})\} d\bar{\tau} ;$$

Notice that the Duhamel integral gives us the time history of the max positive antinode displacement or rotation since we reduce to study an equivalent single dof system for each equation.

As we can see the response is the superposition of many sub-responses of that of a damped oscillator at the generic instant τ forced by a term acting at the instant $\bar{\tau}$. This means that at a generic instant τ the response of the system is given by the superposition of the effects given by all the forcing acting in previous instants.

In order to get the time response in a generic point along the span of the bridge is necessary to return to the definition of the modal decomposition.

$$\tilde{w}_d(\xi, \tau) = \sum_{n=1}^{\infty} \frac{W_n(\xi)}{\tilde{\omega}_{w,n} M_{w,n}} \cdot I_{w,n}(\tau) = \sum_{n=1}^{\infty} F_{w,n}(\xi) \cdot I_{w,n}(\tau) ;$$

$$\tilde{\vartheta}_d(\xi, \tau) = \sum_{m=1}^{\infty} \frac{\Theta_m(\xi)}{\tilde{\omega}_{\vartheta,m} J_{\vartheta,m}} \cdot I_{\vartheta,m}(\tau) = \sum_{m=1}^{\infty} F_{\vartheta,m}(\xi) \cdot I_{\vartheta,m}(\tau) ;$$

Where the new parameters $F_{w,n}(\xi)$ and $F_{\vartheta,m}(\xi)$ can be define as participation factors since represent the response of the system in any position in space when at a generic instant the amplitude of oscillation is unitary meaning that all the forcing terms acting in previous instants gives a global unitary displacement to the system.

In order to get normalised results we will slightly modify the previous definitions as follows.

$$\tilde{w}_d(\xi, \tau) = \sum_{n=1}^{\infty} W_n(\xi) \frac{\tilde{h}_{W,n}}{M_{W,n}} \cdot \frac{I_{W,n}(\tau)}{\tilde{\omega}_{w,n} \cdot \tilde{h}_{W,n}} = \frac{1}{8} \cdot \sum_{n=1}^{\infty} 8 \cdot W_n(\xi) \frac{\tilde{h}_{W,n}}{K_{W,n}} \cdot \tilde{\omega}_{w,n}^2 D_{w,n}(\tau) = \frac{1}{8} \cdot \sum_{n=1}^{\infty} P_{w,n}(\xi) \cdot \tilde{\omega}_{w,n}^2 D_{w,n}(\tau) ;$$

$$\tilde{\vartheta}_d(\xi, \tau) = \sum_{m=1}^{\infty} \Theta_m(\xi) \frac{\tilde{h}_{\Theta,m}}{J_{\Theta,m}} \cdot \frac{I_{\Theta,m}(\tau)}{\tilde{\omega}_{\vartheta,m} \cdot \tilde{h}_{\Theta,m}} = \frac{1}{8} \cdot \sum_{m=1}^{\infty} 8 \cdot \Theta_m(\xi) \frac{\tilde{h}_{\Theta,m}}{K_{\Theta,m}} \cdot \tilde{\omega}_{\vartheta,m}^2 D_{\vartheta,m}(\tau) = \frac{1}{8} \cdot \sum_{m=1}^{\infty} P_{\vartheta,m}(\xi) \cdot \tilde{\omega}_{\vartheta,m}^2 D_{\vartheta,m}(\tau) ;$$

Hence we have defined the displacement and rotation participation parameters slightly different from the participation factors, and a Duhamel parameter slightly different from the corresponding integral. In this way we get normalised parameters with respect to the actual amplitude response of the system.

The main limit of these definitions is that for sinusoidal modals shapes the participation parameters vanish since the stiffening parameter is null. Hence we need to define them as follows.

$$\tilde{w}_d(\xi, \tau) = 2 \sum_{n=1}^{\infty} \sin(\tilde{n}\pi\xi) \cdot D_{w,n}(\tau) ;$$

Where the half-wave number can be odd or even respectively for perfectly flat cables limit condition and skew-symmetric modes.

The other disadvantage is that is required to know the actual dimensionless gyration radius of the deck and cables system \tilde{J}_t , since the torsional eigen frequency appears separately from it. from [31-40] we can state that its value ranges between 0.4 and 0.7.

As previously mentioned the Duhamel integral give us the amplitude in correspondence of the max antinode point that has a different location along the bridge axis for each modal shape. Hence would be meaningless to get the participation factors in that position since cannot be superimposed. Consequently is better to focus the attention on some position along the deck that could be of interest for the structural analysis as for example the displacements and the rotations at midspan and at quarter points.

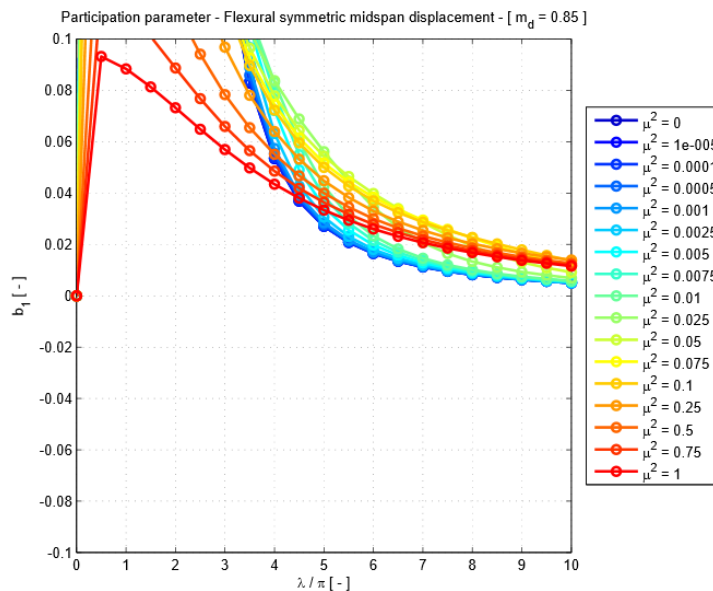


Figure 2.49_Midspan displacement participation parameter for flexural symmetric mode shape 1.

It is evident that increasing the Irvine parameter, displacements decreases due to the higher stiffness of the structure.

Whilst increasing the deck flexural stiffness is important to take in consideration the relative importance of cables and deck contribution. In fact we get increasing displacements as deck stiffness grows just below a certain value for Irvine parameter.

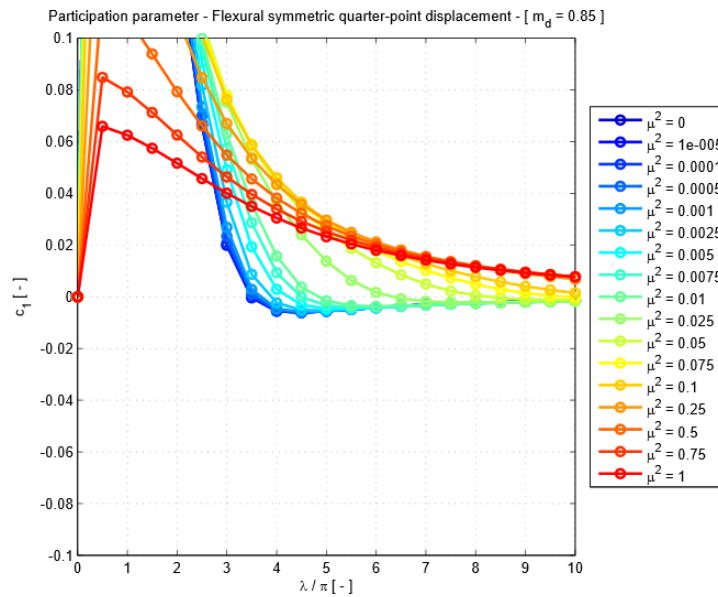


Figure 2.50_Quarter point displacement participation parameter for flexural symmetric mode shape 1.

Considering higher order modes we observe lower displacements and an higher influence of the deck stiffness.

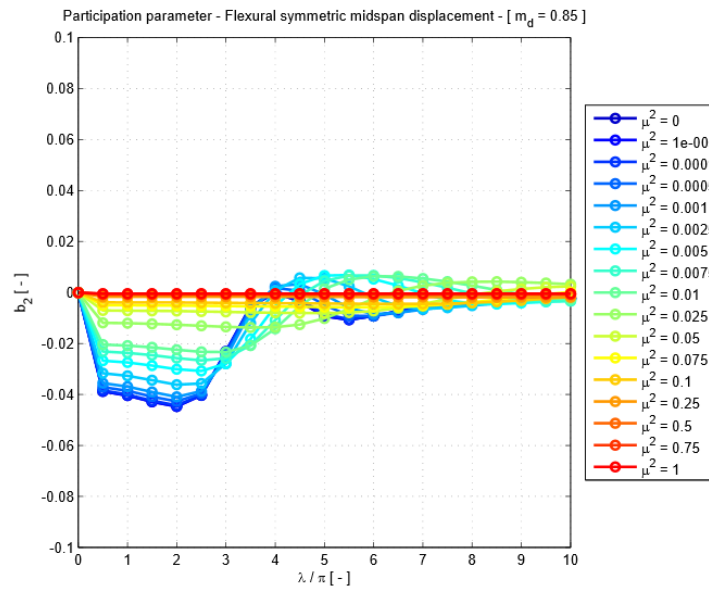


Figure 2.51_Midspan displacement participation parameter for flexural symmetric mode shape 2.

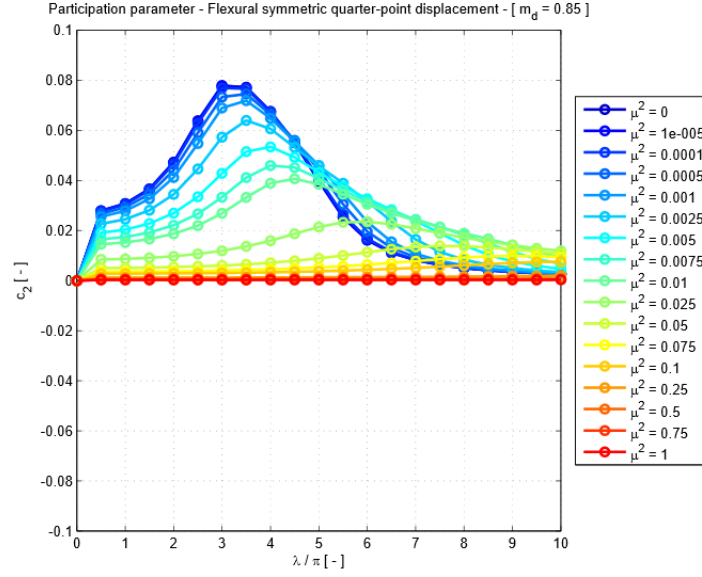


Figure 2.52_Midspan displacement participation parameter for flexural symmetric mode shape 2.

Another important parameter could be the linear stiffening parameter that represent the cables tension increment due to independent flexural and torsional motions and it's defined as follows.

$$h_w = -\frac{E_c A_c}{L_c} y'' \int_0^l w_d(x, t) dx = \frac{H E_c A_c}{8 H L_c} \left(\frac{8f}{l}\right)^2 \int_0^1 \tilde{w}_d(\xi, \tau) d\xi = \frac{H}{8} \lambda_L^2 \sum_{n=1}^{\infty} \int_0^1 F_{w,n}(\xi) d\xi \cdot I_{w,n}(\tau);$$

$$h_{\vartheta} = -\frac{E_c A_c}{L_c} y'' b \int_0^l \vartheta_d(x, t) dx = \frac{H E_c A_c}{8 H L_c} \left(\frac{8f}{l}\right)^2 \int_0^1 \tilde{\vartheta}_d(\xi, \tau) d\xi = \frac{H}{8} \lambda_L^2 \sum_{m=1}^{\infty} \int_0^1 F_{\vartheta,m}(\xi) d\xi \cdot I_{\vartheta,m}(\tau);$$

Or in term of the normalised participation parameters.

$$h_w = H \sum_{n=1}^{\infty} \frac{\lambda_L^2}{8} \int_0^1 P_{w,n}(\xi) d\xi \cdot \tilde{\omega}_{w,n}^2 D_{w,n}(\tau) = H \cdot \frac{1}{8} \sum_{n=1}^{\infty} h_{w,n} \cdot \tilde{\omega}_{w,n}^2 D_{w,n}(\tau);$$

$$h_{\vartheta} = H \sum_{m=1}^{\infty} \frac{\lambda_L^2}{8} \int_0^1 P_{\vartheta,m}(\xi) d\xi \cdot \tilde{\omega}_{\vartheta,m}^2 D_{\vartheta,m}(\tau) = H \cdot \frac{1}{8} \sum_{m=1}^{\infty} h_{\vartheta,m} \cdot \tilde{\omega}_{\vartheta,m}^2 D_{\vartheta,m}(\tau);$$

Hence the new participation parameters $h_{w,n}$ and $h_{\vartheta,m}$ gives us the modal contribution to the tension increment in the cable given by flexural and torsional vibrations respectively, normalised with respect to the initial cable tension H. Notice that the fractional term out of the summation is a residual of the dimensionless convention chosen. Hence we decide to get results independent from that assumption in order to be able to compare the numerical results with similar analysis as those performed by Lo Turmo & Aparicio [5]. In fact they perform the same analysis for the single degree of freedom model of a suspension bridge, hence we have generalised it to the two degree of freedom one.

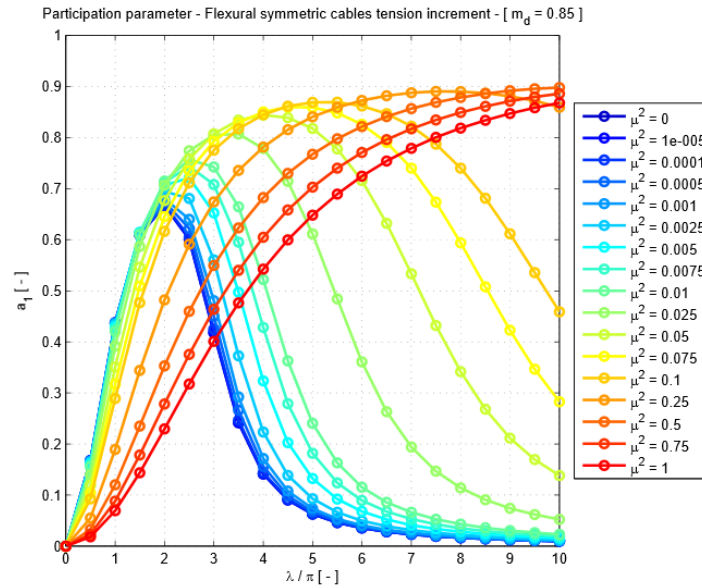


Figure 2.53_Cables tension increment for flexural symmetric mode shape 1.

As we can see as the cables inextensibility is not too high, as the deck stiffness increases the increment in the cables tension reduces since is the deck that holds a high amount of vertical forces not requiring the contribution coming from the cable system. On the contrary as the cables becomes enough rigid the increase of deck stiffness leads to higher values of cables stiffening increment since the deck is not enough rigid to absorb the major amount of external forces. Considering the same deck rigidity we can see that increasing the cables inextensibility remaining below the peak we get increasing tension increments since forces moves to the stiff element of the structure. Whilst above the peak we get a decreasing branch since the modal contribution reduces, being the mode approaching a sinusoidal shape characterised by a lower $h_{w,n}$ or $h_{\theta,m}$.

Further considering higher order modes we can say that the curves slightly increases their peaks and move through higher values for Irvine parameters because in higher order modes there is a larger upward region that reduces the overall cables tension increment. However, as already noticed with the parametric analysis, increasing the Irvine parameter the upward motion should disappear, consequently we get a peak in correspondence of higher λ_L^2 and also we reach higher peak values since the summation of curvatures in the cables is higher than in a single wave mode.

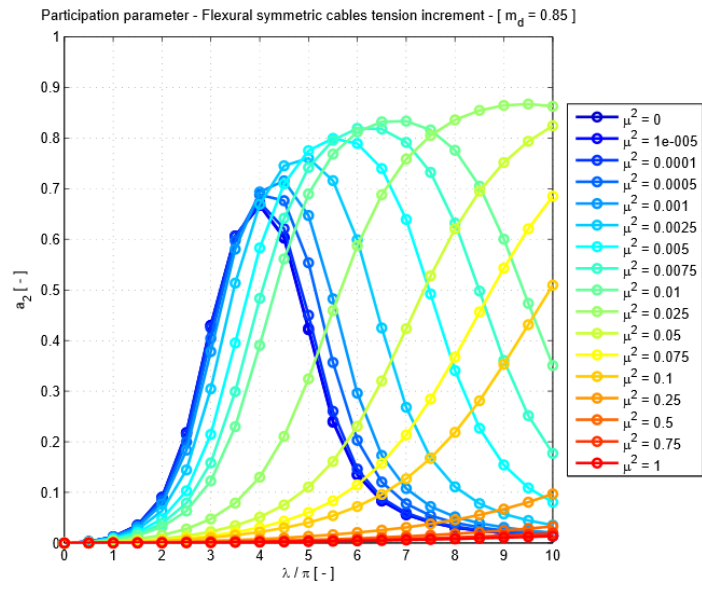


Figure 2.54_Cables tension increment for flexural symmetric mode shape 2.

3. Nonlinear analysis

Up to now, we have analysed first the structural two-dimensional model for a suspension bridge, in order to perform a parametric analysis of linear eigen-properties.

Now we want to solve the complete non-linear coupled system of equations coming from the structural model. We will not analyse the more complex aeroelastic one since it would couple also the linear component of the equations and consequently an analytical treatment will not be feasible. Further, if the structure alone is able to catch the main feature of internal resonances, by means of its quadratic and cubic non-linearities, we can state that the addition of linear coupling term, coming from wind action, will simply enhance these features.

3.1. Direct multiple-scale perturbation technique

The non-linearity of the system of equations of motion of the suspension bridge preclude the exact analytical solution to the problem. Hence, we are forced to resort approximations in order to obtain information about solutions of equations. Among those approximate methods are the so-called perturbation or asymptotic methods, which are able to approximate the solution by means of the first terms (usually no more than three) of an asymptotic expansion. Generally, artificial parameters are introduced representing perturbations, small or large, able to carry out expansion of nonlinear terms. A huge variety of perturbative methods have been developed in the past years in order to study the response of some classical non-linear equations (Van der Pol oscillator, Duffing equation, Klein-Gordon equation). These methods can be divided in few classes: the Straightforward Expansion, the method of Strained Coordinates, the method of Matched and Asymptotic Expansions, the method of Variation of Parameters and Averaging [21, 44]. In the present treatment we will use the so-called multiple time scale method, which is able to give us approximate but accurate solutions in presence of small but finite nonlinearities and belong to the latter class. The solution for the non-dimensional equations of motion of the suspension bridge alone will be search in the following format.

$$\tilde{w}_d(\xi, \tau) = \epsilon \cdot \tilde{w}_1(\xi, T_0, T_1, T_2) + \epsilon^2 \cdot \tilde{w}_2(\xi, T_0, T_1, T_2) + \epsilon^3 \cdot \tilde{w}_3(\xi, T_0, T_1, T_2)$$

$$\tilde{\vartheta}_d(\xi, \tau) = \epsilon \cdot \tilde{\vartheta}_1(\xi, T_0, T_1, T_2) + \epsilon^2 \cdot \tilde{\vartheta}_2(\xi, T_0, T_1, T_2) + \epsilon^3 \cdot \tilde{\vartheta}_3(\xi, T_0, T_1, T_2)$$

Where we introduce the parameter ϵ representing a small but finite perturbation applied to the system, in fact the multiple time scale method is much more accurate in weakly non linear problems. Generally the perturbative term is not completely artificial but it can be associated to the order to magnitude of the actual flexural oscillations.

$$\epsilon = \max(\tilde{w}_d(\xi, \tau)) / \lambda$$

From the last definition, we can state that we will expect higher non-linear contributions to the motion coming from higher order modes, since at equal amplitudes the perturbation parameter increases as the wavelength λ decreases.

We want to stress the fact that we are going to apply the multiple time scale technique in its more general direct approach. In fact, as we can see the unknown functions $\tilde{w}_d(\xi, \tau)$ and $\tilde{\vartheta}_d(\xi, \tau)$ are yet dependent on both time and space variables.

Generally, in order to simplify the treatment other authors facing the same or similar problems [11, 12, 19, 20] apply the perturbative method to the discretized equations, consequently called Discrete approach. This would require the projection of the equations on the modal space, so that the spatial dependence would be hidden inside integral terms, and then the multiple time scale expansion will involve functions dependent only on the time variable. The main differences we can found [45] are that, though both the approaches led to approximate solution in time, the discrete method will be exact in space only accounting for an infinite number of modal shapes. Further, the direct approach is able to give us explicit analytical expressions for the spatial functions eliminating the pitfalls of dealing with spatial series expansion. Usually, in engineering field just few normal modes are of interest, such as those directly excited by external forces or indirectly through internal parametric excitations, since all the others will decay in time as damping exists. Thence, generally finite mode truncation are inevitable and, with the same number of time scale terms, we can get higher convergence with the direct approach having exact spatial functions. Finally, in the discrete approach not only we should choose an infinite number shape functions in order to get the same accuracy of the direct one, but also they have to be a complete set of functions forming a basis, otherwise the convergence would be very poor.

Let's continue with the analytical treatment defining the so-called Time Scale parameter $T_n = \epsilon^n \cdot \tau$, that is a new set of independent variables accounting for the fast and slow time variation of different perturbations. This means that we will obtain a solution that is exact in spatial terms but just approximate in time domain. In fact, the solution will be the superposition of functions characterized by a frequency equal to the natural ones $\tilde{\omega}_{w,n}$ and $\tilde{\omega}_{\vartheta,m}$, the so-called fast time scale functions, and of their submultiples, the slow time scale ones slowed down as n increases. Then T_n can be see as a sort of period of the different time scale functions. Consequently, the derivatives with respect to time requires some further development by means of the chain rule.

$$\frac{d(\cdot)}{d\tau} = \frac{\partial(\cdot)}{\partial T_0} \cdot \frac{dT_0}{d\tau} + \frac{\partial(\cdot)}{\partial T_1} \cdot \frac{dT_1}{d\tau} + \frac{\partial(\cdot)}{\partial T_2} \cdot \frac{dT_2}{d\tau} = D_0 + \epsilon \cdot D_1 + \epsilon^2 \cdot D_2$$

$$\frac{d^2(\cdot)}{d\tau^2} = \left\{ \begin{array}{l} \frac{d}{d\tau} (D_0 + \epsilon \cdot D_1 + \epsilon^2 \cdot D_2) = \\ = (D_0 + \epsilon \cdot D_1 + \epsilon^2 \cdot D_2)^2 = \\ = D_0^2 + 2\epsilon \cdot D_0 D_1 + 2\epsilon^2 \cdot D_0 D_2 + \epsilon^2 \cdot D_1^2 + 2\epsilon^3 \cdot D_1 D_2 + \epsilon^4 \cdot D_2^2 \cong \\ \cong D_0^2 + 2\epsilon \cdot D_0 D_1 + 2\epsilon^2 \cdot D_0 D_2 + \epsilon^2 \cdot D_1^2 \end{array} \right.$$

Where we have introduce a new operator $D_k = \frac{\partial(\cdot)}{\partial T_k}$ that is the counter part of the time derivative in the multiple time scale field. Notice that we have introduced an approximation in the definition of the second order time derivative since we are not interested in perturbation contributions that are too small.

It's now evident that the solutions $\tilde{w}_d(\xi, \tau)$ and $\tilde{\vartheta}_d(\xi, \tau)$ depends both explicitly and implicitly on the time scale T_k . Since each term of the time scale expansion depends on every time scale, hence the truncation will be valid for all instant $\tau < O(\epsilon^{-K})$ where $K = \max(k)$ represents the number of time expansion terms taken in consideration. Beyond these times, we must add further time scales to keep the expansion still valid.

Notice that the introduction of the multiple time scales leads to transform the system from an ordinary to a partial differential equations one, increasing the number of independent variables. Consequently, it's known as the many variables version of the multiple time scale method.

The next step consist in substituting the time scale expansion into the original system of equations and equating coefficients of like powers of ϵ . This allows us to obtain equations for determining each component \tilde{w}_k and $\tilde{\vartheta}_k$ of the time scale expansion. Since the solutions will contain arbitrary functions of different time scales T_k , additional conditions are required. In fact we must remember that we are dealing with perturbations of the system and consequently each higher order term should be a small correction of the corresponding lower one.

$$\tilde{w}_k/\tilde{w}_{k-1} < \infty; \tilde{\vartheta}_k/\tilde{\vartheta}_{k-1} < \infty \quad \forall T_k, k = 1, \dots, K$$

This condition does not requires that each component \tilde{w}_k and $\tilde{\vartheta}_k$ is bounded, but simply that higher order approximations should be no more singular than the first lower order one. This condition is equivalent to the elimination technique used in the Straight-forward expansion method. It allows us to neglect divergent terms of lower order when the time instant overcomes its upper bound beyond which the k_{th} term of the time scale expansion has a contribution to the overall solution comparable to the $k_{th} - 1$ one and hence cannot be more considered a perturbation.

Hence substituting the multiple time scale expansion inside the original structural equations of motion we obtain three new systems, associate to the linear, quadratic and cubic order of the perturbation parameter ϵ . Notice that we will consider expansions up to the third order since, as already mentioned, the system of equations governing the vibrations of the suspension bridge are non-linear up to cubic components.

3.2. Linear contribution

The first component is the linear one being proportional to the first order perturbation ϵ .

$$D_0^2 \tilde{w}_1 + \mu^2 \cdot \tilde{w}_1^{iv} - \tilde{w}_1^{ii} + \lambda_L^2 \cdot \tilde{h}_{w_1} = 0$$

$$\tilde{J}_t \cdot D_0^2 \tilde{\vartheta}_1 + \frac{\beta^2}{\chi^2} \cdot \tilde{\vartheta}_1^{iv} - (1 + \beta^2) \cdot \tilde{\vartheta}_1^{ii} + \lambda_L^2 \cdot \tilde{h}_{\vartheta_1} = 0$$

As we can see we obtain similar equations used in defining the normal modes of the structure. The slight but relevant difference lies in the time variables that this time is not unique but we have a set of three periods T_k . Hence, the following modal expansion will be feasible.

$$\tilde{w}_1(\xi, T_0, T_1, T_2) = \sum_{n=1}^{\infty} W_n(\xi) \cdot z_n(T_0, T_1, T_2) \quad \text{with } n \in \mathbb{N} \setminus \{0\}$$

$$\tilde{\vartheta}_1(\xi, T_0, T_1, T_2) = \sum_{m=1}^{\infty} \Theta_m(\xi) \cdot \gamma_m(T_0, T_1, T_2) \quad \text{with } m \in \mathbb{N} \setminus \{0\}$$

Where Euler approach allows defining the amplitudes variable in time.

$$z_n(T_0, T_1, T_2) = Z_n(T_1, T_2) \cdot \exp(i \cdot \tilde{\omega}_{w,n} \cdot T_0) + \hat{Z}_n(T_1, T_2) \cdot \exp(-i \cdot \tilde{\omega}_{w,n} \cdot T_0)$$

$$\gamma_m(T_0, T_1, T_2) = \Gamma_m(T_1, T_2) \cdot \exp(i \cdot \tilde{\omega}_{\vartheta,m} \cdot T_0) + \hat{\Gamma}_m(T_1, T_2) \cdot \exp(-i \cdot \tilde{\omega}_{\vartheta,m} \cdot T_0)$$

It's of relevance to notice that with respect to the analysis, already performed in order to define the linear eigen-modes, the amplitudes may be not vary periodically in time though any damping is taken in account here. This is because the max amplitudes Z_n and Γ_m are no more constant in time but becomes functions of all the slow time scales T_1, T_2 .

Substituting the modal expansion in the linear systems, we obtain two uncoupled linear equations (the eigen-functions of the system) that allows us to define the linear modal shapes and eigen-frequencies already obtained in the initial structural analysis performed in the first chapter.

It's evident that the presence of additional linear terms coming from the wind-structure interaction will lead to couple also the linear equations of motion making impossible an analytical treatment also of the higher order modes, being dependent on the linear ones as we will see in the following.

3.3. Quadratic contribution

The second order terms are governed by a different set of equations of motion.

$$D_0^2 \tilde{w}_2 + \mu^2 \cdot \tilde{w}_2^{iv} - \tilde{w}_2^{ii} + \lambda_L^2 \cdot \tilde{h}_{w_2} = -2D_0 D_1 \tilde{w}_1 + \lambda_Q^2 \left\{ \begin{array}{l} \tilde{w}_1^{ii} \cdot \tilde{h}_{w_1} + \tilde{\vartheta}_1^{ii} \cdot \tilde{h}_{\vartheta_1} + \\ -\frac{1}{2} \cdot (\tilde{h}_{w_1'w_1'} + \tilde{h}_{\vartheta_1'\vartheta_1'}) \end{array} \right\}$$

$$\tilde{J}_t D_0^2 \tilde{\vartheta}_2 + \frac{\beta^2}{\chi^2} \cdot \tilde{\vartheta}_2^{iv} - (1 + \beta^2) \cdot \tilde{\vartheta}_2^{ii} + \lambda_L^2 \cdot \tilde{h}_{\vartheta_2} = -2\tilde{J}_t D_0 D_1 \tilde{\vartheta}_1 + \lambda_Q^2 \left\{ \begin{array}{l} \tilde{\vartheta}_1^{ii} \cdot \tilde{h}_{w_1} + \tilde{w}_1^{ii} \cdot \tilde{h}_{\vartheta_1} + \\ -\tilde{h}_{w_1'\vartheta_1'} \end{array} \right\}$$

With respect to the linear ones, we get non-homogenous coupled linear ordinary differential equations. Hence substituting the modal expansion proposed for the linear terms we get the following expressions for the right hand side terms of the flexural and torsional equations.

$$(1) = \left\{ \begin{array}{l} -2 \sum_{n=1}^{\infty} \{ i \tilde{\omega}_{w,n} D_1 Z_n \exp(i \cdot \tilde{\omega}_{w,n} \cdot T_0) + c. c. \} W_n(\xi) + \\ \left. \begin{array}{l} \sum_{p,r=1}^{\infty} \left\{ \begin{array}{l} Z_p Z_r \exp(i \cdot (\tilde{\omega}_{w,p} + \tilde{\omega}_{w,r}) \cdot T_0) + \\ Z_p \tilde{Z}_r \exp(i \cdot (\tilde{\omega}_{w,p} - \tilde{\omega}_{w,r}) \cdot T_0) + \\ + c. c. \end{array} \right\} \cdot \left\{ W_p^{ii} \cdot \tilde{h}_{w_r} - \frac{1}{2} \cdot \tilde{h}_{w_p'w_r'} \right\} + \\ \sum_{q,s=1}^{\infty} \left\{ \begin{array}{l} \Gamma_q \Gamma_s \exp(i \cdot (\tilde{\omega}_{\vartheta,q} + \tilde{\omega}_{\vartheta,s}) \cdot T_0) + \\ \Gamma_q \tilde{\Gamma}_s \exp(i \cdot (\tilde{\omega}_{\vartheta,q} - \tilde{\omega}_{\vartheta,s}) \cdot T_0) + \\ + c. c. \end{array} \right\} \cdot \left\{ \Theta_q^{ii} \cdot \tilde{h}_{\vartheta_s} - \frac{1}{2} \cdot \tilde{h}_{\vartheta_q'\vartheta_s'} \right\} \end{array} \right\} \end{array} \right\}$$

$$(2) = \left\{ \begin{array}{l} -2\tilde{J}_t \sum_{m=1}^{\infty} \{i\tilde{\omega}_{\vartheta,m} D_1 \Gamma_m \exp(i \cdot \tilde{\omega}_{\vartheta,m} \cdot T_0) + c. c.\} \theta_m(\xi) + \\ + \lambda_Q^2 \sum_{p,q=1}^{\infty} \left\{ \begin{array}{l} Z_p \Gamma_q \exp(i \cdot (\tilde{\omega}_{w,p} + \tilde{\omega}_{\vartheta,q}) \cdot T_0) + \\ Z_p \tilde{\Gamma}_q \exp(i \cdot (\tilde{\omega}_{w,p} - \tilde{\omega}_{\vartheta,q}) \cdot T_0) + \\ + c. c. \end{array} \right\} \cdot \left\{ \theta_q^{ii} \cdot \tilde{h}_{W_p} + W_p^{ii} \cdot \tilde{h}_{\theta_q} - \tilde{h}_{W_p' \theta_q'} \right\} \end{array} \right\}$$

The solution of these equations is feasible only enforcing additional conditions.

The so-called Solvability Conditions simply enforce that the secular terms vanishes in time, that means the terms associated to the lower order contributions are damped out as time overcome the threshold of validity for them. In mathematical terms this simply requires that the particular integral of the solutions must have any exponential term function of the lower order time scale. Otherwise, the solution will contain a term growing linearly with the lower time scale since the exponential term is already taken in account in the homogeneous contribution that is identical to the linear format. Hence, to avoid that the exponential term function of the lower order time scale would have a multiplicity of two, we need that the right hand side term proportional to it has to vanish.

Things are a little bit more complex since we are dealing with a generic combination of interacting modes also for the same motion component. Thence, we need to make some assumptions to restrict the area of investigations. We will assume to neglect combinational internal resonances of additive and difference (anti-resonance) type, focusing on the so-called one-to-one internal resonance.

However, before proceeding we want just to mention the fact that in order to analyse by means of a mode-by-mode approach the two-to-one internal resonance is necessary to assume that $\tilde{\omega}_{w,n} = 2\tilde{\omega}_{\vartheta,q} + \epsilon^2 \sigma$. The detailed process will be clear in the following treatment for the one-to one resonance. Hence, we will just report the final equations governing the time variation of flexural and torsional amplitudes and phases.

$$D_2 \bar{Z}_n = \frac{1}{2} \left\{ \frac{1}{\tilde{\omega}_{w,n} M_{w,n}} \left(\bar{F}_{w,n} \cdot \sin \delta_w - \frac{1}{2} \alpha \cdot \bar{\Gamma}_n^2 \cdot \sin \delta_1 \right) - \nu_w \bar{Z}_n \right\}$$

$$D_2 \gamma_{w,n} = \frac{1}{2} \frac{1}{\tilde{\omega}_{w,n} M_{w,n}} \left\{ \frac{1}{2} \left[\alpha \cdot \bar{\Gamma}_n^2 / \bar{Z}_n \cdot \cos \delta_1 \right] + \bar{F}_{w,n} \cos \delta_w \right\}$$

$$D_2 \bar{\Gamma}_n = \frac{1}{2} \left\{ \frac{1}{\tilde{J}_t \cdot \tilde{\omega}_{\vartheta,n} M_{\vartheta,n}} \left(\bar{F}_{\vartheta,n} \cdot \sin \delta_{\vartheta} + \alpha \cdot \bar{\Gamma}_n \bar{Z}_n \cdot \sin \delta_1 \right) - \nu_w \bar{\Gamma}_n \right\}$$

$$D_2 \gamma_{\vartheta,n} = \frac{1}{2} \frac{1}{\tilde{J}_t \cdot \tilde{\omega}_{\vartheta,n} M_{\vartheta,n}} \left\{ \alpha \cdot \bar{Z}_n \cdot \cos \delta_1 + \bar{F}_{\vartheta,n} \cos \delta_{\vartheta} \right\}$$

Where.

$$\delta_1 = (2\gamma_{\vartheta,n} - \gamma_{w,n} - \sigma \cdot T_1)$$

$$\delta_w = (\Omega_w - \tilde{\omega}_{w,n}) T_0 - \gamma_{w,n}$$

$$\delta_{\vartheta} = (\Omega_{\vartheta} - \tilde{\omega}_{\vartheta,n}) T_0 - \gamma_{\vartheta,n}$$

$$\alpha = \lambda_Q^2 \left\{ \frac{1}{2} \tilde{h}_{W_n} \cdot \tilde{h}_{\theta_n' \theta_n'} + \tilde{h}_{\theta_n'} \cdot \tilde{h}_{W_n' \theta_n'} \right\}$$

We will not exploit any further analysis towards the two-to-one analysis since computations become very cumbersome. Anyway we report the governing equations that are easy to handle in a numerical integration approach.

Hence, focusing on the one-to one resonance for the flexural motion we can write the constraint on the circular eigen-frequencies and the solvability conditions as follows.

$$\begin{cases} \tilde{\omega}_{w,p} \pm \tilde{\omega}_{w,r} \neq \tilde{\omega}_{w,n} \\ \tilde{\omega}_{\vartheta,q} \pm \tilde{\omega}_{\vartheta,s} \neq \tilde{\omega}_{w,n} \end{cases} \Rightarrow D_1 Z_n = 0 \Rightarrow Z_n = Z_n(T_2)$$

Whilst, for the torsional.

$$\tilde{\omega}_{w,p} \pm \tilde{\omega}_{\vartheta,q} \neq \tilde{\omega}_{\vartheta,m} \Rightarrow D_1 \Gamma_m = 0 \Rightarrow \Gamma_m = \Gamma_m(T_2)$$

As we can see the main consequence is that the amplitudes of vibrations are no more function of the second order time scale T_1 .

Thence, suitable solutions for the quadratic system can be search in the following form.

$$\tilde{w}_2(\xi, T_0, T_2) = \left\{ \begin{array}{l} \sum_{p,r=1}^{\infty} \left\{ \begin{array}{l} Z_p Z_r \exp(i \cdot (\tilde{\omega}_{w,p} + \tilde{\omega}_{w,r}) \cdot T_0) \cdot Y_{pr,1}(\xi) + \\ + Z_p \tilde{Z}_r \exp(i \cdot (\tilde{\omega}_{w,p} - \tilde{\omega}_{w,r}) \cdot T_0) \cdot Y_{pr,2}(\xi) + \\ + c. c. \end{array} \right\} + \\ \\ + \sum_{q,s=1}^{\infty} \left\{ \begin{array}{l} \Gamma_q \Gamma_s \exp(i \cdot (\tilde{\omega}_{\vartheta,q} + \tilde{\omega}_{\vartheta,s}) \cdot T_0) \cdot T_{qs,1}(\xi) + \\ \Gamma_q \tilde{\Gamma}_s \exp(i \cdot (\tilde{\omega}_{\vartheta,q} - \tilde{\omega}_{\vartheta,s}) \cdot T_0) \cdot T_{qs,2}(\xi) + \\ + c. c. \end{array} \right\} \end{array} \right\}$$

$$\tilde{\vartheta}_2(\xi, T_0, T_2) = \sum_{p,q=1}^{\infty} \left\{ \begin{array}{l} Z_p \Gamma_q \exp(i \cdot (\tilde{\omega}_{w,p} + \tilde{\omega}_{\vartheta,q}) \cdot T_0) \cdot H_{pq,1}(\xi) + \\ Z_p \tilde{\Gamma}_q \exp(i \cdot (\tilde{\omega}_{w,p} - \tilde{\omega}_{\vartheta,q}) \cdot T_0) \cdot H_{pq,2}(\xi) + \\ + c. c. \end{array} \right\}$$

Finally substituting in the quadratic equations of motion and collecting similar time dependent terms, we can recognise six independent equations of motion allowing us to find the six unknown functions $Y_{pr,1}(\xi)$, $Y_{pr,2}(\xi)$, $T_{qs,1}(\xi)$, $T_{qs,2}(\xi)$, $H_{pq,1}(\xi)$, $H_{pq,2}(\xi)$. These can be referred as second order corrections of linear modal shapes, hence we will refer to them as to Quadratic Modes. Notice that the global solution of the suspension bridge will be a combination of linear and quadratic modes that vibrates according to different frequencies. Further the quadratic ones will be smoothed out by the scaling factor ϵ , hence the contribution to the overall shape is expected to be just a perturbation of the dominant linear shape. Though we must remember that this perturbation grows as the modal order does.

The six independent equations can be written as follows.

$$\begin{aligned} \mu^2 \cdot Y_{pr,1}^{iv} - Y_{pr,1}^{ii} - (\tilde{\omega}_{w,p} + \tilde{\omega}_{w,r})^2 \cdot Y_{pr,1} + \lambda_L^2 \cdot \tilde{h}_{Y_{pr,1}} &= \lambda_Q^2 \left(W_p^{ii} \cdot \tilde{h}_{W_r} - \frac{1}{2} \cdot \tilde{h}_{W_p'W_r'} \right) \\ \mu^2 \cdot Y_{pr,2}^{iv} - Y_{pr,2}^{ii} - (\tilde{\omega}_{w,p} - \tilde{\omega}_{w,r})^2 \cdot Y_{pr,2} + \lambda_L^2 \cdot \tilde{h}_{Y_{pr,2}} &= \lambda_Q^2 \left(W_p^{ii} \cdot \tilde{h}_{W_r} - \frac{1}{2} \cdot \tilde{h}_{W_p'W_r'} \right) \\ \mu^2 \cdot T_{qs,1}^{iv} - T_{qs,1}^{ii} - (\tilde{\omega}_{\vartheta,q} + \tilde{\omega}_{\vartheta,s})^2 \cdot T_{qs,1} + \lambda_L^2 \cdot \tilde{h}_{T_{qs,1}} &= \lambda_Q^2 \left(\Theta_q^{ii} \cdot \tilde{h}_{\Theta_s} - \frac{1}{2} \cdot \tilde{h}_{\Theta_q'\Theta_s'} \right) \\ \mu^2 \cdot T_{qs,2}^{iv} - T_{qs,2}^{ii} - (\tilde{\omega}_{\vartheta,q} - \tilde{\omega}_{\vartheta,s})^2 \cdot T_{qs,2} + \lambda_L^2 \cdot \tilde{h}_{T_{qs,2}} &= \lambda_Q^2 \left(\Theta_q^{ii} \cdot \tilde{h}_{\Theta_s} - \frac{1}{2} \cdot \tilde{h}_{\Theta_q'\Theta_s'} \right) \\ \left\{ \begin{array}{l} \frac{\beta^2}{\chi^2} \cdot H_{pq,1}^{iv} - (1 + \beta^2) \cdot H_{pq,1}^{ii} + \\ -\tilde{J}_t(\tilde{\omega}_{w,p} + \tilde{\omega}_{\vartheta,q})^2 H_{pq,1} + \lambda_L^2 \cdot \tilde{h}_{H_{pq,1}} \end{array} \right\} &= \lambda_Q^2 \left(\Theta_q^{ii} \cdot \tilde{h}_{W_p} + W_p^{ii} \cdot \tilde{h}_{\Theta_q} - \tilde{h}_{W_p'\Theta_q'} \right) \\ \left\{ \begin{array}{l} \frac{\beta^2}{\chi^2} \cdot H_{pq,2}^{iv} - (1 + \beta^2) \cdot H_{pq,2}^{ii} + \\ -\tilde{J}_t(\tilde{\omega}_{w,p} - \tilde{\omega}_{\vartheta,q})^2 H_{pq,2} + \lambda_L^2 \cdot \tilde{h}_{H_{pq,2}} \end{array} \right\} &= \lambda_Q^2 \left(\Theta_q^{ii} \cdot \tilde{h}_{W_p} + W_p^{ii} \cdot \tilde{h}_{\Theta_q} - \tilde{h}_{W_p'\Theta_q'} \right) \end{aligned}$$

As we can see we obtain six linear non-homogenous ordinary differential equations of fourth order, where the right-hand side term is known as the linear modes has been determined.

In order to solve the whole set of equations we need proper boundary conditions. Since we are dealing with modal shapes we may assume that the same conditions enforced on the linear ones are still valid here. Hence, we will enforce that the functions and their second derivative vanishes at the extremities of the domain. It's evident that the choice of symmetric or skew-symmetric modes strongly influence the shape of the previous equations and then the computations required.

3.1.1 Skew-symmetric modes

Let's assume first of all that the structural parameters are such that the structure vibrates according to skew-symmetric linear modes.

$$W_n(\xi) = \sin(2n\pi \cdot \xi)$$

$$\Theta_m(\xi) = \sin(2m\pi \cdot \xi)$$

Substituting in the equations, we immediately see that all the integrals of the modal shapes vanishes hence remains just the contribution coming from the slopes. We get the same expression commonly found in the Fourier series proof that requires to apply the orthogonality lemma.

$$\int_0^1 \cos(2n\pi \cdot \xi) \cdot \cos(2m\pi \cdot \xi) d\xi = \begin{cases} 0 \Leftrightarrow n \neq m \\ 1/2 \Leftrightarrow n = m \neq 0 \\ 1 \Leftrightarrow n = m = 0 \end{cases}$$

The last case will not be feasible in physical systems, hence let's focus on the first two.

➤ Mode-by-mode vibrations:

In the so-called mode-by-mode oscillation we assume that each quadratic modal configuration interact with itself only. In real life system this is not true but generally should be a good approximation since this is the higher contribution to the overall response. Hence we are in the second case with $n = m \neq 0$.

The solution can be found only making some a priori assumptions on the modal shape and then checking it. Hence we will assume that also the second order correction of skew-symmetric linear modes perform the same symmetries. Consequently $\tilde{h}_{(c)} = 0$, and the equations can be written in the following format.

Let's focus on the first equation.

$$\mu^2 \cdot Y_{n,1}^{iv} - Y_{n,1}^{ii} - 4\tilde{\omega}_{w,n}^2 \cdot Y_{n,1} + \lambda_Q^2 (n\pi/2)^2 = 0$$

As we can see the equation is similar to the one that governs the vibration of flexural linear modes in the general case. The slight modifications concern the constant term and the circular-eigen frequency to be used inside the trigonometric and hyperbolic exponential parameters Ψ and η .

Then with the same procedure performed with linear modes, we get a similar expression obtained for the general symmetric linear modes.

$$Y_{n,1}(\xi) = \frac{\lambda_Q^2 (n\pi/2)^2}{4\tilde{\omega}_{w,n}^2} \cdot \left\{ 1 - \frac{1}{\Psi_{w,n}^2 + \eta_{w,n}^2} \cdot \left(\eta_{w,n}^2 \cdot \frac{\cosh(\Psi_{w,n} \cdot (\xi - \frac{1}{2}))}{\cosh(\frac{\Psi_{w,n}}{2})} + \Psi_{w,n}^2 \cdot \frac{\cos(\eta_{w,n} \cdot (\xi - \frac{1}{2}))}{\cos(\frac{\eta_{w,n}}{2})} \right) \right\}$$

The modal shape just found is not feasible since it does not satisfy the initial hypothesis made that allow us to cancel out $\tilde{h}_{(c)}$.

This means that effectively, in the case of a mode-by mode formulation, the second order correction of a skew-symmetric linear mode is symmetric. Hence assuming $\tilde{h}_{(c)} \neq 0$ we get the following exact modal shape.

$$Y_{n,1}(\xi) = \bar{Y}_{n,1} \cdot \left\{ 1 - \frac{1}{\Psi_{w,n}^2 + \eta_{w,n}^2} \cdot \left(\eta_{w,n}^2 \cdot \frac{\cosh(\Psi_{w,n} \cdot (\xi - \frac{1}{2}))}{\cosh(\frac{\Psi_{w,n}}{2})} + \Psi_{w,n}^2 \cdot \frac{\cos(\eta_{w,n} \cdot (\xi - \frac{1}{2}))}{\cos(\frac{\eta_{w,n}}{2})} \right) \right\}$$

Where.

$$\bar{Y}_{n,1} = \left\{ \frac{\lambda_Q^2 (n\pi/2)^2}{4\tilde{\omega}_{w,n}^2} / \left(1 - \frac{\lambda_L^2}{4\tilde{\omega}_{w,n}^2} \left(1 - \frac{1}{\Psi_{w,n}^2 + \eta_{w,n}^2} \cdot \left(\eta_{w,n}^2 \cdot \frac{\tanh(\Psi_{w,n}/2)}{\Psi_{w,n}/2} + \Psi_{w,n}^2 \cdot \frac{\cos(\eta_{w,n}/2)}{\eta_{w,n}/2} \right) \right) \right) \right\}$$

However, the modal amplitude is not of interest since the shape will be normalised so that $\bar{Y}_{n,1} = 1$.

The solution for $T_{n,1}(\xi)$ and $H_{n,1}(\xi)$ have the same format, but we must pay attention to the fact that the equivalent frequency changes as the expression for Ψ and η .

Notice that though not relevant the expression for modal amplitudes of torsional quadratic modes has to be doubled due to different contribution coming from the slope stiffening term.

$$T_{n,1}(\xi) \Rightarrow 4\tilde{\omega}_{\vartheta,n}^2 \Rightarrow \Psi_{w,n}; \eta_{w,n}$$

$$H_{n,1}(\xi) \Rightarrow \tilde{J}_t(\tilde{\omega}_{w,n} + \tilde{\omega}_{\vartheta,n})^2 \Rightarrow \Psi_{\vartheta,n}; \eta_{\vartheta,n}$$

Though not relevant, for torsional second order contributions we need always to double the modal amplitudes with respect to the expression found for the flexural ones, due to the slight difference in the stiffening slope term in the governing equations.

A different condition can be found for the other three functions since for mode-by-mode approach has null inertial contribution being $\tilde{\omega}_{(\cdot),i} - \tilde{\omega}_{(\cdot),j} = 0$.

$$\mu^2 \cdot Y_{n,2}^{iv} - Y_{n,2}^{ii} + \lambda_L^2 \cdot \tilde{h}_{Y_{n,2}} + \lambda_Q^2 (n\pi/2)^2 = 0$$

Notice that we assume the quadratic mode to be symmetric.

$$Y_{n,2}(\xi) = \bar{Y}_{n,2} \cdot \left\{ \frac{1}{\bar{\lambda}^2} \left(1 - \frac{\cosh(\bar{\lambda}(\xi - \frac{1}{2}))}{\cosh(\bar{\lambda}/2)} \right) - \frac{\xi}{2} \left(\xi - \frac{1}{2} \right) \right\}$$

$$\bar{\lambda} = 1/\mu$$

$$\bar{Y}_{n,2} = \left\{ \lambda_Q^2 (n\pi/2)^2 / \left(1 - \lambda_L^2 \left(\frac{1}{\bar{\lambda}^2} \left(1 - \frac{\tanh(\bar{\lambda}/2)}{\bar{\lambda}/2} \right) - \frac{1}{12} \right) \right) \right\}$$

Hence the hypothesis was true, and we get also in this case a symmetric correction of a skew-symmetric linear shape. The flexural mode $\bar{T}_{n,2}$ has the same expression of $Y_{n,2}$, whilst slight modification occurs for the torsional ones.

$$H_{n,2}(\xi) \Rightarrow \bar{\lambda} = \frac{\beta^2/\chi^2}{1+\beta^2}$$

➤ Multi-mode vibrations

In this case we will consider the effects on quadratic modes coming from the interaction between two different linear modes. Since $n \neq m$ all the governing equations become homogeneous. Hence, we will assume that the second order correction will be skew-symmetric as the associated linear mode, meaning $\tilde{h}_{(\cdot)} = 0$.

$$\mu^2 \cdot Y_{nm,1}^{iv} - Y_{nm,1}^{ii} - (\tilde{\omega}_{w,n} + \tilde{\omega}_{w,m})^2 \cdot Y_{nm,1} = 0$$

We get a governing equation similar to the one for skew-symmetric modes, with a slight different frequency. Hence we can state that with respect to the mode-by-mode approach that gives always symmetric quadratic modes, in the multi-mode one there is a condition that grant the solution function to be skew-symmetric.

This condition concern the equivalent combinational frequency.

$$Y_{nm,1} = \sin(2k\pi \cdot \xi) \Leftrightarrow (\tilde{\omega}_{w,n} + \tilde{\omega}_{w,m}) = 2k\pi \cdot \sqrt{1 + \mu^2 \cdot (2k\pi)^2} \quad \text{with } k = n, m$$

This means that the quadratic correction of two interacting modes is able to shapes itself according to one of the them. Similar expressions holds for the other flexural functions.

$$Y_{nm,2} \Rightarrow (\tilde{\omega}_{w,n} - \tilde{\omega}_{w,m}) = 2k\pi \cdot \sqrt{1 + \mu^2 \cdot (2k\pi)^2}$$

$$T_{nm,1} \Rightarrow (\tilde{\omega}_{\vartheta,n} + \tilde{\omega}_{\vartheta,m}) = 2k\pi \cdot \sqrt{1 + \mu^2 \cdot (2k\pi)^2}$$

$$T_{nm,2} \Rightarrow (\tilde{\omega}_{\vartheta,n} - \tilde{\omega}_{\vartheta,m}) = 2k\pi \cdot \sqrt{1 + \mu^2 \cdot (2k\pi)^2}$$

Whilst the torsional ones becomes as follows.

$$H_{nm,1} \Rightarrow \sqrt{\tilde{J}_t} \cdot (\tilde{\omega}_{w,n} + \tilde{\omega}_{\vartheta,m}) = 2k\pi \cdot \sqrt{1 + \beta^2 + \frac{\beta^2}{\chi^2} \cdot (2k\pi)^2}$$

$$H_{nm,2} \Rightarrow \sqrt{\tilde{J}_t} \cdot (\tilde{\omega}_{w,n} - \tilde{\omega}_{\vartheta,m}) = 2k\pi \cdot \sqrt{1 + \beta^2 + \frac{\beta^2}{\chi^2} \cdot (2k\pi)^2}$$

If the conditions are not satisfied the modal shapes are identical to those obtained in the mode-by-mode approach being normalized with respect to the modal amplitude.

What is important to underline is that in most of the cases the second order correction of skew-symmetric modes is symmetric [24]. This seems to confirm what observed experimentally during oscillations of the Takoma Narrows Bridge just before the collapse and then confirmed by numerical results obtained by means of a simple two dof model of suspension bridge. That is, non-linear oscillations of suspension bridges can lose symmetries and vibrations are characterized by the higher oscillation that moves along the span generating the well-known travelling wave phenomenon. Notice that we cannot have the max amplitude fixed on the same point just to the fact that quadratic modes vibrates with a frequency that is different from the one of linear modes.

3.1.2 Symmetric modes

Let's now focus on the symmetric response of the suspension bridge. As we can see from the governing equations is not possible that the second order correction of symmetric linear mode is skew-symmetric since the right-hand side known term cannot vanish. Hence any travelling waves phenomenon will be expected.

➤ Multi-mode vibrations

Let's start from the flexural motion.

$$Y_{pr,1} = \left\{ \begin{array}{l} \bar{Y}_{1,1} \cdot \frac{\cosh(\Psi_{w,pr} \cdot (\xi - \frac{1}{2}))}{\cosh(\frac{\Psi_{w,pr}}{2})} + \bar{Y}_{1,2} \cdot \frac{\cos(\eta_{w,pr} \cdot (\xi - \frac{1}{2}))}{\cos(\frac{\eta_{w,pr}}{2})} + \\ + \bar{Y}_{1,3} \cdot \left(\frac{\cos(\eta_{w,p} \cdot (\xi - 1/2)) / \cos(\eta_{w,p}/2)}{\mu^2 \cdot \eta_{w,p}^4 + \eta_{w,p}^2 - (\tilde{\omega}_{w,p} + \tilde{\omega}_{w,r})^2} - \frac{\cosh(\Psi_{w,p} \cdot (\xi - 1/2)) / \cosh(\Psi_{w,p}/2)}{\mu^2 \cdot \Psi_{w,p}^4 - \Psi_{w,p}^2 - (\tilde{\omega}_{w,p} + \tilde{\omega}_{w,r})^2} \right) + \bar{Y}_{1,4} \end{array} \right\}$$

Where.

$$\Psi_{w,pr}^2 = \frac{1}{2\mu^2} \left(\sqrt{1 + 4\mu^2 \cdot (\tilde{\omega}_{w,p} + \tilde{\omega}_{w,r})^2} + 1 \right) = \eta_{w,pr}^2 + \frac{1}{\mu^2}$$

$$\Psi_{w,p}^2 = \frac{1}{2\mu^2} \left(\sqrt{1 + 4\mu^2 \cdot \tilde{\omega}_{w,p}^2} + 1 \right) = \eta_{w,p}^2 + \frac{1}{\mu^2}$$

$$\bar{Y}_{1,1} = \frac{1}{\bar{Y}_{1,5}} \left(\frac{\bar{Y}_{1,3}}{\Psi_{w,pr}^2 + \eta_{w,pr}^2} \cdot \left\{ \begin{array}{l} \left[\eta_{w,p}^2 \left[1 - \frac{\lambda_L^2}{(\tilde{\omega}_{w,p} + \tilde{\omega}_{w,r})^2} \left(1 - \frac{\tan(\frac{\eta_{w,pr}}{2})}{(\frac{\eta_{w,pr}}{2})} \right) \right] + \right. \\ \left. - \eta_{w,pr}^2 \left[1 - \frac{\lambda_L^2}{(\tilde{\omega}_{w,p} + \tilde{\omega}_{w,r})^2} \left(1 - \frac{\tan(\frac{\eta_{w,p}}{2})}{(\frac{\eta_{w,p}}{2})} \right) \right] \right] \right\} + \\ \frac{\lambda_Q^2}{2} \frac{\tilde{h}_{Wp}' W_r'}{(\tilde{\omega}_{w,p} + \tilde{\omega}_{w,r})^2} \cdot \eta_{w,pr}^2 \\ + \frac{\left\{ \begin{array}{l} \Psi_{w,p}^2 \left[1 - \frac{\lambda_L^2}{(\tilde{\omega}_{w,p} + \tilde{\omega}_{w,r})^2} \left(1 - \frac{\tanh(\frac{\eta_{w,pr}}{2})}{(\frac{\eta_{w,pr}}{2})} \right) \right] + \right. \\ \left. + \eta_{w,pr}^2 \left[1 - \frac{\lambda_L^2}{(\tilde{\omega}_{w,p} + \tilde{\omega}_{w,r})^2} \left(1 - \frac{\tanh(\frac{\Psi_{w,p}}{2})}{(\frac{\Psi_{w,p}}{2})} \right) \right] \right\}}{\mu^2 \cdot \Psi_{w,p}^4 - \Psi_{w,p}^2 - (\tilde{\omega}_{w,p} + \tilde{\omega}_{w,r})^2} \right)$$

$$\bar{Y}_{1,2} = \frac{1}{\bar{Y}_{1,5}} \left(-\frac{\bar{Y}_{1,3}}{\Psi_{w,pr}^2 + \eta_{w,pr}^2} \cdot \left\{ \frac{\left(\eta_{w,p}^2 \left[1 - \frac{\lambda_L^2}{(\tilde{\omega}_{w,p} + \tilde{\omega}_{w,r})^2} \left(1 - \frac{\tanh\left(\frac{\Psi_{w,pr}}{2}\right)}{\left(\frac{\Psi_{w,pr}}{2}\right)} \right) \right] + \right.}{\mu^2 \cdot \eta_{w,p}^4 + \eta_{w,p}^2 - (\tilde{\omega}_{w,p} + \tilde{\omega}_{w,r})^2} + \right.}{\left. \frac{\left(\Psi_{w,p}^2 \left[1 - \frac{\lambda_L^2}{(\tilde{\omega}_{w,p} + \tilde{\omega}_{w,r})^2} \left(1 - \frac{\tan\left(\frac{\eta_{w,p}}{2}\right)}{\left(\frac{\eta_{w,p}}{2}\right)} \right) \right] \right) + \right.}{\mu^2 \cdot \Psi_{w,p}^4 - \Psi_{w,p}^2 - (\tilde{\omega}_{w,p} + \tilde{\omega}_{w,r})^2} + \right.}{\left. - \Psi_{w,pr}^2 \left[1 - \frac{\lambda_L^2}{(\tilde{\omega}_{w,p} + \tilde{\omega}_{w,r})^2} \left(1 - \frac{\tanh\left(\frac{\Psi_{w,p}}{2}\right)}{\left(\frac{\Psi_{w,p}}{2}\right)} \right) \right] \right) \right\} + \frac{\lambda_Q^2}{2} \frac{\tilde{h}_{w,p}' w_r'}{(\tilde{\omega}_{w,p} + \tilde{\omega}_{w,r})^2} \cdot \Psi_{w,pr}^2 \right)$$

$$\bar{Y}_{1,3} = \frac{\lambda_L^2 \lambda_Q^2 \tilde{h}_{w,p} \tilde{h}_{w,r}}{\tilde{\omega}_{w,p}^2} \cdot \frac{\Psi_{w,p}^2 \eta_{w,p}^2}{\Psi_{w,p}^2 + \eta_{w,p}^2}$$

$$\bar{Y}_{1,4} = \frac{1}{\bar{Y}_{1,5}} \left(\frac{\bar{Y}_{1,3}}{\Psi_{w,pr}^2 + \eta_{w,pr}^2} \cdot \frac{\lambda_L^2}{(\tilde{\omega}_{w,p} + \tilde{\omega}_{w,r})^2} \left\{ \frac{\left(\eta_{w,p}^2 \left(\frac{\tanh\left(\frac{\Psi_{w,pr}}{2}\right)}{\left(\frac{\Psi_{w,pr}}{2}\right)} - \frac{\tan\left(\frac{\eta_{w,pr}}{2}\right)}{\left(\frac{\eta_{w,pr}}{2}\right)} \right) + \right.}{\mu^2 \cdot \eta_{w,p}^4 + \eta_{w,p}^2 - (\tilde{\omega}_{w,p} + \tilde{\omega}_{w,r})^2} + \right.}{\left. - \eta_{w,pr}^2 \left(\frac{\tanh\left(\frac{\Psi_{w,pr}}{2}\right)}{\left(\frac{\Psi_{w,pr}}{2}\right)} - \frac{\tan\left(\frac{\eta_{w,p}}{2}\right)}{\left(\frac{\eta_{w,p}}{2}\right)} \right) + \right.}{\left. - \Psi_{w,pr}^2 \left(\frac{\tan\left(\frac{\eta_{w,pr}}{2}\right)}{\left(\frac{\eta_{w,pr}}{2}\right)} - \frac{\tan\left(\frac{\eta_{w,p}}{2}\right)}{\left(\frac{\eta_{w,p}}{2}\right)} \right) \right) \right\} + \frac{\lambda_Q^2}{2} \frac{\tilde{h}_{w,p}' w_r'}{(\tilde{\omega}_{w,p} + \tilde{\omega}_{w,r})^2} \right)$$

$$\bar{Y}_{1,5} = 1 - \frac{\lambda_L^2}{(\tilde{\omega}_{w,p} + \tilde{\omega}_{w,r})^2} \left\{ 1 - \frac{1}{\Psi_{w,pr}^2 + \eta_{w,pr}^2} \left(\eta_{w,pr}^2 \frac{\tanh\left(\frac{\Psi_{w,pr}}{2}\right)}{\left(\frac{\Psi_{w,pr}}{2}\right)} + \Psi_{w,pr}^2 \frac{\tan\left(\frac{\eta_{w,pr}}{2}\right)}{\left(\frac{\eta_{w,pr}}{2}\right)} \right) \right\}$$

We get similar expression for the other functions with slight modifications.

$$Y_{pr,2} \Rightarrow \begin{cases} (\tilde{\omega}_{w,p} - \tilde{\omega}_{w,r})^2 \Rightarrow \Psi_{w,pr} ; \eta_{w,pr} \\ \tilde{\omega}_{w,p} \Rightarrow \Psi_{w,p} ; \eta_{w,p} ; \tilde{h}_{w,p}' w_r' \end{cases}$$

$$T_{qs,1} \Rightarrow \begin{cases} (\tilde{\omega}_{\vartheta,q} + \tilde{\omega}_{\vartheta,s})^2 \Rightarrow \Psi_{w,qs} ; \eta_{w,qs} \\ \tilde{\omega}_{\vartheta,q}, \tilde{\omega}_{\vartheta,s} \Rightarrow \Psi_{\vartheta,q} ; \eta_{\vartheta,q} ; \tilde{h}_{\vartheta_q' \vartheta_s'} \end{cases}$$

$$T_{qs,2} \Rightarrow \begin{cases} (\tilde{\omega}_{\vartheta,q} - \tilde{\omega}_{\vartheta,s})^2 \Rightarrow \Psi_{w,qs} ; \eta_{w,qs} \\ \tilde{\omega}_{\vartheta,q}, \tilde{\omega}_{\vartheta,s} \Rightarrow \Psi_{\vartheta,q} ; \eta_{\vartheta,q} ; \tilde{h}_{\vartheta_q' \vartheta_s'} \end{cases}$$

The torsional functions have stronger differences.

$$H_{pq,1} = \left\{ \begin{array}{l} \bar{H}_{1,1} \cdot \frac{\cosh(\Psi_{\vartheta,pq}(\xi - \frac{1}{2}))}{\cosh(\frac{\Psi_{\vartheta,pq}}{2})} + \bar{H}_{1,2} \cdot \frac{\cos(\eta_{\vartheta,pq}(\xi - \frac{1}{2}))}{\cos(\frac{\eta_{\vartheta,pq}}{2})} + \\ + \bar{H}_{1,3} \left(\frac{1}{\tilde{\omega}_{w,p}^2} \frac{\Psi_{w,p}^2 \eta_{w,p}^2}{\Psi_{w,p}^2 + \eta_{w,p}^2} \left\{ \begin{array}{l} \frac{\cos(\eta_{w,p}(\xi - \frac{1}{2}))/\cos(\frac{\eta_{w,p}}{2})}{\frac{\beta^2}{\chi^2} \eta_{w,p}^4 + (1 + \beta^2) \cdot \eta_{w,p}^2 - \tilde{J}_t(\tilde{\omega}_{w,p} + \tilde{\omega}_{\vartheta,q})^2} + \\ - \frac{\cosh(\Psi_{w,p}(\xi - 1/2))/\cosh(\Psi_{w,p}/2)}{\frac{\beta^2}{\chi^2} \Psi_{w,p}^4 - (1 + \beta^2) \cdot \Psi_{w,p}^2 - \tilde{J}_t(\tilde{\omega}_{w,p} + \tilde{\omega}_{\vartheta,q})^2} \end{array} \right\} + \right. \\ \left. + \frac{1}{\tilde{J}_t \cdot \tilde{\omega}_{\vartheta,q}^2} \frac{\Psi_{\vartheta,q}^2 \eta_{\vartheta,q}^2}{\Psi_{\vartheta,q}^2 + \eta_{\vartheta,q}^2} \left\{ \begin{array}{l} \frac{\cos(\eta_{\vartheta,q}(\xi - \frac{1}{2}))/\cos(\frac{\eta_{\vartheta,q}}{2})}{\frac{\beta^2}{\chi^2} \eta_{\vartheta,q}^4 + (1 + \beta^2) \cdot \eta_{\vartheta,q}^2 - \tilde{J}_t(\tilde{\omega}_{w,p} + \tilde{\omega}_{\vartheta,q})^2} + \\ - \frac{\cosh(\Psi_{\vartheta,q}(\xi - 1/2))/\cosh(\Psi_{\vartheta,q}/2)}{\frac{\beta^2}{\chi^2} \Psi_{\vartheta,q}^4 - (1 + \beta^2) \cdot \Psi_{\vartheta,q}^2 - \tilde{J}_t(\tilde{\omega}_{w,p} + \tilde{\omega}_{\vartheta,q})^2} \end{array} \right\} \right. \\ \left. + \bar{H}_{1,4} \right\}$$

Where.

$$\Psi_{\vartheta,pq}^2 = \frac{\chi^2}{2\beta^2} \left(\sqrt{(1 + \beta^2)^2 + 4 \frac{\beta^2}{\chi^2} \cdot \tilde{J}_t(\tilde{\omega}_{w,p} + \tilde{\omega}_{\vartheta,q})^2} + (1 + \beta^2) \right) = \eta_{\vartheta,pq}^2 + \frac{\chi^2}{\beta^2} (1 + \beta^2)$$

$$\Psi_{w,p}^2 = \frac{1}{2\mu^2} \left(\sqrt{1 + 4\mu^2 \cdot \tilde{\omega}_{w,p}^2} + 1 \right) = \eta_{w,p}^2 + \frac{1}{\mu^2}$$

$$\Psi_{\vartheta,q}^2 = \frac{\chi^2}{2\beta^2} \left(\sqrt{(1 + \beta^2)^2 + 4 \frac{\beta^2}{\chi^2} \cdot \tilde{J}_t \tilde{\omega}_{\vartheta,q}^2} + (1 + \beta^2) \right) = \eta_{\vartheta,q}^2 + \frac{\chi^2}{\beta^2} (1 + \beta^2)$$

$$\begin{aligned}
\bar{H}_{1,1} &= \frac{1}{\bar{H}_{1,5}} \frac{1}{\Psi_{\vartheta,pq}{}^2 + \eta_{\vartheta,pq}{}^2} \left\{ \bar{H}_{1,3} \left[\frac{1}{\tilde{\omega}_{w,p}{}^2 \Psi_{w,p}{}^2 + \eta_{w,p}{}^2} \left(\left\{ \begin{aligned} &\eta_{w,p}{}^2 \left[1 - \frac{\lambda_L^2}{\tilde{J}_t(\tilde{\omega}_{w,p} + \tilde{\omega}_{\vartheta,q})^2} \left(1 - \frac{\tan\left(\frac{\eta_{\vartheta,pq}}{2}\right)}{\left(\frac{\eta_{\vartheta,pq}}{2}\right)} \right) \right] + \right. \right. \\ &\left. \left. - \eta_{\vartheta,pq}{}^2 \left[1 - \frac{\lambda_L^2}{\tilde{J}_t(\tilde{\omega}_{w,p} + \tilde{\omega}_{\vartheta,q})^2} \left(1 - \frac{\tan\left(\frac{\eta_{w,p}}{2}\right)}{\left(\frac{\eta_{w,p}}{2}\right)} \right) \right] \right] \right\} + \right. \\ &\left. \frac{\beta^2}{\chi^2} \eta_{w,p}{}^4 + (1 + \beta^2) \cdot \eta_{w,p}{}^2 - \tilde{J}_t(\tilde{\omega}_{w,p} + \tilde{\omega}_{\vartheta,q})^2 \right) + \left. \frac{\Psi_{w,p}{}^2 \left[1 - \frac{\lambda_L^2}{\tilde{J}_t(\tilde{\omega}_{w,p} + \tilde{\omega}_{\vartheta,q})^2} \left(1 - \frac{\tan\left(\frac{\eta_{\vartheta,pq}}{2}\right)}{\left(\frac{\eta_{\vartheta,pq}}{2}\right)} \right) \right] + \right. \right. \\ &\left. \left. + \eta_{\vartheta,pq}{}^2 \left[1 - \frac{\lambda_L^2}{\tilde{J}_t(\tilde{\omega}_{w,p} + \tilde{\omega}_{\vartheta,q})^2} \left(1 - \frac{\tanh\left(\frac{\Psi_{w,p}}{2}\right)}{\left(\frac{\Psi_{w,p}}{2}\right)} \right) \right] \right] \right\} + \frac{\beta^2}{\chi^2} \Psi_{w,p}{}^4 - (1 + \beta^2) \cdot \Psi_{w,p}{}^2 - \tilde{J}_t(\tilde{\omega}_{w,p} + \tilde{\omega}_{\vartheta,q})^2 \right) + \\ &+ \frac{1}{\tilde{J}_t \cdot \tilde{\omega}_{\vartheta,q}{}^2 \Psi_{\vartheta,q}{}^2 + \eta_{\vartheta,q}{}^2} \left(\left\{ \begin{aligned} &\eta_{\vartheta,q}{}^2 \left[1 - \frac{\lambda_L^2}{\tilde{J}_t(\tilde{\omega}_{w,p} + \tilde{\omega}_{\vartheta,q})^2} \left(1 - \frac{\tan\left(\frac{\eta_{\vartheta,pq}}{2}\right)}{\left(\frac{\eta_{\vartheta,pq}}{2}\right)} \right) \right] + \right. \\ &\left. - \eta_{\vartheta,pq}{}^2 \left[1 - \frac{\lambda_L^2}{\tilde{J}_t(\tilde{\omega}_{w,p} + \tilde{\omega}_{\vartheta,q})^2} \left(1 - \frac{\tan\left(\frac{\eta_{\vartheta,q}}{2}\right)}{\left(\frac{\eta_{\vartheta,q}}{2}\right)} \right) \right] \right] \right\} + \right. \\ &\left. \frac{\beta^2}{\chi^2} \eta_{\vartheta,q}{}^4 + (1 + \beta^2) \cdot \eta_{\vartheta,q}{}^2 - \tilde{J}_t(\tilde{\omega}_{w,p} + \tilde{\omega}_{\vartheta,q})^2 \right) + \left. \frac{\Psi_{\vartheta,q}{}^2 \left[1 - \frac{\lambda_L^2}{\tilde{J}_t(\tilde{\omega}_{w,p} + \tilde{\omega}_{\vartheta,q})^2} \left(1 - \frac{\tan\left(\frac{\eta_{\vartheta,pq}}{2}\right)}{\left(\frac{\eta_{\vartheta,pq}}{2}\right)} \right) \right] + \right. \right. \\ &\left. \left. + \eta_{\vartheta,pq}{}^2 \left[1 - \frac{\lambda_L^2}{\tilde{J}_t(\tilde{\omega}_{w,p} + \tilde{\omega}_{\vartheta,q})^2} \left(1 - \frac{\tanh\left(\frac{\Psi_{\vartheta,q}}{2}\right)}{\left(\frac{\Psi_{\vartheta,q}}{2}\right)} \right) \right] \right] \right\} + \frac{\beta^2}{\chi^2} \Psi_{\vartheta,q}{}^4 - (1 + \beta^2) \cdot \Psi_{\vartheta,q}{}^2 - \tilde{J}_t(\tilde{\omega}_{w,p} + \tilde{\omega}_{\vartheta,q})^2 \right) \\ &\left. - \lambda_Q^2 \frac{\tilde{h}_{w,p}' \theta_q'}{\tilde{J}_t(\tilde{\omega}_{w,p} + \tilde{\omega}_{\vartheta,q})^2} \eta_{\vartheta,pq}{}^2 \right\}
\end{aligned}$$

$$\begin{aligned}
\bar{\bar{H}}_{1,2} = \frac{1}{\bar{H}_{1,5}} \frac{1}{\Psi_{\vartheta,pq}^2 + \eta_{\vartheta,pq}^2} & \left\{ \bar{\bar{H}}_{1,3} \left[\frac{1}{\tilde{\omega}_{w,p}^2 \Psi_{w,p}^2 + \eta_{w,p}^2} \left(\left\{ \eta_{w,p}^2 \left[1 - \frac{\lambda_L^2}{\tilde{J}_t(\tilde{\omega}_{w,p} + \tilde{\omega}_{\vartheta,q})^2} \left(1 - \frac{\tanh\left(\frac{\Psi_{\vartheta,pq}}{2}\right)}{\left(\frac{\Psi_{\vartheta,pq}}{2}\right)} \right) \right] + \right. \right. \right. \\
& \left. \left. \left. + \Psi_{\vartheta,pq}^2 \left[1 - \frac{\lambda_L^2}{\tilde{J}_t(\tilde{\omega}_{w,p} + \tilde{\omega}_{\vartheta,q})^2} \left(1 - \frac{\tan\left(\frac{\eta_{w,p}}{2}\right)}{\left(\frac{\eta_{w,p}}{2}\right)} \right) \right] \right) \right] + \frac{\beta^2}{\chi^2} \eta_{w,p}^4 + (1 + \beta^2) \cdot \eta_{w,p}^2 - \tilde{J}_t(\tilde{\omega}_{w,p} + \tilde{\omega}_{\vartheta,q})^2 \right. \\
& \left. + \frac{\beta^2}{\chi^2} \Psi_{w,p}^4 - (1 + \beta^2) \cdot \Psi_{w,p}^2 - \tilde{J}_t(\tilde{\omega}_{w,p} + \tilde{\omega}_{\vartheta,q})^2 \right) + \left. \frac{1}{\tilde{J}_t \cdot \tilde{\omega}_{\vartheta,q}^2} \frac{\Psi_{\vartheta,q}^2 \eta_{\vartheta,q}^2}{\Psi_{\vartheta,q}^2 + \eta_{\vartheta,q}^2} \right\} \\
& + \left\{ \frac{1}{\tilde{J}_t \cdot \tilde{\omega}_{\vartheta,q}^2} \frac{\Psi_{\vartheta,q}^2 \eta_{\vartheta,q}^2}{\Psi_{\vartheta,q}^2 + \eta_{\vartheta,q}^2} \left(\left\{ \eta_{\vartheta,q}^2 \left[1 - \frac{\lambda_L^2}{\tilde{J}_t(\tilde{\omega}_{w,p} + \tilde{\omega}_{\vartheta,q})^2} \left(1 - \frac{\tanh\left(\frac{\Psi_{\vartheta,pq}}{2}\right)}{\left(\frac{\Psi_{\vartheta,pq}}{2}\right)} \right) \right] + \right. \right. \right. \\
& \left. \left. \left. + \Psi_{\vartheta,pq}^2 \left[1 - \frac{\lambda_L^2}{\tilde{J}_t(\tilde{\omega}_{w,p} + \tilde{\omega}_{\vartheta,q})^2} \left(1 - \frac{\tan\left(\frac{\eta_{\vartheta,q}}{2}\right)}{\left(\frac{\eta_{\vartheta,q}}{2}\right)} \right) \right] \right) \right] + \frac{\beta^2}{\chi^2} \eta_{\vartheta,q}^4 + (1 + \beta^2) \cdot \eta_{\vartheta,q}^2 - \tilde{J}_t(\tilde{\omega}_{w,p} + \tilde{\omega}_{\vartheta,q})^2 \right. \\
& \left. + \frac{\beta^2}{\chi^2} \Psi_{\vartheta,q}^4 - (1 + \beta^2) \cdot \Psi_{\vartheta,q}^2 - \tilde{J}_t(\tilde{\omega}_{w,p} + \tilde{\omega}_{\vartheta,q})^2 \right) \\
& - \lambda_Q^2 \frac{\tilde{h}_{w_p} \theta_q'}{\tilde{J}_t(\tilde{\omega}_{w,p} + \tilde{\omega}_{\vartheta,q})^2} \Psi_{\vartheta,pq}^2
\end{aligned}$$

$$\bar{\bar{H}}_{1,3} = \lambda_L^2 \lambda_Q^2 \tilde{h}_{w_p} \tilde{h}_{\vartheta_q}$$

$$\begin{aligned}
\bar{H}_{1,4} = \frac{1}{\bar{H}_{1,5}} & \left(\frac{\bar{H}_{1,3}}{\Psi_{\vartheta,pq}^2 + \eta_{\vartheta,pq}^2} \cdot \right. \\
& \left. \cdot \frac{\lambda_L^2}{\tilde{J}_t(\tilde{\omega}_{w,p} + \tilde{\omega}_{\vartheta,q})^2} \right) \\
& + \frac{1}{\tilde{J}_t \cdot \tilde{\omega}_{\vartheta,q}^2} \frac{\Psi_{\vartheta,q}^2 \eta_{\vartheta,q}^2}{\Psi_{\vartheta,q}^2 + \eta_{\vartheta,q}^2} \\
& + \frac{1}{\tilde{\omega}_{w,p}^2} \frac{\Psi_{w,p}^2 \eta_{w,p}^2}{\Psi_{w,p}^2 + \eta_{w,p}^2} \\
& + \frac{\beta^2}{\chi^2} \frac{\Psi_{w,p}^4 - (1 + \beta^2) \cdot \Psi_{w,p}^2 - \tilde{J}_t(\tilde{\omega}_{w,p} + \tilde{\omega}_{\vartheta,q})^2}{\Psi_{w,p}^2 + \eta_{w,p}^2} \\
& + \frac{\beta^2}{\chi^2} \frac{\Psi_{\vartheta,pq}^4 - (1 + \beta^2) \cdot \Psi_{\vartheta,pq}^2 - \tilde{J}_t(\tilde{\omega}_{w,p} + \tilde{\omega}_{\vartheta,q})^2}{\Psi_{\vartheta,pq}^2 + \eta_{\vartheta,pq}^2} \\
& + \frac{\beta^2}{\chi^2} \frac{\Psi_{\vartheta,q}^4 - (1 + \beta^2) \cdot \Psi_{\vartheta,q}^2 - \tilde{J}_t(\tilde{\omega}_{w,p} + \tilde{\omega}_{\vartheta,q})^2}{\Psi_{\vartheta,q}^2 + \eta_{\vartheta,q}^2} \\
& + \frac{\lambda_Q^2 \tilde{h}_{w,p}' \theta_q'}{\tilde{J}_t(\tilde{\omega}_{w,p} + \tilde{\omega}_{\vartheta,q})^2}
\end{aligned}$$

$$\bar{H}_{1,5} = 1 - \frac{\lambda_L^2}{\tilde{f}_t(\tilde{\omega}_{w,p} + \tilde{\omega}_{\vartheta,q})^2} \left(1 - \frac{1}{\Psi_{\vartheta,pq}^2 + \eta_{\vartheta,pq}^2} \left(\eta_{\vartheta,pq}^2 \frac{\tanh\left(\frac{\Psi_{\vartheta,pq}}{2}\right)}{\left(\frac{\Psi_{\vartheta,pq}}{2}\right)} + \Psi_{\vartheta,pq}^2 \frac{\tan\left(\frac{\eta_{\vartheta,pq}}{2}\right)}{\left(\frac{\eta_{\vartheta,pq}}{2}\right)} \right) \right)$$

A similar expression holds also for the other torsional contribution.

$$H_{pq,2} \Rightarrow \begin{cases} \tilde{f}_t \cdot (\tilde{\omega}_{w,p} - \tilde{\omega}_{\vartheta,q})^2 \Rightarrow \Psi_{\vartheta,pq} ; \eta_{\vartheta,pq} \\ \tilde{\omega}_{w,p} \Rightarrow \Psi_{w,p} ; \eta_{w,p} \\ \tilde{\omega}_{\vartheta,q} \Rightarrow \Psi_{\vartheta,q} ; \eta_{\vartheta,q} \end{cases}$$

➤ Mode-by-mode vibrations

Concerning $Y_{pr,1}$, $T_{qs,1}$, $H_{pq,1}$ we can use the same expression found for the multi-mode approach since the governing equation does not lose any term. On the contrary, for the other functions inertial term vanishes and then we need to reformulate the problem. The modal shape we found are the following.

$$Y_{pp,2} = \left\{ \begin{array}{l} \bar{Y}_{2,1} \cdot \frac{\cosh\left(\Psi_{w,pp} \cdot \left(\xi - \frac{1}{2}\right)\right)}{\cosh\left(\frac{\Psi_{w,pp}}{2}\right)} + \bar{Y}_{2,2} \cdot \frac{\xi}{2} \left(\xi - \frac{1}{2}\right) + \\ + \bar{Y}_{2,3} \cdot \left(\frac{\cos(\eta_{w,p} \cdot (\xi - 1/2)) / \cos(\eta_{w,p}/2)}{\eta_{w,p}^2 (\mu^2 \cdot \eta_{w,p}^2 + 1)} - \frac{\cosh(\Psi_{w,p} \cdot (\xi - 1/2)) / \cosh(\Psi_{w,p}/2)}{\Psi_{w,p}^2 (\mu^2 \cdot \Psi_{w,p}^2 - 1)} \right) + \bar{Y}_{2,4} \end{array} \right\}$$

Where.

$$\Psi_{w,pp}^2 = 1/\mu^2$$

$$\Psi_{w,p}^2 = \frac{1}{2\mu^2} \left(\sqrt{1 + 4\mu^2 \cdot \tilde{\omega}_{w,p}^2} + 1 \right) = \eta_{w,p}^2 + \frac{1}{\mu^2}$$

$$\bar{Y}_{2,1} = \frac{1}{\bar{Y}_{2,5}} \frac{1}{\Psi_{w,pp}^2} \bar{Y}_{2,3} \cdot \left(\begin{array}{l} \frac{\eta_{w,p}^2 + \lambda_L^2 \left(1 - \frac{\tan\left(\frac{\eta_{w,p}}{2}\right)}{\left(\frac{\eta_{w,p}}{2}\right)} + \frac{\eta_{w,p}^2}{12} \right)}{\eta_{w,p}^2 (\mu^2 \cdot \eta_{w,p}^2 + 1)} + \\ + \frac{\Psi_{w,p}^2 - \lambda_L^2 \left(1 - \frac{\tanh\left(\frac{\Psi_{w,p}}{2}\right)}{\left(\frac{\Psi_{w,p}}{2}\right)} - \frac{\Psi_{w,p}^2}{12} \right)}{\Psi_{w,p}^2 (\mu^2 \cdot \Psi_{w,p}^2 - 1)} \end{array} \right) - \frac{\lambda_Q^2}{2} \tilde{h}_{W_p'} W_p'$$

$$\bar{Y}_{2,2} = \frac{1}{\bar{Y}_{2,5}} \left(- \frac{\lambda_L^2}{\Psi_{w,pp}^2} \bar{Y}_{2,3} \cdot \left(\begin{array}{l} \frac{\eta_{w,p}^2 \left(1 - \frac{\tanh\left(\frac{\Psi_{w,pp}}{2}\right)}{\left(\frac{\Psi_{w,pp}}{2}\right)} \right) + \Psi_{w,pp}^2 \left(1 - \frac{\tan\left(\frac{\eta_{w,p}}{2}\right)}{\left(\frac{\eta_{w,p}}{2}\right)} \right)}{\eta_{w,p}^2 (\mu^2 \cdot \eta_{w,p}^2 + 1)} + \\ + \frac{\Psi_{w,p}^2 \left(1 - \frac{\tanh\left(\frac{\Psi_{w,pp}}{2}\right)}{\left(\frac{\Psi_{w,pp}}{2}\right)} \right) - \Psi_{w,pp}^2 \left(1 - \frac{\tanh\left(\frac{\Psi_{w,p}}{2}\right)}{\left(\frac{\Psi_{w,p}}{2}\right)} \right)}{\Psi_{w,p}^2 (\mu^2 \cdot \Psi_{w,p}^2 - 1)} \end{array} \right) + \frac{\lambda_Q^2}{2} \tilde{h}_{W_p'} W_p' \right)$$

$$\bar{Y}_{2,3} = \frac{\lambda_L^2 \lambda_Q^2 \tilde{h}_{Wp}^2}{\tilde{\omega}_{w,p}^2} \cdot \frac{\Psi_{w,p}^2 \eta_{w,p}^2}{\Psi_{w,p}^2 + \eta_{w,p}^2}$$

$$\bar{Y}_{2,4} = -\frac{1}{\Psi_{w,pp}^2} \frac{1}{\bar{Y}_{2,5}} \left\{ \bar{Y}_{2,3} \left(\frac{\eta_{w,p}^2 + \Psi_{w,pp}^2 + \lambda_L^2 \left(\frac{\tanh\left(\frac{\Psi_{w,pp}}{2}\right)}{\left(\frac{\Psi_{w,pp}}{2}\right)} - \frac{\tan\left(\frac{\eta_{w,p}}{2}\right)}{\left(\frac{\eta_{w,p}}{2}\right)} + \frac{\eta_{w,p}^2 + \Psi_{w,pp}^2}{12} \right)}{\eta_{w,p}^2 (\mu^2 \cdot \eta_{w,p}^2 + 1)} + \right. \right. \\ \left. \left. + \frac{\Psi_{w,p}^2 - \Psi_{w,pp}^2 - \lambda_L^2 \left(\frac{\tanh\left(\frac{\Psi_{w,pp}}{2}\right)}{\left(\frac{\Psi_{w,pp}}{2}\right)} - \frac{\tanh\left(\frac{\Psi_{w,p}}{2}\right)}{\left(\frac{\Psi_{w,p}}{2}\right)} - \frac{\Psi_{w,p}^2 - \Psi_{w,pp}^2}{12} \right)}{\Psi_{w,p}^2 (\mu^2 \cdot \Psi_{w,p}^2 - 1)} \right) - \frac{\lambda_Q^2}{2} \tilde{h}_{Wp}' \Psi_{w,p}' \right\}$$

$$\bar{Y}_{2,5} = 1 - \lambda_L^2 \left(\frac{1}{\Psi_{w,pp}^2} \left(1 - \frac{\tanh\left(\frac{\Psi_{w,pp}}{2}\right)}{\left(\frac{\Psi_{w,pp}}{2}\right)} \right) - \frac{1}{12} \right)$$

For the other functions we get similar expressions with slight modifications.

$$T_{qq,2} \Rightarrow \begin{cases} \Psi_{w,qq}^2 = 1/\mu^2 \\ \tilde{\omega}_{\vartheta,q} \Rightarrow \Psi_{\vartheta,q}; \eta_{\vartheta,q}; \tilde{h}_{\vartheta,q}' \Psi_{\vartheta,q}' \end{cases}$$

On the contrary we need to define new expressions for the torsional components.

$$H_{pp,2} = \left\{ \begin{aligned} & \bar{H}_{2,1} \cdot \frac{\cosh\left(\Psi_{\vartheta,pp} \cdot \left(\xi - \frac{1}{2}\right)\right)}{\cosh\left(\frac{\Psi_{\vartheta,pp}}{2}\right)} + \bar{H}_{2,2} \cdot \frac{\xi}{2} \left(\xi - \frac{1}{2}\right) + \\ & \frac{1}{\tilde{\omega}_{w,p}^2} \frac{\Psi_{w,p}^2 \eta_{w,p}^2}{\Psi_{w,p}^2 + \eta_{w,p}^2} \left\{ \frac{\cos\left(\eta_{w,p} \cdot \left(\xi - \frac{1}{2}\right)\right) / \cos\left(\frac{\eta_{w,p}}{2}\right)}{\eta_{w,p}^2 \left(\frac{\beta^2}{\chi^2} \eta_{w,p}^2 + (1 + \beta^2)\right)} + \right. \\ & \left. - \frac{\cosh\left(\Psi_{w,p} \cdot \left(\xi - 1/2\right)\right) / \cosh\left(\Psi_{w,p}/2\right)}{\Psi_{w,p}^2 \left(\frac{\beta^2}{\chi^2} \Psi_{w,p}^2 - (1 + \beta^2)\right)} \right\} + \\ & + \bar{H}_{2,3} \left\{ \frac{1}{\tilde{J}_t \cdot \tilde{\omega}_{\vartheta,p}^2} \frac{\Psi_{\vartheta,p}^2 \eta_{\vartheta,p}^2}{\Psi_{\vartheta,p}^2 + \eta_{\vartheta,p}^2} \left\{ \frac{\cos\left(\eta_{\vartheta,p} \cdot \left(\xi - \frac{1}{2}\right)\right) / \cos\left(\frac{\eta_{\vartheta,p}}{2}\right)}{\eta_{\vartheta,p}^2 \left(\frac{\beta^2}{\chi^2} \eta_{\vartheta,p}^2 + (1 + \beta^2)\right)} + \right. \right. \\ & \left. \left. - \frac{\cosh\left(\Psi_{\vartheta,p} \cdot \left(\xi - 1/2\right)\right) / \cosh\left(\Psi_{\vartheta,p}/2\right)}{\Psi_{\vartheta,p}^2 \left(\frac{\beta^2}{\chi^2} \Psi_{\vartheta,p}^2 - (1 + \beta^2)\right)} \right\} + \right. \\ & \left. + \bar{H}_{2,4} \right\} \end{aligned}$$

Where.

$$\Psi_{\vartheta,pp}^2 = \sqrt{(1 + \beta^2)^2 / (\beta^2 / \chi^2)}$$

$$\Psi_{w,p}^2 = \frac{1}{2\mu^2} \left(\sqrt{1 + 4\mu^2 \cdot \tilde{\omega}_{w,p}^2} + 1 \right) = \eta_{w,p}^2 + \frac{1}{\mu^2}$$

$$\Psi_{\vartheta,p}^2 = \frac{\chi^2}{2\beta^2} \left(\sqrt{(1 + \beta^2)^2 + 4 \frac{\beta^2}{\chi^2} \cdot \tilde{J}_t \tilde{\omega}_{\vartheta,p}^2} + (1 + \beta^2) \right) = \eta_{\vartheta,p}^2 + \frac{\chi^2}{\beta^2} (1 + \beta^2)$$

$$\bar{\bar{H}}_{2,1} = \frac{1}{\bar{H}_{2,5}} \frac{1}{\Psi_{\vartheta,pp}^2} \left\{ \bar{\bar{H}}_{2,3} \left\{ \frac{1}{\tilde{\omega}_{w,p}^2} \frac{\Psi_{w,p}^2 \eta_{w,p}^2}{\Psi_{w,p}^2 + \eta_{w,p}^2} \left(\frac{\eta_{w,p}^2 + \lambda_L^2 \left(1 - \frac{\tan\left(\frac{\eta_{w,p}}{2}\right) + \frac{\eta_{w,p}^2}{12}}{\left(\frac{\eta_{w,p}}{2}\right)} \right)}{\eta_{w,p}^2 \left(\frac{\beta^2}{\chi^2} \eta_{w,p}^2 + (1 + \beta^2) \right)} + \frac{\Psi_{w,p}^2 - \lambda_L^2 \left(1 - \frac{\tanh\left(\frac{\Psi_{w,p}}{2}\right) - \frac{\Psi_{w,p}^2}{12}}{\left(\frac{\Psi_{w,p}}{2}\right)} \right)}{\Psi_{w,p}^2 \left(\frac{\beta^2}{\chi^2} \Psi_{w,p}^2 - (1 + \beta^2) \right)} \right) + \frac{1}{\tilde{J}_t \cdot \tilde{\omega}_{\vartheta,p}^2} \frac{\Psi_{\vartheta,p}^2 \eta_{\vartheta,p}^2}{\Psi_{\vartheta,p}^2 + \eta_{\vartheta,p}^2} \left(\frac{\eta_{\vartheta,p}^2 + \lambda_L^2 \left(1 - \frac{\tan\left(\frac{\eta_{\vartheta,p}}{2}\right) + \frac{\eta_{\vartheta,p}^2}{12}}{\left(\frac{\eta_{\vartheta,p}}{2}\right)} \right)}{\eta_{\vartheta,p}^2 \left(\frac{\beta^2}{\chi^2} \eta_{\vartheta,p}^2 + (1 + \beta^2) \right)} + \frac{\Psi_{\vartheta,p}^2 - \lambda_L^2 \left(1 - \frac{\tanh\left(\frac{\Psi_{\vartheta,p}}{2}\right) - \frac{\Psi_{\vartheta,p}^2}{12}}{\left(\frac{\Psi_{\vartheta,p}}{2}\right)} \right)}{\Psi_{\vartheta,p}^2 \left(\frac{\beta^2}{\chi^2} \Psi_{\vartheta,p}^2 - (1 + \beta^2) \right)} \right) \right\} + \left. \begin{array}{l} -\lambda_Q^2 \tilde{h}_{w_p' \vartheta_p'} \end{array} \right\}$$

$$\begin{aligned}
\bar{\bar{H}}_{2,2} = \frac{1}{\bar{\bar{H}}_{2,5}} & \left. \begin{aligned} & - \frac{\lambda_L^2}{\Psi_{w,pp}^2} \bar{\bar{H}}_{2,3} \cdot \\ & + \frac{1}{\tilde{J}_t \cdot \tilde{\omega}_{\vartheta,q}^2} \frac{\Psi_{\vartheta,p}^2 \eta_{\vartheta,p}^2}{\Psi_{\vartheta,p}^2 + \eta_{\vartheta,p}^2} \\ & + \frac{1}{\tilde{\omega}_{w,p}^2} \frac{\Psi_{w,p}^2 \eta_{w,p}^2}{\Psi_{w,p}^2 + \eta_{w,p}^2} \end{aligned} \right\} \\
& \left. \begin{aligned} & \left[\frac{\eta_{w,p}^2 \left(1 - \frac{\tanh\left(\frac{\Psi_{\vartheta,pp}}{2}\right)}{\left(\frac{\Psi_{\vartheta,pp}}{2}\right)} \right) + \Psi_{\vartheta,pp}^2 \left(1 - \frac{\tan\left(\frac{\eta_{w,p}}{2}\right)}{\left(\frac{\eta_{w,p}}{2}\right)} \right)}{\eta_{w,p}^2 \left(\frac{\beta^2}{\chi^2} \eta_{w,p}^2 + (1 + \beta^2) \right)} + \right. \\ & \left. + \frac{\Psi_{w,p}^2 \left(1 - \frac{\tanh\left(\frac{\Psi_{\vartheta,pp}}{2}\right)}{\left(\frac{\Psi_{\vartheta,pp}}{2}\right)} \right) - \Psi_{\vartheta,pp}^2 \left(1 - \frac{\tanh\left(\frac{\Psi_{w,p}}{2}\right)}{\left(\frac{\Psi_{w,p}}{2}\right)} \right)}{\Psi_{w,p}^2 \left(\frac{\beta^2}{\chi^2} \Psi_{w,p}^2 - (1 + \beta^2) \right)} \right] \\ & \left[\frac{\eta_{\vartheta,p}^2 \left(1 - \frac{\tanh\left(\frac{\Psi_{\vartheta,pp}}{2}\right)}{\left(\frac{\Psi_{\vartheta,pp}}{2}\right)} \right) + \Psi_{\vartheta,pp}^2 \left(1 - \frac{\tan\left(\frac{\eta_{\vartheta,p}}{2}\right)}{\left(\frac{\eta_{\vartheta,p}}{2}\right)} \right)}{\eta_{\vartheta,p}^2 \left(\frac{\beta^2}{\chi^2} \eta_{\vartheta,p}^2 + (1 + \beta^2) \right)} + \right. \\ & \left. + \frac{\Psi_{\vartheta,p}^2 \left(1 - \frac{\tanh\left(\frac{\Psi_{\vartheta,pp}}{2}\right)}{\left(\frac{\Psi_{\vartheta,pp}}{2}\right)} \right) - \Psi_{w,pp}^2 \left(1 - \frac{\tanh\left(\frac{\Psi_{\vartheta,p}}{2}\right)}{\left(\frac{\Psi_{\vartheta,p}}{2}\right)} \right)}{\Psi_{\vartheta,p}^2 \left(\frac{\beta^2}{\chi^2} \Psi_{\vartheta,p}^2 - (1 + \beta^2) \right)} \right] \end{aligned} \right\} + \lambda_Q^2 \tilde{h}_{w_p'} \tilde{h}_{\theta_p'}
\end{aligned}$$

$$\bar{\bar{H}}_{2,3} = \lambda_L^2 \lambda_Q^2 \tilde{h}_{w_p} \tilde{h}_{\theta_p}$$

$$\bar{H}_{2,4} = -\frac{1}{\psi_{w,pp}^2} \frac{1}{\bar{H}_{2,5}} \left\{ \bar{H}_{2,3} \left[\frac{1}{\tilde{\omega}_{w,p}^2} \frac{\psi_{w,p}^2 \eta_{w,p}^2}{\psi_{w,p}^2 + \eta_{w,p}^2} \left(\frac{\eta_{w,p}^2 + \psi_{w,pp}^2 + \lambda_L^2 \left(\frac{\tanh\left(\frac{\psi_{w,pp}}{2}\right)}{\left(\frac{\psi_{w,pp}}{2}\right)} - \frac{\tanh\left(\frac{\eta_{w,p}}{2}\right)}{\left(\frac{\eta_{w,p}}{2}\right)} + \right)}{\frac{\eta_{w,p}^2 + \psi_{w,pp}^2}{12}} \right) + \frac{\psi_{w,p}^2 - \psi_{w,pp}^2 + \lambda_L^2 \left(\frac{\tanh\left(\frac{\psi_{w,pp}}{2}\right)}{\left(\frac{\psi_{w,pp}}{2}\right)} - \frac{\tanh\left(\frac{\psi_{w,p}}{2}\right)}{\left(\frac{\psi_{w,p}}{2}\right)} + \right)}{\psi_{w,p}^2 \left(\frac{\beta^2}{\chi^2} \psi_{w,p}^2 - (1 + \beta^2) \right)} \right] + \frac{1}{\tilde{J}_t \tilde{\omega}_{\vartheta,p}^2} \frac{\psi_{\vartheta,p}^2 \eta_{\vartheta,p}^2}{\psi_{\vartheta,p}^2 + \eta_{\vartheta,p}^2} \left(\frac{\eta_{\vartheta,p}^2 + \psi_{\vartheta,pp}^2 + \lambda_L^2 \left(\frac{\tanh\left(\frac{\psi_{\vartheta,pp}}{2}\right)}{\left(\frac{\psi_{\vartheta,pp}}{2}\right)} - \frac{\tanh\left(\frac{\eta_{\vartheta,p}}{2}\right)}{\left(\frac{\eta_{\vartheta,p}}{2}\right)} + \right)}{\frac{\eta_{\vartheta,p}^2 + \psi_{\vartheta,pp}^2}{12}} \right) + \frac{\psi_{\vartheta,p}^2 - \psi_{\vartheta,pp}^2 + \lambda_L^2 \left(\frac{\tanh\left(\frac{\psi_{\vartheta,pp}}{2}\right)}{\left(\frac{\psi_{\vartheta,pp}}{2}\right)} - \frac{\tanh\left(\frac{\psi_{\vartheta,p}}{2}\right)}{\left(\frac{\psi_{\vartheta,p}}{2}\right)} + \right)}{\psi_{\vartheta,p}^2 \left(\frac{\beta^2}{\chi^2} \psi_{\vartheta,p}^2 - (1 + \beta^2) \right)} \right] - \lambda_Q^2 \tilde{h}_{w_p' \vartheta_p'} \right\}$$

$$\bar{H}_{2,5} = 1 - \lambda_L^2 \left(\frac{1}{\psi_{\vartheta,pp}^2} \left(1 - \frac{\tanh\left(\frac{\psi_{\vartheta,pp}}{2}\right)}{\left(\frac{\psi_{\vartheta,pp}}{2}\right)} \right) - \frac{1}{12} \right)$$

3.2 Parametric analysis

As we have done for the linear modes, let's analyse the quadratic modal shapes in correspondence of the main extreme structural conditions.

3.2.1 Taut string ($\lambda_L^2 = \lambda_Q^2 = 0$)

In this particular situation linear modes are always sinusoidal functions with odd or even number of half-waves respectively for symmetric and skew-symmetric modal shapes.

This added to the vanishing of the linear and quadratic Irvine parameter led all the governing equations to become homogenous without any known term. Meaning that quadratic modal shapes are independent from linear ones. Being the governing equations homogeneous and of fourth order we can get sinusoidal shapes for all the functions involved only if proper conditions on frequencies are fulfilled.

Let's start with the multi-modal approach.

$$\mu^2 \cdot Y_{pr,1}^{iv} - Y_{pr,1}^{ii} - (\tilde{\omega}_{w,p} + \tilde{\omega}_{w,r})^2 \cdot Y_{pr,1} = 0$$

$$Y_{pr,1} = \sin(k\pi\xi) \Leftrightarrow (\tilde{\omega}_{w,p} + \tilde{\omega}_{w,r}) = k\pi\sqrt{1 + \mu^2(k\pi)^2}$$

Where k can be even or odd respectively for skew-symmetric and symmetric modes. Similar relations holds for the other functions.

$$Y_{pr,2} \Rightarrow (\tilde{\omega}_{w,p} - \tilde{\omega}_{w,r}) = k\pi\sqrt{1 + \mu^2(k\pi)^2}$$

$$T_{qs,1} \Rightarrow (\tilde{\omega}_{\vartheta,q} + \tilde{\omega}_{\vartheta,s}) = k\pi\sqrt{1 + \mu^2(k\pi)^2}$$

$$T_{qs,2} \Rightarrow (\tilde{\omega}_{\vartheta,q} - \tilde{\omega}_{\vartheta,s}) = k\pi\sqrt{1 + \mu^2(k\pi)^2}$$

$$H_{pq,1} \Rightarrow \sqrt{\tilde{f}_t} \cdot (\tilde{\omega}_{w,p} + \tilde{\omega}_{\vartheta,q}) = 2k\pi \cdot \sqrt{1 + \beta^2 + \frac{\beta^2}{\chi^2} \cdot (2k\pi)^2}$$

$$H_{pq,2} \Rightarrow \sqrt{\tilde{f}_t} \cdot (\tilde{\omega}_{w,p} - \tilde{\omega}_{\vartheta,q}) = 2k\pi \cdot \sqrt{1 + \beta^2 + \frac{\beta^2}{\chi^2} \cdot (2k\pi)^2}$$

For the mode-by-mode vibrations the situation is changes just for the functions with even subscript. In fact in the governing equation vanishes also the inertial term.

$$\mu^2 \cdot Y_{pr,2}^{iv} - Y_{pr,2}^{ii} = 0$$

The equality can be never satisfied since it requires that the combinational frequency vanish. It can be check simply substituting the sinusoidal shape. Hence, this means that the contribution of these functions vanishes applying as mode-by-mode approach.

3.2.2 Inextensible cables

In this extreme structural condition ($\lambda_L^2 = \lambda_Q^2 \rightarrow \infty$) the modal shape can be easily found as the general expressions are known. In fact it's required to neglect all the term not proportional to λ_L^2 and $(\lambda_L^2)^2 \cdot \lambda_Q^2$. This means that the format of the expressions does not change whilst the parameter one does.

First of all let's assume that linear normal modes are symmetric. Then, for the multi-modal approach we get.

$$Y_{pr,1} = \bar{Y}_{1,1} \cdot \frac{\cosh(\psi_{w,pr} \cdot (\xi - \frac{1}{2}))}{\cosh(\frac{\psi_{w,pr}}{2})} + \bar{Y}_{1,2} \cdot \frac{\cos(\eta_{w,pr} \cdot (\xi - \frac{1}{2}))}{\cos(\frac{\eta_{w,pr}}{2})} + \bar{Y}_{1,4}$$

$$\bar{Y}_{1,1} = -\frac{\bar{Y}_{1,3}/\bar{Y}_{1,5}}{\Psi_{w,pr}^2 + \eta_{w,pr}^2} \cdot \frac{1}{(\tilde{\omega}_{w,p} + \tilde{\omega}_{w,r})^2} \left\{ \frac{\eta_{w,p}^2 \left(1 - \frac{\tan\left(\frac{\eta_{w,pr}}{2}\right)}{\left(\frac{\eta_{w,pr}}{2}\right)} \right) - \eta_{w,pr}^2 \left(1 - \frac{\tan\left(\frac{\eta_{w,p}}{2}\right)}{\left(\frac{\eta_{w,p}}{2}\right)} \right)}{\mu^2 \cdot \eta_{w,p}^4 + \eta_{w,p}^2 - (\tilde{\omega}_{w,p} + \tilde{\omega}_{w,r})^2} + \right. \\ \left. + \frac{\Psi_{w,p}^2 \left(1 - \frac{\tanh\left(\frac{\Psi_{w,pr}}{2}\right)}{\left(\frac{\Psi_{w,pr}}{2}\right)} \right) + \eta_{w,pr}^2 \left(1 - \frac{\tanh\left(\frac{\Psi_{w,p}}{2}\right)}{\left(\frac{\Psi_{w,p}}{2}\right)} \right)}{\mu^2 \cdot \Psi_{w,p}^4 - \Psi_{w,p}^2 - (\tilde{\omega}_{w,p} + \tilde{\omega}_{w,r})^2} \right\}$$

$$\bar{Y}_{1,2} = \frac{\bar{Y}_{1,3}/\bar{Y}_{1,5}}{\Psi_{w,pr}^2 + \eta_{w,pr}^2} \cdot \frac{1}{(\tilde{\omega}_{w,p} + \tilde{\omega}_{w,r})^2} \left\{ \frac{\eta_{w,p}^2 \left(1 - \frac{\tanh\left(\frac{\Psi_{w,pr}}{2}\right)}{\left(\frac{\Psi_{w,pr}}{2}\right)} \right) + \Psi_{w,pr}^2 \left(1 - \frac{\tan\left(\frac{\eta_{w,p}}{2}\right)}{\left(\frac{\eta_{w,p}}{2}\right)} \right)}{\mu^2 \cdot \eta_{w,p}^4 + \eta_{w,p}^2 - (\tilde{\omega}_{w,p} + \tilde{\omega}_{w,r})^2} + \right. \\ \left. + \frac{\Psi_{w,p}^2 \left(1 - \frac{\tan\left(\frac{\Psi_{w,pr}}{2}\right)}{\left(\frac{\Psi_{w,pr}}{2}\right)} \right) - \Psi_{w,pr}^2 \left(1 - \frac{\tanh\left(\frac{\Psi_{w,p}}{2}\right)}{\left(\frac{\Psi_{w,p}}{2}\right)} \right)}{\mu^2 \cdot \Psi_{w,p}^4 - \Psi_{w,p}^2 - (\tilde{\omega}_{w,p} + \tilde{\omega}_{w,r})^2} \right\}$$

$$\bar{Y}_{1,3} = \frac{\tilde{h}_{w,p} \tilde{h}_{w,r}}{\tilde{\omega}_{w,p}^2} \cdot \frac{\Psi_{w,p}^2 \eta_{w,p}^2}{\Psi_{w,p}^2 + \eta_{w,p}^2}$$

$$\bar{Y}_{1,4} = \frac{\bar{Y}_{1,3}/\bar{Y}_{1,5}}{\Psi_{w,pr}^2 + \eta_{w,pr}^2} \cdot \frac{1}{(\tilde{\omega}_{w,p} + \tilde{\omega}_{w,r})^2} \left\{ \frac{\left(\eta_{w,p}^2 \left(\frac{\tanh\left(\frac{\Psi_{w,pr}}{2}\right)}{\left(\frac{\Psi_{w,pr}}{2}\right)} - \frac{\tan\left(\frac{\eta_{w,pr}}{2}\right)}{\left(\frac{\eta_{w,pr}}{2}\right)} \right) + \right. \\ \left. - \eta_{w,pr}^2 \left(\frac{\tanh\left(\frac{\Psi_{w,pr}}{2}\right)}{\left(\frac{\Psi_{w,pr}}{2}\right)} - \frac{\tan\left(\frac{\eta_{w,p}}{2}\right)}{\left(\frac{\eta_{w,p}}{2}\right)} \right) + \right. \\ \left. - \Psi_{w,pr}^2 \left(\frac{\tan\left(\frac{\eta_{w,pr}}{2}\right)}{\left(\frac{\eta_{w,pr}}{2}\right)} - \frac{\tan\left(\frac{\eta_{w,p}}{2}\right)}{\left(\frac{\eta_{w,p}}{2}\right)} \right) \right)}{\mu^2 \cdot \eta_{w,p}^4 + \eta_{w,p}^2 - (\tilde{\omega}_{w,p} + \tilde{\omega}_{w,r})^2} + \right. \\ \left. + \frac{\left(\Psi_{w,p}^2 \left(\frac{\tanh\left(\frac{\Psi_{w,pr}}{2}\right)}{\left(\frac{\Psi_{w,pr}}{2}\right)} - \frac{\tan\left(\frac{\eta_{w,pr}}{2}\right)}{\left(\frac{\eta_{w,pr}}{2}\right)} \right) + \right. \\ \left. + \eta_{w,pr}^2 \left(\frac{\tanh\left(\frac{\Psi_{w,pr}}{2}\right)}{\left(\frac{\Psi_{w,pr}}{2}\right)} - \frac{\tanh\left(\frac{\Psi_{w,p}}{2}\right)}{\left(\frac{\Psi_{w,p}}{2}\right)} \right) + \right. \\ \left. + \Psi_{w,pr}^2 \left(\frac{\tan\left(\frac{\eta_{w,pr}}{2}\right)}{\left(\frac{\eta_{w,pr}}{2}\right)} - \frac{\tanh\left(\frac{\Psi_{w,p}}{2}\right)}{\left(\frac{\Psi_{w,p}}{2}\right)} \right) \right)}{\mu^2 \cdot \Psi_{w,p}^4 - \Psi_{w,p}^2 - (\tilde{\omega}_{w,p} + \tilde{\omega}_{w,r})^2} \right\}$$

$$\bar{Y}_{1,5} = -\frac{1}{(\tilde{\omega}_{w,p} + \tilde{\omega}_{w,r})^2} \left\{ 1 - \frac{1}{\Psi_{w,pr}^2 + \eta_{w,pr}^2} \left(\eta_{w,pr}^2 \frac{\tanh\left(\frac{\Psi_{w,pr}}{2}\right)}{\left(\frac{\Psi_{w,pr}}{2}\right)} + \Psi_{w,pr}^2 \frac{\tan\left(\frac{\eta_{w,pr}}{2}\right)}{\left(\frac{\eta_{w,pr}}{2}\right)} \right) \right\}$$

Similar expressions can be obtained for $Y_{pr,2}$, $T_{qs,1}$, $T_{qs,2}$ with the modifications on trigonometric and hyperbolic exponential parameters already mentioned.

$$\bar{\bar{H}}_{1,1} = -\frac{\bar{H}_{1,3}/\bar{H}_{1,5}}{\Psi_{\vartheta,pq}{}^2 + \eta_{\vartheta,pq}{}^2} \frac{1}{\tilde{J}_t(\tilde{\omega}_{w,p} + \tilde{\omega}_{\vartheta,q})^2} \left\{ \frac{1}{\tilde{\omega}_{w,p}{}^2} \frac{\Psi_{w,p}{}^2 \eta_{w,p}{}^2}{\Psi_{w,p}{}^2 + \eta_{w,p}{}^2} \left(\frac{\eta_{w,p}{}^2 \left(1 - \frac{\tan\left(\frac{\eta_{\vartheta,pq}}{2}\right)}{\left(\frac{\eta_{\vartheta,pq}}{2}\right)} \right) - \eta_{\vartheta,pq}{}^2 \left(1 - \frac{\tan\left(\frac{\eta_{w,p}}{2}\right)}{\left(\frac{\eta_{w,p}}{2}\right)} \right)}{\frac{\beta^2}{\chi^2} \eta_{w,p}{}^4 + (1+\beta^2) \cdot \eta_{w,p}{}^2 - \tilde{J}_t(\tilde{\omega}_{w,p} + \tilde{\omega}_{\vartheta,q})^2} + \frac{\Psi_{w,p}{}^2 \left(1 - \frac{\tan\left(\frac{\eta_{\vartheta,pq}}{2}\right)}{\left(\frac{\eta_{\vartheta,pq}}{2}\right)} \right) + \eta_{\vartheta,pq}{}^2 \left(1 - \frac{\tanh\left(\frac{\Psi_{w,p}}{2}\right)}{\left(\frac{\Psi_{w,p}}{2}\right)} \right)}{\frac{\beta^2}{\chi^2} \Psi_{w,p}{}^4 - (1+\beta^2) \cdot \Psi_{w,p}{}^2 - \tilde{J}_t(\tilde{\omega}_{w,p} + \tilde{\omega}_{\vartheta,q})^2} \right) + \frac{1}{\tilde{J}_t \cdot \tilde{\omega}_{\vartheta,q}{}^2} \frac{\Psi_{\vartheta,q}{}^2 \eta_{\vartheta,q}{}^2}{\Psi_{\vartheta,q}{}^2 + \eta_{\vartheta,q}{}^2} \left(\frac{\eta_{\vartheta,q}{}^2 \left(1 - \frac{\tan\left(\frac{\eta_{\vartheta,pq}}{2}\right)}{\left(\frac{\eta_{\vartheta,pq}}{2}\right)} \right) - \eta_{\vartheta,pq}{}^2 \left(1 - \frac{\tan\left(\frac{\eta_{\vartheta,q}}{2}\right)}{\left(\frac{\eta_{\vartheta,q}}{2}\right)} \right)}{\frac{\beta^2}{\chi^2} \eta_{\vartheta,q}{}^4 + (1+\beta^2) \cdot \eta_{\vartheta,q}{}^2 - \tilde{J}_t(\tilde{\omega}_{w,p} + \tilde{\omega}_{\vartheta,q})^2} + \frac{\Psi_{\vartheta,q}{}^2 \left(1 - \frac{\tan\left(\frac{\eta_{\vartheta,pq}}{2}\right)}{\left(\frac{\eta_{\vartheta,pq}}{2}\right)} \right) + \eta_{\vartheta,pq}{}^2 \left(1 - \frac{\tanh\left(\frac{\Psi_{\vartheta,q}}{2}\right)}{\left(\frac{\Psi_{\vartheta,q}}{2}\right)} \right)}{\frac{\beta^2}{\chi^2} \Psi_{\vartheta,q}{}^4 - (1+\beta^2) \cdot \Psi_{\vartheta,q}{}^2 - \tilde{J}_t(\tilde{\omega}_{w,p} + \tilde{\omega}_{\vartheta,q})^2} \right) \right\}$$

$$\bar{\bar{H}}_{1,2} = -\frac{\bar{H}_{1,3}/\bar{H}_{1,5}}{\Psi_{\vartheta,pq}{}^2 + \eta_{\vartheta,pq}{}^2} \frac{1}{\tilde{J}_t(\tilde{\omega}_{w,p} + \tilde{\omega}_{\vartheta,q})^2} \left\{ \frac{1}{\tilde{\omega}_{w,p}{}^2} \frac{\Psi_{w,p}{}^2 \eta_{w,p}{}^2}{\Psi_{w,p}{}^2 + \eta_{w,p}{}^2} \left(\frac{\eta_{w,p}{}^2 \left(1 - \frac{\tanh\left(\frac{\Psi_{\vartheta,pq}}{2}\right)}{\left(\frac{\Psi_{\vartheta,pq}}{2}\right)} \right) + \Psi_{\vartheta,pq}{}^2 \left(1 - \frac{\tan\left(\frac{\eta_{w,p}}{2}\right)}{\left(\frac{\eta_{w,p}}{2}\right)} \right)}{\frac{\beta^2}{\chi^2} \eta_{w,p}{}^4 + (1+\beta^2) \cdot \eta_{w,p}{}^2 - \tilde{J}_t(\tilde{\omega}_{w,p} + \tilde{\omega}_{\vartheta,q})^2} + \frac{\Psi_{w,p}{}^2 \left(1 - \frac{\tanh\left(\frac{\Psi_{\vartheta,pq}}{2}\right)}{\left(\frac{\Psi_{\vartheta,pq}}{2}\right)} \right) - \Psi_{\vartheta,pq}{}^2 \left(1 - \frac{\tanh\left(\frac{\Psi_{w,p}}{2}\right)}{\left(\frac{\Psi_{w,p}}{2}\right)} \right)}{\frac{\beta^2}{\chi^2} \Psi_{w,p}{}^4 - (1+\beta^2) \cdot \Psi_{w,p}{}^2 - \tilde{J}_t(\tilde{\omega}_{w,p} + \tilde{\omega}_{\vartheta,q})^2} \right) + \frac{1}{\tilde{J}_t \cdot \tilde{\omega}_{\vartheta,q}{}^2} \frac{\Psi_{\vartheta,q}{}^2 \eta_{\vartheta,q}{}^2}{\Psi_{\vartheta,q}{}^2 + \eta_{\vartheta,q}{}^2} \left(\frac{\eta_{\vartheta,q}{}^2 \left(1 - \frac{\tanh\left(\frac{\Psi_{\vartheta,pq}}{2}\right)}{\left(\frac{\Psi_{\vartheta,pq}}{2}\right)} \right) + \Psi_{\vartheta,pq}{}^2 \left(1 - \frac{\tan\left(\frac{\eta_{\vartheta,q}}{2}\right)}{\left(\frac{\eta_{\vartheta,q}}{2}\right)} \right)}{\frac{\beta^2}{\chi^2} \eta_{\vartheta,q}{}^4 + (1+\beta^2) \cdot \eta_{\vartheta,q}{}^2 - \tilde{J}_t(\tilde{\omega}_{w,p} + \tilde{\omega}_{\vartheta,q})^2} + \frac{\Psi_{\vartheta,q}{}^2 \left(1 - \frac{\tanh\left(\frac{\Psi_{\vartheta,pq}}{2}\right)}{\left(\frac{\Psi_{\vartheta,pq}}{2}\right)} \right) - \Psi_{\vartheta,pq}{}^2 \left(1 - \frac{\tanh\left(\frac{\Psi_{\vartheta,q}}{2}\right)}{\left(\frac{\Psi_{\vartheta,q}}{2}\right)} \right)}{\frac{\beta^2}{\chi^2} \Psi_{\vartheta,q}{}^4 - (1+\beta^2) \cdot \Psi_{\vartheta,q}{}^2 - \tilde{J}_t(\tilde{\omega}_{w,p} + \tilde{\omega}_{\vartheta,q})^2} \right) \right\}$$

$$\bar{\bar{H}}_{1,3} = \tilde{h}_{w_p} \tilde{h}_{\vartheta_q}$$

$$\begin{aligned}
\bar{H}_{1,4} &= \frac{1}{\bar{H}_{1,5}} \frac{\bar{H}_{1,3}}{\Psi_{\vartheta,pq}^2 + \eta_{\vartheta,pq}^2} \cdot \frac{1}{\tilde{J}_t(\tilde{\omega}_{w,p} + \tilde{\omega}_{\vartheta,q})^2} \left\{ \frac{1}{\tilde{\omega}_{w,p}^2 \Psi_{w,p}^2 + \eta_{w,p}^2} \right. \\
&\quad \left. \left(\left\{ \begin{aligned} &\eta_{w,p}^2 \left(\frac{\tanh\left(\frac{\Psi_{\vartheta,pq}}{2}\right)}{\left(\frac{\Psi_{\vartheta,pq}}{2}\right)} - \frac{\tan\left(\frac{\eta_{\vartheta,pq}}{2}\right)}{\left(\frac{\eta_{\vartheta,pq}}{2}\right)} \right) + \\ &- \eta_{\vartheta,pq}^2 \left(\frac{\tanh\left(\frac{\Psi_{\vartheta,pq}}{2}\right)}{\left(\frac{\Psi_{\vartheta,pq}}{2}\right)} - \frac{\tan\left(\frac{\eta_{w,p}}{2}\right)}{\left(\frac{\eta_{w,p}}{2}\right)} \right) + \\ &- \Psi_{\vartheta,pq}^2 \left(\frac{\tan\left(\frac{\eta_{\vartheta,pq}}{2}\right)}{\left(\frac{\eta_{\vartheta,pq}}{2}\right)} - \frac{\tanh\left(\frac{\Psi_{w,p}}{2}\right)}{\left(\frac{\Psi_{w,p}}{2}\right)} \right) \end{aligned} \right\} + \frac{\beta^2}{\chi^2} \eta_{w,p}^4 + (1+\beta^2) \cdot \eta_{w,p}^2 - \tilde{J}_t(\tilde{\omega}_{w,p} + \tilde{\omega}_{\vartheta,q})^2 \right. \\
&\quad \left. + \frac{\beta^2}{\chi^2} \Psi_{w,p}^4 - (1+\beta^2) \cdot \Psi_{w,p}^2 - \tilde{J}_t(\tilde{\omega}_{w,p} + \tilde{\omega}_{\vartheta,q})^2 \right\} + \\
&\quad \left. \frac{1}{\tilde{J}_t(\tilde{\omega}_{\vartheta,q})^2 \Psi_{\vartheta,q}^2 + \eta_{\vartheta,q}^2} \right\} \\
&\quad \left(\left\{ \begin{aligned} &\eta_{\vartheta,q}^2 \left(\frac{\tanh\left(\frac{\Psi_{\vartheta,pq}}{2}\right)}{\left(\frac{\Psi_{\vartheta,pq}}{2}\right)} - \frac{\tan\left(\frac{\eta_{\vartheta,pq}}{2}\right)}{\left(\frac{\eta_{\vartheta,pq}}{2}\right)} \right) + \\ &- \eta_{\vartheta,pq}^2 \left(\frac{\tanh\left(\frac{\Psi_{\vartheta,pq}}{2}\right)}{\left(\frac{\Psi_{\vartheta,pq}}{2}\right)} - \frac{\tan\left(\frac{\eta_{\vartheta,q}}{2}\right)}{\left(\frac{\eta_{\vartheta,q}}{2}\right)} \right) + \\ &- \Psi_{\vartheta,pq}^2 \left(\frac{\tan\left(\frac{\eta_{\vartheta,pq}}{2}\right)}{\left(\frac{\eta_{\vartheta,pq}}{2}\right)} - \frac{\tan\left(\frac{\eta_{\vartheta,q}}{2}\right)}{\left(\frac{\eta_{\vartheta,q}}{2}\right)} \right) \end{aligned} \right\} + \frac{\beta^2}{\chi^2} \eta_{\vartheta,q}^4 + (1+\beta^2) \cdot \eta_{\vartheta,q}^2 - \tilde{J}_t(\tilde{\omega}_{w,p} + \tilde{\omega}_{\vartheta,q})^2 \right. \\
&\quad \left. + \frac{\beta^2}{\chi^2} \Psi_{\vartheta,q}^4 - (1+\beta^2) \cdot \Psi_{\vartheta,q}^2 - \tilde{J}_t(\tilde{\omega}_{w,p} + \tilde{\omega}_{\vartheta,q})^2 \right\} \left. \right)
\end{aligned}$$

$$\bar{H}_{1,5} = - \frac{1}{\tilde{J}_t(\tilde{\omega}_{w,p} + \tilde{\omega}_{\vartheta,q})^2} \left\{ 1 - \frac{1}{\Psi_{\vartheta,pq}^2 + \eta_{\vartheta,pq}^2} \left(\eta_{\vartheta,pq}^2 \frac{\tanh\left(\frac{\Psi_{\vartheta,pq}}{2}\right)}{\left(\frac{\Psi_{\vartheta,pq}}{2}\right)} + \Psi_{\vartheta,pq}^2 \frac{\tan\left(\frac{\eta_{\vartheta,pq}}{2}\right)}{\left(\frac{\eta_{\vartheta,pq}}{2}\right)} \right) \right\}$$

Similarly we can obtain the expression of parameters for $\bar{H}_{pq,2}$ with proper $\Psi_{\vartheta,pq}$; $\eta_{\vartheta,pq}$ and $\Psi_{w,p}$; $\eta_{w,p}$; $\Psi_{\vartheta,q}$; $\eta_{\vartheta,q}$.

Concerning the mode-by-mode approach we get.

$$\bar{Y}_{2,1} = \frac{1}{\Psi_{w,pp}^2} \bar{Y}_{2,3} / \bar{Y}_{2,5} \cdot \left(\frac{1 - \frac{\tan\left(\frac{\eta_{w,p}}{2}\right) + \frac{\eta_{w,p}^2}{12}}{\left(\frac{\eta_{w,p}}{2}\right)}}{\eta_{w,p}^2(\mu^2 \cdot \eta_{w,p}^2 + 1)} - \frac{1 - \frac{\tanh\left(\frac{\Psi_{w,p}}{2}\right) \Psi_{w,p}^2}{\left(\frac{\Psi_{w,p}}{2}\right)}}{\Psi_{w,p}^2(\mu^2 \cdot \Psi_{w,p}^2 - 1)} \right)$$

$$\bar{Y}_{2,2} = -\frac{1}{\Psi_{w,pp}^2} \bar{Y}_{2,3} / \bar{Y}_{2,5} \cdot \left\{ \begin{array}{l} \frac{\eta_{w,p}^2 \left(1 - \frac{\tanh\left(\frac{\Psi_{w,pp}}{2}\right)}{\left(\frac{\Psi_{w,pp}}{2}\right)}\right) + \Psi_{w,pp}^2 \left(1 - \frac{\tan\left(\frac{\eta_{w,p}}{2}\right)}{\left(\frac{\eta_{w,p}}{2}\right)}\right)}{\eta_{w,p}^2(\mu^2 \cdot \eta_{w,p}^2 + 1)} + \\ + \frac{\Psi_{w,p}^2 \left(1 - \frac{\tanh\left(\frac{\Psi_{w,pp}}{2}\right)}{\left(\frac{\Psi_{w,pp}}{2}\right)}\right) - \Psi_{w,pp}^2 \left(1 - \frac{\tanh\left(\frac{\Psi_{w,p}}{2}\right)}{\left(\frac{\Psi_{w,p}}{2}\right)}\right)}{\Psi_{w,p}^2(\mu^2 \cdot \Psi_{w,p}^2 - 1)} \end{array} \right\}$$

$$\bar{Y}_{2,3} = \frac{\tilde{h}_{wp}^2}{\tilde{\omega}_{w,p}^2} \cdot \frac{\Psi_{w,p}^2 \eta_{w,p}^2}{\Psi_{w,p}^2 + \eta_{w,p}^2}$$

$$\bar{Y}_{2,4} = -\frac{1}{\Psi_{w,pp}^2} \bar{Y}_{2,3} / \bar{Y}_{2,5} \cdot \left(\frac{\frac{\tanh\left(\frac{\Psi_{w,pp}}{2}\right)}{\left(\frac{\Psi_{w,pp}}{2}\right)} - \frac{\tan\left(\frac{\eta_{w,p}}{2}\right)}{\left(\frac{\eta_{w,p}}{2}\right)} + \frac{\eta_{w,p}^2 + \Psi_{w,pp}^2}{12}}{\eta_{w,p}^2(\mu^2 \cdot \eta_{w,p}^2 + 1)} + \frac{\frac{\tanh\left(\frac{\Psi_{w,p}}{2}\right)}{\left(\frac{\Psi_{w,p}}{2}\right)} - \frac{\tanh\left(\frac{\Psi_{w,pp}}{2}\right)}{\left(\frac{\Psi_{w,pp}}{2}\right)} - \frac{\Psi_{w,p}^2 - \Psi_{w,pp}^2}{12}}{\Psi_{w,p}^2(\mu^2 \cdot \Psi_{w,p}^2 - 1)} \right)$$

$$\bar{Y}_{2,5} = -\left(\frac{1}{\Psi_{w,pp}^2} \left(1 - \frac{\tanh\left(\frac{\Psi_{w,pp}}{2}\right)}{\left(\frac{\Psi_{w,pp}}{2}\right)}\right) - \frac{1}{12} \right)$$

Similarly for $\bar{T}_{qs,2}$ with proper $\Psi_{w,qS}$; $\eta_{w,qS}$ and $\Psi_{\vartheta,q}$; $\eta_{\vartheta,q}$.

Then for the torsional component.

$$\bar{H}_{2,1} = \frac{1}{\Psi_{\vartheta,pp}^2} \bar{H}_{2,3} / \bar{H}_{2,5} \cdot \left\{ \begin{array}{l} \frac{1}{\tilde{\omega}_{w,p}^2} \frac{\Psi_{w,p}^2 \eta_{w,p}^2}{\Psi_{w,p}^2 + \eta_{w,p}^2} \left(\frac{\left(1 - \frac{\tan\left(\frac{\eta_{w,p}}{2}\right) + \frac{\eta_{w,p}^2}{12}}{\left(\frac{\eta_{w,p}}{2}\right)}\right)}{\eta_{w,p}^2 \left(\frac{\beta^2}{\chi^2} \eta_{w,p}^2 + (1 + \beta^2)\right)} - \frac{\left(1 - \frac{\tanh\left(\frac{\Psi_{w,p}}{2}\right) \Psi_{w,p}^2}{\left(\frac{\Psi_{w,p}}{2}\right)} - \frac{\Psi_{w,p}^2}{12}\right)}{\Psi_{w,p}^2 \left(\frac{\beta^2}{\chi^2} \Psi_{w,p}^2 - (1 + \beta^2)\right)} \right) + \\ + \frac{1}{\tilde{J}_t \cdot \tilde{\omega}_{\vartheta,p}^2} \frac{\Psi_{\vartheta,p}^2 \eta_{\vartheta,p}^2}{\Psi_{\vartheta,p}^2 + \eta_{\vartheta,p}^2} \left(\frac{\left(1 - \frac{\tan\left(\frac{\eta_{\vartheta,p}}{2}\right) + \frac{\eta_{\vartheta,p}^2}{12}}{\left(\frac{\eta_{\vartheta,p}}{2}\right)}\right)}{\eta_{\vartheta,p}^2 \left(\frac{\beta^2}{\chi^2} \eta_{\vartheta,p}^2 + (1 + \beta^2)\right)} - \frac{\left(1 - \frac{\tanh\left(\frac{\Psi_{\vartheta,p}}{2}\right) \Psi_{\vartheta,p}^2}{\left(\frac{\Psi_{\vartheta,p}}{2}\right)} - \frac{\Psi_{\vartheta,p}^2}{12}\right)}{\Psi_{\vartheta,p}^2 \left(\frac{\beta^2}{\chi^2} \Psi_{\vartheta,p}^4 - (1 + \beta^2)\right)} \right) \end{array} \right\}$$

$$\bar{H}_{2,2} = -\frac{1}{\Psi_{w,pp}^2} \bar{H}_{2,3} / \bar{H}_{2,5} \cdot \left\{ \begin{aligned} & \frac{1}{\tilde{\omega}_{w,p}^2} \frac{\Psi_{w,p}^2 \eta_{w,p}^2}{\Psi_{w,p}^2 + \eta_{w,p}^2} \left(\frac{\eta_{w,p}^2 \left(1 - \frac{\tanh\left(\frac{\Psi_{\vartheta,pp}}{2}\right)}{\left(\frac{\Psi_{\vartheta,pp}}{2}\right)} \right) + \Psi_{\vartheta,pp}^2 \left(1 - \frac{\tanh\left(\frac{\eta_{w,p}}{2}\right)}{\left(\frac{\eta_{w,p}}{2}\right)} \right)}{\eta_{w,p}^2 \left(\frac{\beta^2}{\chi^2} \eta_{w,p}^2 + (1+\beta^2) \right)} + \right. \\ & \left. + \frac{\Psi_{w,p}^2 \left(1 - \frac{\tanh\left(\frac{\Psi_{\vartheta,pp}}{2}\right)}{\left(\frac{\Psi_{\vartheta,pp}}{2}\right)} \right) - \Psi_{\vartheta,pp}^2 \left(1 - \frac{\tanh\left(\frac{\Psi_{w,p}}{2}\right)}{\left(\frac{\Psi_{w,p}}{2}\right)} \right)}{\Psi_{w,p}^2 \left(\frac{\beta^2}{\chi^2} \Psi_{w,p}^2 - (1+\beta^2) \right)} \right) + \\ & + \frac{1}{\tilde{J}_t \cdot \tilde{\omega}_{\vartheta,q}^2} \frac{\Psi_{\vartheta,p}^2 \eta_{\vartheta,p}^2}{\Psi_{\vartheta,p}^2 + \eta_{\vartheta,p}^2} \left(\frac{\eta_{\vartheta,p}^2 \left(1 - \frac{\tanh\left(\frac{\Psi_{\vartheta,pp}}{2}\right)}{\left(\frac{\Psi_{\vartheta,pp}}{2}\right)} \right) + \Psi_{\vartheta,pp}^2 \left(1 - \frac{\tanh\left(\frac{\eta_{\vartheta,p}}{2}\right)}{\left(\frac{\eta_{\vartheta,p}}{2}\right)} \right)}{\eta_{\vartheta,p}^2 \left(\frac{\beta^2}{\chi^2} \eta_{\vartheta,p}^2 + (1+\beta^2) \right)} + \right. \\ & \left. + \frac{\Psi_{\vartheta,p}^2 \left(1 - \frac{\tanh\left(\frac{\Psi_{\vartheta,pp}}{2}\right)}{\left(\frac{\Psi_{\vartheta,pp}}{2}\right)} \right) - \Psi_{w,pp}^2 \left(1 - \frac{\tanh\left(\frac{\Psi_{\vartheta,p}}{2}\right)}{\left(\frac{\Psi_{\vartheta,p}}{2}\right)} \right)}{\Psi_{\vartheta,p}^2 \left(\frac{\beta^2}{\chi^2} \Psi_{\vartheta,p}^2 - (1+\beta^2) \right)} \right) \end{aligned} \right\}$$

$$\bar{H}_{2,3} = \tilde{h}_{W_p} \tilde{h}_{\theta_p}$$

$$\bar{H}_{2,4} = -\frac{1}{\Psi_{w,pp}^2} \bar{H}_{2,3} / \bar{H}_{2,5} \cdot \left\{ \begin{aligned} & \frac{1}{\tilde{\omega}_{w,p}^2} \frac{\Psi_{w,p}^2 \eta_{w,p}^2}{\Psi_{w,p}^2 + \eta_{w,p}^2} \left(\frac{\frac{\tanh\left(\frac{\Psi_{w,pp}}{2}\right)}{\left(\frac{\Psi_{w,pp}}{2}\right)} - \frac{\tanh\left(\frac{\eta_{w,p}}{2}\right)}{\left(\frac{\eta_{w,p}}{2}\right)} + \frac{\eta_{w,p}^2 + \Psi_{w,pp}^2}{12}}{\eta_{w,p}^2 \left(\frac{\beta^2}{\chi^2} \eta_{w,p}^2 + (1+\beta^2) \right)} + \right. \\ & \left. - \frac{\frac{\tanh\left(\frac{\Psi_{w,pp}}{2}\right)}{\left(\frac{\Psi_{w,pp}}{2}\right)} - \frac{\tanh\left(\frac{\Psi_{w,p}}{2}\right)}{\left(\frac{\Psi_{w,p}}{2}\right)} - \frac{\Psi_{w,p}^2 - \Psi_{w,pp}^2}{12}}{\Psi_{w,p}^2 \left(\frac{\beta^2}{\chi^2} \Psi_{w,p}^2 - (1+\beta^2) \right)} \right) + \\ & + \frac{1}{\tilde{J}_t \cdot \tilde{\omega}_{\vartheta,p}^2} \frac{\Psi_{\vartheta,p}^2 \eta_{\vartheta,p}^2}{\Psi_{\vartheta,p}^2 + \eta_{\vartheta,p}^2} \left(\frac{\frac{\tanh\left(\frac{\Psi_{\vartheta,pp}}{2}\right)}{\left(\frac{\Psi_{\vartheta,pp}}{2}\right)} - \frac{\tanh\left(\frac{\eta_{\vartheta,p}}{2}\right)}{\left(\frac{\eta_{\vartheta,p}}{2}\right)} + \frac{\eta_{\vartheta,p}^2 + \Psi_{\vartheta,pp}^2}{12}}{\eta_{\vartheta,p}^2 \left(\frac{\beta^2}{\chi^2} \eta_{\vartheta,p}^2 + (1+\beta^2) \right)} + \right. \\ & \left. - \frac{\frac{\tanh\left(\frac{\Psi_{\vartheta,pp}}{2}\right)}{\left(\frac{\Psi_{\vartheta,pp}}{2}\right)} - \frac{\tanh\left(\frac{\Psi_{\vartheta,p}}{2}\right)}{\left(\frac{\Psi_{\vartheta,p}}{2}\right)} - \frac{\Psi_{\vartheta,p}^2 - \Psi_{\vartheta,pp}^2}{12}}{\Psi_{\vartheta,p}^2 \left(\frac{\beta^2}{\chi^2} \Psi_{\vartheta,p}^2 - (1+\beta^2) \right)} \right) \end{aligned} \right\}$$

$$\bar{H}_{2,5} = -\left(\frac{1}{\Psi_{\vartheta,pp}^2} \left(1 - \frac{\tanh\left(\frac{\Psi_{\vartheta,pp}}{2}\right)}{\left(\frac{\Psi_{\vartheta,pp}}{2}\right)} \right) - \frac{1}{12} \right)$$

Similarly for $\bar{H}_{p,q,2}$ with proper $\Psi_{\vartheta,pq}$; $\eta_{\vartheta,pq}$ and $\Psi_{w,p}$; $\eta_{w,p}$; $\Psi_{\vartheta,q}$; $\eta_{\vartheta,q}$.

As we assume that the linear modes becomes skew-symmetric things change drastically. In fact, for both the multi-modal and mode-by-mode approaches we get the same results obtained for finite values of the linear and quadratic Irvine parameters. This means that the Irvine parameter does not influence the shape of quadratic modal functions only in the special case of skew-symmetric linear modes. This is an important difference between linear and quadratic normal modes, the latter being generally strongly influenced by λ_L^2 and λ_Q^2 whilst the first being completely independent thanks to normalization with respect to the modal amplitude.

3.2.3 Flexible deck

As the deck is no more able to sustain bending moments ($\mu^2 = 0$) the linear flexural modes change shape whilst the torsional one remains in the general format. Further, the governing equation for the flexural quadratic mode lose the fourth order term. Hence, the associated second order correction become as follows.

$$Y_{pr,1} = \bar{Y}_{1,1} \cdot \frac{\cos(\eta_{w,pr} \cdot (\xi - \frac{1}{2}))}{\cos(\frac{\eta_{w,pr}}{2})} + \bar{Y}_{1,2} \cdot \frac{\cos(\eta_{w,p} \cdot (\xi - 1/2)) / \cos(\eta_{w,p}/2)}{\mu^2 \cdot \eta_{w,p}^4 + \eta_{w,p}^2 - (\tilde{\omega}_{w,p} + \tilde{\omega}_{w,r})^2} + \bar{Y}_{1,3}$$

Where.

$$\eta_{w,pr}^2 = (\tilde{\omega}_{w,p} + \tilde{\omega}_{w,r})^2$$

$$\eta_{w,p}^2 = \tilde{\omega}_{w,p}^2$$

$$\bar{Y}_{1,1} = \frac{1}{\bar{Y}_{1,5}} \left(-\bar{Y}_{1,4} \cdot \frac{1 - \frac{\lambda_L^2}{\eta_{w,pr}^2} \left(1 - \frac{\tan(\frac{\eta_{w,p}}{2})}{(\frac{\eta_{w,p}}{2})} \right)}{\eta_{w,p}^2 - \eta_{w,pr}^2} - \frac{\lambda_Q^2 \tilde{h}_{Wp}' W_r'}{2 \eta_{w,pr}^2} \right)$$

$$\bar{Y}_{1,2} = \frac{1}{\bar{Y}_{1,5}} \cdot \left(\bar{Y}_{1,4} \cdot \frac{1 - \frac{\lambda_L^2}{\eta_{w,pr}^2} \left(1 - \frac{\tan(\frac{\eta_{w,p}}{2})}{(\frac{\eta_{w,p}}{2})} \right)}{\eta_{w,p}^2 - \eta_{w,pr}^2} \right)$$

$$\bar{Y}_{1,3} = \frac{1}{\bar{Y}_{1,5}} \left(\bar{Y}_{1,4} \frac{\lambda_L^2}{\eta_{w,pr}} \cdot \frac{\frac{\tan(\frac{\eta_{w,p}}{2})}{(\frac{\eta_{w,p}}{2})} - \frac{\tan(\frac{\eta_{w,pr}}{2})}{(\frac{\eta_{w,pr}}{2})}}{\eta_{w,p}^2 - \eta_{w,pr}^2} + \frac{\lambda_Q^2 \tilde{h}_{Wp}' W_r'}{2 \eta_{w,pr}^2} \right)$$

$$\bar{Y}_{1,4} = \lambda_L^2 \lambda_Q^2 \tilde{h}_{Wp} \tilde{h}_{W_r}$$

$$\bar{Y}_{1,5} = 1 - \frac{\lambda_L^2}{\eta_{w,pr}^2} \left\{ 1 - \frac{\tan(\frac{\eta_{w,pr}}{2})}{(\frac{\eta_{w,pr}}{2})} \right\}$$

We get similar expression for $Y_{pr,2}$ enforcing $\eta_{w,pr}^2 = (\tilde{\omega}_{w,p} - \tilde{\omega}_{w,r})^2$.

$$T_{qs,1} = \left\{ \begin{array}{l} \bar{T}_{1,1} \cdot \frac{\cos(\eta_{w,qs} \cdot (\xi - \frac{1}{2}))}{\cos(\frac{\eta_{w,qs}}{2})} + \\ + \bar{T}_{1,2} \cdot \left(\frac{\cos(\eta_{\vartheta,q} \cdot (\xi - 1/2)) / \cos(\eta_{\vartheta,q}/2)}{\eta_{\vartheta,q}^2 - \eta_{w,qs}^2} + \frac{\cosh(\Psi_{\vartheta,q} \cdot (\xi - 1/2)) / \cosh(\Psi_{\vartheta,q}/2)}{\Psi_{\vartheta,q}^2 + \eta_{w,qs}^2} \right) + \bar{T}_{1,3} \end{array} \right\}$$

Where.

$$\eta_{w,qs}^2 = (\tilde{\omega}_{\vartheta,q} + \tilde{\omega}_{\vartheta,s})^2$$

$$\Psi_{\vartheta,q}^2 = \frac{\chi^2}{2\beta^2} \left(\sqrt{(1 + \beta^2)^2 + 4 \frac{\beta^2}{\chi^2} \cdot \tilde{f}_t \tilde{\omega}_{\vartheta,q}^2} + (1 + \beta^2) \right) = \eta_{\vartheta,q}^2 + \frac{\chi^2}{\beta^2} (1 + \beta^2)$$

$$\bar{T}_{1,1} = \frac{1}{\bar{T}_{1,4}} \left(-\bar{T}_{1,2} \cdot \left\{ \frac{1 - \frac{\lambda_L^2}{\eta_{w,qs}^2} \left(1 - \frac{\tan(\frac{\eta_{\vartheta,q}}{2})}{(\frac{\eta_{\vartheta,q}}{2})} \right)}{\eta_{\vartheta,q}^2 - \eta_{w,qs}^2} + \frac{1 - \frac{\lambda_L^2}{\eta_{w,qs}^2} \left(1 - \frac{\tanh(\frac{\Psi_{\vartheta,q}}{2})}{(\frac{\Psi_{\vartheta,q}}{2})} \right)}{\Psi_{\vartheta,q}^2 - \eta_{w,qs}^2} \right\} - \frac{\lambda_Q^2 \tilde{h}_{w,p}' w_r'}{2 \eta_{w,qs}^2} \right)$$

$$\bar{T}_{1,2} = \frac{\lambda_L^2 \lambda_Q^2 \tilde{h}_{\vartheta,q} \tilde{h}_{\vartheta,s}}{\tilde{f}_t \cdot \tilde{\omega}_{\vartheta,q}^2} \cdot \frac{\Psi_{\vartheta,q}^2 \eta_{\vartheta,q}^2}{\Psi_{\vartheta,q}^2 + \eta_{\vartheta,q}^2}$$

$$\bar{T}_{1,3} = \frac{1}{\bar{T}_{1,4}} \left(-\bar{T}_{1,2} \cdot \frac{\lambda_L^2}{\eta_{w,qs}^2} \left\{ \frac{\frac{\tan(\frac{\eta_{w,qs}}{2})}{(\frac{\eta_{w,qs}}{2})} - \frac{\tan(\frac{\eta_{\vartheta,q}}{2})}{(\frac{\eta_{\vartheta,q}}{2})}}{\eta_{\vartheta,q}^2 - \eta_{w,qs}^2} + \frac{\frac{\tan(\frac{\eta_{w,qs}}{2})}{(\frac{\eta_{w,qs}}{2})} - \frac{\tan(\frac{\Psi_{\vartheta,q}}{2})}{(\frac{\Psi_{\vartheta,q}}{2})}}{\Psi_{\vartheta,q}^2 - \eta_{w,qs}^2} \right\} + \frac{\lambda_Q^2 \tilde{h}_{w,p}' w_r'}{2 \eta_{w,qs}^2} \right)$$

$$\bar{T}_{1,4} = 1 - \frac{\lambda_L^2}{\eta_{w,qs}^2} \left\{ 1 - \frac{\tan(\frac{\eta_{w,qs}^2}{2})}{(\frac{\eta_{w,qs}^2}{2})} \right\}$$

We get similar expression for $T_{qs,2}$ enforcing $\eta_{w,qs}^2 = (\tilde{\omega}_{\vartheta,q} - \tilde{\omega}_{\vartheta,s})^2$.

Concerning the torsional modes we can take the general expression and make simple modifications as follows.

$$H_{pq,1} = \left\{ \begin{array}{l} \bar{H}_{1,1} \cdot \frac{\cosh(\Psi_{\vartheta,pq}(\xi-\frac{1}{2}))}{\cosh(\frac{\Psi_{\vartheta,pq}}{2})} + \bar{H}_{1,2} \cdot \frac{\cos(\eta_{\vartheta,pq}(\xi-\frac{1}{2}))}{\cos(\frac{\eta_{\vartheta,pq}}{2})} + \\ \left(\begin{array}{l} \frac{\cos(\eta_{w,p}(\xi-\frac{1}{2}))/\cos(\frac{\eta_{w,p}}{2})}{\frac{\beta^2}{\chi^2}\eta_{w,p}^4+(1+\beta^2)\eta_{w,p}^2-\tilde{J}_t(\tilde{\omega}_{w,p}+\tilde{\omega}_{\vartheta,q})^2} + \\ + \frac{1}{\tilde{J}_t \cdot \tilde{\omega}_{\vartheta,q}^2} \frac{\Psi_{\vartheta,q}^2 \eta_{\vartheta,q}^2}{\Psi_{\vartheta,q}^2 + \eta_{\vartheta,q}^2} \left\{ \begin{array}{l} \frac{\cos(\eta_{\vartheta,q}(\xi-\frac{1}{2}))/\cos(\frac{\eta_{\vartheta,q}}{2})}{\frac{\beta^2}{\chi^2}\eta_{\vartheta,q}^4+(1+\beta^2)\eta_{\vartheta,q}^2-\tilde{J}_t(\tilde{\omega}_{w,p}+\tilde{\omega}_{\vartheta,q})^2} + \\ - \frac{\cosh(\Psi_{\vartheta,q}(\xi-1/2))/\cosh(\Psi_{\vartheta,q}/2)}{\frac{\beta^2}{\chi^2}\Psi_{\vartheta,q}^4-(1+\beta^2)\Psi_{\vartheta,q}^2-\tilde{J}_t(\tilde{\omega}_{w,p}+\tilde{\omega}_{\vartheta,q})^2} \end{array} \right\} \end{array} \right) + \\ + \bar{H}_{1,4} \end{array} \right\}$$

Where.

$$\Psi_{\vartheta,pq}^2 = \frac{\chi^2}{2\beta^2} \left(\sqrt{(1+\beta^2)^2 + 4\frac{\beta^2}{\chi^2} \cdot \tilde{J}_t(\tilde{\omega}_{w,p} + \tilde{\omega}_{\vartheta,q})^2} + (1+\beta^2) \right) = \eta_{\vartheta,pq}^2 + \frac{\chi^2}{\beta^2} (1+\beta^2)$$

$$\eta_{w,p}^2 = \frac{1}{2\mu^2} \left(\sqrt{1 + 4\mu^2 \cdot \tilde{\omega}_{w,p}^2} - 1 \right)$$

$$\Psi_{\vartheta,q}^2 = \frac{\chi^2}{2\beta^2} \left(\sqrt{(1+\beta^2)^2 + 4\frac{\beta^2}{\chi^2} \cdot \tilde{J}_t \tilde{\omega}_{\vartheta,q}^2} + (1+\beta^2) \right) = \eta_{\vartheta,q}^2 + \frac{\chi^2}{\beta^2} (1+\beta^2)$$

$$\bar{H}_{1,1} = \frac{1}{\bar{H}_{1,5}} \frac{1}{\Psi_{\vartheta,pq}^2 + \eta_{\vartheta,pq}^2} \left\{ \bar{H}_{1,3} \left[\frac{\left(\eta_{w,p}^2 \left[1 - \frac{\lambda_L^2}{\tilde{f}_t(\tilde{\omega}_{w,p} + \tilde{\omega}_{\vartheta,q})^2} \left(1 - \frac{\tan\left(\frac{\eta_{\vartheta,pq}}{2}\right)}{\left(\frac{\eta_{\vartheta,pq}}{2}\right)} \right) \right) + \right.}{\frac{\beta^2}{\chi^2} \eta_{w,p}^4 + (1+\beta^2) \eta_{w,p}^2 - \tilde{f}_t(\tilde{\omega}_{w,p} + \tilde{\omega}_{\vartheta,q})^2} + \right. \right. \\ \left. \left. \frac{\left(-\eta_{\vartheta,pq}^2 \left[1 - \frac{\lambda_L^2}{\tilde{f}_t(\tilde{\omega}_{w,p} + \tilde{\omega}_{\vartheta,q})^2} \left(1 - \frac{\tan\left(\frac{\eta_{\vartheta,p}}{2}\right)}{\left(\frac{\eta_{\vartheta,p}}{2}\right)} \right) \right) \right)}{\frac{\beta^2}{\chi^2} \eta_{\vartheta,q}^4 + (1+\beta^2) \eta_{\vartheta,q}^2 - \tilde{f}_t(\tilde{\omega}_{w,p} + \tilde{\omega}_{\vartheta,q})^2} + \right. \right. \\ \left. \left. + \frac{1}{\tilde{f}_t \tilde{\omega}_{\vartheta,q}^2} \frac{\Psi_{\vartheta,q}^2 \eta_{\vartheta,q}^2}{\Psi_{\vartheta,q}^2 + \eta_{\vartheta,q}^2} \left(\frac{\Psi_{\vartheta,q}^2 \left[1 - \frac{\lambda_L^2}{\tilde{f}_t(\tilde{\omega}_{w,p} + \tilde{\omega}_{\vartheta,q})^2} \left(1 - \frac{\tan\left(\frac{\eta_{\vartheta,pq}}{2}\right)}{\left(\frac{\eta_{\vartheta,pq}}{2}\right)} \right) \right) + \right. \right. \right. \right. \\ \left. \left. \left. + \eta_{\vartheta,pq}^2 \left[1 - \frac{\lambda_L^2}{\tilde{f}_t(\tilde{\omega}_{w,p} + \tilde{\omega}_{\vartheta,q})^2} \left(1 - \frac{\tanh\left(\frac{\Psi_{\vartheta,q}}{2}\right)}{\left(\frac{\Psi_{\vartheta,q}}{2}\right)} \right) \right] \right) \right) \right) \right] + \frac{\beta^2}{\chi^2} \Psi_{\vartheta,q}^4 - (1+\beta^2) \Psi_{\vartheta,q}^2 - \tilde{f}_t(\tilde{\omega}_{w,p} + \tilde{\omega}_{\vartheta,q})^2} \right) \\ - \lambda_Q^2 \frac{\tilde{h}_{w,p'} \theta_{q'}}{\tilde{f}_t(\tilde{\omega}_{w,p} + \tilde{\omega}_{\vartheta,q})^2} \eta_{\vartheta,pq}^2 \right\}$$

$$\bar{H}_{1,2} = \frac{1}{\bar{H}_{1,5}} \frac{1}{\Psi_{\vartheta,pq}^2 + \eta_{\vartheta,pq}^2} \left\{ \bar{H}_{1,3} \left[\frac{\left(\eta_{w,p}^2 \left[1 - \frac{\lambda_L^2}{\tilde{f}_t(\tilde{\omega}_{w,p} + \tilde{\omega}_{\vartheta,q})^2} \left(1 - \frac{\tanh\left(\frac{\Psi_{\vartheta,pq}}{2}\right)}{\left(\frac{\Psi_{\vartheta,pq}}{2}\right)} \right) \right) + \right.}{\frac{\beta^2}{\chi^2} \eta_{w,p}^4 + (1+\beta^2) \eta_{w,p}^2 - \tilde{f}_t(\tilde{\omega}_{w,p} + \tilde{\omega}_{\vartheta,q})^2} + \right. \\ \left. \left. + \Psi_{\vartheta,pq}^2 \left[1 - \frac{\lambda_L^2}{\tilde{f}_t(\tilde{\omega}_{w,p} + \tilde{\omega}_{\vartheta,q})^2} \left(1 - \frac{\tan\left(\frac{\eta_{\vartheta,p}}{2}\right)}{\left(\frac{\eta_{\vartheta,p}}{2}\right)} \right) \right] \right) \right)}{\frac{\beta^2}{\chi^2} \eta_{\vartheta,q}^4 + (1+\beta^2) \eta_{\vartheta,q}^2 - \tilde{f}_t(\tilde{\omega}_{w,p} + \tilde{\omega}_{\vartheta,q})^2} + \right. \\ \left. \left. + \frac{1}{\tilde{f}_t \tilde{\omega}_{\vartheta,q}^2} \frac{\Psi_{\vartheta,q}^2 \eta_{\vartheta,q}^2}{\Psi_{\vartheta,q}^2 + \eta_{\vartheta,q}^2} \left(\frac{\Psi_{\vartheta,q}^2 \left[1 - \frac{\lambda_L^2}{\tilde{f}_t(\tilde{\omega}_{w,p} + \tilde{\omega}_{\vartheta,q})^2} \left(1 - \frac{\tanh\left(\frac{\Psi_{\vartheta,pq}}{2}\right)}{\left(\frac{\Psi_{\vartheta,pq}}{2}\right)} \right) \right) + \right. \right. \right. \\ \left. \left. \left. - \Psi_{\vartheta,pq}^2 \left[1 - \frac{\lambda_L^2}{\tilde{f}_t(\tilde{\omega}_{w,p} + \tilde{\omega}_{\vartheta,q})^2} \left(1 - \frac{\tanh\left(\frac{\Psi_{\vartheta,q}}{2}\right)}{\left(\frac{\Psi_{\vartheta,q}}{2}\right)} \right) \right] \right) \right) \right) \right] + \frac{\beta^2}{\chi^2} \Psi_{\vartheta,q}^4 - (1+\beta^2) \Psi_{\vartheta,q}^2 - \tilde{f}_t(\tilde{\omega}_{w,p} + \tilde{\omega}_{\vartheta,q})^2} \right) \\ - \lambda_Q^2 \frac{\tilde{h}_{w,p'} \theta_{q'}}{\tilde{f}_t(\tilde{\omega}_{w,p} + \tilde{\omega}_{\vartheta,q})^2} \Psi_{\vartheta,pq}^2 \right\}$$

$$\bar{H}_{1,3} = \lambda_L^2 \lambda_Q^2 \tilde{h}_{w,p} \tilde{h}_{\theta,q}$$

$$\bar{H}_{1,4} = \frac{1}{\bar{H}_{1,5}} \left(\frac{\bar{H}_{1,3}}{\Psi_{\vartheta,pq}^2 + \eta_{\vartheta,pq}^2} \cdot \frac{\lambda_L^2}{\tilde{f}_t(\tilde{\omega}_{w,p} + \tilde{\omega}_{\vartheta,q})^2} \right) + \frac{1}{\tilde{f}_t \cdot \tilde{\omega}_{\vartheta,q}^2} \frac{\Psi_{\vartheta,q}^2 \eta_{\vartheta,q}^2}{\Psi_{\vartheta,q}^2 + \eta_{\vartheta,q}^2} + \left(\frac{\eta_{w,p}^2 \left(\frac{\tanh\left(\frac{\Psi_{\vartheta,pq}}{2}\right) - \tan\left(\frac{\eta_{\vartheta,pq}}{2}\right)}{\left(\frac{\Psi_{\vartheta,pq}}{2}\right)} + \frac{\tan\left(\frac{\eta_{\vartheta,pq}}{2}\right)}{\left(\frac{\eta_{\vartheta,pq}}{2}\right)} \right) - \eta_{\vartheta,pq}^2 \left(\frac{\tanh\left(\frac{\Psi_{\vartheta,pq}}{2}\right) - \tan\left(\frac{\eta_{w,p}}{2}\right)}{\left(\frac{\Psi_{\vartheta,pq}}{2}\right)} + \frac{\tan\left(\frac{\eta_{w,p}}{2}\right)}{\left(\frac{\eta_{w,p}}{2}\right)} \right) - \Psi_{\vartheta,pq}^2 \left(\frac{\tan\left(\frac{\eta_{\vartheta,pq}}{2}\right) - \tan\left(\frac{\eta_{w,p}}{2}\right)}{\left(\frac{\eta_{\vartheta,pq}}{2}\right)} - \frac{\left(\frac{\eta_{w,p}}{2}\right)}{\left(\frac{\eta_{w,p}}{2}\right)} \right)}{\frac{\beta^2}{\chi^2} \eta_{w,p}^4 + (1+\beta^2) \cdot \eta_{w,p}^2 - \tilde{f}_t(\tilde{\omega}_{w,p} + \tilde{\omega}_{\vartheta,q})^2} + \frac{\eta_{\vartheta,q}^2 \left(\frac{\tanh\left(\frac{\Psi_{\vartheta,pq}}{2}\right) - \tan\left(\frac{\eta_{\vartheta,pq}}{2}\right)}{\left(\frac{\Psi_{\vartheta,pq}}{2}\right)} + \frac{\tan\left(\frac{\eta_{\vartheta,pq}}{2}\right)}{\left(\frac{\eta_{\vartheta,pq}}{2}\right)} \right) - \eta_{\vartheta,pq}^2 \left(\frac{\tanh\left(\frac{\Psi_{\vartheta,pq}}{2}\right) - \tan\left(\frac{\eta_{\vartheta,q}}{2}\right)}{\left(\frac{\Psi_{\vartheta,pq}}{2}\right)} + \frac{\tan\left(\frac{\eta_{\vartheta,q}}{2}\right)}{\left(\frac{\eta_{\vartheta,q}}{2}\right)} \right) - \Psi_{\vartheta,pq}^2 \left(\frac{\tan\left(\frac{\eta_{\vartheta,pq}}{2}\right) - \tan\left(\frac{\eta_{\vartheta,q}}{2}\right)}{\left(\frac{\eta_{\vartheta,pq}}{2}\right)} - \frac{\left(\frac{\eta_{\vartheta,q}}{2}\right)}{\left(\frac{\eta_{\vartheta,q}}{2}\right)} \right)}{\frac{\beta^2}{\chi^2} \eta_{\vartheta,q}^4 + (1+\beta^2) \cdot \eta_{\vartheta,q}^2 - \tilde{f}_t(\tilde{\omega}_{w,p} + \tilde{\omega}_{\vartheta,q})^2} + \frac{\Psi_{\vartheta,q}^2 \left(\frac{\tanh\left(\frac{\Psi_{\vartheta,pq}}{2}\right) - \tan\left(\frac{\eta_{\vartheta,pq}}{2}\right)}{\left(\frac{\Psi_{\vartheta,pq}}{2}\right)} + \frac{\tan\left(\frac{\eta_{\vartheta,pq}}{2}\right)}{\left(\frac{\eta_{\vartheta,pq}}{2}\right)} \right) + \eta_{\vartheta,pq}^2 \left(\frac{\tanh\left(\frac{\Psi_{\vartheta,pq}}{2}\right) - \tanh\left(\frac{\Psi_{\vartheta,q}}{2}\right)}{\left(\frac{\Psi_{\vartheta,pq}}{2}\right)} + \frac{\tanh\left(\frac{\Psi_{\vartheta,q}}{2}\right)}{\left(\frac{\Psi_{\vartheta,q}}{2}\right)} \right) + \Psi_{\vartheta,pq}^2 \left(\frac{\tan\left(\frac{\eta_{\vartheta,pq}}{2}\right) - \tanh\left(\frac{\Psi_{\vartheta,q}}{2}\right)}{\left(\frac{\eta_{\vartheta,pq}}{2}\right)} - \frac{\left(\frac{\Psi_{\vartheta,q}}{2}\right)}{\left(\frac{\Psi_{\vartheta,q}}{2}\right)} \right)}{\frac{\beta^2}{\chi^2} \Psi_{\vartheta,q}^4 - (1+\beta^2) \cdot \Psi_{\vartheta,q}^2 - \tilde{f}_t(\tilde{\omega}_{w,p} + \tilde{\omega}_{\vartheta,q})^2} + \frac{\lambda_Q^2 \tilde{h}_{w,p} \tilde{\theta}_q'}{\tilde{f}_t(\tilde{\omega}_{w,p} + \tilde{\omega}_{\vartheta,q})^2} \right)$$

$$\bar{H}_{1,5} = 1 - \frac{\lambda_L^2}{\tilde{f}_t(\tilde{\omega}_{w,p} + \tilde{\omega}_{\vartheta,q})^2} \left\{ 1 - \frac{1}{\Psi_{\vartheta,pq}^2 + \eta_{\vartheta,pq}^2} \left(\eta_{\vartheta,pq}^2 \frac{\tanh\left(\frac{\Psi_{\vartheta,pq}}{2}\right)}{\left(\frac{\Psi_{\vartheta,pq}}{2}\right)} + \Psi_{\vartheta,pq}^2 \frac{\tan\left(\frac{\eta_{\vartheta,pq}}{2}\right)}{\left(\frac{\eta_{\vartheta,pq}}{2}\right)} \right) \right\}$$

A similar expression holds also for the other torsional contribution.

$$H_{pq,2} \Rightarrow \begin{cases} \tilde{J}_t \cdot (\tilde{\omega}_{w,p} - \tilde{\omega}_{\vartheta,q})^2 \Rightarrow \Psi_{\vartheta,pq} ; \eta_{\vartheta,pq} \\ \tilde{\omega}_{w,p} \Rightarrow ; \eta_{w,p} \\ \tilde{\omega}_{\vartheta,q} \Rightarrow \Psi_{\vartheta,q} ; \eta_{\vartheta,q} \end{cases}$$

Let's consider then the case of mode-by-mode vibrations. We already know that the functions with odd subscripts maintain the same modal expressions. Whilst the remaining functions change.

$$Y_{pp,2} = \bar{Y}_{2,1} \cdot \frac{\xi}{2} \left(\xi - \frac{1}{2} \right) + \bar{Y}_{2,2} \cdot \left(\frac{\cos(\eta_{w,p} \cdot (\xi - 1/2))}{\cos(\eta_{w,p}/2)} - 1 \right)$$

Where.

$$\eta_{w,p}^2 = \tilde{\omega}_{w,p}^2$$

$$\bar{Y}_{2,1} = \left\{ -\bar{Y}_{2,2} \cdot \lambda_L^2 \left(1 - \frac{\tan\left(\frac{\eta_{w,p}}{2}\right)}{\left(\frac{\eta_{w,p}}{2}\right)} \right) + \frac{\lambda_Q^2}{2} \tilde{h}_{W_p'W_p'} \right\} / \bar{Y}_{2,3}$$

$$\bar{Y}_{2,2} = \frac{\lambda_L^2 \lambda_Q^2 \tilde{h}_{W_p}^2}{\tilde{\omega}_{w,p}^2}$$

$$\bar{Y}_{2,3} = 1 + \frac{\lambda_L^2}{12}$$

Further.

$$T_{qq,2} = \bar{T}_{2,1} \cdot \frac{\xi}{2} \left(\xi - \frac{1}{2} \right) + \bar{T}_{2,2} \cdot \left\{ \Psi_{\vartheta,q} \left(\frac{\cos(\eta_{\vartheta,q} \cdot (\xi - 1/2))}{\cos(\eta_{\vartheta,q}/2)} - 1 \right) + \eta_{\vartheta,q} \left(\frac{\cos(\Psi_{\vartheta,q} \cdot (\xi - 1/2))}{\cos(\Psi_{\vartheta,q}/2)} - 1 \right) \right\}$$

Where.

$$\Psi_{\vartheta,q}^2 = \frac{\chi^2}{2\beta^2} \left(\sqrt{(1 + \beta^2)^2 + 4 \frac{\beta^2}{\chi^2} \cdot \tilde{J}_t \tilde{\omega}_{\vartheta,q}^2} + (1 + \beta^2) \right) = \eta_{\vartheta,q}^2 + \frac{\chi^2}{\beta^2} (1 + \beta^2)$$

$$\bar{T}_{2,1} = \left\{ -\bar{Y}_{2,2} \cdot \lambda_L^2 \left\{ \Psi_{\vartheta,q}^2 \left(1 - \frac{\tan\left(\frac{\eta_{\vartheta,q}}{2}\right)}{\left(\frac{\eta_{\vartheta,q}}{2}\right)} \right) + \eta_{\vartheta,q}^2 \left(1 - \frac{\tanh\left(\frac{\Psi_{\vartheta,q}}{2}\right)}{\left(\frac{\Psi_{\vartheta,q}}{2}\right)} \right) \right\} + \frac{\lambda_Q^2}{2} \tilde{h}_{\Theta_q'\Theta_q'} \right\} / \bar{Y}_{2,3}$$

$$\bar{Y}_{2,2} = \frac{\lambda_L^2 \lambda_Q^2 \tilde{h}_{\Theta_q}^2}{\tilde{J}_t \cdot \tilde{\omega}_{\vartheta,q}^2} \cdot \frac{1}{\Psi_{\vartheta,q}^2 + \eta_{\vartheta,q}^2}$$

$$\bar{Y}_{2,3} = 1 + \frac{\lambda_L^2}{12}$$

Finally.

$$H_{pp,2} = \left\{ \begin{array}{l} \bar{H}_{2,1} \cdot \frac{\cosh(\Psi_{\vartheta,pp}(\xi - \frac{1}{2}))}{\cosh(\frac{\Psi_{\vartheta,pp}}{2})} + \bar{H}_{2,2} \cdot \frac{\xi}{2} \left(\xi - \frac{1}{2} \right) + \\ \left(\begin{array}{l} \frac{\cos(\eta_{w,p}(\xi - \frac{1}{2}))/\cos(\frac{\eta_{w,p}}{2})}{\eta_{w,p}^2 \left(\frac{\beta^2}{\chi^2} \eta_{w,p}^2 + (1 + \beta^2) \right)} + \\ + \frac{1}{\tilde{J}_t \cdot \tilde{\omega}_{\vartheta,p}^2} \frac{\Psi_{\vartheta,p}^2 \eta_{\vartheta,p}^2}{\Psi_{\vartheta,p}^2 + \eta_{\vartheta,p}^2} \left\{ \begin{array}{l} \frac{\cos(\eta_{\vartheta,p}(\xi - \frac{1}{2}))/\cos(\frac{\eta_{\vartheta,p}}{2})}{\eta_{\vartheta,p}^2 \left(\frac{\beta^2}{\chi^2} \eta_{\vartheta,p}^2 + (1 + \beta^2) \right)} + \\ - \frac{\cosh(\Psi_{\vartheta,p}(\xi - 1/2))/\cosh(\Psi_{\vartheta,p}/2)}{\Psi_{\vartheta,p}^2 \left(\frac{\beta^2}{\chi^2} \Psi_{\vartheta,p}^4 - (1 + \beta^2) \right)} \end{array} \right\} + \\ + \bar{H}_{2,4} \end{array} \right) \end{array} \right\}$$

Where.

$$\Psi_{\vartheta,pp}^2 = \sqrt{(1 + \beta^2)^2 / (\beta^2 / \chi^2)}$$

$$\eta_{w,p}^2 = \frac{1}{2\mu^2} \left(\sqrt{1 + 4\mu^2 \cdot \tilde{\omega}_{w,p}^2} \right)$$

$$\Psi_{\vartheta,p}^2 = \frac{\chi^2}{2\beta^2} \left(\sqrt{(1 + \beta^2)^2 + 4 \frac{\beta^2}{\chi^2} \cdot \tilde{J}_t \tilde{\omega}_{\vartheta,p}^2} + (1 + \beta^2) \right) = \eta_{\vartheta,p}^2 + \frac{\chi^2}{\beta^2} (1 + \beta^2)$$

$$\bar{H}_{2,1} = \frac{1}{\bar{H}_{2,5}} \frac{1}{\Psi_{\vartheta,pp}^2} \left\{ \begin{array}{l} \bar{H}_{2,3} \left\{ \begin{array}{l} \frac{\eta_{w,p}^2 + \lambda_L^2 \left(1 - \frac{\tan(\frac{\eta_{w,p}}{2})}{(\frac{\eta_{w,p}}{2})} + \frac{\eta_{w,p}^2}{12} \right)}{\eta_{w,p}^2 \left(\frac{\beta^2}{\chi^2} \eta_{w,p}^2 + (1 + \beta^2) \right)} + \\ \left(\begin{array}{l} \frac{\eta_{\vartheta,p}^2 + \lambda_L^2 \left(1 - \frac{\tan(\frac{\eta_{\vartheta,p}}{2})}{(\frac{\eta_{\vartheta,p}}{2})} + \frac{\eta_{\vartheta,p}^2}{12} \right)}{\eta_{\vartheta,p}^2 \left(\frac{\beta^2}{\chi^2} \eta_{\vartheta,p}^2 + (1 + \beta^2) \right)} + \\ \frac{\Psi_{\vartheta,p}^2 - \lambda_L^2 \left(1 - \frac{\tanh(\frac{\Psi_{\vartheta,p}}{2})}{(\frac{\Psi_{\vartheta,p}}{2})} - \frac{\Psi_{\vartheta,p}^2}{12} \right)}{\Psi_{\vartheta,p}^2 \left(\frac{\beta^2}{\chi^2} \Psi_{\vartheta,p}^4 - (1 + \beta^2) \right)} \end{array} \right) \right\} + \\ - \lambda_Q^2 \tilde{h}_{Wp}' \theta_p' \end{array} \right\}$$

$$\bar{H}_{2,2} = \frac{1}{\bar{H}_{2,5}} \left(-\frac{\lambda_L^2}{\Psi_{w,pp}^2} \bar{H}_{2,3} \cdot \left\{ \begin{aligned} & \frac{\eta_{w,p}^2 \left(1 - \frac{\tanh\left(\frac{\Psi_{\vartheta,pp}}{2}\right)}{\left(\frac{\Psi_{\vartheta,pp}}{2}\right)} \right) + \Psi_{\vartheta,pp}^2 \left(1 - \frac{\tan\left(\frac{\eta_{w,p}}{2}\right)}{\left(\frac{\eta_{w,p}}{2}\right)} \right)}{\eta_{w,p}^2 \left(\frac{\beta^2}{\chi^2} \eta_{w,p}^2 + (1+\beta^2) \right)} + \right. \\ & \left. \frac{1}{\tilde{J}_t \cdot \tilde{\omega}_{\vartheta,q}^2} \frac{\Psi_{\vartheta,p}^2 \eta_{\vartheta,p}^2}{\Psi_{\vartheta,p}^2 + \eta_{\vartheta,p}^2} \left(\frac{\eta_{\vartheta,p}^2 \left(1 - \frac{\tanh\left(\frac{\Psi_{\vartheta,pp}}{2}\right)}{\left(\frac{\Psi_{\vartheta,pp}}{2}\right)} \right) + \Psi_{\vartheta,pp}^2 \left(1 - \frac{\tan\left(\frac{\eta_{\vartheta,p}}{2}\right)}{\left(\frac{\eta_{\vartheta,p}}{2}\right)} \right)}{\eta_{\vartheta,p}^2 \left(\frac{\beta^2}{\chi^2} \eta_{\vartheta,p}^2 + (1+\beta^2) \right)} + \right. \right. \\ & \left. \left. \frac{\Psi_{\vartheta,p}^2 \left(1 - \frac{\tanh\left(\frac{\Psi_{\vartheta,pp}}{2}\right)}{\left(\frac{\Psi_{\vartheta,pp}}{2}\right)} \right) + \Psi_{w,pp}^2 \left(1 - \frac{\tanh\left(\frac{\Psi_{\vartheta,p}}{2}\right)}{\left(\frac{\Psi_{\vartheta,p}}{2}\right)} \right)}{\Psi_{\vartheta,p}^2 \left(\frac{\beta^2}{\chi^2} \Psi_{\vartheta,p}^2 - (1+\beta^2) \right)} \right) \right\} + \lambda_Q^2 \tilde{h}_{w_p' \vartheta_p'} \right)$$

$$\bar{H}_{2,3} = \lambda_L^2 \lambda_Q^2 \tilde{h}_{w_p} \tilde{h}_{\vartheta_p}$$

$$\bar{H}_{2,4} = -\frac{1}{\Psi_{w,pp}^2} \frac{1}{\bar{H}_{2,5}} \bar{H}_{2,3} \left\{ \begin{aligned} & \frac{\eta_{w,p}^2 + \Psi_{w,pp}^2 + \lambda_L^2 \left(\frac{\tanh\left(\frac{\Psi_{w,pp}}{2}\right)}{\left(\frac{\Psi_{w,pp}}{2}\right)} - \frac{\tan\left(\frac{\eta_{w,p}}{2}\right)}{\left(\frac{\eta_{w,p}}{2}\right)} + \frac{\eta_{w,p}^2 + \Psi_{w,pp}^2}{12} \right)}{\eta_{w,p}^2 \left(\frac{\beta^2}{\chi^2} \eta_{w,p}^2 + (1+\beta^2) \right)} + \right. \\ & \frac{1}{\tilde{J}_t \cdot \tilde{\omega}_{\vartheta,p}^2} \frac{\Psi_{\vartheta,p}^2 \eta_{\vartheta,p}^2}{\Psi_{\vartheta,p}^2 + \eta_{\vartheta,p}^2} \left(\frac{\eta_{\vartheta,p}^2 + \Psi_{\vartheta,pp}^2 + \lambda_L^2 \left(\frac{\tanh\left(\frac{\Psi_{\vartheta,pp}}{2}\right)}{\left(\frac{\Psi_{\vartheta,pp}}{2}\right)} - \frac{\tan\left(\frac{\eta_{\vartheta,p}}{2}\right)}{\left(\frac{\eta_{\vartheta,p}}{2}\right)} + \frac{\eta_{\vartheta,p}^2 + \Psi_{\vartheta,pp}^2}{12} \right)}{\eta_{\vartheta,p}^2 \left(\frac{\beta^2}{\chi^2} \eta_{\vartheta,p}^2 + (1+\beta^2) \right)} + \right. \\ & \left. \left. -\lambda_Q^2 \tilde{h}_{w_p' \vartheta_p'} \right) \right\} + \frac{1}{\tilde{J}_t \cdot \tilde{\omega}_{\vartheta,p}^2} \frac{\Psi_{\vartheta,p}^2 \eta_{\vartheta,p}^2}{\Psi_{\vartheta,p}^2 + \eta_{\vartheta,p}^2} \left(\frac{\Psi_{\vartheta,p}^2 - \Psi_{\vartheta,pp}^2 + \lambda_L^2 \left(\frac{\tanh\left(\frac{\Psi_{\vartheta,pp}}{2}\right)}{\left(\frac{\Psi_{\vartheta,pp}}{2}\right)} - \frac{\tanh\left(\frac{\Psi_{\vartheta,p}}{2}\right)}{\left(\frac{\Psi_{\vartheta,p}}{2}\right)} + \frac{\Psi_{\vartheta,p}^2 - \Psi_{\vartheta,pp}^2}{12} \right)}{\Psi_{\vartheta,p}^2 \left(\frac{\beta^2}{\chi^2} \Psi_{\vartheta,p}^2 - (1+\beta^2) \right)} \right) \right)$$

$$\bar{H}_{2,5} = 1 - \lambda_L^2 \left(\frac{1}{\Psi_{\vartheta,pp}^2} \left(1 - \frac{\tanh\left(\frac{\Psi_{\vartheta,pp}}{2}\right)}{\left(\frac{\Psi_{\vartheta,pp}}{2}\right)} \right) - \frac{1}{12} \right)$$

Considering skew-symmetric linear modes, for the multi-mode approach, we get a second order flexural correction equal to the linear symmetric mode in the case of flexible deck as far as the combinational frequency does not satisfy the condition already seen.

$$Y_{pr,1} = \frac{\lambda_L^2}{(\tilde{\omega}_{w,p} + \tilde{\omega}_{w,r})^2} \tilde{h}_{W,n} \cdot \left\{ 1 - \frac{\cos\left((\tilde{\omega}_{w,p} + \tilde{\omega}_{w,r}) \cdot \left(\xi - \frac{1}{2}\right)\right)}{\cos\left(\frac{(\tilde{\omega}_{w,p} + \tilde{\omega}_{w,r})}{2}\right)} \right\}$$

Similarly for $Y_{pr,2}$, $T_{qs,1}$, $T_{qs,2}$ simply changing properly the combinational frequency. Contrary, the two functions $H_{pq,1}$, $H_{pq,2}$ becomes equal to the general format of symmetric linear torsional modes as the combinational frequency does not allow the mode to be sinusoidal.

$$H_{pq,1} = \frac{\lambda_L^2}{\tilde{J}_t \cdot (\tilde{\omega}_{\theta,p} + \tilde{\omega}_{\theta,q})^2} \tilde{h}_{H_{pq,1}} \cdot \left\{ 1 - \frac{1}{\Psi_{\theta,pq}^2 + \eta_{\theta,pq}^2} \cdot \left(\eta_{\theta,pq}^2 \cdot \frac{\cosh\left(\Psi_{\theta,pq} \cdot \left(\xi - \frac{1}{2}\right)\right)}{\cosh\left(\frac{\Psi_{\theta,pq}}{2}\right)} + \Psi_{\theta,pq}^2 \cdot \frac{\cos\left(\eta_{\theta,pq} \cdot \left(\xi - \frac{1}{2}\right)\right)}{\cos\left(\frac{\eta_{\theta,pq}}{2}\right)} \right) \right\}$$

Then passing to the mode-by-mode approach for quadratic modes with odd subscripts, with respect to the multi-mode approach, only the modal amplitude changes but it is not relevant since the mode will be normalized.

Contrary for the remaining functions we get.

$$Y_{pr,2} = \lambda_Q^2 \left(\frac{n\pi}{2}\right)^2 \left(1 - \frac{1}{\lambda_L^2 + 12}\right) \frac{\xi}{2} \left(\xi - \frac{1}{2}\right)$$

Similarly for $T_{qs,2}$, whilst both the torsional ones has the same shape performed in the general case of mode-by-mode approach with skew-symmetric linear modes.

3.2.4 Free warping

Considering a thin walled close cross section deck ($\chi^2 \rightarrow \infty$) we can state that the flexural functions $Y_{pr,1}$, $Y_{pr,2}$ are not affected by the parameter χ^2 . Contrary, for the torsional contribution on the quadratic flexural mode we get similar results obtained for $H_{pq,1}$ for $\mu^2 = 0$.

$$T_{qs,1} = \left\{ \begin{aligned} & \bar{T}_{1,1} \cdot \frac{\cosh\left(\Psi_{\theta,qs} \cdot \left(\xi - \frac{1}{2}\right)\right)}{\cosh\left(\frac{\Psi_{\theta,qs}}{2}\right)} + \bar{T}_{1,2} \cdot \frac{\cos\left(\eta_{\theta,qs} \cdot \left(\xi - \frac{1}{2}\right)\right)}{\cos\left(\frac{\eta_{\theta,qs}}{2}\right)} + \\ & + \bar{T}_{1,3} \cdot \cos\left(\eta_{\theta,q} \cdot \left(\xi - \frac{1}{2}\right)\right) / \cos\left(\frac{\eta_{\theta,q}}{2}\right) + \\ & + \bar{T}_{1,4} \end{aligned} \right\}$$

Where.

$$\Psi_{w,q_s}^2 = \frac{1}{2\mu^2} \left(\sqrt{1 + 4\mu^2 \cdot (\tilde{\omega}_{\vartheta,q} + \tilde{\omega}_{\vartheta,s})^2} - 1 \right) = \eta_{w,q_s}^2 + \frac{1}{\mu^2}$$

$$\eta_{w,q}^2 = \frac{1}{2\mu^2} \left(\sqrt{1 + 4\mu^2 \cdot \tilde{\omega}_{\vartheta,q}^2} - 1 \right)$$

$$\bar{\bar{T}}_{1,1} = \frac{1/\bar{\bar{T}}_{1,5}}{\Psi_{w,q_s}^2 + \eta_{w,q_s}^2} \left\{ \bar{\bar{T}}_{1,3} \left\{ \begin{aligned} & \left[\eta_{\vartheta,q}^2 \left[1 - \frac{\lambda_L^2}{(\tilde{\omega}_{\vartheta,q} + \tilde{\omega}_{\vartheta,s})^2} \left(1 - \frac{\tan(\frac{\eta_{w,q_s}}{2})}{(\frac{\eta_{w,q_s}}{2})} \right) \right] \right] + \right. \\ & \left. - \eta_{w,q_s}^2 \left[1 - \frac{\lambda_L^2}{(\tilde{\omega}_{\vartheta,q} + \tilde{\omega}_{\vartheta,s})^2} \left(1 - \frac{\tan(\frac{\eta_{\vartheta,q}}{2})}{(\frac{\eta_{\vartheta,q}}{2})} \right) \right] \right] \right\} + \left. \begin{aligned} & - \frac{\lambda_Q^2}{2} \frac{\tilde{h}_{\theta_q'} \theta_s'}{(\tilde{\omega}_{\vartheta,q} + \tilde{\omega}_{\vartheta,s})^2} \eta_{w,q_s}^2 \end{aligned} \right\}$$

$$\bar{\bar{T}}_{1,2} = -\frac{1/\bar{\bar{T}}_{1,5}}{\Psi_{w,q_s}^2 + \eta_{w,q_s}^2} \left\{ \bar{\bar{T}}_{1,3} \left\{ \begin{aligned} & \left[\eta_{\vartheta,q}^2 \left[1 - \frac{\lambda_L^2}{(\tilde{\omega}_{\vartheta,q} + \tilde{\omega}_{\vartheta,s})^2} \left(1 - \frac{\tan(\frac{\Psi_{w,q_s}}{2})}{(\frac{\Psi_{w,q_s}}{2})} \right) \right] \right] + \right. \\ & \left. + \Psi_{w,q_s}^2 \left[1 - \frac{\lambda_L^2}{(\tilde{\omega}_{\vartheta,q} + \tilde{\omega}_{\vartheta,s})^2} \left(1 - \frac{\tan(\frac{\eta_{\vartheta,q}}{2})}{(\frac{\eta_{\vartheta,q}}{2})} \right) \right] \right] \right\} + \left. \begin{aligned} & + \frac{\lambda_Q^2}{2} \frac{\tilde{h}_{\theta_q'} \theta_s'}{(\tilde{\omega}_{\vartheta,q} + \tilde{\omega}_{\vartheta,s})^2} \Psi_{w,q_s}^2 \end{aligned} \right\}$$

$$\bar{\bar{T}}_{1,3} = \frac{\lambda_L^2 \lambda_Q^2 \tilde{h}_{\theta_q'} \tilde{h}_{\theta_s'}}{\tilde{J}_t \cdot \tilde{\omega}_{\vartheta,q}^2} \frac{\eta_{\vartheta,q}^2}{\mu^2 \cdot \eta_{\vartheta,q}^4 + \eta_{\vartheta,q}^2 - (\tilde{\omega}_{\vartheta,q} + \tilde{\omega}_{\vartheta,s})^2}$$

$$\bar{\bar{T}}_{1,4} = \frac{\bar{\bar{T}}_{1,3}/\bar{\bar{T}}_{1,5}}{\Psi_{w,q_s}^2 + \eta_{w,q_s}^2} \cdot \frac{\lambda_L^2}{(\tilde{\omega}_{\vartheta,q} + \tilde{\omega}_{\vartheta,s})^2} \left\{ \begin{aligned} & \eta_{\vartheta,q}^2 \left(\frac{\tanh(\frac{\Psi_{w,q_s}}{2})}{(\frac{\Psi_{w,q_s}}{2})} - \frac{\tan(\frac{\eta_{w,q_s}}{2})}{(\frac{\eta_{w,q_s}}{2})} \right) + \\ & - \eta_{w,q_s}^2 \left(\frac{\tanh(\frac{\Psi_{w,q_s}}{2})}{(\frac{\Psi_{w,q_s}}{2})} - \frac{\tan(\frac{\eta_{\vartheta,q}}{2})}{(\frac{\eta_{\vartheta,q}}{2})} \right) + \end{aligned} \right\} + \frac{\lambda_Q^2}{2} \frac{\tilde{h}_{\theta_q'} \theta_s'}{(\tilde{\omega}_{\vartheta,q} + \tilde{\omega}_{\vartheta,s})^2} \left\{ \begin{aligned} & - \Psi_{w,q_s}^2 \left(\frac{\tan(\frac{\eta_{w,q_s}}{2})}{(\frac{\eta_{w,q_s}}{2})} - \frac{\tan(\frac{\eta_{\vartheta,q}}{2})}{(\frac{\eta_{\vartheta,q}}{2})} \right) \end{aligned} \right\}$$

$$\bar{\bar{T}}_{1,5} = 1 - \frac{\lambda_L^2}{(\tilde{\omega}_{\vartheta,q} + \tilde{\omega}_{\vartheta,s})^2} \left\{ 1 - \frac{1}{\Psi_{w,q_s}^2 + \eta_{w,q_s}^2} \left(\eta_{w,q_s}^2 \frac{\tanh(\frac{\Psi_{w,q_s}}{2})}{(\frac{\Psi_{w,q_s}}{2})} + \Psi_{w,q_s}^2 \frac{\tan(\frac{\eta_{w,q_s}}{2})}{(\frac{\eta_{w,q_s}}{2})} \right) \right\}$$

Similar expression holds for $T_{q_s,2}$, while for $H_{p,q,1}$ we get similar result of $T_{q_s,1}$ for $\mu^2 = 0$.

$$H_{pq,1} = \left\{ \begin{aligned} & \bar{H}_{1,1} \cdot \frac{\cos\left(\eta_{\vartheta,pq}\left(\xi - \frac{1}{2}\right)\right)}{\cos\left(\frac{\eta_{\vartheta,pq}}{2}\right)} + \\ & + \bar{H}_{1,2} \cdot \left\{ \frac{1}{\tilde{\omega}_{w,p}^2} \cdot \frac{\Psi_{w,p}^2 \eta_{w,p}^2}{\Psi_{w,p}^2 + \eta_{w,p}^2} \left(\frac{\cos\left(\eta_{w,p}\left(\xi - \frac{1}{2}\right)\right) / \cos\left(\frac{\eta_{w,p}}{2}\right)}{(1+\beta^2) \cdot \eta_{w,p}^2 - \tilde{J}_t(\tilde{\omega}_{w,p} + \tilde{\omega}_{\vartheta,q})^2} + \right. \right. \\ & \left. \left. + \frac{\cosh\left(\Psi_{w,p}\left(\xi - \frac{1}{2}\right)\right) / \cosh\left(\frac{\Psi_{w,p}}{2}\right)}{(1+\beta^2) \cdot \Psi_{w,p}^2 + \tilde{J}_t(\tilde{\omega}_{w,p} + \tilde{\omega}_{\vartheta,q})^2} \right) + \right. \\ & \left. + \frac{\eta_{\vartheta,q}^2}{\tilde{J}_t \cdot \tilde{\omega}_{\vartheta,q}^2} \frac{\cos\left(\eta_{\vartheta,q}\left(\xi - \frac{1}{2}\right)\right) / \cos\left(\frac{\eta_{\vartheta,q}}{2}\right)}{(1+\beta^2) \cdot \eta_{\vartheta,q}^2 - \tilde{J}_t(\tilde{\omega}_{w,p} + \tilde{\omega}_{\vartheta,q})^2} \right\} + \bar{H}_{1,3} \end{aligned} \right\}$$

Where.

$$\eta_{\vartheta,pq}^2 = \tilde{J}_t(\tilde{\omega}_{\vartheta,q} + \tilde{\omega}_{\vartheta,s})^2 / (1 + \beta^2)$$

$$\Psi_{w,p}^2 = \frac{1}{2\mu^2} \left(\sqrt{1 + 4\mu^2 \cdot \tilde{\omega}_{w,p}^2} - 1 \right) = \eta_{w,p}^2 + \frac{1}{\mu^2}$$

$$\eta_{\vartheta,q}^2 = \frac{\chi^2}{2\beta^2} \left(\sqrt{(1 + \beta^2)^2 + 4 \frac{\beta^2}{\chi^2} \cdot \tilde{J}_t \tilde{\omega}_{\vartheta,q}^2} - (1 + \beta^2) \right)$$

$$\bar{H}_{1,1} = -\frac{1}{\bar{H}_{1,4}} \left\{ \bar{H}_{1,2} \left\{ \frac{1}{\tilde{\omega}_{w,p}^2} \frac{\Psi_{w,p}^2 \eta_{w,p}^2}{\Psi_{w,p}^2 + \eta_{w,p}^2} \left(\frac{1 - \frac{\lambda_L^2}{\tilde{J}_t(\tilde{\omega}_{w,p} + \tilde{\omega}_{\vartheta,q})^2} \left(1 - \frac{\tan\left(\frac{\eta_{w,p}}{2}\right)}{\left(\frac{\eta_{w,p}}{2}\right)} \right)}{(1+\beta^2) \cdot \eta_{w,p}^2 - \tilde{J}_t(\tilde{\omega}_{w,p} + \tilde{\omega}_{\vartheta,q})^2} + \right. \right. \\ \left. \left. + \frac{1 - \frac{\lambda_L^2}{\tilde{J}_t(\tilde{\omega}_{w,p} + \tilde{\omega}_{\vartheta,q})^2} \left(1 - \frac{\tanh\left(\frac{\Psi_{w,p}}{2}\right)}{\left(\frac{\Psi_{w,p}}{2}\right)} \right)}{(1+\beta^2) \cdot \Psi_{w,p}^2 + \tilde{J}_t(\tilde{\omega}_{w,p} + \tilde{\omega}_{\vartheta,q})^2} \right) + \right. \\ \left. + \frac{\eta_{\vartheta,q}^2}{\tilde{J}_t \cdot \tilde{\omega}_{\vartheta,q}^2} \cdot \frac{1 - \frac{\lambda_L^2}{\tilde{J}_t(\tilde{\omega}_{w,p} + \tilde{\omega}_{\vartheta,q})^2} \left(1 - \frac{\tan\left(\frac{\eta_{\vartheta,q}}{2}\right)}{\left(\frac{\eta_{\vartheta,q}}{2}\right)} \right)}{(1+\beta^2) \cdot \eta_{w,p}^2 - \tilde{J}_t(\tilde{\omega}_{w,p} + \tilde{\omega}_{\vartheta,q})^2} \right\} + \lambda_Q^2 \frac{\tilde{h}_{w,p}' \theta_q'}{\tilde{J}_t(\tilde{\omega}_{w,p} + \tilde{\omega}_{\vartheta,q})^2} \right\}$$

$$\bar{H}_{1,2} = \lambda_L^2 \lambda_Q^2 \tilde{h}_{w,p} \tilde{h}_{\vartheta,q}$$

$$\bar{H}_{1,3} = \frac{1}{\bar{H}_{1,4}} \left\{ -\bar{H}_{1,2} \frac{\lambda_L^2}{\tilde{J}_t(\tilde{\omega}_{w,p} + \tilde{\omega}_{\theta,q})^2} \left\{ \frac{1}{\tilde{\omega}_{w,p}^2} \frac{\Psi_{w,p}^2 \eta_{w,p}^2}{\Psi_{w,p}^2 + \eta_{w,p}^2} \left(\frac{\tan\left(\frac{\eta_{\theta,pq}}{2}\right) - \tan\left(\frac{\eta_{w,p}}{2}\right)}{\left(\frac{\eta_{\theta,pq}}{2}\right) - \left(\frac{\eta_{w,p}}{2}\right)} \right) \frac{1}{(1+\beta^2) \cdot \eta_{w,p}^2 - \tilde{J}_t(\tilde{\omega}_{w,p} + \tilde{\omega}_{\theta,q})^2} + \frac{\left(\frac{\tan\left(\frac{\eta_{\theta,pq}}{2}\right) - \tanh\left(\frac{\Psi_{w,p}}{2}\right)}{\left(\frac{\eta_{\theta,pq}}{2}\right) - \left(\frac{\Psi_{w,p}}{2}\right)} \right)}{(1+\beta^2) \cdot \Psi_{w,p}^2 + \tilde{J}_t(\tilde{\omega}_{w,p} + \tilde{\omega}_{\theta,q})^2} \right\} + \frac{\lambda_Q^2 \tilde{h}_{w,p'} \theta_{q'}}{\tilde{J}_t(\tilde{\omega}_{w,p} + \tilde{\omega}_{\theta,q})^2} \right\} + \frac{\eta_{\theta,q}^2}{\tilde{J}_t \cdot \tilde{\omega}_{\theta,q}^2 (1+\beta^2) \cdot \eta_{\theta,q}^2 - \tilde{J}_t(\tilde{\omega}_{w,p} + \tilde{\omega}_{\theta,q})^2} \left(\frac{\tan\left(\frac{\eta_{\theta,pq}}{2}\right) - \tan\left(\frac{\eta_{\theta,q}}{2}\right)}{\left(\frac{\eta_{\theta,pq}}{2}\right) - \left(\frac{\eta_{\theta,q}}{2}\right)} \right)$$

$$\bar{H}_{1,4} = 1 - \frac{\lambda_L^2}{\tilde{J}_t(\tilde{\omega}_{w,p} + \tilde{\omega}_{\theta,q})^2} \left\{ 1 - \frac{\tan\left(\frac{\eta_{\theta,pq}}{2}\right)}{\left(\frac{\eta_{\theta,pq}}{2}\right)} \right\}$$

Similarly for $H_{qs,2}$ with proper modification of the combinational resonance.

Then passing to consider the mode-by-mode approach, we can state that $T_{qs,2}$ is modified as $H_{pq,2}$ for $\mu^2 = 0$.

$$T_{q,2} = \left\{ \begin{array}{l} \bar{Y}_{2,1} \cdot \frac{\cosh\left(\Psi_{w,qq} \left(\xi - \frac{1}{2}\right)\right)}{\cosh\left(\frac{\Psi_{w,qq}}{2}\right)} + \bar{Y}_{2,2} \cdot \frac{\xi}{2} \left(\xi - \frac{1}{2}\right) + \\ + \bar{Y}_{2,3} \cdot \cos\left(\eta_{\theta,q} \cdot \left(\xi - \frac{1}{2}\right)\right) / \cos\left(\eta_{\theta,q}/2\right) + \bar{Y}_{2,4} \end{array} \right\}$$

Where.

$$\Psi_{w,qq}^2 = 1/\mu^2$$

$$\eta_{\theta,q}^2 = \frac{\chi^2}{2\beta^2} \left(\sqrt{(1+\beta^2)^2 + 4 \frac{\beta^2}{\chi^2} \cdot \tilde{J}_t \tilde{\omega}_{\theta,q}^2} - (1+\beta^2) \right)$$

$$\bar{T}_{2,1} = \left\{ \frac{1}{\Psi_{w,qq}^2} \bar{T}_{2,3} \cdot \frac{\eta_{\theta,q}^2 + \lambda_L^2 \left(1 - \frac{\tan\left(\frac{\eta_{\theta,q}}{2}\right)}{\left(\frac{\eta_{\theta,q}}{2}\right)} + \frac{\eta_{\theta,q}^2}{12} \right)}{\eta_{\theta,q}^2 (\mu^2 \cdot \eta_{\theta,q}^2 + 1)} - \frac{\lambda_Q^2}{2} \tilde{h}_{\theta_{q'} \theta_{q'}} \right\} / \bar{T}_{2,5}$$

$$\bar{T}_{2,2} = -\frac{\lambda_L^2}{\Psi_{w,qq}^2} \bar{Y}_{2,3} \cdot \eta_{\theta,q}^2 \left(1 - \frac{\tanh\left(\frac{\Psi_{w,qq}}{2}\right)}{\left(\frac{\Psi_{w,qq}}{2}\right)} \right) + \Psi_{w,qq}^2 \left(1 - \frac{\tan\left(\frac{\eta_{\theta,q}}{2}\right)}{\left(\frac{\eta_{\theta,q}}{2}\right)} \right) + \frac{\lambda_Q^2}{2} \tilde{h}_{\theta_{q'} \theta_{q'}}$$

$$\bar{Y}_{2,3} = \frac{\lambda_L^2 \lambda_Q^2 \tilde{h}_{\theta_q}^2}{\tilde{J}_t \cdot \tilde{\omega}_{\theta,q}^2} \cdot \frac{\eta_{\theta,q}^2}{\eta_{\theta,q}^2 (\mu^2 \cdot \eta_{\theta,q}^2 + 1)}$$

$$\bar{Y}_{2,4} = -\frac{1}{\Psi_{w,qq}^2} \frac{1}{\bar{Y}_{2,5}} \left\{ \bar{Y}_{2,3} \left(\eta_{\vartheta,q}^2 + \Psi_{w,qq}^2 + \lambda_L^2 \left(\frac{\tanh\left(\frac{\Psi_{w,qq}}{2}\right) - \tan\left(\frac{\eta_{\vartheta,q}}{2}\right)}{\left(\frac{\Psi_{w,qq}}{2}\right)} + \frac{\eta_{\vartheta,q}^2 + \Psi_{w,qq}^2}{12} \right) \right) - \frac{\lambda_Q^2}{2} \tilde{h}_{\theta_q' \theta_q'} \right\}$$

$$\bar{Y}_{2,5} = 1 - \lambda_L^2 \left(\frac{1}{\Psi_{w,qq}^2} \left(1 - \frac{\tanh\left(\frac{\Psi_{w,qq}}{2}\right)}{\left(\frac{\Psi_{w,qq}}{2}\right)} \right) - \frac{1}{12} \right)$$

Whilst $H_{pp,2}$ changes as $T_{qs,2}$ for $\mu^2 = 0$.

$$H_{pp,2} = \left\{ \begin{array}{l} \bar{H}_{2,1} \cdot \frac{\xi}{2} \left(\xi - \frac{1}{2} \right) + \\ + \frac{\bar{H}_{2,2}}{(1+\beta^2)} \left(\frac{1}{\tilde{\omega}_{w,p}^2} \frac{\Psi_{w,p}^2 \eta_{w,p}^2}{\Psi_{w,p}^2 + \eta_{w,p}^2} \left\{ \frac{\cos\left(\eta_{w,p} \cdot \left(\xi - \frac{1}{2}\right)\right) / \cos\left(\frac{\eta_{w,p}}{2}\right) - 1}{\eta_{w,p}^2} + \right. \right. \\ \left. \left. + \frac{\cosh\left(\Psi_{w,p} \cdot \left(\xi - \frac{1}{2}\right)\right) / \cosh\left(\Psi_{w,p}/2\right) - 1}{\Psi_{w,p}^2} \right\} + \right. \\ \left. + \frac{1}{\tilde{J}_t \cdot \tilde{\omega}_{\vartheta,p}^2} \left\{ \cos\left(\eta_{\vartheta,p} \cdot \left(\xi - \frac{1}{2}\right)\right) / \cos\left(\frac{\eta_{\vartheta,p}}{2}\right) \right\} \right) \end{array} \right\}$$

Where.

$$\Psi_{w,p}^2 = \frac{1}{2\mu^2} \left(\sqrt{1 + 4\mu^2 \cdot \tilde{\omega}_{w,p}^2} + 1 \right) = \eta_{w,p}^2 + \frac{1}{\mu^2}$$

$$\eta_{\vartheta,p}^2 = \frac{\chi^2}{2\beta^2} \left(\sqrt{(1 + \beta^2)^2 + 4 \frac{\beta^2}{\chi^2} \cdot \tilde{J}_t \tilde{\omega}_{\vartheta,p}^2} - (1 + \beta^2) \right)$$

$$\bar{H}_{2,1} = -\frac{\lambda_L^2}{1 + \frac{\lambda_L^2}{12} (1 + \beta^2)} \cdot \left\{ \frac{1}{\tilde{\omega}_{w,p}^2} \frac{\Psi_{w,p}^2 \eta_{w,p}^2}{\Psi_{w,p}^2 + \eta_{w,p}^2} \left(\frac{1 - \frac{\tan\left(\frac{\eta_{w,p}}{2}\right)}{\left(\frac{\eta_{w,p}}{2}\right)}}{\eta_{w,p}^2} + \frac{1 - \frac{\tanh\left(\frac{\Psi_{w,p}}{2}\right)}{\left(\frac{\Psi_{w,p}}{2}\right)}}{\Psi_{w,p}^2} \right) + \right. \\ \left. + \frac{1}{\tilde{J}_t \cdot \tilde{\omega}_{\vartheta,p}^2} \left(1 - \frac{\tan\left(\frac{\eta_{\vartheta,p}}{2}\right)}{\left(\frac{\eta_{\vartheta,p}}{2}\right)} \right) \right\} + \lambda_Q^2 \tilde{h}_{w_p' \theta_p'}$$

$$\bar{H}_{2,2} = \lambda_L^2 \lambda_Q^2 \tilde{h}_{w_p} \tilde{h}_{\theta_p}$$

Considering skew-symmetric linear modes, we get that $\chi^2 \rightarrow \infty$ does not influence the second order correction of flexural modes. Whilst the two functions associated to torsional ones becomes for the multi-modal approach equal to the linear torsional modes for free warping.

$$H_{pq,2} = \frac{\lambda_L^2}{\tilde{J}_t \cdot (\tilde{\omega}_{w,p} + \tilde{\omega}_{\vartheta,q})^2} \tilde{h}_{H_{pq,2}} \cdot \left\{ 1 - \frac{\cos\left(\sqrt{\frac{\tilde{J}_t}{(1+\beta^2)}}(\tilde{\omega}_{w,p} + \tilde{\omega}_{\vartheta,q}) \cdot \left(\xi - \frac{1}{2}\right)\right)}{\cos\left(\frac{1}{2} \sqrt{\frac{\tilde{J}_t}{(1+\beta^2)}}(\tilde{\omega}_{w,p} + \tilde{\omega}_{\vartheta,q})\right)} \right\}$$

In addition, for mode-by-mode becomes parabolic.

$$H_{pp,2} = \lambda_Q^2 \frac{(n\pi)^2}{2} \left(1 - \frac{1}{\lambda_L^2 - 12}\right) \frac{\xi}{2} \left(\xi - \frac{1}{2}\right)$$

Notice that the particular case of torsionally flexible deck is a subcase of the free warping condition simply enforcing $\beta^2 = 0$.

3.4. Cubic contribution

We have mentioned many times that the equations of motion governing the vibration of a two-dof suspension bridge are nonlinear up to cubic terms. Consequently, the last correction with respect to the linear motion will be of third order due to the assumption of neglecting higher order terms in the multiple time scale expansion.

$$D_0^2 \tilde{w}_3 + \mu^2 \cdot \tilde{w}_3^{iv} - \tilde{w}_3^{ii} + \lambda_L^2 \cdot \tilde{h}_{w_3} = \left\{ \begin{array}{l} -2D_0 D_1 \tilde{w}_2 - (D_1^2 + 2D_0 D_2) \tilde{w}_1 - \nu_w D_0 \tilde{w}_1 + F_w \\ \\ + \lambda_Q^2 \left\{ \begin{array}{l} \tilde{w}_1^{ii} \cdot \tilde{h}_{w_2} + \tilde{w}_2^{ii} \cdot \tilde{h}_{w_1} + \\ + \tilde{\vartheta}_1^{ii} \cdot \tilde{h}_{\vartheta_2} + \tilde{\vartheta}_2^{ii} \cdot \tilde{h}_{\vartheta_1} + \\ - (\tilde{h}_{w_1' w_2'} + \tilde{h}_{\vartheta_1' \vartheta_2'}) \end{array} \right\} + \\ \\ + \lambda_C^2 \left\{ \frac{1}{2} \tilde{w}_1^{ii} \cdot (\tilde{h}_{w_1' w_1'} + \tilde{h}_{\vartheta_1' \vartheta_1'}) + \tilde{\vartheta}_1^{ii} \cdot \tilde{h}_{w_1' \vartheta_1'} \right\} \end{array} \right\}$$

$$\left\{ \begin{array}{l} \tilde{J}_t D_0^2 \tilde{\vartheta}_3 + \frac{\beta^2}{\chi^2} \cdot \tilde{\vartheta}_3^{iv} + \\ -(1 + \beta^2) \cdot \tilde{\vartheta}_3^{ii} + \lambda_L^2 \cdot \tilde{h}_{\vartheta_3} \end{array} \right\} = \left\{ \begin{array}{l} -2\tilde{J}_t D_0 D_1 \tilde{\vartheta}_2 - (D_1^2 + 2D_0 D_2) \tilde{\vartheta}_1 - \nu_\vartheta D_0 \tilde{\vartheta}_1 + F_\vartheta + \\ \\ + \lambda_Q^2 \left\{ \begin{array}{l} \tilde{\vartheta}_1^{ii} \cdot \tilde{h}_{w_2} + \tilde{\vartheta}_2^{ii} \cdot \tilde{h}_{w_1} + \\ + \tilde{w}_1^{ii} \cdot \tilde{h}_{\vartheta_2} + \tilde{w}_2^{ii} \cdot \tilde{h}_{\vartheta_1} + \\ - (\tilde{h}_{w_1' \vartheta_2'} + \tilde{h}_{w_2' \vartheta_1'}) \end{array} \right\} + \\ \\ + \lambda_C^2 \left\{ \frac{1}{2} \tilde{\vartheta}_1^{ii} \cdot (\tilde{h}_{w_1' w_1'} + \tilde{h}_{\vartheta_1' \vartheta_1'}) + \tilde{w}_1^{ii} \cdot \tilde{h}_{w_1' \vartheta_1'} \right\} \end{array} \right\}$$

Notice that in the linear component of the right hand side term we have added both flexural and torsional damping and external forcing. In order to make them appear just in the cubic equation and do not affect the lower order ones, making computations further cumbersome, we make the a priori assumption that

dimensionless damping is a second order quantity and dimensionless external forces just perturb the system by means of a third order term.

$$v_{(\cdot)} = \epsilon^2 \cdot \tilde{c}_{(\cdot)}$$

$$F_{(\cdot)} = \epsilon^3 \cdot \tilde{f}_{(\cdot)}$$

This way, we are able to account for wind-structure interaction effects, such as additional damping and vortex shedding forcing. As already mentioned the variation of eigen-frequencies with the wind speed level can be taken in account simply substituting the actual values for the specified wind speed.

In order to explicit the righ-hand side terms we need to substitute the expressions previously found for the linear and quadratic component of motion. After some computations and taking in mind the fact that amplitudes are function only of the quadratic time scale T_2 we get the following expressions.

For the flexural one.

$$(1) = \left\{ \begin{array}{l} -\sum_{n=1}^{\infty} \{ i\tilde{\omega}_{w,n} (2D_2 Z_n + v_w Z_n) \cdot \exp(i\tilde{\omega}_{w,n} T_0) + c.c. \} W_n + \\ \sum_{p,r,t=1}^{\infty} F_{w,prt} + \sum_{q,s,t=1}^{\infty} F_{w,qst} + F_w \end{array} \right\}$$

Where.

$$F_{w,prt} = \left\{ \begin{array}{l} \left(\begin{array}{l} \{ Z_p Z_r Z_t \cdot \exp(i(\tilde{\omega}_{w,p} + \tilde{\omega}_{w,r} + \tilde{\omega}_{w,t}) T_0) + c.c. \} \cdot \\ \left(\lambda_Q^2 (W_t^{ii} \cdot \tilde{h}_{Y_{pr,1}} + Y_{pr,1}^{ii} \cdot \tilde{h}_{W_t} - \tilde{h}_{W_t' Y_{pr,1}'}) + \right. \\ \left. + \frac{\lambda_C^2}{2} (W_t^{ii} \cdot \tilde{h}_{W_p' W_r'}) \right) \end{array} \right) + \\ + \left(\begin{array}{l} \{ Z_p Z_r \hat{Z}_t \cdot \exp(i(\tilde{\omega}_{w,p} + \tilde{\omega}_{w,r} - \tilde{\omega}_{w,t}) T_0) + c.c. \} \cdot \\ \left(\lambda_Q^2 \left(\begin{array}{l} W_t^{ii} \cdot \tilde{h}_{Y_{pr,1}} + Y_{pr,1}^{ii} \cdot \tilde{h}_{W_t} - \tilde{h}_{W_t' Y_{pr,1}'} + \\ + W_r^{ii} \cdot \tilde{h}_{Y_{pt,2}} + Y_{pt,2}^{ii} \cdot \tilde{h}_{W_r} - \tilde{h}_{W_r' Y_{pt,2}'} + \\ + W_p^{ii} \cdot \tilde{h}_{Y_{tr,2}} + Y_{tr,2}^{ii} \cdot \tilde{h}_{W_p} - \tilde{h}_{W_p' Y_{tr,2}'} \end{array} \right) + \right. \\ \left. + \frac{\lambda_C^2}{2} (W_p^{ii} \cdot \tilde{h}_{W_r' W_t'} + W_r^{ii} \cdot \tilde{h}_{W_t' W_p'} + W_t^{ii} \cdot \tilde{h}_{W_r' W_p'}) \right) \end{array} \right) \end{array} \right\}$$

$$F_{w,qst} = \left\{ \begin{aligned} & \left(\left\{ \Gamma_q \Gamma_s Z_p \cdot \exp(i(\tilde{\omega}_{\vartheta,q} + \tilde{\omega}_{\vartheta,s} + \tilde{\omega}_{w,p})T_0) + c.c. \right\} \cdot \right. \\ & \left. \left\{ \lambda_Q^2 \left(W_t^{ii} \cdot \tilde{h}_{T_{qs,1}} + T_{qs,1}^{ii} \cdot \tilde{h}_{W_t} - \tilde{h}_{W_t' T_{qs,1}'} + \right) \right. \right. \\ & \left. \left. + \Theta_q^{ii} \cdot \tilde{h}_{H_{ts,1}} + H_{ts,1}^{ii} \cdot \tilde{h}_{\Theta_q} - \tilde{h}_{\Theta_q' H_{ts,1}'} \right) \right. \\ & \left. \left. + \lambda_C^2 \left(\frac{1}{2} W_t^{ii} \cdot \tilde{h}_{\Theta_q' \Theta_s'} + \Theta_q^{ii} \cdot \tilde{h}_{\Theta_s' W_t'} \right) \right) \right\} + \\ & + \left(\left\{ \hat{\Gamma}_q \Gamma_s Z_p \cdot \exp(i(-\tilde{\omega}_{\vartheta,q} + \tilde{\omega}_{\vartheta,s} + \tilde{\omega}_{w,p})T_0) + c.c. \right\} \cdot \right. \\ & \left. \left\{ \lambda_Q^2 \left(W_t^{ii} \cdot \tilde{h}_{T_{qs,2}} + T_{qs,2}^{ii} \cdot \tilde{h}_{W_t} - \tilde{h}_{W_t' T_{qs,2}'} + \right) \right. \right. \\ & \left. \left. + \Theta_q^{ii} \cdot \tilde{h}_{H_{ts,1}} + H_{ts,1}^{ii} \cdot \tilde{h}_{\Theta_q} - \tilde{h}_{\Theta_q' H_{ts,1}'} \right) \right. \\ & \left. \left. + \lambda_C^2 \left(\frac{1}{2} W_t^{ii} \cdot \tilde{h}_{\Theta_q' \Theta_s'} + \Theta_q^{ii} \cdot \tilde{h}_{\Theta_s' W_t'} \right) \right) \right\} + \\ & + \left(\left\{ \Gamma_q \hat{\Gamma}_s Z_p \cdot \exp(i(\tilde{\omega}_{\vartheta,q} - \tilde{\omega}_{\vartheta,s} + \tilde{\omega}_{w,p})T_0) + c.c. \right\} \cdot \right. \\ & \left. \left\{ \lambda_Q^2 \left(W_t^{ii} \cdot \tilde{h}_{T_{qs,2}} + T_{qs,2}^{ii} \cdot \tilde{h}_{W_t} - \tilde{h}_{W_t' T_{qs,2}'} + \right) \right. \right. \\ & \left. \left. + \Theta_q^{ii} \cdot \tilde{h}_{H_{ts,2}} + H_{ts,2}^{ii} \cdot \tilde{h}_{\Theta_q} - \tilde{h}_{\Theta_q' H_{ts,2}'} \right) \right. \\ & \left. \left. + \lambda_C^2 \left(\frac{1}{2} W_t^{ii} \cdot \tilde{h}_{\Theta_q' \Theta_s'} + \Theta_q^{ii} \cdot \tilde{h}_{\Theta_s' W_t'} \right) \right) \right\} + \\ & + \left(\left\{ \Gamma_q \Gamma_s \hat{Z}_p \cdot \exp(i(\tilde{\omega}_{\vartheta,q} + \tilde{\omega}_{\vartheta,s} - \tilde{\omega}_{w,p})T_0) + c.c. \right\} \cdot \right. \\ & \left. \left\{ \lambda_Q^2 \left(W_t^{ii} \cdot \tilde{h}_{T_{qs,1}} + T_{qs,1}^{ii} \cdot \tilde{h}_{W_t} - \tilde{h}_{W_t' T_{qs,1}'} + \right) \right. \right. \\ & \left. \left. + \Theta_q^{ii} \cdot \tilde{h}_{H_{ts,2}} + H_{ts,2}^{ii} \cdot \tilde{h}_{\Theta_q} - \tilde{h}_{\Theta_q' H_{ts,2}'} \right) \right. \\ & \left. \left. + \lambda_C^2 \left(\frac{1}{2} W_t^{ii} \cdot \tilde{h}_{\Theta_q' \Theta_s'} + \Theta_q^{ii} \cdot \tilde{h}_{\Theta_s' W_t'} \right) \right) \right\} \end{aligned} \right\}$$

For the torsional one.

$$(2) = \left\{ \begin{aligned} & -\sum_{m=1}^{\infty} \{ i\tilde{\omega}_{\vartheta,m} (2D_2 \Gamma_m + \nu_{\vartheta} \Gamma_m) \cdot \exp(i\tilde{\omega}_{\vartheta,m} T_0) + c.c. \} \Theta_m + \\ & \sum_{p,r,v=1}^{\infty} F_{\vartheta,prv} + \sum_{q,s,v=1}^{\infty} F_{w,qsv} + F_{\vartheta} \end{aligned} \right\}$$

Where.

$$F_{\vartheta,prv} = \left\{ \begin{aligned} & \left(\left\{ Z_p Z_r \Gamma_v \cdot \exp(i(\tilde{\omega}_{w,p} + \tilde{\omega}_{w,r} + \tilde{\omega}_{\vartheta,v})T_0) + c.c. \right\} \cdot \right. \\ & \left. \left\{ \lambda_Q^2 \left(\begin{aligned} & \Theta_v^{ii} \cdot \tilde{h}_{Y_{pr,1}} + Y_{pr,1}^{ii} \cdot \tilde{h}_{\Theta_v} - \tilde{h}_{\Theta_v' Y_{pr,1}'} \\ & + W_r^{ii} \tilde{h}_{H_{pv,1}} + H_{pv,1}^{ii} \cdot \tilde{h}_{W_r} - \tilde{h}_{W_r' H_{pv,1}'} \end{aligned} \right) + \right. \right. \\ & \left. \left. + \lambda_C^2 \left(\frac{1}{2} \Theta_v^{ii} \cdot \tilde{h}_{W_p' W_r'} + W_p^{ii} \cdot \tilde{h}_{W_r' \Theta_v'} \right) \right\} \right) + \\ & + \left(\left\{ \hat{Z}_p Z_r \Gamma_v \cdot \exp(i(-\tilde{\omega}_{w,p} + \tilde{\omega}_{w,r} + \tilde{\omega}_{\vartheta,v})T_0) + c.c. \right\} \cdot \right. \\ & \left. \left\{ \lambda_Q^2 \left(\begin{aligned} & \Theta_v^{ii} \cdot \tilde{h}_{Y_{pr,2}} + Y_{pr,2}^{ii} \cdot \tilde{h}_{\Theta_v} - \tilde{h}_{\Theta_v' Y_{pr,2}'} \\ & + W_r^{ii} \tilde{h}_{H_{pv,2}} + H_{pv,2}^{ii} \cdot \tilde{h}_{W_r} - \tilde{h}_{W_r' H_{pv,2}'} \end{aligned} \right) + \right. \right. \\ & \left. \left. + \lambda_C^2 \left(\frac{1}{2} \Theta_v^{ii} \cdot \tilde{h}_{W_p' W_r'} + W_p^{ii} \cdot \tilde{h}_{W_r' \Theta_v'} \right) \right\} \right) + \\ & + \left(\left\{ Z_p \hat{Z}_r \Gamma_v \cdot \exp(i(\tilde{\omega}_{w,p} - \tilde{\omega}_{w,r} + \tilde{\omega}_{\vartheta,v})T_0) + c.c. \right\} \cdot \right. \\ & \left. \left\{ \lambda_Q^2 \left(\begin{aligned} & \Theta_v^{ii} \cdot \tilde{h}_{Y_{pr,2}} + Y_{pr,2}^{ii} \cdot \tilde{h}_{\Theta_v} - \tilde{h}_{\Theta_v' Y_{pr,2}'} \\ & + W_r^{ii} \tilde{h}_{H_{pv,1}} + H_{pv,1}^{ii} \cdot \tilde{h}_{W_r} - \tilde{h}_{W_r' H_{pv,1}'} \end{aligned} \right) + \right. \right. \\ & \left. \left. + \lambda_C^2 \left(\frac{1}{2} \Theta_v^{ii} \cdot \tilde{h}_{W_p' W_r'} + W_p^{ii} \cdot \tilde{h}_{W_r' \Theta_v'} \right) \right\} \right) + \\ & + \left(\left\{ Z_p Z_r \hat{\Gamma}_v \cdot \exp(i(\tilde{\omega}_{w,p} + \tilde{\omega}_{w,r} - \tilde{\omega}_{\vartheta,v})T_0) + c.c. \right\} \cdot \right. \\ & \left. \left\{ \lambda_Q^2 \left(\begin{aligned} & \Theta_v^{ii} \cdot \tilde{h}_{Y_{pr,1}} + Y_{pr,1}^{ii} \cdot \tilde{h}_{\Theta_v} - \tilde{h}_{\Theta_v' Y_{pr,1}'} \\ & + W_r^{ii} \tilde{h}_{H_{pv,2}} + H_{pv,2}^{ii} \cdot \tilde{h}_{W_r} - \tilde{h}_{W_r' H_{pv,2}'} \end{aligned} \right) + \right. \right. \\ & \left. \left. + \lambda_C^2 \left(\frac{1}{2} \Theta_v^{ii} \cdot \tilde{h}_{W_p' W_r'} + W_p^{ii} \cdot \tilde{h}_{W_r' \Theta_v'} \right) \right\} \right) \end{aligned} \right\}$$

$$F_{w,qsv} = \left\{ \begin{array}{l} \left(\left\{ \Gamma_q \Gamma_s \Gamma_v \cdot \exp(i(\tilde{\omega}_{\vartheta,q} + \tilde{\omega}_{\vartheta,s} + \tilde{\omega}_{\vartheta,v})T_0) + c.c. \right\} \cdot \right. \\ \left. \left(\left\{ \lambda_Q^2 \left(\Theta_v^{ii} \cdot \tilde{h}_{T_{qs,1}} + T_{qs,1}^{ii} \cdot \tilde{h}_{\Theta_v} - \tilde{h}_{\Theta_v'} T_{qs,1}' \right) + \right. \right. \right. \\ \left. \left. \left. + \lambda_C^2 \left(\frac{1}{2} \Theta_q^{ii} \cdot \tilde{h}_{\Theta_s' \Theta_v'} \right) \right\} \right) \right) + \\ + \left(\left\{ \Gamma_q \Gamma_s \hat{\Gamma}_v \cdot \exp(i(\tilde{\omega}_{\vartheta,q} + \tilde{\omega}_{\vartheta,s} - \tilde{\omega}_{\vartheta,v})T_0) + c.c. \right\} \cdot \right. \\ \left. \left(\left\{ \lambda_Q^2 \left(\Theta_v^{ii} \cdot \tilde{h}_{T_{qs,1}} + T_{qs,1}^{ii} \cdot \tilde{h}_{\Theta_v} - \tilde{h}_{\Theta_v'} T_{qs,1}' + \right. \right. \right. \\ \left. \left. \left. + \Theta_s^{ii} \cdot \tilde{h}_{T_{qv,2}} + T_{qv,2}^{ii} \cdot \tilde{h}_{\Theta_s} - \tilde{h}_{\Theta_s'} T_{qv,2}' + \right. \right. \right. \\ \left. \left. \left. + \Theta_q^{ii} \cdot \tilde{h}_{T_{vs,2}} + T_{vs,2}^{ii} \cdot \tilde{h}_{\Theta_q} - \tilde{h}_{\Theta_q'} T_{vs,2}' \right\} \right) + \right. \\ \left. \left. \left(+ \frac{\lambda_C^2}{2} \left(\Theta_q^{ii} \cdot \tilde{h}_{\Theta_s' \Theta_v'} + \Theta_s^{ii} \cdot \tilde{h}_{\Theta_v' \Theta_q'} + \Theta_v^{ii} \cdot \tilde{h}_{\Theta_s' \Theta_q'} \right) \right) \right) \right) \end{array} \right\}$$

We have finally found the explicit expressions for the equations governing the third order contribution to oscillations. The format is the most general as possible since we are dealing with multi-modal approach. However, analytical solutions are feasible only making some assumptions on the modal interaction. In fact, in the general case we should consider any possible combination between three different modes. Hence to simplify the treatment in the following we will focus just on the mode-by-mode vibrations that are a particular condition for the multi-modal approach and generally gives a contribution that is dominant. This means that in the following we will not be able to detect combinational resonances but only parametric one. We remember that this kind of assumption was introduced first in the definition of the first solvability condition in the analysis of quadratic equations.

The main advantage of this assumption is that equations simplifies very much since we can collect all terms under the same summation operator.

3.4.1 Flexural equation

Let's analyse the mode-by-mode cubic flexural equation of motion for the suspension bridge model.

$$(1) = \sum_{n=1}^{\infty} \left\{ -\{i\tilde{\omega}_{w,n}(2D_2 Z_n + \nu_w Z_n) \cdot \exp(i\tilde{\omega}_{w,n}T_0) + c.c.\} W_n + \right. \\ \left. (F_{w,1})_n + (F_{w,2})_n \right\} + F_w$$

Where.

$$\begin{aligned}
(F_{w,1})_n = & \left\{ \left(\begin{aligned} & \{Z_n^3 \cdot \exp(i3\tilde{\omega}_{w,n}T_0) + c.c.\} \cdot \\ & \left(\lambda_Q^2 (W_n^{ii} \cdot \tilde{h}_{Y_{1,n}} + Y_{1,n}^{ii} \cdot \tilde{h}_{W_n} - \tilde{h}_{W_n'Y_{1,n}'} + \right. \right. \\ & \quad \left. \left. + \frac{\lambda_c^2}{2} (W_n^{ii} \cdot \tilde{h}_{W_n'W_n'}) \right) \right) \right\} + \\ & + \left\{ \left(\begin{aligned} & \{Z_n^2 \hat{Z}_n \cdot \exp(i\tilde{\omega}_{w,n}T_0) + c.c.\} \cdot \\ & \lambda_Q^2 \left(\begin{aligned} & W_n^{ii} \cdot \tilde{h}_{Y_{1,n}} + Y_{1,n}^{ii} \cdot \tilde{h}_{W_n} - \tilde{h}_{W_n'Y_{1,n}'} + \\ & + 2 (W_n^{ii} \cdot \tilde{h}_{Y_{2,n}} + Y_{2,n}^{ii} \cdot \tilde{h}_{W_n} - \tilde{h}_{W_n'Y_{2,n}'} + \\ & + \frac{3}{2} \lambda_c^2 W_n^{ii} \cdot \tilde{h}_{W_n'W_n'} \end{aligned} \right) \right) \right\} \right\} \\ \\
(F_{w,2})_n = & \left\{ \left(\begin{aligned} & \{\Gamma_n^2 Z_n \cdot \exp(i(2\tilde{\omega}_{\vartheta,n} + \tilde{\omega}_{w,n})T_0) + c.c.\} \cdot \\ & \left(\lambda_Q^2 \left(\begin{aligned} & W_n^{ii} \cdot \tilde{h}_{T_{1,n}} + T_{1,n}^{ii} \cdot \tilde{h}_{W_n} - \tilde{h}_{W_n'T_{1,n}'} + \\ & + \Theta_n^{ii} \cdot \tilde{h}_{H_{1,n}} + H_{1,n}^{ii} \cdot \tilde{h}_{\Theta_n} - \tilde{h}_{\Theta_n'H_{1,n}'} \end{aligned} \right) \right) \right) \right\} + \\ & + \left\{ \left(\begin{aligned} & \{\hat{\Gamma}_n \Gamma_n Z_n \cdot \exp(i\tilde{\omega}_{w,n}T_0) + c.c.\} \cdot \\ & \lambda_Q^2 \left(\begin{aligned} & 2 (W_n^{ii} \cdot \tilde{h}_{T_{2,n}} + T_{2,n}^{ii} \cdot \tilde{h}_{W_n} - \tilde{h}_{W_n'T_{2,n}'} + \\ & + \Theta_n^{ii} \cdot (\tilde{h}_{H_{1,n}} + \tilde{h}_{H_{2,n}}) + (H_{1,n}^{ii} + H_{2,n}^{ii}) \cdot \tilde{h}_{\Theta_n} + \\ & - (\tilde{h}_{\Theta_n'H_{1,n}'} + \tilde{h}_{\Theta_n'H_{2,n}'} \end{aligned} \right) \right) \right) \right\} + \\ & + \left\{ \left(\begin{aligned} & + 2\lambda_c^2 \left(\frac{1}{2} W_n^{ii} \cdot \tilde{h}_{\Theta_n'\Theta_n'} + \Theta_n^{ii} \cdot \tilde{h}_{\Theta_n'W_n'} \right) \right) \right\} \right\} + \\ \\
& + \left\{ \left(\begin{aligned} & \{\Gamma_n^2 \hat{Z}_n \cdot \exp(i(2\tilde{\omega}_{\vartheta,n} - \tilde{\omega}_{w,n})T_0) + c.c.\} \cdot \\ & \left(\lambda_Q^2 \left(\begin{aligned} & W_n^{ii} \cdot \tilde{h}_{T_{1,n}} + T_{1,n}^{ii} \cdot \tilde{h}_{W_n} - \tilde{h}_{W_n'T_{1,n}'} + \\ & + \Theta_n^{ii} \cdot \tilde{h}_{H_{2,n}} + H_{2,n}^{ii} \cdot \tilde{h}_{\Theta_n} - \tilde{h}_{\Theta_n'H_{2,n}'} \end{aligned} \right) \right) \right) \right\} + \\ & + \left\{ \left(\begin{aligned} & + \lambda_c^2 \left(\frac{1}{2} W_n^{ii} \cdot \tilde{h}_{\Theta_n'\Theta_n'} + \Theta_n^{ii} \cdot \tilde{h}_{\Theta_n'W_n'} \right) \right) \right\} \right\}
\end{aligned}
\end{aligned}$$

In order to decouple flexural and torsional motion we introduce a detuning parameter σ that allows us to link the respective frequencies.

$$\tilde{\omega}_{w,n} = \tilde{\omega}_{\vartheta,n} + \epsilon^2 \cdot \sigma$$

The meaning of the last expression is that flexural and torsional frequencies are closely spaced. Hence we are implicitly going to analyse the so-called one-to-one internal resonance.

Substituting in the mode-by-mode cubic flexural equation we notice that appear some further exponential terms proportional to the flexural eigen-frequency $\tilde{\omega}_{w,n}$. These are the so-called secular terms that has to vanish as the actual time instant overcomes the limit proper for the linear time scale.

Let's write just the terms that can become Secular.

$$\left. \begin{aligned} & -i\tilde{\omega}_{w,n}(2D_2Z_n + \nu_w Z_n)W_n + \\ & + Z_n^2 \hat{Z}_n \cdot \left\{ \lambda_Q^2 \left(\begin{aligned} & W_n^{ii} \cdot \tilde{h}_{Y_{1,n}} + Y_{1,n}^{ii} \cdot \tilde{h}_{W_n} - \tilde{h}_{W_n'Y_{1,n}'} + \\ & + 2(W_n^{ii} \cdot \tilde{h}_{Y_{2,n}} + Y_{2,n}^{ii} \cdot \tilde{h}_{W_n} - \tilde{h}_{W_n'Y_{2,n}'}) + \end{aligned} \right) + \right. \\ & \quad \left. + \frac{3}{2}\lambda_C^2 W_n^{ii} \cdot \tilde{h}_{W_n'W_n'} \right\} + \\ & + \hat{\Gamma}_n \Gamma_n Z_n \cdot \left\{ \lambda_Q^2 \left(\begin{aligned} & 2(W_n^{ii} \cdot \tilde{h}_{T_{2,n}} + T_{2,n}^{ii} \cdot \tilde{h}_{W_n} - \tilde{h}_{W_n'T_{2,n}'}) + \\ & + \Theta_n^{ii} \cdot (\tilde{h}_{H_{1,n}} + \tilde{h}_{H_{2,n}}) + (H_{1,n}^{ii} + H_{2,n}^{ii}) \cdot \tilde{h}_{\Theta_n} + \\ & - (\tilde{h}_{\Theta_n'H_{1,n}'} + \tilde{h}_{\Theta_n'H_{2,n}'}) \end{aligned} \right) + \right. \\ & \quad \left. + 2\lambda_C^2 \left(\frac{1}{2}W_n^{ii} \cdot \tilde{h}_{\Theta_n'\Theta_n'} + \Theta_n^{ii} \cdot \tilde{h}_{\Theta_n'W_n'} \right) \right\} + \\ & + \Gamma_n^2 \hat{Z}_n \cdot \exp(-i2\sigma T_2) \left\{ \lambda_Q^2 \left(\begin{aligned} & W_n^{ii} \cdot \tilde{h}_{T_{1,n}} + T_{1,n}^{ii} \cdot \tilde{h}_{W_n} - \tilde{h}_{W_n'T_{1,n}'} + \\ & + \Theta_n^{ii} \cdot \tilde{h}_{H_{2,n}} + H_{2,n}^{ii} \cdot \tilde{h}_{\Theta_n} - \tilde{h}_{\Theta_n'H_{2,n}'} \end{aligned} \right) + \right. \\ & \quad \left. + \lambda_C^2 \left(\frac{1}{2}W_n^{ii} \cdot \tilde{h}_{\Theta_n'\Theta_n'} + \Theta_n^{ii} \cdot \tilde{h}_{\Theta_n'W_n'} \right) \right\} + \\ & + \frac{1}{2}\bar{F}_w \cdot \exp(i(\Omega_w - \tilde{\omega}_{w,n})T_0) + c. c. \end{aligned} \right\} \exp(i\tilde{\omega}_{w,n}T_0)$$

Notice that the external forcing has been expanded in Fourier series by means of Euler exponential notation for complex numbers. Hence \bar{F}_w will be the forcing magnitude tuned by a trigonometric function with circular frequency equal to Ω_w . As we can see, the model is able to catch also external linear resonance as it's satisfied the condition $\Omega_w = \tilde{\omega}_{w,n}$.

The following step requires to assume a solution format also for the cubic flexural equation.

$$\tilde{w}_3(\xi, T_0, T_2) = \sum_{n=1}^{\infty} \{ \Phi_{S,n}(\xi, T_0, T_2) \cdot \exp(i\tilde{\omega}_{w,n}T_0) + \Phi_{NS,n}(\xi, T_0, T_2) + c. c. \}$$

Where we simply assume that the cubic flexural solution will be equal to the superposition of a secular function Φ_S and a non-secular one Φ_{NS} .

Substituting in the left-hand side term of the governing equation and considering just the secular contribution we get.

$$\sum_{n=1}^{\infty} \{ \mu^2 \cdot \Phi_{S,n}^{iv} - \Phi_{S,n}^{ii} - \tilde{\omega}_{w,n}^2 \Phi_{S,n} + \lambda_L^2 \cdot \tilde{h}_{\Phi_{S,n}} \} \exp(i\tilde{\omega}_{w,n} T_0)$$

Since the corresponding homogeneous equation has a non-trivial solution we need to satisfy a proper solvability condition in order to solve the complete problem.

To do that we introduce an adjoin solution $u(\xi)$ that will be defined later. This unknown function multiplies both the left and right-hand side $F_w(\xi)$ terms of the governing equation that then has to be integrated in the unitary spatial domain of interest at which extremities boundary conditions has to be enforced.

Hence considering a mode per time and simplifying the exponential $\exp(i\tilde{\omega}_{w,n} T_0)$ we get.

$$\left\{ \begin{array}{l} \mu^2 \int_0^1 u(\xi) \cdot \Phi_{S,n}^{iv} d\xi - \int_0^1 u(\xi) \cdot \Phi_{S,n}^{ii} d\xi + \\ -\tilde{\omega}_{w,n}^2 \int_0^1 u(\xi) \cdot \Phi_{S,n} d\xi + \lambda_L^2 \int_0^1 u(\xi) \cdot \tilde{h}_{\Phi_{S,n}} d\xi \end{array} \right\} = \int_0^1 u(\xi) \cdot F_w(\xi) d\xi$$

Then integration by parts allows us to pass the derivative from $\Phi_{S,n}$ to $u(\xi)$.

$$\left\{ \begin{array}{l} \int_0^1 (\mu^2 \cdot u^{iv} - u^{ii} - \tilde{\omega}_{w,n}^2 \cdot u + \lambda_L^2 \tilde{h}_u) \Phi_{S,n} d\xi + \\ \left[\mu^2 \cdot \left(u \cdot \Phi_{S,n}^{iii} - u^i \cdot \Phi_{S,n}^{ii} + \right. \right. \\ \left. \left. + u^{ii} \cdot \Phi_{S,n}^i - u^{iii} \cdot \Phi_{S,n} \right) + -u \cdot \Phi_{S,n}^i + u^i \cdot \Phi_{S,n} \right]_0^1 \end{array} \right\} = \int_0^1 u(\xi) \cdot F_w(\xi) d\xi$$

The so-called adjoin homogenous equation ($\mu^2 \cdot u^{iv} - u^{ii} - \tilde{\omega}_{w,n}^2 \cdot u + \lambda_L^2 \tilde{h}_u = 0$) is self-adjoin since the coefficients are the same of the original governing equation of $\Phi_{S,n}$.

To define explicitly the function $u(\xi)$ we need to assume $F_w(\xi) = 0$ and enforce the vanishing of $\Phi_{S,n}$ and its second derivative at the boundary of the domain.

$$\left[\mu^2 \cdot \left(u \cdot \Phi_{S,n}^{iii} - u^i \cdot \Phi_{S,n}^{ii} + \right. \right. \\ \left. \left. + u^{ii} \cdot \Phi_{S,n}^i - u^{iii} \cdot \Phi_{S,n} \right) + -u \cdot \Phi_{S,n}^i + u^i \cdot \Phi_{S,n} \right]_0^1 = 0$$

That can be rewritten as.

$$\mu^2 \cdot [u]_0^1 \cdot \Phi_{S,n}^{iii} + \mu^2 \cdot [u^{ii} - u]_0^1 \cdot \Phi_{S,n}^i = 0$$

Assuming that each coefficient vanish independently we get proper boundary conditions for $u(\xi)$ that are the same previously mentioned for $\Phi_{S,n}$. Thence, we have define the complete self-adjoin problem that it's equal to the one defined for the linear eigen-properties. Consequently.

$$u(\xi) = W_n(\xi)$$

The initial purpose was to define proper solvability conditions for the original cubic secular equation. Hence substituting in the modal projection of the secular cubic equation the self-adjoint one for $u(\xi)$ and the boundary conditions for $u(\xi)$ and $\Phi_{S,n}$ we get the Solvability condition.

$$\int_0^1 W_n(\xi) \cdot F_w(\xi) d\xi = 0$$

Integration by parts allows us to reduce the order of spatial derivative down to the first order and enforce the well-known boundary conditions on linear modal shapes $W_n(\xi)$.

Summing up common terms the solvability condition gives us the one of the ordinary differential equation governing the time variation (T_2) of flexural and torsional amplitudes.

$$\left\{ \begin{aligned} & i\tilde{\omega}_{w,n}(2D_2Z_n + \nu_w Z_n) \cdot M_{w,n} + Z_n^2 \hat{Z}_n \cdot \alpha_{1,w} + \\ & + \hat{\Gamma}_n \Gamma_n Z_n \cdot \alpha_{2,w} + \Gamma_n^2 \hat{Z}_n \cdot \exp(-i2\sigma T_2) \cdot \alpha_{3,w} \end{aligned} \right\} = \frac{1}{2} \bar{\bar{F}}_{w,n} \cdot \exp(i(\Omega_w - \tilde{\omega}_{w,n})T_0)$$

Where we define the modal mass $M_{w,n}$ and force $\bar{\bar{F}}_{w,n}$, plus other constant parameters.

$$M_{w,n} = \int_0^1 W_n^2 d\xi$$

$$\alpha_{1,w} = \lambda_Q^2 \left\{ 2 \left[\tilde{h}_{W_n} (\tilde{h}_{W_n'Y_{1,n}'} + 2\tilde{h}_{W_n'Y_{2,n}'}) \right] + \tilde{h}_{W_n'W_n'} (\tilde{h}_{Y_{1,n}} + 2\tilde{h}_{Y_{2,n}'}) \right\} + \frac{3}{2} \lambda_C^2 (\tilde{h}_{W_n'W_n'})^2$$

$$\alpha_{2,w} = \lambda_Q^2 \left\{ \begin{aligned} & 2\tilde{h}_{W_n'W_n'} \tilde{h}_{T_{2,n}} + \tilde{h}_{W_n} (4\tilde{h}_{W_n'T_{2,n}'} + \tilde{h}_{\theta_n'H_{1,n}'} + \tilde{h}_{\theta_n'H_{2,n}'}) + \\ & + \tilde{h}_{W_n'\theta_n'} (\tilde{h}_{H_{1,n}} + \tilde{h}_{H_{2,n}}) + \tilde{h}_{\theta_n} (\tilde{h}_{W_n'H_{1,n}'} + \tilde{h}_{W_n'H_{2,n}'}) \end{aligned} \right\} + \lambda_C^2 \left\{ \begin{aligned} & \tilde{h}_{W_n'W_n'} \tilde{h}_{\theta_n'\theta_n'} + \\ & + 2(\tilde{h}_{W_n'\theta_n'})^2 \end{aligned} \right\}$$

$$\alpha_{3,w} = \lambda_Q^2 \left\{ \begin{aligned} & \tilde{h}_{W_n'W_n'} \tilde{h}_{T_{1,n}} + \tilde{h}_{W_n} (2\tilde{h}_{W_n'T_{1,n}'} + \tilde{h}_{\theta_n'H_{2,n}'}) + \\ & \tilde{h}_{W_n'\theta_n'} \tilde{h}_{H_{2,n}} + \tilde{h}_{\theta_n} \tilde{h}_{W_n'H_{2,n}'} \end{aligned} \right\} + \lambda_C^2 \left\{ \begin{aligned} & \frac{1}{2} \tilde{h}_{W_n'W_n'} \tilde{h}_{\theta_n'\theta_n'} + \\ & + (\tilde{h}_{W_n'\theta_n'})^2 \end{aligned} \right\}$$

$$\bar{\bar{F}}_{w,n} = \int_0^1 W_n \bar{\bar{F}}_w d\xi$$

3.4.2 Torsional equation

Notice that we obtain an equation that contains both the flexural and torsional amplitudes. Then we need to define also the torsional companion of that equation.

$$(2) = \sum_{n=1}^{\infty} \left\{ \begin{aligned} & -\{i\tilde{\omega}_{\vartheta,n}(2D_2\Gamma_n + \nu_{\vartheta}\Gamma_n) \cdot \exp(i\tilde{\omega}_{\vartheta,n}T_0) + c. c. \} \theta_n + \\ & (F_{\vartheta,1})_n + (F_{\vartheta,2})_n \end{aligned} \right\} + F_{\vartheta}$$

Where.

$$\begin{aligned}
(F_{\vartheta,1})_n = & \left\{ \left(\begin{aligned} & \{Z_n^2 \Gamma_n \cdot \exp(i(2\tilde{\omega}_{w,n} + \tilde{\omega}_{\vartheta,n})T_0) + c.c.\} \cdot \\ & \left(\lambda_Q^2 \left(\begin{aligned} & \Theta_n^{ii} \cdot \tilde{h}_{Y_{1,n}} + Y_{1,n}^{ii} \cdot \tilde{h}_{\Theta_n} - \tilde{h}_{\Theta_n'Y_{1,n}'} \\ & + W_n^{ii} \tilde{h}_{H_{1,n}} + H_{1,n}^{ii} \cdot \tilde{h}_{W_n} - \tilde{h}_{W_n'H_{1,n}'} \end{aligned} \right) + \right) \\ & + \lambda_C^2 \left(\frac{1}{2} \Theta_n^{ii} \cdot \tilde{h}_{W_n'W_n'} + W_n^{ii} \cdot \tilde{h}_{W_n'\Theta_n'} \right) \end{aligned} \right) \right\} + \\
& + \left\{ \left(\begin{aligned} & \{\hat{Z}_n Z_n \Gamma_n \cdot \exp(i\tilde{\omega}_{\vartheta,n}T_0) + c.c.\} \cdot \\ & \left(\lambda_Q^2 \left(\begin{aligned} & 2 \left(\Theta_n^{ii} \cdot \tilde{h}_{Y_{2,n}} + Y_{2,n}^{ii} \cdot \tilde{h}_{\Theta_n} - \tilde{h}_{\Theta_n'Y_{2,n}'} \right) \\ & + W_n^{ii} (\tilde{h}_{H_{1,n}} + \tilde{h}_{H_{2,n}}) + (H_{1,n}^{ii} + H_{2,n}^{ii}) \cdot \tilde{h}_{W_n} + \\ & - (\tilde{h}_{W_n'H_{1,n}'} + \tilde{h}_{W_n'H_{2,n}'} \end{aligned} \right) + \right) \\ & + 2\lambda_C^2 \left(\frac{1}{2} \Theta_n^{ii} \cdot \tilde{h}_{W_n'W_n'} + W_n^{ii} \cdot \tilde{h}_{W_n'\Theta_n'} \right) \end{aligned} \right) \right\} + \\
& + \left\{ \left(\begin{aligned} & \{Z_n^2 \hat{\Gamma}_n \cdot \exp(i(2\tilde{\omega}_{w,n} - \tilde{\omega}_{\vartheta,n})T_0) + c.c.\} \cdot \\ & \left(\lambda_Q^2 \left(\begin{aligned} & \Theta_n^{ii} \cdot \tilde{h}_{Y_{1,n}} + Y_{1,n}^{ii} \cdot \tilde{h}_{\Theta_n} - \tilde{h}_{\Theta_n'Y_{1,n}'} \\ & + W_n^{ii} \tilde{h}_{H_{2,n}} + H_{2,n}^{ii} \cdot \tilde{h}_{W_n} - \tilde{h}_{W_n'H_{2,n}'} \end{aligned} \right) + \right) \\ & + \lambda_C^2 \left(\frac{1}{2} \Theta_n^{ii} \cdot \tilde{h}_{W_n'W_n'} + W_n^{ii} \cdot \tilde{h}_{W_n'\Theta_n'} \right) \end{aligned} \right) \right\} \\
(F_{\vartheta,2})_n = & \left\{ \left(\begin{aligned} & \{\Gamma_n^3 \cdot \exp(i3\tilde{\omega}_{\vartheta,q}T_0) + c.c.\} \cdot \\ & \left(\lambda_Q^2 \left(\Theta_n^{ii} \cdot \tilde{h}_{T_{1,n}} + T_{1,n}^{ii} \cdot \tilde{h}_{\Theta_n} - \tilde{h}_{\Theta_n'T_{1,n}'} \right) + \right) \\ & + \lambda_C^2 \left(\frac{1}{2} \Theta_n^{ii} \cdot \tilde{h}_{\Theta_n'\Theta_n'} \right) \end{aligned} \right) \right\} + \\
& + \left\{ \left(\begin{aligned} & \{\Gamma_n^2 \hat{\Gamma}_n \cdot \exp(i\tilde{\omega}_{\vartheta,n}T_0) + c.c.\} \cdot \\ & \left(\lambda_Q^2 \left(\begin{aligned} & \Theta_n^{ii} \cdot \tilde{h}_{T_{1,n}} + T_{1,n}^{ii} \cdot \tilde{h}_{\Theta_n} - \tilde{h}_{\Theta_n'T_{1,n}'} + \\ & + 2 \left(\Theta_n^{ii} \cdot \tilde{h}_{T_{2,n}} + T_{2,n}^{ii} \cdot \tilde{h}_{\Theta_n} - \tilde{h}_{\Theta_n'T_{2,n}'} \right) \end{aligned} \right) + \right) \\ & + \frac{3}{2} \lambda_C^2 \Theta_n^{ii} \cdot \tilde{h}_{\Theta_n'\Theta_n'} \end{aligned} \right) \right\}
\end{aligned}$$

Substituting $\tilde{\omega}_{w,n} = \tilde{\omega}_{\vartheta,n} + \epsilon^2 \cdot \sigma$ we get the secular terms from the right-hand side of the governing equation.

$$\sum_{n=1}^{\infty} \left\{ \begin{aligned} & -\{i\tilde{\omega}_{\vartheta,n}(2D_2\Gamma_n + \nu_{\vartheta}\Gamma_n) + c.c.\}\Theta_n + \\ & \Gamma_n^2 \hat{\Gamma}_n \cdot \left\{ \lambda_Q^2 \left(\begin{aligned} & \Theta_n^{ii} \cdot \tilde{h}_{T_{1,n}} + T_{1,n}^{ii} \cdot \tilde{h}_{\Theta_n} - \tilde{h}_{\Theta_n'T_{1,n}'} + \\ & + 2(\Theta_n^{ii} \cdot \tilde{h}_{T_{2,n}} + T_{2,n}^{ii} \cdot \tilde{h}_{\Theta_n} - \tilde{h}_{\Theta_n'T_{2,n}'}) \end{aligned} \right) + \right. \\ & \left. + \frac{3}{2}\lambda_C^2 \Theta_n^{ii} \cdot \tilde{h}_{\Theta_n'\Theta_n'} \right\} + \\ & Z_n Z_n \Gamma_n \cdot \left\{ \lambda_Q^2 \left(\begin{aligned} & 2(\Theta_n^{ii} \cdot \tilde{h}_{Y_{2,n}} + Y_{2,n}^{ii} \cdot \tilde{h}_{\Theta_n} - \tilde{h}_{\Theta_n'Y_{2,n}'}) \\ & + W_n^{ii}(\tilde{h}_{H_{1,n}} + \tilde{h}_{H_{2,n}}) + (H_{1,n}^{ii} + H_{2,n}^{ii}) \cdot \tilde{h}_{W_n} + \\ & - (\tilde{h}_{W_n'H_{1,n}'} + \tilde{h}_{W_n'H_{2,n}'}) \end{aligned} \right) + \right. \\ & \left. + \lambda_C^2(\Theta_n^{ii} \cdot \tilde{h}_{W_n'W_n'} + 2W_n^{ii} \cdot \tilde{h}_{W_n'\Theta_n'}) \right\} + \\ & Z_n^2 \hat{\Gamma}_n \cdot \exp(i2\sigma T_2) \left\{ \lambda_Q^2 \left(\begin{aligned} & \Theta_n^{ii} \cdot \tilde{h}_{Y_{1,n}} + Y_{1,n}^{ii} \cdot \tilde{h}_{\Theta_n} - \tilde{h}_{\Theta_n'Y_{1,n}'} \\ & + W_n^{ii} \tilde{h}_{H_{2,n}} + H_{2,n}^{ii} \cdot \tilde{h}_{W_n} - \tilde{h}_{W_n'H_{2,n}'} \end{aligned} \right) + \right. \\ & \left. + \lambda_C^2 \left(\frac{1}{2}\Theta_n^{ii} \cdot \tilde{h}_{W_n'W_n'} + W_n^{ii} \cdot \tilde{h}_{W_n'\Theta_n'} \right) \right\} \\ & + \frac{1}{2}\bar{F}_{\vartheta} \cdot \exp(i(\Omega_{\vartheta} - \tilde{\omega}_{\vartheta,n})T_0) + c.c. \end{aligned} \right\} \cdot \exp(i\tilde{\omega}_{\vartheta,n}T_0)$$

Then assuming the solution format.

$$\tilde{\vartheta}_3(\xi, T_0, T_2) = \sum_{n=1}^{\infty} \{ \Psi_{S,n}(\xi, T_0, T_2) \cdot \exp(i\tilde{\omega}_{\vartheta,n}T_0) + \Psi_{NS,n}(\xi, T_0, T_2) + c.c. \}$$

Substituting the solution in the left-hand side term, considering just secular contributions $\Psi_{S,n}$, multiplying both the right $F_{\vartheta}(\xi)$ and left hand side terms by the adjoin function $v(\xi)$ and integrating on the unitary domain we get.

$$\left\{ \begin{aligned} & \left(\frac{\beta^2}{\chi^2} \int_0^1 v(\xi) \cdot \Psi_{S,n}^{iv} d\xi - (1 + \beta^2) \int_0^1 v(\xi) \cdot \Psi_{S,n}^{ii} d\xi + \right. \\ & \left. - \tilde{f}_t \tilde{\omega}_{\vartheta,n}^2 \int_0^1 v(\xi) \cdot \Psi_{S,n} d\xi + \lambda_L^2 \int_0^1 v(\xi) \cdot \tilde{h}_{\Psi_{S,n}} d\xi \right) \end{aligned} \right\} = \int_0^1 v(\xi) \cdot F_{\vartheta}(\xi) d\xi$$

Integrating by parts we get.

$$\left\{ \int_0^1 \left(\frac{\beta^2}{\chi^2} v^{iv} - (1 + \beta^2) v^{ii} - \tilde{f}_t \tilde{\omega}_{\vartheta,n}^2 v + \lambda_L^2 \tilde{h}_v \right) \Psi_{S,n} d\xi + \left[\frac{\beta^2}{\chi^2} \cdot \left(v \cdot \Psi_{S,n}^{iii} - v^i \cdot \Psi_{S,n}^{ii} + v^{ii} \cdot \Psi_{S,n}^i - v^{iii} \cdot \Psi_{S,n} \right) - (1 + \beta^2) \cdot (v \cdot \Psi_{S,n}^i + v^i \cdot \Psi_{S,n}) \right]_0^1 \right\} = \int_0^1 v(\xi) \cdot F_{\vartheta}(\xi) d\xi$$

Enforcing that the secular function $\Psi_{S,n}$ vanishes with its second derivative at the domain boundaries we get the self-adjoint homogeneous equation $\left(\frac{\beta^2}{\chi^2} v^{iv} - (1 + \beta^2) v^{ii} - \tilde{f}_t \tilde{\omega}_{\vartheta,n}^2 v + \lambda_L^2 \tilde{h}_v = 0 \right)$ and proper boundary conditions for $v(\xi)$ defining the complete adjoint problem. The problem is identical to the one analysed for torsional linear eigen-properties, hence it admits the same solution.

$$v(\xi) = \Theta_n(\xi)$$

Then the solvability condition required becomes as follows.

$$\int_0^1 \Theta_n(\xi) \cdot F_{\vartheta}(\xi) d\xi = 0$$

Integrating by part and exploiting the boundary conditions proper for torsional linear modes we get the second ordinary differential equation governing the time variation (T_2) of flexural and torsional amplitudes.

$$\left\{ \begin{aligned} & i\tilde{\omega}_{\vartheta,n} (2D_2\Gamma_n + \nu_{\vartheta}\Gamma_n) \cdot M_{\vartheta,n} + \Gamma_n^2 \hat{\Gamma}_n \cdot \alpha_{1,\vartheta} + \\ & + \hat{Z}_n Z_n \Gamma_n \cdot \alpha_{2,\vartheta} + Z_n^2 \hat{\Gamma}_n \cdot \exp(i2\sigma T_2) \cdot \alpha_{3,\vartheta} \end{aligned} \right\} = \frac{1}{2} \bar{F}_{\vartheta,n} \cdot \exp(i(\Omega_{\vartheta} - \tilde{\omega}_{\vartheta,n})T_0)$$

Where we define the modal mass $M_{\vartheta,n}$ and force $\bar{F}_{\vartheta,n}$, plus other constant parameters.

$$M_{\vartheta,n} = \int_0^1 \Theta_n^2 d\xi$$

$$\alpha_{1,\vartheta} = \lambda_Q^2 \left\{ 2 \left[\tilde{h}_{\Theta_n} (\tilde{h}_{\Theta_n' T_{1,n}'} + 2\tilde{h}_{\Theta_n' T_{2,n}'}) \right] + \tilde{h}_{\Theta_n' \Theta_n'} (\tilde{h}_{T_{1,n}} + 2\tilde{h}_{T_{2,n}'}) \right\} + \frac{3}{2} \lambda_C^2 (\tilde{h}_{\Theta_n' \Theta_n'})^2$$

$$\alpha_{2,\vartheta} = \lambda_Q^2 \left\{ \begin{aligned} & 2\tilde{h}_{\Theta_n' \Theta_n'} \tilde{h}_{Y_{2,n}} + \tilde{h}_{\Theta_n} (4\tilde{h}_{\Theta_n' Y_{2,n}'} + \tilde{h}_{W_n' H_{1,n}'} + \tilde{h}_{W_n' H_{2,n}'}) + \\ & + \tilde{h}_{W_n' \Theta_n'} (\tilde{h}_{H_{1,n}} + \tilde{h}_{H_{2,n}}) + \tilde{h}_{W_n} (\tilde{h}_{\Theta_n' H_{1,n}'} + \tilde{h}_{\Theta_n' H_{2,n}'}) \end{aligned} \right\} + \lambda_C^2 \left\{ \begin{aligned} & \tilde{h}_{W_n' W_n'} \tilde{h}_{\Theta_n' \Theta_n'} + \\ & + 2(\tilde{h}_{W_n' \Theta_n'})^2 \end{aligned} \right\}$$

$$\alpha_{3,\vartheta} = \lambda_Q^2 \left\{ \begin{aligned} & \tilde{h}_{\Theta_n' \Theta_n'} \tilde{h}_{Y_{1,n}} + \tilde{h}_{\Theta_n} (2\tilde{h}_{\Theta_n' Y_{1,n}'} + \tilde{h}_{W_n' H_{2,n}'}) + \\ & \tilde{h}_{W_n' \Theta_n'} \tilde{h}_{H_{2,n}} + \tilde{h}_{W_n} \tilde{h}_{\Theta_n' H_{2,n}'} \end{aligned} \right\} + \lambda_C^2 \left\{ \begin{aligned} & \frac{1}{2} \tilde{h}_{\Theta_n' W_n'} \tilde{h}_{\Theta_n' \Theta_n'} + \\ & + (\tilde{h}_{W_n' \Theta_n'})^2 \end{aligned} \right\}$$

$$\bar{F}_{\vartheta,n} = \int_0^1 \Theta_n \bar{F}_{\vartheta} d\xi$$

3.5. Governing equations

We have already mentioned that the modal amplitudes are not constant in time. Hence assuming a sinusoidal variation, we can express the flexural and torsional amplitudes in polar form by means of the well-known Euler exponential complex formulation.

This way we are able to distinguish explicitly between the actual amplitude and the phase lag.

$$Z_n(T_2) = \frac{1}{2} \bar{Z}_n(T_2) \cdot \exp(i\gamma_{w,n}T_0)$$

$$\Gamma_n(T_2) = \frac{1}{2} \bar{\Gamma}_n(T_2) \cdot \exp(i\gamma_{\vartheta,n}T_0)$$

Substituting in the solvability conditions, we are able to distinguish the real from the imaginary part of equations.

Finally, we come to a governing system of four ordinary differential equations of first order.

$$D_2 \bar{Z}_n = \frac{1}{2} \left\{ \frac{1}{\tilde{\omega}_{w,n}} \left(\bar{F}_{w,n} \cdot \sin \delta_w - \frac{1}{4} \alpha_{3,w} \cdot \bar{Z}_n \bar{\Gamma}_n^2 \cdot \sin \delta_1 \right) - \nu_w \bar{Z}_n \right\}$$

$$D_2 \gamma_{w,n} = \frac{1}{2} \frac{1}{\tilde{\omega}_{w,n}} \left\{ \frac{1}{4} \left[\alpha_{1,w} \cdot \bar{Z}_n^2 + \bar{\Gamma}_n^2 (\alpha_{2,w} + \alpha_{3,w} \cdot \cos \delta_1) \right] - \bar{F}_{w,n} / \bar{Z}_n \cos \delta_w \right\}$$

$$D_2 \bar{\Gamma}_n = \frac{1}{2} \left\{ \frac{1}{\tilde{\omega}_{\vartheta,n}} \left(\bar{F}_{\vartheta,n} \cdot \sin \delta_\vartheta + \frac{1}{4} \alpha_{3,\vartheta} \cdot \bar{\Gamma}_n \bar{Z}_n^2 \cdot \sin \delta_1 \right) - \nu_w \bar{\Gamma}_n \right\}$$

$$D_2 \gamma_{\vartheta,n} = \frac{1}{2} \frac{1}{\tilde{\omega}_{\vartheta,n}} \left\{ \frac{1}{4} \left[\alpha_{1,\vartheta} \cdot \bar{\Gamma}_n^2 + \bar{Z}_n^2 (\alpha_{2,\vartheta} + \alpha_{3,\vartheta} \cdot \cos \delta_1) \right] - \bar{F}_{\vartheta,n} / \bar{\Gamma}_n \cos \delta_\vartheta \right\}$$

Where we have define some new parameters in order to get autonomous equations (implicit time dependence).

$$\delta_1 = 2(\gamma_{\vartheta,n} - \gamma_{w,n} - \sigma \cdot T_2)$$

$$\delta_w = (\Omega_w - \tilde{\omega}_{w,n})T_0 - \gamma_{w,n}$$

$$\delta_\vartheta = (\Omega_\vartheta - \tilde{\omega}_{\vartheta,n})T_0 - \gamma_{\vartheta,n}$$

3.5.1 Free undamped vibrations

The case without external forcing and any damping sources will be analysed since it's the simpler one and allows us to study the possibility of internal energy exchange between different modes due to one-to-one internal resonance.

The governing equations can be written as follows.

$$D_2 \bar{Z}_n = -\frac{1}{8} \frac{1}{\tilde{\omega}_{w,n}} \alpha_{3,w} \cdot \bar{Z}_n \bar{\Gamma}_n^2 \cdot \sin \delta_1$$

$$D_2\gamma_{w,n} = \frac{1}{8} \frac{1}{\tilde{\omega}_{w,n}} \left\{ \alpha_{1,w} \cdot \bar{Z}_n^2 + \bar{\Gamma}_n^2 (\alpha_{2,w} + \alpha_{3,w} \cdot \cos\delta_1) \right\}$$

$$D_2\bar{\Gamma}_n = \frac{1}{8} \frac{1}{\tilde{\omega}_{\vartheta,n}} \alpha_{3,\vartheta} \cdot \bar{\Gamma}_n \bar{Z}_n^2 \cdot \sin\delta_1$$

$$D_2\gamma_{\vartheta,n} = \frac{1}{8} \frac{1}{\tilde{\omega}_{\vartheta,n}} \left\{ \alpha_{1,\vartheta} \cdot \bar{\Gamma}_n^2 + \bar{Z}_n^2 (\alpha_{2,\vartheta} + \alpha_{3,\vartheta} \cdot \cos\delta_1) \right\}$$

Further.

$$D_2\delta_1 = 2(D_2\gamma_{\vartheta,n} - D_2\gamma_{w,n} - \sigma) = \frac{1}{4} \left\{ \begin{aligned} & \left(\frac{\alpha_{2,\vartheta}}{\tilde{\omega}_{\vartheta,n} \cdot M_{\vartheta,n}} - \frac{\alpha_{1,w}}{\tilde{\omega}_{w,n} \cdot M_{w,n}} \right) \bar{Z}_n^2 + \\ & + \left(\frac{\alpha_{1,\vartheta}}{\tilde{\omega}_{\vartheta,n} \cdot M_{\vartheta,n}} - \frac{\alpha_{2,w}}{\tilde{\omega}_{w,n} \cdot M_{w,n}} \right) \bar{\Gamma}_n^2 + \\ & + \left(\frac{\alpha_{3,\vartheta}}{\tilde{\omega}_{\vartheta,n} \cdot M_{\vartheta,n}} \bar{Z}_n^2 - \frac{\alpha_{3,w}}{\tilde{\omega}_{w,n} \cdot M_{w,n}} \bar{\Gamma}_n^2 \right) \cdot \cos\delta_1 \end{aligned} \right\} - 2\sigma$$

Let's focus on particular conditions for which analytical solutions are feasible.

a) Dominant flexural mode

In this situation we are analysing the classical condition for suspension bridges. In fact we are searching for the torsional perturbation coming from a flexural vibration. Hence we will assume that there is no evident energetic exchange between the two motion, consequently the second order correction of flexural amplitude remains constant in time ($\bar{Z}_n(T_2) = \bar{Z}_{n,0}$) and the torsional one null ($\bar{\Gamma}_n(T_2) = 0$). Consequently we get that.

$$\gamma_{w,n} = \frac{1}{2} (\epsilon \cdot \bar{Z}_{n,0})^2 \frac{\alpha_{1,w}}{4 \cdot \tilde{\omega}_{w,n} \cdot M_{w,n}} \tau + \gamma_{w,n0}$$

Notice that the subscript zero indicates initial conditions.

Exploiting the polar form for vibration amplitudes and substituting these two conditions and inside the expressions for the linear w_1, ϑ_1 and quadratic w_2, ϑ_2 components of motion, we get the resultant vertical motion of the bridge's deck axis.

$$w_d(\xi, \tau) = \left\{ \begin{aligned} & (\epsilon \cdot \bar{Z}_{n,0}) \cdot \cos(\tilde{\omega}_{w,n}^{NL} \cdot \tau + \gamma_{w,n0}) \cdot W_n(\xi) + \\ & + \frac{1}{2} (\epsilon \cdot \bar{Z}_{n,0})^2 \cdot \{ \cos[2(\tilde{\omega}_{w,n}^{NL} \cdot \tau + \gamma_{w,n0})] \cdot Y_{1,n}(\xi) + Y_{2,n}(\xi) \} \end{aligned} \right\} + o(\epsilon^3)$$

Where we have introduced the nonlinear circular frequency.

$$\tilde{\omega}_{w,n}^{NL} = \tilde{\omega}_{w,n} + \epsilon^2 D_2\gamma_{w,n} = \tilde{\omega}_{w,n} + \frac{1}{2} (\epsilon \cdot \bar{Z}_{n,0})^2 \cdot \frac{\alpha_{1,w}}{4 \cdot \tilde{\omega}_{w,n} \cdot M_{w,n}} + o(\epsilon^3)$$

This is better known as the frequency-amplitude equation since it's able to trace the variation of frequencies as the amplitudes of oscillations changes. This is a typical feature of nonlinear systems that can lead to the Jump Phenomenon according which not all the curve can be traced since the system prefer to minimize energy in a more stable configuration. In fact the classical straight line of linear system, that represent a constant frequency for any amplitudes, as the latter grow it is curved toward higher frequencies, if the nonlinear system has a stiffening behaviour, and toward lower frequencies, if the system has a softening behaviour. This means that as the downward motion is dominant we expect a hardening of the suspension bridge because cable stiffening behaviour grows, contrary a softening one as dominant upward motion occurs. This is known a priori simply checking the sign of $\alpha_{1,w}$ since would be positive for hardening and negative for softening behaviour. In the particular case in which $\alpha_{1,w} = 0$ we get a linear response since nonlinearities balance themselves.

We notice that vertical oscillations are a superposition of dominant linear oscillation with frequency $\tilde{\omega}_{w,n}^{NL}$ and a second order correction oscillating with double frequency with a phase shift $\gamma_{w,0}$ constant in time. Further the latter introduce a vertical translation of displacements $Y_{2,n}(\xi)$, meaning that the bridge will not oscillate around the undeformed configuration $w_d = 0$.

Finally it's fundamental to notice that flexural motion is not able to give any contribution to the torsional motion. This is due to the fact that the flexural motion alone is not able to introduce sectional asymmetries in the response of the suspension bridge, since cables perform the same stiffening behaviour, that is both hardening or softening.

b) Dominant torsional mode

The initial assumption $\bar{\Gamma}_n(T_2) = \bar{\Gamma}_{n,0}$ and $\bar{Z}_n(T_2) = 0$ allow us to write.

$$\gamma_{\vartheta,n} = \frac{1}{2}(\epsilon \cdot \bar{\Gamma}_{n,0})^2 \frac{\alpha_{1,\vartheta}}{4 \cdot \tilde{\omega}_{\vartheta,n} \cdot M_{\vartheta,n}} \tau + \gamma_{\vartheta,n0}$$

Exploiting polar form for amplitudes and the two assumptions made we get the following resultant motions.

$$w_d(\xi, \tau) = \frac{1}{2}(\epsilon \cdot \bar{\Gamma}_{n,0})^2 \{(\epsilon \cdot \bar{Z}_{n,0}) \cdot \cos[2(\tilde{\omega}_{\vartheta,n}^{NL} \cdot \tau + \gamma_{\vartheta,n0})]\} \cdot T_{1,n}(\xi) + T_{2,n}(\xi) + o(\epsilon^3)$$

$$\vartheta_d(\xi, \tau) = (\epsilon \cdot \bar{\Gamma}_{n,0}) \cdot \cos(\tilde{\omega}_{\vartheta,n}^{NL} \cdot \tau + \gamma_{\vartheta,n0}) \cdot \Theta_n(\xi) + o(\epsilon^3)$$

Where the nonlinear torsional frequency becomes.

$$\tilde{\omega}_{\vartheta,n}^{NL} = \tilde{\omega}_{\vartheta,n} + \epsilon^2 D_2 \gamma_{\vartheta,n} = \tilde{\omega}_{\vartheta,n} + \frac{1}{2}(\epsilon \cdot \bar{\Gamma}_{n,0})^2 \cdot \frac{\alpha_{1,\vartheta}}{4 \cdot \tilde{\omega}_{\vartheta,n} \cdot M_{\vartheta,n}} + o(\epsilon^3)$$

It's interesting to notice that torsional motion has just the linear contribution. In fact, as just torsional motion is present the additional stiffness given by cables nonlinear behaviour vanishes since each cable gives equal contribution but with opposite sign. Contrary torsional vibrations are able to perturb the flexural ones by means of a second order contribution. This is because the reference system is positioned in the mass centre of the deck section, not in the stiffness one. Consequently, a torsional motion is able to introduce an asymmetric response in the section that led the centre of mass to move in the vertical direction since the stiffness centre changes position as amplitudes vary. Notice that the vertical oscillations are two time faster than the torsional ones but start with the same phase lag, being activated by the latter. Further $T_{2,n}(\xi)$ drift the flexural motion to vibrate not in the neighbourhood of the initial undeformed configuration. Once again the sign of $\alpha_{1,\vartheta}$ govern the hardening and softening behaviour of the response.

c) Modal energy exchange

This time we will consider the more general condition, for which both the flexural and the torsional motions are activated and internal energy exchange occurs between the two. Consequently nor $\bar{Z}_n(T_2)$ nor $\bar{\Gamma}_n(T_2)$ assume a priori constant values with passing of time.

Recalling that the operator D_2 simply represent the first order derivative with respect to the second order time scale T_2 , we can write the ratio between the equations governing the time variation of \bar{Z}_n and $\bar{\Gamma}_n$.

$$D_2 \bar{Z}_n / D_2 \bar{\Gamma}_n = d\bar{Z}_n / d\bar{\Gamma}_n = -\alpha_{3,w} / \alpha_{3,\vartheta} \cdot \tilde{\omega}_{\vartheta,n} / \tilde{\omega}_{w,n} \cdot M_{\vartheta,n} / M_{w,n} \cdot \bar{\Gamma}_n / \bar{Z}_n$$

Separating variables and integrating with respect to amplitudes we get.

$$\bar{Z}_n^2 + \{(\alpha_{3,w} \cdot \tilde{\omega}_{\vartheta,n} \cdot M_{\vartheta,n}) / (\alpha_{3,\vartheta} \cdot \tilde{\omega}_{w,n} \cdot M_{w,n})\} \cdot \bar{\Gamma}_n^2 = \bar{E}_0$$

Where the constant of integration \bar{E}_0 is proportional to the initial total energy stored by the isolated system. Notice that as far as $\alpha_{3,w}$ and $\alpha_{3,\vartheta}$ have the same sign, \bar{E}_0 must be positive definite at any time instant. This means that the system is isolated, and consequently flexural and torsional amplitudes are bounded being the system energetic level of the system constant. Conversely, as the two parameters has opposite signs then the initial energy is no more positive definite, meaning that in the system there are regenerative elements like sources and sinks of energy. Being the system no more isolated, oscillations can grow or decrease indefinitely.

In the following, for sake of simplicity, we will consider systems completely isolated.

Let's transform the energetic relation. First, introduce some differential equalities. Making use of the differential format for the energetic equation we get.

$$d\left(\frac{1}{8} \frac{1}{\tilde{\omega}_{\vartheta,n}} \alpha_{3,\vartheta} \cdot \bar{\Gamma}_n^2 \bar{Z}_n^2 \cdot \cos\delta_1\right) = \left\{ \begin{array}{l} \frac{1}{4} \left(\frac{\alpha_{3,\vartheta}}{\tilde{\omega}_{\vartheta,n} \cdot M_{\vartheta,n}} \bar{Z}_n^2 - \frac{\alpha_{3,w}}{\tilde{\omega}_{w,n} \cdot M_{w,n}} \bar{\Gamma}_n^2 \right) \cdot \cos\delta_1 \cdot \bar{\Gamma}_n d\bar{\Gamma}_n + \\ - \frac{1}{8} \frac{1}{\tilde{\omega}_{\vartheta,n}} \alpha_{3,\vartheta} \cdot \bar{\Gamma}_n^2 \bar{Z}_n^2 \cdot \sin\delta_1 \cdot d\delta_1 \end{array} \right\}$$

Further explicating T_2 from the equation governing the time variation of the torsional amplitude we get.

$$\bar{\Gamma}_n D_2 \delta_1 = \bar{\Gamma}_n (d\delta_1 / dT_2) = \frac{1}{8} \frac{1}{\tilde{\omega}_{\vartheta,n}} \alpha_{3,\vartheta} \cdot \bar{\Gamma}_n^2 \bar{Z}_n^2 \cdot \sin\delta_1 \cdot d\delta_1 / d\bar{\Gamma}_n$$

Then explicating the definition of $D_2 \delta_1$, making use of the energetic relation between \bar{Z}_n^2 and $\bar{\Gamma}_n^2$ and exploiting the first differential relation just found we get, after integration with respect to $\bar{\Gamma}_n$.

$$\frac{1}{8} \frac{1}{\tilde{\omega}_{\vartheta,n}} \alpha_{3,\vartheta} \cdot \bar{\Gamma}_n^2 \bar{Z}_n^2 \cdot \cos\delta_1 = \left\{ \begin{array}{l} \left[\frac{1}{4} \left(\frac{\alpha_{1,w}}{\tilde{\omega}_{w,n} \cdot M_{w,n}} - \frac{\alpha_{2,\vartheta}}{\tilde{\omega}_{\vartheta,n} \cdot M_{\vartheta,n}} \right) \bar{E}_0 + 2\sigma \right] \frac{\bar{\Gamma}_n^2}{2} + \\ + \frac{1}{4} \left[\begin{array}{l} \left(\frac{\alpha_{2,w}}{\tilde{\omega}_{w,n} \cdot M_{w,n}} - \frac{\alpha_{1,\vartheta}}{\tilde{\omega}_{\vartheta,n} \cdot M_{\vartheta,n}} \right) + \\ - \left(\frac{\alpha_{1,w}}{\tilde{\omega}_{w,n} \cdot M_{w,n}} - \frac{\alpha_{2,\vartheta}}{\tilde{\omega}_{\vartheta,n} \cdot M_{\vartheta,n}} \right) \left(\frac{\alpha_{3,w}}{\tilde{\omega}_{w,n} \cdot M_{w,n}} / \frac{\alpha_{3,\vartheta}}{\tilde{\omega}_{\vartheta,n} \cdot M_{\vartheta,n}} \right) \end{array} \right] \frac{\bar{\Gamma}_n^2}{4} + C \end{array} \right\} \quad (a)$$

In order to decouple variables \bar{Z}_n and $\bar{\Gamma}_n$ we may introduce a unique parameter able to define both of them.

Thanks to the fact that initial energy \bar{E}_0 remains the same, we can take as reference parameter the exchange ratio between the flexural and torsional modes, called ζ .

$$\bar{\Gamma}_n^2 = \zeta \cdot \bar{E}_0 \Rightarrow \bar{Z}_n^2 = (\alpha_{3,\vartheta} \cdot \tilde{\omega}_{w,n} \cdot M_{w,n}) / (\alpha_{3,w} \cdot \tilde{\omega}_{\vartheta,n} \cdot M_{\vartheta,n}) \cdot (1 - \zeta) \bar{E}_0$$

Consequently, we can write.

$$D_2 \bar{\Gamma}_n^2 = 2 \bar{\Gamma}_n D_2 \bar{\Gamma}_n = 4 \left(\frac{\alpha_{3,w}}{8 \tilde{\omega}_{w,n} \cdot M_{w,n}} \right)^2 \left(\frac{\alpha_{3,\vartheta}}{\tilde{\omega}_{\vartheta,n} \cdot M_{\vartheta,n}} / \frac{\alpha_{3,w}}{\tilde{\omega}_{w,n} \cdot M_{w,n}} \right)^2 \zeta^2 (1 - \zeta)^2 \bar{E}_0^4 \sin^2 \delta_1$$

Then exploiting the latter energetic relations in the relation (a), adding and subtracting to $D_2 \bar{\Gamma}_n^2$ the right and left hand side term of the same equality (a) we get.

$$(D_2 \zeta)^2 = \left(\frac{\alpha_{3,\vartheta}}{4 \tilde{\omega}_{\vartheta,n} \cdot M_{\vartheta,n}} \right)^2 \bar{E}_0^2 \cdot \{F^2(\zeta) - G^2(\zeta)\}$$

Where.

$$F^2(\zeta) = \zeta^2 (1 - \zeta)^2$$

$$G^2(\zeta) = \left\{ \begin{array}{l} \left\{ \frac{1}{8} \left(\frac{\alpha_{1,w}}{\tilde{\omega}_{w,n} \cdot M_{w,n}} - \frac{\alpha_{2,\vartheta}}{\tilde{\omega}_{\vartheta,n} \cdot M_{\vartheta,n}} \right) \bar{E}_0 + \sigma \right\} \left(\frac{\alpha_{3,\vartheta}}{\tilde{\omega}_{\vartheta,n} \cdot M_{\vartheta,n}} \right) (1 - \zeta) \bar{E}_0 + \\ + \frac{1}{16} \left[\begin{array}{l} \left(\frac{\alpha_{2,w}}{\tilde{\omega}_{w,n} \cdot M_{w,n}} - \frac{\alpha_{1,\vartheta}}{\tilde{\omega}_{\vartheta,n} \cdot M_{\vartheta,n}} \right) + \\ - \left(\frac{\alpha_{1,w}}{\tilde{\omega}_{w,n} \cdot M_{w,n}} - \frac{\alpha_{2,\vartheta}}{\tilde{\omega}_{\vartheta,n} \cdot M_{\vartheta,n}} \right) \left(\frac{\alpha_{3,w}}{\tilde{\omega}_{w,n} \cdot M_{w,n}} \right) \end{array} \right] \left(\frac{\alpha_{3,\vartheta}}{\tilde{\omega}_{\vartheta,n} \cdot M_{\vartheta,n}} \right)^2 (1 - \zeta)^2 \bar{E}_0^2 + C \right\} \left(\frac{\alpha_{3,w}}{\tilde{\omega}_{w,n} \cdot M_{w,n}} \right)^2 \frac{\left(\frac{\alpha_{3,\vartheta}}{\tilde{\omega}_{\vartheta,n} \cdot M_{\vartheta,n}} \right)^4 \bar{E}_0^4}{\left(\frac{\alpha_{3,w}}{\tilde{\omega}_{w,n} \cdot M_{w,n}} \right)^4 \bar{E}_0^4} \right\}^2$$

Hence we need to perform numerical integration of a nonlinear ordinary differential equation to get the transient path.

$$\int_{\zeta_0}^{\zeta} d\zeta / \sqrt{F^2(\zeta) - G^2(\zeta)} = \left(\frac{\alpha_{3,\vartheta}}{4 \tilde{\omega}_{\vartheta,n} \cdot M_{\vartheta,n}} \right) \bar{E}_0 T_2$$

Notice that to get real amplitudes we need a positive radicand, meaning $F^2(\zeta) > G^2(\zeta)$. Whilst stationary response can be defined analytically as $T_2 \rightarrow \infty$ leading to $F^2(\zeta) = G^2(\zeta)$. This does not mean that amplitudes remains constant in time but can still vary though in a regular path.

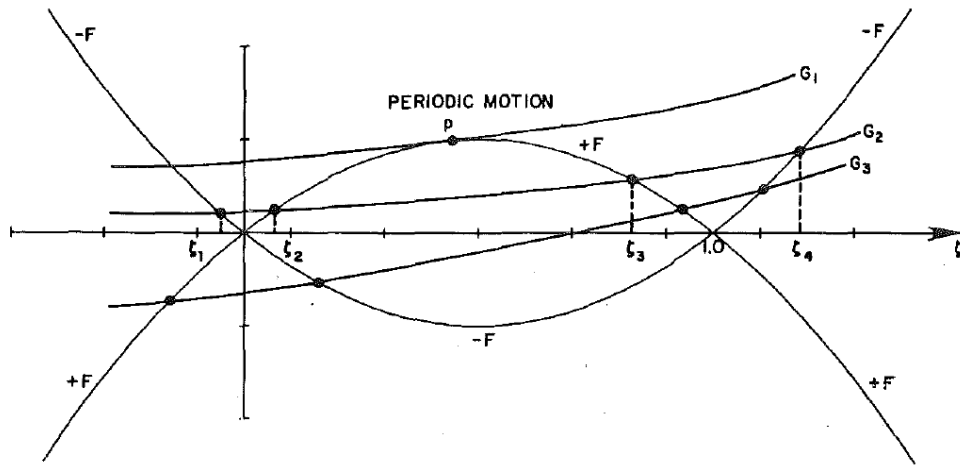


Figure 3.1_ Functions governing the internal energy exchange.

Let's consider some particular conditions.

➤ Amplitude and phase modulation

The stationary condition is a fourth order equation leading to four roots. Hence we may assume that $\zeta_i < \zeta_{i+1}$ with $i = 1, \dots, 4$. However since the system is isolated, only the roots satisfying $0 < \zeta_i < 1$ are feasible. Hence we can say that ζ must oscillates periodically between ζ_2 and ζ_3 at passing of time. In fact energy transfer occurs, and consequently flexural and torsional amplitudes vary periodically in time leading to an aperiodic motion in terms of w_d and ϑ_d since amplitudes are modulated like in the beatment phenomenon.

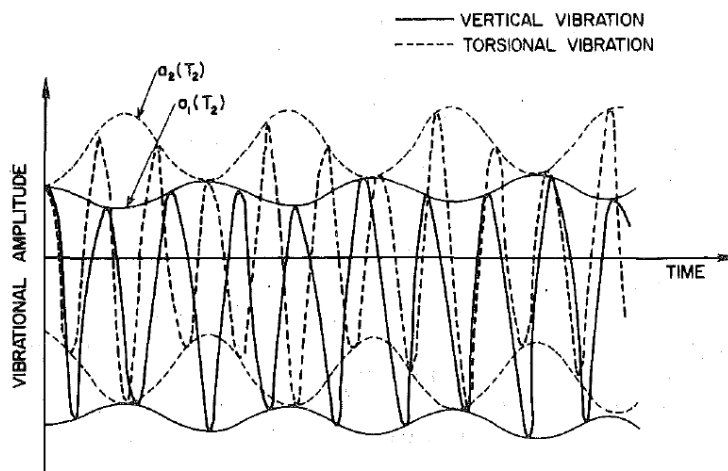


Figure 3.2_ Amplitude modulation in time.

Since the equations governing the phase modulation in time are strictly dependent on amplitudes, we can say that also phase lags are aperiodic.

➤ Phase modulation

This particular condition occurs only in the case in which the stationary condition gives only one root, leading to constant amplitudes. This does not mean that amplitudes remain equal to the ones dictated by initial conditions. In fact the initial energy, during the transitory, can flow through the flexural and torsional amplitudes as the system prefer in order to minimize potential energy. Once a stable condition is reached, amplitudes does not vary any more since initial repartition of energy is fixed.

Hence enforcing constancy of amplitudes ($D_2\bar{Z}_n = D_2\bar{\Gamma}_n = 0$) we get that the condition is satisfied as far as $\delta_1 = n\pi$ with $n \in N$. Consequently, $\cos\delta_1 = \pm 1$ depending on the choice of n . Hence substituting in the equation governing the phase lags, lead to a linear growth in time of $\gamma_{w,n}$ and $\gamma_{\vartheta,n}$ being $D_2\bar{Z}_n$ and $D_2\bar{\Gamma}_n$ constant. The fact that amplitudes remains constant grant the nonlinear frequencies to be constant in time too.

Further, another phenomenon can be observed.

$$\tilde{\omega}_{\vartheta,n}^{NL} - \tilde{\omega}_{w,n}^{NL} = (\tilde{\omega}_{\vartheta,n} - \tilde{\omega}_{w,n}) + \epsilon^2(D_2\gamma_{\vartheta,n} - D_2\gamma_{w,n}) = \epsilon^2(D_2\gamma_{\vartheta,n} - D_2\gamma_{w,n} - \sigma) = \frac{1}{2}\epsilon^2 D_2\delta_1$$

Being $\delta_1 = n\pi$ lead to $\tilde{\omega}_{\vartheta,n}^{NL} = \tilde{\omega}_{w,n}^{NL}$ meaning that nonlinearities adjust the phase lag between the flexural and torsional motion so that the respective frequencies coalesce. This is the well-known Synchronization or Entrainment phenomenon and has been a great issue to be solved in the past, when clock pendulum where the only available instruments for time measurement at least during daytime.

➤ Amplitude modulation

We are looking for stationary phases enforcing $D_2\gamma_{w,n} = D_2\gamma_{\vartheta,n} = 0$. Explicating both the conditions with respect to $\cos\delta_1$ and equating the two expressions found we get.

$$\left\{ \alpha_{1,w}\alpha_{3,\vartheta}\bar{Z}_n^4 + (\alpha_{2,w}\alpha_{3,\vartheta} - \alpha_{2,\vartheta}\alpha_{3,w})\bar{Z}_n^2\bar{\Gamma}_n^2 - \alpha_{1,\vartheta}\alpha_{3,w}\bar{\Gamma}_n^4 \right\} / \left(\bar{Z}_n^2\bar{\Gamma}_n^2\alpha_{3,w}\alpha_{3,\vartheta} \right) = 0$$

That together with the energetic relation between amplitudes is able to give us the time variation of \bar{Z}_n and $\bar{\Gamma}_n$. Since the governing equations are not directly dependent on time, the system gives us constant amplitudes as in periodic motion. We conclude saying that is not possible to have just pure amplitude modulation.

Slight different is the condition for the phase lag δ_1 to be periodic, meaning $D_2\gamma_{w,n} - D_2\gamma_{\vartheta,n} = 0$ hence the stationarity of phases is just a special subcase.

$$D_2\delta_1 = 0 \Leftrightarrow d\zeta^2 + e\zeta + f = 0$$

Where.

$$d = \left\{ \begin{array}{l} \left(\frac{\alpha_{1,w}}{\tilde{\omega}_{w,n}M_{w,n}} - \frac{\alpha_{2,\vartheta}}{\tilde{\omega}_{\vartheta,n}M_{\vartheta,n}} \right) \left[\frac{3}{2} + 2 \frac{\alpha_{3,w}}{\alpha_{3,\vartheta}} \frac{\tilde{\omega}_{\vartheta,n}M_{\vartheta,n}}{\tilde{\omega}_{w,n}M_{w,n}} \right] + \\ - \frac{1}{2} \left(\frac{\alpha_{2,w}}{\tilde{\omega}_{w,n}M_{w,n}} - \frac{\alpha_{1,\vartheta}}{\tilde{\omega}_{\vartheta,n}M_{\vartheta,n}} \right) / \left(\frac{\alpha_{3,w}}{\alpha_{3,\vartheta}} \frac{\tilde{\omega}_{\vartheta,n}M_{\vartheta,n}}{\tilde{\omega}_{w,n}M_{w,n}} \right) + \frac{8}{\bar{E}_0} \left(\frac{2C}{\bar{E}_0} - \sigma \right) \left(\frac{\alpha_{3,w}}{\alpha_{3,\vartheta}} \frac{\tilde{\omega}_{\vartheta,n}M_{\vartheta,n}}{\tilde{\omega}_{w,n}M_{w,n}} \right) \end{array} \right\}$$

$$e = \left\{ \begin{array}{l} - \left(2 + \frac{\alpha_{3,w} \tilde{\omega}_{\vartheta,n} M_{\vartheta,n}}{\alpha_{3,\vartheta} \tilde{\omega}_{w,n} M_{w,n}} \right) + \\ + \left(\frac{\alpha_{2,w}}{\tilde{\omega}_{w,n} M_{w,n}} - \frac{\alpha_{1,\vartheta}}{\tilde{\omega}_{\vartheta,n} M_{\vartheta,n}} \right) / \left(\frac{\alpha_{3,w} \tilde{\omega}_{\vartheta,n} M_{\vartheta,n}}{\alpha_{3,\vartheta} \tilde{\omega}_{w,n} M_{w,n}} \right) + \frac{8}{\bar{E}_0} \left(\frac{2C}{\bar{E}_0} - \sigma \right) \left(\frac{\alpha_{3,w} \tilde{\omega}_{\vartheta,n} M_{\vartheta,n}}{\alpha_{3,\vartheta} \tilde{\omega}_{w,n} M_{w,n}} \right) \end{array} \right\}$$

$$f = \left\{ \begin{array}{l} \frac{1}{2} \left(\frac{\alpha_{1,w}}{\tilde{\omega}_{w,n} M_{w,n}} - \frac{\alpha_{2,\vartheta}}{\tilde{\omega}_{\vartheta,n} M_{\vartheta,n}} \right) + \\ - \frac{1}{2} \left(\frac{\alpha_{1,w}}{\tilde{\omega}_{w,n} M_{w,n}} - \frac{\alpha_{2,\vartheta}}{\tilde{\omega}_{\vartheta,n} M_{\vartheta,n}} \right) / \left(\frac{\alpha_{3,w} \tilde{\omega}_{\vartheta,n} M_{\vartheta,n}}{\alpha_{3,\vartheta} \tilde{\omega}_{w,n} M_{w,n}} \right) - \frac{8}{\bar{E}_0} C \left(\frac{\alpha_{3,w} \tilde{\omega}_{\vartheta,n} M_{\vartheta,n}}{\alpha_{3,\vartheta} \tilde{\omega}_{w,n} M_{w,n}} \right) \end{array} \right\}$$

Let's analyse the steady response in time of the system as different initial conditions are enforced. First, let's write the stationarity condition in a compact format.

$$\pm F(\zeta) = G(\zeta) \Rightarrow \pm \zeta(1 - \zeta) = a(1 - \zeta) + b(1 - \zeta)^2 + c$$

Where.

$$a = \left\{ \frac{1}{8} \left(\frac{\alpha_{1,w}}{\tilde{\omega}_{w,n} M_{w,n}} - \frac{\alpha_{2,\vartheta}}{\tilde{\omega}_{\vartheta,n} M_{\vartheta,n}} \right) \bar{E}_0 + \sigma \right\} / \left(\frac{\alpha_{3,\vartheta}}{8 \tilde{\omega}_{\vartheta,n} M_{\vartheta,n}} \bar{E}_0 \right)$$

$$b = \frac{1}{16} \left\{ \begin{array}{l} \left(\frac{\alpha_{2,w}}{\tilde{\omega}_{w,n} M_{w,n}} - \frac{\alpha_{1,\vartheta}}{\tilde{\omega}_{\vartheta,n} M_{\vartheta,n}} \right) + \\ - \left(\frac{\alpha_{1,w}}{\tilde{\omega}_{w,n} M_{w,n}} - \frac{\alpha_{2,\vartheta}}{\tilde{\omega}_{\vartheta,n} M_{\vartheta,n}} \right) \left(\frac{\alpha_{3,w}}{\tilde{\omega}_{w,n} M_{w,n}} \right) / \left(\frac{\alpha_{3,\vartheta}}{\tilde{\omega}_{\vartheta,n} M_{\vartheta,n}} \right) \end{array} \right\} / \left(\frac{\alpha_{3,w}}{8 \tilde{\omega}_{w,n} M_{w,n}} \right)$$

$$c = C \left\{ \frac{\alpha_{3,w}}{8 \tilde{\omega}_{w,n} M_{w,n}} / \left(\frac{\alpha_{3,\vartheta}}{8 \tilde{\omega}_{\vartheta,n} M_{\vartheta,n}} \bar{E}_0 \right)^2 \right\}$$

The solutions can be written as.

$$\zeta_{1,2} = \left((a + 2b \pm 1) \pm \sqrt{(a + 2b \pm 1)^2 - 4(b \pm 1)(a + b + c)} \right) / (2(b \pm 1))$$

Searching for periodic solutions we get that $\zeta_1 = \zeta_2$ as long as the radicand vanishes.

$$\zeta_{1,2} = \zeta_p = (a + 2b \pm 1) / (2(b \pm 1)) \Leftrightarrow c = (1 + a^2 \mp 2a) / (4(b \pm 1))$$

In order to explicit this condition we need first recall the fact that the constant C depends on initial energetic conditions.

$$C = \left(\frac{\alpha_{3,\vartheta}}{8 \tilde{\omega}_{\vartheta,n} M_{\vartheta,n}} \bar{E}_0 \right)^2 / \left(\frac{\alpha_{3,w}}{8 \tilde{\omega}_{w,n} M_{w,n}} \right) \{ \zeta_0(1 - \zeta_0) \cos \delta_{1,0} - a(1 - \zeta_0) - b(1 - \zeta_0)^2 \}$$

Hence we can explicit the periodicity condition as follows.

$$\{\zeta_0(1 - \zeta_0)\cos\delta_{1,0} - a(1 - \zeta_0) - b(1 - \zeta_0)^2\} = (1 + a^2 \mp 2a)/(4(b \pm 1))$$

Since periodicity of amplitudes means $D_2\bar{Z}_n = D_2\bar{\Gamma}_n = 0$, as already seen, we get from both the governing differential equations that $\delta_1 = \delta_{1,0} = n\pi$ and hence the periodic solutions can be defined.

$$\zeta_{0,p} = \zeta_p \left\{ 1 \pm \sqrt{1 - (b + (-1)^n)/(b \pm 1)} \right\} = \zeta_p \Leftrightarrow \begin{cases} F(\zeta) = G(\zeta); n \text{ even} \\ F(\zeta) = -G(\zeta); n \text{ odd} \end{cases}$$

This means that the periodic condition can be reached only in the case in which the initial repartition of energy is already the one that would be at steady state periodic conditions. Meaning that periodic conditions are very unstable and rare to occur, but anyway feasible.

Let's analyse the extreme values reached by the constant C as initial conditions vary.

$$\partial C / \partial \delta_{1,0} = 0 \Leftrightarrow \begin{cases} \zeta_0 = 0 \Rightarrow \partial C / \partial \zeta_0 = 0 \Leftrightarrow \cos\delta_{1,0} = -(a + 2b) \Rightarrow \zeta_{st} = [0; \zeta_L = 2\zeta_{0,p}] \\ \zeta_0 = 1 \Rightarrow \partial C / \partial \zeta_0 = 0 \Leftrightarrow \cos\delta_{1,0} = a \Rightarrow \zeta_{st} = [\zeta_U = \frac{a+b}{b \pm 1}; 1] \\ \delta_{1,0} = n\pi \Rightarrow \partial C / \partial \zeta_0 = 0 \Leftrightarrow \zeta_0 = \zeta_p \end{cases}$$

Where we have introduced the so-called lower and upper aperiodic regime thresholds ζ_L and ζ_U , where as the name suggest there will be exchange of energy between modes at passing of time. Notice that we must pay attention to chose a sign for ζ_U granting ζ to be bounded between 0 and 1. Further it's clear that as initial conditions are stationary points for $C(\zeta_0, \delta_{1,0})$ then the steady state conditions of the system will oscillate between two configurations of which one is represented by the initial condition itself. Hence the system will return periodically to the initial conditions. Then looking for the concavity of the stationary points for $C(\zeta_0, \delta_{1,0})$.

Being.

$$\begin{cases} \partial^2 C / \partial \delta_{1,0}^2 > 0 \Leftrightarrow \cos\delta_{1,0} < -b \\ \partial^2 C / \partial \zeta_0^2 > 0 \Leftrightarrow \cos\delta_{1,0} < 0 \end{cases}$$

Then we can say that.

$$\left\{ \begin{array}{l} \zeta_0 = 0 ; \cos\delta_{1,0} = -(a + 2b) \Rightarrow \partial^2 C / \partial \delta_{1,0}^2 = 0 ; \partial^2 C / \partial \zeta_0^2 > 0 \\ \zeta_0 = 1 ; \cos\delta_{1,0} = a \Rightarrow \partial^2 C / \partial \delta_{1,0}^2 = 0 ; \partial^2 C / \partial \zeta_0^2 > 0 \Leftrightarrow a < -b \\ \delta_{1,0} = n\pi ; \zeta_0 = \zeta_p \Rightarrow \partial^2 C / \partial \delta_{1,0}^2 > 0 \Leftrightarrow n \text{ odd} ; \partial^2 C / \partial \zeta_0^2 > 0 \Leftrightarrow \begin{cases} b < -1 ; n \text{ even} \\ b > 1 ; n \text{ odd} \end{cases} \end{array} \right.$$

Let's perform a simple parametric analysis of initial conditions.

$$\zeta_0 = 0 \Rightarrow \left\{ \begin{array}{l} \zeta_L = 0 \Leftrightarrow a + 2b \pm 1 = 0 \Leftrightarrow \bar{E}_0 = \bar{E}_{0,1} \\ \zeta_L = 1 \Leftrightarrow a + b = 0 \Leftrightarrow \bar{E}_0 = \bar{E}_{0,2} \end{array} \right.$$

$$\zeta_0 = 1 \Rightarrow \left\{ \begin{array}{l} \zeta_U = 0 \Leftrightarrow a + b = 0 \Leftrightarrow \bar{E}_0 = \bar{E}_{0,3} \\ \zeta_U = 1 \Leftrightarrow a = \pm 1 \Leftrightarrow \bar{E}_0 = \bar{E}_{0,2} \end{array} \right.$$

$$\zeta_0 = \zeta_p \Rightarrow \left\{ \begin{array}{l} \zeta_p = 0 \Leftrightarrow a + 2b \pm 1 = 0 \Leftrightarrow \bar{E}_0 = \bar{E}_{0,1} \\ \zeta_p = 1 \Leftrightarrow a = \pm 1 \Leftrightarrow \bar{E}_0 = \bar{E}_{0,2} \end{array} \right.$$

Where.

$$\bar{E}_{0,1} = \sigma \frac{\alpha_{3,w} \tilde{\omega}_{\vartheta,n} M_{\vartheta,n}}{\alpha_{3,\vartheta} \tilde{\omega}_{w,n} M_{w,n}} / \left\{ \left(\frac{\alpha_{1,w}}{\tilde{\omega}_{w,n} M_{w,n}} - \frac{\alpha_{2,\vartheta}}{\tilde{\omega}_{\vartheta,n} M_{\vartheta,n}} \right) \mp \frac{\alpha_{3,w}}{\tilde{\omega}_{w,n} M_{w,n}} \right\}$$

$$\bar{E}_{0,2} = 2 \sigma \frac{\alpha_{3,w}}{\tilde{\omega}_{w,n} M_{w,n}} / \left\{ \frac{\alpha_{3,\vartheta}}{\tilde{\omega}_{\vartheta,n} M_{\vartheta,n}} \left(\frac{\alpha_{1,\vartheta}}{\tilde{\omega}_{\vartheta,n} M_{\vartheta,n}} - \frac{\alpha_{2,w}}{\tilde{\omega}_{w,n} M_{w,n}} \right) - \frac{\alpha_{3,w}}{\tilde{\omega}_{w,n} M_{w,n}} \left(\frac{\alpha_{1,w}}{\tilde{\omega}_{w,n} M_{w,n}} - \frac{\alpha_{2,\vartheta}}{\tilde{\omega}_{\vartheta,n} M_{\vartheta,n}} \right) \right\}$$

$$\bar{E}_{0,3} = \sigma / \left\{ \pm \frac{\alpha_{3,\vartheta}}{\tilde{\omega}_{\vartheta,n} M_{\vartheta,n}} - \left(\frac{\alpha_{1,w}}{\tilde{\omega}_{w,n} M_{w,n}} - \frac{\alpha_{2,\vartheta}}{\tilde{\omega}_{\vartheta,n} M_{\vartheta,n}} \right) \right\}$$

Hence, we have found the initial total energy required to get pure translational and rotational vibrations, and the one that grant periodic transition between the two extreme conditions.

Finally, we can perform a stability analysis of initial conditions simply analysing the perturbed configuration.

$$\zeta = \zeta_0 + \Delta\zeta$$

$$\delta_1 = \delta_{1,0} + \Delta\delta$$

Since the perturbations $\Delta\zeta = \Delta\zeta(T_2)$ and $\Delta\delta = \Delta\delta(T_2)$ vary in time, the expressions for $D_2(\bar{Z}_n)^2$ and $D_2\delta$ can be written in terms of energy ratio ζ as follows.

Further assuming small but finite perturbations we can focus just on linear terms and make the usual simplifications for trigonometric functions in presence of small angles.

$$D_2 \Delta \zeta = -\frac{\alpha_{3,\vartheta}}{4\tilde{\omega}_{\vartheta,n} \cdot M_{\vartheta,n}} \bar{E}_0 \cdot \zeta(1-\zeta) \cdot \sin \delta_1 \cong -\frac{\alpha_{3,\vartheta}}{4\tilde{\omega}_{\vartheta,n} \cdot M_{\vartheta,n}} \bar{E}_0 \cdot \left\{ \begin{aligned} &[(1-2\zeta_0) \cdot \sin \delta_{1,0}] \Delta \zeta + \\ &+ [\zeta_0(1-\zeta_0) \cdot \cos \delta_{1,0}] \Delta \delta \end{aligned} \right\}$$

$$D_2 \Delta \delta = \frac{1}{4} \left\{ \begin{aligned} &\left(\frac{\alpha_{2,\vartheta}}{\tilde{\omega}_{\vartheta,n} \cdot M_{\vartheta,n}} - \frac{\alpha_{1,w}}{\tilde{\omega}_{w,n} \cdot M_{w,n}} \right) \bar{E}_0 \zeta + \\ &\left(\frac{\alpha_{1,\vartheta}}{\tilde{\omega}_{\vartheta,n} \cdot M_{\vartheta,n}} - \frac{\alpha_{2,w}}{\tilde{\omega}_{w,n} \cdot M_{w,n}} \right) / \left(\frac{\alpha_{3,w}}{\alpha_{3,\vartheta}} \frac{\tilde{\omega}_{\vartheta,n} \cdot M_{\vartheta,n}}{\tilde{\omega}_{w,n} \cdot M_{w,n}} \right) \bar{E}_0 (1-\zeta) + \\ &-\frac{\alpha_{3,\vartheta}}{\tilde{\omega}_{\vartheta,n} \cdot M_{\vartheta,n}} \bar{E}_0 (1-2\zeta) \cdot \cos \delta_1 \end{aligned} \right\} - 2\sigma$$

$$\cong \frac{\bar{E}_0}{4} \cdot \left\{ \begin{aligned} &\left[\begin{aligned} &\frac{\alpha_{2,\vartheta}}{\tilde{\omega}_{\vartheta,n} \cdot M_{\vartheta,n}} - \frac{\alpha_{1,w}}{\tilde{\omega}_{w,n} \cdot M_{w,n}} + \\ &-\left(\frac{\alpha_{1,\vartheta}}{\tilde{\omega}_{\vartheta,n} \cdot M_{\vartheta,n}} - \frac{\alpha_{2,w}}{\tilde{\omega}_{w,n} \cdot M_{w,n}} \right) / \left(\frac{\alpha_{3,w}}{\alpha_{3,\vartheta}} \frac{\tilde{\omega}_{\vartheta,n} \cdot M_{\vartheta,n}}{\tilde{\omega}_{w,n} \cdot M_{w,n}} \right) + \Delta \zeta + \\ &+ 2 \frac{\alpha_{3,\vartheta}}{\tilde{\omega}_{\vartheta,n} \cdot M_{\vartheta,n}} \cdot \cos \delta_{1,0} \end{aligned} \right] \Delta \zeta + \\ &+ \left[\frac{\alpha_{3,\vartheta}}{\tilde{\omega}_{\vartheta,n} \cdot M_{\vartheta,n}} (1-2\zeta_0) \cdot \cos \delta_{1,0} \right] \Delta \delta \end{aligned} \right\}$$

Assuming the usual polar format for perturbations $\Delta \zeta = \bar{\Delta} \bar{\zeta} \cdot \exp(\lambda T_2)$ and $\Delta \delta = \bar{\Delta} \bar{\delta} \cdot \exp(\lambda T_2)$ we can enforce the vanishing of the determinant for the previous linear homogeneous system in order to get non-trivial solutions. Hence, we find the analytical expression for the exponential parameter.

$$\lambda = \pm \frac{\bar{E}_0}{4} \frac{\alpha_{3,\vartheta}}{\tilde{\omega}_{\vartheta,n} \cdot M_{\vartheta,n}} \sqrt{(1-2\zeta_0)^2 \sin^2 \delta_{1,0} - \left(\frac{\partial^2 C}{\partial \delta_{1,0}^2} \frac{\partial^2 C}{\partial \zeta_0^2} \right) / \left[\left(\frac{\alpha_{3,\vartheta}}{8\tilde{\omega}_{\vartheta,n} \cdot M_{\vartheta,n}} \bar{E}_0 \right)^2 / \left(\frac{\alpha_{3,w}}{8\tilde{\omega}_{w,n} \cdot M_{w,n}} \right) \right]^2}$$

Necessary and sufficient condition to get bounded response of the system is the exponential parameter to be imaginary.

$$\frac{\partial^2 C}{\partial \delta_{1,0}^2} \frac{\partial^2 C}{\partial \zeta_0^2} > \left[\left(\frac{\alpha_{3,\vartheta}}{\tilde{\omega}_{\vartheta,n} \cdot M_{\vartheta,n}} \bar{E}_0 \right)^2 / 8 \left(\frac{\alpha_{3,w}}{\tilde{\omega}_{w,n} \cdot M_{w,n}} \right) \right]^2 (1-2\zeta_0)^2 \sin^2 \delta_{1,0}$$

Hence, the most general stability condition can be written more synthetically.

$$2\zeta_0(1-\zeta_0) \cdot \cos \delta_{1,0} (b + \cos \delta_{1,0}) > (1-2\zeta_0)^2 \sin^2 \delta_{1,0}$$

It's evident the important role played by the curvature of the function $C(\zeta_0, \delta_{1,0})$ that we have deeply analysed.

Let's analyse the main possible initial conditions.

$$\zeta_0 = \frac{1}{2} \text{ and/or } \delta_{1,0} = n\pi \Rightarrow \frac{\partial^2 c}{\partial \delta_{1,0}^2} \frac{\partial^2 c}{\partial \zeta_0^2} > 0 \Leftrightarrow \cos \delta_{1,0} < \min\{-b; 0\}$$

$$\zeta_0 = [0; 1] \Rightarrow 0 > \sin^2 \delta_{1,0} \Rightarrow \text{never stable}$$

$$\delta_{1,0} = (2n + 1)\frac{\pi}{2} \Rightarrow 0 > \pm(1 - 2\zeta_0)^2 \Leftrightarrow \begin{cases} \text{always stable for } n \text{ odd} \\ \text{never stable for } n \text{ even} \end{cases}$$

Notice that we are able just to detect the regions where stability is granted, hence when initial conditions does not grant it we cannot say that conditions are surely unstable since may be indifferent. Further in general we can talk of strong instability when both the perturbations grows in time, whilst we have weak instability as $\delta_{1,0}$ diverges and $\zeta_0 \rightarrow 0$.

4. Slackening of hangers

As we have mentioned many times in the previous treatment, that the proposed model is a continuous 2 dof representation of a generic suspension bridge. Hence we make very restrictive hypothesis as for example we neglect the third degree of freedom associated to lateral displacement of the deck since it has generally small effects on the critical Flutter threshold due to the fact that the lateral displacement given by drag aeroelastic forces introduces small rotation of the deck cross sections. Another important hypothesis is the assumption of perfectly rigid pylons in order to neglect their relative displacement in correspondence of the main cables, assumption that allow us to neglect longitudinal displacements of cables and hence ensure that the non-local cables stiffening contribution to be a constant term.

Since the main goal of the present work is to obtain a reliable simple but sufficiently accurate sectional nonlinear model of a generic suspension bridge the previous two contributions can be easily neglected. What we continue to neglect in the equivalent sectional model is the possibility that hangers undergo to slackening. Since this contribution has an important effect on the structural response both during large oscillations and at Flutter threshold, due to the fact that it introduces a high variation of the actual stiffness of the structural system, we want to make our model capable to catch this phenomenon.

Previously we mentioned the fact that to model precisely the actual behaviour of hangers it's necessary to increase the number of the dof from 2 to 4. In fact just in the latter kind of models is possible to introduce an appropriate constitutive model that is able to capture the linear elastic response of hangers in tension and their slackening in compression due to the very high slenderness that characterised these structural elements. For better representation of the actual behaviour of hangers is also possible to introduce a constitutive model properly tuned so that it is able to catch the initial stretch induced by self-weight of the stiffening girder. Notice that we want to consider just non linearity coming from geometrical effects hence all material hardening or softening behaviour and yielding condition will be neglected.

Hence in order to remain in the field of a 2 dof model we need to introduce some simplifications in the hangers' behaviour.

Up to now we make the easiest assumption considering hangers perfectly rigid both in tension and in compression, in order to neglect all problems related to their slackening.

The further and immediate improvement of the model would be to model the hangers as perfectly rigid in tension and perfectly flexible in compression. This assumption is a crude representation of the actual behaviour of hangers, but it's able to catch the main feature of their structural response. In fact is a good representation of both the tension response of real bridges during serviceability conditions where hangers remains in the linear branch also during large displacements and of the compression response once the displacements are enough large to grant slackening, overcoming the initial tensile stretch. In terms of constitutive model it's like if we introduce a perfectly tenso-rigid material behaviour.

The current assumption allows us to consider hangers as uniformly smeared along the bridge's span, losing the actual local effect due to their effective location. Hence the local contribution given by slackening of hanger is approximate also in term of the actual position in which hangers could effectively undergo to slackening.

The first step is to find out a proper limit condition able to distinguish between taut and slack hangers. As long as hangers remains taut, thanks to the tenso-rigid model assumed, they are able to transfer the loads acting on the stiffening girder to the main cable of pertinence depending on the side of the deck to which it belongs to. While in those region where the vertical displacement on one side of the bridge, due to the combination of flexural and torsional vibrations, are so high that slackening occurs consequently the loads acting on the deck cannot be sustained by the deck and cables system. In fact locally one or both cables are no more loaded by the action of external forces, hence this surplus of energy has to be absorbed by the remaining stiff part of the deck and cables system. Hence as usual a flow of forces occurs and it moves from the flexible elements towards stiff ones.

4.1 Modified equations of motion

In order to find out a proper threshold condition for slackening initiation is necessary to reformulate the equations of motion from the beginning starting from the Total Potential Energy Variation.

$$\Delta V(w_d, \vartheta_d, q, m) = \left\{ \begin{array}{l} \int_0^l \left(\frac{1}{2} E_d I_d \cdot w_d''^2 + \frac{1}{2} E_d \Gamma_d \cdot \vartheta_d''^2 + \frac{1}{2} G_d J_d \cdot \vartheta_d'^2 - q \cdot w_d - m \cdot \vartheta_d \right) dx + \\ + \int_0^{l_R^+} \left\{ \frac{1}{2} H \cdot (w_d' + b\vartheta_d')^2 + \int_0^{w_R'} h^+(w_R) \cdot (y' + w_R') dw_R' \right\} dx + \\ + \int_0^{l_L^+} \left\{ \frac{1}{2} H \cdot (w_d' - b\vartheta_d')^2 + \int_0^{w_L'} h^+(w_L) \cdot (y' + w_L') dw_L' \right\} dx \end{array} \right\};$$

Notice that with respect the initial formulation, this time we cannot collect all terms under the same sign of integration since each of them has a different domain in which it is able to make work.

Since we need to integrate the contribution of cables along a piecewise continuous domain the following definition holds.

$$\int_0^{l^+} \{\cdot\} dx = \sum \int_{x_1}^{x_2} \{\cdot\} dx \quad \text{with} \quad (x_1, x_2) \in [0, l];$$

The stiffening terms are define as follows.

$$h^+(w_R) = \int_0^{l_R^+} \frac{E_c A_c}{L_c} \left\{ \left(y' w_d' + \frac{w_d'^2}{2} \right) + b(y' + w_d') \vartheta_d' + \frac{(b\vartheta_d')^2}{2} \right\} dx = h^+_{w_R} + h^+_{w\vartheta_R} + h^+_{\vartheta_R};$$

$$h^+(w_L) = \int_0^{l_L^+} \frac{E_c A_c}{L_c} \left\{ \left(y' w_d' + \frac{w_d'^2}{2} \right) - b(y' + w_d') \vartheta_d' + \frac{(b\vartheta_d')^2}{2} \right\} dx = h^+_{w_L} + h^+_{w\vartheta_L} + h^+_{\vartheta_L};$$

Then integration by parts of the differential of the TPE leads to the following equality.

$$\delta V = \left\{ \begin{array}{l} \int_0^l \{ (E_d I_d \cdot w_d'''' - q) \cdot dw_d + (E_d \Gamma_d \cdot \vartheta_d'''' - G_d J_d \cdot \vartheta_d'' - m) \cdot d\vartheta_d \} dx + \\ - \int_0^{l_R^+} \left\{ \begin{array}{l} (H \cdot (w_d'' + b\vartheta_d'') + h^+(w_R) \cdot (y'' + w_d'' + b\vartheta_d'')) \cdot dw_d + \\ + b(H \cdot (w_d'' + b\vartheta_d'') + h^+(w_R) \cdot (y'' + w_d'' + b\vartheta_d'')) \cdot d\vartheta_d \end{array} \right\} dx + \\ - \int_0^{l_L^+} \left\{ \begin{array}{l} (H \cdot (w_d'' - b\vartheta_d'') + h^+(w_L) \cdot (y'' + w_d'' - b\vartheta_d'')) \cdot dw_d + \\ + b(H \cdot (w_d'' - b\vartheta_d'') + h^+(w_L) \cdot (y'' + w_d'' - b\vartheta_d'')) \cdot d\vartheta_d \end{array} \right\} dx \end{array} \right\};$$

Exploiting the stationarity of the TPE variational we get the nonlinear equations of equilibrium.

$$\delta_{w_d} V = 0 \quad \forall \delta w_d \Leftrightarrow \left\{ \begin{array}{l} \int_0^l \{ E_d I_d \cdot w_d'''' - q(x) \} dx + \\ - \int_0^{l_R^+} \{ H \cdot (w_d'' + b\vartheta_d'') + h^+(w_R) \cdot (y'' + w_d'' + b\vartheta_d'') \} dx + \\ - \int_0^{l_L^+} \{ H \cdot (w_d'' - b\vartheta_d'') + h^+(w_L) \cdot (y'' + w_d'' - b\vartheta_d'') \} dx \end{array} \right\} = 0 ;$$

$$\delta_{\vartheta_d} V = 0 \quad \forall \delta \vartheta_d \Leftrightarrow \left\{ \begin{array}{l} \int_0^l \{ E_d \Gamma_d \cdot \vartheta_d'''' - G_d J_d \cdot \vartheta_d'' - m(x) \} dx + \\ - \int_0^{l_R^+} b \{ H \cdot (w_d'' + b\vartheta_d'') + h^+(w_R) \cdot (y'' + w_d'' + b\vartheta_d'') \} dx + \\ - \int_0^{l_L^+} b \{ H \cdot (w_d'' - b\vartheta_d'') + h^+(w_L) \cdot (y'' + w_d'' - b\vartheta_d'') \} dx \end{array} \right\} = 0 ;$$

4.2 Slackening development

Let's consider just the linear components of the equations of motion adding the inertial terms.

$$\left\{ \begin{array}{l} \int_0^l \{ m_d \cdot \ddot{w}_d + E_d I_d \cdot w_d'''' - q(x, t) \} dx + \\ - \int_0^{l_R^+} \left\{ -m_c \cdot (\ddot{w}_d + b\ddot{\vartheta}_d) + H \cdot (w_d'' + b\vartheta_d'') - \int_0^{l_R^+} \frac{E_c A_c}{L_c} y''^2 (w_d + b\vartheta_d) dx \right\} dx + \\ - \int_0^{l_L^+} \left\{ -m_c \cdot (\ddot{w}_d - b\ddot{\vartheta}_d) + H \cdot (w_d'' - b\vartheta_d'') - \int_0^{l_L^+} \frac{E_c A_c}{L_c} y''^2 (w_d - b\vartheta_d) dx \right\} dx \end{array} \right\} = 0 ;$$

$$\left\{ \begin{array}{l} \int_0^l \{ J_t \ddot{\vartheta}_d + E_d \Gamma_d \cdot \vartheta_d'' - G_d J_d \cdot \vartheta_d'' - m(x, t) \} dx + \\ -b \int_0^{l_R^+} \left\{ -m_c \cdot (\ddot{w}_d + b \ddot{\vartheta}_d) + H \cdot (w_d'' + b \vartheta_d'') - \int_0^{l_R^+} \frac{E_c A_c}{L_c} y''^2 (w_d + b \vartheta_d) dx \right\} dx + \\ -b \int_0^{l_L^+} \left\{ -m_c \cdot (\ddot{w}_d - b \ddot{\vartheta}_d) + H \cdot (w_d'' - b \vartheta_d'') - \int_0^{l_L^+} \frac{E_c A_c}{L_c} y''^2 (w_d - b \vartheta_d) dx \right\} dx \end{array} \right\} = 0 ;$$

Let's write the forces and couples transmitted by the deck to the cables system, from initial to perturbed condition, and hence including the self-weight of the girder.

$$\bar{F}_d(t) = \int_0^l F_d(x, t) dx = \int_0^l \{ m_d \cdot g + q(x, t) - m_d \cdot \ddot{w}_d(x, t) - E_d J_d \cdot w_d''(x, t) \} dx ;$$

$$\bar{C}_d(t) = \int_0^l C_d(x, t) dx = \int_0^l \{ m(x, t) - J_t \cdot \ddot{\vartheta}_d(x, t) - E_d \Gamma_d \cdot \vartheta_d''(x, t) + G_d J_d(x) \cdot \vartheta_d''(x, t) \} dx ;$$

Notice that we assume that the deck has a symmetric section as usually happens in real structures, hence, before external actions initiate to work, the deck is able to transfer only a vertical static load to the cables system. This assumption would be relevant for further conclusions.

Taking in consideration the linear component of the equilibrium equation we can rewrite the previous relations as follows.

$$\bar{F}_d(t) = \int_0^l (m_d \cdot g) dx - \int_0^{l_R^+} \left\{ \begin{array}{l} -m_c \cdot (\ddot{w}_d + b \ddot{\vartheta}_d) + \\ + H \cdot (w_d'' + b \vartheta_d'') + \\ - \int_0^{l_R^+} \frac{E_c A_c}{L_c} y''^2 (w_d + b \vartheta_d) dx \end{array} \right\} dx - \int_0^{l_L^+} \left\{ \begin{array}{l} -m_c \cdot (\ddot{w}_d - b \ddot{\vartheta}_d) + \\ + H \cdot (w_d'' - b \vartheta_d'') + \\ - \int_0^{l_L^+} \frac{E_c A_c}{L_c} y''^2 (w_d - b \vartheta_d) dx \end{array} \right\} dx ;$$

$$\bar{C}_d(t) = -b \int_0^{l_R^+} \left\{ \begin{array}{l} -m_c \cdot (\ddot{w}_d + b \ddot{\vartheta}_d) + \\ + H \cdot (w_d'' + b \vartheta_d'') + \\ - \int_0^{l_R^+} \frac{E_c A_c}{L_c} y''^2 (w_d + b \vartheta_d) dx \end{array} \right\} dx - b \int_0^{l_L^+} \left\{ \begin{array}{l} -m_c \cdot (\ddot{w}_d - b \ddot{\vartheta}_d) + \\ + H \cdot (w_d'' - b \vartheta_d'') + \\ - \int_0^{l_L^+} \frac{E_c A_c}{L_c} y''^2 (w_d - b \vartheta_d) dx \end{array} \right\} dx ;$$

Notice that even if we are dealing with the only linear terms anyway the equations of motion are coupled due to the asymmetric response of the two main cables.

Let's pass to the dimensionless format. It's evident that though each cable has a different contribution due to different domains, the analytical expressions under integral sign are similar.

$$F_c^i(x, t) = \left\{ \begin{array}{l} -m_c \cdot (\ddot{w}_d \pm b \ddot{\vartheta}_d) + \\ + H \cdot (w_d'' \pm b \vartheta_d'') + \\ - \int_0^{l_i^+} \frac{E_c A_c}{L_c} y''^2 (w_d \pm b \vartheta_d) dx \end{array} \right\} = \left\{ \begin{array}{l} -m_c f \cdot \left(\frac{d^2 \tilde{w}_d}{dt^2} \pm \frac{d^2 \tilde{\vartheta}_d}{dt^2} \right) + \\ + H \frac{f}{l^2} \cdot (\tilde{w}_d'' \pm \tilde{\vartheta}_d'') + \\ - \frac{E_c A_c}{L_c} y''^2 f l \alpha_h^i \int_0^1 (\tilde{w}_d \pm \tilde{\vartheta}_d) d\xi \end{array} \right\} ;$$

Notice that we have introduced a new parameter representing the ratio between the contributions coming from the residual fraction of the span where the deck is still able to transfer forces and couples to the main cables, and the ideal condition without slackening. In general this fraction would be different for each side of the deck section, hence α^R refers to the right side and α^L to the left one.

$$\alpha_h^R = \int_0^{l_R^+} (w_d \pm \vartheta_d) dx / \int_0^l (w_d \pm \vartheta_d) dx ;$$

$$\alpha_h^L = \int_0^{l_L^+} (w_d \pm \vartheta_d) dx / \int_0^l (w_d \pm \vartheta_d) dx ;$$

Notice that the subscript refers to the cables tension increment and not to hangers response.

Other similar parameters allow us to get simpler expression for the previous definitions collecting all terms under the same integral sign.

$$\alpha_c^R = \int_0^{l_R^+} F_c^R(x, t) dx / \int_0^l F_c^R(x, t) dx ;$$

$$\alpha_c^L = \int_0^{l_L^+} F_c^L(x, t) dx / \int_0^l F_c^L(x, t) dx ;$$

In the following we will refer to these parameters and we will call them generally slackening parameters.

Hence substitution in the forces and couples expression lead to the following relations.

$$\bar{F}_d(t) = \int_0^l \left\{ m_d \cdot g - \alpha_c^R \cdot \begin{pmatrix} -m_c f \cdot \left(\frac{d^2 \tilde{w}_d}{dt^2} + \frac{d^2 \tilde{\vartheta}_d}{dt^2} \right) + \\ + H \frac{f}{l^2} \cdot (\tilde{w}_d'' + \tilde{\vartheta}_d'') + \\ - \frac{E_c A_c}{L_c} y''^2 f l \alpha_h^R \int_0^1 (\tilde{w}_d + \tilde{\vartheta}_d) d\xi \end{pmatrix} - \alpha_c^L \cdot \begin{pmatrix} -m_c f \cdot \left(\frac{d^2 \tilde{w}_d}{dt^2} - \frac{d^2 \tilde{\vartheta}_d}{dt^2} \right) + \\ + H \frac{f}{l^2} \cdot (\tilde{w}_d'' - \tilde{\vartheta}_d'') + \\ - \frac{E_c A_c}{L_c} y''^2 f l \alpha_h^L \int_0^1 (\tilde{w}_d - \tilde{\vartheta}_d) d\xi \end{pmatrix} \right\} dx ;$$

$$\bar{C}_d(t) = -b \int_0^l \left\{ \alpha_c^R \cdot \begin{pmatrix} -m_c f \cdot \left(\frac{d^2 \tilde{w}_d}{dt^2} + \frac{d^2 \tilde{\vartheta}_d}{dt^2} \right) + \\ + H \frac{f}{l^2} \cdot (\tilde{w}_d'' + \tilde{\vartheta}_d'') + \\ - \frac{E_c A_c}{L_c} y''^2 f l \alpha_h^R \int_0^1 (\tilde{w}_d + \tilde{\vartheta}_d) d\xi \end{pmatrix} + \alpha_c^L \cdot \begin{pmatrix} -m_c f \cdot \left(\frac{d^2 \tilde{w}_d}{dt^2} - \frac{d^2 \tilde{\vartheta}_d}{dt^2} \right) + \\ + H \frac{f}{l^2} \cdot (\tilde{w}_d'' - \tilde{\vartheta}_d'') + \\ - \frac{E_c A_c}{L_c} y''^2 f l \alpha_h^L \int_0^1 (\tilde{w}_d - \tilde{\vartheta}_d) d\xi \end{pmatrix} \right\} dx ;$$

Then introducing the definition of dimensionless time we can get the local format of the previous relations.

$$\tilde{F}_d(\xi, \tau) = \frac{F_d \cdot l^2}{Hf} = 16 \cdot \tilde{m}_d - \alpha_c^R \cdot \begin{pmatrix} -(1 - \tilde{m}_d) \cdot \left(\frac{d^2 \tilde{w}_d}{d\tau^2} + \frac{d^2 \tilde{\vartheta}_d}{d\tau^2} \right) + \\ + (\tilde{w}_d'' + \tilde{\vartheta}_d'') + \\ - \alpha_h^R \cdot \lambda_L^2 \int_0^1 (\tilde{w}_d + \tilde{\vartheta}_d) d\xi \end{pmatrix} - \alpha_c^L \cdot \begin{pmatrix} -(1 - \tilde{m}_d) \cdot \left(\frac{d^2 \tilde{w}_d}{d\tau^2} - \frac{d^2 \tilde{\vartheta}_d}{d\tau^2} \right) + \\ + (\tilde{w}_d'' - \tilde{\vartheta}_d'') + \\ - \alpha_h^L \cdot \lambda_L^2 \int_0^1 (\tilde{w}_d - \tilde{\vartheta}_d) d\xi \end{pmatrix} ;$$

$$\tilde{C}_d(\xi, \tau) = \frac{c_d \cdot l^2}{Hfb} = - \left\{ \alpha_c^R \cdot \left(\begin{array}{l} -(1 - \tilde{m}_d) \cdot \left(\frac{d^2 \tilde{w}_d}{d\tau^2} + \frac{d^2 \tilde{\vartheta}_d}{d\tau^2} \right) + \\ + (\tilde{w}_d'' + \tilde{\vartheta}_d'') + \\ - \alpha_h^R \cdot \lambda_L^2 \int_0^1 (\tilde{w}_d + \tilde{\vartheta}_d) d\xi \end{array} \right) + \alpha_c^L \cdot \left(\begin{array}{l} -(1 - \tilde{m}_d) \cdot \left(\frac{d^2 \tilde{w}_d}{d\tau^2} - \frac{d^2 \tilde{\vartheta}_d}{d\tau^2} \right) + \\ + (\tilde{w}_d'' - \tilde{\vartheta}_d'') + \\ - \alpha_h^L \cdot \lambda_L^2 \int_0^1 (\tilde{w}_d - \tilde{\vartheta}_d) d\xi \end{array} \right) \right\};$$

In order to define the new dimensionless term inside the vertical force component we need first to recall the initial equilibrium condition of cables under the self-weight of the deck.

$$-2Hy'' = (m_d + 2m_c) \cdot g \Rightarrow 2H \frac{8f}{l^2} = (m_d + 2m_c) \cdot g \Rightarrow H \frac{f}{l^2} = \frac{(m_d + 2m_c)}{16} \cdot g;$$

Consequently the following definitions for the dimensionless masses hold.

$$\tilde{m}_d = \frac{m_d}{(m_d + 2m_c)} = 1 - \frac{2m_c}{(m_d + 2m_c)} = 1 - 2\tilde{m}_c;$$

We choose to take the dimensionless mass of the deck as only variable since in literature is much more easy to find data referred to this parameter with respect to those of cables, for which when present is not in general clear if they refer to the single cable or to both of them.

Hence the critical conditions for the initiation of slackening correspond to those amplitude that induces negative forces and null couples in the cables system. Consequently hangers undergoes to slackening and the external actions cannot more be transfer from the stiffening girder to the main cables.

$$\tilde{F}_d(\xi, \tau) = 16 \cdot \tilde{m}_d + \tilde{C}_d(\xi, \tau) \leq 0;$$

$$\tilde{C}_d(\xi, \tau) = 0;$$

Notice that for the torsional couple the slackening condition is much more restrictive than for vertical forces since the cables system is able to sustain both positive and negative couples but only stretching forces. It's also evident that the two condition cannot be satisfied at the same time. This means that even if locally the hangers are no more able to transfer the vertical forces coming from the deck anyway are able to transfer couples, and vice versa.

The further step required is the exploitation of the modal expansion.

$$\tilde{w}_d(\xi, \tau) = \sum_{n=1}^{\infty} W_n(\xi) \cdot z_n(\tau) \quad \text{with } n \in \mathbb{N} \setminus \{0\};$$

$$\tilde{\vartheta}_d(\xi, \tau) = \sum_{m=1}^{\infty} \theta_m(\xi) \cdot \gamma_m(\tau) \quad \text{with } m \in \mathbb{N} \setminus \{0\};$$

It's evident that the actual formulation is too complex to be handled analytically. In fact the interaction between at least two modes, one vertical and the other torsional, requires to consider not only the superposition in space of the effect given by each mode but also in time. In fact each of them would have a proper circular frequency and phase lag that shift the response in time and make superposition of effects very complicate. Also numerical investigations are not so simple since the slackening parameters are a priori unknown, hence iterative methods are required.

In order to analyse simpler cases let's study separately the flexural and the torsional motion.

➤ Flexural vibrations:

As the torsional components becomes negligible the vertical slackening condition reduces to the following relation.

$$\tilde{F}_d(\xi, \tau) \leq 0 \Leftrightarrow 8 \cdot \tilde{m}_d + \alpha_c \cdot \left\{ (1 - \tilde{m}_d) \cdot \frac{d^2 \tilde{w}_d}{d\tau^2} - \tilde{w}_d'' + \alpha_h \cdot \lambda_L^2 \int_0^1 \tilde{w}_d d\xi \right\} \leq 0 ;$$

Is possible to consider a common slackening parameter because under pure vertical motions the contribution of each cable is equal, in fact is the torsional component that introduces asymmetry in the response of the cables.

Consequently the slackening parameters are equal on the two side of the bridge section and then the previous relation holds.

$$\alpha_c^R = \alpha_c^L \quad \text{and} \quad \alpha_h^R = \alpha_h^L ;$$

Notice that under pure flexural vibrations the torsional slackening condition simply requires that each cable contribution should be null. Albeit this the hangers system is still able to transfer vertical forces due to the initial stretch given by self-weight.

$$\tilde{C}_d(\xi, \tau) = 0 \Leftrightarrow \alpha_c \cdot \left\{ (1 - \tilde{m}_d) \cdot \frac{d^2 \tilde{w}_d}{d\tau^2} - \tilde{w}_d'' + \alpha_h \cdot \lambda_L^2 \int_0^1 \tilde{w}_d d\xi \right\} = 0 ;$$

➤ Torsional vibrations:

When only the asymmetric sectional motion occurs the slackening threshold reduces to the following equality.

$$\tilde{C}_d(\xi, \tau) = 0 \Leftrightarrow \alpha_c^R \cdot \left\{ (1 - \tilde{m}_d) \cdot \frac{d^2 \tilde{\vartheta}_d}{d\tau^2} - \tilde{\vartheta}_d'' + \alpha_h^R \cdot \lambda_L^2 \int_0^1 \tilde{\vartheta}_d d\xi \right\} = \alpha_c^L \cdot \left\{ (1 - \tilde{m}_d) \cdot \frac{d^2 \tilde{\vartheta}_d}{d\tau^2} - \tilde{\vartheta}_d'' + \alpha_h^L \cdot \lambda_L^2 \int_0^1 \tilde{\vartheta}_d d\xi \right\} ;$$

Can be rewritten in a more synthetic form.

$$(\alpha_c^R - \alpha_c^L) \cdot \left\{ (1 - \tilde{m}_d) \cdot \frac{d^2 \tilde{\vartheta}_d}{d\tau^2} - \tilde{\vartheta}_d'' \right\} = (\alpha_c^R \cdot \alpha_h^R - \alpha_c^L \cdot \alpha_h^L) \cdot \lambda_L^2 \int_0^1 \tilde{\vartheta}_d d\xi$$

It's evident that under pure torsional motion each cable response can be different from the other since the one characterised by a dominant upward motion will have lower slackening parameters.

$$\alpha_c^R \neq \alpha_c^L \quad \text{and} \quad \alpha_h^R \neq \alpha_h^L ;$$

As a consequence of this statement the cable system could have a net vertical contribution even if the hangers system is not able to transfer torsional moments. Once again this contribution is given by initial stretch given by self-weight.

$$\tilde{F}_d(\xi, \tau) \leq 0 \Leftrightarrow 16 \cdot \tilde{m}_d + \tilde{C}_d(\xi, \tau) \leq 0 ;$$

Hence it's now evident that the symmetry of the stiffening girder section avoids that both the conditions could be satisfied at the same time. Conversely an additional contribution to initial stretching given by the eccentricity of the deck centre of mass should be accidentally tuned in order to get that dangerous condition. Anyway this condition can occur also in the very unfortunate case in which some of the hangers break introducing an asymmetry in the cable system stiffness.

4.3 Slackening initiation

The presence of the slackening terms does not allow us to get further information on the problem. Hence before passing to numerical investigations is better to search for the threshold condition of slackening. This allows us to get analytical solutions of the following limit conditions without the need for defining any slackening parameters.

$$\tilde{F}_d(\xi, \tau) = 16 \cdot \tilde{m}_d + \tilde{C}_d(\xi, \tau) = 0 ;$$

$$\tilde{C}_d(\xi, \tau) = 0 ;$$

In fact up to the slackening initiation all the hangers are still taut, condition that allows us to integrate the cable system contribution on the whole length of the bridge's span.

$$\alpha_c^R = \alpha_c^L = 1 \quad \text{and} \quad \alpha_h^R = \alpha_h^L = 1 ;$$

Since some terms drop out thanks to the symmetry of the cables response is not sufficient to substitute the last two equalities into the slackening condition. Hence is necessary to reformulate the problem starting from the linear equations of motion found in the initial chapters where the flexural and torsional response are completely decoupled.

Hence let's write the forces and couples transmitted by the deck to the cables system.

$$F_d(x, t) = m_d \cdot g + q(x, t) - m_d \cdot \ddot{w}_d(x, t) - E_d I_d \cdot w_d''''(x, t) ;$$

$$C_d(x, t) = m(x, t) - J_t \cdot \ddot{\vartheta}_d(x, t) - E_d \Gamma_d \cdot \vartheta_d''''(x, t) + G_d J_d(x) \cdot \vartheta_d''(x, t) ;$$

Notice that this time is possible to get immediately the local values of the deck actions since we can collect both the contributions coming from the deck and the two cables under the same integral.

Replacing the deck contributions with those coming from the cable system we finally get the following relations.

$$F_d(x, t) = m_d \cdot g + 2m_c \cdot \ddot{w}_d(x, t) - 2H \cdot w_d''(x, t) - 2h_w \cdot y'' ;$$

$$C_d(x, t) = 2m_c b^2 \cdot \ddot{\vartheta}_d(x, t) - 2H b^2 \cdot \vartheta_d''(x, t) - 2h_\vartheta b \cdot y'' ;$$

Let's pass to the dimensionless format.

$$F_d(x, t) = m_d g + 2m_c f \frac{2H}{l^2(m_d+2m_c)} \cdot \frac{d^2 \tilde{w}_d}{d\tau^2}(\xi, \tau) - 2H \frac{f}{l^2} \cdot \tilde{w}_d''(\xi, \tau) + 2 \frac{E_c A_c}{L_c} y''^2 f l \int_0^1 \tilde{w}_d(\xi, \tau) d\xi ;$$

$$C_d(x, t) = 2m_c b^2 \frac{f}{b} \frac{2H}{l^2(m_d+2m_c)} \cdot \frac{d^2 \tilde{\vartheta}_d}{d\tau^2}(\xi, \tau) - 2H b^2 \frac{f}{b l^2} \cdot \tilde{\vartheta}_d''(\xi, \tau) + 2 \frac{E_c A_c}{L_c} y''^2 f l b \int_0^1 \tilde{\vartheta}_d(\xi, \tau) d\xi ;$$

Hence we get the dimensionless forces and couples transferred to the cables.

$$\tilde{F}_d(\xi, \tau) = F_d \cdot \frac{l^2}{2Hf} = m_d \frac{l^2}{2Hf} g + \frac{2m_c}{(m_d+2m_c)} \cdot \frac{d^2 \tilde{w}_d}{d\tau^2}(\xi, \tau) - \tilde{w}_d''(\xi, \tau) + \frac{E_c A_c}{H} \frac{l}{L_c} \left(\frac{8f}{l}\right)^2 \int_0^1 \tilde{w}_d(\xi, \tau) d\xi ;$$

$$\tilde{C}_d(\xi, \tau) = C_d \cdot \frac{l^2}{2Hbf} = \frac{2m_c}{(m_d+2m_c)} \cdot \frac{d^2 \tilde{\vartheta}_d}{d\tau^2}(\xi, \tau) - \tilde{\vartheta}_d''(\xi, \tau) + \frac{E_c A_c}{H} \frac{l}{L_c} \left(\frac{8f}{l}\right)^2 \int_0^1 \tilde{\vartheta}_d(\xi, \tau) d\xi ;$$

Again in order to define some dimensionless masses we need first to recall the initial equilibrium condition of cables under the self-weight of the deck. Consequently we obtain the same expressions for the deck and cables dimensionless masses previously defined.

Hence finally we get the conditions for slackening initiation.

$$\tilde{F}_d(\xi, \tau) = 8 \cdot \tilde{m}_d + (1 - \tilde{m}_d) \cdot \frac{d^2 \tilde{w}_d}{d\tau^2}(\xi, \tau) - \tilde{w}_d''(\xi, \tau) + \lambda_L^2 \tilde{h}_w = 0 ;$$

$$\tilde{C}_d(\xi, \tau) = (1 - \tilde{m}_d) \cdot \frac{d^2 \tilde{\vartheta}_d}{d\tau^2}(\xi, \tau) - \tilde{\vartheta}_d''(\xi, \tau) + \lambda_L^2 \tilde{h}_\vartheta = 0 ;$$

It's evident that with respect to previous more general conditions that get into the slackening domain thanks to some additional parameters, here the formulation is very much simpler.

The main reason is that the critical conditions are completely independent since they take trace just of the motion proper of the deck axis and not of the actual position of cables. This is a direct consequence of the fact that skew-symmetric some terms coming from cables torsional contributions drop out. Not all of them can vanish otherwise the cables system contribution to torsion would be null.

Hence we can have really two distinct critical conditions for slackening initiation; one associated to pure vertical and the second to pure torsional vibrations.

Let's now exploit the modal expansion of the actual structural response.

$$\tilde{F}_{d,n} = 8 \cdot \tilde{m}_d + \{(1 - \tilde{m}_d) W_n(\xi) \cdot \lambda_{w,n}^2 - W_n''(\xi) + \lambda_L^2 \tilde{h}_{w,n}\} \cdot Z_n e^{\lambda_{w,n} \tau} + c. c. ;$$

$$\tilde{C}_{d,m} = \{(1 - \tilde{m}_d) \Theta_m(\xi) \cdot \lambda_{\vartheta,m}^2 - \Theta_m''(\xi) + \lambda_L^2 \tilde{h}_{\vartheta,m}\} \cdot \Gamma_m e^{\lambda_{\vartheta,m} \tau} + c. c. ;$$

The following simple relations hold.

$$\lambda^2_{w,n} Z_n e^{\lambda_{w,n} \tau} + c.c. = \left\{ \begin{aligned} & (\alpha_{w,n}^2 - \tilde{\omega}_{w,n}^2 + i2\alpha_{w,n}\tilde{\omega}_{w,n})(Z_n^R + iZ_n^I)[\cos(\tilde{\omega}_{w,n}\tau) + i\sin(\tilde{\omega}_{w,n}\tau)] \cdot e^{\alpha_{w,n}\tau} + c.c. = \\ & = 2 \cdot \left\{ \begin{aligned} & [Z_n^R(\alpha_{w,n}^2 - \tilde{\omega}_{w,n}^2) - Z_n^I 2\alpha_{w,n}\tilde{\omega}_{w,n}] \cos(\tilde{\omega}_{w,n}\tau) + \\ & - [Z_n^I(\alpha_{w,n}^2 - \tilde{\omega}_{w,n}^2) + Z_n^R 2\alpha_{w,n}\tilde{\omega}_{w,n}] \sin(\tilde{\omega}_{w,n}\tau) \end{aligned} \right\} \cdot e^{\alpha_{w,n}\tau} = \\ & = Z_{n,1} \cos(\tilde{\omega}_{w,n}\tau + \varphi_{wn,1}) \cdot e^{\alpha_{w,n}\tau} \end{aligned} \right\};$$

$$Z_n e^{\lambda_{w,n} \tau} + c.c. = \left\{ \begin{aligned} & (Z_n^R + iZ_n^I)[\cos(\tilde{\omega}_{w,n}\tau) + i\sin(\tilde{\omega}_{w,n}\tau)] \cdot e^{\alpha_{w,n}\tau} + c.c. = \\ & = 2 \cdot \{Z_n^R \cos(\tilde{\omega}_{w,n}\tau) - Z_n^I \sin(\tilde{\omega}_{w,n}\tau)\} \cdot e^{\alpha_{w,n}\tau} = \\ & = Z_{n,2} \cos(\tilde{\omega}_{w,n}\tau + \varphi_{wn,2}) \cdot e^{\alpha_{w,n}\tau} \end{aligned} \right\};$$

Where we have defined the following vibrations amplitudes and phase lags.

$$Z_{n,1} = 2\sqrt{\{Z_n^R(\alpha_{w,n}^2 - \tilde{\omega}_{w,n}^2) - Z_n^I 2\alpha_{w,n}\tilde{\omega}_{w,n}\}^2 + \{Z_n^I(\alpha_{w,n}^2 - \tilde{\omega}_{w,n}^2) + Z_n^R 2\alpha_{w,n}\tilde{\omega}_{w,n}\}^2};$$

$$\tan(\varphi_{wn,1}) = \frac{Z_n^R(\alpha_{w,n}^2 - \tilde{\omega}_{w,n}^2) - Z_n^I 2\alpha_{w,n}\tilde{\omega}_{w,n}}{Z_n^I(\alpha_{w,n}^2 - \tilde{\omega}_{w,n}^2) + Z_n^R 2\alpha_{w,n}\tilde{\omega}_{w,n}};$$

$$Z_{n,2} = 2\sqrt{\{Z_n^R\}^2 + \{Z_n^I\}^2};$$

$$\tan(\varphi_{wn,2}) = \frac{Z_n^R}{Z_n^I};$$

Similar relations hold also for the torsional counterpart. Hence substituting in the general expression we can get the modal limit conditions.

$$\tilde{F}_{d,n} = 8 \cdot \tilde{m}_d + \left\{ \begin{aligned} & (1 - \tilde{m}_d)W_n(\xi) \cdot Z_{n,1} \cos(\tilde{\omega}_{w,n}\tau + \varphi_{wn,1}) + \\ & - (W_n''(\xi) - \lambda_L^2 \tilde{h}_{W,n}) \cdot Z_{n,2} \cos(\tilde{\omega}_{w,n}\tau + \varphi_{wn,2}) \end{aligned} \right\} \cdot e^{\alpha_{w,n}\tau};$$

$$\tilde{C}_{d,m} = \left\{ \begin{aligned} & (1 - \tilde{m}_d)\Theta_m(\xi) \cdot \Gamma_{m,1} \cos(\tilde{\omega}_{\vartheta,m}\tau + \varphi_{\vartheta m,1}) + \\ & - (\Theta_m''(\xi) - \lambda_L^2 \tilde{h}_{\Theta,m}) \cdot \Gamma_{m,2} \cos(\tilde{\omega}_{\vartheta,m}\tau + \varphi_{\vartheta m,2}) \end{aligned} \right\} \cdot e^{\alpha_{\vartheta,m}\tau};$$

It's evident that the general damped motion is more reliable but it doesn't allow to get analytical results in term of max admissible amplitude of vibrations due to the presence of the real exponential term that introduce phase lag and tune the vibrations.

Hence let's make a further assumption that is consider undamped vibrations. Consequently the time evolution of modes can be described by a simple trigonometric function with constant amplitude.

The previous limit conditions require just a slight modification, due to the following definitions.

$$\lambda_{w,n} = i\tilde{\omega}_{w,n} ;$$

$$\lambda_{\vartheta,m} = i\tilde{\omega}_{\vartheta,m} ;$$

Hence we get simpler critical conditions identical to that obtained by [5] for the only vertical component.

$$\tilde{F}_{d,n} = 8 \cdot \tilde{m}_d - \{(1 - \tilde{m}_d)\tilde{\omega}_{w,n}^2 \cdot W_n(\xi) + W_n''(\xi) - \lambda_L^2 \tilde{h}_{w,n}\} \cdot Z_n \cos(\tilde{\omega}_{w,n}\tau + \varphi_{wn}) = 0 ;$$

$$\tilde{C}_{d,m} = \{(1 - \tilde{m}_d)\tilde{\omega}_{\vartheta,m}^2 \cdot \Theta_m(\xi) + \Theta_m''(\xi) - \lambda_L^2 \tilde{h}_{\vartheta,m}\} \cdot \Gamma_m \cos(\tilde{\omega}_{\vartheta,m}\tau + \varphi_{\vartheta m}) = 0 ;$$

Now we are able to find out the critical flexural and torsional amplitude that is able to fix the limit between the linear response of the system and the non-linear one induced by hangers slackening.

Two observations have to be made.

First of all, since we are searching for a critical condition that has to be valid for any instant in the time domain, we can neglect the trigonometric terms. This corresponds to consider only the instant in which the trigonometric function reaches its maximum without tuning the amplitude.

Secondly, as a consequence of neglecting damping effects, the vibration response will be identical after any cycle. Since to do that has to pass by its symmetric configuration we must take the time dependent contributions in absolute value in order to consider the worst situation.

This is not sufficient since the cable's system contribution varies along the span, hence in order to catch the first point undergoing to slackening we must consider the one in correspondence of which the cable system contribution reaches its minimum, that in general corresponds to the one with the maximum displacement.

Hence the max antinode critical conditions can be found.

$$\tilde{F}_{d,n} = 0 \Leftrightarrow Z_{cr,n} = 8 \cdot \tilde{m}_d \cdot \min \left\{ |(1 - \tilde{m}_d)\tilde{\omega}_{w,n}^2 \cdot W_n(\xi) + W_n''(\xi) - \lambda_L^2 \tilde{h}_{w,n}|^{-1} \right\} ;$$

$$\tilde{C}_{d,m} = 0 \Leftrightarrow \Theta_m''(\xi) = \lambda_L^2 \tilde{h}_{\vartheta,m} - (1 - \tilde{m}_d)\tilde{\omega}_{\vartheta,m}^2 \cdot \Theta_m(\xi) ;$$

Notice that we are able to define a critical amplitude threshold just for the flexural vibration component. This is the main consequence of the fact that hangers are prestretched by a symmetric force given by deck self-weight. The absence of an asymmetry in the initial sectional configuration as already said avoids that both the critical conditions can occur at the same time, and drastically modifies the critical threshold condition. Consequently concerning the torsional limit, we can say that the cable system is no more able to sustain any torque in all the points where the deck reaches a critical warping independently on the actual max antinode rotation.

Since the antinode displacement varies its position along the span not only as different modes are taken into account but also tuning the structural parameters. Hence we can give a more general definition.

$$Z_n = \frac{Z_n(\bar{\xi}_a)}{W_n(\bar{\xi}_a)} \Rightarrow Z_{cr,n}(\bar{\xi}_a) = 8 \cdot \tilde{m}_d \cdot \min \left\{ \left| (1 - \tilde{m}_d) \tilde{\omega}_{w,n}^2 \cdot W_n(\xi) + W_n''(\xi) - \lambda_L^2 \tilde{h}_{w,n} \right|^{-1} \right\} \cdot W_n(\bar{\xi}_a);$$

Notice that even if we get an analytical expression for the flexural critical amplitude, there are two subcases for which the previous expression further simplifies.

These conditions are the cases of skew-symmetric modes and perfectly flat cable limit condition that grant a simple sinusoidal modal shape.

$$W_n(\xi) = \sin(\tilde{n}\pi\xi);$$

$$\tilde{\omega}_{w,n} = \tilde{n}\pi \cdot \sqrt{1 + \mu^2 \cdot (\tilde{n}\pi)^2};$$

Where the number of half-waves can be odd or even respectively for the two particular cases analysed.

Consequently the stiffening term vanishes and the flexural critical condition give us the following amplitude.

$$Z_{cr,n}(\bar{\xi}_a) = 8 \cdot \tilde{m}_d \cdot \min \{ (\tilde{n}\pi)^2 \cdot |(1 - \tilde{m}_d) \cdot (1 + \mu^2 \cdot (\tilde{n}\pi)^2) - 1| \cdot \sin(\tilde{n}\pi\xi) \}^{-1};$$

Hence.

$$Z_{cr,n}(\bar{\xi}_a) = \left\{ \frac{(\tilde{n}\pi)^2}{8} \cdot \left| \left(\frac{1}{\tilde{m}_d} - 1 \right) \cdot \mu^2 \cdot (\tilde{n}\pi)^2 - 1 \right| \right\}^{-1};$$

Before going into the numerical analysis we want to focus the attention on the fact that it's important to check the reliability of the results. In order to do that we will compute the modal participation parameter for the cables stiffening term associate to the actual critical flexural amplitude. Then we will consider acceptable only the amplitudes that grant a variation of the cables initial tension far enough from unity. The others results will be neglected since the fact that the stiffening term becomes comparable with the initial tension means that the slackening of hangers occurs at vibration amplitudes larger than that required for the slackening of the main cables. We can say a priori that this cannot happen for any amplitude in the case of sinusoidal modal shapes since the stiffening term vanishes anyway.

Hence since the critical amplitude is the maximum value that the vibration history will assume, let's write the tension increment associate to vertical vibrations as follows.

$$h_{w,cr} = \frac{H}{8} \lambda_L^2 \int_0^1 \tilde{w}_d(\xi, \tau) d\xi = \frac{H}{8} \lambda_L^2 \sum_{n=1}^{\infty} \int_0^1 W_n(\xi) d\xi \cdot z_n(\tau) = \frac{H}{8} \lambda_L^2 \sum_{n=1}^{\infty} \tilde{h}_{w,n} \cdot Z_{cr,n}(\bar{\xi}_a);$$

Or in term of the normalised participation parameters.

$$h_w = H \sum_{n=1}^{\infty} \frac{\lambda_L^2}{8} \int_0^1 P_{w,n}(\xi) d\xi \cdot \tilde{\omega}_{w,n}^2 D_{w,n}(\tau) = H \cdot \frac{1}{8} \sum_{n=1}^{\infty} h_{w,n} \cdot \tilde{\omega}_{w,n}^2 D_{w,n}(\tau);$$

First analyse the main feature of the antinode displacements associated to the first slackening of the flexural mode of order one.

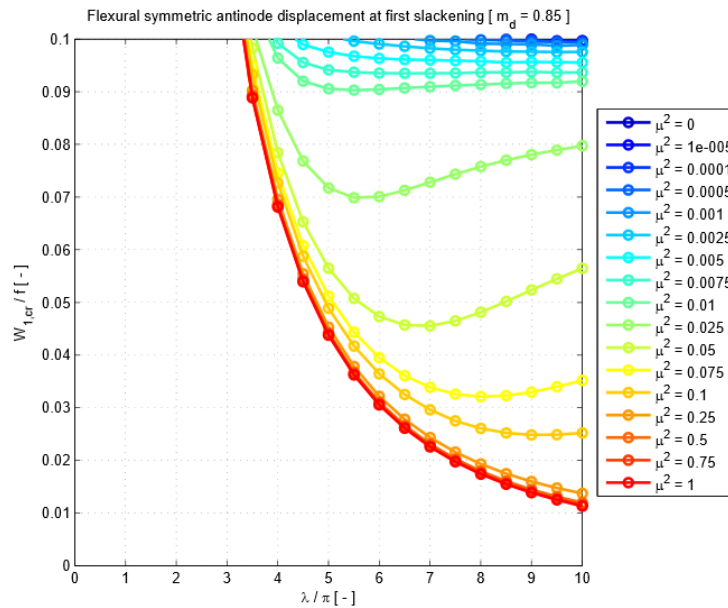


Figure 4.1_Antinode displacement at first slackening for flexural mode 1.

As we can see increasing the flexural deck stiffness requires higher antinode displacements for slackening onset. Whilst increasing the cables inextensibility we get decreasing limits only if the deck stiffness is enough stiff. In fact for values of μ^2 that are not too much high we get as λ_L^2 increases, first the slack displacement decreases and then increase tending to a horizontal asymptote.

Let's now compare the slackening amplitudes associated to modal shapes of different order considering the second one.

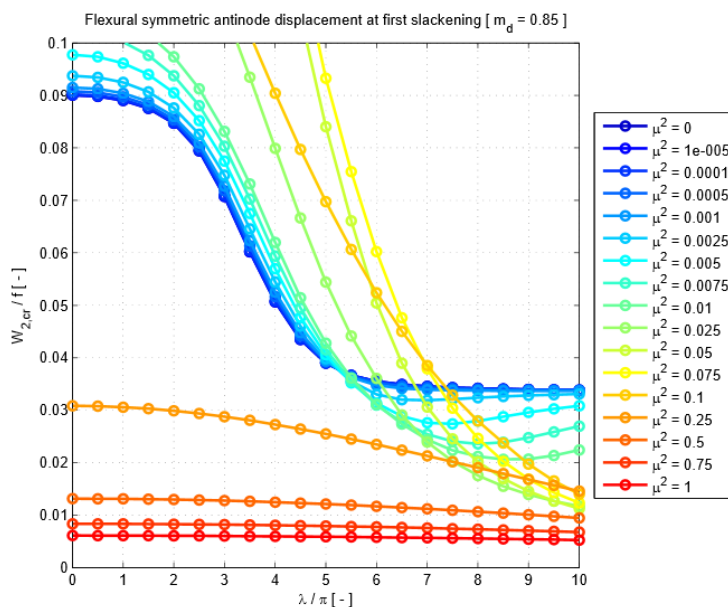


Figure 4.2_Antinode displacement at first slackening for flexural mode 2.

It's evident that slack amplitudes rapidly decreases as the modal order increases, since the moving upward regions extend to a larger part of the deck.

Further the variation of the slack displacements changes since become monotonically decreasing as λ_L^2 increases for $\mu^2 > 0.1$ whilst as μ^2 do we get can get an initial increase followed by a rapid reduction. Analyse the cable system tension increment for both the first and the second order mode.

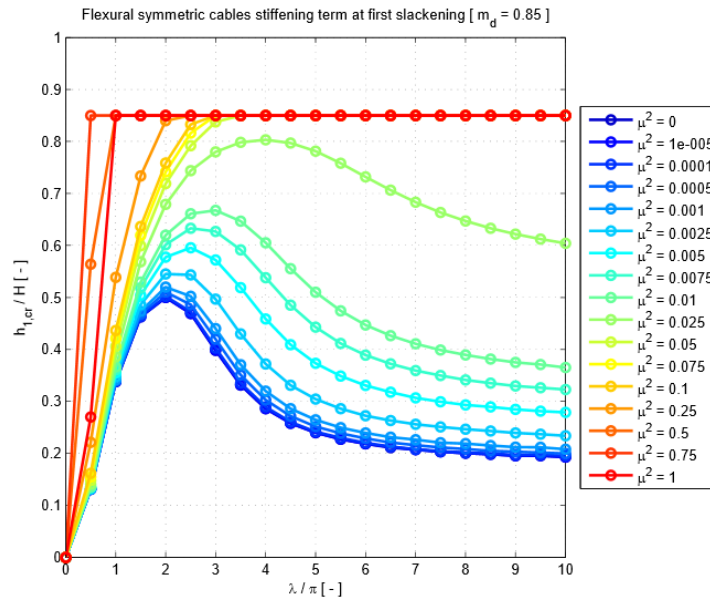


Figure 4.3_ Cable tension increment at first slackening for flexural mode 1.

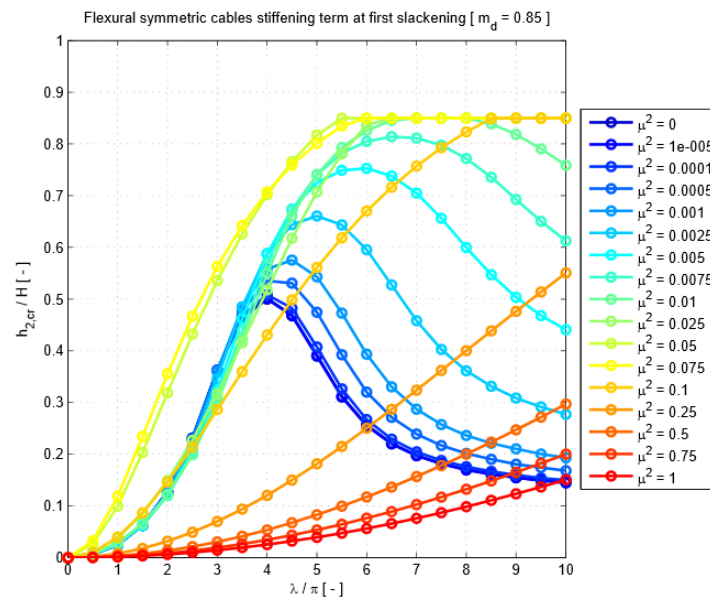


Figure 4.4_ Cable tension increment at first slackening for flexural mode 2.

In both the first and second mode we can recognise a similar behaviour, leading the cable tension to increase initially reaching a peak and then decreasing tending to a horizontal asymptote as the cables inextensibility increases. Whilst as the deck stiffness grows we get for the first case a monotonic increase of the slack flexural amplitude and for the second one a rapid decrease as $\mu^2 > 0.075$.

However the most important feature is the fact that the slack displacement has a fixed upper bound that can be reached only in correspondence of particular structural conditions. We observe that this upper value is always the same for any choice of the modal order and it coincides exactly with the dimensionless deck mass ($\tilde{m}_d = 0.85$) assumed. This fact not only can be easily explained but lead to an interesting conclusion.

Let's enforce the condition we have just observed for a generic mode.

$$h_{w,cr}/H = \frac{1}{8} \lambda_L^2 \cdot \tilde{h}_{W,n} \cdot Z_{cr,n} = \frac{\lambda_L^2 \cdot \tilde{h}_{W,n}}{\max\{[(1-\tilde{m}_d)\tilde{\omega}_{w,n}^2 \cdot W_n(\xi) + W_n''(\xi) - \lambda_L^2 \tilde{h}_{W,n}]\}} \cdot \tilde{m}_d$$

Hence.

$$h_{w,cr}/H = \tilde{m}_d \Leftrightarrow \max\{[(1-\tilde{m}_d)\tilde{\omega}_{w,n}^2 \cdot W_n(\xi) + W_n''(\xi) - \lambda_L^2 \tilde{h}_{W,n}]\} = \lambda_L^2 \cdot \tilde{h}_{W,n}$$

This condition generally can be satisfied only punctually for a particular choice of the structural parameters that are a priori unknowns. However the positions where this condition holds are certainly the two ends of the deck, where due to the particular boundary conditions assumed both the inertial and curvature contributions vanish.

Let's analyse the modal shape of second order and a particular structural condition, decoupling the total force transmitted to the cable system into the inertial $((1-\tilde{m}_d)\tilde{\omega}_{w,n}^2 \cdot W_n(\xi))$, curvature $(W_n''(\xi))$ and stiffening $(\lambda_L^2 \cdot \tilde{h}_{W,n})$ contributions.

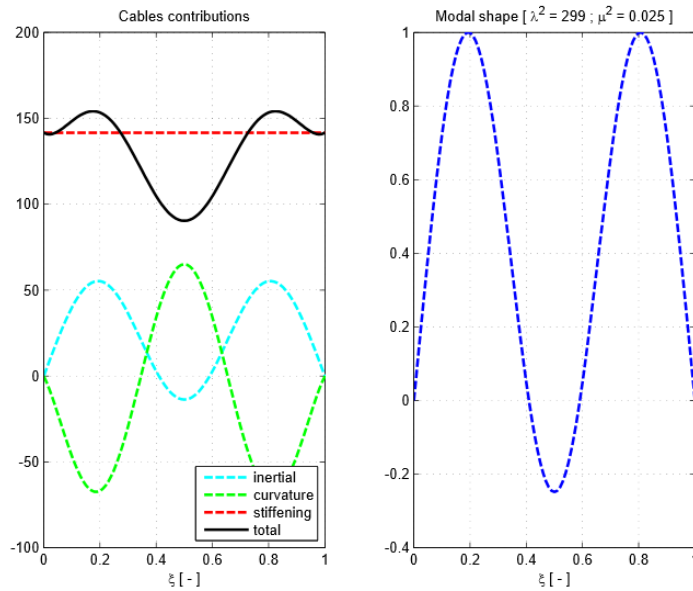


Figure 4.5_Deck to cables forces before critical conditions.

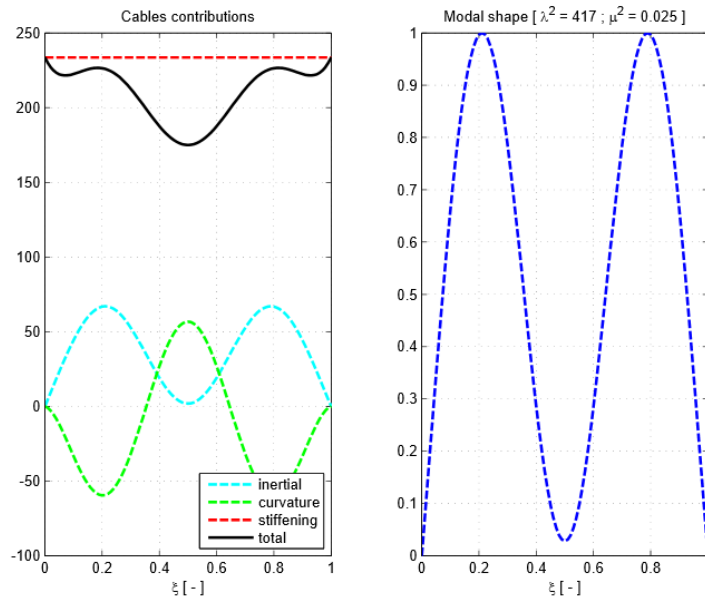


Figure 4.6_ Deck to cables forces after critical conditions.

Assuming λ_L^2 as the variable parameter we can say that as it is below a limit critical value the slackening condition occurs in a generic position inside the deck span that varies as λ_L^2 does. On the contrary as the Irvine parameter exceeds a critical upper bound the hangers will initiate to slack in correspondence of the two extreme sections of the deck for any further increase of λ_L^2 , since the maximum force transmitted from the deck to the cables will be always in correspondence of that position. However in correspondence of higher deck stiffness we can get a secondary critical condition for which the slackening returns to initiate in along the span of the bridge.

The critical condition for the actual condition analysed can be sketched as follows.

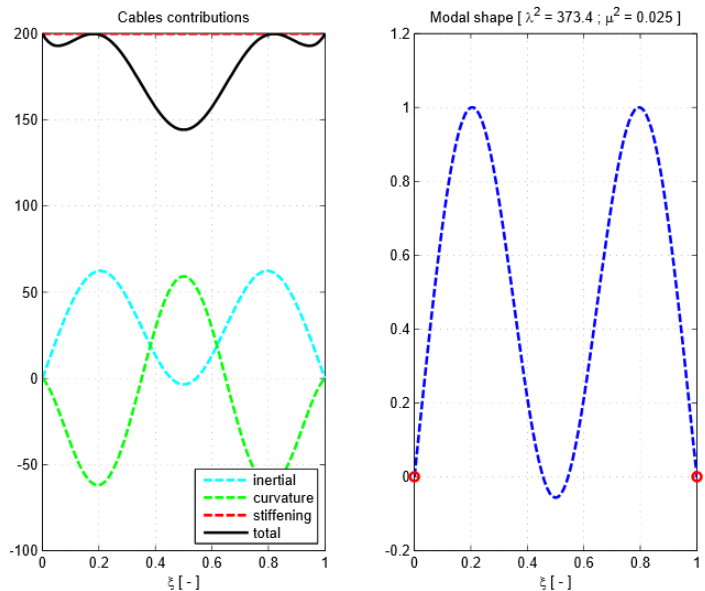


Figure 4.7_ Critical condition for slackening initiation.

Since in real life bridges the central span is supported by the pylons at the two extremities, the results just obtained simply state that there exist some particular structural conditions such that slackening initiation cannot occur.

But this statement can be misleading since increasing further the antinode displacement the regions immediately near the deck ends will slack since the curves representing the total deck to cable forces undergoes simply to an homothetic amplification. Hence it's better to say that there exist particular structural conditions such that hangers start to slack in the neighbourhood of pylons.

However we can say that these are extreme conditions that real life bridges do not perform. Further increasing the modal order this condition will disappear.

5. Aeroelastic model

Once we have deeply analysed the structural response of the bridge alone we want to study the effects that wind forces may have on such a slender structure. Hence we will analyse the so called wind-structure interaction and its effects on the linear eigen-properties of the model.

5.1. Fluid dynamics tools

Consider the unsteady motion of a fluid consisting of a single substance (to exclude mixtures and chemical reactions) characterized by fundamental unknown properties such as speed u , density ρ and pressure P variables with regularity in space and time. For simplicity, we assume that a negligible dynamic viscosity characterizes the fluid.

$$\mu = \rho\nu \cong 0 ;$$

Fixed, in an inertial reference system, the position of a reference finite volume V and the corresponding surface of the closed contour S is possible to write the fundamental equations that govern the dynamics of the flow.

5.1.1. Conservation of mass

Mathematically translates the absence of wells or springs of mass of the fluid in the domain V considered, equating the rate of change of the mass of fluid in the reference volume and the net flow of the incoming fluid through the border S .

$$\int_V \frac{\partial \rho(\vec{r}, t)}{\partial t} dV = - \oint_S \rho(\vec{r}, t) \vec{u}(\vec{r}, t) \cdot \hat{n}(\vec{r}) dS ;$$

Applying the divergence theorem turns the surface integral into a volume one, so it is useful to introduce the operator Nabla allowing a concise notation operators gradient, divergence and curl.

$$\vec{\nabla} = \left(\frac{\partial}{\partial x} \quad \frac{\partial}{\partial y} \quad \frac{\partial}{\partial z} \right)^T ;$$

$$grad(s) = \vec{\nabla} s ;$$

$$div(\vec{v}) = \vec{\nabla} \cdot \vec{v} ;$$

$$rot(\vec{v}) = \vec{\nabla} \times \vec{v} ;$$

$$\int_V \left[\frac{\partial \rho}{\partial t} + \vec{\nabla} \cdot (\rho \vec{u}) \right] dV = 0 ;$$

Because of the arbitrariness of the control volume chosen, we can express the equation in a local form.

$$\frac{\partial \rho}{\partial t} + \vec{\nabla} \cdot (\rho \vec{u}) = 0 ;$$

Note that the notation "continuity equation" can be misleading because the equation of conservation of mass is also valid when the speed and / or density are discontinuous functions.

5.1.2. Conservation of momentum

From the fundamental law of dynamics (Newton's second law) for inertial systems is possible to match the rate of change of momentum in the volume V with the resultant of the forces acting on it (mainly the force of gravity) and on its surface S (pressure alone, having assumed negligible viscosity of the fluid).

$$\int_V \frac{\partial(\rho \vec{u})}{\partial t} dV = - \oint_S \rho \vec{u} * (\vec{u} \cdot \hat{n}) dS - \oint_S P \hat{n} dS + \int_V \rho \vec{g} dV ;$$

Where the * operator indicates that the operation must be performed for each component of the vector in separate equations along the three Cartesian directions.

Let's transform the surface integrals into volume ones for both vector and scalar quantities respectively using the divergence and the gradient theorems. Pay attention to the fact that we cannot apply directly the divergence theorem to a vector quantity. Therefore, it is necessary to consider separately each Cartesian component of $\rho \vec{u}$ and only finally add vectorially the different contributions.

$$\oint_S \rho u_i (\vec{u} \cdot \hat{n}) dS = \int_V \vec{\nabla} \cdot (\rho u_i \vec{u}) dV = \int_V [\rho \vec{u} \cdot \vec{\nabla} u_i + u_i \vec{\nabla} \cdot (\rho \vec{u})] dV ;$$

$$\oint_S \rho \vec{u} * (\vec{u} \cdot \hat{n}) dS = \int_V [\rho (\vec{u} \cdot \vec{\nabla}) * \vec{u} + \vec{u} * \vec{\nabla} \cdot (\rho \vec{u})] ;$$

Developing the time derivative and substituting the equation of conservation of mass will simplify some terms.

$$\int_V \left\{ \begin{array}{l} \rho \frac{\partial \vec{u}}{\partial t} + [\vec{u} \frac{\partial \rho}{\partial t} + \vec{u} * \vec{\nabla} \cdot (\rho \vec{u})] + \\ + \rho (\vec{u} \cdot \vec{\nabla}) * \vec{u} + \vec{\nabla} P - \rho \vec{g} \end{array} \right\} dV = \int_V \left\{ \rho \frac{\partial \vec{u}}{\partial t} + \rho (\vec{u} \cdot \vec{\nabla}) * \vec{u} + \vec{\nabla} P - \rho \vec{g} \right\} dV = 0 ;$$

Exploiting the arbitrariness of V and collecting ρ , we obtain a partial differential equation, which appears to be non-linear due to the presence of the quadratic term $(\vec{u} \cdot \nabla) \vec{u}$ and the presence of the unknown variable ρ in the denominator.

$$\frac{\partial \vec{u}}{\partial t} + (\vec{u} \cdot \vec{\nabla}) * \vec{u} + \frac{\nabla P}{\rho} = \vec{g};$$

5.1.3. Conservation of total energy

The unknowns of the problem are two scalar quantity $\rho(\vec{r}, t)$, $P(\vec{r}, t)$ and a vector one $\rho(\vec{r}, t)$. Hence to solve the problem in closed form is necessary to introduce an additional scalar equation representing the balance of the total energy in the fluid volume.

This equation is a function of two additional unknowns, namely the temperature $T(\vec{r}, t)$ and internal energy $e(\vec{r}, t)$. Therefore, it is necessary to introduce two state equations to express the pressure and the temperature as a function of internal energy and density. These expressions vary according to the thermodynamic properties of the fluid under consideration.

Neglecting the viscosity of the fluid can simplify the equation of energy balance since the contribution to the internal energy coming from the viscous friction vanishes. In addition to its introduction would require a special formulation of the stress-strain relation, which for Newtonian fluids (in which the relationship involves first derivatives of the speed) results in the model proposed by Stokes.

5.1.4. Inviscid incompressible flows

The condition of incompressibility imposes an external constraint on the velocity field that should prove to be solenoidal at each instant in each point of the domain.

$$\vec{\nabla} \cdot \vec{u} = 0;$$

It is interesting to observe the consequences of this hypothesis when applied to the equation of mass balance.

$$\frac{\partial \rho}{\partial t} + \vec{u} \cdot \vec{\nabla} \rho = 0;$$

The above expression is an equation of mass transport per unit volume (namely ρ). Consequently, only in the particular case where the initial density of the fluid is uniformly distributed in the entire control volume, it is possible to assume $\rho(\vec{r}, t) = \bar{\rho} = \text{const}$ as a solution of the equation. Otherwise, the density variation in time and space is defined by the equation itself.

Therefore, it is important to underline the fact that the condition of incompressibility is an external constraint that cannot be interpreted as an alternative equation of the mass balance. Should not mislead the fact that it is possible to derive the condition of the solenoidal field motion writing the mass balance with the condition that the density of the fluid is always and everywhere constant. In fact, the latter constraint is related to a physical property of the fluid, then turns out to be an unacceptable forcing if imposed a priori. Therefore, only when the flow is incompressible and with uniform density is permissible to refer to a fluid characterized by constant density.

The equations that govern the motion of an inviscid incompressible flow with uniform density are called "Euler equations for incompressible currents". They bind the balance of momentum to the condition of incompressibility.

$$\frac{\partial \vec{u}}{\partial t} + (\vec{u} \cdot \vec{\nabla}) * \vec{u} + \frac{\vec{\nabla} P}{\rho} = \vec{g};$$

$$\vec{\nabla} \cdot \vec{u} = 0;$$

Key aspect is that, in order to satisfy the additional constraint of incompressibility disappears the dependence of the solution of the problem by thermodynamics, expressed by the equation of energy balance and state equations. Consequently, it is distorted the original meaning of the pressure and the one that appears in the equation of momentum balance is not a function of temperature and density of the fluid. In fact, it simply represents the Lagrange multiplier associated with the constraint of incompressibility, which allows solving the system of four equations (otherwise indeterminate considering only three Cartesian components of the velocity). Therefore, the system of Euler equations refers exclusively to an ideal fluid whose viscosity and thermal conductivity are negligible (to be distinguished from the perfect gas, whereby the pressure keeps its thermodynamics valence, persisting the relation $P = \rho RT$).

Therefore, although the model of incompressible flow is completely unrealistic, because it loses the physical meaning of the fluid pressure, for low flow velocity that model is able to represent adequately accurate prediction of experimental results. Usually to verify the validity of the previous finding refers to the Mach number that expresses the ratio between the average velocity of the flow and that of sound (in the same fluid at rest and in thermodynamic standard conditions).

$$Ma := \frac{U}{c} < 0.3 ;$$

In general, the speed that can be achieved respecting the condition of incompressibility are high enough to make a reasonable approximation of inviscid fluid. In fact, for Reynolds numbers high enough you can focus all the effects of viscosity in a very thin fluid layer at the interface with solid walls, said Viscous Boundary Layer. In this way, the flow can be studied separately in the area of the boundary layer and in that away from it, respectively, with suitable laws of the wall and through the Euler equations.

$$Re := \frac{\rho U D}{\mu} = \frac{U D}{\nu} ;$$

Euler equations containing partial derivatives both temporal and spatial, therefore, to determine fully the unknowns of the problem (speed and pseudo-fluid pressure) is necessary to provide appropriate initial and boundary conditions.

Respectively express the distribution of the velocity field at the initial time in each point of the control volume and the distribution of the normal component to the surface S of the domain at any time subsequent to the initial one.

$$\vec{u}(\vec{r}, 0) = \vec{u}_0(\vec{r}) ;$$

$$\vec{u}(\vec{r}_S, t) \cdot \hat{n} = \vec{u}_n(\vec{r}_S, t) ;$$

It 'important to note that it is possible to impose a condition solely on the normal component of the velocity at the boundary, because, from the hypothesis of inviscid flow, the tangential component is free to assume any distribution. Therefore, it is good to note that the speed should not be forced to be orthogonal to the boundary. In fact, in the case where the contour represents a still and waterproof wall, holds $\vec{u}_n(\vec{r}_S, t) = 0$, so the only motion granted to the flow is to slip on the solid surface.

It highlights the fact that you have not set any conditions on the initial pseudo-pressure, because it lacks the time dependence in the condition of incompressibility.

The fact that the couple $\vec{u}(\vec{r}, t)$ and $P(\vec{r}, t) + C(t)$ represents a complete solution to the problem for any choice of the arbitrary function $C(t)$ is a consequence of the fact that the flow is incompressible and that the normal component of the velocity is prescribed on the entire contour of the reference volume. In purely mathematical terms it is observed that in the system of equations never appears directly the pseudo-pressure but only the gradient, therefore, the form taken by the flow field is irrelevant. This condition is typical in the current confined in which the flow is completely contained within impermeable and rigid walls.

From the thermodynamic point of view it would have drastic consequences if the pressure field was defined up to a reference value variable in time. In fact, it would introduce arbitrary variations of the absolute pressure that strongly affects all the physical characteristics of the fluid. This is one more reason to exclude from any thermodynamic consideration the pressure that appears in the Euler equations and consider it as a simple additional variable of little physical meaning.

On the other hand, in the case of open flows is necessary to specify the pressure distribution on the boundary portion in which is not indicated any condition on the normal speed. In this way, in the governing equations appears directly a pressure value that is taken as a reference for every moment after the initial one, so that the distribution appears uniquely defined.

The presence of the incompressibility constraint must also be met by the initial and boundary conditions, which implies a direct link between the two.

$$\vec{\nabla} \cdot \vec{u}_0(\vec{r}_S) = 0;$$

$$\vec{u}_0(\vec{r}_S) \cdot \hat{n} = \vec{u}_n(\vec{r}_S, 0);$$

The fact that the flow field is solenoidal has not only local effects as observed so far. In fact, it is possible to impose a condition of global compatibility on the entire border.

$$\int_S \vec{u}(\vec{r}_S, t) \cdot \hat{n} dS = \int_V \vec{\nabla} \cdot \vec{u}(\vec{r}, t) dV = 0 \Rightarrow \int_S \vec{u}_n(\vec{r}_S, t) dS = 0;$$

In the case in which the external force field \vec{g} is conservative, it's possible to express it as the gradient of the corresponding potential ϵ . In the particular case where ϵ represents the action of gravitation per unit volume of fluid, it is possible to write the equation of momentum balance, in the formulation of Euler, in function of the known "Bernoulli's Trinomio".

$$\vec{\nabla}(\vec{a} \cdot \vec{b}) = \vec{a} \times \vec{\nabla} \times \vec{b} + \vec{b} \times \vec{\nabla} \times \vec{a} + (\vec{a} \cdot \vec{\nabla}) * \vec{b} + (\vec{b} \cdot \vec{\nabla}) * \vec{a};$$

$$\vec{a} = \vec{b} = \vec{u} \Rightarrow \frac{\vec{\nabla}(|u|^2)}{2} = \vec{u} \times \vec{\nabla} \times \vec{u} + (\vec{u} \cdot \vec{\nabla}) * \vec{u} \Rightarrow (\vec{u} \cdot \vec{\nabla}) * \vec{u} = \frac{\vec{\nabla}(|u|^2)}{2} - \vec{u} \times \vec{\nabla} \times \vec{u} = \frac{\vec{\nabla}(|u|^2)}{2} - (\vec{\nabla} \times \vec{u}) \times \vec{u};$$

$$\frac{\partial \vec{u}}{\partial t} + (\vec{u} \cdot \vec{\nabla}) * \vec{u} + \frac{\vec{\nabla} \tilde{p}}{\rho} = \vec{g} \Rightarrow \frac{\partial \vec{u}}{\partial t} + (\vec{\nabla} \times \vec{u}) \times \vec{u} + \vec{\nabla} \left(\frac{\tilde{p}}{\rho} + \frac{|u|^2}{2} \right) = \vec{g};$$

$$\vec{g} = -g\hat{z} \Rightarrow \vec{\nabla} \epsilon = -\vec{\nabla}(gz) \Rightarrow \epsilon = -g \Rightarrow \frac{\partial \vec{u}}{\partial t} + (\vec{\nabla} \times \vec{u}) \times \vec{u} = -\vec{\nabla} H;$$

$$H := \frac{\tilde{p}}{\rho} + \frac{|u|^2}{2} + g;$$

5.1.5. Potential flows

By definition, the rotor of the velocity field of a flow is said vorticity field.

$$\vec{\omega} := \vec{\nabla} \times \vec{u};$$

This magnitude represents a local index than a fluid particle is rotating around its own axis (it can be shown that the vorticity is exactly equal to twice the angular velocity). However, we must not think that flows characterized by current lines (lines tangent to the velocity field) curved are associated to values of the local vorticity always different from zero, or vice versa it is possible that rectilinear current lines have not null vorticity. Therefore, there is no link between the intensity of the vorticity and shape of the field lines of current flow.

By definition of vorticity can immediately rewrite the Euler equation of balance of momentum.

$$\frac{\partial \vec{u}}{\partial t} + \vec{\omega} \times \vec{u} = -\vec{\nabla} \tilde{H};$$

$$\tilde{H} := \frac{\tilde{p}}{\rho} + \frac{|\vec{u}|^2}{2} + \epsilon;$$

The application of the rotor and a simple mathematical identity allows to obtain the so-called "equation of vorticity" in which disappears the dependence from the pressure field.

$$\vec{\nabla} \times (\vec{a} \times \vec{b}) = \vec{a} * \vec{\nabla} \cdot \vec{b} - \vec{b} * \vec{\nabla} \cdot \vec{a} - (\vec{a} \cdot \vec{\nabla}) * \vec{b} + (\vec{b} \cdot \vec{\nabla}) * \vec{a};$$

$$\vec{a} = \vec{\omega}; \vec{b} = \vec{u} \Rightarrow \vec{a} * \vec{\nabla} \cdot \vec{b} = 0; \vec{b} * \vec{\nabla} \cdot \vec{a} = 0 \Rightarrow \vec{\nabla} \times (\vec{\omega} \times \vec{u}) = -(\vec{\omega} \cdot \vec{\nabla}) * \vec{u} + (\vec{u} \cdot \vec{\nabla}) * \vec{\omega};$$

$$\vec{\omega} \times \left(\frac{\partial \vec{u}}{\partial t} + \vec{\omega} \times \vec{u} \right) = \vec{\omega} \times (-\vec{\nabla} \tilde{H}) \Rightarrow \frac{\partial \vec{\omega}}{\partial t} + \vec{\nabla} \times (\vec{\omega} \times \vec{u}) = 0 \Rightarrow \frac{\partial \vec{\omega}}{\partial t} + (\vec{u} \cdot \vec{\nabla}) * \vec{\omega} = (\vec{\omega} \cdot \vec{\nabla}) * \vec{u};$$

The last expression is a transport equations of vorticity and allows you to translate on the fly an additional external constraint that you can force the flow. In fact, the vanishing of the vorticity at the initial time of each particle of the fluid is an index of irrotational motion field at each point of the domain and for each subsequent instant.

$$\vec{\omega}_0 = 0 \Rightarrow \vec{\nabla} \times \vec{u} = \vec{0};$$

This is a direct consequence of the fact that we are neglecting the viscosity of the fluid, which is the only mechanism that allows the transfer of vorticity between particles. Therefore, we can say that in the presence of external conservative forcing also the vorticity is conserved.

In reality, this statement is valid even in the viscous fluid flows provided they are not in contact with any solid wall, where it generates the large part of vorticity, and speed ensures a Reynolds number sufficiently high, to neglect the viscosity of the flow far from the wall.

In any case, it is a condition very useful because it allows extending the irrotational uniform flow condition, which typically it's assumed to come from infinity, in the neighbourhood of the body that is immersed, where the motion field loses its uniformity and nothing guarantees a priori the vanishing of its rotor.

Substituting this condition in the formulation of Euler under the assumption of conservative forces field is further simplifies the equation of momentum balance.

$$\frac{\partial \vec{u}}{\partial t} = -\vec{\nabla} \left(\frac{\tilde{p}}{\rho} + \frac{|\vec{u}|^2}{2} + \epsilon \right);$$

$$\vec{\nabla} \cdot \vec{u} = 0;$$

$$\vec{\nabla} \times \vec{u} = \vec{0};$$

It is noted that having considered a generic conservative force field, it is not possible to introduce the definition of Bernoulli's Trinomio H, only valid for the gravitational forces field.

An irrotational velocity field, in the particular case where the domain considered is simply connected, is definitely conservative, therefore, is expressed by the gradient of a scalar function called "Kinetic Potential".

$$\vec{u} = \vec{\nabla}\phi ;$$

The main advantage of this change of variables is mainly because from an unknown three-component vector we switch to a single scalar one. The price to pay is the increase of the order of the system of solving equations by one point.

In fact, the condition of incompressibility is transformed into the homogeneous Laplace equation, a second order partial derivatives equation.

$$\vec{\nabla} \cdot \vec{u} = \vec{\nabla} \cdot \vec{\nabla}\phi = 0 \Rightarrow \nabla^2\phi = 0 ;$$

The full definition of the solution requires suitable boundary conditions, which result in only Neumann condition on normal gradient at each point of the border.

$$\vec{u}(\vec{r}_S, t) \cdot \vec{n} = \vec{\nabla}\phi(\vec{r}_S, t) \cdot \vec{n} = \vec{u}_n(\vec{r}_S, t) \Rightarrow \frac{\partial\phi(\vec{r}_S, t)}{\partial n} = \vec{u}_n(\vec{r}_S, t) ;$$

Consequently, the system of two scalar equations is said "Neumann problem" and is harmonic, i.e. an elliptic problem in the particular case in which the governing equation is homogeneous.

Since the boundary condition is time-variant, we have at every moment a different problem. Therefore, the temporal evolution of $\phi(\vec{r}, t)$ and of all quantities dependent from it, are closely dominated by the instantaneous distribution of the normal speed at the border of the domain.

The expression of the condition of global compatibility entire boundary of the domain does not undergo formal changes.

$$\int_S \vec{u}_n(\vec{r}_S, t) dS = 0;$$

This condition guarantees the existence of the solution but not its uniqueness. In fact, similarly to what said for the pseudo-pressure, also the kinetic potential of the resulting solution of the Neumann problem is defined up to an arbitrary function of time, in consequence of the fact that in the equations always appears with at least one derivative of order greater than the first. But even in this case the velocity field is unique because it is not affected by this under determination being dependent on the gradient of the kinetic potential. This explains why it was not necessary to impose any conditions of Dirichlet for the distribution of the potential on the boundary of the domain.

Once that has been calculated, the function $\phi(\vec{r}, t)$ can be defined separately both the velocity field that the distribution of pressure. In fact, the momentum balance equation can be also written as a function only of the kinetic potential.

$$\frac{\partial(\vec{\nabla}\phi)}{\partial t} = -\vec{\nabla}\left(\frac{\tilde{p}}{\rho} + \frac{|\vec{\nabla}\phi|^2}{2} + \epsilon\right) \Rightarrow \vec{\nabla}\left(\frac{\partial\phi}{\partial t} + \frac{\tilde{p}}{\rho} + \frac{|\vec{\nabla}\phi|^2}{2} + \epsilon\right) = 0 \Rightarrow \frac{\partial\phi}{\partial t} + \frac{\tilde{p}}{\rho} + \frac{|\vec{\nabla}\phi|^2}{2} + \epsilon = C(t) ;$$

The equation just determined expresses the so-called "Bernoulli theorem for non-stationary irrotational potential flows" and allows to derive directly at each instant the pressure at any point of the domain simply by knowing $\phi(\vec{r}, t)$

It concludes by emphasizing the fact that the introduction of the kinetic potential is granted only when you disappear from the equation of momentum balance the nonlinear term $\vec{\omega} \times \vec{u} = (\vec{\nabla} \times \vec{u}) \times \vec{u}$. This allows to completely decoupling the determination of the velocity field from the pressure one.

Consequently to the fact that the problem is completely dependent on one scalar function $\Phi(\vec{r}, t)$ it is called "flow potential" but we must remember the basic assumptions that lie behind this concise definition.

- unsteady flow;
- inviscid fluid;
- incompressible flow in uniform density;
- irrotational velocity field;
- conservative force field;
- domain simply connected;

5.1.6. Multi connected domains

Effectively the need to have a simply connected domain is a forcing difficult to find in many problems of interest for applications in which is interesting to analyse the interaction of the flow with an immersed body. In fact, when the axial extent of a cylindrical body is much larger than its size in cross section, it is reasonable to consider a sectional model of the body, for simplicity assumed infinitely extended. This way we can be traced back to the condition of the planar motion but you lose the domain mono- connectivity.

For this purpose we introduce a new quantity called "Circulation" representative of the circulation of the velocity field along a closed path entirely contained in the fluid domain.

$$\Gamma := \oint_{\partial S} \vec{u}(\vec{r}, t) \cdot \hat{t} ds = \oint_{\partial S} \vec{u}(\vec{r}, t) \cdot d\vec{r};$$

There is a close link between circulation and vorticity that can be expressed using the Stokes theorem of the rotor, which allows you to switch from the integral of line to that on the surface that the closed path borders and within which the flow field is defined and regular. It stresses the importance of having a regular domain (no singularity) in order to apply the above theorem.

$$\oint_{\partial S} \vec{u}(\vec{r}, t) \cdot d\vec{r} = \int_S \vec{\nabla} \times \vec{u} \cdot \hat{n} dS \Rightarrow \Gamma = \int_S \vec{\omega} \cdot \hat{n} dS ;$$

Therefore, in order to be able to express the velocity field in terms of the gradient of a potential, the vanishing of vorticity in the whole domain is a sufficient condition, as can be deduced from the second equation written, equivalent to the condition of conservative field.

$$\vec{\omega} = \vec{0} \Rightarrow \Gamma = 0 \Rightarrow \oint_{\partial S} \vec{u}(\vec{r}, t) \cdot d\vec{r} = 0 \Rightarrow \int_{\partial S_1} \vec{u}(\vec{r}, t) \cdot d\vec{r} = \int_{\partial S_2} \vec{u}(\vec{r}, t) \cdot d\vec{r} ;$$

Instead is strictly necessary that the circulation vanishes along any closed path within that domain. Therefore, in the case of multi connected domains it is necessary that the chosen path never concatenates the source of circulation. This condition can be satisfied if you apply a cut to the fluid domain such that, starting from the external border, reaches the edge of the solid so that any closed path chosen is reducible to a point without departing from the stream. Usually, this cut is to coincide with the wake of the flow when it is sufficiently thin, so that only a small perturbation in the solution is introduced.

5.1.7. Kelvin theorem

It is now considered a more general situation of non-viscous fluid whose incompressible constant density flow field is regular and subject to a system of conservative forces. The calculation of the circulation by definition in this case is based on a Lagrangian approach choosing a closed path that moves with the flow.

$$\Gamma := \oint_{\partial \tilde{S}} \vec{u}(\vec{r}, t) \cdot d\vec{r} ;$$

It replaces the Euler equation, valid for the above conditions, the expression of the circulation differentiated with respect to time, remembering that also the contour of interaction moves with the flow.

$$\frac{\partial \vec{u}}{\partial t} + (\vec{\nabla} \times \vec{u}) \times \vec{u} = -\vec{\nabla} \left(\frac{\tilde{P}}{\rho} + \frac{|\vec{u}|^2}{2} + \epsilon \right) ;$$

$$\frac{d\Gamma}{dt} = \frac{d}{dt} \oint_{\partial \tilde{S}} \vec{u}(\vec{r}, t) \cdot d\vec{r} = \oint_{\partial \tilde{S}} \left[\frac{\partial \vec{u}}{\partial t} + (\vec{\nabla} \times \vec{u}) \times \vec{u} \right] \cdot d\vec{r} = - \oint_{\partial \tilde{S}} \vec{\nabla} \left(\frac{\tilde{P}}{\rho} + \frac{|\vec{u}|^2}{2} + \epsilon \right) \cdot d\vec{r} = - \oint_{\partial \tilde{S}} d \left(\frac{\tilde{P}}{\rho} + \frac{|\vec{u}|^2}{2} + \epsilon \right) ;$$

Since we chose a regular motion field the integral over a closed line of a scalar must vanish.

$$\frac{d\Gamma}{dt} = 0 ;$$

The condition derived summarizes the statement of the "Kelvin's Theorem" which can be generalized to the case of regular barotropic flow (in which the density can vary with pressure alone) of an inviscid fluid subjected to a conservative force field. In these conditions, the theorem shows that the circulation around a closed perimeter that moves with the flow remains constant in time. This condition explains a very important physical phenomenon that occurs in the wake of bodies immersed in a flow. In fact, it is observed that each vortex generated on the profile corresponds to one opposite in the wake (called starter) so that the total circulation remains null along the closed path that embraces both and the theorem is satisfied.

5.1.8. Elementary solutions for planar potential flows

The Laplace equation and associated boundary conditions have the distinction of being all linear equations. Consequently applies the fundamental properties of superposition that allows formulating a new solution to the linear problem simply by linearly combining an arbitrary number of elementary solutions. The same approach is the basis of the method of separation of variables in which the choice of the number of necessary elementary solutions must take in account of the complexity of the problem, which in turn is primarily related to the geometry of the domain under consideration. Although the available solutions form a very narrow set, to get a wider basis is sufficient a spatial translation of available solutions. The optimal arrangement of such solutions is of fundamental importance in order to build a solution that reproduce as closely as possible the actual response of the system. In addition, for those solutions that have a primary point of indeterminacy it is necessary that the placement be such that the singular point does not belong to the fluid domain where the motion field is defined. Further, also the choice of the positions in which impose boundary conditions greatly affects the accuracy of the solution, as they change the values of the coefficients of the linear combination determined by them. Instead, the number of conditions to be imposed is dictated by that of the solutions used.

The elementary solutions of relevant importance available for the Laplace equation in terms of plane motion are those relating to cases of uniform current, straight source, straight doublet and straight vortex.

For brevity will be treated only those that later will prove useful in the treatment.

Due to the planarity of the problem, it is convenient to refer, at least initially, to a cylindrical reference system for the definition of the flow field of the governing equation.

$$\vec{r} = R\hat{R} + z\hat{z};$$

$$\vec{u}(\vec{R}) = \vec{u}(R, \theta) = u_R(R, \theta)\hat{r}(\theta) + u_\theta(R, \theta)\hat{\theta}(\theta);$$

$$\Phi = \Phi(R, \theta) \Rightarrow u_R(R, \theta) = \frac{\partial\Phi}{\partial R}; u_\theta(R, \theta) = \frac{1}{R} \frac{\partial\Phi}{\partial\theta};$$

$$\nabla^2\Phi = \frac{1}{R} \frac{\partial}{\partial R} \left(R \frac{\partial\Phi}{\partial R} \right) + \frac{1}{R^2} \frac{\partial^2\Phi}{\partial\theta^2} = 0;$$

We consider first a rectilinear source characterized by a plane motion field having constant intensity speed along each circle centred on the axis of the source from which each particle branches off radially. Consequently, to the cylindrical symmetry of the flow field also the kinetic potential will be a function of only the radial coordinate.

$$\vec{u}(R, \theta) = u_R(R, \theta)\hat{r}(\theta);$$

$$\Phi = \Phi(R) \Rightarrow u_R(R, \theta) = \frac{d\Phi}{dR}; u_\theta(R, \theta) = 0;$$

The Laplace equation simplifies accordingly.

$$\nabla^2\Phi = \frac{1}{R} \frac{\partial}{\partial R} \left(R \frac{\partial\Phi}{\partial R} \right) + \frac{1}{R^2} \frac{\partial^2\Phi}{\partial\theta^2} = \frac{1}{R} \frac{d}{dR} \left(R \frac{d\Phi}{dR} \right) = \frac{1}{R} \frac{d}{dR} (R u_R) = 0 \xrightarrow{\forall R \neq 0} u_R(R, \theta) = \frac{C}{R};$$

The solution of the equation leads to explicit the expression of the radial component of velocity, the intensity of which is deduced to be inversely proportional to the distance from the axis of the source.

The integration constant C can be related to volumetric flow rate per unit length λ through a cylindrical surface surrounding the axis of the source.

$$Q_V = \int_S \vec{u}(R, \theta) \cdot \hat{n} dS = \int_S \frac{C}{R} \hat{r} \cdot \hat{n} dS = \frac{C}{R} \int_S \hat{r} \cdot \hat{r} dS = \frac{C}{R} \int_S dS = \frac{C}{R} 2\pi RL = 2\pi CL;$$

$$\lambda = \frac{Q_V}{L} = 2\pi C \Rightarrow C = \frac{\lambda}{2\pi};$$

$$\vec{u}_s(R, \theta) = \frac{\lambda}{2\pi R} \hat{r}(\theta) \Rightarrow \Phi_s(R) = \int_0^R u_R(R, \theta) dR = \int_0^R \frac{\lambda}{2\pi R} dR \Rightarrow \Phi_s(R) = \frac{\lambda}{2\pi} \ln R;$$

This emphasizes the fact that the solution has a singularity point at the axis of the source, which therefore must be suitably positioned outside of the domain of definition of the flow field.

Let's now consider the elementary case of rectilinear vortex with reference to a particular whirling structure that generates a velocity field characterized by cylindrical symmetry in which the particles of the fluid move on circular paths around a fixed axis with a speed inversely proportional to the distance from the axis.

$$\vec{u}(R, \theta) = u_\theta(R)\hat{\theta} = \frac{C}{R} \hat{\theta};$$

The vortex, as it is defined, has the particularity to be irrotational in fact, even though following circular trajectories, the particles do not rotate on their own, except along the axis where, however, the motion field is not defined.

$$|\vec{\omega}|_{R \neq 0} = |\vec{V} \times \vec{u}| = \frac{1}{R} \frac{\partial(Ru_\theta)}{\partial R} - \frac{1}{R} \frac{\partial u_R}{\partial \theta} = \frac{1}{R} \frac{d(Ru_\theta)}{dR} = \frac{1}{R} \frac{dC}{dR} = 0 ;$$

So along any closed path that does not concatenate the axis of the vortex you can apply the theorem of Stokes as it encloses a regular domain, therefore the circulation is null as the vorticity. The same theorem is no longer valid when the closed path concatenates the cylinder axis, therefore the circulation expressed as by definition in general doesn't vanish.

$$\Gamma = \oint_L \vec{u}(R, \theta) \cdot d\vec{R} = \oint_L \frac{C}{R} \hat{\theta} \cdot d\vec{R} = \int_0^{2\pi} \frac{C}{R} R d\theta = 2\pi C ;$$

It is observed immediately that the circulation of the velocity field is not cancelled along a path that surrounds the axis of the rectilinear vortex, further is constant for any shape and size of the path as long as the concatenation is unique.

Therefore, the intensity of the vortex represented by the arbitrary constant C can be directly linked to the physical constant Γ .

$$C = \frac{\Gamma}{2\pi} \Rightarrow \vec{u}_v(R, \theta) = \frac{\Gamma}{2\pi R} \hat{\theta} ;$$

Note that also in this case the solution has a singularity at the swirling axis.

To determine the expression of the kinetic potential let's proceed integrating the definition of the velocity components in cylindrical coordinates.

$$u_R(R, \theta) = \frac{d\Phi}{dR} = 0 \Rightarrow \Phi(\theta) = f(\theta) ;$$

$$u_\theta(R, \theta) = \frac{1}{R} \frac{\partial \Phi}{\partial \theta} = \frac{\Gamma}{2\pi R} \Rightarrow \Phi(\theta) = \frac{\Gamma \theta}{2\pi} + g(R) ;$$

Equating the two possible expressions for the potential and assuming to be null the arbitrary constant of integration we obtain the following expression.

$$\Phi(\theta) = \frac{\Gamma \theta}{2\pi} + g(R) = f(\theta) \Leftrightarrow g(R) = C \Rightarrow C = 0 \Rightarrow \Phi_v(\theta) = \frac{\Gamma \theta}{2\pi} ;$$

The expression just found is a biunique function of the plan only when the angular coordinate ranges within the first round angle. Because we want the solution to be periodic exactly of that angle, because generally we consider problems in which the fluid wets the entire contour of the body that is immersed, it will be necessary to introduce in the previous expression a suitable angular coordinate curtailed of the first round angle.

Since the translation of the singular points outside of the fluid domain is easier if it has to do with Cartesian coordinates, it is necessary to express in such coordinates the elementary expressions thus far found. To do this we will use some well-known polar transformations.

$$x = R \cos \theta ; y = R \sin \theta \Rightarrow R = \sqrt{x^2 + y^2} ; \tan \theta = \frac{y}{x} ;$$

$$\Phi_s(x, y) = \frac{\lambda}{2\pi} \ln \sqrt{x^2 + y^2} ;$$

$$\Phi_v(x, y) = \frac{\Gamma}{2\pi} \tan^{-1} \left(\frac{y}{x} \right) ;$$

It points out the need to pay attention to the reversal of the tangent function because you can lose the information on the dial where you are actually therefore should take the necessary precautions.

In this way, any translation requires a simple change of variables in the above formulas.

$$x \rightarrow x - x_0 ;$$

$$y \rightarrow y - y_0 ;$$

We must pay attention to the fact that in general performing a translation you lose the symmetry of the solution with respect to at least one of the two axes.

5.1.9. Stream functions

Current lines represent the lines of the instantaneous velocity vector field therefore cannot be crossed by the flow. This, in the particular case in which the flow is incompressible and planar, can be described by a scalar function called current function and defined as the volumetric flow rate, per unit length perpendicular to the plane, of the fluid flowing between a generic point and another taken as a reference.

$$\Psi(x, y, t) := \int_{(x_0, y_0)}^{(x, y)} \vec{u}(x, y, t) \cdot \hat{n}(x, y) ds ;$$

By choosing a closed path that encloses a flow domain simply connected you can apply the divergence theorem.

$$\oint_{\partial S} \vec{u}(x, y, t) \cdot \hat{n}(x, y) ds = \int_S \vec{\nabla} \cdot \vec{u} dS ;$$

Thanks to the incompressibility of the flow, it can be shown that the velocity field is conservative.

$$\oint_{\partial S_1} \vec{u}(x, y, t) \cdot \hat{n}(x, y) ds = \oint_{\partial S_2} \vec{u}(x, y, t) \cdot \hat{n}(x, y) ds ;$$

The same applies also in the case in which the path considered surrounds a multiply connected fluid domain when the outline of the region, alien to the flow, is waterproof. In fact, in this case, it is necessary to consider also the contour that encloses that region where, however, the normal component of velocity at each point vanishes, and then the conservation condition is automatically satisfied.

The last equation expresses the conservativeness of the motion field normal to a generic path and consequently the definition of the current function depends only on the choice of the end points of the path along which it is defined.

Expressing the unit normal by the scalar product between the other two components of the intrinsic triad.

$$\Psi(x, y, t) = \int_{(x_0, y_0)}^{(x, y)} \vec{u}(x, y, t) \cdot \hat{t} \times \hat{z} ds = \int_{(x_0, y_0)}^{(x, y)} \vec{u}(x, y, t) \times \hat{t} \cdot \hat{z} ds = \int_{(x_0, y_0)}^{(x, y)} [\vec{u}(x, y, t) \times d\hat{r}]_z ;$$

Recalling that the motion field is flat, the only non-zero component of the vector product is the one belonging to the plane of the flow.

$$\Psi(x, y, t) = \int_{(x_0, y_0)}^{(x, y)} [u(x, y, t) dy - v(x, y, t) dx];$$

From the differentiation of the current function can be derived expressions for the two components of the fluid velocity.

$$u(x, y, t) = \frac{\partial \Psi}{\partial y};$$

$$v(x, y, t) = -\frac{\partial \Psi}{\partial x};$$

Expressions just obtained can be rewritten synthetically in vector terms.

$$\vec{u} = \vec{\nabla} \Psi \times \hat{z};$$

The vector notation has a more general value, in fact, can also be used in systems of plane coordinates different from the Cartesian one.

For example, in the frequent case of cylindrical symmetry is particularly advantageous to express the current function in terms of a radial and an angular coordinate.

$$\Psi = \Psi(R, \theta);$$

Consequently, also the velocity components associated with it must take account of the change of variables in the expression of the derivatives.

$$u_R(R, \theta, t) = \frac{1}{R} \frac{\partial \Psi}{\partial \theta};$$

$$u_\theta(R, \theta, t) = -\frac{\partial \Psi}{\partial R};$$

It is observed immediately that the velocity field thus defined automatically satisfies the condition of incompressibility, thanks to equality of the second mixed derivatives of the scalar function guaranteed by the Schwatz theorem.

$$\vec{\nabla} \cdot \vec{u} = \frac{1}{R} \frac{\partial (R u_R)}{\partial R} + \frac{1}{R} \frac{\partial u_\theta}{\partial \theta} = \frac{1}{R} \frac{\partial}{\partial R} \left(\frac{\partial \Psi}{\partial \theta} \right) + \frac{1}{R} \frac{\partial}{\partial \theta} \left(-\frac{\partial \Psi}{\partial R} \right) = 0;$$

It must be stressed that what is said in this paragraph is valid whatever the viscosity of the fluid considered, in fact, no hypothesis has been made in this regard.

In the case where the flow is irrotational the stream function is the solution of the Laplace equation.

$$\vec{\nabla} \times \vec{u} = \frac{\partial (u_\theta)}{\partial R} - \frac{1}{R} \frac{\partial (u_R)}{\partial \theta} = \frac{\partial}{\partial R} \left(-\frac{\partial \Psi}{\partial R} \right) - \frac{1}{R} \frac{\partial}{\partial \theta} \left(\frac{1}{R} \frac{\partial \Psi}{\partial \theta} \right) = -\nabla^2 \Psi = 0;$$

As has already been determined expressions for the components of the flow field of a plane potential flow is possible to define a direct link between the kinetic potential and stream function.

$$u_R(R, \theta, t) = \frac{\partial \Phi}{\partial R} = \frac{1}{R} \frac{\partial \Psi}{\partial \theta};$$

$$u_\theta(R, \theta, t) = \frac{1}{R} \frac{\partial \Phi}{\partial \theta} = -\frac{\partial \Psi}{\partial R};$$

Which implies that the family of equipotential lines and $\Psi = \text{const}$ are orthogonal, simply by checking the condition of orthogonality of the respective gradients.

$$\vec{\nabla} \Phi = \frac{\partial \Phi}{\partial R} \hat{R} + \frac{1}{R} \frac{\partial \Phi}{\partial \theta} \hat{\theta};$$

$$\vec{\nabla} \Psi = \frac{\partial \Psi}{\partial R} \hat{R} + \frac{1}{R} \frac{\partial \Psi}{\partial \theta} \hat{\theta};$$

$$\vec{\nabla} \Phi \cdot \vec{\nabla} \Psi = \left(\frac{\partial \Phi}{\partial R} \right) \left(\frac{\partial \Psi}{\partial R} \right) + \left(\frac{1}{R} \frac{\partial \Phi}{\partial \theta} \right) \left(\frac{1}{R} \frac{\partial \Psi}{\partial \theta} \right) = 0;$$

Besides, the elementary solutions previously obtained can be rewritten in terms of the stream function by integrating the relationships just viewed and taking null arbitrary constants of integration for simplicity.

$$\Phi_s(R) = \frac{\lambda}{2\pi} \ln R \Rightarrow \frac{\partial \Phi_s}{\partial R} = \frac{\lambda}{2\pi R} = \frac{1}{R} \frac{\partial \Psi_s}{\partial \theta} \Rightarrow \Psi_s(R) = \frac{\lambda}{2\pi} \theta \Rightarrow \Psi_s(x, y) = \frac{\lambda}{2\pi} \tan^{-1} \left(\frac{y}{x} \right);$$

$$\Phi_v(\theta) = \frac{\Gamma \theta}{2\pi} \Rightarrow \frac{1}{R} \frac{\partial \Phi}{\partial \theta} = \frac{\Gamma}{2\pi R} = -\frac{\partial \Psi_v}{\partial R} \Rightarrow \Psi_v(R) = -\frac{\Gamma}{2\pi} \ln R \Rightarrow \Psi_v(x, y) = -\frac{\Gamma}{2\pi} \ln \sqrt{x^2 + y^2};$$

5.2. Two dimensional stationary lifting flow around a circular cylinder

It is considered a cylinder of length ideally infinite with circular section, so as to be able to study the problem in two dimensions by considering a generic section of the solid. The plane flow, steady, incompressible with uniform density and irrotational of a non-viscous fluid invest the body perpendicularly to its axis with uniform velocity in space and time average intensity equal to U.

From the analysis you want to determine the distribution of the velocity field and pressure around the generic section of the body, rigidly constrained to the global reference system of cylindrical coordinates (R, θ , z), with z outgoing from the plane along the axis of cylinder. For convenience we introduce two auxiliary Cartesian axes to form a right-handed triad with z, where x is directed as U.

In consequence of the fact that the velocity field around the cylinder must be planar, the expression of vorticity is simplified and the condition of irrotational flow is rewritten in another form.

$$\vec{u}(R, \theta) = u_R(R, \theta) \hat{r} + u_\theta(R, \theta) \hat{\theta} \Rightarrow \vec{\omega} = \vec{\nabla} \times \vec{u} = \omega \hat{z} = 0 \Leftrightarrow \hat{z} \cdot \vec{\omega} = 0;$$

We write the equations governing the problem, namely the condition of incompressible and irrotational flow, in cylindrical coordinates.

$$\vec{\nabla} \cdot \vec{u} = 0 \Rightarrow \frac{1}{R} \frac{\partial(Ru_R)}{\partial R} + \frac{1}{R} \frac{\partial u_\theta}{\partial \theta} = 0 \Rightarrow \frac{\partial(Ru_R)}{\partial R} + \frac{\partial u_\theta}{\partial \theta} = 0 ;$$

$$\vec{\nabla} \times \vec{u} = 0 \Rightarrow \frac{1}{R} \frac{\partial(Ru_\theta)}{\partial R} - \frac{1}{R} \frac{\partial u_R}{\partial \theta} = 0 \Rightarrow \frac{\partial(Ru_\theta)}{\partial R} - \frac{\partial u_R}{\partial \theta} = 0 ;$$

In order to solve the linear first order differential system of two equations, are needed suitable boundary conditions that translate mathematically the impermeability of the surface of the cylinder and restore the undisturbed condition infinitely upstream of the body (set for simplicity on a single component of the velocity field).

$$\hat{n} = \hat{r} \Rightarrow u_R(\bar{R}, \theta) = 0 ;$$

$$\lim_{R \rightarrow \infty} u_R(R, \theta) = U \cos \theta ;$$

We emphasize the fact that the initial conditions are not necessary since it considers the stationary regime condition.

Substituting the expression for $\frac{\partial u_\theta}{\partial \theta}$ obtained from the first equation into the second specifically derivate with respect to θ there can be traced back to a single differential equation of second order.

$$\frac{\partial}{\partial \theta} \left[\frac{\partial(Ru_\theta)}{\partial R} - \frac{\partial u_R}{\partial \theta} \right] = \frac{\partial}{\partial R} \left(R \frac{\partial u_\theta}{\partial R} \right) - \frac{\partial^2 u_R}{\partial \theta^2} = 0 ;$$

$$\frac{\partial u_\theta}{\partial \theta} = - \frac{\partial(Ru_R)}{\partial R} \Rightarrow \frac{\partial}{\partial R} \left[R \frac{\partial(Ru_R)}{\partial R} \right] - \frac{\partial^2 u_R}{\partial \theta^2} = 0 ;$$

The search for elementary solutions of the equation is addressed by means of the method of separation of variables in which the velocity field is described by the product of two unknown functions dependent each by a single variable between R and θ . This is a very strong hypothesis that dramatically narrows the range of validity of each elementary solution obtained. Therefore, it is imperative to exploit the linearity of the problem, and overlap the effects of various elementary solutions through a linear combination to obtain a new solution of the problem which is better suited to the boundary conditions. This is allowed by the fact that the number of elementary solutions is large enough to be considered a base.

$$u_R(R, \theta) = f(R)g(\theta) ;$$

$$\frac{\partial}{\partial R} \left[R \frac{\partial(Ru_R)}{\partial R} \right] - \frac{\partial^2 u_R}{\partial \theta^2} = g \frac{d}{dR} \left[R \frac{d(Rf)}{dR} \right] - f \frac{d^2 g}{d\theta^2} = g \frac{d}{dR} \left[Rf + R^2 \frac{df}{dR} \right] - f \frac{d^2 g}{d\theta^2} = \left\{ g \left(\begin{array}{l} f + Rf' + \\ + 2Rf'' + R^2 f''' \end{array} \right) + fg' \right\} = 0 ;$$

$$\frac{1}{f} (f + Rf' + 2Rf'' + R^2 f''') = - \frac{g'}{g} \Rightarrow F(R) = -G(\theta) \quad \forall (R, \theta) ;$$

The equality of two functions dependent on different variables can be satisfied only in the case where both are constants.

Thus, the problem reduces to two ordinary differential equations, in independent variables (but linked by the constant separation σ), of second order and with constant coefficients.

$$g'' + \sigma g = 0;$$

$$R^2 f'' + 3Rf' + (1 - \sigma)f = 0;$$

The solutions to the first equation in exponential form can be searched using the method proposed by Euler.

$$g(\theta) = e^{\lambda\theta};$$

Substituting in the equation and remembering that the exponential does not vanish for any value of λ and θ , it comes down to an algebraic equation in the unknown λ .

$$\lambda^2 + \sigma = 0;$$

We must distinguish three different solutions depending on the value assumed by σ .

$$\sigma < 0 \Rightarrow \sigma = -k^2 \Rightarrow \lambda_{1,2} = \pm k \Rightarrow g(\theta) = C_1 e^{k\theta} + C_2 e^{-k\theta};$$

$$\sigma = 0 \Rightarrow \lambda_{1,2} = 0 \Rightarrow g(\theta) = C_1 + C_2 \theta;$$

$$\sigma > 0 \Rightarrow \sigma = k^2 \Rightarrow \lambda_{1,2} = \pm ik \Rightarrow g_k(\theta) = A_{1,k} \sin(k\theta) + A_{2,k} \cos(k\theta);$$

The choice must fall back to that which guarantees a periodic solution of 2π around the cross section of the cylinder. It is noted immediately that the first solution should be discarded because as θ grows it is divergent, the same problem is avoided in the second assuming to be null the second integration constant. Therefore, the solution should have the same form of the third equation that appears to be periodic of a round angle only if the arbitrary constant k is an integer, including zero.

Given the range of variability of k turns out to be uniquely defined also the one for σ , then you can proceed to the resolution of the second ordinary differential equation dependent only on R .

To begin with let's consider the particularly simple case in which k is zero.

$$\frac{1}{f} \frac{d}{dR} \left[R \frac{d(Rf)}{dR} \right] = -\frac{1}{g} \frac{d^2 g}{d\theta^2} = \sigma;$$

$$k = 0 \Rightarrow \sigma = 0 \Rightarrow \frac{1}{f_0} \frac{d}{dR} \left[R \frac{d(Rf_0)}{dR} \right] = 0 \Rightarrow \frac{d(Rf_0)}{dR} = \frac{B_{1,0}}{R} \Rightarrow f_0(R) = \frac{B_{1,0} \log_e R}{R} + \frac{B_{2,0}}{R};$$

For any other value assumed by k , the ordinary differential equation takes the form of an "equi-dimensional" or Euler equation, so called because it is characterized by being composed of the terms in which the order is equal to the degree of differentiation.

$$k > 0 \Rightarrow R^2 f'' + 3Rf' + (1 - k^2)f = 0 \leftrightarrow ax^2 \frac{d^2 y}{dx^2} + bx \frac{dy}{dx} + cy = 0;$$

Seeking elementary solutions suitable for a development in power series of the final solution.

$$f(R) = R^n;$$

Substituting in the governing equation it reduces to an algebraic equation as a function of the unknown parameter n (confirming that the solution never vanishes for any value taken by the exponent).

$$n(n-1) + 3n + (1-k^2) = n^2 + 2n + 1 - k^2 = 0 \Rightarrow (n+1)^2 = k^2 \Rightarrow n_{1,2} = \pm k - 1;$$

$$f_k(R) = C_{1,k} R^{k-1} + C_{2,k} \frac{1}{R^{k+1}};$$

Leveraging the ability to overlay the effects of the special conditions so far analysed, you can write a final shape of the solution to the original second order partial differential equation with separate variables.

$$u_R(R, \theta) = f(R)g(\theta) = f_0(R)g_0(\theta) + \sum_{k=1}^{\infty} f_k(R)g_k(\theta);$$

$$u_R(R, \theta) = \frac{B_{1,0} \log_e R}{R} + \frac{B_{2,0}}{R} + \sum_{k=1}^{\infty} \left(C_{1,k} R^{k-1} + C_{2,k} \frac{1}{R^{k+1}} \right) [A_{1,k} \sin(k\theta) + A_{2,k} \cos(k\theta)];$$

Note that the second term corresponds to the elementary solution of Laplace's equation previously determined for the case of linear source where $B_{2,0} = \frac{\lambda}{2\pi}$.

Now it is possible to determine the expressions taken from the integration constants in order to satisfy the boundary conditions of the problem.

$$\lim_{R \rightarrow \infty} u_R(R, \theta) < \infty \Leftrightarrow \lim_{R \rightarrow \infty} R^{k-1} < \infty \Leftrightarrow k = 1 \Rightarrow C_{1,k>1} = 0 \text{ and } C_{1,1} \neq 0;$$

You collect integration constants to define new ones.

$$\sum_{k=1}^{\infty} \left(\begin{array}{l} C_{1,k} R^{k-1} + \\ C_{2,k} \frac{1}{R^{k+1}} \end{array} \right) \left[\begin{array}{l} A_{1,k} \sin(k\theta) + \\ A_{2,k} \cos(k\theta) \end{array} \right] = A_1 \sin \theta + A_2 \cos \theta + \sum_{k=1}^{\infty} a_{1,k} \frac{\sin(k\theta)}{R^{k+1}} + a_{2,k} \frac{\cos(k\theta)}{R^{k+1}};$$

Consequently, the condition undisturbed flow indefinitely upstream of the cylinder can be imposed.

$$\lim_{R \rightarrow \infty} u_R(R, \theta) = A_1 \sin \theta + A_2 \cos \theta = U \cos \theta \Leftrightarrow A_1 = 0 \text{ and } A_2 = U;$$

The water resistance of the cylinder determines the vanishing of the orthogonal velocity to the body surface along a generic direction.

$$u_R(\bar{R}, \theta) = \frac{B_{1,0} \log_e \bar{R}}{\bar{R}} + \frac{B_{2,0}}{\bar{R}} + U \cos \theta + \sum_{k=1}^{\infty} a_{1,k} \frac{\sin(k\theta)}{\bar{R}^{k+1}} + a_{2,k} \frac{\cos(k\theta)}{\bar{R}^{k+1}} = 0;$$

$$\frac{B_{1,0} \log_e \bar{R}}{\bar{R}} + \frac{B_{2,0}}{\bar{R}} = 0 \Leftrightarrow B_{2,0} = -B_{1,0} \log_e \bar{R};$$

$$U \cos \theta + a_{2,1} \frac{\cos \theta}{\bar{R}^2} = 0 \Leftrightarrow a_{2,1} = -\bar{R}^2 U;$$

$$\sum_{k=1}^{\infty} a_{1,k} \frac{\text{sen}(k\theta)}{\bar{R}^{k+1}} + \sum_{k=2}^{\infty} a_{2,k} \frac{\cos(k\theta)}{\bar{R}^{k+1}} = 0 \Leftrightarrow a_{1,k>0} = 0 ; a_{2,k>1} = 0 ;$$

It finally gets the final expression for the radial component of the velocity field of the flow.

$$u_R(R, \theta) = \frac{C \log_e R/\bar{R}}{R} + U \left(1 - \frac{\bar{R}^2}{R^2}\right) \cos \theta ;$$

From the condition of incompressibility is extracted term derived with respect to the coordinate θ .

$$\frac{\partial(Ru_R)}{\partial R} + \frac{\partial u_\theta}{\partial \theta} = 0 \Rightarrow \frac{\partial u_\theta}{\partial \theta} = -\frac{\partial(Ru_R)}{\partial R} = -\frac{\partial}{\partial R} \left\{ R \left[\frac{C \log_e R/\bar{R}}{R} + U \left(1 - \frac{\bar{R}^2}{R^2}\right) \cos \theta \right] \right\} = -\frac{\partial}{\partial R} \left[C \log_e \frac{R}{\bar{R}} + U \left(R - \frac{\bar{R}^2}{R} \right) \cos \theta \right] = -\frac{C}{R} - U \left(1 + \frac{\bar{R}^2}{R^2} \right) \cos \theta ;$$

The integration of the previous expression is used to define the angular component of velocity of the flow.

$$u_\theta(R, \theta) = -\frac{C\theta}{R} - U \left(1 + \frac{\bar{R}^2}{R^2} \right) \text{sen } \theta + F(R) ;$$

The integration constant C is defined by recalling that the final solution should be periodic by 2π .

$$u_\theta(R, \theta) = u_\theta(R, \theta + 2\pi) \Leftrightarrow -\frac{C\theta}{R} - U \left(1 + \frac{\bar{R}^2}{R^2} \right) \text{sen } \theta = -\frac{C(\theta+2\pi)}{R} - U \left(1 + \frac{\bar{R}^2}{R^2} \right) \text{sen}(\theta + 2\pi) ;$$

$$\sin \theta = \sin(\theta + 2\pi) \Rightarrow \frac{2\pi C}{R} = 0 \Leftrightarrow C = 0 ;$$

$$u_R(R, \theta) = U \left(1 - \frac{\bar{R}^2}{R^2} \right) \cos \theta ;$$

$$u_\theta(R, \theta) = -U \left(1 + \frac{\bar{R}^2}{R^2} \right) \text{sen } \theta + F(R) ;$$

The integration with respect to θ has introduced an arbitrary function depends only on the radial coordinate, the expression of which can be defined by the irrotational condition of the velocity field expressed by the equations so far found.

$$\frac{\partial(Ru_\theta)}{\partial R} - \frac{\partial u_R}{\partial \theta} = 0 \Rightarrow \frac{\partial(Ru_\theta)}{\partial R} = \frac{\partial u_R}{\partial \theta} = -U \left(1 - \frac{\bar{R}^2}{R^2} \right) \text{sen } \theta ;$$

Integrating with respect to R another expression for the angular component of the flow is obtained.

$$u_\theta(R, \theta) = -U \left(1 + \frac{\bar{R}^2}{R^2} \right) \text{sen } \theta + \frac{G(\theta)}{R} ;$$

In this case the arbitrary function appears to be dependent only on angular coordinate.

So that the expression for $u_\theta(R, \theta)$ to be unique is necessary that the two arbitrary functions above are linked appropriately to each other.

$$F(R) = \frac{G(\theta)}{R} \Leftrightarrow G(\theta) = B = \text{cost} ;$$

$$u_{\theta}(R, \theta) = -U \left(1 + \frac{\bar{R}^2}{R^2} \right) \text{sen } \theta + \frac{B}{R};$$

To give a physical meaning to the constant just introduced is appropriate to recall the definition of rectilinear vortex, whose velocity field contributes to the definition of the flow in the tangential direction around the cylinder section previously obtained.

$$\vec{u}_v(R, \theta) = u_{\theta}(R) \hat{\theta} = \frac{\Gamma}{2\pi R} \hat{\theta} \Rightarrow B = \frac{\Gamma}{2\pi};$$

Ultimately, you can write the final formulation for the angular component of velocity.

$$u_{\theta}(R, \theta) = -U \left(1 + \frac{\bar{R}^2}{R^2} \right) \text{sen } \theta + \frac{\Gamma}{2\pi R};$$

By overlaying the two scalar components is obtained the total vector flow field around the circular cylinder.

$$\vec{u}(R, \theta) = \left[U \left(1 - \frac{\bar{R}^2}{R^2} \right) \cos \theta \right] \hat{r} + \left[\frac{\Gamma}{2\pi R} - U \left(1 + \frac{\bar{R}^2}{R^2} \right) \text{sen } \theta \right] \hat{\theta};$$

Given the arbitrariness of the parameter Γ exists a family of infinite possible solutions that properly describe the flow field around the body. This emphasizes the fact that the non-uniqueness of the solution is valid for any form of the section of the cylinder being Γ independent from it.

In summary, the presence of the infinitely extended solid body makes multiply connected fluid domain, which does not allow to apply the Stokes theorem since in the region occupied by the solid is not defined any flow. The circulation cannot, therefore, be determined by the vorticity, for which it would be null like in any mono-connected domain, but by means of its definition it reveals the arbitrariness. Consequently, the solution loses the uniqueness, the motion field is not conservative, being a priori Γ not null, and therefore cannot be expressed by the gradient of a scalar function, since it has no kinematic potential.

As for the loss of uniqueness of the solution is linked to the idealization of non-viscous fluid. In fact, every real fluid is always characterized by even a small viscosity, concentrated in the boundary layer, which in conditions of stationary flow makes it unique solution by fixing the circulation, the value of which, however, depends on the shape of the section of the cylinder and on the past history of the momentum field. At the physical level, the circulation generated in the viscous boundary layer grows until the flow moves in stationary conditions. From here onwards is maintained constant thanks to the fact that the flow is well described by the Euler equations in most of the domain, which can be written in terms of vorticity to explain the condition of preservation of the circulation.

Being known the velocity field is also possible to determine the one associated to the pressure applying the Bernoulli theorem in the stationary version. The formulation of the previously determined theorem is valid for incompressible (with uniform density) and irrotational currents in the simply connected domain that has permission to write the speed as a function of a kinetic potential. This is no longer possible because the domain is multi connected and the circulation of the flow is non-zero for each path traced around the body that there is immersed. Therefore, in this case, the motion field is not conservative and consequently the Bernoulli theorem is not associated with a potential.

$$\frac{\partial \vec{u}}{\partial t} = -\vec{\nabla} \left(\frac{\bar{p}}{\rho} + \frac{|\vec{u}|^2}{2} + \epsilon \right) = 0;$$

It is assumed that there are no other external forcing except from the fluid pressure, which can be expressed by a dimensionless pressure coefficient.

This is equal to the difference between the pressure reached by the fluid near the cylinder and the one at the inlet of the body, where the speed is uniform and can be defined a kinetic energy per unit volume taken as a parameter for normalization.

$$\vec{\nabla} \left(\frac{\tilde{P}}{\rho} + \frac{|\vec{u}|^2}{2} \right) = 0 \Leftrightarrow \frac{\tilde{P}}{\rho} + \frac{|\vec{u}|^2}{2} = C = \text{const} \Rightarrow \tilde{P}(R, \theta) = \bar{\rho}C - \frac{1}{2}\bar{\rho}|\vec{u}|^2 \Rightarrow \tilde{P}_\infty = \tilde{P}(R \rightarrow \infty) = \bar{\rho}C - \frac{1}{2}\bar{\rho}U^2 ;$$

$$C_{\tilde{P}}(R, \theta) = \frac{\tilde{P}(R, \theta) - \tilde{P}_\infty}{\frac{1}{2}\bar{\rho}U^2} = 1 - \frac{|\vec{u}(R, \theta)|^2}{U^2} ;$$

It is evident that the pressure coefficient can be at most equal to unity, the condition reached only in the stagnation point where it cancels the local velocity.

From the previously calculated expression for the velocity field you can define the module in cylindrical coordinates.

$$u_R(R, \theta) = U \left(1 - \frac{\bar{R}^2}{R^2} \right) \cos \theta ;$$

$$u_\theta(R, \theta) = -U \left(1 + \frac{\bar{R}^2}{R^2} \right) \sin \theta + \frac{\Gamma}{2\pi R} ;$$

$$\begin{aligned} |\vec{u}(R, \theta)|^2 &= u_R(R, \theta)^2 + u_\theta(R, \theta)^2 = U^2 \left(1 - 2\frac{\bar{R}^2}{R^2} + \frac{\bar{R}^4}{R^4} \right) \cos^2 \theta + U^2 \left(1 + 2\frac{\bar{R}^2}{R^2} + \frac{\bar{R}^4}{R^4} \right) \sin^2 \theta - \\ &\frac{\Gamma U}{\pi R} \left(1 + \frac{\bar{R}^2}{R^2} \right) \sin \theta + \left(\frac{\Gamma}{2\pi R} \right)^2 = U^2 \left(1 + \frac{\bar{R}^4}{R^4} \right) + 2U^2 \frac{\bar{R}^2}{R^2} (\sin^2 \theta - \cos^2 \theta) - \frac{\Gamma U}{\pi R} \left(\frac{R^2 + \bar{R}^2}{R^2} \right) \sin \theta + \left(\frac{\Gamma}{2\pi R} \right)^2 = \\ &U^2 \left(1 + \frac{\bar{R}^4}{R^4} \right) - 2U^2 \frac{\bar{R}^2}{R^2} \cos(2\theta) - \frac{\Gamma U \bar{R}}{\pi R^2} \left(\frac{R}{\bar{R}} + \frac{\bar{R}}{R} \right) \sin \theta + \left(\frac{\Gamma}{2\pi R} \right)^2 ; \end{aligned}$$

The pressure coefficient is now immediately defined in the coordinates adopted.

$$C_{\tilde{P}}(R, \theta) = -\frac{\bar{R}^2}{R^2} \left[\frac{\bar{R}^2}{R^2} - 2 \cos(2\theta) - \frac{\Gamma}{\pi \bar{R} U} \left(\frac{R}{\bar{R}} + \frac{\bar{R}}{R} \right) \sin \theta + \left(\frac{\Gamma}{2\pi \bar{R} U} \right)^2 \right] ;$$

The pressure coefficient reveals that the circulation makes the pressure around the cylinder asymmetrical with respect to the plane aligned with the undisturbed upstream flow.

This becomes clearer if one refers to the pressure exerted on the body surface.

$$u_R(\bar{R}, \theta) = 0 ;$$

$$u_\theta(\bar{R}, \theta) = -2U \sin \theta + \frac{\Gamma}{2\pi \bar{R}} ;$$

$$|\vec{u}(\bar{R}, \theta)|^2 = u_R(R, \theta)^2 + u_\theta(R, \theta)^2 = 4U^2 \sin^2 \theta - \frac{2\Gamma U}{\pi \bar{R}} \sin \theta + \left(\frac{\Gamma}{2\pi \bar{R}} \right)^2 ;$$

$$C_{\tilde{P}}(\bar{R}, \theta) = 1 - \frac{|\vec{u}(\bar{R}, \theta)|^2}{U^2} = 1 - 4 \sin^2 \theta - \frac{2\Gamma}{\pi \bar{R} U} \sin \theta + \left(\frac{\Gamma}{2\pi \bar{R} U} \right)^2 ;$$

The expression just found contains two terms related to the circulation of the fluid, of which the one constant with the angle has no effect against the net force on the body, instead of the other, varying with the sine of the angular coordinate, introduces an asymmetry in the distribution of pressure at the surface of the body.

Consequently, by integrating the pressure field along the contour of the section of the cylinder is possible to calculate the net force, per unit length, acting on it in the direction orthogonal to the upstream flow.

$$\vec{f} = \int_0^{2\pi} \tilde{P}(\bar{R}, \theta) [-\hat{r}(\theta)] \bar{R} d\theta = -\bar{R} \int_0^{2\pi} \tilde{P}(\bar{R}, \theta) (\cos\theta \hat{x} + \sin\theta \hat{y}) \bar{R} d\theta ;$$

Determining the direction of this force is immediate if one considers the fact that the pressure distribution was obtained through the Bernoulli theorem. In the particular case considered, the theorem expresses a relationship of mutual balance between the flow field and the pressure distribution of the flow, in such a way that the sum of the two contributions is kept constant. Since the circulation is due to the presence of a rectilinear vortex, the velocity field is perturbed by Γ which increases the intensity in those locations where the symmetrical component of the velocity is concordant with the direction of rotation of the flow and otherwise it reduces. The asymmetry of the flow is therefore linked to the variation of relative direction between these two velocity components along the profile of the section. In consequence of the above theorem, there is respectively a decrease and an increase of the pressure on the cylinder, which then turns out to be not symmetrically distributed.

Substituting the expression of pressure and remembering some trigonometric identities the formulation for the total force acting on the cylinder is simplified.

$$\vec{f} = -\bar{R} \int_0^{2\pi} \left\{ \bar{\rho} C - \frac{1}{2} \bar{\rho} \left[4U^2 \sin^2 \theta - \frac{2\Gamma U}{\pi \bar{R}} \sin \theta + \left(\frac{\Gamma}{2\pi \bar{R}} \right)^2 \right] \right\} (\cos\theta \hat{x} + \sin\theta \hat{y}) \bar{R} d\theta ;$$

$$\int_0^{2\pi} \sin^2 \theta \cos\theta d\theta = \int_0^{2\pi} \sin \theta \cos\theta d\theta = \int_0^{2\pi} \cos\theta d\theta = \int_0^{2\pi} \sin^3 \theta d\theta = \int_0^{2\pi} \sin\theta d\theta = 0 ;$$

$$\vec{f} = -\frac{\bar{\rho}\Gamma U}{\pi} \left(\int_0^{2\pi} \sin^2 \theta d\theta \right) \hat{y} = -\bar{\rho}\Gamma U \hat{y};$$

Since you are considering a plane motion in which the average velocity of the undisturbed flow is directed perpendicular to the cylinder axis along which the circulation can be represented as a vector, is easily found the general expression of the so called "Kutta-Joukowski Theorem " .

$$\vec{f} = \bar{\rho} \vec{U} \times \vec{\Gamma} ;$$

The theorem provides intensity, direction and orientation of the lift force per unit length for a cylinder having a section of any shape. More specifically we speak of lift and downforce depending on whether the force is directed respectively upwards or downwards, depending on the direction of rotation of the straight vortex and the direction of the undisturbed velocity field.

This emphasizes the fact that in the case in which the circulation were null, as happens for symmetrical flow, the previous expression is transformed into the paradox of d'Alembert. According to which bodies invested by a stationary, irrotational, incompressible with constant density and negligible viscosity flows offer no resistance to the motion of the fluid itself, that is, are not lifting. As already mentioned, in the real applications this is not possible mainly by the fact that the viscosity of the fluid is never completely null, at least in the boundary layer, and this fact always introduces a contribution to the swirling motion, which in steady state becomes constant.

The last statement has important consequences for the velocity and pressure fields that can actually develop around a body of infinitely extended of generic section immersed in a fluid.

In this regard, it is considered a flat plate placed in incidence uniform, incompressible with uniform density, irrotational and with null circulation flow for any path that concatenates the section of the solid.

In these conditions, the tracking of the trajectories allows to identify two stagnation points located respectively on the lower part of the abdomen front and rear upper back. The trajectories near either end of the back and of the abdomen have a distortion at the output region. The presence of the body, in fact, force the particles to follow a given path with an influence increasingly louder as you get closer to the solid wall. Consequently, only the particles closer to the plate are bound to move from the stagnation point on the back of the one in the belly. In order to reach the second stagnation point must pass a sharp edge and travel a stretch in the opposite direction to the uniform flow. In the reversal point has a concentration of trajectories that involves a speed unrealistically tending to infinity. For this reason, it is necessary to consider the effects of viscosity which, by introducing a component of circulatory motion, move the stagnation points, particularly the one on back moves in correspondence with the sharp edge output. This prevents the inversion of the trajectories for the particles in output, which quite simply follow the direction suggested by the airfoil, and thus no longer has the singularity in the motion field. Instead, the stagnation point in entry remains on the belly of the foil and the trajectories become more uneven, which greatly increases the speed at the sharp edge; for this reason the airfoils have a rounded leading edge that regulates the flow field.

Since the phenomena that regulate the output conditions of a real flow are very complex in general, to stay within non-viscous fluids, reference is made to "Kutta condition" which states that the velocity at the trailing edge must be finite. This simplification constraint can be satisfied by imposing a boundary condition on the speed, which typically introduces an additional circulation to the motion field that simulates the effect of viscosity in the stationary flow of a real fluid. In general, the vorticity necessary to satisfy the Kutta condition is determined iteratively until the tail stagnation point coincides with the trailing edge.

5.3. Conformal mapping of Joukowski

Any-one correspondence between two sets of complex coordinates can be defined as a transformation, which defines a link between the points (images) of the two plans considered. More specifically speaking of conformal transformation when two curves at the point of intersection keep unchanged the angle, in terms of amplitude and direction, and the ratio between the lengths passing from one plane to another in a neighbourhood of the point d ' interest. It can be shown that any holomorphic function conforms at all points of the plane in which is characterised by non-zero and finite first derivative.

As the transformations are not unique but have three degrees of freedom, are required suitable boundary conditions. Typically these require that infinitely far away from the body match points and speed.

$$\lim_{z \rightarrow \infty} \frac{\omega(z)}{z} = \lim_{z \rightarrow \infty} \frac{d\omega(z)}{dz} = 1 ;$$

Since each condition imposes two constraints is necessary to introduce a further degree of freedom leaving free the scale factor between a plane and the other.

For this reason, in the following we will refer exclusively to complex plans in which it is convenient to express the position of the points in polar coordinates rather than Cartesian. The transition is immediate by simply applying Euler's formula.

$$z = x + iy = Re^{i\vartheta} = R \cos \theta + i \cdot R \sin \theta ;$$

$$R = \sqrt{x^2 + y^2} ;$$

$$\vartheta = \tan^{-1} \left(\frac{y}{x} \right) ;$$

It introduces a complex potential, in which precisely the real and imaginary part are respectively represented by the kinetic potential and the stream function defined for a uniform, incompressible and irrotational flow of a non-viscous fluid in uniform density. The relationships that have allowed us to affirm the orthogonality of the equipotential lines and $\Psi = \text{const}$, actually translate the Cauchy-Riemann condition, which guarantees the independence of the complex derivative with respect to the chosen direction in the neighbourhood of the point considered.

$$\frac{\partial \Phi}{\partial x} = \frac{\partial \Psi}{\partial y};$$

$$\frac{\partial \Phi}{\partial y} = -\frac{\partial \Psi}{\partial x};$$

These, together with the condition that the real and imaginary components of the complex potential are real functions characterized by continuous first derivative in the neighbourhood of the point of interest, are sufficient to ensure that the function of a complex variable considered is holomorphic in the same point, said regular.

$$\omega = \Phi + i\Psi;$$

Otherwise, it comes to singular point when the complex function is not holomorphic at that point.

The holomorphic condition for the complex potential is very important because it ensures that its components are harmonic solutions of the Laplace equation and ensures that the composition of several analytic functions is another analytic function.

The elementary solutions of the Laplace equation previously analysed can now be obtained through the complex potential by introducing an appropriate transformation of general validity.

$$\omega = m \cdot \ln z = m \cdot \ln R e^{i\vartheta} = m \cdot \ln R + i \cdot m\vartheta = m \cdot \ln \sqrt{x^2 + y^2} + i \cdot m \tan^{-1} \left(\frac{y}{x} \right);$$

Varying the expression assumed by the parameter m is possible to obtain simultaneously the expressions for the kinetic potential and current function for the different elementary cases analysed.

- source:

$$m = \frac{\lambda}{2\pi} \Rightarrow \omega = \Phi + i\Psi = \frac{\lambda}{2\pi} \cdot \ln \sqrt{x^2 + y^2} + i \cdot \frac{\lambda}{2\pi} \tan^{-1} \left(\frac{y}{x} \right);$$

- vortex:

$$m = -i \cdot \frac{\Gamma}{2\pi} \Rightarrow \omega = \Phi + i\Psi = -i \cdot \frac{\Gamma}{2\pi} \cdot \ln \sqrt{x^2 + y^2} + \frac{\Gamma}{2\pi} \tan^{-1} \left(\frac{y}{x} \right);$$

Of greater practical interest is the case when you want to describe the condition in which a circular section of generic radius \bar{R} is hit by a uniform flow with unitary speed.

The presence of the body introduces changes in the real fluid dynamic lattice that can be mapped by a uniform flow in the complex plane of the above scalar functions using an appropriate conformal transformation, called Joukowski transform.

$$\omega = z + \frac{\bar{R}^2}{z};$$

$$\omega = R e^{i\theta} + \frac{\bar{R}^2}{R} e^{-i\theta} ;$$

Going back to Cartesian coordinates through the Euler formula.

$$\omega = \Phi + i\Psi = R \left(1 + \frac{\bar{R}^2}{R}\right) \cos \theta + i \cdot R \left(1 - \frac{\bar{R}^2}{R}\right) \sin \theta = \left(1 + \frac{\bar{R}^2}{R}\right) x + i \cdot \left(1 - \frac{\bar{R}^2}{R}\right) y ;$$

Reversing the expression you determine immediately the coordinates of the complex potential around the circular section.

$$x = \frac{\Phi}{\left(1 + \frac{\bar{R}^2}{R}\right)} = \sqrt{R^2 - y^2} ;$$

$$y = \frac{\Psi}{\left(1 - \frac{\bar{R}^2}{R}\right)} = \sqrt{R^2 - x^2} ;$$

These relations allow you to track easily in the original plane the equipotential lines when you set a certain value for Φ through the first expression and the current lines from the second one once it is fixed Ψ . In fact, in conformal transform the complex potential maintains the same values on corresponding lines of the original and transformed plan. So also solid surfaces and other boundary conditions remain the same going from one plane to another.

Operate with transformations in succession to obtain a new holomorphic function can lead to expressions capable of describing phenomena much more complex. The first attempts were made by Joukowski that initially applied in two phases of the just view homonymous transformation. A first time by applying the reversed version to obtain the coordinates of the transformed points as a function of Φ and Ψ ; a second to transform these coordinates in another complex plane where the representation of the problem turns out to be more simple.

$$\omega = z_1 + \frac{\bar{R}^2}{z_1} \Rightarrow z_1 = x_1 + iy_1 \Rightarrow z = z_1 + \frac{\bar{R}^2}{z_1} ;$$

Substituting the coordinates of diametrically opposite points on the circumference of the section immersed we obtained coordinates in the transformed plane belonging to the real axis.

$$z_1 = \pm \bar{R} \Rightarrow z = \pm 2\bar{R} ;$$

$$z_1 = \pm i\bar{R} \Rightarrow z = 0 ;$$

This indicates that the points belonging to the circumference of the immersed section are mapped in the transformed plane through a section of a thin foil of width $4\bar{R}$, represented by a segment belonging to the abscissa axis. This particular type of transformation is defined as homothetic since it involves any rotation or translation, but only a stretching.

Consequently, when the flow is aligned with the real axis, the current lines are all parallel to the airfoil, while the equipotential lines are normal to it for the property of orthogonality already discussed.

$$z = x + iy = x_1 + iy_1 + \frac{\bar{R}^2}{x_1 + iy_1} = x_1 + iy_1 + \frac{\bar{R}^2}{R_1^2} (x_1 - iy_1) = \left(1 + \frac{\bar{R}^2}{R_1^2}\right) x_1 + i \left(1 - \frac{\bar{R}^2}{R_1^2}\right) y_1 ;$$

Subsequently, the author has proposed other solutions that take into account many more factors and allow to analytically describing the flow around airfoils said precisely as Joukowski ones.

You first need to modify the expression of the complex field ω in order to clarify the actual average speed of the uniform flow, which invests the object of interest.

Moreover, as has been previously shown to overcome the paradox of d'Alembert is necessary to take into account the vorticity that is formed around the body immersed and that, by introducing an asymmetry in the flow field, guarantees not null lift even for the particularly flow analysed that is incompressible, irrotational and steady for an inviscid and uniform density fluid. Moreover, the presence of circulation is strictly necessary in order to satisfy the Kutta condition on the speed at the trailing edge. It's important to note that the circulation keeps in the turned plane the same values along closed paths that assumed in the original plan. So first we calculate the complex potential associated to the flow around the circular cross-section.

$$\omega = U \left(z_1 + \frac{\bar{R}^2}{z_1} \right) - i \frac{\Gamma}{2\pi} \ln z_1 ;$$

Besides, we must consider that the incident flux is never parallel to the rope that joins the leading with the trailing edge (called nose and tail of the airfoils) section. Is detected, then, an angle α between the two directions said angle of attack. To take this into account it is necessary to introduce a transformation intermediate between those seen previously that rotates properly the flow.

$$z_2 = z_1 e^{-i\alpha} ;$$

It underlines the fact that the compliance of the transformation keeps unchanged the angle of attack going from one plane to another.

It is clear now that the circulation necessary to satisfy the Kutta condition also depends on the angle of attack. It should however keep in mind the fact that the lift calculated using the Kutta-Joukowski theorem is purely theoretical. Experimentally it shows that the lift force vanishes when the angle of attack reaches values close to that of the stall, specifically for the section in question but that with a good approximation can be taken equal to 10° . This is mainly due to vortex shedding from the upper side of profile generating turbulence that break down the lift.

However, it is not all because to be able to deal with cases of real practical interest than the simple flat plate is possible to introduce a translation of the centre of the circle just defined. In the complex plane are eligible two translations orthogonal along the real axis and the imaginary one that respectively allow to take into account the tapered shape and curvature (asymmetry) of the rope in the real section.

$$\Delta = m + in ;$$

$$\omega = z + \frac{(\bar{R}-m)^2}{z} ;$$

For simplicity, the translation is written for the basic transformation for which is simpler to notice that the centre of the circle cannot translate.

In fact, the first derivative of the analytical function ω with respect to complex variable z vanishes, then at that point the transformation cannot be conformal and the section assumes a typical teardrop shape.

$$f'(z)|_{z=\bar{R}-\Delta} = \left. \frac{d\omega}{dz} \right|_{z=\bar{R}-m} = \left[1 - \frac{(\bar{R}-m)^2}{z^2} \right]_{z=\bar{R}-m} = 0;$$

Returning to the more general case the translation of the circle translates otherwise.

$$z_3 = z_2 + \Delta;$$

Finally last applies the transformation of Joukowsky.

$$z = z_3 + \frac{(\bar{R}-m)^2}{z_3};$$

At the end of this section is to stress that the importance of conformal transforms lies in the simplicity with which make it possible to study problems particularly complex starting from the known solutions of the elementary simpler cases as the flow around a circular section. The main simplification concerns the geometry of the real problem which is reduced to a much simpler one to be analyse and the solution of which is defined analytically.

5.4. Theory of Theodorsen

The present theory wants to provide an analytical formulation to aeroelastic forces acting on a wing section when immersed in an unsteady potential flow, in order to identify the conditions that lead to instability of the system. To do this you need to equip the body of at least two degrees of freedom, one vertical translation and one torsional around the stiffness axis of the profile. In fact, in the case in which they were present only the vertical oscillations, these would be damped by fluid dynamic forces. For simplicity, we want to consider the conditions that lead to instability without investigating the post critical response of the system, so it is permissible to assume that the oscillations around the equilibrium condition are infinitely small. This condition is very important in the fluid dynamic field because it is the basis of the concept of small perturbations, which allows linearizing the aeroelastic problem. In the following, the discussion is restricted to the case where the motion induced by the aeroelastic action is sinusoidal. This is an ideal condition but in general is a good estimate of the actual response. In fact, on the one hand, the structural damping induces small perturbations to the motion, and moreover hen it's neglected you are in favour of safety, on the other hand is not interested in describing a divergent response since, as already mentioned, but it's interesting to identify the conditions that lead to its onset.

Let's consider a thin flat plate parallel to the potential flow that invests starting from undisturbed uniform but non-stationary conditions, and that generates a wake equally thin. The configuration can be further complicated by overlapping the solution found regarding a stationary flux incident on a thin profile curved and separately for the flow incidence. Moreover, the assumption of flat wake has little influence on the results when considering small oscillations. The flat section can be mapped into a circular unit radius obtained by a conformal transformation of Joukowsky. In fact, considering a reference system X,Y centred at the origin of the circular section, the position of each point in the plane can be described by means of cylindrical coordinates expressed by the real and imaginary part of a complex number Z.

Then, applying the above transformation is possible to pass to the transformed plan x,y centred at the midpoint of the thin plate of width $2b$ equal to four times the radius of the circle.

$$z = Z + \frac{\bar{R}^2}{Z};$$

$$b = 2\bar{R};$$

It is noted that both the points that describe the flux lines around the circle that those associated to the direct internal flow between corresponding sources and sinks are transformed in the plane of the thin plate into flow lines which affect the entire domain. In fact very small or very large values of Z map points tending to infinity in z . So the transformed plane is mapped twice by different Riemann surfaces. The transition from one surface to the other is accomplished by crossing the circumference of the circle or the thickness of the thin plate. More specifically to the points on the upper and lower side of the thin plate correspond respectively those belonging to the upper and lower semi-circumference of the circle, instead the points of the top and bottom of the rectilinear wake become respectively the external and internal points of the same circle.

Theodorsen uses the so-called method of singularities, which consists of the superposition of the effects caused by different elementary entities whose solutions, as has been shown previously, present a singular point. To this end are applied rectilinear sources of intensity $\pm\lambda$ on the circumference of the section respectively in correspondence of the points with the same abscissa but opposite ordinates, representative of the upper and lower surface of the flat plate. In addition, to take account of the presence of vorticity in the flow, straight vortices are inserted with intensity equal to $\pm 2\Gamma$ places on the horizontal axis, respectively, within the circle and in its wake, indefinitely extended, in points that map to those of the upper and bottom surface of the wake associated with the sheet.

We highlight the fact that in the plane of the thin plate although sources and vortices of opposite intensity match, their contributions cannot cancel due to the fact that they belong to different Riemann surfaces, and so it is not granted any type of contact between opposing contributions.

The analysis of the problem, thanks to the validity of the principle of superimposition of the effects, may be divided into two phases.

5.4.1. Non-circulatory flow component

The contribution of the component of the circulatory flow is represented by the distribution of sources and sinks along the circumference of the circular section.

Each pair of source and sinks is a primary mathematical entity called doublet. Each of these elements has, by definition, an intensity proportional to the intensity of the source and the distance from the pit.

$$k = \lambda d;$$

Since each of them can move freely along the circumference of the section, it follows that the overall distribution of doublets varies in time and space. This is essential because it allows you to keep track of the continuous variation of the flow around the flat plate due not so much to the unsteadiness of the flow, which you can keep track already by the time variation of its local velocity, but to the aeroelastic response of the system. In fact, the characteristics of the motion of the foil and the flow influencing each other.

In order to determine the relationship between the intensity of the rectilinear sources and the motion of the system is required that the distribution of doublets meets at each instant on the solid surface of the foil both the condition of impermeability and the absence of cavitations resulting from the assumption of very small fluctuations.

This request results in the Neumann condition that in this case enforces the pointwise equality on the surface of the foil between the normal component of the flow velocity and that of the body in the same direction. In this regard, we consider the equation that describes in time the configuration of the surface of the foil.

$$F(x, y, z, t) = 0 ;$$

If we consider a more general case of the present one in which the geometry of the section also depends on the out of plane coordinated z , it is possible to separate the variables of dependence.

$$F(x, y, z, t) = y - y_s(x, z, t) = 0 \Rightarrow y = y_s(x, z, t) ;$$

In order to establish the absence of cavitation is useful to introduce the mathematical entity defined as substantial derivative, that in analytical level is nothing but the composite derivative of a functional, but that translates a very important physical concept. It takes into account the variability of the field not only as function of time but also of the fact that each point has its own temporal history and that the observer is moving in the same field. This method is known in the literature as Lagrangian approach, and is distinguished from the Eulerian just for the fact that the observer moves together with a particle of the field.

$$\frac{DF}{Dt} = \frac{\partial F}{\partial t} + u \frac{\partial F}{\partial x} + v \frac{\partial F}{\partial y} + w \frac{\partial F}{\partial z} ;$$

So the Neumann condition is expressed in cancelling the previously said derivative.

$$\frac{DF}{Dt} = 0 \Rightarrow v(x, y, z, t) = \frac{\partial y_s}{\partial t} + u \frac{\partial y_s}{\partial x} + w \frac{\partial y_s}{\partial y} ;$$

Consequence of the small perturbations approach, the fluctuating components of velocity of the flow are infinitesimal compared to the average undisturbed speed, and the rotations of the body represented by the spatial derivatives are always much smaller than unit. So, being allowed neglecting infinitesimals of higher order than the first, the above expression is simplified.

$$v(x, y, z, t) = \frac{\partial y_s}{\partial t} + (U + u') \frac{\partial y_s}{\partial x} + w \frac{\partial y_s}{\partial y} \cong \frac{\partial y_s}{\partial t} + U \frac{\partial y_s}{\partial x} ;$$

The equation just written is valid in general because it is able to describe the speed on the surface of a body of any sectional geometry. Typically, however, it tends to approximate the actual geometry with that of a thin profile when its dimensions permit. In this way, the equation refers directly to the axis of the profile.

In the present case, not only the thickness is negligible, but also since the motion field is two-dimensional, the displacement of the foil is identical for any values of the out of plane coordinate z , with respect to which the function is independent.

$$v_a(x, t) = \frac{\partial y_a}{\partial t} + U \frac{\partial y_a}{\partial x} ;$$

To describe appropriately the oscillations of the flow around the foil were introduced sources.

The expression of the kinetic potential for a single rectilinear source has already been defined and is written here introducing a generic translation along the horizontal axis in the plane of the thin plate.

$$\Phi_s(x, y, t) = \frac{\lambda(x_0, y_0, t)}{2\pi} \ln \sqrt{(x - x_0)^2 + y^2} = \frac{\lambda(x_0, y_0, t)}{4\pi} \ln[(x - x_0)^2 + y^2];$$

Assume that the source distribution on the surface of a generic sheet is sufficiently thick as to be able to describe the intensity per unit length by a continuous function $\tilde{\lambda}(x, y, t)$. In this way, the potential at a generic point of the domain can be calculated through the integration of the different contributions from distributed sources with continuity along the whole extension of the foil.

$$\Phi'(x, y, t) = \frac{1}{4\pi} \int_{-b}^b \tilde{\lambda}(\xi, y, t) \ln[(\xi - x_0)^2 + y^2] d\xi;$$

In calculating the speed of oscillation of the foil in the y direction is necessary to pay attention to which area is being considered; for now it is assumed to be the top one.

$$v_a(x, 0^+, t) = \frac{\partial \Phi}{\partial y} = \frac{1}{4\pi} \lim_{y \rightarrow 0^+} \frac{\partial}{\partial y} \int_{-b}^b \tilde{\lambda}^+(\xi, t) \ln[(\xi - x_0)^2 + y^2] d\xi = \frac{1}{2\pi} \lim_{y \rightarrow 0^+} y \int_{-b}^b \frac{\tilde{\lambda}^+(\xi, t)}{[(\xi - x_0)^2 + y^2]} d\xi;$$

Since the speed tends to cancel approaching the axis of the foil with the exception of the case in which you tend simultaneously to the centre of the source, the only non-negligible contribution it has in the neighbourhood of that point.

$$v_a(x, 0^+, t) = \frac{1}{2\pi} \lim_{y \rightarrow 0^+} y \int_{x-\epsilon}^{x+\epsilon} \frac{\tilde{\lambda}^+(\xi, t)}{[(\xi - x_0)^2 + y^2]} d\xi;$$

The intensity function being continuous can vary only an infinitesimal amount in the neighbourhood considered, therefore, hence it is legitimate to consider constant and equal to the value assumed in the generic point along the horizontal axis.

$$v_a(x, 0^+, t) = \frac{\tilde{\lambda}^+(x, t)}{2\pi} \lim_{y \rightarrow 0^+} \int_{-\epsilon}^{\epsilon} \frac{y}{[\xi'^2 + y^2]} d\xi' = \frac{\tilde{\lambda}^+(x, t)}{2\pi} \lim_{y \rightarrow 0^+} \left[\tan^{-1} \left(\frac{\epsilon}{y} \right) - \tan^{-1} \left(-\frac{\epsilon}{y} \right) \right];$$

Now it is necessary that together with the abscissa also the around tends to zero though less rapidly, so that the limits of inverse trigonometric functions prove respectively equal to $\pm \pi / 2$ and are negligible the effects of the other sources in the neighbourhood considered. This way you can go back to a discrete formulation of the problem.

$$v_a(x, 0^+, t) = \frac{\tilde{\lambda}^+(x, t)}{2};$$

Since in this case the intensity of the sources is equal to the double of those considered for the general case it is possible to write immediately the previous relation for both the sources with positive and negative intensity.

$$v_a(x, 0^+, t) = \pm \lambda^\pm(x, t);$$

The fact that sources and sinks are discretely distributed on different surfaces allows the calculation of the intensity of one regardless of the presence of the other. Indeed, the current lines of a doublet are represented by the circles passing through the source and the pit associated with it. A special flow line exactly coincides

with the circumference of the circle that is transformed as seen in the contour of the foil so that it coincides with a stream line. The particular case considered shows clearly that the vertical velocities of sources and doublets do not affect each other as it is not allowed no direct connection between the two that would require to be able to cross the thickness of the plate.

The last equation written states that the vertical component of the speed of the foil determines the pointwise intensity required to the distribution of sources and sinks.

Therefore, it is of fundamental importance to know the expression of that speed. In this case, the degrees of freedom, both of which refer to the stiffness axis of the foil, are represented by a vertical translation in the positive direction opposite to the y axis (pointing upwards) and a clockwise rotation. The axis of rotation is positioned in the point of abscissa \bar{x}_α proportional to half of the total length of the lamina.

$$\bar{x}_\alpha = \varepsilon_\alpha b ;$$

$$y_\alpha(x, t) = -h_\alpha(t) - \alpha(t)(x - \bar{x}_\alpha) ;$$

It replaces the expression just given for the vertical component of movement of the rope in the expression previously obtained for the velocity in the same direction.

$$v_\alpha(x, t) = \frac{\partial y_\alpha}{\partial t} + U \frac{\partial y_\alpha}{\partial x} = -\dot{h}_\alpha - \dot{\alpha}(x - \bar{x}_\alpha) - U\alpha ;$$

It is therefore immediately determine the kinetic potential of the circle as a function of the kinematics of the foil having already obtained the relation between its vertical speed to the intensity of the sources.

For now we will just define the infinitesimal component around the origin of a generic point of source or pit of the flow.

Since reference is now made to the circumference of the circle is also well introduce a translation in the vertical component and to remember that the sources used have intensity twice that of reference.

$$d\Phi' = \frac{\tilde{\lambda}(X, Y, t)}{4\pi} \ln[(X - X_0)^2 + (Y - Y_0)^2] = \frac{\lambda(X, Y, t)}{2\pi} \ln[(X - X_0)^2 + (Y - Y_0)^2] ;$$

Considering the intensity of the pair source-sink, placed symmetrically on the circumference to the horizontal axis, you must add the two contributions of opposite intensity.

$$d\Phi' = \frac{\lambda(X, Y, t)}{2\pi} \frac{\ln[(X - X_0)^2 + (Y - Y_0)^2]}{\ln[(X - X_0)^2 + (Y + Y_0)^2]} ;$$

Exploiting the relationship between the ordinate of the points belonging to the circumference, the kinetic potential is defined as a function of a single variable.

$$Y = \sqrt{\bar{R}^2 - X^2} ;$$

To determine the potential associated with the full distribution of sources and sinks is necessary to integrate the infinitesimal contributions along the outline of the complete circle. Thanks to the fact we have written it all as a function of the only abscissa the integral ranges exclusively within the diameter of the circle.

$$\Phi' = \frac{1}{2\pi} \int_{-\bar{R}}^{\bar{R}} \lambda(X, Y, t) \frac{\ln[(X - X_0)^2 + (Y - Y_0)^2]}{\ln[(X - X_0)^2 + (Y + Y_0)^2]} dX ;$$

Substituting to the intensity of the elementary entity the vertical component of the velocity of the foil and suitably transforming the coordinates in the plane of the lamina is obtained an expression fully defined. The integration is reduced to the following expression valid for sources when you see the positive sign and negative for sinks.

$$\Phi_{nc}'(x, t) = \left[\dot{h}_\alpha + \dot{\alpha} \left(\frac{x}{2} - \bar{x}_\alpha \right) + U\alpha \right] \sqrt{b^2 - x^2};$$

It is emphasized that the potential just determined relates to the fluctuating component of the incident flux on the foil.

Being known the expression of the kinetic potential is possible to determine immediately that relating to the distribution of pressure along the circumference of the circle. This requires to apply the formula of Bernoulli's theorem, has already been treated previously, for the case of non-stationary incompressible and irrotational flow of a non-viscous fluid with uniform density, in the absence of external force ($\epsilon = 0$).

$$\frac{\partial \Phi'}{\partial t} + \frac{\tilde{P}}{\rho} + \frac{|\vec{u}|^2}{2} = C(t);$$

Where instead of the absolute value of the gradient of the kinetic potential has replaced the local velocity of the total flow. The same should be done for the first term but, being derived in time, the contribution of the average velocity vanishes. The expression can be made explicit by recalling that the plate is struck by a horizontal flow, so the velocity components transverse to its chord are usually negligible for small displacements and rotations of the immersed profile.

$$|\vec{u}| = \sqrt{(U + u')^2 + v^2 + w^2} \cong U + \frac{\partial \Phi'}{\partial x};$$

It is observed that in this case the velocity of flow concerns the entire domain surrounding the foil and then the Neumann condition, which prevents the phenomenon of cavitation, does not bind the speeds of all the points considered to be equal to those of the foil.

Thus it is possible to explain the Bernoulli theorem in function of pressure, refers to that which is infinitely far away from the lamina where the motion is uniform, although variable in time. This can be done for both the upper and lower side of the blade by simply changing the sign to the kinetic potential, taking advantage of the skew symmetry of the velocity field.

$$P_\infty = \bar{\rho} C(t);$$

$$(\tilde{P} - P_\infty)^\pm = -\bar{\rho} \left[\pm \frac{\partial \Phi'}{\partial t} + \frac{1}{2} \left(U \pm \frac{\partial \Phi'}{\partial x} \right)^2 \right];$$

Since we want to determine the force acting on the foil, is of interest the only difference in pressure between the top surface and the bottom.

$$\left(U \pm \frac{\partial \Phi'}{\partial x} \right)^2 = U^2 \pm 2U \frac{\partial \Phi'}{\partial x} + \frac{\partial \Phi'}{\partial x}^2;$$

$$\Delta \tilde{P} = (\tilde{P} - P_\infty)^+ - (\tilde{P} - P_\infty)^- = -2\bar{\rho} \left[\frac{\partial \Phi'}{\partial t} + U \frac{\partial \Phi'}{\partial x} \right];$$

The calculation of the total lift acting on the blade due to the circulatory flow component requires the non-simple integration of the pressure difference over the entire width of the foil.

Attention should be paid to the fact that as it was written for the pressure difference is necessary to consider positive lift associated with a jump of negative pressure so that it is concordant with the direction chosen for the y-axis.

$$F_{L,nc} = - \int_{-b}^b \Delta \tilde{P} dx = 2\bar{\rho} \int_{-b}^b \left[\frac{\partial \Phi'}{\partial t} + U \frac{\partial \Phi'}{\partial x} \right] dx = 2\bar{\rho} \int_{-b}^b \frac{\partial \Phi'}{\partial t} dx + 2\bar{\rho} U [\Phi'(b, t) - \Phi'(-b, t)];$$

Since the velocity field of the flow depends on the first derivative in space of the kinetic potential, it is not affected by the change of a constant term in the potential. This allows to assume that the potential vanishes in correspondence with the entrance of the foil. In addition, since there are no circulatory contributions, the potential is uniquely defined so that the constant has been assumed null must be the same whatever the number of times we move on the contour of the foil. It follows that the potential also vanishes at the end of the output.

$$\Phi'(\pm b, t) = 0;$$

$$F_{L,nc} = 2\bar{\rho} \frac{\partial}{\partial t} \left(\int_{-b}^b \Phi'(x, t) dx \right);$$

We note that the lift will cancel in the general case in which the flow is steady, confirming what has already been found in deriving the Kutta-Joukowski theorem for stationary flows without circulation.

Specializing the solution to the present case, the time variation of the integral in the space of the kinetic potential completely defines the out of plane lift per unit length of the foil.

$$F_{L,nc}(t) = \pi \bar{\rho} b^2 [\ddot{h}_\alpha(t) - \bar{x}_\alpha \ddot{\alpha}(t) + U \dot{\alpha}(t)];$$

The non-circulatory contribution to the torsional moment around the axis of rotation of the blade requires roughly the same steps already seen, remembering to considered positive aerodynamic couples only if clockwise.

$$M_{z,nc}(t) = \int_{-b}^b \Delta \tilde{P} \cdot (x - \bar{x}_\alpha) dx = -2\bar{\rho} \int_{-b}^b \left[\frac{\partial \Phi'}{\partial t} + U \frac{\partial \Phi'}{\partial x} \right] (x - \bar{x}_\alpha) dx;$$

Developing the product is recognized in the last term the direct contribution of the lift, it is also possible to operate an integration by parts the second term to eliminate the contributions coming from the ends of the plate.

$$\int_{-b}^b \frac{\partial \Phi'}{\partial x} x dx = [\Phi' x]_{-b}^b - \int_{-b}^b \Phi' dx = 2b\Phi'(b, t) - \int_{-b}^b \Phi' dx = - \int_{-b}^b \Phi' dx;$$

$$M_{z,nc}(t) = -2\bar{\rho} \frac{\partial}{\partial t} \int_{-b}^b \Phi'(x, t) x dx + 2\bar{\rho} U \int_{-b}^b \Phi' dx + F_{L,nc}(t) \bar{x}_\alpha;$$

It replaces the general expression for the lift already found.

$$F_{L,nc} = 2\bar{\rho} \frac{\partial}{\partial t} \left(\int_{-b}^b \Phi'(x, t) dx \right);$$

$$M_{z,nc}(t) = -2\bar{\rho} \frac{\partial}{\partial t} \int_{-b}^b \Phi'(x, t) (x - \bar{x}_\alpha) dx + 2\bar{\rho} U \int_{-b}^b \Phi' dx;$$

Finally, it is explained the kinetic potential for the present case and develop the integrals in the plane of the foil to obtain the out of plane torque per unit length.

$$M_{z,nc}(t) = \pi b^2 \bar{\rho} \left[\bar{x}_\alpha \dot{h}_\alpha(t) + U \dot{h}_\alpha(t) - \left(\frac{b^2}{8} + \bar{x}_\alpha^2 \right) \ddot{\alpha}(t) + U^2 \alpha(t) \right];$$

5.4.2. Circulatory flow component

Unless consider very specific kinematics, and of little practical interest, the circulatory component alone is not able to satisfy the constraint of finite speed at the output end of the profile. This need is dictated by the Kutta condition and as a direct consequence of this is that, the point of detachment of the flow takes place precisely at the tail of the profile.

To this end it is necessary to superimpose a motion field characterized by not null circulation obtained by introducing a distribution of vortices fixed on the surface of the thin plate, and a counter-vortices that move away from it at the speed of the uniform flow following the route traced by the wake that is extends to infinity. The last statement translates what is commonly called the hypothesis of Taylor, which states that, with good approximation, the turbulence, and therefore all the vorticity in the flow, is transported by the average undisturbed stream as suspension particles. The approximation is to neglect the interaction between the different structures that are formed in the flow, going to consider only those of larger dimensions.

This particular distribution of vortices of positive intensity and against-vortices of negative intensity allows to satisfy also the theorem of Kelvin with which it binds the total circulation in a closed path, which moves with the current, to remain constant in time. In fact, to an increase of the circulation on the foil corresponds to an increase of counter-circulation in the wake. This underlines the importance of the wake in the study of forcing acting on a submerged body, which would otherwise be strongly overestimated as it is in the quasi-static approach. This fact will be extensively discussed at the end of the paragraph.

This emphasizes the fact that the theorem of Kelvin do not prevent the possibility that the sources of vorticity are both variable in time and in space, as has been done for the sources, in fact, this condition appears to be strictly necessary in order to correctly model the aeroelastic response of the system.

So that on the surface of the foil and then the circle one is again satisfied the condition of impermeability is necessary that both surfaces coincide with stream lines, which as we know cannot be crossed by the flow. To this end, has been shown to be necessary that each counter-clockwise against-vortex in place X_0^- on the horizontal axis passing through the center of the circle of radius \bar{R} is associated with a vortex positioned X_0^+ on the same axis, that in the complex plane is translated into the following condition.

$$X_0^- = \frac{\bar{R}^2}{X_0^+};$$

It is evident the analogy with the conformal transformed of Joukowsky which in effect is formed by two components of which the first is the uniform current lines and the second the curve around a circle. Of course, the two components have different areas of influence where their contribution becomes more important, respectively away and in the neighbourhood of the immersed body.

In the following, to identify the pair of vortices, it will always refer to the position of the vortex with negative circulation.

It is observed that as the position of the vortex moves toward the centre of the circle are generated counter-vortices in the wake increasingly distant from the body.

The fact of positioning the axis of the vortices exclusively inside the circle or in the wake is not random but allows you can isolate these singular points outside the stream. In fact, as has already been mentioned, to make the domain simply connected we need to introduce a cut in the domain in correspondence of the wake, thus introducing an approximation, however, is that more and more negligible as the wake and then the cut is thin. That said, it has the added benefit of placing the singular points outside the domain, a fundamental requirement for the applicability of many theorems used in the treatment.

In the present case, considering a flat wake, the procedure to reduce to a simply connected domain is definitely acceptable and the absence of singularities allows to apply without problems Stokes theorem that guarantees the existence of kinetic potential for an irrotational flow, as previously been shown.

We proceed now with the definition of the potential associated to the component of the circulatory flow, and recalling the expression already obtained for the single rectilinear vortex is imprinted a translation along the horizontal axis in the plane of the foil.

$$\Phi_v(X, Y, X_0, t) = \frac{\Gamma(X_0, t)}{2\pi} \tan^{-1} \left(\frac{Y}{X - X_0} \right);$$

It is observed that the intensities of all the vortices should be independent from the vertical coordinate being all positioned on the horizontal axis.

As for the sources also for the vortices is considered a pair of elementary entities linked by a kinematic constraint on the mutual position. So is immediate calculate the potential associated to a system formed by associated vortex and counter-vortex, recalling the relationship between the position of the two elements.

$$\Phi(X, Y, X_0, t) = \frac{\Gamma(X_0, t)}{2\pi} \left[\tan^{-1} \left(\frac{Y}{X - X_0} \right) - \tan^{-1} \left(\frac{Y}{X - \bar{R}^2/X_0} \right) \right] = \frac{\Gamma(X_0, t)}{2\pi} \tan^{-1} \left[\frac{(X_0 - \bar{R}^2/X_0) \cdot Y}{X^2 - (X_0 + \bar{R}^2/X_0) \cdot X + Y^2 + 1} \right];$$

We introduce a new parameter.

$$\frac{X_0}{\bar{R}} + \frac{\bar{R}}{X_0} = 2 \frac{X_0}{\bar{R}};$$

After a few steps, you leads back to a simpler expression of the potential in the plane of the foil.

$$\Phi_c(x, \bar{x}_0, t) = -\frac{\Gamma(\bar{x}_0, t)}{2\pi} \tan^{-1} \left[\frac{\sqrt{b^2 - x^2} \sqrt{\bar{x}_0^2 - b^2}}{b^2 - x\bar{x}_0} \right];$$

This emphasizes the fact that the trailing edge of the foil the kinetic potential is not cancelled.

Therefore, confirms what has been said previously for the single vortex, that to each path of 360 ° around it the potential increases by a constant amount.

To determine the pressure jump through the foil is exploited again the same expression used for the component of the non-circulatory motion being this again antisymmetric with respect to the horizontal axis.

$$\Delta \bar{P} = -2\bar{\rho} \left[\frac{\partial \Phi'}{\partial t} + U \frac{\partial \Phi'}{\partial x} \right];$$

Assuming to be valid the hypothesis proposed by Taylor in respect of the propagation of turbulence, it is possible to explain the time derivative of the kinetic potential in a simpler form by the average speed of the flow.

$$\frac{\partial \Phi'}{\partial t} = \frac{\partial \Phi'}{\partial \bar{x}_0} U ;$$

$$\Delta \tilde{P} = -2\bar{\rho}U \left[\frac{\partial \Phi'}{\partial \bar{x}_0} + \frac{\partial \Phi'}{\partial x} \right] ;$$

Substituting the expression previously determined for the kinetic potential, after a few passages it is possible to obtain the expression of the pointwise change of pressure generated by a pair of counter-rotating vortices of the same intensity. The effect is measured in a generic point of the blade, corresponding to the counterpart on the circular perimeter in the complex plane.

$$\Delta \tilde{P}(x, \bar{x}_0, t) = -\bar{\rho}U \frac{\Gamma(\bar{x}_0, t)}{\pi} \left[\frac{\bar{x}_0 + x}{\sqrt{b^2 - x^2} \sqrt{\bar{x}_0^2 - b^2}} \right] ;$$

To determine the effect of a single vortex pair in terms of lift over the entire plate is necessary to integrate on the surface of the section (corresponding to the outline of the circular one in the complex plane). Once again, as it was written the pressure difference is necessary to consider positive lift associated with a negative pressure jump.

$$F_{L,c}(\bar{x}_0, t) = -\int_{-b}^b \Delta \tilde{P}(x, \bar{x}_0, t) dx = \bar{\rho}U \frac{\Gamma(\bar{x}_0, t)}{\pi \sqrt{\bar{x}_0^2 - b^2}} \int_{-b}^b \left[\frac{\bar{x}_0 + x}{\sqrt{b^2 - x^2}} \right] dx = \bar{\rho}U \Gamma(\bar{x}_0, t) \frac{\bar{x}_0}{\sqrt{\bar{x}_0^2 - b^2}} ;$$

Note that as the position of the negative vortex moves away along the trail, the lift tends to that of a single vortex in accordance with the formulation of the theorem of Kutta-Joukowski.

Subsequently it is necessary to overlap the contributions of each pair of vortices in order to obtain the total lift. To do this we need to integrate the above expression along the entire trail for hypothesis extends indefinitely from the tail of the profile. In fact if you consider a finite time interval is sufficient to integrate up to where it was transported the first vortex generated on the surface of the foil, that is $b + U \cdot t_0$.

$$F_{L,c}(t) = \int_b^{+\infty} F_{L,c}(\bar{x}_0, t) = \bar{\rho}U \int_b^{+\infty} \frac{\bar{x}_0}{\sqrt{\bar{x}_0^2 - b^2}} \Gamma(\bar{x}_0, t) ;$$

Since you are implicitly integrating over the circulation introduced by each pair of vortices, it is useful to assume, as had been done for doublets, a sufficiently dense distribution to consider the vorticity continuously variable.

$$\Gamma(\bar{x}_0, t) = \gamma(\bar{x}_0, t) d\bar{x}_0 ;$$

The new parameter introduced is the intensity per unit length of the circulation generated by the pairs of counter-rotating vortices. Since the hypothesis of Taylor ensures that the vorticity moves at constant intensity in the space, to meet this condition it is necessary γ to be variable not only in space but also in time.

Only in the particular case in which the reference frame is moving along with the flow we will not resent of any variation of the density of circulation due to the passing of time but only the fact that there is moving away from the first vortex

$$\gamma(\bar{x}_0, t) = \gamma(U \cdot t - \bar{x}_0) ;$$

The above expression simply resumes the hypothesis of Taylor, in fact, the time dependence is of fundamental importance in order to define the current position of the vortex that is previously detached from \bar{x}_0 . Since the time axis starts at the instants of the first motion of the fluid we are considering the distance from the first vortex that is formed in the flow.

Redefining the components immediately circulatory potential, pressure difference and importance.

$$\Phi_c(x, t) = -\frac{1}{2\pi} \int_b^{+\infty} \tan^{-1} \left[\frac{\sqrt{b^2-x^2} \sqrt{\bar{x}_0^2-b^2}}{b^2-x\bar{x}_0} \right] \gamma(\bar{x}_0, t) d\bar{x}_0 ;$$

$$\Delta\tilde{P}(x, t) = -\bar{\rho}U \frac{1}{\pi\sqrt{b^2-x^2}} \int_b^{+\infty} \frac{\bar{x}_0+x}{\sqrt{\bar{x}_0^2-b^2}} \gamma(\bar{x}_0, t) d\bar{x}_0 ;$$

$$F_{L,c}(t) = \bar{\rho}U \int_b^{+\infty} \frac{\bar{x}_0}{\sqrt{\bar{x}_0^2-b^2}} \gamma(\bar{x}_0, t) d\bar{x}_0 ;$$

The circulatory component of the aerodynamic torque around the centre of stiffness due to a single pair of vortices is obtained by the following integral.

In this case the clockwise sign convention requires no change of sign of the pressure difference.

$$\begin{aligned} M_{z,c}(\bar{x}_0, t) &= \int_{-b}^b \Delta\tilde{P}(x, \bar{x}_0, t) \cdot (x - \bar{x}_\alpha) dx = -\bar{\rho}U(t) \frac{\Gamma(\bar{x}_0, t)}{\pi \cdot \sqrt{\bar{x}_0^2-b^2}} \int_{-b}^b \frac{\bar{x}_0+x}{\sqrt{b^2-x^2}} (x - \bar{x}_\alpha) dx = \\ &= -\bar{\rho}U(t) \Gamma(\bar{x}_0, t) \frac{b^2}{\sqrt{\bar{x}_0^2-b^2}} \left(\frac{1}{2} - \frac{\bar{x}_0 \cdot x_\alpha}{b^2} \right) ; \end{aligned}$$

Integrating once again but on the length of the wake travelled by the first vortex generated, one obtains the total torque generated by all the detached vortices so far from the body.

$$\begin{aligned} M_{z,c}(t) &= \int_b^{+\infty} M_{z,c}(\bar{x}_0, t) = -\bar{\rho}U(t) b^2 \int_b^{+\infty} \frac{1}{\sqrt{\bar{x}_0^2-b^2}} \cdot \left(\frac{1}{2} - \frac{\bar{x}_0 \cdot x_\alpha}{b^2} \right) \cdot \gamma(\bar{x}_0, t) d\bar{x}_0 = \\ &= -\bar{\rho}U(t) b \int_b^{+\infty} \left[\frac{\frac{1}{2}(b+\bar{x}_0)}{\sqrt{\bar{x}_0^2-b^2}} - \left(\frac{x_\alpha}{b} + \frac{1}{2} \right) \frac{\bar{x}_0}{\sqrt{\bar{x}_0^2-b^2}} \right] \gamma(\bar{x}_0, t) d\bar{x}_0 = -\bar{\rho}U(t) b \int_b^{+\infty} \left[\frac{1}{2} \sqrt{\frac{\bar{x}_0+b}{\bar{x}_0-b}} - \right. \\ &\quad \left. \left(\varepsilon_\alpha + \frac{1}{2} \right) \frac{\bar{x}_0}{\sqrt{\bar{x}_0^2-b^2}} \right] \gamma(\bar{x}_0, t) d\bar{x}_0 ; \end{aligned}$$

In the integral previous some terms are grouped so as to highlight the fact that the lift and the aerodynamic torque depend on the same integrals appropriately weighed.

5.4.3. Circulatory intensity

It now goes to the most important phase of the theory developed by Theodorsen, namely the determination of the intensity of the circulation. To do this it is necessary to impose the Kutta condition constraining the total velocity at the trailing edge of the profile to be finite. Since you are considering a simple geometry you can narrow it down to only the horizontal component of the velocity, lined with the foil. In order to determine the total speed of the flow you must first define the total potential, composed by the contribution of duplets and of vortex pairs.

$$\Phi_{tot}(x, t) = \Phi'_{nc} + \Phi_c = \left[\dot{h}_\alpha + \dot{\alpha} \left(\frac{x}{2} - \bar{x}_\alpha \right) + U\alpha \right] \sqrt{b^2 - x^2} - \frac{1}{2\pi} \int_b^{+\infty} \tan^{-1} \left[\frac{\sqrt{b^2 - x^2} \sqrt{\bar{x}_0^2 - b^2}}{b^2 - x\bar{x}_0} \right] \gamma(\bar{x}_0, t) d\bar{x}_0$$

Differentiating with respect to the abscissa in the plane of the thin plate is obtained the expression for the horizontal component of the local velocity.

$$u(x, t) = \frac{\partial \Phi_{tot}}{\partial x} = - \left[\dot{h}_\alpha - \dot{\alpha} \bar{x}_\alpha + U\alpha \right] \frac{x}{\sqrt{b^2 - x^2}} + \frac{\dot{\alpha}}{2} \left(\sqrt{b^2 - x^2} - \frac{x^2}{\sqrt{b^2 - x^2}} \right) + \frac{1}{2\pi} \int_b^{+\infty} \frac{\sqrt{\bar{x}_0^2 - b^2}}{(\bar{x}_0 - x) \sqrt{b^2 - x^2}} \gamma(\bar{x}_0, t) d\bar{x}_0;$$

It is observed that the common denominator tends to zero as it approaches to the trailing edge of the foil. So in order to avoid that the intensity of the speed explodes, it is necessary that the numerator decreases faster than the previous term.

It is estimated, therefore, the expression of the numerator at abscissa $x = b$ and imposes that vanishes.

$$Q(t) = \left[\dot{h}_\alpha - \dot{\alpha} \left(\bar{x}_\alpha - \frac{b}{2} \right) + U\alpha \right] = \frac{1}{2\pi b} \int_b^{+\infty} \sqrt{\frac{\bar{x}_0 + b}{\bar{x}_0 - b}} \gamma(\bar{x}_0, t) d\bar{x}_0;$$

The relation just given is the most important result of the theory of Theodorsen and must be respected in order to satisfy the Kutta condition. This imposes a constraint to the circuitry whose intensity can now be defined.

Furthermore we introduce a function $C(t)$, which collects all of the terms under the integral appearing in the expressions of the forcing that it can be defined in a concise expression. This is obtained simply by multiplying and dividing the circulatory components of lift and torque by the factor $Q(t)$ just defined.

$$F_{L,c}(t) = \bar{\rho} U \int_b^{+\infty} \frac{\bar{x}_0}{\sqrt{\bar{x}_0^2 - b^2}} \gamma(\bar{x}_0, t) d\bar{x}_0 = 2\pi b \bar{\rho} U Q(t) C(t);$$

$$M_{z,c}(t) = -\bar{\rho} U b \int_b^{+\infty} \left[\frac{1}{2} \sqrt{\frac{\bar{x}_0 + b}{\bar{x}_0 - b}} - \left(\varepsilon_\alpha + \frac{1}{2} \right) \frac{\bar{x}_0}{\sqrt{\bar{x}_0^2 - b^2}} \right] \gamma(\bar{x}_0, t) d\bar{x}_0 = -2\pi b^2 \bar{\rho} U Q(t) \left[\frac{1}{2} - \left(\varepsilon_\alpha + \frac{1}{2} \right) C(t) \right];$$

The exact expression of the new time dependent parameter introduced is as follows.

$$C(t) = \frac{\int_b^{+\infty} \frac{\bar{x}_0}{\sqrt{\bar{x}_0^2 - b^2}} \gamma(\bar{x}_0, t) d\bar{x}_0}{\int_b^{+\infty} \sqrt{\frac{\bar{x}_0 + b}{\bar{x}_0 - b}} \gamma(\bar{x}_0, t) d\bar{x}_0};$$

In order to determine the value of $C(t)$ at each time instant is of fundamental importance to provide a reasonable expression to the intensity per unit length of the circuitry.

It really is not easy to identify a function $\gamma(\bar{x}_0, t)$ a priori; for this it is convenient to choose a time trend of the motion of the plate and from this calculate the intensity distribution of circuitry.

The choice of the more reasonable flow field appears to be the sinusoidal one; in fact it was observed that for small oscillations of the foil the variation of vorticity follows a sinusoid in the stretch of the wake immediately downstream of the trailing edge.

Having chosen a temporal history sinusoidal generic, both components of motion of the foil can be expressed by making use of the Euler notation for complex numbers, thanks to the fact that we are in the linear range for the hypothesis of small oscillations.

$$h_\alpha(t) = h_{\alpha,0} \cdot e^{i\omega t};$$

$$\alpha(t) = \alpha_0 \cdot e^{i\omega t};$$

It is emphasized that the stationary terms may be complex numbers to be able to track the spatial phase shift between the different points of the plan.

Until now it was only assumed that the oscillations were so small as to linearize the geometry of the problem, but with the kinematic constraint just introduced we can obtain exact solutions only in the case where the motion is actually sinusoidal or at least stationary (corresponding to a infinite period).

The same applies to the intensity of circuitry per unit length, since it is linked to the components of motion by the equality that translates the Kutta condition.

$$\gamma(\bar{x}_0, t) = \gamma_0 \cdot e^{i\omega \cdot \left(t - \frac{\bar{x}_0}{U}\right)};$$

A direct consequence is that now the vorticity not only is periodic in space but also in time. In fact, the two coordinates are well connected to each other by the hypothesis of Taylor on the propagation of eddies along the trail.

$$\gamma(\bar{x}_0, t) = \gamma(\bar{x}_0 + U \cdot T, t) = \gamma(\bar{x}_0, t + T);$$

The two equalities are merely to indicate that moving along the trail of a stretch equal to that travelled by a vortex transported by the average speed of the flow or waiting for a period of time equal to the period of the sinusoidal motion of the foil, we will observe the same conditions. This causes the wavelength of the motion is closely related to the average speed of the flow.

$$\lambda = U \cdot T;$$

$$T = \frac{2\pi}{\omega};$$

The last observation made allows us to link the speed of the mean flow to the motion of the foil through the angular wave number k , with respect to the dimensionless semi-chord b . In fact, it is possible to reformulate the expression of the phase angle at the imaginary exponent of $\gamma(\bar{x}_0, t)$ choosing an instant and a position in the wake generic as shown below.

$$\omega \cdot \left(t - \frac{\bar{x}_0}{U}\right) = \frac{\omega}{U} (Ut - \bar{x}_0) = \frac{2\pi}{\lambda} (Ut - \bar{x}_0) = k(Ut - \bar{x}_0) = kb \left(\frac{U}{b}t - \frac{\bar{x}_0}{b}\right) = \tilde{k} \left(\frac{U}{b}t - \xi_0\right);$$

$$\gamma(\bar{x}_0, t) = \gamma_0 \cdot \exp \left\{ i\tilde{k} \left(\frac{U}{b}t - \xi_0\right) \right\};$$

$$\bar{x}_0 = \xi_0 \cdot b ;$$

Now it is possible to reformulate the expression given previously for $C(t)$ that after some simplifications is no longer a function of time but only the wave number k , and also is clear to be a complex function.

$$C(k^*) = \frac{\int_1^{+\infty} \frac{\xi_0}{\sqrt{\xi_0^2 - 1}} e^{-ik^* \xi_0} d\xi_0}{\int_1^{+\infty} \frac{\xi_0 + 1}{\sqrt{\xi_0 - 1}} e^{-ik^* \xi_0} d\xi_0} ;$$

5.4.4. Bessel and Theodorsen functions

At this point in the discussion you need to open a small parenthesis to recall the main properties of the Bessel functions.

First define a complex function.

$$K_n(z) = \int_0^{\infty} e^{-x \cdot \cosh(t)} \cosh(nt) dt ;$$

Such that.

$$K_n(t) = e^{\frac{i n \pi}{2}} G_n(it) ;$$

Where a new complex function is expressed as follows.

$$G_n(it) = -\bar{Y}_n(x) + \left(\ln 2 - \gamma + i \frac{\pi}{2} \right) \cdot J_n(x) ;$$

Defining.

$$\bar{Y}_n(x) = \frac{\pi}{2} Y_n(x) + (\ln 2 - \gamma) \cdot J_n(x) ;$$

The above function can be rewritten.

$$G_n(x) = -\frac{\pi}{2} [Y_n(x) - i \cdot J_n(x)] ;$$

You can now determine the values of the first function above defined as $K_n(z)$.

$$K_0(-ik) = \int_0^{\infty} e^{ik \cdot \cosh(t)} dt = \int_1^{\infty} \frac{e^{ikx}}{\sqrt{x^2 - 1}} dx = \int_1^{\infty} \frac{\cos(kx)}{\sqrt{x^2 - 1}} dx + i \int_1^{\infty} \frac{\sin(kx)}{\sqrt{x^2 - 1}} dx ;$$

Because.

$$G_0(k) = -\frac{\pi}{2} [Y_0(k) - i \cdot J_0(k)] = K_0(-ik) ;$$

There are two conditions that allow to determine the two unknown functions simply equating the real and imaginary parts.

$$Y_0(k) = -\frac{2}{\pi} \int_1^{\infty} \frac{\cos(kx)}{\sqrt{x^2-1}} dx ;$$

$$J_0(k) = \frac{2}{\pi} \int_1^{\infty} \frac{\text{sen}(kx)}{\sqrt{x^2-1}} dx ;$$

Continuing to sample the functions in the same way just seen, you switch to the next term.

$$K_1(-ik) = \int_0^{\infty} e^{ik \cdot \cosh(t)} \cosh(t) dt = \int_1^{\infty} \frac{x e^{ikx}}{\sqrt{x^2-1}} dx = \int_0^{\infty} \frac{x \cdot \cos(kx)}{\sqrt{x^2-1}} dx + i \int_0^{\infty} \frac{x \cdot \text{sen}(kx)}{\sqrt{x^2-1}} dx ;$$

$$G_1(k) = -\frac{\pi}{2} [Y_1(k) - i \cdot J_1(k)] = \frac{K_1(-ik)}{i} ;$$

$$Y_1(k) = -\frac{2}{\pi} \int_1^{\infty} \frac{x \cdot \text{sen}(kx)}{\sqrt{x^2-1}} dx ;$$

$$J_1(k) = -\frac{2}{\pi} \int_1^{\infty} \frac{x \cdot \cos(kx)}{\sqrt{x^2-1}} dx ;$$

The functions just formed are known in the literature as Bessel functions of order n (1 and 2), respectively of the first J_n and second Y_n species. These can be linearly combined to form complex functions used in the study of radiation known as Hankel functions.

$$H_n^{(2)}(k) = J_n(k) - iY_n(k) ;$$

You arrive at the conclusion of this parenthesis rewriting the function C (k) as follows.

$$C(\tilde{k}) = \frac{H_1^{(2)}(\tilde{k})}{H_1^{(2)}(\tilde{k}) + iH_0^{(2)}(\tilde{k})} ;$$

This expression can be drastically simplified by rationalizing the denominator to clearly separate the real from the imaginary part.

$$C(\tilde{k}) = \frac{[J_1(\tilde{k}) - iY_1(\tilde{k})]}{[J_1(\tilde{k}) - iY_1(\tilde{k})] + i[J_0(\tilde{k}) - iY_0(\tilde{k})]} = \frac{[J_1(\tilde{k}) - iY_1(\tilde{k})]}{[J_1(\tilde{k}) + Y_0(\tilde{k})] - i[Y_1(\tilde{k}) - J_0(\tilde{k})]} = F(\tilde{k}) + i \cdot G(\tilde{k}) ;$$

$$F(\tilde{k}) = \frac{J_1(\tilde{k})[J_1(\tilde{k}) + Y_0(\tilde{k})] + Y_1(\tilde{k})[Y_1(\tilde{k}) - J_0(\tilde{k})]}{[J_1(\tilde{k}) + Y_0(\tilde{k})]^2 + [Y_1(\tilde{k}) - J_0(\tilde{k})]^2} ;$$

$$G(\tilde{k}) = -\frac{J_1(\tilde{k}) \cdot J_0(\tilde{k}) + Y_1(\tilde{k}) \cdot Y_0(\tilde{k})}{[J_1(\tilde{k}) + Y_0(\tilde{k})]^2 + [Y_1(\tilde{k}) - J_0(\tilde{k})]^2} ;$$

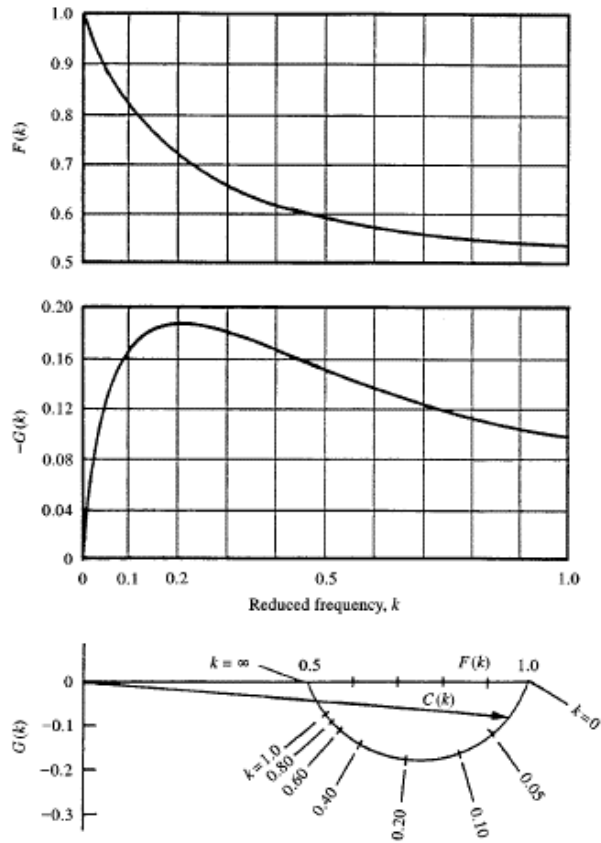


Figure 5.1_ Real and imaginary part of the complex Theodorsen function.

The two functions just defined represent the true goal of the entire study so far conducted, so that $C(k)$ is known as a function of the circuitry of Theodorsen. This can be seen as a filter capable of damp down more consistently the aerodynamic forces acting on the body when it oscillates at very high frequencies (high wave number k). From the physical point of view, the function just defined is able to take into account the aeroelastic interaction existing between the motion of the fluid vein and that of the body. This is also a big difference compared with the Quasi- Stationary approach, which has been mentioned at the beginning of treatment. In fact, as the name itself suggests the Stationary Theory provides reliable results only when the frequency with which the immersed body moves is much lower than that required by a particle of fluid to cross the characteristic dimension (aligned with the mean flow) of the body itself. The parameter that promptly provides that information is said "reduced speed".

$$U^* = \frac{U}{fB};$$

This is an important parameter when you want to carry out wind tunnel tests, in fact when making scale models is a must to ensure that the model maintains the same reduced speed of the real structure. Therefore, when the wind speed and the mechanical characteristics of the structure to the true are such as to use the Quasi- Stationary Theory, you can measure the dimensionless aerodynamic coefficients in the wind tunnel on simple rigid models. This way you avoid having to realise a complex aeroelastic model that is able to faithfully reproduce the inertial characteristics and the stiffness of the structure to the true, the cost of which in terms of realisation and testing are significantly higher. In general, for simplicity arises a practical threshold equal to $U^* = 10-20$ over which is applicable.

You immediately notice the similarity between the expression of the angular wave number and the reduced velocity.

$$\tilde{k} = \frac{2\pi fb}{U} = \frac{\pi}{U^*};$$

It is observed then that in making k dimensionless has followed an unusual path, in fact, the normalization term is not the full length of the foil but only its half.

In wind engineering applications is typical also refer to another dimensionless parameter said reduced frequency, corresponding to the ratio between the frequency of the body and that of the flow, or coincides with the inverse of the reduced speed.

$$f^* = \frac{fB}{U} = \frac{1}{U^*};$$

So you can see k^* as a kind of dimensionless reduced frequency.

$$\tilde{k} = \pi f^*;$$

Further, the number of Strouhal allows to link the frequency of vortex shedding to the average speed of the wind and to the characteristic size of the body.

$$f_s = St \frac{U}{B};$$

Since the phenomenon of vortex shedding is self-excited the body immersed in the flow oscillates more when the frequency of vortex shedding frequency is close to his own. So it is possible to determine a critical speed of the flow for which this phenomenon takes place, said speed of Strouhal.

$$U_{st} = \frac{f_s B}{St};$$

You notice immediately that switching to reduced speed you have a direct link with the number of Strouhal therefore coincides with the reduced frequency at the vortex shedding.

$$U_{st}^* = \frac{1}{St};$$

5.4.5. Aeroelastic forces

Now we are able to determine fully the components of the circulatory lift and the aerodynamic torque.

$$F_{L,c}(t) = 2\pi b \bar{\rho} U Q(t) C(\tilde{k});$$

$$M_{z,c}(t) = -2\pi b^2 \bar{\rho} U Q(t) \left[\frac{1}{2} - \left(\varepsilon_\alpha + \frac{1}{2} \right) C(\tilde{k}) \right];$$

We have reached the end of the discussion proposed by Theodorsen, in fact have been completely defined the aerodynamic forcing in their two components circulatory and not.

Now it only remains to superimpose effects.

$$L(t) = F_{L,nc}(t) + F_{L,c}(t) ;$$

Hence.

$$L(t) = \pi b^2 \bar{\rho} [\ddot{h}_\alpha(t) - \bar{x}_\alpha \ddot{\alpha}(t) + U \dot{\alpha}(t)] + 2\pi b \bar{\rho} U C(\tilde{k}) \left[\dot{h}_\alpha - \dot{\alpha} \left(\bar{x}_\alpha - \frac{b}{2} \right) + U \alpha \right] ;$$

In the expression of the aerodynamic torque, you have simplify common terms between the components circulatory and not. Specifically cancel out the second and fourth component of the non-circulatory that are replaced with the residual coming from the circulatory contribution.

$$M(t) = M_{z,nc}(t) + M_{z,c}(t) = \pi b^2 \bar{\rho} \left[\bar{x}_\alpha \ddot{h}_\alpha(t) + U \dot{h}_\alpha(t) - \left(\frac{b^2}{8} + \bar{x}_\alpha^2 \right) \ddot{\alpha}(t) + U^2 \alpha(t) \right] - 2\pi b^2 \bar{\rho} U \left[\frac{1}{2} - \left(\varepsilon_\alpha + \frac{1}{2} \right) C(\tilde{k}) \right] \left[\dot{h}_\alpha - \dot{\alpha} \left(\bar{x}_\alpha - \frac{b}{2} \right) + U \alpha \right] ;$$

Hence.

$$M(t) = \pi b^2 \bar{\rho} \left[\bar{x}_\alpha \ddot{h}_\alpha(t) - \left(\frac{b^2}{8} + \bar{x}_\alpha^2 \right) \ddot{\alpha}(t) + U \dot{\alpha} \left(\bar{x}_\alpha - \frac{b}{2} \right) \right] + 2\pi b \bar{\rho} U \left(\bar{x}_\alpha + \frac{b}{2} \right) C(\tilde{k}) \left[\dot{h}_\alpha - \dot{\alpha} \left(\bar{x}_\alpha - \frac{b}{2} \right) + U \alpha \right] ;$$

You can now see that not only the not-circulatory contribution of the flow introduces terms proportional to the second derivative of the two free coordinates of the system. These terms represent the added aerodynamic mass that must be summed up to that of the structural system. In fact, at the physical level this added mass represents the portion of fluid that participates in the body motion increasing its inertia. Indeed, since the speed of the body is transmitted to the fluid, there being no dissipative internal resources (such as viscosity, neglected here) it is necessary that the increase of kinetic energy is converted completely into work required to move the fluid. Because the forcing that change the internal energy of the fluid are generally outside the system, this additional kinetic energy can be taken into account by simply considering the balance of forces acting on the immersed body characterized however by increased mass and inertia. Finally, we note that these apparent masses are not only characteristics of the particular geometry of the immersed solid but also depend on the inclination of along or around which it moves. You also have to take special care when dealing with complex kinematics where multiple degrees of freedom contribute to the same component of apparent mass.

It is noted that this contribution is given only by not-circulatory terms, then it is not to depend on the reduced frequency (or wave number) of the aeroelastic system through the function of Theodorsen. Despite this, their contribution in the energy balance of the immersed body becomes increasingly dominant with as its acceleration grows. This is to indicate that at very high oscillation frequencies the participating mass is expected to grow very much, but in many cases under these conditions collapses the hypothesis of incompressibility and we must treat typical problems of sound waves propagation.

In the literature there are references in which this apparent mass is associated with that of a cylinder having a radius equal to the semi-chord of the foil. In reality, this analogy is valid as regards the lift exerted on the fluid. In fact, a cylinder of this size is characterized by a moment of inertia completely different from the not-circulatory contribution present in the aerodynamic torque, but it would be necessary to have a cylinder characterized by a much smaller diameter of $\sqrt{2}b$.

This emphasizes the fact that when dealing with low density fluids such as air ($\bar{\rho} = 1.18 \text{ kg/m}^3$), the contribution of the apparent mass is generally negligible compared to that structural, unless it has to do with particular structures (such as sails of boats).

With respect to the terms proportional to the speed is important to emphasize the fact that their weight on the total aero-mechanical damping strongly depends on the velocity of the fluid. Therefore, it is a good rule not to neglect the effects of the aerodynamic component, which typically already for wind speed not excessively high exceeds the purely structural contribution (unless that are provided special dissipation devices). Without, in fact, it would cause a valuation in favour of safety of the structural response but an underestimation of the resources of the complete aero-mechanical system would be excessive.

Now you bring back the aeroelastic forces just determined to matrix form more appropriate numerical implementation.

$$\underline{M}_{aero} = \pi b^2 \rho \begin{bmatrix} 1 & -\bar{x}_\alpha \\ \bar{x}_\alpha & -\left(\frac{b^2}{8} + \bar{x}_\alpha^2\right) \end{bmatrix};$$

$$\underline{C}_{aero} = \pi b \rho U \begin{bmatrix} 2 \cdot C(\tilde{k}) & b - 2\left(\bar{x}_\alpha - \frac{b}{2}\right) \cdot C(\tilde{k}) \\ 2\left(\bar{x}_\alpha + \frac{b}{2}\right) \cdot C(\tilde{k}) & b\left(\bar{x}_\alpha - \frac{b}{2}\right) - 2\left(\bar{x}_\alpha^2 - \frac{b^2}{4}\right) \cdot C(\tilde{k}) \end{bmatrix};$$

$$\underline{K}_{aero} = 2\pi b \rho U^2 \cdot C(\tilde{k}) \begin{bmatrix} 0 & 1 \\ 0 & \left(\bar{x}_\alpha + \frac{b}{2}\right) \end{bmatrix};$$

These represent respectively the aerodynamic matrices of mass, damping and stiffness that will add to the structural counterparts to form the complete aeroelastic system. In fact, you can go to the frequency domain by introducing the idea of sinusoidal oscillations, replacing the coordinate's expressions already seen in terms of complex exponentials.

$$\underline{M}_{stru} \cdot \underline{\ddot{q}} + \underline{C}_{stru} \cdot \underline{\dot{q}} + \underline{K}_{stru} \cdot \underline{q} = \underline{F}_{aero};$$

$$\underline{q}(t) = \begin{bmatrix} h_\alpha(t) \\ \alpha(t) \end{bmatrix} = \begin{bmatrix} h_{\alpha,0} \\ \alpha_0 \end{bmatrix} e^{i\omega t} = \underline{q}_0 \cdot e^{i\omega t};$$

$$[-\omega^2(\underline{M}_{stru} - \underline{M}_{aero}) + i\omega(\underline{C}_{stru} - \underline{C}_{aero}) + (\underline{K}_{stru} - \underline{K}_{aero})] \cdot \underline{q}_0 = \underline{0};$$

It is observed that once defined the aero-mechanical matrices the system becomes homogeneous since there is no component of the aerodynamic forcing that does not depend on the motion of the foil. In general, when it approaches the problem with the Quasi- Stationary Theory always remains a static component of the forcing, which determines the stationary configuration of the system, and another associated with the turbulent components of the incident flow that leads to a structural response variable in time, known as Buffeting.

Despite this lack, easily remedied, the usefulness of this theoretical formulation is undoubted whenever you approach the problem of determining the critical conditions leading to a flutter kind of instability. For which only the dynamic components of the flow are of interest, which depend directly on the configuration assumed by the body instantaneously. So the static component turns out to be of little interest since it does not affect in any way the onset of instability. While the dynamic component of buffeting forces is strongly dependent on the instantaneous configuration of the body, but generally it is permissible to linearize this dependence in the neighbourhood the static configuration. So that these forcing depend exclusively on the

turbulent components of the flow velocity and consequently don't affect directly the mass, damping and structural rigidity matrices, which affect the critical flutter conditions.

In fact, the solving system has a non-trivial solution only in the case where the determinant of the complete aeroelastic matrix vanishes. This is precisely defined Flutter Determinant and the solution requires an iterative approach having to solve a nonlinear system of two equations. In fact, the said determinant is a complex entity, then the vanishing of the real and imaginary part provide respectively the frequency and the corresponding average flow velocity in correspondence of the instability onset of the system. This coincides with the vanishing of the aeroelastic damping that, becoming negative at speeds exceeding that of flutter just determined, introduces energy into the system instead of dissipating it.

However, we doubt that the introduction of the kinematic constraint of sinusoidal oscillations is strong enough to introduce an approximation comparable to what you would have using a simpler approach such as Steady Theory.

In this regard, please note that you have perfectly sinusoidal oscillations only in special cases such as in the presence of free oscillations (absence of forcing, structural and aerodynamic damping) or external sinusoidal forcing. Since as mentioned above the critical flutter speed conventionally arises at the vanishing of the aeromechanical damping, and from then the response becomes self-excited with sinusoidal behaviour, then the frequency and the critical speed of flutter so calculated are exact results the analytical problem. It therefore underlines the fact that the results are accurate only at the exact critical condition, so it is not possible to refer to the results obtained for different speeds from flutter. This is not to say, however, even the variation of the eigenvalues of the problem with the average wind speed is completely unreliable, but only that it is not exact because the shape functions used to describe the motion of the foil only approximates the real ones.

Typically for observation already made previously, since the Stationary Theory overestimate the aerodynamic forces then the critical flutter speed determined by the approach of Theodorsen are less on safe side since it allows to reach higher intensities as the analytical model reproduces more faithfully the physics of the problem.

Deepen now the main differences observed between the approach of Quasi- Stationary Theory and the one proposed by Theodorsen. First, as already mentioned the Stationary one completely ignores the effect that the wake has on the aerodynamic forcing, leading to an excessive overestimation of their effects on the immersed body (as the onset of the flutter instability) in terms also very significant. Instead, the theory presented so far holds strongly considering the contribution of the vortices that are detached from the body immersed. In fact, in the discussion above, was given great importance to the contribution of the circulatory flow for which immediately was emphasized the importance of placing counter-vortices in wake so that we can meet the balance between generated and dissipated circulation required by Kelvin theorem. The theory of Theodorsen simplifies the physics of the phenomenon but the assumptions introduced represent in a sufficiently accurate way real phenomena. Numerical analysis with complex computational codes introduce approximations comparable to the simplifications introduced by an analytical approach, due for example to the impossibility of knowing a priori the point where the vortex shedding occurs exactly. Besides being very expensive algorithms, in computational terms, their use, at least in the early stages of analysis, can be inconvenient having to simulate the response of the system each time a parameter has to be changed.

We have already discussed the importance of the reduced angular wave number k^* that can be taken as the prince parameter capable of synthesizing the fundamental information regarding the transient component of the aeroelastic interaction between the flow and the foil. Now we want to investigate the substantial difference between the analytical method proposed by Theodorsen and those generally used in the simplified design, the so-called Quasi-Static approach.

In fact, when an unsteady phenomenon is characterized by a reduced frequency sufficiently low it is possible to neglect a large part of the interaction between the motion of the incident flow and the thin plate. The first and simplest is undoubtedly the pure stationary approach in which the forcing are determined as a function of static configuration reached by the body instantaneously to vary the angle of attack of the flow.

$$L(t) \cong 2\pi b \bar{\rho} U [\dot{h}_\alpha + U\alpha];$$

$$M(t) \cong -F_L(t)b \left(\varepsilon_\alpha + \frac{1}{2} \right);$$

It is noted that the speed with which the foil translates vertically is essential to grasp the variation of the angle of attack, while moving by itself has no effect on the forcing, which are expressed in terms of only the circulatory components essential to define the intensity.

The second difference is more sophisticated and, as has already been mentioned earlier, simplifies the treatment as it ignores the effect of the wake. Of course we are talking of the Quasi- Stationary approach, for which the formulation of aerodynamic forcing reproduces exactly the one proposed by Theodorsen but neglects the influence of the motion of the foil on that of the particles of the fluid letting the function $C(k^*)$ to tend to unity.

$$C(\tilde{k}) = 1;$$

Again, this is granted when the reduced frequency is sufficiently low. Previously by referring to the reduced speed was reported a threshold of $U^* = 10-20$ over which the Stationary Theory provides reliable results. In terms of reduced frequency, this empirical limit corresponds to $f^* = 0.05-0.1$ below which it must remain.

Therefore, the function of Theodorsen plays a crucial role in defining the aerodynamic forcing agents on the foil. The reasons are essentially two and affect the circulatory flow component alone, the only one that suffers the effects of the function $C(k^*)$.

The first reason, which has been already discussed, is the most obvious. In fact, if one considers only the function $F(k^*)$, being generally of interest the real component of the intensity, it always takes values less than unity. This result in a reduction of both the aerodynamic lift and couple passing from the Stationary to the more complete Theodorsen Theory. It is observed that the reduction may be very substantial and shows a maximum of 50% in the limit condition $U^* = 0$, which is reached exactly only when the flow speed is zero and thus the oscillation of the body strongly affects the local motion of fluid particles that are in its vicinity. Referring to what stated above in respect of the field of applicability of the Stationary Theory is observed that in correspondence with the practical threshold $U^* = 10-20$ have very high over-estimation of aerodynamic forcing ranging respectively between 40 and 25%. Therefore, when using the Stationary approach is good to keep in mind this observation, noting that the results obtained in terms of structural performance are enormously in favour of safety. Of course the approach of Theodorsen exactly represent the quasi-static one in the limit condition for which the reduced speed tents to infinity, to indicate the complete absence of aeroelastic interaction for $C(k^*) = 1$.

The second reason is inherent in the fact that the same function $C(k^*)$ is a complex entity. Because if the quasi-static forces are real, and therefore in phase with the movements associated with them, multiplying these actions by $C(k^*)$ are generated some negative phase shifts (due to the sign of $G(k^*)$) that rotate in clock-wise sense the aerodynamic resultants.

$$\theta = \text{artan}[G(\tilde{k})/F(\tilde{k})];$$

It is observed that the amount of rotation is very limited, since the function $G(\tilde{k})$, that governs the phenomenon, after a very small maximum equal to 0.2 in correspondence of $U^* = 5\pi$, it shows a trend that levels very rapidly around 0.1. Despite this, this effect cannot be neglected when the energy introduced into the oscillating structural system appears to be strongly influenced by the angle of incidence of the flow. So studying issues related to the phenomena of dynamic instability such as flutter is well to bear in mind that the Stationary Theory loses essential information, which in this case may lead to an underestimation of the critical condition.

At the experimental level have been conducted many tests on thin layer in order to verify the accuracy of the theory of Theodorsen. From studies of Halfman, Greidanus, van der Bergh Vooren and shows that below $k^*=0.4$ the error that the theoretical approximations commit is negligible being of the same order of the experimental. Except for the torsional component of the lift, which turns out to be overestimated by 10-15% by the theoretical approach. Beyond this threshold, the experimental results diverge very quickly from the theoretical ones. These differences are largely because with increasing the reduced frequency you accentuate the discrepancies of the theoretical model, which no longer able to satisfy instantly the Kutta condition and the assumption of flat wake becomes unrealistic.

5.5. Static torsional divergence

In order to provide an upper limit to the admissible wind speed to be taken in account for Flutter analysis, let's first focus on the limit condition of static divergence. As usually happens the static unstable limit requires higher extreme conditions than its dynamic counterpart. Hence, we will assume the static ones as a threshold beyond which is no more interesting to investigate further the dynamic instability problem since the system undergoes first to a static unstable condition.

Another important feature of static aeroelastic problems is the fact that are characterised by several simplifying features. By definition, time does not appear as an independent variable and, as result, vibratory inertial forces are eliminated from the equilibrium equations. Also, aerodynamic forces can be based upon well-known steady flow results rather than more complex unsteady flow theories.

In order to comprehend the basic phenomena of static aeroelasticity, let's consider the behaviour of a rigid wing segment, elastically restrained in a two-dimensional flow, similar to that used by Theodorsen with the only difference that in this situation we have just the torsional degree of freedom.

The wing is characterised by a constant chord c and an area S , its twisting is opposed by a linear coiled spring attached at the elastic axis, located at a distance e behind the aerodynamic centre, where forces' resultants apply. Notice that due to the fact that we are dealing with a thin airfoil the sectional area and the chord are coincident.

$$e = x_\alpha + \frac{b}{2};$$

$$S = c = 2b ;$$

The total angle of attack ϑ measured from the zero lift condition, is taken as the sum of an initial angle ϑ_0 and the elastic twist contribution ϑ_{el} .

$$\vartheta = \vartheta_0 + \vartheta_{el} ;$$

Since the elastic twist is proportional to the external aerodynamic torque about the elastic axis by means of the torsional flexibility coefficient of the coiled spring equal to the inverse of its stiffness.

$$\vartheta_{el} = C_{\vartheta} \cdot T = T/K_{\vartheta} ;$$

Notice that we have to consider the total torque, that is the sum of the direct contribution coming from the external aerodynamic couple and lift about the elastic axis. Hence, the lift force has a torsional contribution because of the fact that it's acting on the aerodynamic axis that is not coincident with the elastic one.

$$T = M + L \cdot e ;$$

Then is necessary to introduce some simple steady state relations allowing us to define aerodynamic forces in a straightforward way by means of the dynamic pressure q notion.

$$T = \frac{1}{2} \rho_a U^2 S \cdot (C_M \cdot S + C_L \cdot e) = qS \cdot (C_M \cdot S + C_L \cdot e) ;$$

We are able to link the total lift coefficient to the total angle of attack, and we can assume that it vanishes as ϑ does if we are dealing with a thin foil. In fact, the resultant lift force acting on a horizontal plate is null as its thickness tends to vanish.

$$C_L(\vartheta) = C_L(0) + \frac{\partial C_L}{\partial \vartheta} \cdot \vartheta = \frac{\partial C_L}{\partial \vartheta} \cdot (\vartheta_0 + \vartheta_{el}) ;$$

Where the slope of the lift curve can be determined by means of wind tunnel tests on rigid models at different angle inclinations, being valid the assumption of quasi-static condition. Anyway, for simple sectional shapes of the wing is possible to get analytical expression also for the aerodynamic coefficients. Indeed, for the case of thin plate in steady motion can be demonstrate [14] that the lift coefficient grows linearly with the angle of attack proportionally to a factor of a round angle.

$$C_L(\vartheta) = 2\pi \cdot \vartheta \Rightarrow \frac{\partial C_L}{\partial \vartheta} = 2\pi ;$$

Consequently, it's possible to define the actual elastic component of the total angle of attack simply exploiting the previous definition given to it and to the total torque.

$$\vartheta_{el} = T/K_{\vartheta} = \frac{qS}{K_{\vartheta}} \cdot \left\{ C_M \cdot 2b + \left[C_L(0) + \frac{\partial C_L}{\partial \vartheta} \cdot (\vartheta_0 + \vartheta_{el}) \right] \cdot e \right\} ;$$

Hence, obtaining an implicit equality we need to make in evidence the only important parameter that is the elastic torsional angle.

$$\vartheta_{el} = \left\{ C_M \cdot 2b + \left[C_L(0) + \frac{\partial C_L}{\partial \vartheta} \cdot \vartheta_0 \right] \cdot e \right\} / \left\{ \frac{K_{\vartheta}}{qS} - \frac{\partial C_L}{\partial \vartheta} \cdot e \right\} ;$$

It's evident that exists a particular value for the dynamic pressure such that the elastic torsional angle explodes. This particular condition known as Torsional Divergence.

$$\vartheta_{el} \rightarrow \infty \Leftrightarrow \frac{K_{\vartheta}}{qS} - \frac{\partial C_L}{\partial \vartheta} \cdot e = 0 \Rightarrow q_D = K_{\vartheta} / \left(\frac{\partial C_L}{\partial \vartheta} \cdot S \cdot e \right);$$

Finally recalling the definition of dynamic pressure, we are able to define the wind speed threshold for static divergence onset.

$$q_D = \frac{1}{2} \rho_a U_D^2 \Rightarrow U_D = \sqrt{K_{\vartheta} / \left(\frac{1}{2} \rho_a S e \cdot \frac{\partial C_L}{\partial \vartheta} \right)};$$

Notice that up to now we deal with a generic wing section, and the fact that the initial inelastic angle of attack does not play any role in the definition of the critical condition.

For the particular condition of thin flat plate section, the previous expression further simplifies.

$$U_D = \sqrt{K_{\vartheta} / \left(\frac{1}{2} \rho_a S e \cdot \frac{\partial C_L}{\partial \vartheta} \right)} = \sqrt{K_{\vartheta} / \left\{ \frac{1}{2} \rho_a \cdot 2b \cdot \left(x_{\alpha} + \frac{b}{2} \right) \cdot 2\pi \right\}} = \sqrt{K_{\vartheta} / \{ \pi \rho_a b \cdot (2x_{\alpha} + b) \}};$$

We have already underline the fact that the proposed 2-dof model of suspension bridge is characterised by nonlinearities up to cubic terms. Consequently is not possible to know a priori the exact position of the elastic axis being dependent on the actual configuration of the bridge. Hence, we need to refer all the quantities, such as displacements and rotations, to the geometric axis of the bridge symmetric section. The actual values found will consequently contain also contributions related to the lever arm present between the elastic and the geometrical axis.

The exact position of the pressure point (aerodynamic centre) where all the external aerodynamic forces act, requires a numerical analysis of the wind-structure interaction. Usually as proposed by Theodorsen its position is fixed to the first quarter of the airfoil chord. For sake of simplicity and to be on safe side we will assume the aerodynamic centre coincide with the nose of the foil.

$$x_{\alpha} = 0 \Rightarrow e = 2x_{\alpha} + b = b \Rightarrow U_D = \sqrt{K_{\vartheta} / (\pi \rho_a b^2)};$$

Notice that the divergence speed is very much influenced by the relative position of elastic and aerodynamic axis. In fact as the latter goes aft the first one, the lift force gives a stabilising contribution to the overall system. As we can see as the pressure centre coincide with the elastic one we get an infinite divergence speed.

As already notice, the static divergence condition is independent from the initial angle of attack. Hence, static divergence occurs as the increase of aerodynamic total torque due to an arbitrary change of the angle of attack is equal to the elastic restoring moment.

$$\Delta M_{el} = \Delta \vartheta / C_{\vartheta} = \Delta M_{aero} = q \cdot \Delta \vartheta \cdot S \cdot e \cdot \frac{\partial C_L}{\partial \vartheta};$$

Since the elastic moment is constant with the initial angle of attack and the aerodynamic couple grows linearly with it, equilibrium in small rotation is no more granted beyond a critical angle.

The same problem holds in the lateral instability of columns with initial eccentricity, hence we are not dealing with a hidden instability.

Lets' try to pass to the dimensionless format for the static divergence speed, trying to use the modal quantities such as mass and stiffness. This allow us to pass from the continuous formulation to the discrete one of a 2-dofs oscillator. Hence making use of the definitions of dimensionless torsional circular eigen-frequency and gyration radius we get the following expression for the dimensional torsional stiffness.

$$K_{\vartheta,m} = \tilde{\omega}_{\vartheta,m}^2 \cdot J_{\vartheta,m} \Rightarrow K_{\vartheta} = \left\{ \tilde{\omega}_{\vartheta,m}^2 / \left(l^2 \cdot \frac{m_d + 2m_c}{2H} \right) \right\} \cdot \{ \tilde{J}_t \cdot (m_d + 2m_c) \cdot b^2 \};$$

Hence the divergence speed can be rewritten as follows.

$$U_{D,m} = \sqrt{K_{\vartheta} / (\pi \rho_a b^2)} = \sqrt{\tilde{J}_t \cdot \tilde{\omega}_{\vartheta,m}^2} \cdot \sqrt{\frac{2H}{\pi \rho_a l^2}};$$

Finally we get the dimensionless format.

$$\tilde{U}_{D,m} = U_{D,m} \cdot \sqrt{\frac{\pi \rho_a l^2}{2H}} = \sqrt{\tilde{J}_t} \cdot \tilde{\omega}_{\vartheta,m};$$

Notice that the values assumed by the dimensionless torsional divergence speed are equal to that of the corresponding circular eigen-frequencies of the structural model. In order to stress the fact that these frequencies are independent from the wind speed level, in the following we will write it in uppercase.

$$\tilde{U}_{D,m} = \sqrt{\tilde{J}_t} \cdot \tilde{\Omega}_{\vartheta,m}$$

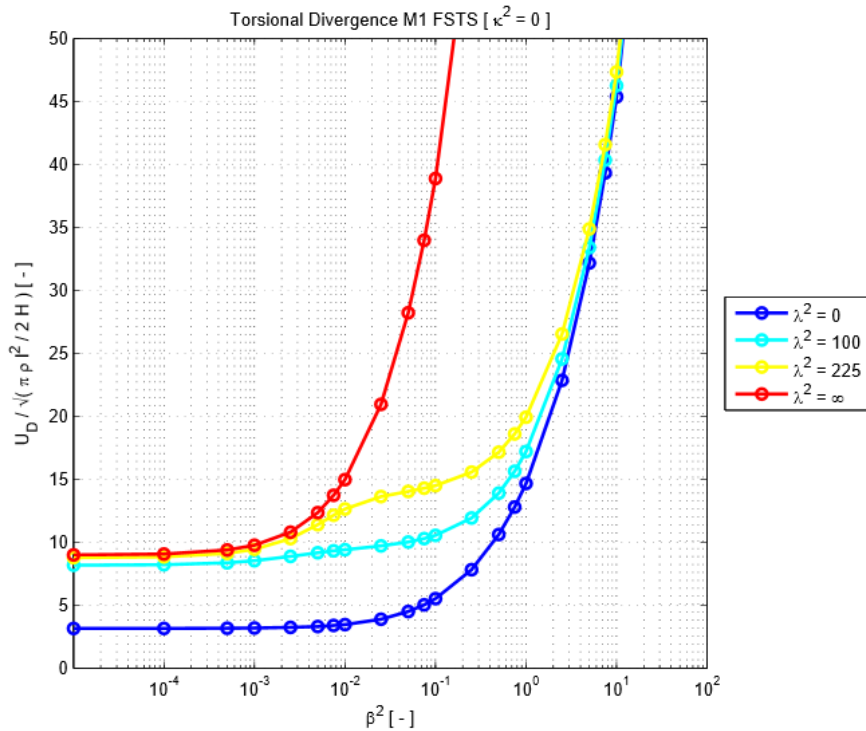


Figure 5.2_Torsional static divergence wind speed of Mode 1 for $\chi^2 = 0$.

From the available data taken from literature [31-40] we can get an estimation of the variation range of the dimensional factor just collected.

$$\sqrt{\frac{\pi\rho_a l^2}{2H}} \cong (4 \div 10) \text{ [m/s]};$$

Therefore, we need to take in consideration that the dimensional counterpart of the following Divergence Speed has to be incremented by that scaling factor to get reliable values.

Notice that we limit the plotting of the dimensionless wind speed up to values of 50 since generally real critical Flutter conditions onset at speed never above 100 m/s.

5.6. Dynamic flutter instability

Now we are able to write down the analytical formulation for the complete aeroelastic model of a suspension bridge.

We have already found the equations of motion governing the flexural and torsional vibrations in the undamped but forced situation. Thence, we need to define explicitly the aerodynamic forcing just found and add structural equivalent viscous damping. In fact, as we will see in the following, the presence of aerodynamic damping doesn't allow us to neglect the influence of the velocity on the overall response of the bridge. Hence adding also the structural contribution does not make the computations more cumbersome than they are. Indeed, we expect the appearance of imaginary terms linked not only to the presence of damping but also to the presence of Theodorsen complex function inside the aerodynamic contributions.

5.6.1. Analytical formulation

The theory developed by Theodorsen it's able to model the mean wind actions on a rigid section of a plate. The forces arising from these actions are linear with the system's configuration, hence can be included in the linear equations governing the forced-damped bridge's motion.

$$(m_d + 2m_c) \cdot \ddot{w}_d + c_w \cdot \dot{w}_d + E_d J_d \cdot w_d'''' - 2H \cdot w_d'' - 2y'' h_w = -L(t);$$

$$(J_t + 2m_c b^2) \cdot \ddot{\vartheta}_d + c_\theta \cdot \dot{\vartheta}_d + E_d \Gamma_d \cdot \vartheta_d'''' - (G_d J_d + 2H b^2) \cdot \vartheta_d'' - 2y'' b h_\theta = M(t);$$

Where:

$$L(t) = \pi b^2 \rho_a \cdot (\ddot{w}_d - x_\alpha \ddot{\vartheta}_d) + 2\pi b \rho_a U \cdot \left\{ C_w \dot{w}_d + \left[\frac{b}{2} - \left(x_\alpha - \frac{b}{2} \right) C_\theta \right] \dot{\vartheta}_d \right\} + 2\pi b \rho_a U^2 C_\theta \theta_d;$$

$$M(t) = \left\{ \begin{array}{l} \pi b^2 \rho_a \cdot \left[x_\alpha \ddot{w}_d - \left(\frac{b^2}{8} + x_\alpha^2 \right) \ddot{\vartheta}_d \right] + \\ + 2\pi b \rho_a U \cdot \left\{ \left(x_\alpha + \frac{b}{2} \right) C_w \dot{w}_d + \left[\frac{b}{2} \left(x_\alpha - \frac{b}{2} \right) - \left(x_\alpha^2 - \frac{b^2}{4} \right) C_\theta \right] \dot{\vartheta}_d \right\} + \\ + 2\pi b \rho_a U^2 \left(x_\alpha + \frac{b}{2} \right) C_\theta \theta_d \end{array} \right\};$$

Before proceeding, let's make few considerations.

In the previous treatment, that allows us to define analytically the forces arising from the wind-structure interaction, we assume a sign convention such that are positive upward lifting displacements and clock-wise rotations. In the structural model, nothing change regarding the rotational convention, but on the contrary, we need to reverse the flexural one. Consequently, in order to refer to the structural convention we need to change the sign of the lift force.

In fact, the aerodynamic lift and couple for Theodorsen Theory are positive respectively upward and clockwise, hence the first one has negative sign with respect to downward sign convention for flexural coordinate used in the structural model.

The Theodorsen theory refers the plate's motion to its centre of stiffness since it's tailored on a linear model of a wing. Since the model of the bridge takes in account the nonlinear geometrical behaviour of the main cables, the position of the centre of stiffness in each bridge's section is a priori unknown. This requires referring the principal coordinates to the centre of mass, whose position falls on the vertical axis passing through the geometric midpoint of the deck + cables system' section. Practically this requires to cancel out x_α terms that appears in aerodynamic forces. Immediate consequence is that the mass matrix becomes diagonal, but the inertial forces still indirectly couples the flexural-torsional motion. This operation simply hide a translation of the reference system and a change of variables, in fact we know that any rigid displacement can be reduced to a rigid roto-translation, hence it's allowed.

$$L(t) = \pi b^2 \rho_a \cdot \ddot{w}_d + 2\pi b \rho_a U \cdot \left\{ C_w \cdot \dot{w}_d + \frac{b}{2} (1 + C_\theta) \cdot \dot{\theta}_d \right\} + 2\pi b \rho_a U^2 C_\theta \cdot \theta_d ;$$

$$M(t) = -\frac{\pi}{8} b^4 \rho_a \cdot \ddot{\vartheta}_d + \pi b^2 \rho_a U \cdot \left\{ C_w \cdot \dot{w}_d + \frac{b}{2} (1 - C_\theta) \cdot \dot{\theta}_d \right\} + \pi b^2 \rho_a U^2 C_\theta \cdot \theta_d ;$$

As we can see, the wind actions are constant along the span of the bridge since the formulation proposed by Theodorsen refers to a generic section of a thin infinite wing. This could be not a good approximation in the study of real wing, where side effects given by the finite length can be relevant. However, concerning suspension bridges where the span length ranges from 20 to 80 times the deck's width [31-40] neglecting side effect is a must when dealing with the main span.

In real problems wind properties cannot be constant along all the main bridges span due to the randomness of the phenomenon, hence the previous assumptions allows us to get results on the safe side.

We can say that this assumption is similar to the one that allow us to consider constant sectional properties of the structural system.

Further we must remember the fact that, Theodorsen, in order to be able to define the circulation intensity in a simple way, assumes a pure sinusoidal motion for the airfoil both in flexure and in torsion. From this, two further remarks follow.

First, sinusoidal motion is strictly possible only in absence of damping, hence when the aerodynamic contribution degrades the structural one in correspondence of Flutter condition. In the following will be considered generic conditions following the path to reach Flutter onset, then will be assumed the theory proposed by Theodorsen to be valid also for wind speeds lower than the critical one.

Notice that is the presence aerodynamic damping that makes oscillations approximately but not exactly sinusoidal. In fact, if the structural contribution to equivalent viscous damping is in general negligible in absence of special dissipative devices; on the other hand the aerodynamic one can reach significant values above 10% with respect the critical condition.

Hence, in order to better approximate the actual response of the suspension bridge immersed in a viscous fluid, we need a slight modification the definition of Theodorsen function. Can be demonstrate [14] that the integral that define the function $C(k^*)$ still converges as we substitute to the reduced frequency the following definition.

$$\text{undamped} : \tilde{k} = \frac{\omega b}{U} \Rightarrow \text{damped} : \tilde{k} = (\omega - i\alpha) \frac{b}{U};$$

The previous statement simply makes possible to consider damped oscillations of the following kind.

$$q(t) = q_0 \cdot e^{(\alpha+i\omega)t};$$

This modification slightly changes the shape of the real and imaginary part of Theodorsen Function. Generally, we can say that it has negligible influence since affect only very low reduced frequencies where the Quasi- Stationary Theory gives reliable results. From numerical analysis is possible to state that the presence of damping introduce considerable modification only in correspondence of dimensionless circular frequencies lower than unit, meaning that it affect strongly the response of very stiff bridges.

The second remark concern the fact that up to now we have considered a unique circular eigen-frequency. This assumption is typical when dealing with coupled linear systems. In fact the presence of aerodynamic forces makes coupled also the linear component of the structural response, while the nonlinearities coming from the cables behaviour just couple higher order terms of second and third degree. Hence in order to make a clear distinction between flexural and torsional contribution the following definitions hold.

$$C_w = C(\tilde{k}_w) \text{ with } \tilde{k}_w = (\omega_w - i\alpha_w) \frac{b}{U};$$

$$C_\theta = C(\tilde{k}_\theta) \text{ with } \tilde{k}_\theta = (\omega_\theta - i\alpha_\theta) \frac{b}{U};$$

Notice that in the definition of the reduced frequencies we have the dimensional circular eigen-frequencies.

Let's now find out the dimensionless format for the linear equations of motion for the complete aeroelastic system.

First of all we sum up the structural and the aerodynamic contributions in terms of mass, damping and stiffness.

$$\left\{ \begin{array}{l} (m_d + 2m_c + \pi b^2 \rho_a) \cdot \ddot{w}_d + \\ + (c_w + 2\pi b \rho_a U C_w) \cdot \dot{w}_d + \pi b^2 \rho_a U (1 + C_\theta) \cdot \dot{\theta}_d \\ + E_d I_d \cdot w_d^{iv} - 2H \cdot w_d'' - 2y'' h_w + 2\pi b \rho_a U^2 C_\theta \cdot \theta_d \end{array} \right\} = 0;$$

$$\left\{ \begin{array}{l} (J_t + 2m_c b^2 + \frac{\pi}{8} b^4 \rho_a) \cdot \ddot{\vartheta}_d + \\ + [c_\theta + \frac{\pi}{2} b^3 \rho_a U (1 - C_\theta)] \cdot \dot{\theta}_d - \pi b^2 \rho_a U C_w \cdot \dot{w}_d \\ + E_d \Gamma_d \cdot \theta_d^{iv} - (G_d J_d + 2H b^2) \cdot \vartheta_d'' - \pi b^2 \rho_a U^2 C_\theta \cdot \theta_d - 2y'' b h_\theta \end{array} \right\} = 0;$$

Then introduce the fundamental dimensionless quantity already define for the structural model.

$$(1 + \tilde{m}_a) \cdot \frac{d^2 \tilde{w}_d}{d\tau^2} + \tilde{c}_{ww} \cdot \frac{d\tilde{w}_d}{d\tau} + \tilde{c}_{w\theta} \cdot \frac{d\tilde{\theta}_d}{d\tau} + \mu^2 \cdot \tilde{w}_d{}^{''v} - \tilde{w}_d{}'' + \lambda_L^2 \tilde{h}_w + 2\tilde{k}_{\theta\theta} \cdot \theta_d = 0 ;$$

$$(\tilde{J}_t + \tilde{J}_a) \cdot \frac{d^2 \tilde{\theta}_d}{d\tau^2} + \tilde{c}_{\theta\theta} \cdot \frac{d\tilde{\theta}_d}{d\tau} + \tilde{c}_{\theta w} \cdot \frac{d\tilde{w}_d}{d\tau} + \frac{\beta^2}{\chi^2} \cdot \tilde{\theta}_d{}^{''v} - (1 + \beta^2) \cdot \tilde{\theta}_d{}'' - \tilde{k}_{\theta\theta} \cdot \theta_d + \lambda_L^2 \tilde{h}_\theta = 0 ;$$

The new parameters introduced can be define as follows.

First, let's introduce the dimensionless aeroelastic participating mass and torsional inertia.

$$\tilde{m}_a = \pi b^2 \rho_a / (m_d + 2m_c) ;$$

$$\tilde{J}_a = \frac{\pi}{8} b^4 \rho_a / [(m_d + 2m_c) \cdot b^2] ;$$

We can say immediately that the additional mass coming from the fluid participating to the motion of the structure is negligible. From literature [31-40] we can state that, with respect to the deck and cables contribution, the aeroelastic mass ranges from 0.02 to 0.07 while the torsional inertia drop down by an order of magnitude ranging between 0.004 to 0.01 with respect to the structural one \tilde{J}_t .

$$\tilde{J}_t \cong 0.6 ;$$

We want to underline the fact that in the following we will neglect the aeroelastic contributions, but we are not making any change in the definition of the dimensionless parameters. In fact doing that it's like if we are defining a new time parameter in which we take in account also the participating mass. This would not be possible otherwise, the results coming from the structural analysis cannot be compared to the ones coming from the aeroelastic analysis.

$$\frac{d^2 \tilde{w}_d}{d\tau^2} + \tilde{c}_{ww} \cdot \frac{d\tilde{w}_d}{d\tau} + \tilde{c}_{w\theta} \cdot \frac{d\tilde{\theta}_d}{d\tau} + \mu^2 \cdot \tilde{w}_d{}^{''v} - \tilde{w}_d{}'' + \lambda_L^2 \tilde{h}_w + 2\tilde{k}_{\theta\theta} \cdot \theta_d = 0 ;$$

$$\tilde{J}_t \cdot \frac{d^2 \tilde{\theta}_d}{d\tau^2} + \tilde{c}_{\theta\theta} \cdot \frac{d\tilde{\theta}_d}{d\tau} + \tilde{c}_{\theta w} \cdot \frac{d\tilde{w}_d}{d\tau} + \frac{\beta^2}{\chi^2} \cdot \tilde{\theta}_d{}^{''v} - (1 + \beta^2) \cdot \tilde{\theta}_d{}'' - \tilde{k}_{\theta\theta} \cdot \theta_d + \lambda_L^2 \tilde{h}_\theta = 0 ;$$

Then, write the damping contributions.

$$\tilde{c}_{ww} = (c_w + 2\pi b \rho_a U C_w) \cdot l / \sqrt{2H \cdot (m_d + 2m_c)} ;$$

$$\tilde{c}_{w\theta} = \pi b \rho_a U (1 + C_\theta) \cdot l / \sqrt{2H \cdot (m_d + 2m_c)} ;$$

$$\tilde{c}_{\theta\theta} = \left[c_\theta + \frac{\pi}{2} b^3 \rho_a U (1 - C_\theta) \right] \cdot l / [b^2 \cdot \sqrt{2H \cdot (m_d + 2m_c)}] ;$$

$$\tilde{c}_{\theta w} = -\pi b \rho_a U C_w \cdot l / \sqrt{2H \cdot (m_d + 2m_c)} ;$$

Finally the stiffness one.

$$\tilde{k}_{\theta\theta} = \pi \rho_a U^2 C_\theta \cdot l^2 / 2H ;$$

Let's make some consideration regarding the positive or negative contributions of the last terms. First, we must remember the variation range of the original Theodorsen function.

$$C = F + iG \quad \text{where } F \in [0.5, 1) ; G \in (-0.2, 0] ;$$

The direct flexural damping \tilde{c}_{ww} has a real part that will be always positive and an imaginary part always negative. Where always means for any value reached by the wind speed.

The torsional contribution on the flexural $\tilde{c}_{w\theta}$ and torsional $\tilde{c}_{\theta\theta}$ motion has both the real and the imaginary parts positive for any U.

While the flexural contribution on the torsional motion $\tilde{c}_{\theta w}$ has always a negative real part and a positive imaginary one.

More interesting is the aerodynamic contribution on the torsional stiffness parameter $\tilde{k}_{\theta\theta}$ that has a positive real part and a negative imaginary one. This means that increasing the wind speed it is able on one hand to increase its contribution to the stiffness of the flexural motion while on the other hand it reduces the torsional one.

Hence, we can state that this last parameter is the fundamental one responsible of the so called Torsional Degradation phenomenon. Notice that not only it reduces the torsional stiffness but also increases the flexural one with a contribution two times higher. Consequently, as the wind speed increases the structure becomes very stiff in with respect to flexural motion and slack with respect the torsional one. Thence we will expect that the bridge will prefer to transfer energy from the flexural to the torsional motion where the TPE is lower.

Before proceeding we want to write the previous dimensionless parameters in a more compact format. First reformulate a term common to all these parameters.

$$\pi b l \rho_a U / \sqrt{2H \cdot (m_d + 2m_c)} = \frac{U}{U_D} \cdot \sqrt{\tilde{J}_t} \cdot \tilde{\Omega}_\theta \cdot \sqrt{\frac{2H}{\pi \rho_a l^2}} \cdot \frac{\pi b l \rho_a}{\sqrt{2H \cdot (m_d + 2m_c)}} = \sqrt{\tilde{J}_t} \cdot \tilde{\Omega}_\theta \cdot \sqrt{\tilde{m}_a} \cdot \tilde{u} ;$$

To this end let's introduce the notion of dimensionless wind speed u , that is the generic one U normalised with respect to the Divergence Speed U_D proper for the structural condition under consideration.

$$\tilde{u} = U / U_D ;$$

Notice that the aeroelastic mass appears again but this time cannot be neglected since there is any term of comparison. Thence in the following numerical analysis will be important to give it a representative value for the most common situation, taken from the bibliographical references previously mentioned.

$$\tilde{m}_a \cong 4\% ;$$

Further from the analysis of a single degree of freedom damped oscillator we can state some relations between the dimensionless damping parameter and the associate ratios.

$$c_w \frac{l}{\sqrt{2H \cdot (m_d + 2m_c)}} = \tilde{c}_w = 2 \cdot \xi_w \cdot \tilde{\omega}_w \cdot (1 + \tilde{m}_a) \cong 2 \cdot \xi_w \cdot \tilde{\omega}_w ;$$

$$c_\theta \frac{l}{b^2 \cdot \sqrt{2H \cdot (m_d + 2m_c)}} = \tilde{c}_\theta = 2 \cdot \xi_\theta \cdot \tilde{\omega}_\theta \cdot (\tilde{J}_t + \tilde{J}_a) \cong 2 \cdot \xi_\theta \cdot \tilde{\omega}_\theta \cdot \tilde{J}_t ;$$

Consequently, we are able to define the damping and stiffness dimensionless parameters as follows.

$$\begin{aligned}\tilde{c}_{ww} &= 2 \left(\xi_w \cdot \tilde{\omega}_w + \sqrt{\tilde{J}_t \cdot \tilde{m}_a} \cdot \tilde{\Omega}_\vartheta \cdot \tilde{u} \cdot C_w \right); \\ \tilde{c}_{w\vartheta} &= \sqrt{\tilde{J}_t \cdot \tilde{m}_a} \cdot \tilde{\Omega}_\vartheta \cdot \tilde{u} \cdot (1 + C_\theta); \\ \tilde{c}_{\vartheta\vartheta} &= 2\sqrt{\tilde{J}_t} \cdot \left\{ \xi_\vartheta \cdot \sqrt{\tilde{J}_t} \cdot \tilde{\omega}_\vartheta + \frac{1}{4} \cdot \sqrt{\tilde{m}_a} \cdot \tilde{\Omega}_\vartheta \cdot \tilde{u} \cdot (1 - C_\theta) \right\}; \\ \tilde{c}_{\vartheta w} &= -\sqrt{\tilde{J}_t \cdot \tilde{m}_a} \cdot \tilde{\Omega}_\vartheta \cdot \tilde{u} \cdot C_w; \\ \tilde{k}_{\vartheta\vartheta} &= \tilde{J}_t \cdot \tilde{\Omega}_\vartheta^2 \cdot \tilde{u}^2 \cdot C_\theta;\end{aligned}$$

It's evident that the introduction of the dimensionless wind speed normalised with respect to the Static Divergence condition is a powerful tool that avoid us the need to know the actual value of many structural parameters not always so simple to found in literature. Notice the difference between $\tilde{\Omega}_\vartheta$ that refers to the response of the structure alone and $\tilde{\omega}_\vartheta$ associated to the complete aeroelastic model, hence it varies as the wind speed changes.

Now we are ready also to define the reduced frequency in function of all dimensionless quantities introducing the quantities introduced up to now.

$$\tilde{k} = (\omega - i\alpha) \frac{b}{U} = (\tilde{\omega} - i\tilde{\alpha}) \cdot \frac{1}{l} \sqrt{\frac{2H}{m_d + 2m_c}} \cdot b \cdot \frac{U_D}{U} \cdot \frac{1}{\sqrt{\tilde{J}_t \cdot \tilde{\Omega}_\vartheta}} \sqrt{\frac{\pi \rho_a l^2}{2H}} = (\tilde{\omega} - i\tilde{\alpha}) \cdot \sqrt{\tilde{m}_a} / (\sqrt{\tilde{J}_t} \cdot \tilde{\Omega}_\vartheta \cdot \tilde{u});$$

Now we are ready to pass to the modal space simply performing two steps. The first consist in the modal expansion of the approximate dimensionless equation of motion where we assume to neglect the fluid mass contributions.

$$\begin{aligned}\tilde{w}_d(\xi, \tau) &= \sum_{n=1}^{\infty} W_n(\xi) \cdot (Z_n e^{\lambda_{w,n}\tau} + c.c.) \quad \text{with } n \in \mathbb{N} \setminus \{0\}; \quad \lambda_{w,n} = \alpha_{w,n} + i\omega_{w,n}; \\ \tilde{\vartheta}_d(\xi, \tau) &= \sum_{m=1}^{\infty} \Theta_m(\xi) \cdot (\Gamma_m e^{\lambda_{\vartheta,m}\tau} + c.c.) \quad \text{with } m \in \mathbb{N} \setminus \{0\}; \quad \lambda_{\vartheta,m} = \alpha_{\vartheta,m} + i\omega_{\vartheta,m};\end{aligned}$$

Notice that we need to consider damped vibrations hence the exponential term has both the real and imaginary parts. Consequently, in order to get real vibrations we need a complex amplitude and the associated conjugate counterpart.

Substituting we get two modal equations that are not useful for our purpose due to their spatial dependence. Then we can pass to the second step consisting in the complete modal projection of the original dimensionless equations of motion. To do that we need to multiply respectively the first and the second modal equations by the flexural and the torsional modes and then integrate over the whole length of the dimensionless span.

Finally, we obtain two linear coupled equations of motion similar to that of a 2-dof degree of freedom oscillator.

$$\left\{ \left[\begin{aligned} &(M_{w,n} \cdot \lambda_{w,n}^2 + \tilde{c}_{ww} \cdot M_{w,n} \cdot \lambda_{w,n} + K_{w,n}) \cdot Z_n e^{\lambda_{w,n} \tau} + \\ &+ (\tilde{c}_{w\vartheta} \cdot \lambda_{\vartheta,m} + 2\tilde{k}_{\vartheta\vartheta}) \cdot \tilde{h}_{w,n,\vartheta_m} \cdot \Gamma_m e^{\lambda_{\vartheta,m} \tau} \end{aligned} \right] + c. c. \right\} = 0 \quad \forall(n, m);$$

$$\left\{ \left[\begin{aligned} &(J_{\vartheta,m} \cdot \lambda_{\vartheta,m}^2 + \tilde{c}_{\vartheta\vartheta} \cdot M_{\vartheta,m} \cdot \lambda_{\vartheta,m} + K_{\vartheta,m} - \tilde{k}_{\vartheta\vartheta} \cdot M_{\vartheta,m}) \cdot \Gamma_m e^{\lambda_{\vartheta,m} \tau} + \\ &+ (\tilde{c}_{w\vartheta} \cdot \lambda_{w,n}) \cdot \tilde{h}_{w,n,\vartheta_m} \cdot Z_n e^{\lambda_{w,n} \tau} \end{aligned} \right] + c. c. \right\} = 0 \quad \forall(n, m);$$

Where the new parameters defined are modal masses, stiffness and coupling term.

$$M_{w,n} = \int_0^1 W_n^2(\xi) d\xi;$$

$$M_{\vartheta,m} = \int_0^1 \Theta_m^2(\xi) d\xi \Rightarrow J_{\vartheta,m} = \tilde{J}_t M_{\vartheta,m};$$

$$K_{w,n} = \int_0^1 W_n(\xi) \cdot [\mu^2 \cdot W_n''(\xi) - W_n''(\xi)] d\xi + \lambda_L^2 \tilde{h}_{w,n}^2 = \tilde{\Omega}_{w,n}^2 \cdot M_{w,n};$$

$$K_{\vartheta,m} = \int_0^1 \Theta_m(\xi) \cdot \left[\frac{\beta^2}{\chi^2} \cdot \Theta_m''(\xi) - (1 + \beta^2) \cdot \Theta_m''(\xi) \right] d\xi + \lambda_L^2 \tilde{h}_{\vartheta,m}^2 = \tilde{\Omega}_{\vartheta,m}^2 \cdot J_{\vartheta,m};$$

$$\tilde{h}_{w,n,\vartheta_m} = \int_0^1 W_n(\xi) \cdot \Theta_m(\xi) d\xi;$$

Once again notice that the uppercase circular frequencies are constant with the wind speed since refers to the structural model.

From the modal projection of the equations of motion it is evident that the term $\tilde{h}_{w,n,\vartheta_m}$ is the fundamental parameter giving us the actual order of magnitude of the coupling between a flexural and a torsional mode. Its definition allows us to state that we will expect higher coupling between similar modal shapes. In fact, in the limit condition, the product between two identical modes will give us the maximum expected coupling since the function to be integrated will be only positive. In all the other cases, the function will have both positive and negative sign, hence, the integral will decrease. The opposite limit condition refers to the case when two sinusoidal modes, one symmetric and the other skew-symmetric, of the same order interact, leading to the vanishing of the coupling term.

$$\tilde{h}_{w,n,\vartheta_m} = \int_0^1 \sin(n\pi\xi) \cdot \sin(m\pi\xi) d\xi = 0;$$

Therefore, in the following Flutter analysis will be crucial to identify the modal combination that would lead first the structure to the unstable threshold. A priori, we can assume that the worst combination will be that with the maximum coupling term, hence we would perform a mode by mode analysis between modal shape of the same order and with the same symmetries.

Another interesting feature of the modal equations of motion is that both the complex conjugate parts are in turn complex expressions because of the presence of the Theodorsen function. Hence is important to underline the fact that the notation *c. c.* refers only to the time variation of oscillations and not to the function $C(k^*)$.

Let's proceed writing the modal equations of motion in matrix form, exploiting the definition of modal mass, stiffness and coupling term just given.

$$F \cdot q = 0 ;$$

Where we have introduced the so-called Flutter matrix and the vector of generalised coordinate.

$$F = \begin{pmatrix} (\lambda_{w,n}^2 + \tilde{c}_{ww} \cdot \lambda_{w,n} + \tilde{\Omega}_{w,n}^2) \cdot M_{w,n} & (\tilde{c}_{w\vartheta} \cdot \lambda_{\vartheta,m} + 2\tilde{k}_{\vartheta\vartheta}) \cdot \tilde{h}_{w,n,\vartheta,m} \\ (\tilde{c}_{\vartheta w} \cdot \lambda_{w,n}) \cdot \tilde{h}_{w,n,\vartheta,m} & (\tilde{J}_t \cdot \lambda_{\vartheta,m}^2 + \tilde{c}_{\vartheta\vartheta} \cdot \lambda_{\vartheta,m} + \tilde{J}_t \cdot \tilde{\Omega}_{\vartheta,m}^2 - \tilde{k}_{\vartheta\vartheta}) \cdot M_{\vartheta,m} \end{pmatrix} ;$$

$$q = \begin{pmatrix} Z_n e^{\lambda_{w,n}\tau} & \tilde{Z}_n e^{\tilde{\lambda}_{w,n}\tau} \\ \Gamma_m e^{\lambda_{\vartheta,m}\tau} & \tilde{\Gamma}_m e^{\tilde{\lambda}_{\vartheta,m}\tau} \end{pmatrix} ;$$

The complex linear system of two equations just found is homogeneous; hence we can find a non-trivial solution only enforcing the vanishing of the so-called Flutter Determinant.

$$\det(F) = 0 ;$$

In its general format, the Flutter determinant cannot be solved analytically because all the terms are implicit and non-linear functions of the solution.

First, we need to notice that all the terms depend on the λ parameter referred to the flexural or the torsional motion. In fact, on one hand the aeroelastic terms depend on it by the Theodorsen function through the definition of reduced frequency, and on the other the modal terms by means of the modal shapes. For both the groups the dependence is indirect and non-linear.

Consequently, the main unknowns of the problem are the real and the imaginary part of the exponential terms, both for the flexural and the torsional vibrations. Hence, it seems that the problem cannot be solved because we have a number of unknowns higher than the number of equations. In reality this is not so because as the modal system is quadratic with the unknowns frequencies, the Flutter Determinant has to be of the fourth order because of the cross multiplication between the terms of the matrix of coefficients.

Hence, the vanishing of the Flutter Determinant is able to give us both the flexural and torsional exponential parameters λ .

The problem is a little bit more complicated since all the aeroelastic terms depend on the actual wind speed. This means that at each value of U we get a different system to be solved, that give us the flexural and torsional exponential terms associated to that particular wind speed level. For example assuming null wind speed all aerodynamic terms will vanish, except the ones associated to direct damping given by the structural contribution. Thence neglecting the structural damping also the last ones vanish and the Flutter Determinant reduces to the following fourth order expression.

$$\det(F) = (\lambda_{w,n}^2 + \tilde{\Omega}_{w,n}^2) \cdot (\tilde{J}_t \cdot \lambda_{\vartheta,m}^2 + \tilde{J}_t \cdot \tilde{\Omega}_{\vartheta,m}^2) \cdot M_{w,n} M_{\vartheta,m} = 0 ;$$

It's evident that in the absence of any fluid motion the structural response is identical to the one already analysed in the previous chapter.

$$\det(F) = 0 \Leftrightarrow \lambda_{w,n} = \tilde{\Omega}_{w,n} \quad \text{and} \quad \lambda_{\vartheta,m} = \tilde{\Omega}_{\vartheta,m} ;$$

In all the other conditions when the wind speed is not null, we need to solve a fourth order implicit equation by means of appropriate iterative methods.

In this regard we must remember the fact that the Flutter matrix is complex because of Theodorsen function. Hence, once we fix the wind speed, in order to zeroing the Flutter Determinant we need to split it into real and imaginary parts. This means that in order to solve the Flutter system we need to pass from a single non-linear quadratic complex equation to two real ones.

Since we are not able to write down a code able to find out the solution of a non-linear system of equations in two unknowns, we will rely on the available solver *fsolve* implemented in the commercial software Matlab. The only important note is that the solver is able to find out just the nearest zero to the initial conditions proposed, hence we need to solve it twice, once starting near the flexural vibrating conditions and then near the torsional one. We want to stress the fact that we solve the Flutter Determinant twice since we need to assume each time that the flexural and torsional oscillations are identical. This is only an assumption needed every time we have a coupled vibrating system. Hence, the two unknowns to be found are the real and imaginary part of the flexural or torsional exponential parameter.

Therefore, since the goal of the Flutter analysis is to identify the critical wind speed corresponding to the unstable response onset, we need to assume iteratively different wind speeds until we reach Flutter conditions.

It's evident the advantage to have introduced dimensionless wind speed normalised with respect to the Static Divergence onset. In fact, it gives us priori an upper limit beyond which is useless to investigate further Flutter conditions.

Let's focus on the critical conditions for Flutter onset we have just mentioned. Since Flutter is a phenomenon that brings the structure to undergo to self-sustained oscillations. Consequently, if external conditions still stand for a sufficient elapse of time the oscillations of the structure will diverge in time. The reason why oscillations pass from a stable condition to an unstable one is that the wind speed is enough high that the aerodynamic damping becomes enough negative to overcome the positive structural one. Thence the structure is no more able to dissipate part of the energy introduced by the wind action, but nay it pump additional energy even if the external forcing does not change.

Hence, the first straightforward way is to map the equivalent viscous damping of the complete aeroelastic system at each wind speed analysed. The Flutter onset will coincide with the wind speed that grants null total damping. This can be deduce directly from the zeroing of the Flutter Determinant by means of the following simple relations coming from the single dof damped oscillator.

$$\alpha = -\xi\omega_D \quad , \quad \omega_D = \omega\sqrt{1-\xi^2} \quad , \quad \xi = \frac{c}{c_{cr}} = -\frac{\alpha}{\sqrt{\omega^2+\alpha^2}} \quad , \quad c_{cr} = 2\sqrt{k_{eq}m_{eq}} ;$$

This approach will be used to define the Flutter using the automatic solver for the zeroing of the Flutter Determinant. Hence we will refer to the combination of both as to the New Approach.

The previous critical condition is strongly based on the physics of the problem, but there exists also another one a little bit more mathematical. As we have previously mentioned, the Flutter determinant has a real and an imaginary part because of Theodorsen function.

Hence we reach the Flutter onset as the solution of the imaginary part coincide with one of the real one. Classical solutions of Flutter determinant are based on this procedure and for simplicity assume undamped oscillations though the presence of the relevant aerodynamic contribution. This way the zeroing of two independent non-linear equations allows us to find out the three relevant positive roots. The first two relate to the real part and the third to the imaginary part of the Flutter Determinant, since only the first one ensure two positive roots. Notice that the roots has to be positive since are representative of aeroelastic circular eigen-frequency.

Thence as the wind speed increases we expect the imaginary solution to move towards one of the two real roots. As it reaches on of them, we get the Flutter onset of flexural or torsional kind depending on whatever motion is representing the real root reached. This can be detected simply following the variation of both the two circular eigen-frequency as the wind speed grows. It's evident that we don't need to map the damping parameter in order to find out critical thresholds. Anyway, it's possible to get an estimation of it simply substituting the circular eigen-frequency found from the real roots into the direct aeroelastic damping contributions. In the following, we will refer to the actual procedure as to the Old Approach.

We want to underline the fact that we are able to map both the damping and the circular eigen-frequency of the aeroelastic system. Hence, we can find out also the variation of the modal shapes as the wind speed grows. In the following we will refer to these as to Aeroelastic Modes to be distinguished from the Structural ones dependent only on geometrical and mechanical properties of the bridge and not on the wind speed level. Notice that we will assume that only the symmetric modal shapes can be influenced by the wind action, indirectly through the variation of the circular eigen-frequency. Instead, the skew-symmetric ones will not change shape but only frequency of vibration since the definition of the modal shape is feasible only when the circular frequency assumes particular values.

Before proceeding we want to hint that in the following we will analyse different aerodynamic models for the wind actions on the structure. We will refer to the Theodorsen and Steady-State analysis respectively to the one modelling the wind effect by means of the complete Theodorsen Theory and to that with the simplification of assuming unitary the complex function $C(k^*)$.

A further kind of analysis will be based on the so-called Quasi-Static modelling of wind forces. According to this approach the aerodynamic lift and couple are proportional to appropriate homonymous coefficients.

$$L(t) = 2\pi b \rho_a U \cdot (\dot{w}_d + U \cdot \dot{\theta}_d) = C_L b \rho_a U \cdot (\dot{w}_d + U \cdot \dot{\theta}_d);$$

$$M(t) = L(t) \cdot \left(x_\alpha + \frac{b}{2}\right) = 2C_M b \rho_a U \cdot (\dot{w}_d + U \cdot \dot{\theta}_d) \cdot \left(x_\alpha + \frac{b}{2}\right);$$

Notice that the expression for the aerodynamic coefficients are the same previously analysed for the Static Divergence onset. Hence are valid only for the case of a thin plate in a potential flow, in all the other case a wind tunnel tests are required.

Is important to notice that the lift force accounts for the instantaneous angle of attack thanks to the vertical speed \dot{w}_d . Generally this term can be neglected when approximate solutions are sufficiently accurate.

Following the same procedure seen for the Transient Approach we get the following Flutter matrix.

$$F = \left\{ \begin{array}{cc} \left(\lambda_{w,n}^2 + \tilde{c}_{ww} \cdot \lambda_{w,n} + \tilde{D}_{w,n}^2 \right) \cdot M_{w,n} & 2\tilde{k}_{\vartheta\vartheta} \cdot \tilde{h}_{w,n,\vartheta m} \\ \left(\tilde{c}_{\vartheta w} \cdot \lambda_{w,n} \right) \cdot \tilde{h}_{w,n,\vartheta m} & \left(\tilde{J}_t \cdot \lambda_{\vartheta,m}^2 + \tilde{c}_{\vartheta\vartheta} \cdot \lambda_{\vartheta,m} + \tilde{J}_t \cdot \tilde{D}_{\vartheta,m}^2 - \tilde{k}_{\vartheta\vartheta} \right) \cdot M_{\vartheta,m} \end{array} \right\};$$

Where the definition of some parameters slightly change.

$$\tilde{c}_{ww} = 2 \left(\xi_w \cdot \tilde{\omega}_w + \sqrt{\tilde{J}_t \cdot \tilde{m}_a} \cdot \tilde{\Omega}_\vartheta \cdot \tilde{u} \right);$$

$$\tilde{c}_{\vartheta\vartheta} = 2\tilde{J}_t \cdot \tilde{\omega}_\vartheta \cdot \xi_\vartheta;$$

$$\tilde{c}_{\vartheta w} = -\frac{1}{2} [\tilde{c}_{ww}]_{\xi_w=0};$$

$$\tilde{k}_{\vartheta\vartheta} = \tilde{J}_t \cdot \tilde{\Omega}_\vartheta^2 \cdot \tilde{u}^2;$$

Let's introduce some further simplifications neglecting first of all the vertical speed on the actual angle of attack and secondly the effect of damping on the response of the system also the structural one. Accordingly, the aeroelastic damping parameters vanish and the unknowns are the only flexural and torsional circular eigen-frequencies.

$$F = \left\{ \begin{array}{cc} \left(-\tilde{\omega}_{F, nm}^2 + \tilde{\Omega}_{w, n}^2 \right) \cdot M_{w, n} & 2\tilde{k}_{\vartheta\vartheta} \cdot \tilde{h}_{w, n, \vartheta m} \\ 0 & \left(-\tilde{J}_t \cdot \tilde{\omega}_{F, nm}^2 + \tilde{J}_t \cdot \tilde{\Omega}_{\vartheta, m}^2 - \tilde{k}_{\vartheta\vartheta} \right) \cdot M_{\vartheta, m} \end{array} \right\};$$

Hence, the vanishing of the Flutter determinant leads to the following statement.

$$\det(F) = (K_{w, n} - \tilde{\omega}_{F, nm}^2 \cdot M_{w, n}) \cdot (K_{\vartheta, n} - \tilde{\omega}_{F, nm}^2 \cdot J_{\vartheta, m} - \Gamma_{\vartheta, m}) = 0;$$

We can solve it analytically as follows.

$$(M_{w, n} \cdot J_{\vartheta, m}) \cdot \tilde{\omega}_{F, nm}^4 - (K_{w, n} \cdot J_{\vartheta, m} + K_{\vartheta, n} \cdot M_{w, n} - \Gamma_{\vartheta, m} \cdot M_{w, n}) \cdot \tilde{\omega}_{F, nm}^2 + K_{w, n} \cdot (K_{\vartheta, n} - \Gamma_{\vartheta, m}) = 0;$$

Collect the modal equivalent masses.

$$\tilde{\omega}_{F, nm}^4 - \left(\tilde{\Omega}_{w, n}^2 + \tilde{\Omega}_{\vartheta, m}^2 - \frac{\Gamma_{\vartheta, m}}{J_{\vartheta, m}} \right) \cdot \tilde{\omega}_{F, nm}^2 + \tilde{\Omega}_{w, n}^2 \cdot \left(\tilde{\Omega}_{\vartheta, m}^2 - \frac{\Gamma_{\vartheta, m}}{J_{\vartheta, m}} \right) = 0;$$

Define the relative flutter to torsional and the flexural to torsional squared circular eigen-frequency ratios.

$$\left\{ \begin{array}{l} \varepsilon = (\omega_{F, nm} / \tilde{\Omega}_{\vartheta, m})^2 \\ \delta = (\tilde{\Omega}_{w, n} / \tilde{\Omega}_{\vartheta, m})^2 \end{array} \right. \Rightarrow \varepsilon^2 - \left(1 + \delta - \frac{\Gamma_{\vartheta, m}}{K_{\vartheta, m}} \right) \cdot \varepsilon + \delta \cdot \left(1 - \frac{\Gamma_{\vartheta, m}}{K_{\vartheta, m}} \right) = 0$$

Hence, we can find directly the analytical solution for the aeroelastic frequencies.

$$\varepsilon_{1,2} = \frac{1}{2} \left\{ \left(1 + \delta - \frac{\Gamma_{\vartheta, m}}{K_{\vartheta, m}} \right) \pm \sqrt{\left(1 + \delta - \frac{\Gamma_{\vartheta, m}}{K_{\vartheta, m}} \right)^2 - 4\delta \cdot \left(1 - \frac{\Gamma_{\vartheta, m}}{K_{\vartheta, m}} \right)} \right\};$$

From the last expression is possible to extrapolate two extreme conditions. The first one refers to the Static Divergence condition that can be found simply enforcing null Flutter circular frequency since any motion is required.

$$\omega_{F,nm} = 0 \Rightarrow \varepsilon = 0 \Leftrightarrow \left(1 - \frac{\Gamma_{\vartheta,m}}{K_{\vartheta,m}}\right) = 0 \Rightarrow \Gamma_{\vartheta,m} = K_{\vartheta,m} \Rightarrow \tilde{J}_t \cdot \tilde{\Omega}_{\vartheta}^2 \cdot \tilde{u}^2 \cdot M_{\vartheta,m} = K_{\vartheta,m} \Rightarrow \tilde{u}_D = 1 ;$$

Meaning that the actual definition give to the dimensional Divergence speed is exact, since no dimensionless speed can overcome it, being normalised with respect to it.

In order to define the Flutter condition onset is necessary to enforce that the two roots found are identical, as we have done in the Old Approach.

$$\varepsilon_1 = \varepsilon_2 \Leftrightarrow \left(1 - \frac{\Gamma_{\vartheta,m}}{K_{\vartheta,m}} + \delta\right)^2 - 4\delta \cdot \left(1 - \frac{\Gamma_{\vartheta,m}}{K_{\vartheta,m}}\right) = 0 \Rightarrow \left(1 - \frac{\Gamma_{\vartheta,m}}{K_{\vartheta,m}} - \delta\right)^2 = 0 \Rightarrow \Gamma_{\vartheta,m} = K_{\vartheta,m} \cdot (1 - \delta) ;$$

Then recall some known definitions.

$$\tilde{J}_t \cdot \tilde{\Omega}_{\vartheta}^2 \cdot \tilde{u}^2 \cdot M_{\vartheta,m} = K_{\vartheta,m} \cdot (1 - \delta) \Rightarrow \tilde{u}_{QS} = \sqrt{1 - \delta} ;$$

The Quasi-Static Approach allows analytical solution but due to its simplicity it does not allow to say if the Flutter onset will be of flexural or torsional kind. The ratio between the flexural and torsional structural circular eigen-frequencies plays a fundamental role, in fact as it decreases we get Flutter speed approaching the limit Divergence condition. This happens as the flexural stiffness is sufficiently high with respect to the torsional one. Notice that implicit assumption is that the bridge is always much more slack with respect to torsional vibrations than flexural one, as usually happens in real structures. In fact, as the condition reverses we would get a negative radicand. Hence the parameter δ must range between 0 and 1.

5.6.2. Numerical results

Before starting to comment the Flutter limit curves let's make few considerations on the numerical methods implemented.

We have already explained the main features of the methods we have called New and Old Approach, now we want to sketch some representative images in order to see how the codes work.

First of all we analyse the main feature of the New Approach focusing on the variation of the circular eigenfrequency and of the damping ratio for the complete aeroelastic system.

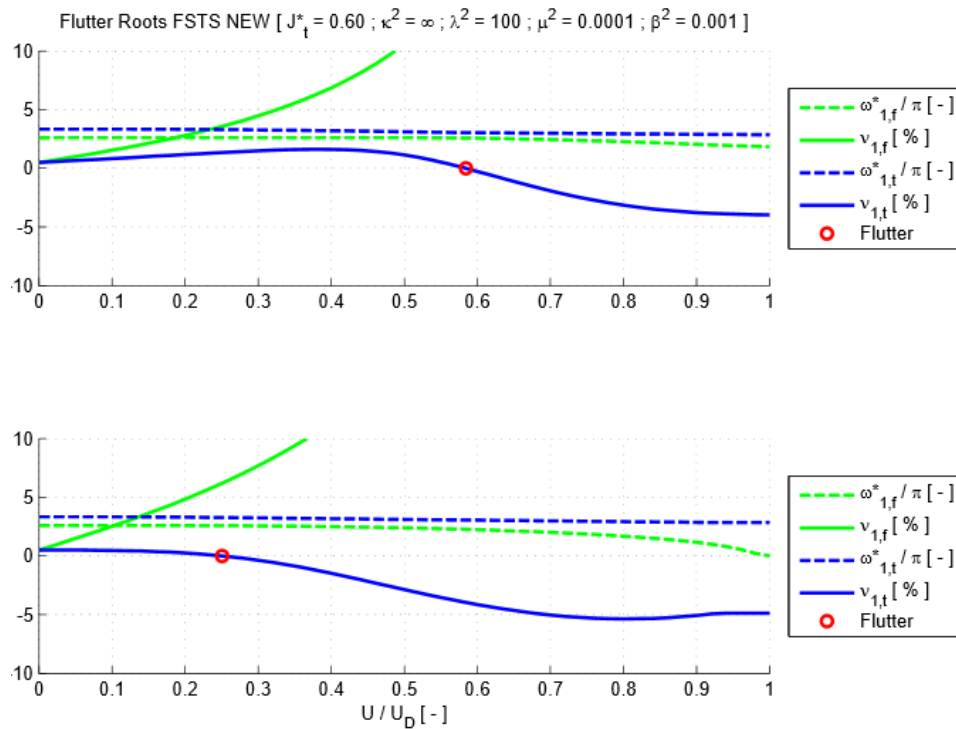


Figure 5.3_Aeroelastic frequency and damping of Mode 1 for Theodorsen and Steady-State formulation.

The first thing we notice is that there is a huge difference between the so-called Theodorsen formulation and the Steady-State one. The only difference is that in the second one we assume the complex Theodorsen function to be constant and unitary. Therefore, it's evident that its influence on the Flutter speed threshold is very important, because neglecting its dependence on the actual reduced frequency means lose too much fundamental information. In fact, we are not able to feel the difference between the structural vibration frequency and the one required to the fluid to overpass the whole bridge's sectional width. The fact that with the Steady-State formulation we assume the reduced frequency to be very high means that the structural vibrations are much more slow than the wind ones. Therefore, we are losing the information concerning the interaction between the fluid flow and the motion of the bridge section that modifies the direction of the stream lines. Consequently, the Steady-State approach overestimate very much the wind forces and hence we get lower admissible Flutter speed limits. We can state that it is a method a little bit easier than the Transient one, but simplifications means also less reliable models since to get simple results we cannot exploit all the structural resources that can be appreciated only by a more complicate but accurate model of the wind-structure interaction such as the Theodorsen formulation. Generally we can state that the safe factor is about 50 % or higher.

As we can see, results confirm what we have already stated concerning the contribution coming from the aeroelastic damping. In fact, starting from the initial value of 0.5 %, assumed to be representative of real life bridges without special dissipative devices, associated to the pure structural contribution, it's evident that both the damping branches at least double it within very low wind speed levels. The stable branch, the flexural one in this case, grows very fast and in correspondence of Flutter onset it overcome 10 % and 5 % respectively for the Theodorsen and the Steady-State formulation in all cases analysed.

Regarding the unstable branch we want to underline two fundamental features. The first one concern the fact that in both the formulations is evident a change of curvature slightly after the reaching of the Flutter onset. This means that if the wind speed increases monotonically from zero, the divergent damping branch will pass from stable to unstable conditions but then the structure will return to stable one. This is a theoretical possibility in fact in all cases analysed the wind speed required to return to the stable condition is higher than the Static Divergence threshold. Anyway in the present treatment also if possible is not of interest because we want to catch just the limit onset of the Flutter instability, in fact we are not assuming any wind speed time history meaning that for us wind speed is constant along the time axis.

Focusing on the unstable branch of the only Steady-State approach, we want to underline the fact that assuming a null structural damping would be not possible. In fact, the curve has an initial slope slightly negative that will led the structure to become unstable as the wind speed becomes different from zero. Thence the choice of a very small but not null initial structural damping should appear to be useless but in reality it is not. This is true at least for the Steady-State formulation, instead for the Transient one it become useless, because the unstable damping branch initially grows.

Further, another important information we can get analysis the unstable damping branch is the slope characterising the curve near the Flutter onset. In fact, it gives a qualitative measure of how much is violent and sudden the passage from stable to unstable oscillations under accelerate wind action. This in general is a very important aspect to be taken in consideration, particularly regarding accelerate flight of aileron.

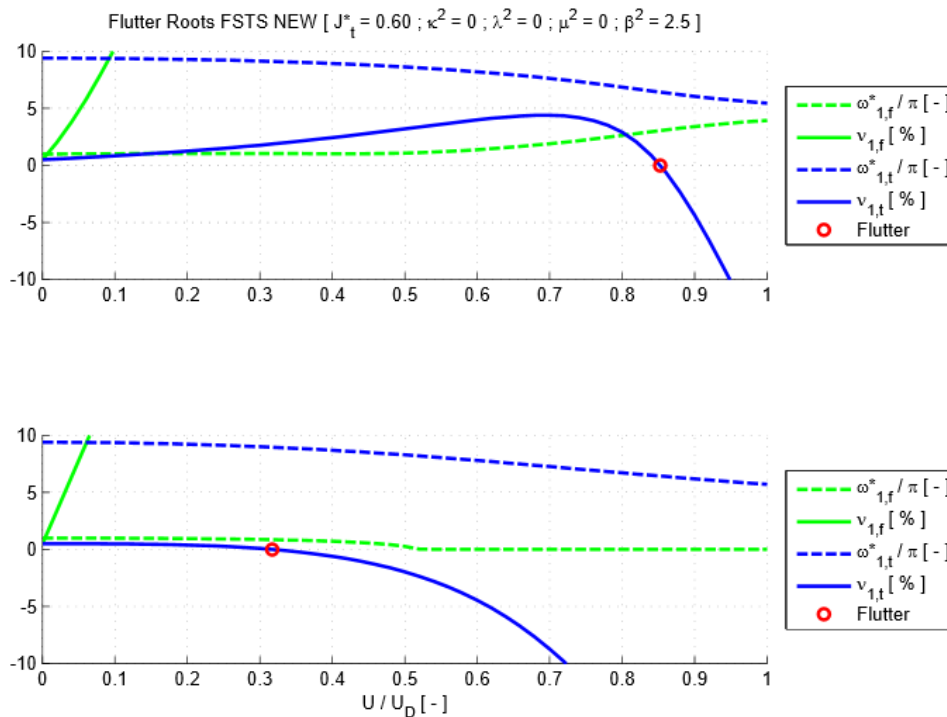


Figure 5.4_Damping slope of Mode 1 for Theodorsen and Steady-State formulation.

As we can see this feature depends strongly on the geometrical and mechanical properties of the structure. In fact as the torsional stiffness is much more higher than the flexural one, the Flutter speed approaches the Divergence threshold and the structure enters in the unstable branch more and more suddenly and violently. Notice also that as the initial values of circular eigen-frequencies are more different from each other, then overlapping effect due to aeroelastic forces increases.

The aeroelastic response of any coupled structure has another important peculiarity, that is, starting from more or less distinct values, the frequency of oscillations of the main two interacting modes tend to converge as the wind speed grows. Notice that this phenomenon has its maximum effect in an around of the Flutter onset, where we have the highest modal energy exchange.

Now we want to show how the Old Approach works in finding the Flutter limit conditions. First of all we need to plot both the real and imaginary part of the Flutter determinant as function of the only circulat eigenfrequency.

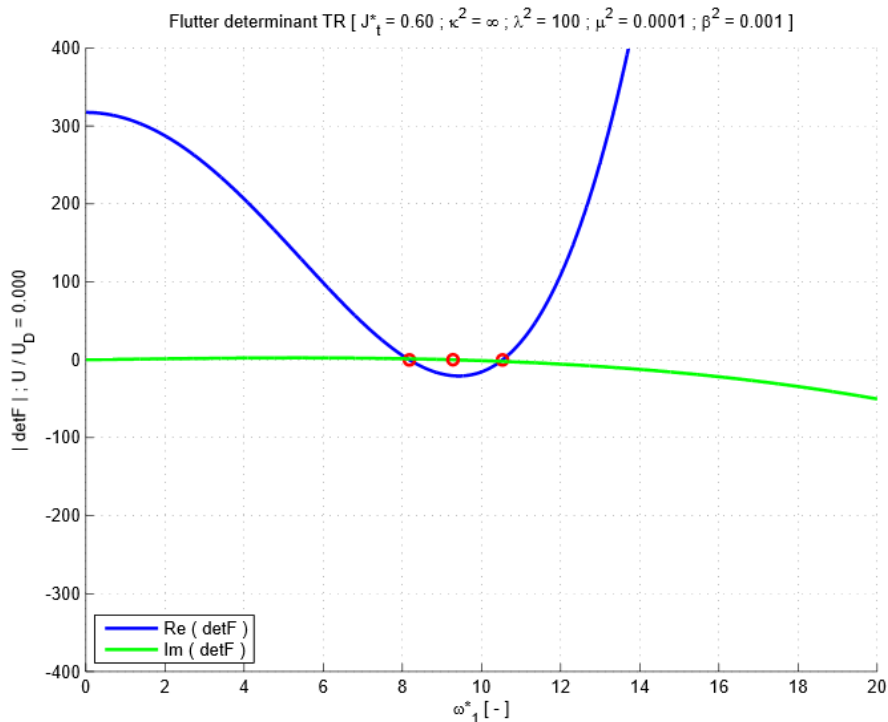


Figure 5.5_ Flutter determinant of Mode 1 for generic structural conditions at null wind speed.

As we can see as the wind speed is null we get two roots from the zeroing of the real part of the Flutter determinant corresponding to the flexural and torsional one of the only structure, and a unique root from the imaginary part in between the previous two.

Then as the wind speed increases also the properties of the aeroleastic system change, consequently we get different masses, stiffness and damping that change the frequencies of oscillations.

There particular structural condition for which one of the real root is so near vanishing that increasing the wind speed we get just one real root meaning that the previous frequency collapses to zero.

Others cases concern the ones in which the two real frequencies are very near to each other, hence as the wind speed increases we can get a unique real root meaning that the two are coincident and then return to separate again. We assume that frequencies cannot exchange, that means the min frequency remains so for any value of wind speed. This is an important aspect to be taken in account when the two real roots coincide at certain wind speed.

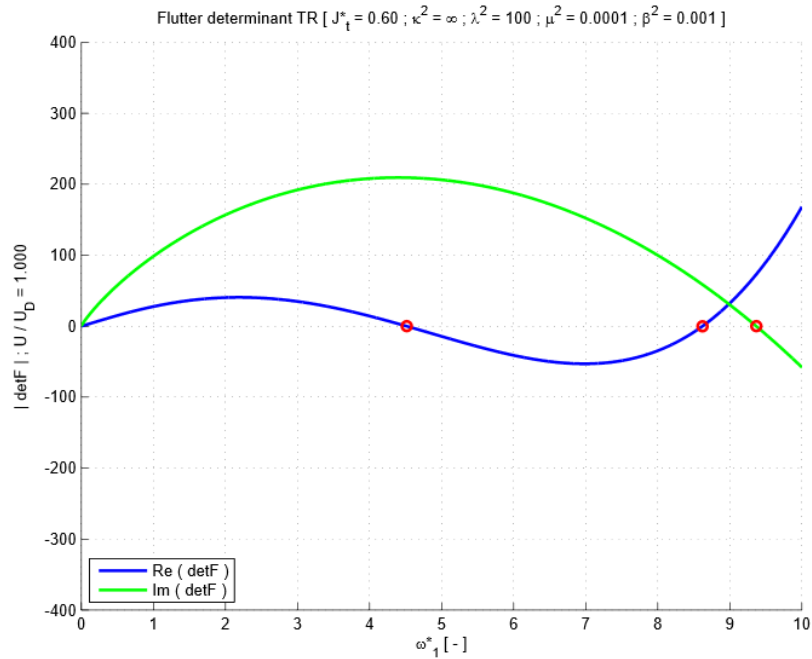


Figure 5.6_Flutter determinant of Mode 1 for generic structural conditions at Divergent wind speed.

As the wind speed reaches the threshold corresponding to the Static Divergence condition, we notice that the imaginary root overtake one of the two real roots, the higher or the lower one. This means that there exist a wind speed level at which the imaginary and one of the real root coincide; this is the Flutter onset condition. In fact at this wind speed level the Flutter Determinant exactly vanishes.

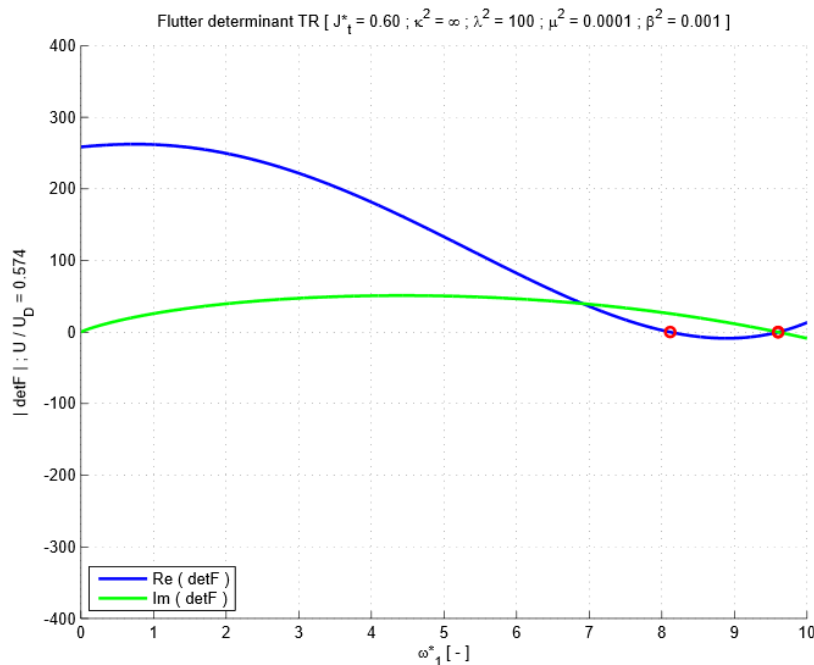


Figure 5.7_Flutter determinant of Mode 1 for generic structural conditions at Flutter wind speed.

Thence, once we find for each wind speed the three roots we can trace the difference between the imaginary and the real ones in order to find out, which is overtaken to know if it is a flexural or torsional Flutter condition, and in correspondence of which wind speed.

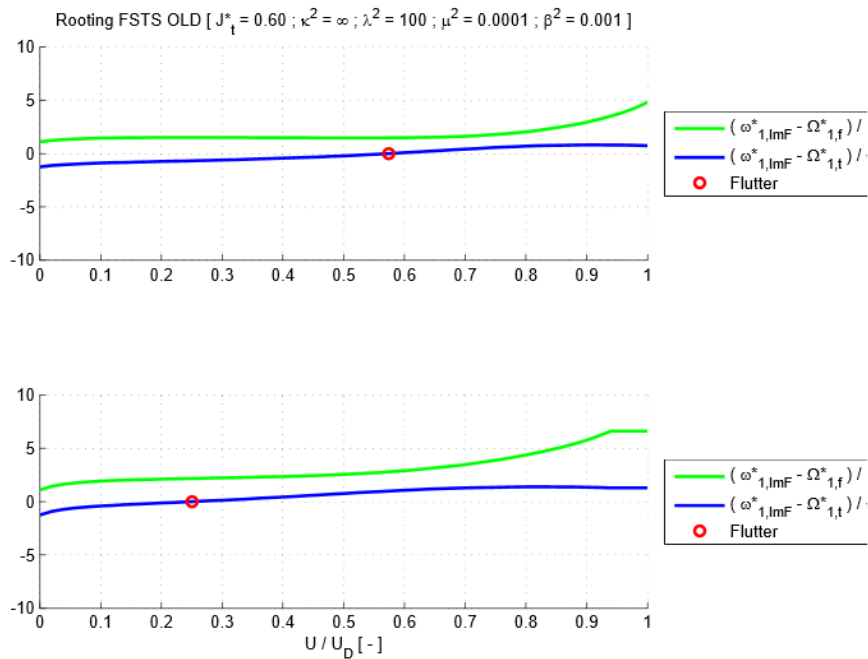


Figure 5.8 _Flutter onset of Mode 1 for Theodorsen and Steady-State formulation.

Finally after detecting the Flutter condition we can get also the path followed both by the circular eigenfrequencies and by the damping ratios.

This last plot allow us to compare the Flutter onset condition obtained with both the Approaches implemented. As we can see the results are practically identical, in fact we can notice just a slight difference that makes the Old approach slightly on the safe side. This is because in the zeroing process the latter does not consider the contributions coming from the aeroelastic damping. Consequently the aerodynamic forces are a little bit higher with respect to the one obtained with the New Approach. Hence we can state that the Old Approach is simpler in the formulation but longer in the numerical process with respect to the New one, and result are coincident for engineering applications.

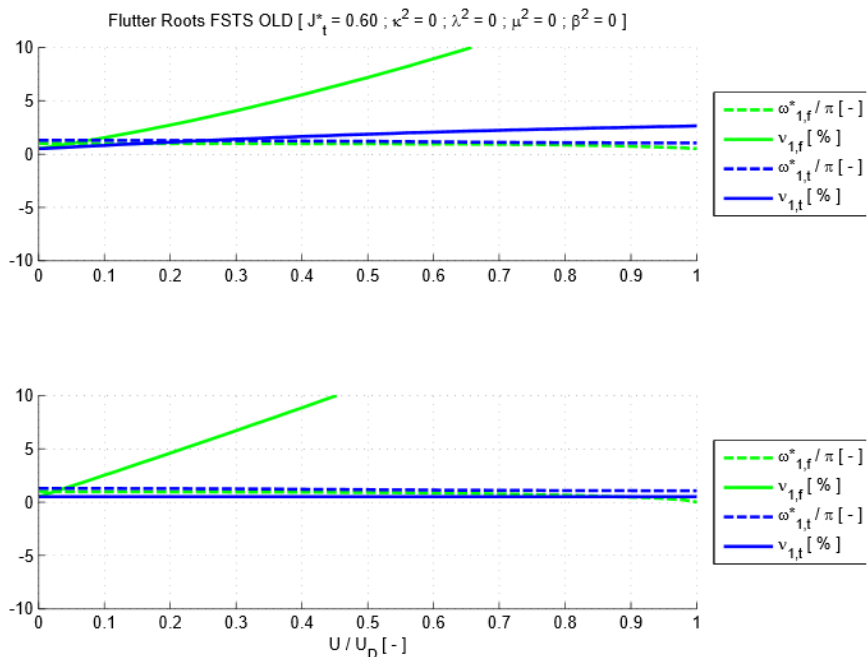


Figure 5.9 _Aeroelastic frequency and damping of Mode 1 for Theodorsen and Steady-State formulation.

With respect to the New Approach it's evident that the damping ratios are strongly different due to the fact that we are computing them on the basis of the only direct aeroelastic damping parameter, hence losing some important contributions coming from the other dof motion. In fact one on all, we cannot distinguish any divergent damping branch. Notice that in the Steady-State formulation we get constant damping due to the simplified formulation of the complex Theodorsen function than is now independent from the reduced frequency. On the other hand both the frequencies branches are quite similar to the ones we obtain with the New Approach.

Further we want to analyse the variation of the modal shapes as the wind speed increases. In fact we as we have previously stated, modes depend indirectly from the actual circular eigen-frequency that we have just seen is an aeroelastic property. Notice that we have assumed that only the non-sinusoidal modal shapes can be tuned by the presence of wind actions.

In the following we will plot not the whole set of modals shapes corresponding to the wind speed considered, but only the ones corresponding to the structural one in absence of wind as reference, the one with minimum and maximum participating mass to get the lower and upper limit for modal shapes and the one so-called Flutter modal shape in correspondence of Flutter onset.

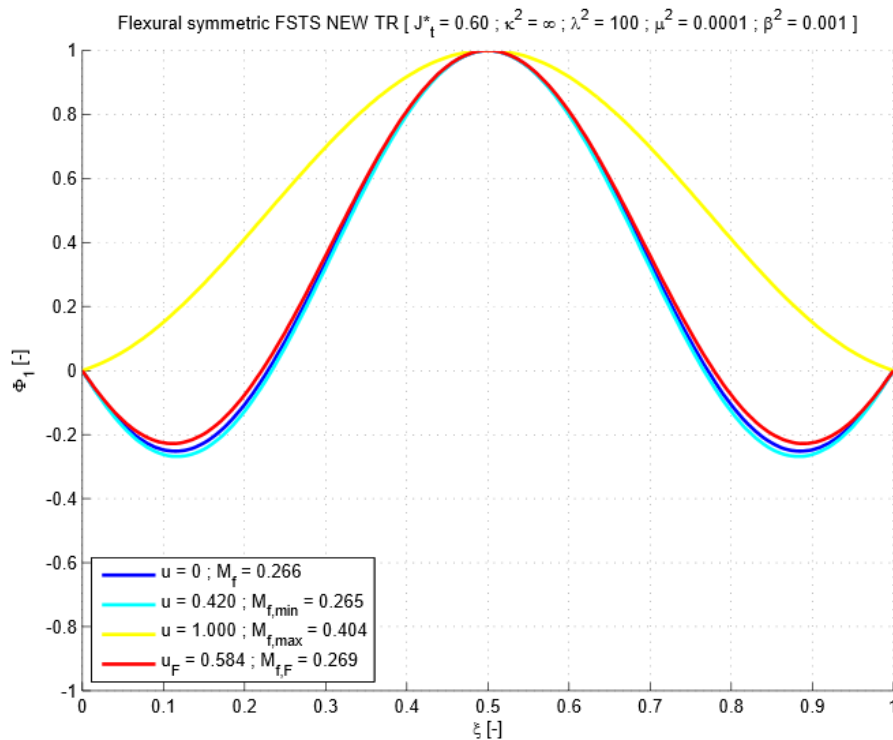


Figure 5.10_Aeroelastic modal shape of Mode 1 for generic structural conditions.

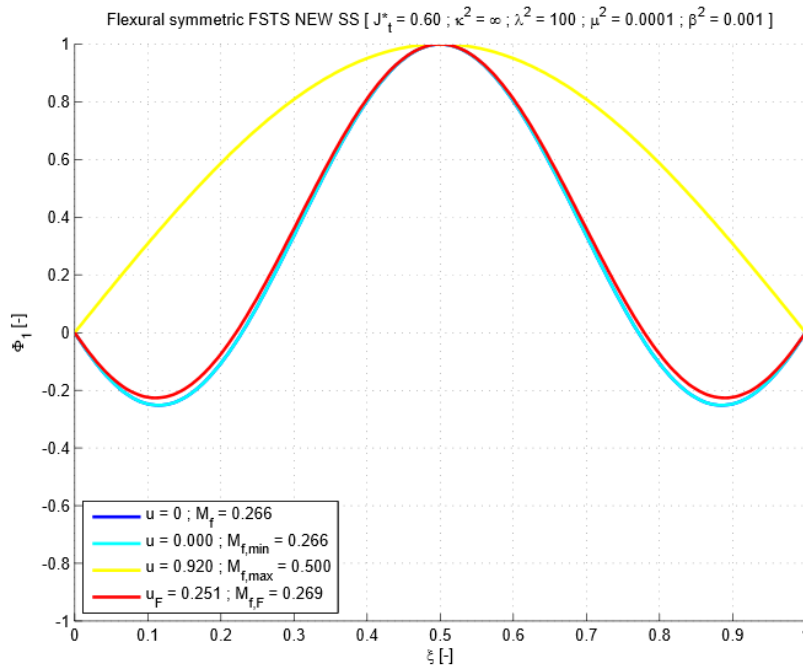


Figure 5.11_Aeroelastic modal shape of Mode 1 for generic structural conditions.

It's evident that as Flutter condition exist the modal shape with the highest participating mass will be never reached. In all the cases analysed we notice a slight modification of the circular eigen-frequencies up to Flutter condition when it exist, consequently the variation of modal shapes with wind speed conditions is not so crucial.

The choice between Theodorsen and Steady-State formulation is not so important regarding the shapes of the modes up to the Flutter condition but can be relevant beyond it.

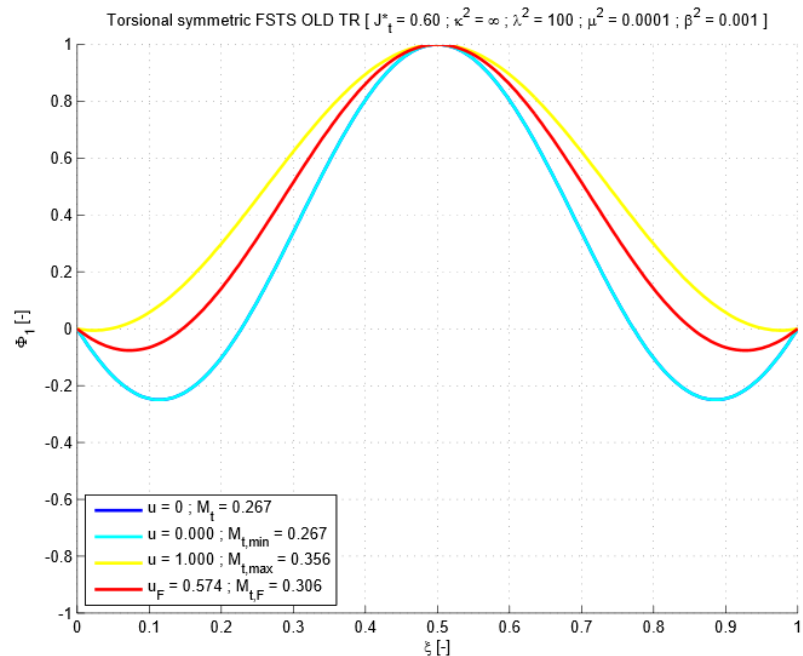


Figure 5.12_Aeroelastic modal shape of Mode 1 for generic structural conditions.

On the other hand the slight difference between the New and Old Approach in the Flutter condition onset, affects the shapes of eigen-modes strongly also up to Flutter condition.

Notice that the wind has the same effect on modal shape of reducing on one hand the cables inextensibility or on the other the flexural or torsional relative stiffness.

Now we are ready to analyse the results coming from the Flutter analysis in terms of wind speed limits. First let's see the simpler approach, that is the Quasy-Static formulation of the problem. As we can see from the following plotting, we decide to sketch different curves for each value of the deck to cables flexural stiffness ratio μ^2 since the Quasy-Static formulation is not able to say if the divergence would be flexural or torsional, hence we choose the deck to cables torsional stiffness β^2 as reference parameter. As we can see the curves are strongly non-linear and some are not monotonically growing with the β^2 parameter. The latter feature is reasonable if we think to the simple formulation given by the Quasi-Static formulation to the Flutter wind speed limit.

$$\tilde{u}_{QS} = \sqrt{1 - \delta} = \sqrt{1 - (\tilde{\omega}_{w,n} / \tilde{\omega}_{\vartheta,m})^2};$$

We have already pointed out that it implicitly assumes that the δ cannot be higher than one, meaning that the flexural frequency need to be always lower than the torsional one.

This assumption precludes the possibility to trace flexural unstable branches for Flutter speed.

In the code, in order to avoid a negative radicand, we take the absolute value of the radicand since the previous condition is not always satisfied particularly as the flexural stiffness becomes very high.

Hence, the branches that decreases with as the parameter β^2 grows represent flexural unstable branches, while the other growing ones relates all to torsional vibrations.

In general the path followed by the curves was expected since would be reasonable that once μ^2 is fixed increasing the torsional relative stiffness we expect higher and higher torsional Flutter wind speeds since the energetic level respectively for the flexural and torsional motion differ more and more. The opposite behaviour is expected increasing the flexural relative stiffness since energetic levels comes nearer. This is true for torsional unstable branches that are feasible only when the relative torsional stiffness reaches values enough high.

On the other hand as the structural system becomes enough rigid in the flexural direction, then as the low torsional stiffness grows the energetic levels tends to align hence flexural Flutter will occur at lower wind speed.

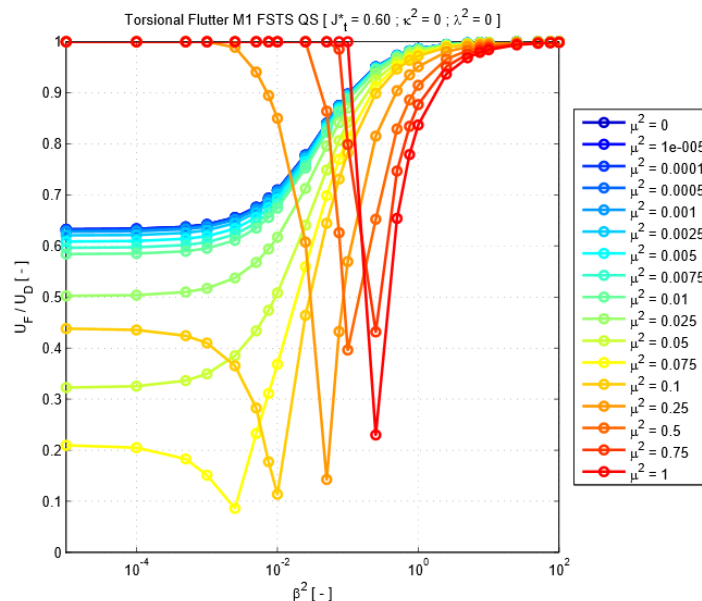


Figure 5.13_Flutter curves of Mode 1 for Quasi-Static formulation with $\chi^2 = 0$.

As the cables inextensibility increases, to see the passage from flexural to torsional unstable branches, we need higher relative flexural stiffness μ^2 and lower torsional limit parameter β^2 . This is a consequence of the fact that, as cables stiffness increases, the global flexural stiffness reduces and hence we need higher contributions coming from the deck so that flexural frequencies of oscillations overtake the torsional ones. The reduction of flexural stiffness contribution coming from the cables system is because increasing their axial inextensibility we are limiting the stiffening behaviour directly linked to deformations. On the other hand the cables inextensibility has lower effect on torsional oscillations in correspondence of high and low values of β^2 respectively for the stiff $\chi^2 = 0$ and free $\chi^2 = \infty$ warping limit condition. As main consequence of these two aspects the coupling factor $\tilde{h}_{w_n, \vartheta_m}$ decreases as the cables inextensibility is higher and higher.

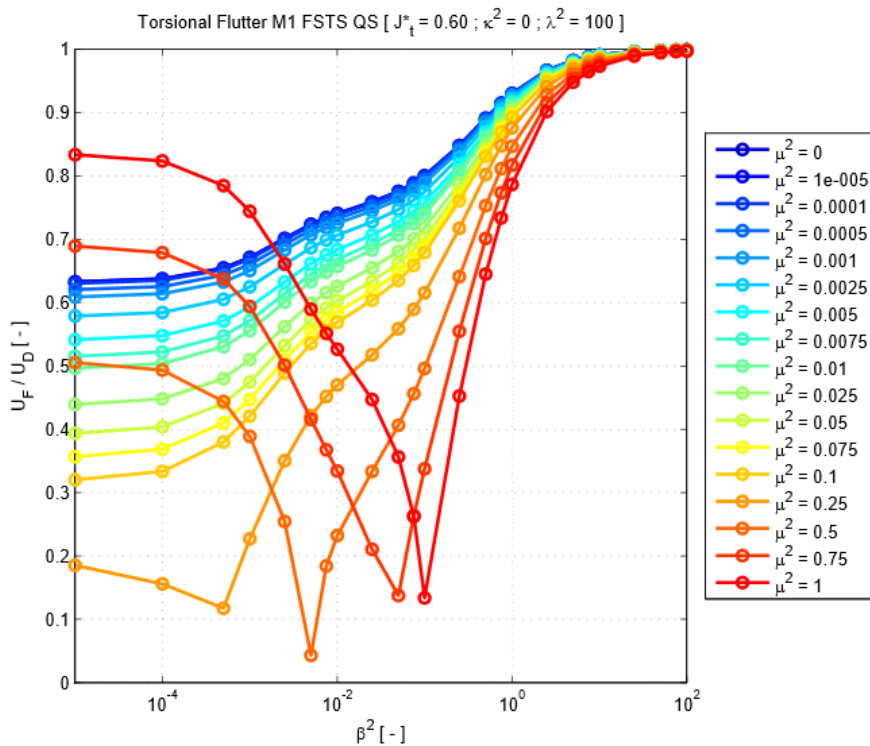


Figure 5.14_Flutter curves of Mode 1 for Quasi-Static formulation with $\chi^2 = 0$.

We notice also that we have a higher variation between different curves in correspondence of low torsional stiffness β^2 , meaning that the relative flexural parameter this parameter μ^2 has an higher effect on the Flutter onset when the torsional one is not too much high, otherwise any tuning of the first one will be less influent.

The Irvine cables parameter λ^2 influences results turns away the curves increasing the scattering. But notice that the upper limit curve does not present so evident differences with respect the previous one, hence the increase of cables inextensibility leads to an higher influence of the relative flexural stiffness parameter μ^2 . This is due again to the fact that there is an higher influence on flexural modes than torsional ones, as previously stated regarding the coupling factor.

Also it decreases and increases Flutter speed respectively at the highest and lowest range of β^2 .

Both effect are due to the fact that the higher is λ^2 the more the cables are inextensible and consequently the structure is more rigid and any tuning of the structural parameters has less influence on its response.

Considering the case of $\chi^2 = \infty$ we get similar shapes of the curves with the important difference that critical conditions move toward higher values of β^2 , with a translation of two order of magnitude.

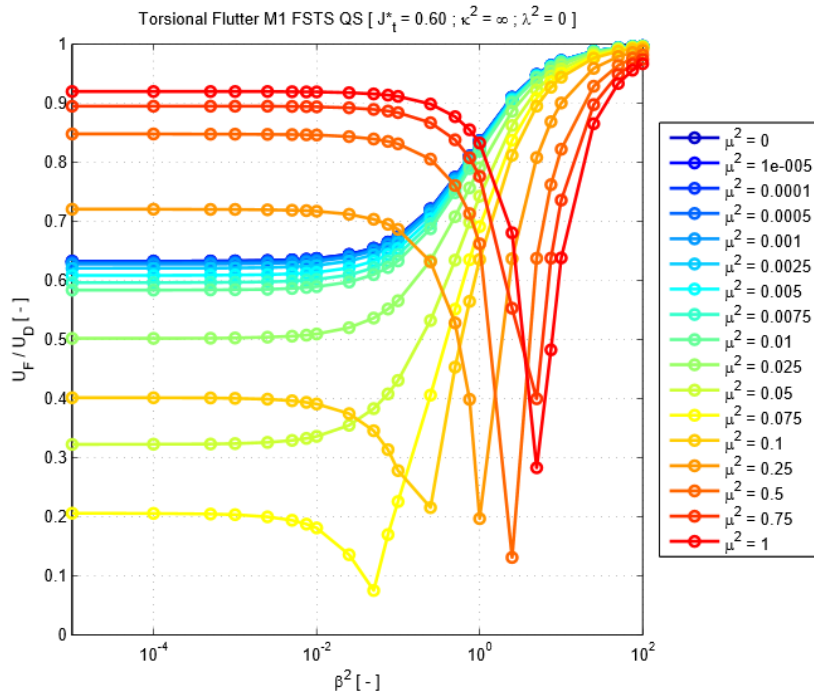


Figure 5.15_Flutter curves of Mode 1 for Quasi-Static formulation with $\chi^2 = \infty$.

Regarding the results obtained by means of the Theodorsen and Steady-State formulation we can state that there are just slight differences between the ones obtained by the New and Old approach. The only remarkable one is that from the latter we never get Flutter conditions of flexural type with the parameter used in the numerical simulations.

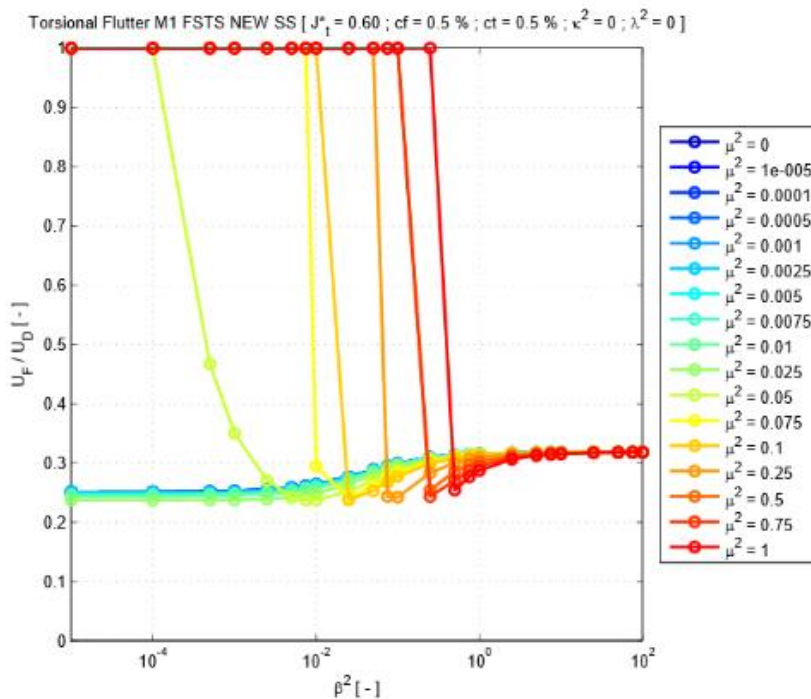


Figure 5.16_Flutter curves of Mode 1 Steady-State formulation.

At a first sight we can see that the main feature noticed in the Quasi-Static formulation are relevant also for both the other approaches. In fact, curves are non-linear and we notice that are not monotonically growing. However, this time the decreasing branches are not associated to flexural oscillations. Consequently, we can state that as the flexural stiffness is high enough the bridge can reach higher wind speed limit when the torsional stiffness is low than when it is very high. We noticed this same phenomenon previously in the Quasi-Static formulation for the flexural branches. Hence, the main difference is that only with the Transient and Steady-State formulation we are able to say exactly if the Flutter condition will be of torsional or flexural type.

From this observation we learn that is not important which frequency is lower and which is higher to choose if the Flutter onset will be of torsional or flexural kind. What really and only governs the choice is the Flutter determinant and the damping ratio of the complete aeroelastic system.

As we can see from the Transient results we get slightly lower Flutter speed with respect to the Quasi-Static condition since the latter one lose too much information regarding the interaction between modes. In fact it consider just the frequencies and not also the modal shape similarities and further any damping contribution is taken in account. Hence although it's the simplest method taken in account it gives not the more safe results.

As the cables inextensibility increases we get the same behaviour previously commented, that is an higher influence of flexural parameter μ^2 . This time both for the Transient and Steady-State approach we notice an increase of the scatter between curves mainly in correspondence of mean values of the relative torsional parameter β^2 in the range 0.01-10. Hence in that region we get that higher Flutter speeds increases and lower ones decreases for the same reason that the Irvine parameter modifies modal shapes in different ways for flexural and torsional motion, and the latter one is more influenced in correspondence of high and low values of β^2 respectively for the stiff $\chi^2 = 0$ and free $\chi^2 = \infty$ warping limit condition. Consequently the coupling terms $\tilde{h}_{w_n, \vartheta_m}$ changes in different ways depending on the actual structural conditions.

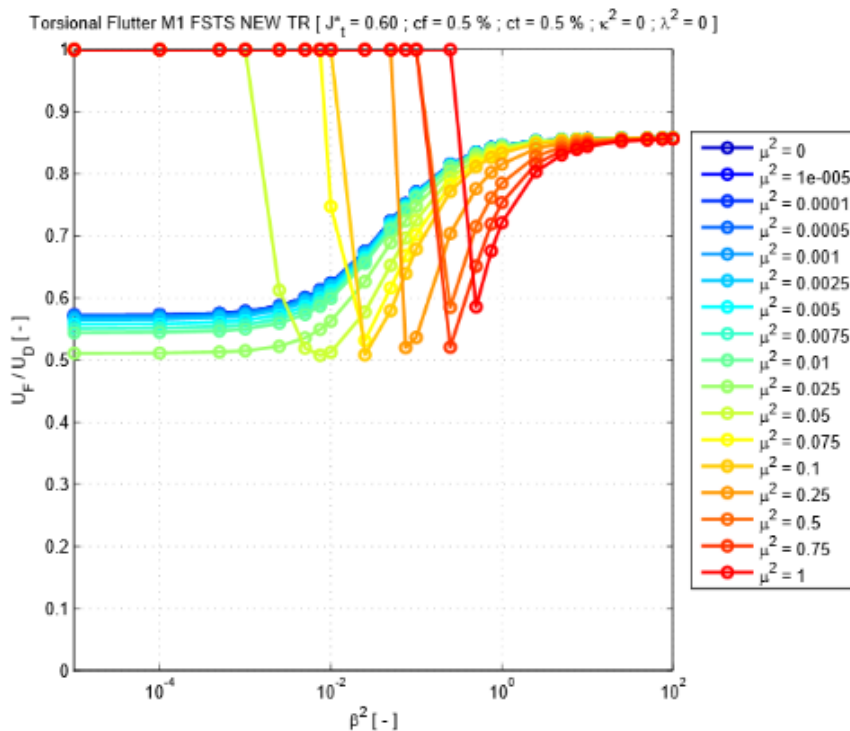


Figure 5.17_Flutter curves of Mode 1 Theodorsen formulation.

Regarding the differences between Transient and Steady-State results we can say that the latter one gives us Flutter speed that are really on safe side being lower of above 50 % with respect to the ones obtained with the complete Theodorsen formulation. On the other hand the main feature are the same in the two formulation, and also the critical values for flexural and torsional parameters are practically the same.

Finally we report also the flexural ranch of the Flutter curves, that as we have already stated, we can get it only from Transient formulation. It's evident that we can get flexural unstable branches only in a very limited set of situations. This mainly happens when the flexural stiffness is very low and the torsional one too much high so that the latter one is not able to vibrate enough to pump energy inside the system. Hence the flexural one do that but only at very high wind speed level as the flexural parameter μ^2 reaches reliable values.

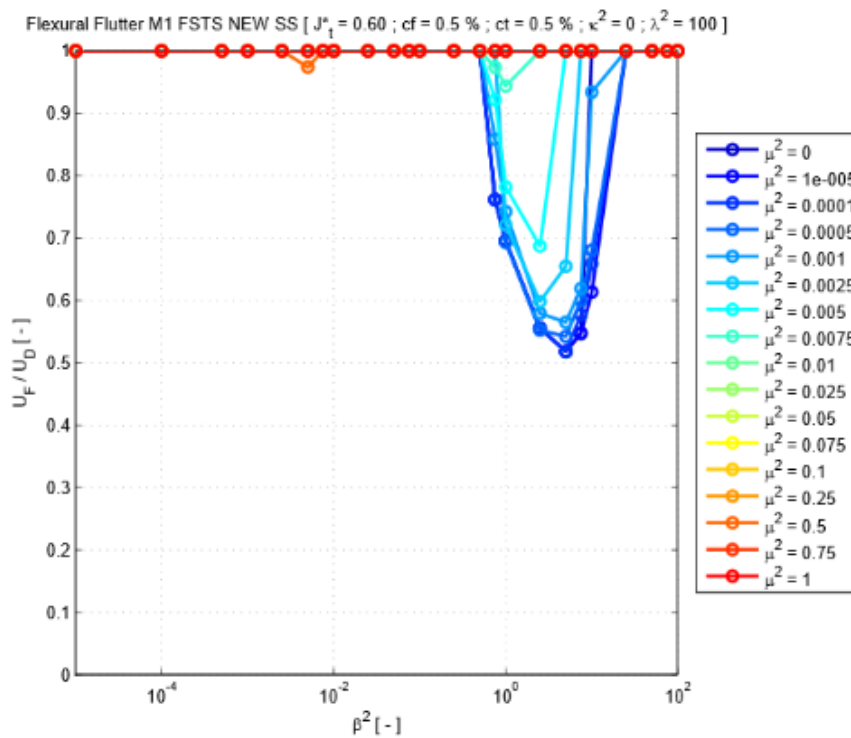


Figure 5.18_ Flutter curves of Mode 1 Theodorsen formulation.

6. Parametric resonance

6.1 Floquet theory

6.1.1 The theorem

The classical theory proposed by Floquet allows us to study the stability of linear systems with periodic coefficients.

Let's consider a system of first order n linear equations.

$$x' = A(t) \cdot x ;$$

Where $x = (x_1 \dots x_n)$ be the vector of unknowns, $t \in (-\infty, +\infty)$ the time variable and $A(t)$ the $(n \times n)$ matrix of continuous periodic functions of period T .

$$A(t + T) = A(t) ;$$

A system of this kind does not have necessarily a non-trivial periodic solution of period T , as can be show considering the simple $n = 1$ case.

$$x' = a(t) \cdot x \Rightarrow x(t) = c \cdot \exp\left(\int_0^t a(t) dt\right) \Rightarrow x(t + T) = x(t) \Leftrightarrow c \neq 0 \text{ and } \int_0^T a(t) dt = 0 ;$$

Floquet states the following theorem [28].

“A system $x' = A(t) \cdot x$ with $A(t + T) = A(t)$ has at least one non-zero solution $x(t)$ such that $x(t + T) = \lambda \cdot x(t)$ for any t where λ is a convenient non-vanishing constant (real or complex).”

Hence, let's prove that statement. Consider first a fundamental $(n \times n)$ system which columns are the n solutions of the problem.

$$X(t) = \{x_{ik}(t)\} = \{col[x_{1k}(t), \dots, x_{nk}(t)]\} ;$$

Consequently thanks to Abel Theorem we get $\det[X(t)] \neq 0$. Then, from the Jacobi-Liouville formula we can write the following relations.

$$\det[X(t)] = \det[X(t_0)] \cdot \exp\left(\int_{t_0}^t \text{tr}(A) dt\right) ;$$

Assuming $t_0 = 0$ we get that as long as $\det[X(0)] \neq 0 \Rightarrow \det[X(t)] \neq 0 \Rightarrow \det[X(t + T)] \neq 0$ for any t . In fact, the vanishing of the determinant is not linked to the choice of the time instant but only on initial conditions.

$$\det[X(t + T)] = \det[X(t_0)] \cdot \exp\left(\int_{t_0}^{t+T} \text{tr}(A) dt\right) ;$$

Consequently also $X(t + T)$ is a fundamental system of solutions and it can be seen as a linear combination of $X(t)$.

$$X(t + T) = C \cdot X(t) \Rightarrow x_{ik}(t + T) = \sum_{j=1}^n c_{jk} \cdot x_{ij}(t);$$

Where C is a $(n \times n)$ constant matrix, hence exploiting the relations just obtained we get another fundamental relation.

$$\det[X(t + T)] = \det[C] \cdot \det[X(t)] = \det[X(0)] \cdot \exp\left(\int_0^t \text{tr}(A) dt\right) \neq 0;$$

Consequently as $\det[X(0)] \neq 0$.

$$\det[C] = \exp\left(\int_0^t \text{tr}(A) dt\right) \neq 0;$$

Now we want to discuss whether there are non-zero solutions, such that $x(t + T) = \lambda \cdot x(t)$ holds.

If such a solution $x(t) = (x_1 \dots x_n)$ exists, then for some non-zero vector $m = (m_1 \dots m_n)$ we must have the following relations.

$$x_s(t) = \sum_{k=1}^n m_k \cdot x_{sk}(t);$$

Hence exploiting the previous relation.

$$x_s(t + T) = \sum_{k=1}^n m_k \cdot x_{sk}(t + T) = \sum_{k=1}^n m_k \cdot \sum_{j=1}^n c_{jk} \cdot x_{sj}(t) = \sum_{j=1}^n \left\{ \sum_{k=1}^n c_{jk} \cdot m_k \right\} \cdot x_{sj}(t);$$

Finally, in order to satisfy the fundamental condition we get.

$$x_s(t + T) = \lambda \cdot x_s(t) \Leftrightarrow \sum_{k=1}^n c_{jk} \cdot m_k = \lambda \cdot m_j \quad \text{for } j = 1, \dots, n;$$

Consequently we can state that the factors or multipliers λ are the characteristic roots of the matrix C . In fact, the previous relation can be written in the classical matrix form.

$$[C - \lambda \cdot I] \cdot m = 0 \quad \text{with } I = \text{diag}(1, \dots, 1);$$

It represents a classical eigen-value problem that allows us to find out the characteristic eigen-values and eigen-vector of a linear problem as long as the vector m does not vanish simply zeroing the determinant of the left hand side matrix and the solving the linear system.

$$\det[C - \lambda \cdot I] = 0 \Rightarrow \lambda = (\lambda_1, \dots, \lambda_n) \Rightarrow [C - \lambda_i \cdot I] \cdot m_j = 0 \Rightarrow m_j \Rightarrow x_i(t);$$

From the condition that avoids the determinant of the matrix C we get that, no multipliers λ_s can vanish.

$$\det[C] = \prod_{i=1}^n \lambda_i \neq 0 \Leftrightarrow \lambda_i \neq 0 \quad \text{for } i = 1, \dots, n;$$

Hence if all the characteristic roots λ_i are distinct then there exist also n distinct solutions $x_i(t)$ forming a fundamental system. Otherwise if only m multipliers λ_i are distinct, with $1 \leq m \leq n$, then there exist just m distinct solutions. Consequently the theorem is proved.

We notice that the multipliers λ_i are independent from the choice of the fundamental system of solutions. To see this, let Y be another fundamental system of solutions such that $Y = M \cdot X$ where matrix M is not singular. This assumption is fundamental for the following relations.

$$X(t + T) = C \cdot X(t) \Rightarrow M^{-1} \cdot Y(t + T) = M^{-1}C \cdot Y(t) \Rightarrow Y(t + T) = M^{-1}CM \cdot Y(t) = C' \cdot Y(t) ;$$

It's evident that the characteristic roots of C and C' have to be the same since we have performed just a simple change of variables.

Generally the numbers λ_i are called characteristic multipliers or factors of the system, and can be written in exponential format as $\lambda_i = \exp(r_i \cdot T)$ where the real or complex numbers r_i are called characteristic exponents of the system and are defined up to multiples of $i\omega = \sqrt{-1} \cdot 2\pi/T$. Consequently, we can write the solutions in the following format.

$$x_i(t) = p_i(t) \cdot \exp(r_i \cdot t) ;$$

Exploiting the fundamental relation for the solutions and the definition of characteristic multipliers we get.

$$x_i(t + T) = p_i(t + T) \cdot \exp[r_i \cdot (t + T)] = \lambda_i \cdot p_i(t + T) \cdot \exp(r_i \cdot t) = \lambda_i \cdot x_i(t) ;$$

Hence also the new function is periodic of period T .

$$p_i(t + T) = p_i(t) ;$$

Finally we can conclude that the linear system $x' = A(t) \cdot x$ has at least , $1 \leq m \leq n$, periodic linearly independent solutions in the form $x_i(t) = p_i(t) \cdot \exp(r_i \cdot t)$, $1 \leq i \leq m$ of period T .

Let's proceed by considering a particular fundamental system $X(t)$ such that $X(0) = I$.

$$X(t + T) = C \cdot X(t) \Rightarrow C = X(T) ;$$

Hence we define for the first time the so called Monodromy matrix C that give a quantitative measure of the variation of the solution $x(t)$ after a period T . Consequently, it can be defined numerically simply integrating the equations along the time axis up to the period of the periodic term.

$$\det[C] = \det[X(T)] \Rightarrow \prod_{i=1}^n \lambda_i = \det[X(0)] \cdot \exp\left(\int_{t_0}^T \text{tr}(A) dt\right) ;$$

Finally we get the definition for the characteristic exponents.

$$\exp(\sum_{i=1}^n r_i \cdot T) = \exp\left(\int_{t_0}^T \text{tr}(A) dt\right) \Rightarrow \sum_{i=1}^n r_i = \int_{t_0}^T \text{tr}(A) dt / T ;$$

Now we search for a convenient choice of the fundamental matrix $X(T)$ in order to be able to write the Monodromy matrix in canonical form, i.e as the sum of n Companion matrices of the generic characteristic root λ_s of order n_s uniquely defined up to an arbitrary permutation as proved by Jordan's Theorem .

$$C = J = P^{-1}AP = \sum_{s=1}^m C_s = [c_{ij}] \text{ s. t. } \begin{cases} c_{i,i} = \lambda_s \\ c_{i,i+1} = 1 \text{ with } 1 \leq i \leq n_s ; \\ c_{i,j} = 0 \end{cases}$$

Where J is the so-called Jordan canonical matrix and P arbitrary complex non-singular Permutation matrix. Notice that because of the particular definition given to the Companion matrices, the associate characteristic multiplier λ_s has a multiplicity equal to $\mu_s = \sum_{s=1}^m n_s$ since we repeat each along the main diagonal of C_s . Consequently, for each Companion matrix the associate Fundamental system has n_s solutions $x_s(t)$

$$X_s(t + T) = C_s \cdot X_s(t) \Rightarrow x_k(t + T) = \lambda_s \cdot x_k(t) - x_{k-1}(t) ;$$

Let's write the Monodromy matrix as an exponential one by means of a $(n \times n)$ canonical matrix D .

$$C = \exp(D \cdot T) \text{ where } D = \sum_{s=1}^m D_s = [d_{ij}] \text{ s. t. } \begin{cases} d_{i,i} = d \\ d_{i,i+1} = 1 \text{ with } 1 \leq i \leq n ; \\ d_{i,j} = 0 \end{cases}$$

Assume a particular form for each Companion matrix.

$$D_s = dI + Z \text{ where } Z = [z_{ij}] \text{ s. t. } \begin{cases} z_{i,j} = 0 \\ z_{i,i+1} = 1 \end{cases} \text{ with } 1 \leq i \leq n ;$$

Consequently the Z matrix elevated at the generic power gives.

$$Z^h = [z_{ij}^{(h)}] \text{ s. t. } \begin{cases} z_{i,j}^{(h)} = 0 \\ z_{i,i+h}^{(h)} = 1 \end{cases} \text{ if } 1 \leq h \leq n_s - 1 ; z_{i,j}^{(h)} = 0 \text{ if } h \geq n_s ;$$

Hence, we can take its exponential to get a polynomial expression for Z .

$$\exp(Z) = [\xi_{ij}^{(h)}] \text{ s. t. } \begin{cases} \xi_{i,i} = 1 \\ \xi_{i,j>i} = 1/j! ; \\ \xi_{i,j<i} = 0 \end{cases}$$

Finally we can write the Monodromy matrix as follows.

$$C = \exp(D \cdot T) = \sum_{s=1}^m \exp(D_s \cdot T) = \sum_{s=1}^m \exp[(dI + Z) \cdot T] ;$$

Hence recalling that.

$$c_{i,i} = \exp(d_{i,i} \cdot T) \Rightarrow \lambda_s = \exp(d \cdot T) ;$$

Then.

$$C_s = \exp(D_s \cdot T) = [g_{ij}] \text{ s.t. } \begin{cases} g_{i,i} = \lambda_s \\ g_{i,j>i} = \lambda_s \cdot T^j / j! \text{ with } 1 \leq i \leq n ; \\ g_{i,j<i} = 0 \end{cases}$$

Now we can prove the periodicity of all the functions $p_k(t)$.

$$x_k(t) = p_k(t) \cdot \exp(r_k \cdot t) \Rightarrow X(t) = P(t) \cdot \exp(D \cdot t) ;$$

Since.

$$X(t + T) = P(t + T) \cdot \exp(D \cdot t) \cdot \exp(D \cdot T) = C \cdot X(t) \Leftrightarrow P(t + T) = P(t) ;$$

Finally assuming $M(t) = \exp(D \cdot t)$ we get the fundamental system in a more compact form.

$$X(t) = P(t) \cdot M(t) ;$$

It states that, the fundamental solution of a linear differential system with periodic coefficients is given by the product between a periodic function $P(t)$ and the solution of the associate system with constant coefficient $M(t)$.

Hence, it's immediate to check the stability of all the solutions of the system that is completely dictated by $M(t)$ being $P(t)$ periodic bounded.

$$x(t) \rightarrow 0 \text{ as } t \rightarrow +\infty \Leftrightarrow |\lambda_i| = |\exp(r_i \cdot t)| < 1 \Rightarrow \text{Re}(r_i) < 0 ;$$

$$x(t) < \infty \text{ as } t \rightarrow +\infty \Leftrightarrow |\lambda_i| \leq 1 \text{ with } \mu_i = \nu_i \text{ as } |\lambda_i| = 1 ;$$

$$x(t) = x(t + T) \quad \forall t \Leftrightarrow |\lambda_i| = 1 \text{ at least once ;}$$

Where μ_i is the multiplicity of the root λ_i for the equation $\det[C - \lambda \cdot I]$, and ν_i is the nullity of the associate matrix $C - \lambda_i \cdot I$.

Before proceeding let's focus on the periodicity of the solution when at least one root satisfies $|\lambda_i| = 1$.

$$x(t + T) = \lambda \cdot x(t) \Rightarrow \begin{cases} \text{if } \lambda = 1 \Rightarrow x(t + T) = x(t) \Rightarrow \text{period } T \\ \text{if } \lambda = -1 \Rightarrow x(t + 2T) = -x(t + T) = x(t) \Rightarrow \text{period } 2T \end{cases} ;$$

We can deduce that the period of the solution is strongly influenced by the value assumed by the characteristic multiplier. In general is valid the following relation.

$$x(t + nT) = \lambda^n \cdot x(t) \Rightarrow \text{period } nT ;$$

6.1.2 Hill's equation

A case in which the application of the Floquet theory has been particularly fruitful is the Hill's equation.

$$x'' + p(t) \cdot x = 0 ;$$

It can be also generalised to the damped case as follows.

$$y'' + q(t) \cdot y' + p^*(t) \cdot y = 0 ;$$

Where both $q(t)$ and $p(t)$ are periodic functions of period T . The second one can be reduced to the first form simply by means the following transformation.

$$y = x \cdot \exp\left(-\frac{1}{2} \int_0^t q(t) dt\right) ;$$

So that.

$$y' = \left\{ x' - \frac{1}{2} \cdot x \cdot q(t) \right\} \cdot \exp\left(-\frac{1}{2} \int_0^t q(t) dt\right) ;$$

$$y'' = \left\{ x'' - x' \cdot q(t) + \frac{1}{2} \cdot x \cdot \left[\frac{1}{2} \cdot q(t)^2 - q'(t) \right] \right\} \cdot \exp\left(-\frac{1}{2} \int_0^t q(t) dt\right) ;$$

Substituting we get.

$$x'' + p(t) \cdot x = 0 \text{ where } p(t) = p^*(t) - \frac{1}{4} \cdot q(t)^2 - \frac{1}{2} \cdot q'(t) ;$$

In order to reduce the system to a first order one we need some further transformations.

$$x = x_1 \text{ and } x' = x_2 ;$$

Hence, we reduce the order of the differential equation but we increase the number of unknowns.

$$\begin{cases} x_1' = x_2 \\ x_2' = -p(t) \cdot x_1 \end{cases} \Rightarrow z' = Az \text{ with } z = \begin{pmatrix} x_1 \\ x_2 \end{pmatrix} ; A = \begin{bmatrix} 0 & 1 \\ -p(t) & 1 \end{bmatrix} ;$$

Let's choose the fundamental system $X(t) = (x_1, x_2)$ such that.

$$x_{11}(0) = x_{22}(0) = 1 ;$$

$$x_{21}(0) = x_{12}(0) = 0 ;$$

Hence the determinant of the initial fundamental system of solutions is unitary.

$$\det[X(0)] = 1 ;$$

Since the trace of the matrix of coefficients vanishes and the initial conditions determinant is one then also the determinant of the Monodromy matrix has to be unitary.

$$\text{tr}(A) = 0 \Rightarrow \det(C) = \det[X(0)] \cdot \exp(\text{tr}(A)) = 1 ;$$

Notice that in all Hamiltonian systems the last relation holds.

Before proceeding let's find out the characteristic roots of the Monodromy matrix.

$$\det[C - \lambda \cdot I] = 0 \Leftrightarrow \lambda^2 - \lambda \cdot \text{tr}(C) + \det(C) = 0 ;$$

Since each component of the solutions can be written in the form $x_{ik}(t + T) = \sum_{j=1}^{n=2} c_{jk} \cdot x_{i,j}(t)$, then exploiting the assumed particular initial conditions to $x_{ik}(T) = \sum_{j=1}^{n=2} c_{jk} \cdot x_{i,j}(0) = \sum_{j=1}^{n=2} c_{jk}$

$$2B = \text{tr}(C) = c_{11} + c_{22} = x_{11}(T) + x_{22}(T) ;$$

Finally, we get the following quadratic form.

$$\lambda^2 - 2\lambda \cdot B + 1 = 0 \Leftrightarrow \lambda_{1,2} = B \pm \sqrt{B^2 - 1} ;$$

Hence we need to study the sign of the determinant $B^2 - 1$.

$$\text{if } B^2 < 1 \Rightarrow -1 < B < 1 \Rightarrow |\lambda_{1,2}| = |B \pm i\sqrt{1 - B^2}| < 1 \Rightarrow x(t) \text{ bounded} ;$$

$$\text{if } B^2 = 1 \Rightarrow B = \pm 1 \Rightarrow |\lambda_{1,2}| = 1 \Rightarrow x(t) \text{ periodic of } (T \text{ or } 2T) ;$$

$$\text{if } B^2 > 1 \Rightarrow B < -1; B > 1 \Rightarrow |\lambda_{1,2}| = |B \pm \sqrt{B^2 - 1}| > 1 \Rightarrow x(t) \text{ unbounded} ;$$

Hence we can conclude that stable and unstable solutions are separated by two particular situations that grant periodic solutions. In order to find out more precisely where these regions are we need further considerations.

Before we want to mention the results obtained by Liapunov concerning the stability thresholds of for the solution.

$$\text{if } p(t) \leq 0 \Rightarrow 0 < \lambda_1 < 1 < \lambda_2 \Rightarrow x(t) \text{ unbounded};$$

$$\text{if } p(t) > 0 \text{ and } \int_0^T p(t)dt \leq 4/T \Rightarrow \lambda_{1,2} = \exp(\pm i\theta) \text{ with } \theta > 0 \Rightarrow x(t) \text{ bounded};$$

Then pass exploiting the relation $\lambda = \exp(\mu \cdot T)$ in order to define the determinant and the trace of the Monodromy matrix.

$$\det(C) = \lambda_1 \cdot \lambda_2 = 1 \Rightarrow \mu_1 + \mu_2 = 0 \Rightarrow \mu_1 = -\mu_2;$$

$$\text{tr}(C) = 2B = \lambda_1 + \lambda_2 \Rightarrow \exp(\mu_1 \cdot T) + \exp(\mu_2 \cdot T) = \exp(\mu_1 \cdot T) + \exp(-\mu_1 \cdot T);$$

Exploiting the exponential definition of the hyperbolic cosine function, we get.

$$\cosh(\alpha) = \frac{1}{2} \cdot (e^\alpha + e^{-\alpha}) \Rightarrow B = \cosh(\mu_1 \cdot T);$$

Let's analyse first the case $-1 < B < 1$. Assuming $B = \cos(\sigma \cdot T^*)$ with $0 < \sigma \cdot T^* < \pi$ we get.

$$\lambda_{1,2} = B \pm \sqrt{B^2 - 1} = \cos(\sigma \cdot T^*) \pm i \cdot \sin(\sigma \cdot T^*) = \exp(\pm i \cdot \sigma T^*);$$

Hence, we need to consider a complex amplitude and take in account both the complex conjugate terms to get real pseudo-periodic solutions, which consequently are stable.

$$x(t) = \exp(\pm i \cdot \sigma T^*) \cdot [q(t) \pm i \cdot r(t)] + c.c.;$$

Notice that the pseud-period of the solution is $T^* = 2\pi/\sigma$, hence as it becomes equal to a multiple of the period of the forcing periodic term, we get that.

$$T^* = nT \Rightarrow \sigma = 2\pi/nT \text{ with } n = 1,2 \text{ (for } \lambda = \pm 1);$$

Further, since we have $B \neq \pm 1$ it follows that.

$$\cos(\sigma \cdot T) \neq \pm 1 \Leftrightarrow \sigma \cdot T \neq m\pi \text{ with } m = 0,1,2 \Rightarrow T^* \neq 2T/m;$$

Hence at resonance a k multiple of T^* has to be equal or twice the forcing one T .

$$kT = k \cdot 2\pi/\sigma = nT \Leftrightarrow \sigma = \frac{n}{k} \cdot \frac{2\pi}{T};$$

The second case refers to $B > 1$.

$$\lambda_{1,2} = B \pm \sqrt{B^2 - 1} \Rightarrow \lambda_1 > 1 > \lambda_2 > 0;$$

Since $\det(C) = \lambda_1 \cdot \lambda_2 = 1 \Rightarrow \lambda_2 = 1/\lambda_1$ hence being $\mu_1 = -\mu_2$ we get an unstable solution due to the explosion of the first exponential term.

$$x(t) = C_1 \cdot \exp(\mu_1 \cdot t) \cdot p_1(t) + C_2 \cdot \exp(-\mu_1 \cdot t) \cdot p_2(t);$$

The third when $B = 1 \Rightarrow \lambda_{1,2} = 1$. Hence we get an unstable solutions due to an harmonic instability of period T .

$$x(t) = (C_1 + C_2 \cdot t) \cdot p_1(t) + C_2 \cdot p_2(t);$$

The fourth case is characterised by $B < -1$. Hence assuming a periodic solution of period $2T$ we get.

$$\lambda_{1,2} = B \pm \sqrt{B^2 - 1} \Rightarrow \lambda_1 < -1 < \lambda_2 < 0 \Rightarrow \mu_1 = \varphi + i \cdot \frac{\pi}{T};$$

Consequently the first exponential diverges in time.

$$x(t) = C_1 \cdot \exp(\varphi t) \cdot p_1(t) \cdot \exp\left(i \cdot \frac{\pi}{T} t\right) + C_2 \cdot \exp(-\varphi t) \cdot p_2(t) \cdot \exp\left(-i \cdot \frac{\pi}{T} t\right);$$

Finally the fifth refers to the case $B = -1 \Rightarrow \lambda_{1,2} = -1$. We get an unstable solution of period $2T$, hence we can call it subharmonic resonance since the structural period is an higher multiple of the forcing term.

$$x(t) = (C_1 + C_2 \cdot t) \cdot p_1(t) \cdot \exp\left(i \cdot \frac{\pi}{T} t\right) + C_2 \cdot p_2(t) \cdot \exp\left(-i \cdot \frac{\pi}{T} t\right);$$

6.2 Modal projection of aeroelastic equations of motion

We want to apply the Floquet Theory to the complete aeroelastic model of suspension bridges treated in the previous chapter. The goal will be to determine which structural parameters play an important role in the stability of vibrations.

First, we need to consider the complete system of non-linear coupled equations in the dimensionless format.

$$\left\{ \begin{array}{l} \frac{d^2 \tilde{w}_d}{d\tau^2} + \tilde{c}_{ww} \cdot \frac{d\tilde{w}_d}{d\tau} + \tilde{c}_{w\vartheta} \cdot \frac{d\tilde{\vartheta}_d}{d\tau} + \mu^2 \cdot \tilde{w}_d'' - \tilde{w}_d'' + \lambda_L^2 \tilde{h}_w + 2\tilde{k}_{\vartheta\vartheta} \cdot \theta_d + \\ -\lambda_Q^2 \cdot \left[\tilde{h}_w \cdot \tilde{w}_d'' + \tilde{h}_\vartheta \cdot \tilde{\vartheta}_d'' - \frac{1}{2} (\tilde{h}_{w'w'} + \tilde{h}_{\vartheta'\vartheta'}) \right] + \\ -\lambda_C^2 \cdot \left[\frac{1}{2} (\tilde{h}_{w'w'} + \tilde{h}_{\vartheta'\vartheta'}) \cdot \tilde{w}_d'' + \tilde{h}_{w'\vartheta'} \cdot \tilde{\vartheta}_d'' \right] \end{array} \right\} = \tilde{q}(\xi, \tau);$$

$$\left\{ \begin{aligned} & \left[\tilde{J}_t \cdot \frac{d^2 \tilde{\vartheta}_d}{dt^2} + \tilde{c}_{\vartheta\vartheta} \cdot \frac{d \tilde{\vartheta}_d}{d\tau} + \tilde{c}_{\vartheta w} \cdot \frac{d \tilde{w}_d}{d\tau} + \frac{\beta^2}{\chi^2} \cdot \tilde{\vartheta}_d'^v - (1 + \beta^2) \cdot \tilde{\vartheta}_d'' + \lambda_L^2 \tilde{h}_\vartheta - \tilde{k}_{\vartheta\vartheta} \cdot \theta_d + \right. \\ & \quad \left. - \lambda_Q^2 \cdot [\tilde{h}_\vartheta \cdot \tilde{w}_d'' + \tilde{h}_w \cdot \tilde{\vartheta}_d'' - \tilde{h}_{w'\vartheta'}] + \right. \\ & \quad \left. - \lambda_C^2 \cdot [\tilde{h}_{w'\vartheta'} \cdot \tilde{w}_d'' + \frac{1}{2}(\tilde{h}_{w'w'} + \tilde{h}_{\vartheta'\vartheta'}) \cdot \tilde{\vartheta}_d''] \right] \end{aligned} \right\} = \tilde{m}(\xi, \tau);$$

Notice that we still have right hand side terms since in the following we need to introduce an additional external forcing term.

Next, we need to perform a modal expansion of both the vertical and the torsional vibrations.

$$\tilde{w}_d(\xi, \tau) = \sum_{n=1}^{\infty} W_n(\xi) \cdot z_n(\tau) \quad \text{with } n \in \mathbb{N} \setminus \{0\};$$

$$\tilde{\vartheta}_d(\xi, \tau) = \sum_{m=1}^{\infty} \Theta_m(\xi) \cdot \gamma_m(\tau) \quad \text{with } m \in \mathbb{N} \setminus \{0\};$$

Notice that we don't need to specify the time function hence it would be determined numerically.

However, in order to get the equations of motion of an equivalent 2-dof pendulum we need to avoid the direct dependence on the spatial coordinate. Hence we project the equations of motion in the modal space simply multiplying the flexural and the torsional one by the respective modal shape and then integrate over the unitary domain of the dimensionless span.

The flexural vibrations.

$$\left\{ \begin{aligned} & M_{w,n} \cdot \ddot{z}_n + C_{w,n} \cdot \dot{z}_n + C_{w\vartheta,nm} \cdot \dot{\gamma}_m + K_{w,n}^{(L)} \cdot z_n + K_{w\vartheta,nm}^{(L)} \cdot \gamma_m + \\ & \quad + K_{w,n}^{(Q)} \cdot z_n^2 + K_{w\vartheta,nm}^{(Q)} \cdot \gamma_m^2 + \\ & \quad + K_{w,n}^{(C)} \cdot z_n^3 + K_{w\vartheta,nm}^{(C)} \cdot z_n \cdot \gamma_m^2 \end{aligned} \right\} = \Gamma_{w,n};$$

Where.

$$M_{w,n} = \int_0^1 W_n^2(\xi) d\xi;$$

$$C_{w,n} = \tilde{c}_{ww} \cdot M_{w,n};$$

$$C_{w\vartheta,nm} = \tilde{c}_{w\vartheta} \cdot \tilde{h}_{W_n\Theta_m};$$

$$K_{w,n}^{(L)} = \int_0^1 W_n(\xi) \cdot [\mu^2 \cdot W_n'^v(\xi) - W_n''(\xi)] d\xi + \lambda_L^2 \cdot \tilde{h}_{W_n}^2;$$

$$K_{w\vartheta,nm}^{(L)} = 2\tilde{k}_{\vartheta\vartheta} \cdot \tilde{h}_{W_n\Theta_m};$$

$$K_{w,n}^{(Q)} = -\lambda_Q^2 \cdot \tilde{h}_{W_n} \cdot \left\{ \int_0^1 W_n(\xi) \cdot W_n''(\xi) d\xi - \frac{1}{2} \cdot \tilde{h}_{W_n'^2} \right\} = \frac{3}{2} \cdot \lambda_Q^2 \cdot \tilde{h}_{W_n} \cdot \tilde{h}_{W_n'^2};$$

$$K_{w\vartheta, nm}^{(Q)} = -\lambda_Q^2 \cdot \left\{ \begin{array}{l} \tilde{h}_{\vartheta_m} \cdot \int_0^1 W_n(\xi) \cdot \Theta_m''(\xi) d\xi + \\ -\frac{1}{2} \cdot \tilde{h}_{W_n} \cdot \tilde{h}_{\vartheta_m'^2} \end{array} \right\} = \lambda_Q^2 \cdot \left\{ \tilde{h}_{\vartheta_m} \cdot \tilde{h}_{W_n', \vartheta_m'} + \frac{1}{2} \cdot \tilde{h}_{W_n} \cdot \tilde{h}_{\vartheta_m'^2} \right\};$$

$$K_{w, n}^{(C)} = -\frac{1}{2} \cdot \lambda_C^2 \cdot \tilde{h}_{W_n'^2} \cdot \int_0^1 W_n(\xi) \cdot W_n''(\xi) d\xi = \frac{1}{2} \cdot \lambda_C^2 \cdot (\tilde{h}_{W_n'^2})^2;$$

$$K_{w\vartheta, nm}^{(C)} = -\lambda_C^2 \cdot \left\{ \begin{array}{l} \frac{1}{2} \cdot \tilde{h}_{\vartheta_m'^2} \cdot \int_0^1 W_n(\xi) \cdot W_n''(\xi) d\xi + \\ + \tilde{h}_{W_n', \vartheta_m'} \cdot \int_0^1 W_n(\xi) \cdot \Theta_m''(\xi) d\xi \end{array} \right\} = \lambda_C^2 \cdot \left\{ \frac{1}{2} \cdot \tilde{h}_{\vartheta_m'^2} \cdot \tilde{h}_{W_n'^2} + (\tilde{h}_{W_n', \vartheta_m'})^2 \right\};$$

$$\Gamma_{w, n} = \int_0^1 W_n(\xi) \cdot \tilde{q}(\xi, \tau) d\xi$$

We remember that all the operator \tilde{h} simply perform the integration of the product between the term at the subscript, along the dimensionless span length.

Moreover, the torsional ones.

$$\left\{ \begin{array}{l} J_{\vartheta, m} \cdot \dot{\gamma}_m + C_{\vartheta, m} \cdot \dot{\gamma}_m + C_{\vartheta w, mn} \cdot \dot{z}_n + K_{\vartheta, m}^{(L)} \cdot \gamma_m + \\ + K_{\vartheta w, mn}^{(Q)} \cdot \gamma_m \cdot z_n + \\ + K_{\vartheta, m}^{(C)} \cdot \gamma_m^3 + K_{\vartheta w, mn}^{(C)} \cdot \gamma_m \cdot z_n^2 \end{array} \right\} = \Gamma_{\vartheta, m}(\xi, \tau);$$

Where.

$$M_{\vartheta, m} = \int_0^1 \Theta_m^2(\xi) d\xi \Rightarrow J_{\vartheta, m} = \tilde{J}_t \cdot M_{\vartheta, m};$$

$$C_{\vartheta, m} = \tilde{c}_{\vartheta\vartheta} \cdot M_{\vartheta, m};$$

$$C_{\vartheta w, mn} = \tilde{c}_{\vartheta w} \cdot \tilde{h}_{W_n, \vartheta_m};$$

$$K_{\vartheta, m}^{(L)} = \int_0^1 \Theta_m(\xi) \cdot \left[\frac{\beta^2}{\chi^2} \cdot \Theta_m^{''v}(\xi) - (1 + \beta^2) \cdot \Theta_m''(\xi) \right] d\xi + \lambda_L^2 \cdot \tilde{h}_{\vartheta_m}^2 - \tilde{k}_{\vartheta\vartheta} \cdot M_{\vartheta, m};$$

$$K_{\vartheta w, mn}^{(Q)} = -\lambda_Q^2 \cdot \left\{ \begin{array}{l} \tilde{h}_{\vartheta_m} \cdot \left(\int_0^1 \Theta_m(\xi) \cdot W_n''(\xi) d\xi + \right. \\ \left. - \tilde{h}_{W_n', \vartheta_m'} \right) + \\ \left. + \tilde{h}_{W_n} \cdot \int_0^1 \Theta_m(\xi) \cdot \Theta_m''(\xi) d\xi \right\} = \lambda_Q^2 \cdot \left\{ \begin{array}{l} 2 \cdot \tilde{h}_{\vartheta_m} \cdot \tilde{h}_{W_n', \vartheta_m'} + \\ + \tilde{h}_{W_n} \cdot \tilde{h}_{\vartheta_m'^2} \end{array} \right\};$$

$$K_{\vartheta, m}^{(C)} = -\lambda_C^2 \cdot \tilde{h}_{\vartheta_m'^2} \cdot \int_0^1 \Theta_m(\xi) \cdot \Theta_m''(\xi) d\xi = \lambda_C^2 \cdot (\tilde{h}_{\vartheta_m'^2})^2;$$

$$K_{\vartheta w, mn}^{(C)} = -\lambda_C^2 \cdot \left\{ \begin{aligned} &\tilde{h}_{W_n', \vartheta_m'} \cdot \int_0^1 \Theta_m(\xi) \cdot W_n''(\xi) d\xi + \\ &+ \frac{1}{2} \cdot \tilde{h}_{W_n'^2} \cdot \int_0^1 \Theta_m(\xi) \cdot \Theta_m''(\xi) d\xi \end{aligned} \right\} = \lambda_C^2 \cdot \left\{ (\tilde{h}_{W_n', \vartheta_m'})^2 + \frac{1}{2} \cdot \tilde{h}_{W_n'^2} \cdot \tilde{h}_{\vartheta_m'^2} \right\};$$

$$\Gamma_{\vartheta, m} = \int_0^1 \Theta_m(\xi) \cdot \tilde{m}(\xi, \tau) d\xi$$

Notice that in the modal torsional equation of motion we are not able to define a second order term that is independent from the flexural component. This is an important difference with respect to the vertical counterpart and is due to the fact that rotations of the deck introduces an asymmetric response of the two main cables, but this response depend strongly on the flexural amplitude of vibration that affect the stiffness of the cables system. This property of the system will be fundamental in the following in order to study the stability of vibrations.

6.3 Vortex shedding modelling

The forcing terms Γ represent the modal counter part of external unsteady forces. For the complete aeroelastic model, they can represent any unsteady aerodynamic action such as gusts, buffeting or vortex shedding.

An accurate modelling of unsteady forces coming from the detachment of vortices from the bridge's deck is a very complex procedure.

Vortex shedding is perhaps one of the most studied phenomena of fluid mechanics, especially its interaction with circular cylinders

When a vortex is formed on one side of the immersed body, it immediately increases flow velocity on the opposite side, which results, according to Bernoulli theory, in a pressure reduction

The process of vortex shedding can only be explained if the effect of viscosity is considered. In fact, only a viscous fluid will satisfy the no-slip condition of its particles on the surface of a body immersed in the flow-. Even if viscosity is very small this condition will hold but its influence on the flow regime will be confined to a small region, which is the boundary layer along the body. Within this layer the velocity of the fluid changes from zero on the surface to the free-stream velocity of the flow.

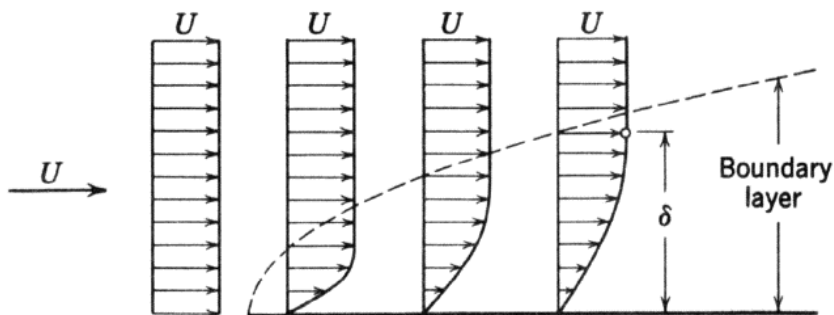


Figure 6.1_ Boundary layer on a flat plate.

While the free stream is pulling the boundary layer forward, the skin friction at the solid wall is retarding it. At surfaces with high curvature, there can also be an adverse pressure gradient adding contributions to the retarding action, which may cause the flow to be interrupted entirely and the boundary layer may detach from the wall, called separation. Notice that streamlined bodies can still experience separation if the angle of attack between the free stream and the surface is large enough.

It's clear from the physical understanding of the separation process, that viscosity and free stream velocity have an important influence and can be collected in the Reynolds number. It expresses the ratio between the inertia and the friction forces acting on the fluid.

$$Re := \frac{\rho U D}{\mu} = \frac{U D}{\nu};$$

Considering the flow past a circular cylinder, a great variety of changes in the nature of the flow occur with increasing Reynolds number.

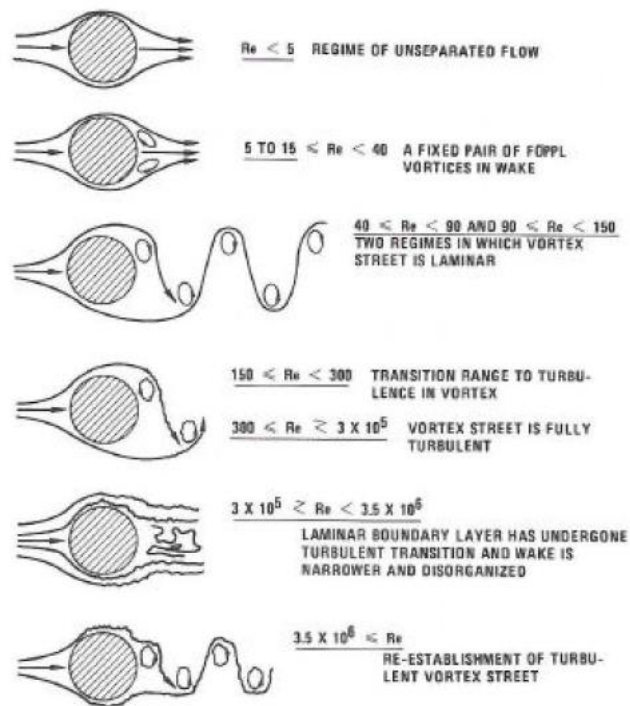


Figure 6.2_ Reynolds number effect on trailing vortex street.

At very low Reynold number, say below 0.5, the inertia effects are negligible and the flow pattern is very similar to that for laminar flow, the pressure recovery being nearly complete. This means, that the pressure drag is also negligible and effective drag on the body is entirely due to skin friction.

At increased Re, approximately between 2 and 30, separation of the boundary layer occurs at two points at the back of the cylinder. There symmetrical eddies are formed which rotate in opposite direction. They remain fixed and the flow closes behind them.

Further increase of the Reynolds number elongate the fixed vortices, which then begins to oscillate until they break away at a Re of around 90.

The breaking away occurs alternatively from one and the other side, then the eddies travel downstream. This process is intensified with further increase of Re while the shedding of vortices from alternate sides of the cylinder is regular. This leads to formation of the characteristic wake which is known as Von Karman vortex street. The eddying motion is periodic both in space and time. The pressure drag at this stage is already larger than the profile drag. Having passed a transition range where the regularity of shedding decreases, above a Re of 300 vortex shedding becomes irregular. However, there still is a predominant frequency but the amplitude appears to be random. Notice that the critical regime can be anticipated as the roughness of the body surface increases.

At very high level of Reynolds number from about $3 \cdot 10^5$ the separation point moves rearward on the cylinder, consequently the drag coefficient decreases appreciably. The flow in the wake becomes so turbulent that the vortex street pattern is no longer recognisable.

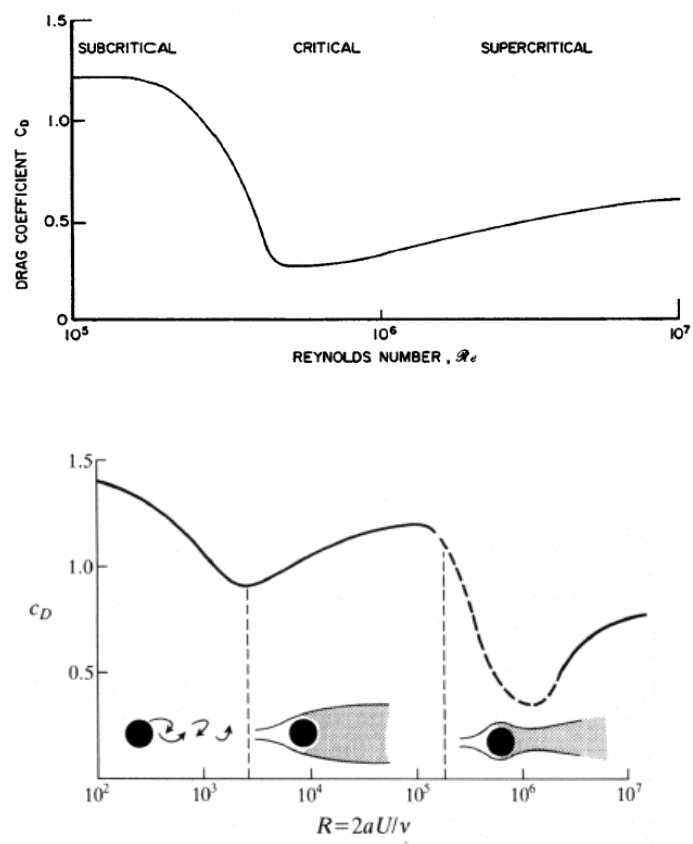


Figure 6.3_ Reynolds number effect on drag coefficient.

Hence it's clear that the process of vortex shedding and its dependence on the Reynolds number is highly complex, which makes analytical as well as numerical treatment very challenging.

Since vortex shedding process is able to exert a fluctuating force on the body, this can be very interesting when studying the body oscillations. To characterise this process, Strouhal defined a dimensionless shedding frequency, called Strouhal number.

$$St = f \cdot D/U ;$$

Where D is the generic cross flow dimension of the immersed body. For circular cylinders this formula applies to $250 < Re < 2 \cdot 10^5$. As we know air has a kinematic viscosity at 20°C is about $\nu = 1.5 \cdot 10^{-5} \text{ m}^2/\text{s}$, hence for suspension bridges taking the sectional height of the deck as reference cross flow dimension we are sure to be in that range of Reynolds number for any wind speed, being $D = 3 \div 8 \text{ m}$.

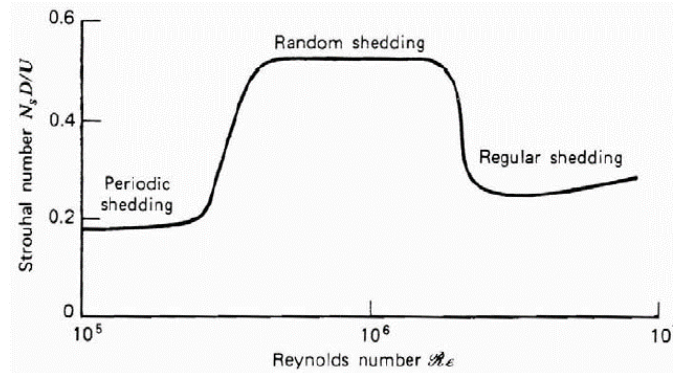


Figure 6.4_ Reynolds number effect on Strouhal number.

After Strouhal's observations, subsequent investigations found the Strouhal number to be highly dependent on the cross-sectional geometry of the body and accordingly focused on determining so called universal Strouhal numbers, which would be independent of the geometry. The most widely used is that proposed by Roshko [46].

The most important physical parameter of a two-dimensional body exhibiting vortex-induced oscillations is the size and shape of its after-body, which is the part of the cross-section downstream of the separation points. For vortex-induced or galloping type excitation the pressure loading occurs principally on the after-body surface. Accordingly, body with a very short after-body, e.g. a semi-circular cylinder with the flat face downstream, will only be weakly excited. On the contrary, the same cylinder mounted the other way round can experience considerable oscillations under the same conditions.

Deniz and Staubli [47] compare results obtained from investigations on the effect of body geometry on the vortex shedding process. They notice sudden jumps of the Strouhal number occurring at elongation ratios of approximately $B/D = 2 \div 3$ and $B/D = 4 \div 7$, which mark the limits of three different flow regimes due to reattachment of the separated flow. The first class refers to leading-edge vortex shedding, the second to impinging leading edge vortices and the third to trailing-edge vortex shedding.

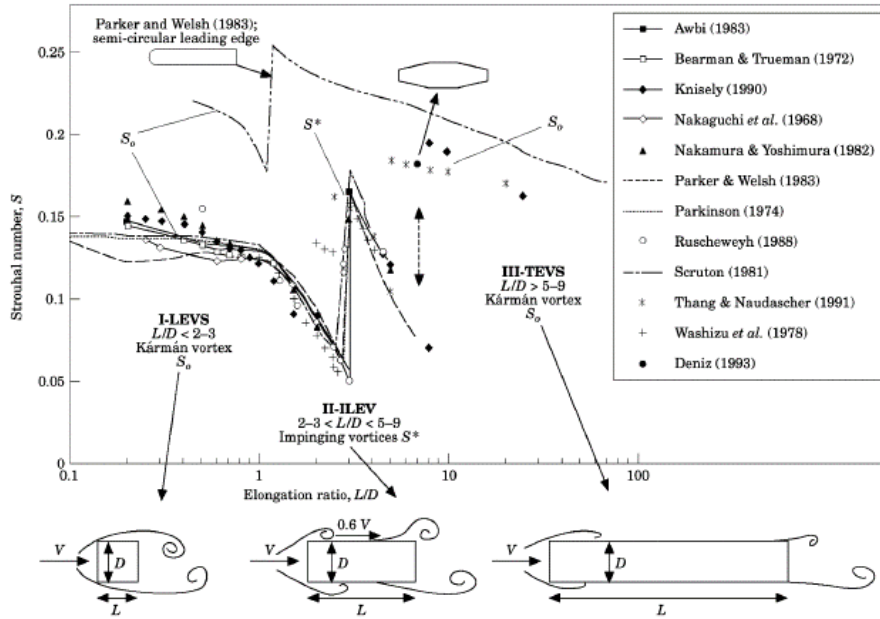


Figure 6.5_ Sectional aspect ratio effect on Strouhal number.

Hence concerning large structures, like suspension bridges, where the cross sectional aspect ratio ranges between $B/D = 4 \div 12$ [31-40], we can state that we fall in the Third class of trailing edge eddies.

Notice that also the angle of attack plays a fundamental role in the separation flow, seems to render universal Strouhal number inapplicable.

Further the curvature of the body surface is very important since it has the same effect of a non-null angle of attack. Civil engineering structures have generally bluff body sections characterised by sharp edges that are preferential separation points. Since those points are generally fixed consequently the vortex-shedding phenomenon is not actually influenced by Reynolds number.

The Strouhal number describe the process of vortex-shedding and depends on the geometry and the Reynolds number. The frequency of the shedding is also that of the alternating forces acting transversely to the flow on the body whereas the forces in flow direction have a frequency twice. Notice that the latter force component would be useless in the proposed 2-dof model of the suspension bridge since we are neglecting all drag component coming from the wind action.

$$F_L = \frac{1}{2} \cdot \rho_a \cdot B \cdot U^2 \cdot C_L \cdot \sin(\omega_{St} \cdot t) ;$$

$$\omega_{St} = 2\pi \cdot St \cdot U/D ;$$

Where we have introduced the lift coefficient being the actual transversal force associate to upward or downward motion of the immersed body. Further, notice that we chose as reference surface the upper deck face where resulting lift forces directly acts, and then normalised it to get the same quantity per unit length.

$$S_{deck} = B \cdot l \Rightarrow S_{ref} = B = 2 \cdot b ;$$

It should be noted, that this only describes the principal oscillating forces, since the time-history actually applied on the body is much more complex with a rich frequency spectrum.

If the structure is elastically mounted the periodic force exerted by the process of vortex-shedding gives rise to oscillations. These will also influence the flow pattern and a complex interaction takes place. Further if the structure is considerably deformable under the pressure forces it will not only act as a rigid body, giving rise to aeroelastic conditions.

It's obvious that considerable excitation of the body only occurs at the shedding frequencies close to the natural frequency of the body in the across-flow direction. However, it's important to note, that even in the case of resonance the amplitude always remains limited, as shown experimentally in studies of oscillating cylinders. Vortex-induced vibrations are thus a response problem opposed to Flutter being a stability problem. The aim is either to predict the frequency of the aerodynamic forces and then to design the structure for the caused oscillations or to make sure the characteristics of the structures are such that it will not be excited. In limit state terminology this type of oscillations can be considered as serviceability problem because the levels of vibrations need to be limited to ensure comfort of the users and to avoid fatigue problem in the long term.

By experimental investigations, it had soon realised that the wake behind a bluff body is altered if the body exerts an oscillation. The main finding was, that the oscillations alter the vortex pattern in that spacing between vortices in the wake changes. Subsequent investigations then studied elastically mounted bodies, mainly cylinders. An important phenomenon observed in those occurs at shedding frequencies close to resonance. Here the shedding process becomes controlled by the natural frequency of the structure even if variations in the flow velocity tend to shift it away. This is commonly referred to as lock-in phenomenon.

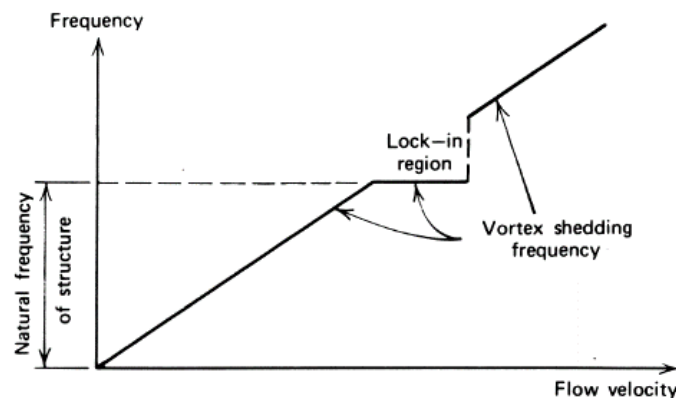


Figure 6.6_ Strouhal model and lock-in phenomenon.

While the influence of the frequency of oscillation on vortex shedding process is well investigated, the influence of the amplitude is less well known. Visualisation of the flow field around a transversally oscillating cylinder by Griffin and Ramberg [48] shows well organised shedding for amplitude of $0.5 \cdot D$ and an oscillation frequency near the natural vortex-shedding frequency. An increase in amplitude to D at the same frequency of oscillation leads to a disorganisation of the wake. This can be thought as a self-limitation of the vortex-induced excitation. Generally we can take as $0.2 \cdot D$ the reference maximum admissible amplitude of oscillation induced by vortex detaching from circular cylinders.

Another important parameter affecting the vortex-shedding phenomenon is the mass-damping ratio, which generally is well represented by the Scruton number.

$$Sc = 4\pi \cdot m \cdot \xi_{tot} / \rho_a \cdot D^2 ;$$

Notice that we need to consider both the structural and the aerodynamic damping contributions. Experimental investigations show that as the Scruton number increases the lock-in region moves towards lower flow velocities and it becomes thinner. Notice that generally it ranges between $U/U_{St} = 0.8 \div 1.5$. However, more important is its effect on the maximum amplitude of oscillation induced by vortex-shedding. In fact, is possible to limit the oscillations simply increasing Sc by means of proper damping devices, like a tuned mass damper (TMD).

Further, it influences the flow regime, in fact experimental investigations show that can be detected three main regimes. The first where vibrations are forced mainly by the random nature of vortex-shedding, the second is a transition zone where there is a considerable increase of the root mean square response and finally the third characterised by self-sustained vibrations due to lock-in phenomenon.

By last, we want to mention the fact that the turbulence intensity of the flow strongly influence the oscillations of the body. In fact, mainly in aeroelastic phenomena turbulence is able to reduce very much the correlation of wind action between different points of the structure, which vibrations consequently decreases in amplitude.

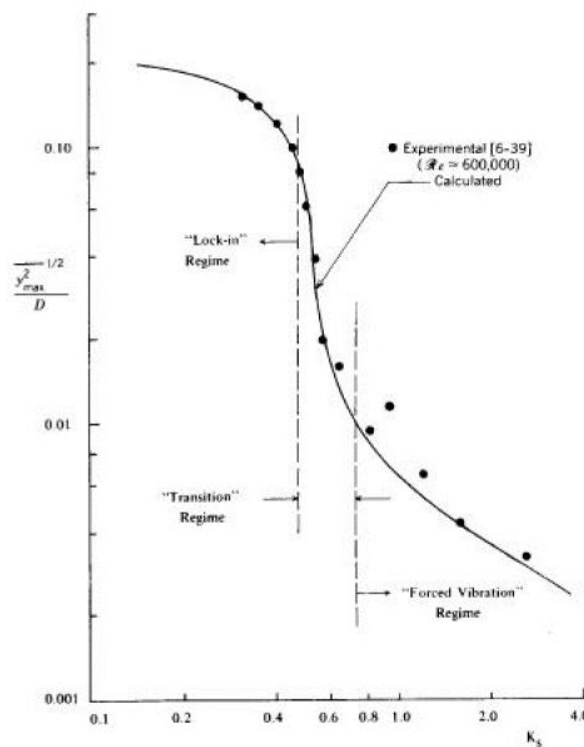


Figure 6.7_ Scruton number effect on response of cylinder.

In order to define completely the transversal lift force generated by the vortex-shedding phenomenon we give some numerical results [49] for generic bridge cross sections. Notice that an average value of the Strouhal number for circular cylinder is around 0.18.






Steady state load coefficients and flow field at time $tU/B = 10$	C_D	C_L^{rms}	St
 G1	0.08	0.07	0.17
 G2	0.08	0.08	0.17
 G3	0.10	0.08	0.10
 G4	0.08	0.12	0.17
 G5	0.27	0.33	0.11

Figure 6.8_ Drag, Lift and Strouhal parameters for different cross sections.

6.4 Stability analysis of the complete aeroelastic model

Now we are ready to define the unsteady forcing terms comparing in the right hand-side of the modal equations of motion of the complete aeroelastic model for the suspension bridge.

Before proceeding let's recall the fact that concerning suspension bridge's deck, thanks to the high cross sectional aspect ratio B/D the eddies detachment phenomenon falls in the third class, that of trailing-edge vortex shedding. Hence, the fact that the periodic resultant forces arising are not applied in the centre of stiffness of the deck section, means that we can reduce them to a vertical force and a torque. Consequently, vortex-shedding will perturb the structural systems both with a flexural and a torsional component.

But due to the fact that the structural model is not linear and then the centre of stiffness is a priori unknown we need to refer to the centre of mass that thanks to the symmetry of the section is well known.

$$\Gamma_{w,n} = \int_0^1 W_n(\xi) \cdot \tilde{q}(\xi, \tau) d\xi = \int_0^1 W_n(\xi) \cdot F_L \cdot l^2 / 2Hf d\xi = \Gamma_0 \cdot \tilde{h}_{W_n} \cdot \sin(\tilde{\omega}_{St} \cdot \tau) ;$$

$$\Gamma_{\vartheta,m} = \int_0^1 \Theta_m(\xi) \cdot \tilde{m}(\xi, \tau) d\xi = \int_0^1 \Theta_m(\xi) \cdot F_L b \cdot l^2 / 2Hfb d\xi = \Gamma_0 \cdot \tilde{h}_{\Theta_m} \cdot \sin(\tilde{\omega}_{St} \cdot \tau) ;$$

Where the forcing term can be written in function of the dimensionless wind speed.

$$\Gamma_0 = \frac{1}{2} \cdot \rho_a \cdot B \cdot U^2 \cdot C_L \cdot l^2 / 2Hf = \tilde{B} \cdot \tilde{c}_L \cdot \tilde{J}_t \cdot \tilde{\Omega}_{\vartheta,m}^2 \cdot \tilde{u}^2 ;$$

Once again we need to introduce few new parameters easily available from literature [31-40], such as the deck sectional aspect ratio, the dimensionless deck's height and the lift coefficient normalised with respect to the flat plate condition.

$$\tilde{\alpha} = B/D = 2b/D = 4 \div 12 ;$$

$$\tilde{B} = B/f = 0.17 \div 0.51 ;$$

$$\tilde{c}_L = C_L(\theta_d)/2\pi ;$$

In order to fix these values we will take the average value for $\tilde{\alpha} \cong 7$ and $\tilde{B} \cong 0.32$, whilst since up to now we dealt with flat plate limit condition let's assume for sake of simplicity $\tilde{c}_L = 1$. Notice that the actual lift coefficient depends upon the dimensional deck torsional configuration only since we assume the wind blowing aligned with the chord of the deck section at rest.

Furthermore, we need to define the dimensionless counterpart of the Strouhal circular frequency and critical speed.

$$\tilde{\omega}_{St} = \omega_{St} \cdot l \sqrt{\frac{(m_d+2m_c)}{2H}} = 2\pi \cdot St \cdot U/D \cdot l \sqrt{\frac{(m_d+2m_c)}{2H}} = \pi \cdot St \cdot (\tilde{\alpha}/\sqrt{\tilde{m}_a}) \cdot \sqrt{\tilde{J}_t} \cdot \tilde{\Omega}_{\vartheta,m} \cdot \tilde{u} ;$$

$$\tilde{\omega}_{St} = \tilde{\omega}_w \Leftrightarrow \tilde{u}_{St} = \tilde{\omega}_w / (\pi \cdot St \cdot (\tilde{\alpha}/\sqrt{\tilde{m}_a}) \cdot \sqrt{\tilde{J}_t} \cdot \tilde{\Omega}_{\vartheta,m}) ;$$

Hence we need to define a representative value for the Strouhal number taking $St \cong 0.1$, according to the values reported in the previous figure for different sectional shape.

Notice that the most important parameter is the deck sectional aspect ratio; in fact, it can vary in a large range and then it can affect strongly the results.

Before proceeding, we want to stress the fact that in order to model the self-limiting behaviour of vortex induced vibrations would be necessary to slightly modify the simple formula proposed for vortex-shedding forcing. What is generally done is to introduce a damping term dependent on the vibration itself, like a Van der Pol oscillator [30].

$$F_L = \frac{1}{2} \cdot \rho_a \cdot U^2 \cdot B \cdot \left\{ \tilde{k} \cdot H_0(\tilde{k})/U \cdot \frac{d\tilde{w}_d}{d\tau} + C_L \cdot \sin(\omega_{St} \cdot t) \right\} ;$$

Where $H_0(\tilde{k})$ is the Flutter derivative, function of the reduced frequency, associate to the direct flexural damping. Since in the aeroelastic model we have already taken in account of it in the flutter formulation, we will not consider it twice.

The goal now is to study the stability of the suspension bridge when it undergoes to dominant flexural motion. Hence we will proceed following the procedure used in the work by Herrmann and Hauger [29]

$$z_n(t) < \varepsilon \Rightarrow z_n^2(t) ; z_n^3(t) \cong 0 ;$$

$$\gamma_m(t) \cong 0 \Rightarrow \tilde{c}_L = C_L(\theta_d = 0)/2\pi ;$$

Notice that though dominant, flexural vibrations are anyway small, consequently non-linear terms are negligible and we can study the response of a single degree of freedom linear and damped oscillator under the action of external sinusoidal forcing. Whilst the fact that torsional oscillations are negligible allows us to take the lift coefficient corresponding to a zero angle of attack, that for the assumption of aligned wind flow, means null deck torsion.

$$M_{w,n} \cdot \ddot{z}_n + C_{w,n} \cdot \dot{z}_n + K_{w,n}^{(L)} \cdot z_n = \Gamma_0 \cdot \tilde{h}_{w_n} \cdot \sin(\tilde{\omega}_{St} \cdot \tau) ;$$

First, let's study the homogeneous which solution is well known.

$$z_{n,o} = C \cdot \exp(\hat{\alpha}_{w,n} \cdot \tau) \cdot \cos(\hat{\omega}_{w,n} \cdot \tau + \varphi_{w,n}) ;$$

$$\hat{\alpha}_{w,n} = -\tilde{c}_{ww}/2 ;$$

$$\hat{\omega}_{w,n} = \sqrt{\tilde{\omega}_{w,n}^2 - \hat{\alpha}_{w,n}^2} ;$$

Where the constant amplitude and the phase lag can be define from initial conditions. Since we are looking for unstable conditions we can neglect the homogeneous term since it will always be damped down by passing of time. This is not true just if the wind speed is already so high that the Flutter onset has been already reached, and hence negative damping grant self-sustained oscillations. Since we know a priori that this is an unstable condition we will not consider it further.

Hence the only term that will be taken in account is the particular integral, which can be determined simply passing to the complex domain taking in account also for a fictitious cosine forcing.

Exploiting $K_{w,n}^{(L)} = \tilde{\Omega}_{w,n}^2 \cdot M_{w,n}$ we get.

$$\left\{ \begin{array}{l} \left(\ddot{z}_{n,p} + \tilde{c}_{ww} \cdot \dot{z}_{n,p} + \tilde{\Omega}_{w,n}^2 \cdot z_{n,p} = \Gamma_0/M_{w,n} \cdot \tilde{h}_{w_n} \cdot \sin(\tilde{\omega}_{St} \cdot \tau) \right) \cdot i + \\ \left(\ddot{s}_{n,p} + \tilde{c}_{ww} \cdot \dot{s}_{n,p} + \tilde{\Omega}_{w,n}^2 \cdot s_{n,p} = \Gamma_0/M_{w,n} \cdot \tilde{h}_{w_n} \cdot \cos(\tilde{\omega}_{St} \cdot \tau) \right) = \\ \left(\dot{y}_{n,p} + \tilde{c}_{ww} \cdot \dot{y}_{n,p} + \tilde{\Omega}_{w,n}^2 \cdot y_{n,p} = \Gamma_0/M_{w,n} \cdot \tilde{h}_{w_n} \cdot \exp(i \cdot \tilde{\omega}_{St} \cdot \tau) \right) \end{array} \right. ;$$

Hence assume the particular integral in the following form.

$$y_{n,p} = \Gamma_0/M_{w,n} \cdot \tilde{h}_{w_n} \cdot H(\delta) \cdot \exp(i \cdot \tilde{\omega}_{St} \cdot \tau) ;$$

$$\delta = \tilde{\omega}_{St}/\tilde{\Omega}_{w,n} ;$$

Substituting we get the so-called complex dynamic amplification factor.

$$H(\delta) = \left\{ \tilde{\Omega}_{w,n}^2 \cdot (1 - \delta^2 + i \cdot (\tilde{c}_{ww}/\tilde{\Omega}_{w,n}) \cdot \delta) \right\}^{-1} = |H(\delta)| \cdot \exp(-i \cdot \varphi) ;$$

Since the direct flexural damping is a complex parameter because of Theodorsen function dependence, we need to split it into its real and imaginary component in order to define the modulus and the phase lag of $H(\delta)$.

$$|H(\delta)| = \left\{ \tilde{\Omega}_{w,n}^2 \cdot \sqrt{(1 - \delta^2 - (\tilde{c}_{ww}^I / \tilde{\Omega}_{w,n}) \cdot \delta)^2 + ((\tilde{c}_{ww}^R / \tilde{\Omega}_{w,n}) \cdot \delta)^2} \right\}^{-1};$$

$$tg(\varphi) = (\tilde{c}_{ww}^R / \tilde{\Omega}_{w,n}) \cdot \delta / (1 - \delta^2 - (\tilde{c}_{ww}^I / \tilde{\Omega}_{w,n}) \cdot \delta);$$

Notice that thanks to damping the oscillation amplitudes are finite also in correspondence of linear primary resonance, while in same conditions the phase lag is exactly equal to $\pi/2$.

But the most important thing is that actually this formulation will not take in account the wind effect on the primary linear resonance since the dynamic amplification factor depends upon $\tilde{\Omega}_{w,n}$.

Then in order to consider just the actual external sinusoidal forcing we need to take just the imaginary part of $y_{n,p}$.

$$z_{n,p} = Im(y_{n,p}) = z_{n,0} \cdot \sin(\tilde{\omega}_{St} \cdot \tau - \varphi);$$

$$z_{n,0} = \Gamma_0 \cdot \tilde{h}_{W_n} \cdot |H(\delta)| / M_{w,n};$$

Since vortex-shedding is a self-limited phenomenon in the following numerical analysis we will assume as upper bound for $z_{n,0} = 0.2 \cdot D/f = 0.2 \cdot \tilde{d} \cong 0.009$.

Having defined the perturbation in terms of amplitudes we can use it to perturb the complete system, assuming it small enough but not vanishing in order to neglect just the non-linear perturbed terms.

$$z_n(t) = z_{n,0} \cdot \sin(\tilde{\omega}_{St} \cdot \tau - \varphi) + z_{p,n}(t) \quad \text{with } z_{p,n}(t) < \varepsilon;$$

$$\gamma_m(t) = \gamma_{p,m}(t) \quad \text{with } \gamma_{p,m}(t) < \varepsilon;$$

Substituting in the complete non-linear aeroelastic system of equations of motion we get the following Variational System of equations.

$$M_{w,n} \cdot \ddot{z}_{p,n} + C_{w,n} \cdot \dot{z}_{p,n} + C_{w\vartheta,nn} \cdot \dot{\gamma}_{p,m} + K_{w,n}^{(L)} \cdot z_{p,n} + K_{w\vartheta,nn}^{(L)} \cdot \gamma_{p,m} = 0;$$

$$J_{\vartheta,m} \cdot \ddot{\gamma}_{p,m} + C_{\vartheta,m} \cdot \dot{\gamma}_{p,m} + C_{\vartheta w,mm} \cdot \dot{z}_{p,n} + \left\{ K_{\vartheta,m}^{(L)} + K_{\vartheta w,mm}^{(Q)} \cdot z_{n,0} \cdot \sin(\tilde{\omega}_{St} \cdot \tau - \varphi) \right\} \cdot \gamma_{p,m} = 0;$$

Notice that the fact that the second order term of torsional motion is dependent on both linear motion while the flexural one has the two quadratic contributions in two independent terms, make possible that a small but not vanishing vertical perturbation influences the torsional response. In fact any residual of the periodic perturbation vanishes in the flexural equation of motion since its contributions has been already satisfied. This kind of phenomena are known as Parametric excitation.

We have stressed many times the fact that being a self-limiting phenomenon, vortex shedding is able to induce just small flexural perturbations. However, due to the fact that their effects on torsional vibrations is amplified by the quadratic coupled modal stiffness $K_{\vartheta w,mm}^{(Q)}$ it will be of fundamental importance to understand its influence on the system response.

Consequently, we can say that in the design process will be useful whether is possible to tune the geometrical and mechanical properties of the suspension bridge in order to minimise that cross stiffness.

Notice that the Variational Equations contains both the Aerodynamic ($z_{n,0} = 0$) and the Parametric ($U = 0$). Hence though it accounts for just the fundamental parameter associated to parametric excitation, being a simplification of the original complete non-linear coupled aeroelastic model, it's able to catch both phenomena.

Hence we obtain a system of two linear coupled second order differential equations with periodic coefficients that recall a generalised Hill's equation and that can be solved exploiting the Floquet Theory previously treated.

In order to proceed with numerical investigations we need to reduce the Hill's system to the first order by a simple change of variables. Thence, let's write it in matrix form.

$$M \cdot \ddot{q} + C \cdot \dot{q} + K \cdot q = 0 ;$$

$$q = \begin{Bmatrix} Z_{P,n} \\ Y_{P,m} \end{Bmatrix} ;$$

$$M = \begin{Bmatrix} M_{w,n} & 0 \\ 0 & J_{\vartheta,m} \end{Bmatrix} ;$$

$$D = \begin{Bmatrix} C_{w,n} & C_{w\vartheta, nm} \\ C_{\vartheta w, mn} & C_{\vartheta, m} \end{Bmatrix} ;$$

$$K = \begin{Bmatrix} K_{w,n}^{(L)} & K_{w\vartheta, nm}^{(L)} \\ 0 & K_{\vartheta, m}^{(L)} + K_{\vartheta w, mn}^{(Q)} \cdot z_{n,0} \cdot \sin(\tilde{\omega}_{St} \cdot \tau - \varphi) \end{Bmatrix} ;$$

Then.

$$\ddot{q} = -M^{-1} \cdot D \cdot \dot{q} - M^{-1} \cdot K \cdot q = 0$$

Assuming.

$$x = \begin{Bmatrix} x_1 \\ x_2 \end{Bmatrix} \text{ where } x_1 = q \text{ and } x_2 = \dot{x}_1 ;$$

Thence we get.

$$\dot{x} = J \cdot x ;$$

Where we have introduced the Jacobian matrix, that from the previous treatment we know it is periodic of the same period of the periodic term, hence $T = 2\pi$.

$$J = \begin{Bmatrix} 0 & I \\ -M^{-1} \cdot K & -M^{-1} \cdot D \end{Bmatrix} ;$$

The numerical analysis requires some simple steps.

First, we need to define the Monodromy matrix simply performing a numerical integration of the equations of motion over the period and take the value assumed by the oscillation amplitude and velocity in correspondence of $t = T$. Since we need to assume proper initial conditions for both the velocity and the amplitude of both flexural and torsional oscillations we will assume unitary one by one so that the fundamental matrix at initial instant will be the unitary matrix $X(0) = I$ and we can exploit $C = X(T)$. In this way the first column of the Monodromy matrix will be filled as follows.

$$C = X(T) = \{[x(T)]_{z=1} \quad [x(T)]_{\gamma=1} \quad [x(T)]_{\dot{z}=1} \quad [x(T)]_{\dot{\gamma}=1}\};$$

Then we need just to compute the eigenvalues of the Monodromy matrix in order to get the characteristic multipliers of the problem.

Finally, we get stable conditions as long as the maximum absolute value of the characteristic roots is lower than one. Otherwise, at least one of the degree of freedom will diverge in time.

In the following, we will comment some numerical result obtained in the form of stability maps. They allows us to distinguish in an easy and synthetic way stable from unstable regions. Each condition will be fully characterised by the circular frequency of vortex shedding Ω_{VS} and by a wind speed level. Notice that a priori these two will be completely separate in order to be able to catch unstable regions independently from any model able to link the two previous parameters. Only secondly we will introduce the Strouhal linear model enriched by the lock-in effect, in order to able to say under which conditions vortex shedding phenomenon is able to explain unstable conditions.

Two model will be analyse.

The first is called Structural one, since it accounts for geometrical and mechanical properties of the suspension bridge only. This preliminary analysis is useful in order to check if the non-linearities of the dynamic system are enough to find out resonance conditions different from the primary linear one. Hence in this model the term playing a fundamental role is $K_{\vartheta w, mn}^{(Q)}$ since it's the only one able to couple the equations of motion. In fact all damping and stiffening terms coming from aeroelastic effects will not be taken in account.

On the other hand, we will refer to second one as to the Aeroelastic model, where both structural and aerodynamic parameters will be of relevance. The task of this model is to find out if and under which conditions, wind effect on suspension bridges, coupled with parametric resonance, is able to lead the structure to unstable conditions. Results will be of relevance only if the structure reaches those critical conditions in correspondence of a wind speed lower than Flutter one.

Notice that to be rigorous we can deal with only external resonances since the system is driven by the external action of vortex shedding. However, since we want to study the stability of the perturbed system this external forcing does not appear directly in the equations of motion, but it introduces in the linear system a cross coupling periodic term linked to flexural vibrations. Hence regarding the perturbed system we are dealing with a structural model characterised by periodic coefficients, and the fact that periodicity is driven by an external excitation is of secondary importance. What really matters is to find out the amplitudes and the frequencies of vertical motion able to lead the system to unstable conditions.

Consequently, we can talk indifferently about external or internal resonance since simply the first refers to the cause and the second to the effects of wind actions on the structure.

In both the model we will analyse different resonance conditions besides the linear primary one, such as subharmonic and superharmonic of order two for both the flexural and the torsional vibrations, and further combinational of sum and difference type.

$$\text{primary linear} : \Omega_{VS} = \omega_i ;$$

$$\text{subharmonic} : \Omega_{VS} = 2 \cdot \omega_i ;$$

$$\text{superharmonic} : \Omega_{VS} = \omega_i / 2 ;$$

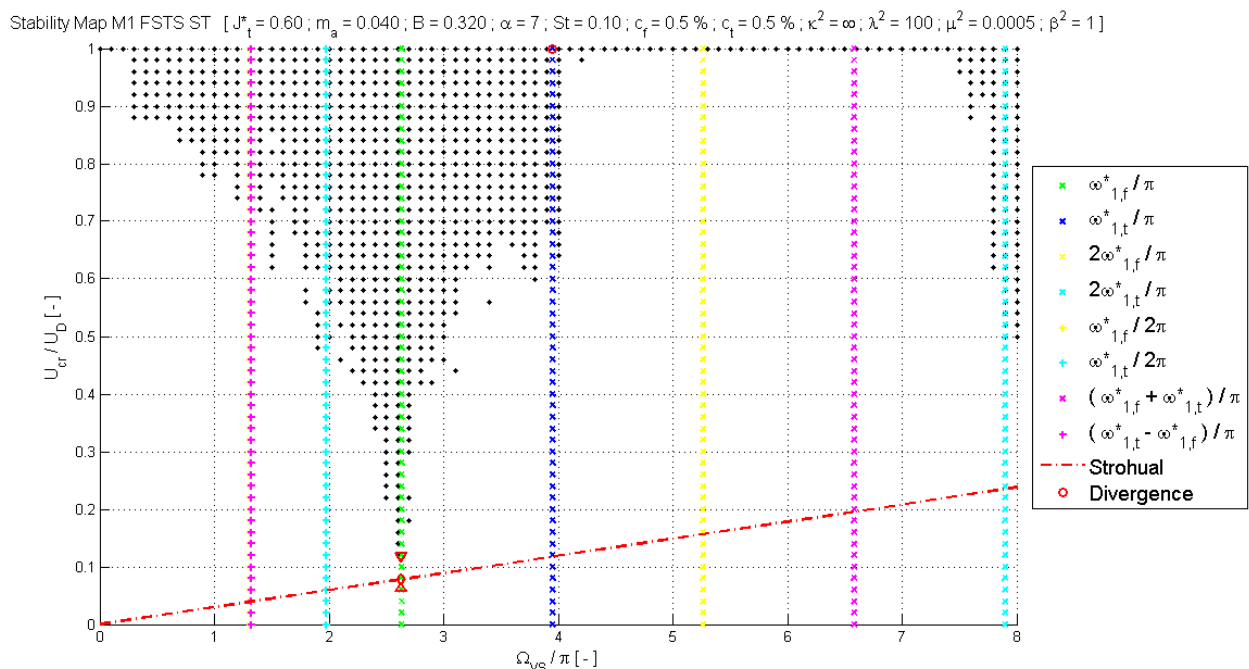
$$\text{combiational sum} : \Omega_{VS} = \omega_w + \omega_g ;$$

$$\text{combiational difference} : \Omega_{VS} = |\omega_w - \omega_g| ;$$

We choose to consider just the second order type of internal resonance since we want to catch just the most important and critical conditions near the classical primary linear resonance.

We know that all the other kind of resonances are feasible only in non-linear systems, but we have stressed many times that the perturbed model is linear. This is true but non-linearities are hidden inside the periodic coupling term where flexural vibrations appear.

Let's analyse some numerical results starting from the Structural model.



As we can see, the Structural model is able to catch the main resonance of the system. In fact, besides the primary linear flexural one the system undergoes in resonance also as the vertical motion frequency is near the torsional one. This kind of phenomenon is called internal resonance of kind 1:1. Further is able to catch also the so called 2:1 internal resonance as the flexural motion is characterised by a frequency that doubles the torsional one. On the other hand, the effect of other kind of resonances are less evident.

Notice that the presence of internal resonances reduces drastically the critical wind speed level that in the case of the simple structural model alone is represented by the torsional divergence speed.

But, it's evident that in this case the vortex-shedding phenomenon seems not be able to explain any of the previous unstable conditions. In fact the linear model proposed by Strouhal never reaches the critical conditions in terms of frequencies and amplitudes (wind speed) that lead the system response to diverge in time.

As already mentioned in the definition of the dimensionless Strouhal circular frequency plays a relevant role the deck sectional aspect ratio. In fact it strongly modifies the slope of the Strouhal curve, that consequently under certain geometrical conditions can enter unstable regions.

This means that in the design process is fundamental to take in consideration this fact, since the choice of the sectional dimensions of the deck will be of fundamental importance for the dynamic stability of the overall structure.

As we can see reducing the aspect ratio down to $\tilde{\alpha} = 3$ the vortex shedding phenomenon is able to explain the main resonant unstable conditions that are the flexural primary linear one and the second order subharmonic internal torsional one.

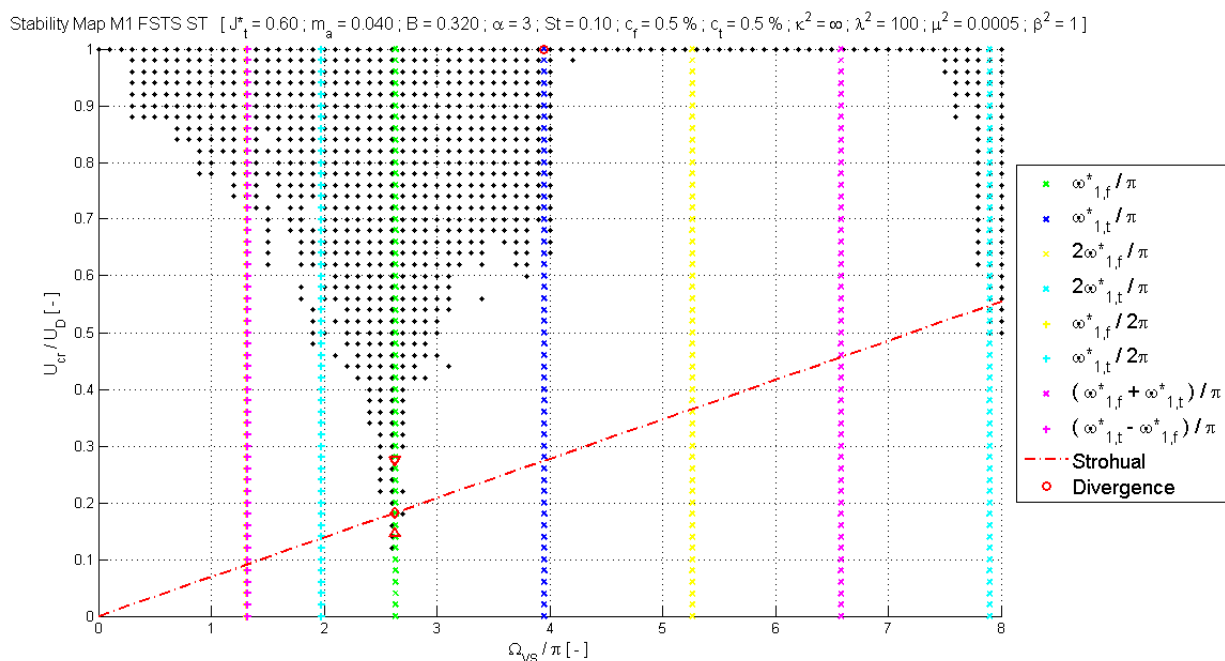


Figure 6.10_ Stability map for the Structural Model with bluff deck section.

Hence, we can conclude that very bluff deck sections can be useful to increase torsional and flexural stiffness of the suspension bridge but lead the structure to be more susceptible to instabilities due to vortex shedding.

Let's now analyse the Aeroelastic model accounting for the fluid-structure interaction effects on the dynamic stability if the system.

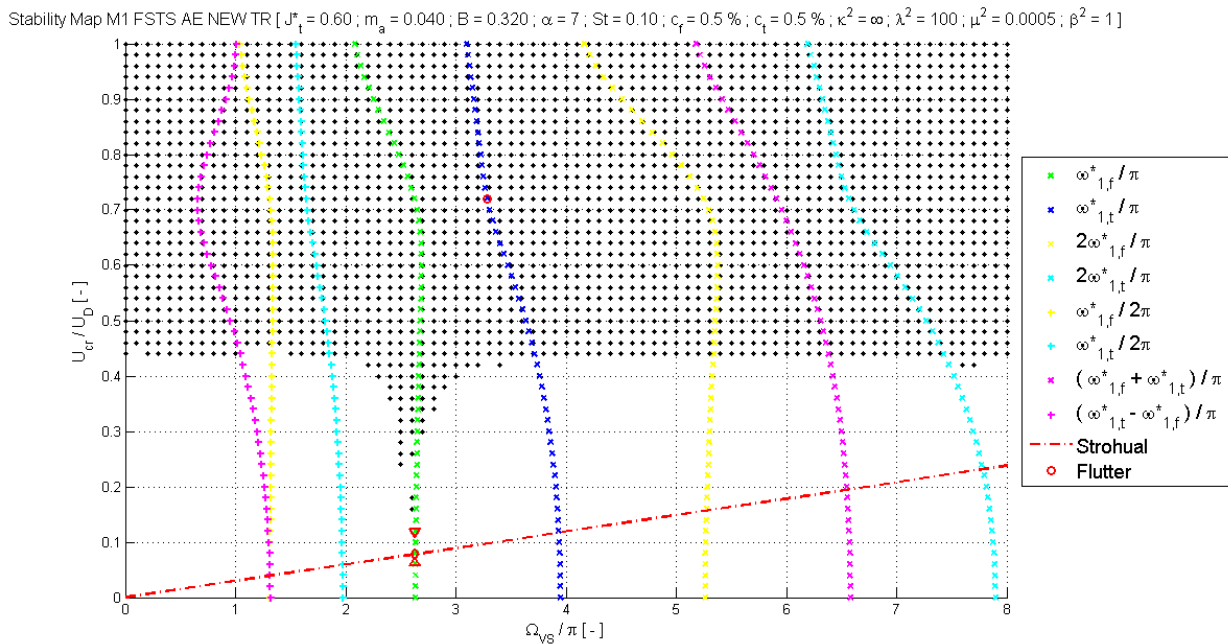


Figure 6.11_ Stability map for the Aeroelastic Model with slender deck section.

As already mentioned in the Flutter analysis, the fluid-structure interaction makes the frequencies being dependent on the actual wind speed level, consequently we see curved lines representing the main internal or external resonance conditions.

Further and more important is that the wind-structure interaction enlarges unstable regions. This valid also for wind speed very much lower than the one required to reach the critical Flutter condition. Hence, the interaction between Aeroelasticity and Parametric resonance can lead to unexpected unstable conditions.

Notice that though the unstable region is more merged than in the pure structural model, we still recognise the main resonances, which are the linear primary and the 2:1 internal ones. The presence of wind not only obscures the stability maps but also it reduces and increases respectively the critical wind speed required to reach the torsional 2:1 internal and the flexural 1:1 external resonances. In fact as we can see the Flutter instability is of torsional kind.

Another interesting feature is that near the curve of combinational resonance of difference type we get always a larger stable region. In fact as reported also in different articles [41], the so called anti-parametric resonance with respect to the parametric and additive parametric resonances has a stabilising effect on the dynamic response of the system. This is due primary to the fact that this phenomenon is able to increase significantly the damping of the system. This particular property can be exploit trying to find the optimal geometrical and mechanical parameters able to maximise this intrinsic damping effect. The physical explanation of this phenomenon hides behind the fact that as parametric excitation occur there is energy transfer between the two main interacting modes. Consequently, as higher order modes are characterised by higher damping ratios, then the system is able to dissipate faster that energy with respect to the system without Parametric excitation. Notice that we are dealing with an energetic exchange; hence, being the energy transfer not unidirectional we should observe modulated vibrations.

As we can see as long as the deck is slender enough vortex shedding is not sufficient to bring the structure to unstable conditions, while as the deck sectional aspect ratio reduces, the dynamic response diverges as the wind speed reaches levels that are much lower than those expected by the only Flutter analysis.

Stability Map M1 FSTS AE NEW TR [$J_1^* = 0.60$; $m_a = 0.040$; $B = 0.320$; $\alpha = 3$; $St = 0.10$; $c_r = 0.5\%$; $c_l = 0.5\%$; $\kappa^2 = \infty$; $\lambda^2 = 100$; $\mu^2 = 0.0005$; $\beta^2 = 1$]

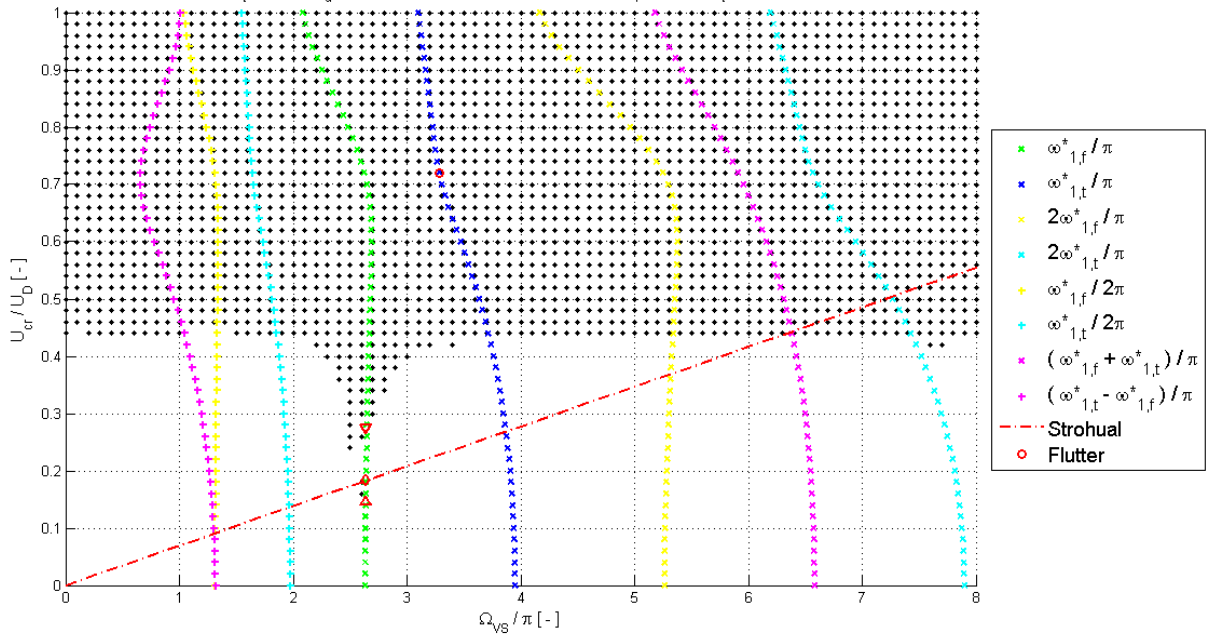


Figure 6.12_ Stability map for the Aeroelastic Model with bluff deck section.

Now we are able to transform the previous information in terms of flexural antinodal displacements by means the singles degree of freedom oscillator formulation. In fact once we define the wind speed and the shedding frequency we know respectively the forcing term T_0 and the complex dynamic amplification factor $H(\delta)$.

Stability Map M1 FSTS ST [$J_1^* = 0.60$; $m_a = 0.040$; $B = 0.320$; $\alpha = 7$; $St = 0.10$; $c_r = 0.5\%$; $c_l = 0.5\%$; $\kappa^2 = \infty$; $\lambda^2 = 100$; $\mu^2 = 0.0005$; $\beta^2 = 1$]

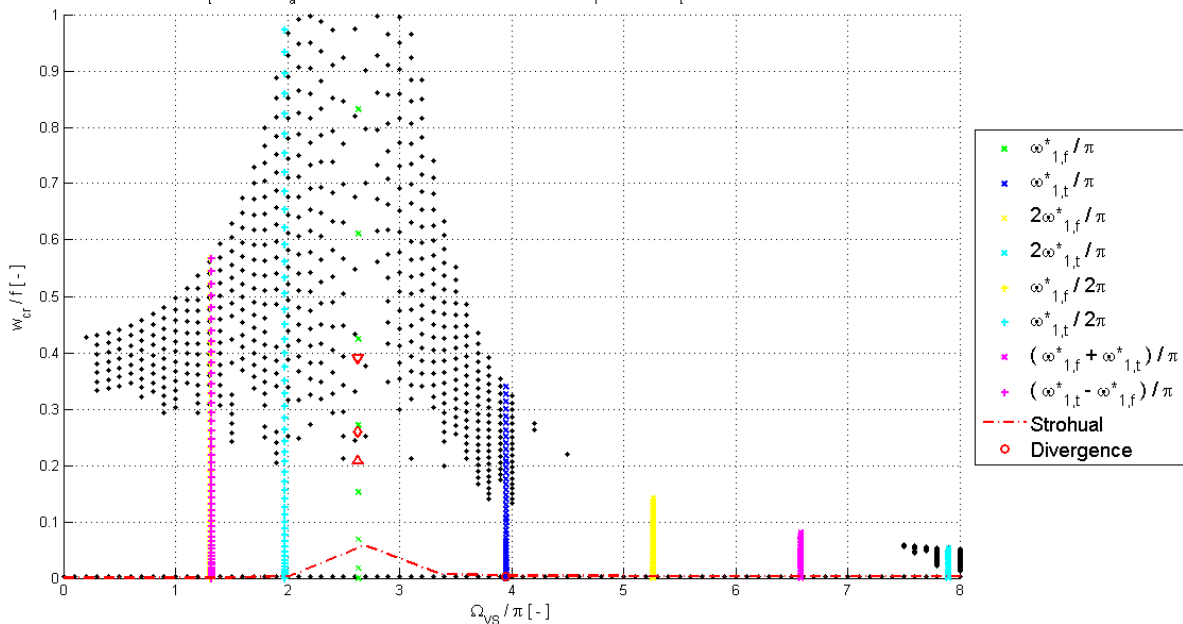


Figure 6.13_ Unstable antinodal displacements for the Structural Model with slender deck section.

Stability Map M1 FSTS AE NEW TR [$J_1^* = 0.60$; $m_a = 0.040$; $B = 0.320$; $\alpha = 7$; $St = 0.10$; $c_f = 0.5\%$; $c_t = 0.5\%$; $\kappa^2 = \infty$; $\lambda^2 = 100$; $\mu^2 = 0.0005$; $\beta^2 = 1$]

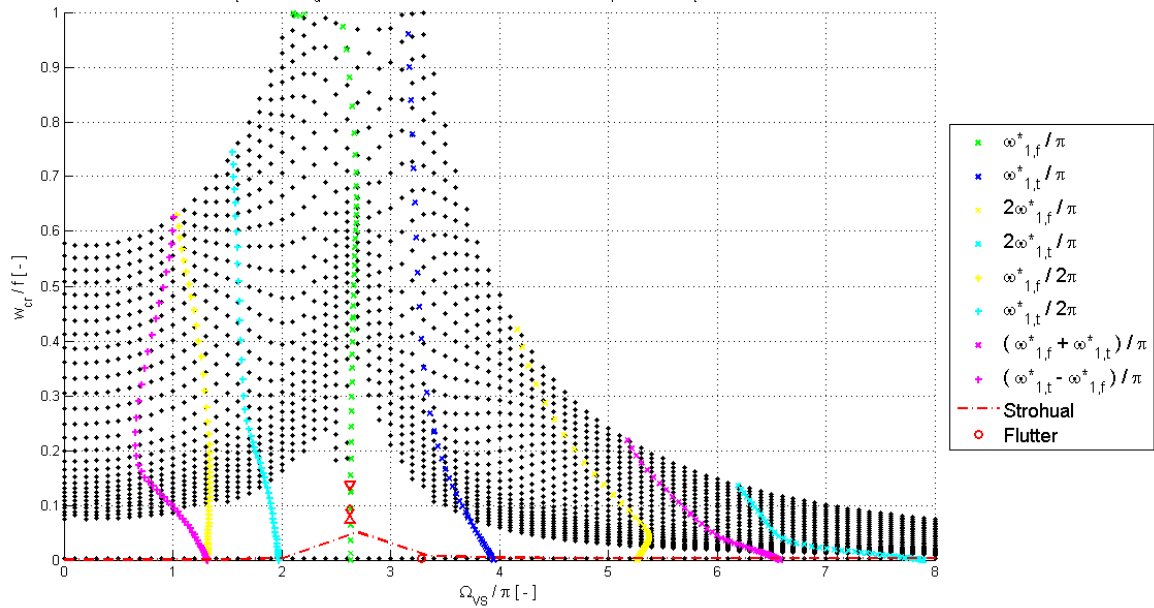


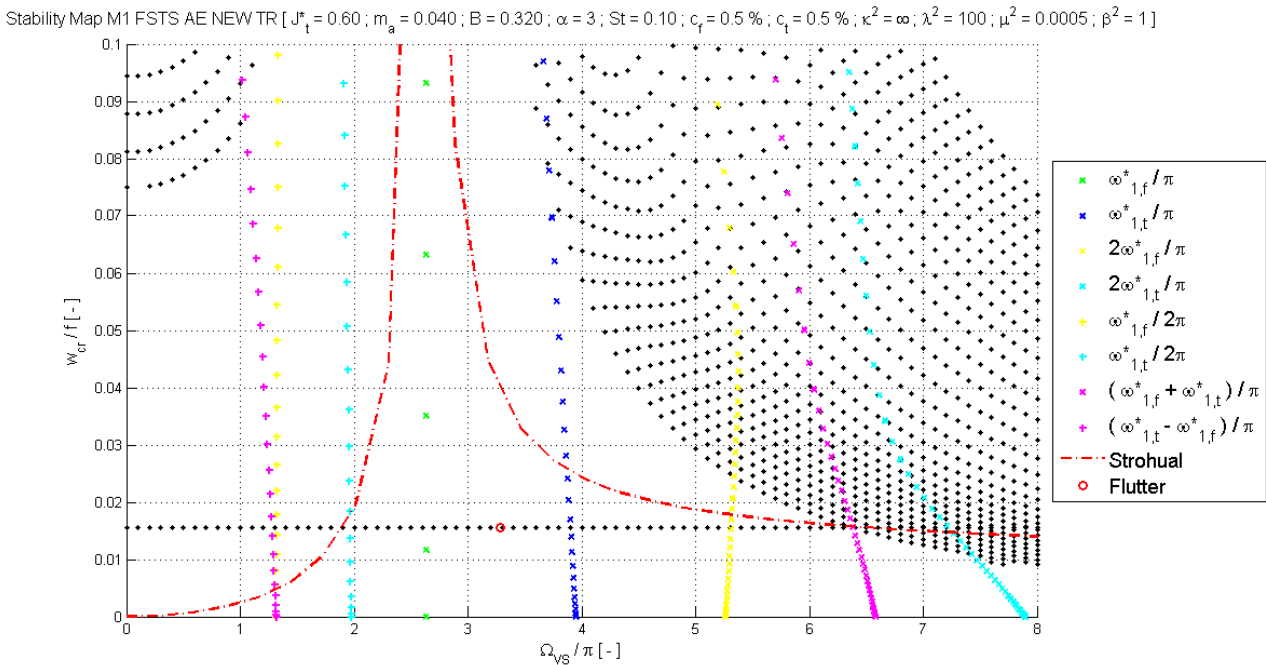
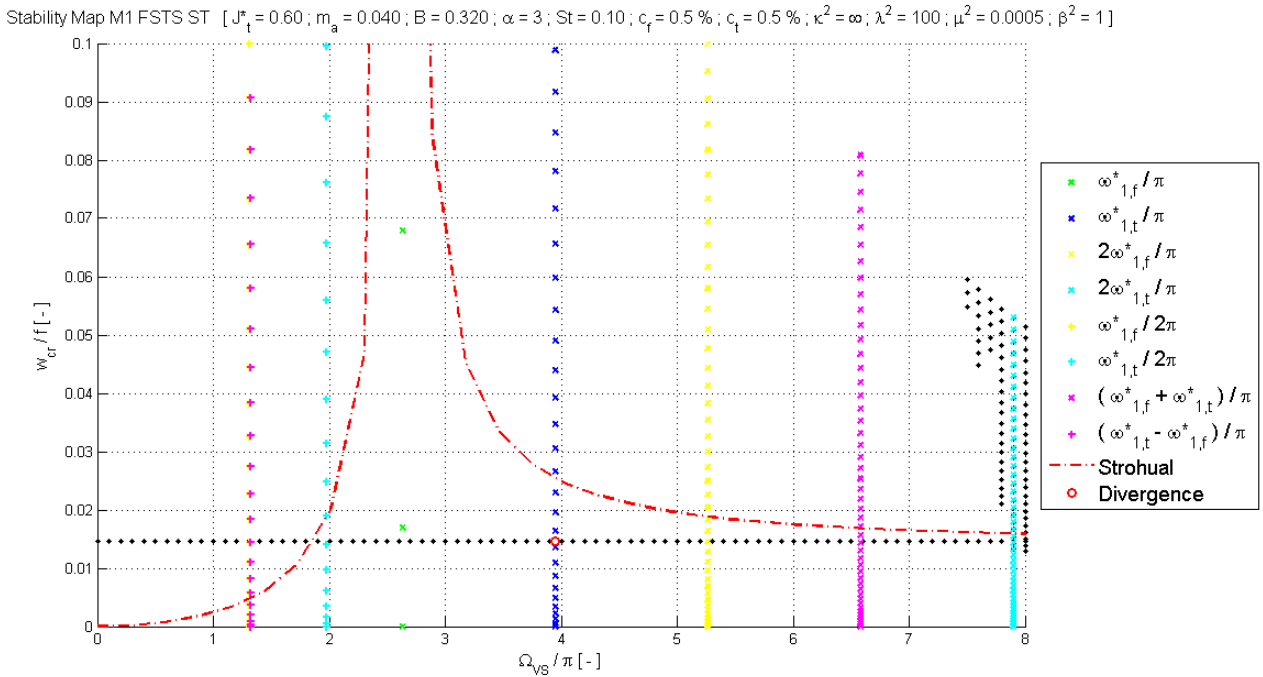
Figure 6.14_ Unstable antinodal displacements for the Aeroelastic Model with slender deck section.

We recognise immediately the usual shape performed by any single dof forced oscillator. We must remind that it's also damped only in the latter figure, where we reach limited oscillations in the case of primary linear resonance. In fact, it's evident that the amplitudes reached in the lock-in interval are much higher when neglecting aerodynamic damping.

Anyway, the total damping is never high enough to limit flexural oscillations to be lower than the cable's initial sag.

On the contrary according to Strouhal conditions we should reach amplitudes that are always lower than the more conventional 10% with respect f .

Is more interesting to analyse the results associate to bluff decks where unstable conditions are feasible, focusing on amplitudes up to $0.1 \cdot f$.



First notice that regarding amplitudes we have a lower bound representing the flexural motion in correspondence of torsional Divergence and Flutter respectively for the Structural and the Aeroelastic model.

What is important to underline is that according to Strohual linear law, only in correspondence of 2:1 internal resonances unstable conditions are feasible for both the models. In fact, all the other situations require too much high antinodal displacements that are difficult to observe.

Secondly, it's evident that the critical amplitudes just obtained are just slightly different with respect to the Divergence or Flutter ones. This simply remind us that dealing with parametric excitation the amplitudes of the forcing mode are fundamental but not sufficient to exploit unstable conditions. In fact, a proper frequency of oscillation is required to the flexural motion in order to make the system divergent in time.

Notice that the critical amplitudes obtained are small enough to fulfil approximately the empirical limit threshold $z_{max} = 0.2 \cdot D/f \cong 0.009$ reminding us that vortex-shedding is a self-limiting phenomenon.

Further we can observe that for the actual example analyse the amplitudes are low enough that hangers remains taut. In fact the antinodal displacement induced by vortex-shedding does not overcome the one required for slackening initiation of about $0.105 \cdot f$. Hence the stiffness contribution coming from the cable system has to be taken in account on the overall length of the suspension bridge.

6.5 Application to the Tacoma Narrow Bridge

The collapse of the central span of the original Tacoma suspension bridge on 7 November 1940 has been studied in many papers. The first one has a thorough report (the "Carmody Report"), written by a governmental committee consisting of O.H. Ammann, T. Von Karman, and G.B. Woodruff in 1941 [52].

Clark Eldridge, a bridge engineer for the Washington State Toll Bridge Authority, proposed a design in 1938. The central span was 853.4m long and 11.9m wide, with two lanes. A truss below the roadway was 7.6m deep to stiffen the deck against vertical, lateral, and torsional displacements. The design was submitted to the US Public Works Authority (PWA), which was to provide a grant for 45 percent of the cost, with the remainder to be borrowed from the Reconstruction Finance Corporation and paid back from tolls. The estimated cost was \$11 million. The PWA wanted to lower the cost, and a well-known consultant, Leon Moisseiff of New York, was hired. He replaced the truss in Eldridge's design with two vertical (stiffening) silicon-steel plate girders along the sides, extending 1.22m above and below the roadway. Stringers and laterals with a chevron (K) configuration were placed below the deck. The new estimated cost was \$6.4 million. The Washington State engineers accepted the new deck so that they could get a bridge over the Tacoma Narrows.

As an aside, a replacement bridge was built on the site 10 years after the collapse, for \$14 million. It has four lanes. The deck is 18.3m wide and 10.1m deep, with a stiffening truss below the roadway and with three sets of diagonal shock absorbers on each side at midspan. An adjacent bridge with three lanes opened in 2007, at a cost of \$849 million.

The original Tacoma suspension bridge was opened on 1 July 1940 and since the opening day vertical oscillations appeared due to lateral winds whose speed reached more than 22m/s. In those cases the amplitude ranges from 0.4m up to 0.76m [26]. Those vertical oscillations were not considered dangerous and they died away due damping forces when the velocity of wind dropped down. On 7 November 1940 the wind speed of 19 m/s was measured. The motion of the deck before 10 a.m. was vertical with an amplitude not more than 0.5 m. The frequency of the motion was 36–38 cycles per minute, which was significantly higher than previously measured frequencies. Around 10 a.m. the motion of the central span switched into a torsional mode with a single nod at the midspan. The torsional oscillations appeared after the loosening of the midspan cable band on one main cable. The initial frequency was 14 cycles per minute, but after a short time it decreased to 12 cycles per minute, perhaps due to some damage within the deck.

The motion of the central span changed form during the subsequent hour, but it was primarily a one-noded torsional oscillation. The maximum twist angle was about 35° and the corresponding maximum vertical amplitude was about 4.3 m. The bridge collapsed at 11:10 a.m. and the central span fell into the Tacoma Narrows. From the parameters of the original Tacoma bridge [40,50] it follows that the hangers are sufficiently stiff to be considered inextensible in tension and completely slack in compression.

There have been presented many theories discussing reasons which led to the collapse. The influence of aerodynamic forces has been intensively studied together with some nonlinear phenomena connected with the construction of suspension bridges, namely the nonlinearity of cable systems. Scanlan's approach has resulted in an estimate of the critical flutter velocity for the Tacoma Narrows bridge of approximately 20 m/s [51], which is approximately the wind speed measured on the actual bridge on 7 November 1940.

In the present work we want to consider not only the nonlinearities introduced by the cable system and the ones coming from wind action, but also the effects of parametric flexural excitation of the bridge.

From the available data of the structure [40,50] we can define first the fundamental dimensionless parameters entering in the governing equation of motion.

$$\lambda_L^2 = 168.3$$

$$\chi^2 = 0.3$$

$$\mu^2 = 3.8 \cdot 10^{-4}$$

$$\beta^2 = 1.2 \cdot 10^{-4}$$

With these values we are able to completely define the eigen-properties of the bridge. The ones of interest are the circular frequencies associated to the fifth symmetric flexural mode and to the first skew-symmetric torsional one. In fact just before collapse the bridge oscillates according to a dominant flexural motion characterised by 8 internal nodes that is associated to a fifth order symmetric mode, and once the snap occurs, torsional oscillations of a central one node mode appears.

$$\tilde{\omega}_{w,5} = 32.315$$

$$\tilde{\omega}_{t,1} = 9.187$$

By means of the definition given in Chapter 1 for the dimensionless circular eigen-frequency, we are able to define the frequencies associated to the modes of interest.

$$f_{w,5} = 0.681 \text{ Hz}$$

$$f_{t,1} = 0.194 \text{ Hz}$$

Comparing the numerical results with those observed during the collapse [26,51,52,53] we can state that the flexural frequency just computed is higher than the measured one (of about 0.617 Hz) whilst the computed torsional frequency is slightly lower than the one observed (about 1.94 Hz). The reason is that the proposed model neglects the contribution coming from the motion of pylons assumed to be perfectly rigid and the ones coming from the hangers for which a tenso-rigid constitutive model applies, both make the structure

stiffer in the flexural and torsional direction. On the other hand the assumption of perfectly hinged ends neglects the stiffening contribution coming from cables inertia and mainly from the two side spans. Consequently we can state that on the flexural motion the combination of all these contributions makes the response stiffer whilst the torsional one become softer. The reason hides behind the fact that practically the whole torsional stiffness comes from the two main cables, hence the stiffening contribution coming from hangers deformability is of less relevance than in the flexural response.

Further we are able to estimate the critical wind speed level that is able to lead the structure both at torsional divergence and to Flutter onset.

$$U_D = 41.7 \text{ m/s}$$

Since we are looking for the lowest critical wind speed, we have performed the numerical analysis focusing on the interaction between similar modal shapes characterised by a low order. Hence we have concluded that the lowest threshold is given by the interaction between the first flexural and torsional skew-symmetric modes.

$$U_F = 27.6 \text{ m/s}$$

The results obtained are in accordance with those obtained numerically ($U_F = 20 \text{ m/s}$) by a recent (2004) study of Scanlan [20,51] but not with the experimental ones by Farquhardson [53] in 1954 on a full model 1:50 scale dynamic wind tunnel test ($U_F = 7.1 \text{ m/s}$).

Finally we can focus on the stability conditions analysing the stability map associated to the aeroelastic model for the TNB. In order to compare numerical results with those measured during the collapse we need to take in consideration the fifth order symmetric flexural mode, characterising the structure just before the sudden snap condition, and the first order skew-symmetric torsional one, leading the structure to collapse.

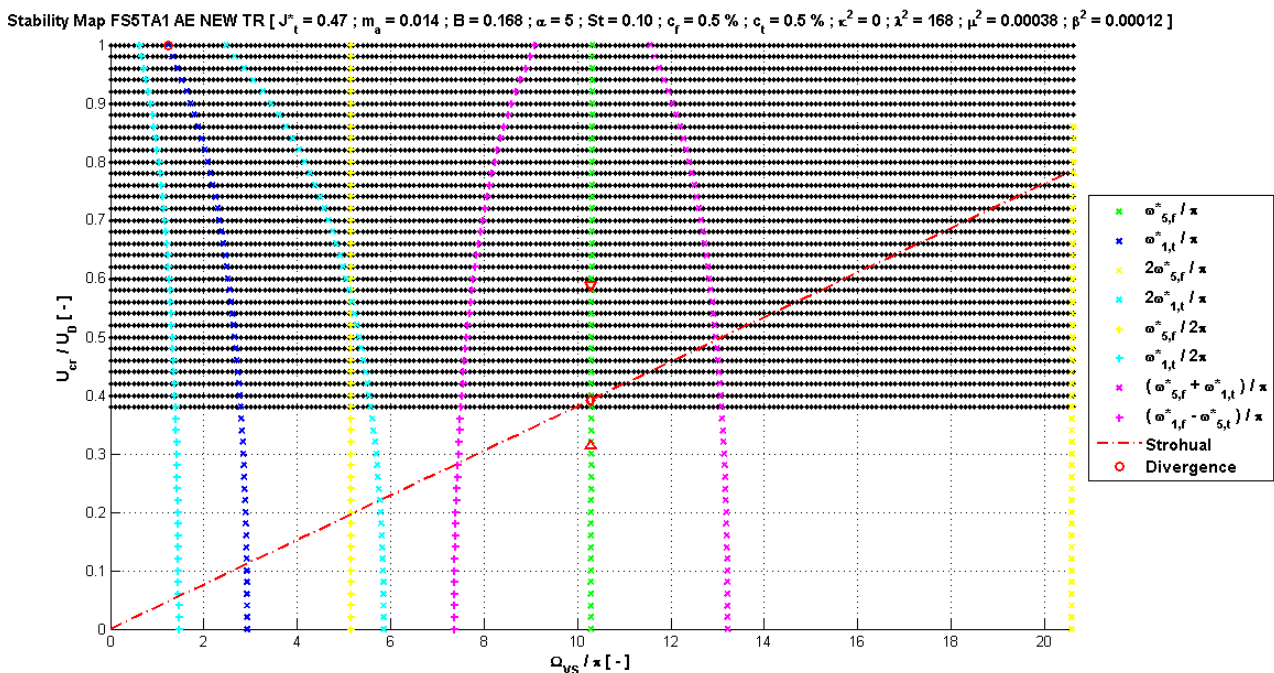


Figure 6.17_ Stability map for the Aeroelastic Model of the Tacoma Narrow Bridge.

First of all we should notice that the interaction between these two modes alone is not able to lead the structure to Flutter onset before the static Divergence condition occurs since the modal shapes are too much different. Secondly we notice immediately that the torsional frequencies are lower than the flexural one due to the fact that are associated to modes of the first and of the fifth order, respectively.

We have not reported the figure associated to the only structural model since the absence of aeroelastic effects preclude the possibility of appearance of unstable conditions in the wind speed range below the static divergence limit.

According to the Strouhal model as vortex shedding frequencies reaches the one proper of the flexural motion of the bridge, the first unstable condition occurs. This does not necessarily mean that lock-in phenomenon occurs since generally, for suspension bridges and all heavy bodies, is the structure itself that governs the vortex shedding frequency. Hence we can interpret the result saying that as the structure excited by vortex shedding vibrates according to the fifth order flexural symmetric mode, the response diverges in time due to the internal parametric interaction with the first order skew-symmetric torsional mode. However what really makes evident the strength of the interaction between aeroelastic effects and internal parametric excitation is the critical wind speed necessary for the onset of unstable conditions.

$$U_{cr} = 0.4 \cdot U_D = 16.7 \text{ m/s}$$

As already noticed in the previous paragraph, accounting for both the aeroelastic and parametric excitation phenomena a drastic reduction of the critical wind speed occurs. In this particular case the reduction is about the 40%.

We can say that the numerical results we have just found for the TNB are reasonable according to the onset registered just before collapse when the wind blow approximately to 19m/s.

Let's now focus on the vertical antinode displacements necessary for the onset of unstable conditions.

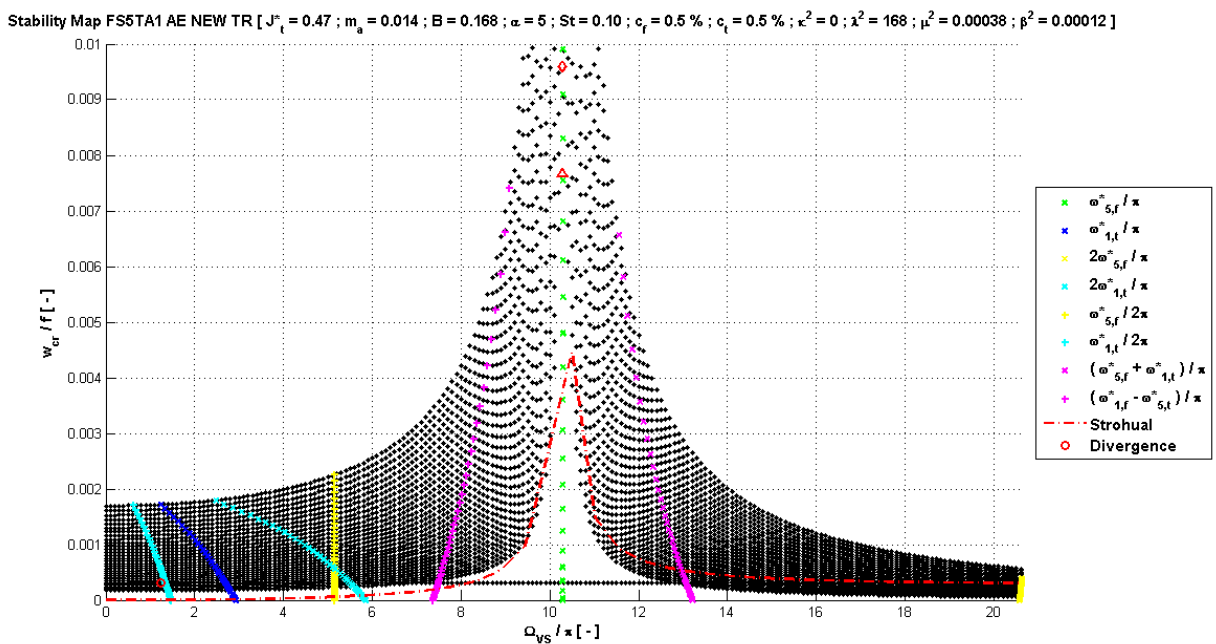


Figure 6.18_ Unstable antinodal displacements for the Tacoma Narrow Bridge.

First notice that, in correspondence of the lock-in point, the unstable antinode displacement is about 0.775% (54cm) the initial cables sag. This is an important data since allows us to state that the hangers does not undergoes to slackening conditions being the initiation threshold for the fifth order flexural symmetric mode equal to 1.033% (73cm) the initial sag. Consequently we can avoid to take in consideration any stiffness reduction due to slackening of hangers and compute all the modal quantities integrating all over the length of the suspension bridge.

Again concerning the comparison with real phenomenon we can state that effectively during collapse of the TNB in the central span no hangers seems to slack. Further just before the bridge motion snaps to the dominant torsional motion, vertical oscillations of about 0.5m were observed, very similarly to those just determined.

7. Conclusion

In this work, a non-linear dynamic model of a suspension bridge is devised, with the purpose of providing a unified framework for the study of aeroelastic and internal parametric resonance instabilities.

An initial insight into cables statics makes possible to detect the main relevant terms governing their elongation and stiffening behaviour. This makes possible to state, first, that only considering higher than one half-wave number would be necessary to consider both the linear and the quadratic contribution; second, that neglecting the cable's slope in the definition of its curvature we will introduce an overestimation of the overall elongation, higher as the modal order increases; and finally as the order of modal shapes increases the total elongation of cables reduces drastically.

Following the classical Deflection Theory, it has been possible to write the nonlinear static flexural response of a suspension bridge. The next step has consisted in the generalization of the displacement field in order to account for the torsional response of the deck-cables system. Hence by means of variational formulation we achieve the self-adjoint system of two equations of motion. The presence of quadratic and cubic nonlinear terms make the equations coupled. Once the dimensionless equations governing the motion of the bridge have been determined, we have been able to perform a modal expansion necessary to define the analytical expression for both the eigen-frequencies and the modal shapes. We notice that the functions governing the eigen-value problem are defined through trigonometric and hyperbolic tangents, characterised by vertical asymptotes, which makes difficult to recognise numerically the roots of the problem. In fact, as the order of modal shapes increases the eigen-roots tend to coalesce on these vertical asymptotes. Concerning modal shapes the fundamental term governing the distinction between symmetric and skew-symmetric configurations is the so-called stiffening term, which vanishes in the latter situation. Symmetric modes' expression contains not only a trigonometric cosine function but also its hyperbolic counterpart. The latter term makes the spatial solution to diverge from the simpler sinusoidal shape introducing additional moving "upward" regions near the bridge span ends and reducing the amplitudes of the negative unitary antinode displacements, characterising also the skew-symmetric shapes. These on the contrary are defined by a sinusoidal function, typically used for Fourier series expansions.

A parametric analysis allows us to detect the main extreme structural conditions such as Flat Cables, Inextensible Cables, Flexible Deck, Rigid Deck, Free Warping Deck, Stiff Warping Deck and all the possible combinations. For each of them we have been able to define both the eigen-values (frequencies) and the eigen-vectors (modal shapes). From a bibliographical research we have been able to define typical values for the dimensionless terms governing the equations of motion such as λ_L^2 , μ^2 , β^2 , χ^2 .

We have concluded that frequencies of vibrations increase more rapidly with the stiffness of the deck (in terms of μ^2 or χ^2 , β^2) as also the cables' inextensibility does. On one hand there exist a critical value for deck stiffness below which the contribution coming from the cable system (λ_L^2) is so relevant that frequencies remain constant. This threshold reduces as the cables contribution or the modal order increases. On the other hand as the deck's stiffness overcomes a certain critical value, the cables' initial tension is no more able to affect the frequencies of vibrations of the system that coalesce to the ones characterising the case of Flat Cables. It has been possible to define a critical combination of cable inextensibility and deck stiffness able to lead the structure to switch from a symmetric to a skew-symmetric mode. This is known from literature as Cross Over Frequency (COF).

Concerning the influence of structural parameters on modal shapes we can say that the bridge performs higher upward motions as the inextensibility of cables increases. In fact as λ_L^2 grows, the cables govern the spatial response of the suspension bridges making deck flexibility less relevant. Further as the deck stiffness increases the antinodal upward and downward motions tend to get farther from the deck midspan. For each generic symmetric modal shape of order n , it's possible to define some critical threshold beyond which it switches from a $2(n - 1)$ to a 0, from a 0 to a $2(n - 1)$ and finally from a $2(n - 1)$ to a $2n$ internal noded mode. Respectively the conditions to be enforced are the vanishing of the midspan upward antinode motion, of the span ends slope, and of the vanishing of the midspan displacement once again.

By analogy we called these conditions Cross Over Modes. We notice that for the first order mode the COF condition is coincident with the $2(n - 1)$ -to-0 and the 0-to- $2(n - 1)$ COM conditions, which appear in correspondence of the same structural conditions. Even more specifically for the case of Free Warping deck the COF and the unique COM condition of torsional mode 1 coalesce on the same curve. Whilst for any modal order we can say that both the COF and all the COM conditions holds for the same value of the tuning parameter λ_L^2 only in correspondence of the Flexible Deck condition. Further it is possible to detect some critical values for the deck stiffness beyond which any level of the cables initial tension would be not sufficient in order to reach any of the COF or COM conditions.

Finally performing the modal expansion of the linear damped-forced equations of motion and applying the well-known Duhamel convolution integral, we have been able to find out some modal participation parameters. The analysis of the one associated to antinodal displacements, relevant for the mode considered, confirm the fact that increasing or decreasing both the deck' stiffness and the cables' inextensibility would not be the better solution. There exist, in fact, an optimal combination of structural parameters able to minimise or maximise the modal displacement in certain position of interest. The same conclusion holds for the participation parameter associated to cables tension increment, although we can recognise that, as the modal order increases, higher levels of cables inextensibility are required to reach peak values of tension increment.

The direct application of the Multiple-Scale perturbation technique allows us to study analytically the main features of the complete nonlinear system of coupled equations. The choice of applying the direct approach ensures the possibility to get analytical expressions for the so-called Quadratic Modes, that are no more than the second order correction of the classical linear ones. The same parametric analysis performed for the linear modes allows us to explain the well-known phenomenon of Travelling Waves, which can be observed from experimental and numerical testing on suspension bridges. In fact, we found that only under very special conditions the second order correction of linear skew-symmetric modal shapes is skew-symmetric too. In all the other, and more common, situations we get symmetric second order corrections to linear skew-symmetric modes. Considering this and the fact that Quadratic Modes varies in time according to a multiple of the non non-linear frequency characterising the Linear Ones, superimposing the two contributions we would observe a higher amplitude of oscillation that moves along the bridge span.

Then we focus on the particular case of the so-called mode-by-mode approach, neglecting interaction between modes of different order, for the special case of 1:1 internal resonance. Hence, we obtain the equations governing the time variation of amplitudes and phase lag for the flexural and the torsional motion. In order to simplify further the treatment we analyse just the steady state response in the case of perfectly isolated system, neglecting any source of dissipation (damping) or excitation (external forces). First we consider the case of dominant flexural or torsional motion. We conclude that the system can perform both a hardening and softening behaviour according to the sign of a parameters collecting all the information regarding the structural data. As already mentioned the structure will vibrates according to a nonlinear frequency that changes as the amplitudes of oscillations, with the risk of performing the well-known Jump Phenomenon. For flexural and torsional dominant motion we observe that the second order correction of modal shapes vibrates according to a frequency that doubles the nonlinear one associated to Linear Modes. Further, Quadratic contribution will not vibrates around the undeformed configuration, hence the overall motion would be drifted apart by a small quantity.

Then analysing the more generic condition of interacting flexural and torsional modes we were able to write the equations of motion in terms of the so-called Energy Exchange Ratio, which allows us to simplify the analysis. Particular cases have been analysed; such as pure Phase Modulation that can be performed as long as amplitudes remains constant in time, leading to the so-called Entrainment phenomenon. On the contrary pure Amplitude Modulation is not feasible. Generally suspension bridges perform a combination of phase an amplitudes modulation typical of internal energetic exchange phenomena.

Then find out the initial conditions required to get periodic solutions in the steady state response, concluding that periodicity is a very unstable condition, meaning that the system generally prefers internal energy exchange.

Focusing on initial conditions we observe that the system will oscillates between the initial condition and the so-called upper or lower aperiodic regime threshold. Then performing a parametric analysis of initial conditions we were able to define the initial energy required to get pure flexural or torsional motion, and the one that grants the periodic passage from one to the other.

Finally we perform a simple stability analysis perturbing the equations of motion by means of a small amount of additional energy and phase lag. We obtain a general condition of stability. Consequently for those initial conditions for which that condition is not satisfied the response could be unstable but also indifferent to perturbations. Hence the results are not so satisfactory.

A perfectly tenso-rigid constitutive model for hangers has been assumed in order to take into account the nonlinearities coming from the Slackening phenomenon. Starting from the Variational Formulation has been possible to reformulate the complete system of equations governing the response of the suspension bridges taking in account both the non-local, coming from the main cables, and the local, from the hangers, sources of nonlinearities. In order to take in consideration the fact that, in those regions where hangers undergoes to slackening, the cables stiffening contribution vanishes, we have introduce proper reduction parameters. We notice that only in the case of pure torsional vibration the slackening condition would be pointwise.

Then, passing to the modal projection of equations, we focus on the slackening onset, writing down the analytical expression for the critical antinode amplitude required for both the flexural and torsional motion. Focusing on the more interesting case of pure flexural motion, we get the critical amplitudes that reduces drastically as the modal order increases. Whilst the effect of structural parameters is much more complicate, in fact there exist critical structural configuration able to minimise the slackening amplitude making the structure much more susceptible to that phenomenon. Generally those critical conditions require to have high level of cables inextensibility and of deck' stiffness.

The analysis of cables tension increment, associate to the antinode amplitude required to get first slackening of hangers, had initially the scope of neglecting those amplitudes leading to too high reduction of cables initial tension, with the risk of slackening of the cables system itself. However it unexpectedly reveals also that under particular structural condition the initiation of slackening would be located in correspondence of the pylons. Obviously this is not admissible being, there, the bridge supported directly by the vertical elements. Fortunately this particular condition will not be feasible with real life structural parameters.

A deep insight in analytical aerodynamic field paves the way for the study of aeroelastic effects treated by means of the well-known Thodorsen Theory for an airfoil immersed in a potential flow. Wind forces introduce additional mass, damping and stiffness that not only couples the linear equations of motion but also led the system to be no more self-adjoin. In fact, it loses its symmetries both in damping and stiffness matrices, making the structure susceptible respectively to flutter instabilities and static divergence problems.

The comparison between different approaches to the Flutter problem allows us to analyse the main differences. In fact, comparing the original formulation proposed by Theodorsen with the so-called Steady-State we get a relevant reduction of the critical wind speed. The unique difference between the two formulations is that the latter one assume a priori a unitary value for the well-known Complex Theodorsen Function. Hence, results confirm the importance of maintaining the actual reduced frequency of the aeroelastic system, in order to account for the effects that the structural motion has on the surrounding flow. From the analysis of the frequencies and the damping of the aeroelastic system we notice that as the flexural and torsional frequencies of the structural system alone are increasingly different, the Flutter onset occurs for wind speed nearer to the Static Divergence condition. This fact can be explained considering that the higher is the similarity of the two main interacting modes the higher is the interaction, and then the lower is the Flutter critical speed. Further, the slope of the damping curve of the unstable branch (usually the torsional one) increases as the difference between flexural and torsional structural frequencies does; meaning that the onset of Flutter condition would be less possible, but as it occurs it would be increasingly violent and sudden.

The fact that frequencies varies with the wind speed level allows us to find out so-called aeroelastic modal shapes. Anyway we conclude that the variation with respect to the structural frequencies and modal shapes is negligible up to the Flutter onset.

The non-linear system has been treated in the framework of Floquet stability theory, thus achieving the stability maps in terms of wind speed and frequency of vortex shedding. After a thorough examination of the achieved results, we can conclude saying that parametric resonance is a critical phenomenon that can be activated by vortex-shedding as far as the sectional shape factor is low enough. This should warn very much engineers, since a phenomenon like vortex-shedding is usually taken in consideration just concerning serviceability limit states. On the contrary, we have just found that under certain conditions such a phenomenon may lead to very strong and critical unstable conditions in correspondence of wind speed that can be considered safe with respect to classical static divergence or dynamic flutter instabilities.

Finally, the classical application to the Tacoma Narrow Bridges is performed considering the interaction between the fifth flexural symmetric mode and the first torsional skew-symmetric one. Results in terms of frequencies match with those observed just before the collapse of the TNB. Whilst the lowest Flutter speed, obtained numerically by the skew-symmetric modes of first order, seems to overestimate the results obtained by experimental test on the full model scaled bridge. However, the stability map for the TNB confirm that parametric resonance and aeroelastic effects, together, lead the structural response to diverge in time in correspondence of wind speed level that is considerably lower than flutter speed. Further the threshold obtained numerically seems to be comparable to that measured during the collapse, both in terms of wind speed level and flexural amplitudes.

The present study can be improved accounting for the possible slackening of vertical hangers directly in the code written to construct the stability maps, which may introduce an additional non-linearity to the system. In fact, the structural model considered herein is based on perfectly bilateral behaviour of hangers, so that the deck displacement parameters are univocally connected to the cable displacements. In the presence of large upward displacement, slackening may occur, thus leading to a loss of stiffness for the whole system. In spite of this limitation, the model still provides valid results: in fact in the cases analysed the unstable behaviour corresponds to displacements that are lower than the ones necessary for slackening initiation. In the future development of this work, when dealing with higher modes in the framework of multi modal approach, it will be unavoidable to introduce the loss of stiffness due to slackening, since as we have observed initiation will be much easily feasible.

References

- [1] A. Pugsley, *The theory of suspension bridges*. 2nd ed. Edward Arnold, 1968.
- [2] D.B. Steinman, *A practical treatise on suspension bridges*. Wiley, 1953.
- [3] F. Bleich, C. McCulloch, R. Rosecrans, G. Vincent, *The mathematical theory of vibration in suspension bridges*, U.S. Government Printing Office, 1950.
- [4] D. B. Steinman, A generalized deflection theory for suspension bridges, *Transaction of ASCE*, 100, 1133-1234, 1935.
- [5] J. Luco, J. Turmo, Linear vertical vibrations of suspension bridges: A review of continuum models and some new results, *Soil Dynamics and Earthquake Engineering*, 30, 769–781, 2010.
- [6] H. Irvine, *Cable structures*, MITpress, 1981.
- [7] A. M. Abdel-Ghaffar, Vertical vibration analysis of suspension bridges, *ASCE Journal of Structural Division*, 106, 2053-2075, 1980.
- [8] A. M. Abdel-Ghaffar, Free torsional vibrations of suspension bridges, *ASCE Journal of Structural Division*, 105, 767–788, 1979.
- [9] A. M. Abdel-Ghaffar, Free lateral vibrations of suspension bridges, *ASCE Journal of Structural Division*, 104, 503-525, 1978.
- [10] A. M. Abdel-Ghaffar, Suspension bridge vibration: continuum formulation, *ASCE Journal of the Engineering Mechanics Division*, 108, 1215–1232, 1982.
- [11] A.M. Abdel-Ghaffar, L. Rubin, Nonlinear free vibrations of suspension bridges: Theory, *Journal of Engineering Mechanics*, 109, 313–329, 1983.
- [12] A.M. Abdel-Ghaffar, L. Rubin, Nonlinear free vibrations of suspension bridges: Application, *Journal of Engineering Mechanics*, 109, 330–345, 1983.
- [13] O.H. Ammann, T. Von Kármán, G.B. Woodruff, The failure of the Tacoma Narrows Bridge : a report to the honorable John M. Carmody, Federal Works Agency, 1941.
- [14] R. L. Bisplinghoff, H. Ashley, R. L. Halfman, *Aeroelasticity*, Addison-Wesley, 1955.
- [15] T. Theodorsen, General theory of aerodynamic instability and the mechanism of flutter, NACA Report n. 496, 1979.
- [16] L. Salvatori, C. Borri, Frequency- and time-domain methods for the numerical modeling of full-bridge aeroelasticity, *Computers and Structures*, 85, 675-687, 2007.
- [17] A. Arena, W. Lacarbonara, Nonlinear parametric modeling of suspension bridges under aeroelastic forces: torsional divergence and flutter, *Nonlinear Dynamics*, 70, 2487-2510, 2012.
- [18] D. Sado, Energy transfer in two-degree-of-freedom vibrating system : a survey, *Journal of Theoretical and Applied Mechanics*, 31, 151-173, 1993.
- [19] Y. A. Rossikhin, M. V. Shitikova, Analysis of nonlinear free vibrations of suspension bridges, *Journal of Sound and Vibration*, 186, 369-393, 1995.
- [20] M. Cevik, M. Pakdemirli, Non linear vibrations of suspension bridges with external excitation, *International Journal of Nonlinear Mechanics*, 40, 901-923, 2005.
- [21] A. H. Nayfeh, Introduction to perturbation techniques, Wiley, 1993.
- [22] G. Airolì, F. Gazzola, A new mathematical explanation of what triggered the catastrophic torsional mode of the Tacoma Narrows Bridge, *Applied Mathematical Modelling*, 39, 901-912, 2015.
- [23] K. S. Moore, Large torsional oscillations in a suspension bridge: Multiple periodic solutions to a nonlinear wave equation, *SIAM Journal on Mathematical Analysis*, 33, 1411-1429, 2002.

- [24] P.J. McKenna, Large torsional oscillations in suspension bridges revised: Fixing an old approximation, *American Mathematics Monthly*, 106, 1-18, 1999.
- [25] D. Jacover, P. J. McKenna, Nonlinear torsional flexing in a periodically forced suspended beam, *Journal of Computational and Applied Mathematics*, 52, 241-265, 1994.
- [26] R.H. Plaut, Snap loads and torsional oscillations of the original Tacoma Narrows Bridge, *Journal of Sound and Vibration*, 309, 613–636, 2008.
- [27] R.H. Plaut, F.M. Davis, Sudden lateral asymmetry and torsional oscillations of section models of suspension bridges, *Journal of Sound and Vibration* 307, 2007, 894–905, 2007
- [28] L. Cesari, Asymptotic behaviour and stability problems in ordinary differential equations, Springer, 1971.
- [29] G. Herrmann, W. Hauger, On the interrelation of divergence, flutter and auto-parametric resonance, *Ingenieur-Archiv*, 42, 81-88, 1973.
- [30] E. Simiu, R.H. Scanlan, *Wind effects on structures*, Wiley, 1996.
- [31] J. M. W. Brownjohn, F. Magalhaes, E. Caetano, A. Cunha, Ambient vibration re-testing and operational modal analysis of the Humber Bridge, *Engineering Structures*, 32, 2003-2018, 2010.
- [32] F. Nieto, S. Hernandez, J. A. Jurado, A. Mosquera, Analytical approach to sensitivity analysis of flutter speed in bridges considering deck mass, *Advances in Engineering Software*, 42, 117-129, 2011.
- [33] S. Adnur, M. Gunaydin, A. C. Altunisik, B. Sevim, Construction stage analysis of Humber suspension bridge, *Applied Mathematical Modelling*, 36, 5492-5505, 2012.
- [34] K. Kaptan, S. Tezacn, S. Altin, S. Cherry, Dynamic analysis of suspension bridges and full scale testing, *Procedia Engineering*, 14, 1065-1070, 2011.
- [35] N. M. Apaydin, Earthquake performance assessment and retrofit investigations of two suspension bridges in Istanbul, *Soil Dynamics and Earthquake Engineering*, 30, 702-710, 2010.
- [36] F. Ubertini, Effects of cables damage on vertical and torsional eigenproperties of suspension bridges, *Journal of Sound and Vibrations*, 333, 2404-2421, 2014.
- [37] H. Wang, T. Tao, R. Zhou, X. Hua, A. Kareem, Parameter sensitivity study on flutter stability of long-span triple-tower suspension bridge, *Journal of Wind Engineering and Industrial Aerodynamics*, 128, 12-21, 2014.
- [38] D. Cobo del Arco, A. C. Aparicio, Preliminary static analysis of suspension bridges, *Engineering Structures*, 23, 1096-1103, 2001.
- [39] R. Karoumi, Some modelling aspects in the nonlinear finite element analysis of cable supported bridges, *Computer and Structures*, 71, 397-412, 1999.
- [40] J. Malik, Sudden lateral asymmetric and torsional oscillations in the original Tacoma suspension bridge, *Journal of Sound and Vibration*, 332, 3772-3789, 2013.
- [41] J. Welte, T. Kniffka, H. Ecker, Parametric excitation in a two degree of freedom MEMS system, *Shock and Vibrations*, 20, 1113-1124, 2013.
- [42] S. Deniz, T. Staubli, Oscillating rectangular and octagonal profiles: interaction of leading- and trailing-edge vortex formation, *Journal of Fluids and Structures*, 11, 3–31, 1997.
- [43] A. Larsen, J. H. Walther, Discrete vortex simulation of flow around five generic bridge deck sections, *Journal of Wind Engineering and Industrial Aerodynamics*, 77-78, 591-602, 1998.
- [44] A. H. Nayfeh, *Perturbation methods*, Wiley, 1973.
- [45] M. Pakdemirli, H. Boyaci, Comparison of direct- perturbation methods with discretization-methods for non-linear vibrations, *Journal of sound and vibration*, 186, 835-845, 1994.
- [46] A. Roshko, On the drag and shedding frequency of two dimensional bluff bodies, National Advisory Committee for Aeronautics, NACA Technical Note 3169, 1954.

- [47] S. Deniz, T. Staubli, Oscillating rectangular and octagonal profiles: interaction of leading and trailing-edge vortex formation, *Jurnal of Fluids and Structures*, 11, 3-31, 1997.
- [48] O. M. Griffin, S. E. Ramberg, Thevortex-street wakes of vibrating cylinders, *Journal of Fluid Mechanics*, 66, 553-576, 1974.
- [49] A. Larsen, J. H. Walther, Discrete simulation of flow around five generic bridge deck sections, *Journal of Wind Engineering and Industrial Aerodynamics*, 77-78, 591-602, 1998.
- [50] P. Bergot, L. Civati, Dynamic structural instability in suspension bridges, Master Thesis, F. Gazzola, 2014.
- [51] R. H. Scanlan, E. Simiu, Aeroelasticity of civil engineering structures, in: E. H. Dowell (Ed.), *A Modern Course in Aeroelasticity*, 4th reviewed and enlarged edition, Kluwer Academic Publishers, 2004.
- [52] O.H. Ammann, T. von Karman, G.B. Woodruff, The failure of the Tacoma Narrows Bridge: a report to the Honorable John M Carmody, Administrator, Federal Works Agency, Washington, DC, March 28, 1941. Also in: *The Failure of the Tacoma Narrows Bridge: A Reprint of Original Reports*, Advisory Board on the Investigation of Suspension Bridges, Bulletin No. 78 of the Agricultural and Mechanical College of Texas, Fourth Series, Vol. 15, No. 1, School of Engineering, Texas Engineering Experiment Station College Station, Texas, January 1, 1944.
- [53] K.Y. Billah, R.H. Scanlan, Resonance, Tacoma Narrows Bridge failure, and undergraduate physics textbooks, *American Journal of Physics*, 59, 118–124, 1991.
- [54] D. Baccarin, Suspension Bridges - Conceptual analysis and model arrangement, Master Thesis, A. Capsoni, 2014.